ISSN: 2152-7385 Volume 6, Number 1, January 2015

Scientific Research Publishing

Applied Mathematics

Journal Editorial Board

ISSN Print: 2152-7385 ISSN Online: 2152-7393
http://www.scirp.org/journal/am

Applied Mathematics, 2015, 6, 1-220
Published Online January 2015 in SciRes. http://www.scirp.org/journal/am

Table of Contents

Volume 6 Number 1 January 2015

Applied Mathematics, 2015, 6, 1-220
Published Online January 2015 in SciRes. http://www.scirp.org/journal/am

Applied Mathematics (AM)

Journal Information

SUBSCRIPTIONS

The *Applied Mathematics* (Online at Scientific Research Publishing, www.SciRP.org) is published monthly by Scientific Research Publishing, Inc., USA.

Subscription rates:

Print: $89 per copy.
To subscribe, please contact Journals Subscriptions Department, E-mail: sub@scirp.org

SERVICES

Advertisements
Advertisement Sales Department, E-mail: service@scirp.org

Reprints (minimum quantity 100 copies)
Reprints Co-ordinator, Scientific Research Publishing, Inc., USA.
E-mail: sub@scirp.org

COPYRIGHT

PRODUCTION INFORMATION

For manuscripts that have been accepted for publication, please contact:
E-mail: am@scirp.org

Applied Mathematics, 2015, 6, 1-6
Published Online January 2015 in SciRes. http://www.scirp.org/journal/am
http://dx.doi.org/10.4236/am.2015.61001

Generalization of Some Problems with *s*-Separation

Beih El-Sayed El-Desouky, Mohamed Moustafa Gad, Shimaa El-Eraqy

Department of Mathematics, Faculty of Science, Mansoura University, Mansoura, Egypt
Email: b_desouky@yahoo.com

Received 29 October 2014; revised 26 November 2014; accepted 18 December 2014

Abstract

In this article we apply and discuss El-Desouky technique to derive a generalization of the problem of selecting *k* balls from an *n*-line with no two adjacent balls being *s*-separation. We solve the problem in which the separation of the adjacent elements is not having odd and even separation. Also we enumerate the number of ways of selecting *k* objects from *n*-line objects with no two adjacent being of separations *m*, *m* + 1, ⋯, *pm*, where *p* is positive integer. Moreover we discuss some applications on these problems.

Keywords

Probability Function, *s*-Separation, *s*-Successions, *n*-Line, *n*-Circle

1. Introduction

Kaplansky [1] (see also Riordan ([2] p. 198, lemma) and Moser [3]) studied the problem of selecting k objects from n objects arranged in a line (called n-line) or a circle (called n-circle) with no two selected objects being consecutive. Let $f(x,y)$ and $g(x,y)$ denote the number of ways of such selections for n-line and n-circle respectively. Kaplansky proved that

$$f(n,k)=\begin{cases}\binom{n-k+1}{k}, & 0\le k\le n\\ 0, & \text{otherwise,}\end{cases} \tag{1.1}$$

and

$$g(n,k)=\begin{cases}\frac{n}{k}\binom{n-k-1}{k-1}, & n\ge 2k+1\\ 0, & 1\le n\le k.\end{cases} \tag{1.2}$$

How to cite this paper: El-Desouky, B.S., Gad, M.M. and El-Eraqy, S. (2015) Generalization of Some Problems with *s*-Separation. *Applied Mathematics*, **6**, 1-6. http://dx.doi.org/10.4236/am.2015.61001

El-Desouky [4] studied another related problem with different techniques and proved that

$$l(n,k)=\begin{cases}\sum_{i=0}^{\lambda}\binom{k-1}{i}\binom{n-k+1-i}{i+1}, & \lambda=\min\left(k-1,\left[\frac{n-k}{2}\right]\right),\ 0\le k\le n\\ 0, & \text{otherwise,}\end{cases} \tag{1.3}$$

where $l(n,k)$ is the number of ways of selecting *k* balls from *n* balls arranged in a line with no two adjacent balls being unit separation.

In the following we adopt some conventions: $\left[x^n\right]f(x)$ denotes the coefficient of x^n in the formal power series $f(x)$; $\left[x^n y^m\right]f(x,y)$ denotes the coefficient of $x^n y^m$ in the series $f(x,y)$; $[x]$ is the largest integer less than or equal to *x*, $N=\{0,1,\cdots\}$ and $N_n=\{1,2,3,\cdots\}$.

Also, El-Desouky [5] derived a generalization of the problem given in [4] as follows: let $l_s(n,k)$ denote the number of ways of selecting *k* balls from *n* balls arranged in a line with no two adjacent balls from the *k* selected balls being *s*-separation; two balls have separation *s* if they are separated by exactly *s* balls. Let $d_s(n,k)$ denote the number of ways of selecting *k* balls from *n* balls arranged in a circle with no two adjacent balls from the *k* selected balls being *s*-separation

Let $l_s(n,k)$ be as defined before. Then $l_s(n,k)$ is equal to the number of *k*-subsets of N_n where the difference $s+1$ is not allowed, so

$$l_s(n,k)=\sum_{i=0}^{\nu}(-1)^i\binom{k-1}{i}\binom{n-(s+1)i}{k-i}$$
$$\text{where } \nu=\min\left(k-1,\left[\frac{n-k}{s}\right]\right),\ 0\le k\le n,\ \text{and } s=0,1,\cdots,n-k. \tag{1.4}$$

Let $d_s(n,k)$ be as defined before. Then the difference $s+1$ is not allowed, so

$$d_s(n,k)=\frac{n}{k}\sum_{i=0}^{\beta}(-1)^i\binom{k}{i}\binom{n-(s+1)i-1}{k-i-1},$$
$$\text{where } \beta=\min\left(k,\left[\frac{n-k}{s}\right]\right),\ 0\le k\le n,\ \text{and } s=0,1,\cdots,n-k. \tag{1.5}$$

Let $l_s(n,k,m)$ be the number of ways of selecting *k* balls from *n* balls arranged in a line with exactly *m* adjacent balls being of separation *s* or $(s\text{-successions})$, which gives a generalization of (4.1) in El-Desouky [4]. Thus,

$$l_s(n,k,m)=\sum_{i=m}^{\mu'}\sum_{j=0}^{k-1-i}(-1)^i\binom{k-1}{i}\binom{k-1-i}{j}\binom{n-(s+1)i-sj}{k-m},$$
$$\text{where } \mu'=\min\left(k-1,\left[\frac{n-k+m}{s+1}\right]\right),\ m=0,1,\cdots,k-1,\ s=0,1,\cdots,n-k. \tag{1.6}$$

For more details on such problems, see [3] [6] [7].

2. Main Results

We use El-Desouky technique to solve two problems in the linear case, with new restrictions. That is if the separation of any two adjacent elements from the *k* selected elements being of odd separation and of even separation. Moreover, we enumerate $M_s(n,k;m,pm)$ which denotes the number of ways of selecting *k* objects from *n* objects arrayed in a line where any two adjacent objects from the *k* selected objects are not being of *m*, *m* + 1, ⋯, *pm* separations, where *p* is positive integer.

2.1. No Two Adjacent Being Odd Separation

Let $y_o(n,k)$ denote the number of ways of selecting *k* balls from *n* balls arranged in a line, where the separation of any two adjacent balls from the k selected balls being of odd separation. say s, *i.e.* $s = 1,3,5,\cdots$. This means that no two adjacent being of 2, 4, 6, $\cdots$ differences, see **Table 1**.

So, following Decomposition (2.3.14) see [8] (p. 55), $y_o(n,k)$ is equal to the number of k-subsets of N_n where the differences $s+1$, $s = 1,3,5,\cdots$ are not allowed, hence $y_o(n,k) = \left[x^n\right] f(x)$, where

$$\begin{aligned} f(x) &= \left(x + x^2 + \cdots\right)\left[x + x^2 + \cdots - \left(x^2 + x^4 + \cdots\right)\right]^{k-1}\left(1 + x + \cdots\right) \\ &= \frac{x}{1-x}\left[\frac{x}{1-x} - \left(x^2 + x^4 + \cdots\right)\right]^{k-1}\frac{1}{1-x} \\ &= \frac{x}{(1-x)^2}\frac{x^{k-1}}{(1-x)^{k-1}}\left[1 - (1-x)\left(x + x^3 + \cdots\right)\right]^{k-1} \\ &= x^k (1-x)^{-(k+1)}(1-x)^{-(k+1)}, \end{aligned}$$

hence

$$f(x) = \sum_{i=0}^{\infty}\sum_{j=0}^{\infty}(-1)^j x^k \binom{k+i}{i} x^i \binom{k+j-2}{j} x^j = \sum_{i=0}^{\infty}\sum_{j=0}^{\infty}(-1)^j \binom{k+i}{i}\binom{k+j-2}{j} x^{i+j+k}.$$

Setting $n = i + j + k$ $j = n - i - k$ we have

$$f(x) = \sum_{n=k}^{\infty}\sum_{i=0}^{n-k}(-1)^{n-i-k}\binom{k+i}{i}\binom{k+n-i-k-2}{n-i-k}x^n = \sum_{n=k}^{\infty}\sum_{i=0}^{n-k}(-1)^{n-i-k}\binom{k+i}{i}\binom{n-i-2}{n-i-k}x^n.$$

Therefore, the coefficient of x^n gives

$$y_o(n,k) = \sum_{i=0}^{n-k}(-1)^{n-i-k}\binom{k+i}{i}\binom{n-i-2}{k-2}.$$

A calculated table for the values of $y_o(n,k)$ is given in **Table 1**, where $1 \le n$, $k \le 10$.

Remark 1. *It is easy to conclude that* $y_o(n,k)$ *satisfies the following recurrence relation*

$$y_o(n,k) = y_o(n-1,k-1) + y_o(n-2,k), \quad n,\ k \ge 2 \ \text{ and } \ y_o(n,k) = 0 \ \text{ for } \ k > n \tag{2.1}$$

with the convention $y_o(n,1) = n$, $n \ge 1$.

Table 1. A calculated table for the values of $y_o(n,k)$.

n \ k	1	2	3	4	5	6	7	8	9	10
1	1	0	0	0	0	0	0	0	0	0
2	2	1	0	0	0	0	0	0	0	0
3	3	2	1	0	0	0	0	0	0	0
4	4	4	2	1	0	0	0	0	0	0
5	5	6	5	2	1	0	0	0	0	0
6	6	9	8	6	2	1	0	0	0	0
7	7	12	14	10	7	2	1	0	0	0
8	8	16	20	20	12	8	2	1	0	0
9	9	20	30	30	27	14	9	2	1	0
10	10	25	40	50	42	35	16	10	2	1

2.2. No Two Adjacent Being Even Separation

Let $y_e(n,k)$ denote the number of ways of selecting k balls from n balls arranged in a line, where the separation of any two adjacent balls from the k selected balls are not being of even separation, say s *i.e.* $s = 0, 2, 4, \cdots$. This means that no two adjacent being of 1, 3, 5,$\cdots$ differences.

So, following Decomposition (2.3.14) see [8] (p. 55) then $y_e(n,k)$ is equal to the number of k-subsets of N_n where the differences $s+1$, $s = 0, 2, 4, \cdots$ are not allowed, hence $y_e(n,k) = \left[x^n\right] f(x)$, where

$$\begin{aligned} f(x) &= \left(x + x^2 + \cdots\right)\left[x + x^2 + \cdots - \left(x + x^3 + \cdots\right)\right]^{k-1}(1 + x + \cdots) \\ &= \frac{x}{1-x}\left[\frac{x}{1-x} - \left(x + x^3 + \cdots\right)\right]^{k-1}\frac{1}{1-x} \\ &= \frac{x}{(1-x)^2}\frac{x^{k-1}}{(1-x)^{k-1}}\left[1 - (1-x)\left(1 + x^2 + \cdots\right)\right]^{k-1} \\ &= \frac{x^{2k-1}}{(1-x)^{k+1}(1+x)^{k-1}} \\ &= x^{2k-1}(1-x)^{-(k-1)}(1+x)^{-(k-1)}, \end{aligned}$$

hence

$$f(x) = \sum_{i=0}^{\infty}\sum_{j=0}^{\infty}(-1)^j x^{2k-1}\binom{k+i}{i}x^i\binom{k+j-2}{j}x^j = \sum_{i=0}^{\infty}\sum_{j=0}^{\infty}(-1)^j\binom{k+i}{i}\binom{k+j-2}{j}x^{2k-1+i+j}.$$

Setting $n = 2k-1+i+j$, $j = n-2k+1-i$ we get

$$f(x) = \sum_{j=0}^{\infty}\sum_{i=0}^{n-2k+1}(-1)^{n+1-i}\binom{k+i}{i}\binom{k+n-2k+1-i-2}{n-2k+1-i}x^n = \sum_{j=0}^{\infty}\sum_{i=0}^{n-2k+1}(-1)^{n+1-i}\binom{k+i}{i}\binom{n-k-i-1}{k-2}x^n.$$

Therefore, the coefficient of x^n gives

$$y_e(n,k) = \sum_{i=0}^{n-2k+1}(-1)^{n+1-i}\binom{k+i}{i}\binom{n-k-i-1}{k-2}. \tag{2.2}$$

Moreover in the next subsection, we use our technique to enumerate $M_s(n,k;m,pm)$ the number of ways of selecting k objects from n objects arrayed in a line such that no two adjacent elements have the differences $m + 1$, $m + 2$, $\cdots$, $pm + 1$ *i.e.* no two adjacent element being of m, $m + 1$, $\cdots$, pm separations, where p is positive integer.

2.3. Explicit Formula for $M_s(n,k;m,pm)$

Let $M_s(n,k;m,pm)$ be the number of ways of selecting k objects from n objects arrayed in a line where any two adjacent objects from the k selected objects are not being of m, $m + 1$, $\cdots$, pm separations, where p is positive integer, hence $M_s(n,k;m,pm) = \left[x^n\right] f(x)$, where

$$\begin{aligned} f(x) &= \left(x + x^2 + \cdots\right)\left[x + x^2 + \cdots - \left(x^{m+1} + x^{m+2} + \cdots + x^{pm+1}\right)\right]^{k-1}\frac{1}{1-x} \\ &= \frac{x^k}{(1-x)^2}\left[\frac{1-x^m}{1-x} + x^{pm+1}(1-x)^{-1}\right]^{k-1} \\ &= x^k(1-x)^{-(k+1)}\left[1 - x^m\left(1 - x^{pm-m+1}\right)\right]^{k-1} \\ &= \sum_{i=0}^{\infty}\sum_{j=0}^{\infty}\sum_{l=0}^{\infty}(-1)^{i+j}\binom{k-1}{i}\binom{i}{j}x^{j(pm-m+1)+mi}x^l\binom{k+l}{l}x^k. \end{aligned}$$

Setting $n = j(pm-m+1)+mi+l+k$ it is easy to find the coefficient of x^n hence

$$M_s(n,k;m,pm)=\sum_{i=0}^{k-1}\sum_{j=0}^{i}(-1)^{i+j}\binom{k-1}{i}\binom{i}{j}\binom{n-j(pm-m+1)-mi}{k}. \tag{2.3}$$

3. Some Applications

Let n urns be set out along a line, that is, one-dimensional.

Suppose we have m balls of which m_i are of colour c_i, $i=1,2,\cdots,k$ and we assign these balls to urns so that, see Pease [9]:

i) No urn contains more than one ball.

ii) All m_i balls of colour c_i are in consecutive urns, $i=1,2,\cdots,k$.

El-Desouky proved that if the order of colours of the groups is specified, the number of arrangement is just $\binom{n-m+k}{k}$. Hence if the total number of balls $\sum_{i=1}^{k}m_i=2k-1,$ the number of arrangements is $l_o(n,k)=f(n,k)=\binom{n-k+1}{k}$ as a special case of El-Desouky results [5].

It is of practical interest to find the asymptotic behavior of $f(n,k)$ or the probability $p(n,k)=f(n,k)\Big/\binom{n}{k}$ for large n and k.

Let X be a random variable having the probability function $p(n,k)$ then

$$P(X=k)=p(n,k)=\frac{\binom{n-k+1}{k}}{\binom{n}{k}},$$

so

$$\begin{aligned}\ln P(X=k)&=\ln\left[\left(1-\frac{k-1}{n}\right)\left(1-\frac{k}{n}\right)\cdots\left(1-\frac{2(k-1)}{n}\right)\right]-\ln\left[\left(1-\frac{1}{n}\right)\left(1-\frac{2}{n}\right)\cdots\left(1-\frac{k-2}{n}\right)\left(1-\frac{k-1}{n}\right)\right]\\&\simeq\left[-\frac{k-1}{n}-\frac{k}{n}-\cdots-\frac{2(k-1)}{n}\right]-\left[-\frac{1}{n}-\frac{2}{n}-\cdots-\frac{k-2}{n}-\frac{k-1}{n}\right]\\&=-\frac{3k(k-1)}{2n}+\frac{k(k-1)}{2n}=-\frac{k(k-1)}{n},\end{aligned}$$

where we used the first aproximation

$$\ln(1-x)=-x.$$

Therefore,

$$P(X=k)=\mathrm{e}^{-\frac{k(k-1)}{n}}.$$

Putting $Y=\frac{X}{\sqrt{n}}$ we have

$$\begin{aligned}P(Y=t)&=P\left(\frac{X}{\sqrt{n}}=t\right)=P\left(X=\sqrt{n}t\right)\\&=\mathrm{e}^{\frac{-\sqrt{n}t\left(\sqrt{n}t-1\right)}{n}},\ \text{hence}\end{aligned}$$

$$\lim_{n\to\infty} P(Y=t) = \mathrm{e}^{-t^2}.$$

Maosen [10] considered the following problem. Let t be any nonnegative integer.

If we want to select k balls from an n-line or an n-circle under the restriction that any two adjacent selected balls are not t-separated, how many ways are there to do it? He solved these problems by means of a direct structural analysis. For the two kinds of problems, he used $F_t(n,k)$ to denote the number of ways of selecting k balls from n balls arranged in a line with no two adjacent selected balls being t-separation and $G_t(n,k)$ to denote the number of ways of selecting k balls from an n-circle with no two adjacent selected being t-separation. He proved that

$$F_t(n,k) = \sum_{t\ge 0} (-1)^t \binom{k-1}{l}\binom{n-l(t+1)}{k-1}, \tag{3.2}$$

$$G_t(n,k) = \frac{n}{k}\left\{(-1)^j \binom{k}{j}\binom{n-j(t+1)-1}{k-1-j} + (-1)^k \delta\left[n,k(1+t)\right]\right\}. \tag{3.3}$$

Remark 2. *In fact El-Desouky* [5] *has proved* (3.2) *in* 1988.

References

[1] Kplansky, I. (1943) Solution of the “Problems des Ménages”. *Bulletin of the American Mathematical Society*, **49**, 784-785. http://dx.doi.org/10.1090/S0002-9904-1943-08035-4

[2] Riordan, J. (1958) An Introduction to Combinatorial Analysis. Wiley, New York.

[3] Moser, W.O.J. (1986) The Number of Subsets without a Fixed Circular Distance. *Journal of Combinatorial Theory*, *Series A*, **43**, 130-132. http://dx.doi.org/10.1016/0097-3165(86)90030-0

[4] El-Desouky, B.S. (1988) On Selecting k Balls from an n-Line without Unit Separation. *Indian Journal of Pure and Applied Mathematics*, **19**, 145-148.

[5] El-Desouky, B.S. (1988) Selecting k Balls without s-Separation. *The* 23*rd Annual Conference on Statistics*, *Computer Science*, *Operations Research and Mathematics*, Cairo, December 1988, 40-46.

[6] Mansour, T. and Sun, Y.D. (2008) On Selecting the Number of Combinations without Certain Separations. *European Journal of Combinatorics*, **29**, 1200-1206. http://dx.doi.org/10.1016/j.ejc.2007.06.024

[7] Mansour, T. (2014) Set Partitions with Circular Successions. *European Journal of Combinatorics*, **41**, 207-216. http://dx.doi.org/10.1016/j.ejc.2014.06.008

[8] Gourden, J.P. and Jackson, D.M. (1993) Combinatorial Enumeration. Wiley, New York.

[9] Pease, R.W. (1975) General Solution to the Occupancy Problem with Variably Sized Runs of Adjacent Cells Occupied by Single Balls. *Mathematics Magazine*, **48**, 131-134. http://dx.doi.org/10.2307/2689693

[10] Maosen, J. (1995) On Selecting k Balls from an n-Line or n-Circle without t-Separations. *Northeastern Mathematical Journal*, **11**, 355-364.

Applied Mathematics, 2015, 6, 7-19
Published Online January 2015 in SciRes. http://www.scirp.org/journal/am
http://dx.doi.org/10.4236/am.2015.61002

Scientific Research Publishing

Higher-Order Minimizers and Generalized (F,ρ)-Convexity in Nonsmooth Vector Optimization over Cones

S. K. Suneja[1], Sunila Sharma[1], Malti Kapoor[2*]

[1]Department of Mathematics, Miranda House, University of Delhi, Delhi, India
[2]Department of Mathematics, Motilal Nehru College, University of Delhi, Delhi, India
Email: *maltikapoor1@gmail.com

Received 1 November 2014; revised 29 November 2014; accepted 16 December 2014

Abstract

In this paper, we introduce the concept of a (weak) minimizer of order *k* for a nonsmooth vector optimization problem over cones. Generalized classes of higher-order cone-nonsmooth (*F*, *ρ*)-convex functions are introduced and sufficient optimality results are proved involving these classes. Also, a unified dual is associated with the considered primal problem, and weak and strong duality results are established.

Keywords

Nonsmooth Vector Optimization over Cones, (Weak) Minimizers of Order *k*, Nonsmooth (*F*, *ρ*)-Convex Function of Order *k*

1. Introduction

It is well known that the notion of convexity plays a key role in optimization theory [1] [2]. In the literature, various generalizations of convexity have been considered. One such generalization is that of a ρ-convex function introduced by Vial [3]. Hanson and Mond [4] defined the notion of an *F*-convex function. As an extended unification of the two concepts, Preda [5] introduced the concept of a (F,ρ)-convex function. Antczak gave the notion of a locally Lipschitz (F,ρ)-convex scalar function of order *k* [6] and a differentiable (F,ρ)-convex vector function of order 2 [7].

L. Cromme [8] defined the concept of a strict local minimizer of order *k* for a scalar optimization problem. This concept plays a fundamental role in convergence analysis of iterative numerical methods [8] and in stability

*Corresponding author.

How to cite this paper: Suneja, S.K., Sharma, S. and Kapoor, M. (2015) Higher-Order Minimizers and Generalized (*F*, *ρ*)-Convexity in Nonsmooth Vector Optimization over Cones. *Applied Mathematics*, **6**, 7-19.
http://dx.doi.org/10.4236/am.2015.61002

results [9]. The definition of a strict local minimizer of order 2 is generalized to the vectorial case by Antczak [7].

Recently, Bhatia and Sahay [10] introduced the concept of a higher-order strict minimizer with respect to a nonlinear function for a differentiable multiobjective optimization problem. They proved various sufficient optimality and mixed duality results involving generalized higher-order strongly invex functions.

The main purpose of this paper is to extend the concept of a higher-order minimizer to a nonsmooth vector optimization problem over cones. The paper is organized as follows. We begin in Section 2 by recalling some known concepts in the literature. We then define the notion of a (weak) minimizer of order *k* for a nonsmooth vector optimization problem over cones. Thereafter, we introduce various new generalized classes of cone-nonsmooth (F,ρ)-convex functions of higher-order. In Section 3, we study several optimality conditions for higher-order minimizers via the introduced classes of functions. In Section 4, we associate a unified dual to the considered problem and establish weak and strong duality results.

2. Preliminaries and Definitions

Let $S \subseteq \mathbf{R}^n$ be a nonempty open subset of $\mathbf{R}^n$. Let $K \subseteq \mathbf{R}^m$ be a closed convex cone with nonempty interior and let $\operatorname{int}K$ denote the interior of *K*. The dual cone K^* of *K* is defined as

$$K^* = \left\{ y^* \in \mathbf{R}^m : \left\langle y, y^* \right\rangle \geq 0 \ \text{ for all } \ y \in K \right\}.$$

The strict positive dual cone K^{s^*} of *K* is given by

$$K^{s^*} = \left\{ y^* \in \mathbf{R}^m : \left\langle y, y^* \right\rangle > 0 \ \text{ for all } \ y \in K \setminus \{0\} \right\}.$$

A function $\psi : S \to \mathbf{R}$ is said to be locally Lipschitz at a point $u \in S$ if for some $l > 0$, $\left\| \psi(x) - \psi(\bar{x}) \right\| \leq l \left\| x - \bar{x} \right\| \quad \forall x, \ \bar{x}$ within a neighbourhood of *u*.

A function ψ is said to be locally Lipschitz on *S* if it is locally Lipschitz at each point of *S*.

Definition 2.1. [11] Let $\psi : S \to \mathbf{R}$ be a locally Lipschitz function, then $\psi^0(u;v)$ denotes the Clarke's generalized directional derivative of ψ at $u \in S$ in the direction v and is defined as

$$\psi^0(u;v) = \limsup_{\substack{y \to u \\ t \to 0^+}} \frac{\psi(y+tv) - \psi(y)}{t}.$$

The Clarke's generalized gradient of ψ at *u* is denoted by $\partial\psi(u)$ and is defined as

$$\partial\psi(u) = \left\{ \xi \in \mathbf{R}^n : \psi^0(u;v) \geq \langle \xi, v \rangle \ \text{ for all } \ v \in \mathbf{R}^n \right\}.$$

Let $f : S \to \mathbf{R}^m$ be a vector valued function given by $f = \left(f_1, f_2, \cdots, f_m \right)^t$, $f_i : S \to \mathbf{R}$. Then *f* is said to be locally Lipschitz on *S* if each f_i is locally Lipschitz on *S*. The generalized directional derivative of a locally Lipschitz function $f : S \to \mathbf{R}^m$ at $u \in S$ in the direction v is given by

$$f^0(u;v) = \left(f_1^0(u;v), f_2^0(u;v), \cdots, f_m^0(u;v) \right)^t.$$

The generalized gradient of *f* at *u* is the set

$$\partial f(u) = \partial f_1(u) \times \cdots \times \partial f_m(u),$$

where $\partial f_i(u)$ is the generalized gradient of f_i at *u* for $i = 1, 2, \cdots, m$.

Every element $A = \left(A_1, \cdots, A_m \right)^t \in \partial f(u)$ is a continuous linear operator from $\mathbf{R}^n$ to $\mathbf{R}^m$ and $Au = \left(A_1^t u, \cdots, A_m^t u \right)^t \in \mathbf{R}^m$ for all $u \in S$.

A functional $F : S \times S \times \mathbf{R}^n \to \mathbf{R}$ is sublinear with respect to the third variable if, for all $(x,u) \in S \times S$,

(i) $F(x,u;A_1 + A_2) \leq F(x,u;A_1) + F(x,u;A_2)$ for all $A_1, A_2 \in \mathbf{R}^n$, and

(ii) $F(x,u;\alpha A) = \alpha F(x,u;A)$ for all $\alpha \in \mathbf{R}_+$.

(i) and (ii) together imply $F(x,u;0)=0$. (1)

We consider the following nonsmooth vector optimization problem

$$\text{(NVOP)} \quad K\text{-minimize} \quad f(x)$$

$$\text{subject to} \quad -g(x)\in Q,$$

where $f=(f_1,\cdots,f_m)^t:S\to\mathbf{R}^m$, $g=(g_1,\cdots,g_p)^t:S\to\mathbf{R}^p$, K and Q are closed convex cones with nonempty interiors in $\mathbf{R}^m$ and $\mathbf{R}^p$ respectively. We assume that f_i for each $i\in\{1,\cdots,m\}$ and g_j for each $j\in\{1,\cdots,p\}$ are locally Lipschitz on S.

Let $S_0=\{x\in S:-g(x)\in Q\}$ denote the set of all feasible solutions of (NVOP).

The following solution concepts are well known in the literature of vector optimization theory.

Definition 2.2. A point $\bar{x}\in S_0$, is said to be

(i) a weak minimizer (weakly efficient solution) of (NVOP) if for every $x\in S_0$,

$$f(x)-f(\bar{x})\notin-\operatorname{int}K;$$

(ii) a minimizer (efficient solution) of (NVOP) if for every $x\in S_0$,

$$f(x)-f(\bar{x})\notin-K\setminus\{0\}.$$

With the idea of analyzing the convergence and stability of iterative numerical methods, L. Cromme [8] introduced the notion of a "strict local minimizer of order *k*". As a recent advancement on this platform, Bhatia and Sahay [10] defined the concept of a higher-order strict minimizer with respect to a nonlinear function for a differentiable multiobjective optimization problem. We now generalize this concept and give the definition of a higher-order (weak) minimizer with respect to a function ω for a nonsmooth vector optimization problem over cones.

Definition 2.3. A point $\bar{x}\in S_0$ is said to be

(i) a weak minimizer of order $k\geq 1$ for (NVOP) with respect to ω, if there exists a vector $\beta\in\operatorname{int}K$ such that, for every $x\in S_0$

$$f(x)-f(\bar{x})-\beta\|\omega(x,\bar{x})\|^k\notin-\operatorname{int}K;$$

(ii) a minimizer of order $k\geq 1$ for (NVOP) with respect to ω, if there exists a vector $\beta\in\operatorname{int}K$ such that, for every $x\in S_0$

$$f(x)-f(\bar{x})-\beta\|\omega(x,\bar{x})\|^k\notin-K\setminus\{0\}.$$

Remark 2.1. (1) If f is a scalar valued function, $K=\mathbf{R}_+$ and $\omega(x,\bar{x})=x-\bar{x}$, the definition of a weak minimizer of order *k* reduces to the definition of a strict minimizer of order *k* (see [8] [9] [12] [13]).

(2) If $K=\mathbf{R}^m_+$, $k=2$ and $\omega(x,\bar{x})=x-\bar{x}$, the definition of a (weak) minimizer of order *k* becomes the definition of a vector strict global (weak) minimizer of order 2 given by Antczak [7].

(3) If $K=\mathbf{R}^m_+$ the definition of a weak minimizer of order *k* reduces to the definition of a strict minimizer of order *k* given by Bhatia and Sahay [10].

Remark 2.2. (1) Clearly a minimizer of order *k* for (NVOP) with respect to ω is also a weak minimizer of order *k* for (NVOP) with respect to the same ω.

(2) A direct implication of the fact that $\beta\in\operatorname{int}K$ is that, a (weak) minimizer of order *k* for (NVOP) with respect to ω is a (weak) minimizer for (NVOP).

(3) Note that if $\bar{x}$ is a (weak) minimizer of order *k* for (NVOP) with respect to ω, then for all $\ell>k$, it is also a (weak) minimizer of order ℓ for (NVOP) with respect to the same ω.

In the sequel, for a vector function $f:S\to\mathbf{R}^m$ and $A=(A_1,\cdots,A_m)^t\in\partial f(u)$, $F(x,u;A)$ denotes the vector $(F(x,u;A_1),\cdots,F(x,u;A_m))^t$.

We now define various classes of nonsmooth (F,ρ)-convex functions of higher-order over cones.

Definition 2.4. A locally Lipschitz function $f:S\to\mathbf{R}^m$ is said to be *K*-nonsmooth (F,ρ)-convex of order *k* with respect to ω at $u\in S$ on *S* if there exist a sublinear (with respect to the third variable) functional

$F : S \times S \times \mathbf{R}^n \to \mathbf{R}$ and a vector $\rho = (\rho_1, \rho_2, \cdots, \rho_m) \in \mathbf{R}^m$ such that, for each $A \in \partial f(u)$ and all $x \in S$

$$f(x) - f(u) - F(x,u;A) - \rho\|\omega(x,u)\|^k \in K .$$

If the above relation holds for every $u \in S$ then f is said to be K-nonsmooth (F,ρ)-convex of order k with respect to ω on S.

Remark 2.3. (1) If f is a scalar valued function and $K = \mathbf{R}_+$, the above definition reduces to the definition of a (locally Lipschitz) (F,ρ)-convex function of order k with respect to ω given by Antczak [6].

(2) If f is a differentiable function, $K = \mathbf{R}_+^m$, $k = 2$ and $\omega(x,\bar{x}) = x - \bar{x}$ the definition of a K-nonsmooth (F,ρ)-convex function of order k with respect to ω becomes the definition of a vector (F,ρ)-convex function of order 2 given in [7].

(3) If $K = \mathbf{R}_+^m$, $F(x,u;A) = A\eta(x,u)$ for some function $\eta : S \times S \to \mathbf{R}^n$ and $k = 2$, K-nonsmooth (F,ρ)-convexity of order k with respect to ω reduces to $\rho-(\eta,\theta)$-invexity, where $\omega(x,\bar{x}) = \theta(x,\bar{x})$, introduced by Nahak and Mohapatra [14].

(4) If f is a differentiable function, $K = \mathbf{R}_+^m$ and $F(x,u;a) = a^t\eta(x,u)$, $a \in \mathbf{R}^n$, for some function $\eta : S \times S \to \mathbf{R}^n$, the above definition becomes the definition of a higher-order strongly invex function given by Bhatia and Sahay [10].

Definition 2.5. A locally Lipschitz function $f : S \to \mathbf{R}^m$ is said to be K-nonsmooth (F,ρ)-pseudoconvex type I of order k with respect to ω at $u \in S$ on S if there exist a sublinear (with respect to the third variable) functional $F : S \times S \times \mathbf{R}^n \to \mathbf{R}$ and a vector $\rho \in \mathbf{R}^m$ such that, for each $A \in \partial f(u)$ and all $x \in S$,

$$-F(x,u;A) \notin \operatorname{int}K \Rightarrow -\left[f(x) - f(u) - \rho\|\omega(x,u)\|^k \right] \notin \operatorname{int}K .$$

Equivalently,

$$f(x) - f(u) - \rho\|\omega(x,u)\|^k \in -\operatorname{int}K \Rightarrow F(x,u;A) \in -\operatorname{int}K .$$

If f is K-nonsmooth (F,ρ)-pseudoconvex type I of order k with respect to ω at every $u \in S$ then f is said to be K-nonsmooth (F,ρ)-pseudoconvex type I of order k with respect to ω on S.

Clearly, if f is K-nonsmooth (F,ρ)-convex of order k with respect to ω, then f is K-nonsmooth (F,ρ)-pseudoconvex type I of order k with respect to the same ω, however the converse may not be true as shown by the following example.

Example 2.1. Consider the following nonsmooth function $f : S \to \mathbf{R}^2$, $S = (-2,2) \subseteq \mathbf{R}$, $f(x) = (f_1(x), f_2(x))$ and $K = \{(x,y) : x \geq 0, y \leq x\}$

$$f_1(x) = \begin{cases} -2x, & x < 0 \\ -x^6 - x, & x \geq 0 \end{cases} \qquad f_2(x) = \begin{cases} x^3 - x/2, & x < 0 \\ -x/3, & x \geq 0 \end{cases}$$

Here $\partial f_1(0) = [-2,-1]$ and $\partial f_2(0) = \left[-\frac{1}{2}, -\frac{1}{3}\right]$.

Define $F : S \times S \times \mathbf{R} \to \mathbf{R}$ as

$$F(x,u;a) = a\left(\sqrt{x} - \sqrt{u}\right).$$

Let $\omega : S \times S \to R$ be given by $\omega(x,u) = x^2 - u^2$, $k = 3$ and $\rho = (-1,0)$.

Then, at $u = 0$.

$$f(x) - f(u) - \rho\|\omega(x,u)\|^k \in -\operatorname{int}K \Rightarrow x > 0 \Rightarrow F(x,u;A) \in -\operatorname{int}K ,$$

for every $x \in S$ and $A \in \partial f(0)$.

Hence, f is K-nonsmooth (F,ρ)-pseudoconvex type I of order 3 with respect to ω at u on S.
However, for $x = 1$ and $A = (-1,-1/2)$.

$$f(x) - f(u) - F(x,u;A) - \rho\|\omega(x,u)\|^k \notin K ,$$

so that f is not K-nonsmooth (F,ρ)-convex of order 3 at u on S.

Definition 2.6. A locally Lipschitz function $f:S\to\mathbf{R}^m$ is said to be K-nonsmooth (F,ρ)-pseudoconvex type II of order k with respect to ω at $u\in S$ on S if there exist a sublinear (with respect to the third variable) functional $F:S\times S\times\mathbf{R}^n\to\mathbf{R}$ and a vector $\rho\in\mathbf{R}^m$ such that, for each $A\in\partial f(u)$ and all $x\in S$,

$$-\left[F(x,u;A)+\rho\|\omega(x,u)\|^k\right]\notin \operatorname{int}K \Rightarrow -\left[f(x)-f(u)\right]\notin \operatorname{int}K$$

Equivalently,

$$f(x)-f(u)\in -\operatorname{int}K \Rightarrow \left[F(x,u;A)+\rho\|\omega(x,u)\|^k\right]\in -\operatorname{int}K .$$

If the above relation holds for every $u\in S$, then f is said to be K-nonsmooth (F,ρ)-pseudoconvex type II of order k with respect to ω on S.

We now give an example to show that a K-nonsmooth (F,ρ)-pseudoconvex type II function of order k with respect to ω may fail to be a K-nonsmooth (F,ρ)-convex function of order k with respect to ω.

Example 2.2. Consider the following nonsmooth function $f:S\to\mathbf{R}^2$, $S=(0,2)\subseteq\mathbf{R}$, $f(x)=\left(f_1(x),f_2(x)\right)$ and $K=\{(x,y):x\le 0, y\ge x\}$

$$f_1(x)=\begin{cases}-x, & x\le 1\\ -x^2, & x>1\end{cases},\quad f_2(x)=\begin{cases}x/4, & x\le 1\\ (x-1/2)^2, & x>1\end{cases}$$

Here $\partial f_1(1)=[-2,-1]$ and $\partial f_2(1)=\left[\frac{1}{4},1\right]$.

Let $F:S\times S\times\mathbf{R}\to\mathbf{R}$ be given by $F(x,u;a)=a\left(\mathrm{e}^x-\mathrm{e}^u\right)$.

$$\omega(x,u)=x^2-u^2-\frac{9}{16} \text{ and } \rho=(1,-1).$$

Then, at $u=1$,

$$f(x)-f(u)\in -\operatorname{int}K \Rightarrow x\le 1 \Rightarrow F(x,u;A)+\rho\|\omega(x,u)\|^k\in -\operatorname{int}K ,$$

for every $k\ge 1$, $x\in S$ and $A\in\partial f(1)$.

Therefore, f is K-nonsmooth (F,ρ)-pseudoconvex type II of order $k\ge 1$ with respect to ω at u on S.

However, for $x=5/4$ and $A=(-2,\alpha_2)$, $\alpha_2\in[1/4,1]$,

$$f(x)-f(u)-F(x,u;A)-\rho\|\omega(x,u)\|^k\notin K .$$

Thus, f is not K-nonsmooth (F,ρ)-convex of any order k with respect to ω at u on S.

Definition 2.7. A locally Lipschitz function $f:S\to\mathbf{R}^m$ is said to be K-nonsmooth (F,ρ)-quasiconvex type I of order k with respect to ω at $u\in S$ on S if there exist a sublinear (with respect to the third variable) functional $F:S\times S\times R^n\to R$ and a vector $\rho\in R^m$ such that, for each $A\in\partial f(u)$ and all $x\in S$,

$$\left[f(x)-f(u)\right]\notin \operatorname{int}K \Rightarrow -\left[F(x,u;A)+\rho\|\omega(x,u)\|^k\right]\in K .$$

If the above relation holds at every $u\in S$, then f is said to be K-nonsmooth (F,ρ)-quasiconvex type I of order k with respect to ω on S.

Definition 2.8. A locally Lipschitz function $f:S\to\mathbf{R}^m$ is said to be K-nonsmooth (F,ρ)-quasiconvex type II of order k with respect to ω at $u\in S$ on S if there exist a sublinear (with respect to the third variable) functional $F:S\times S\times\mathbf{R}^n\to\mathbf{R}$ and a vector $\rho\in\mathbf{R}^m$ such that, for each $A\in\partial f(u)$ and all $x\in S$,

$$\left[f(x)-f(u)-\rho\|\omega(x,u)\|^k\right]\notin \operatorname{int}K \Rightarrow -F(x,u;A)\in K .$$

If f is K-nonsmooth (F,ρ)-quasiconvex type II of order k with respect to ω at every $u\in S$, then f is said to be K-nonsmooth (F,ρ)-quasiconvex type II of order k with respect to ω on S.

Remark 2.4. When f is a differentiable function, $K=\mathbf{R}_+^m$ and $F(x,u;a)=a^t\eta(x,u)$, $a\in\mathbf{R}^n$ for some function $\eta: S\times S\to\mathbf{R}^n$, Definition 2.4 - 2.7 take the form of the corresponding definitions given by Bhatia and Sahay [10].

3. Optimality

In this section, we obtain various nonsmooth Fritz John type and Karush-Kuhn-Tucker (KKT) type necessary and sufficient optimality conditions for a feasible solution to be a (weak) minimizer of order k for (NVOP).

On the lines of Craven [15] we define Slater-type cone constraint qualification as follows:

Definition 3.1. The problem (NVOP) is said to satisfy Slater-type cone constraint qualification at $\bar{x}$ if, for all $B\in\partial g(\bar{x})$, there exists a vector $\xi\in R^n$ such that $B\xi\in-\mathrm{int}Q$.

Remark 3.1. The following inclusion relation is worth noticing.

For $\lambda=(\lambda_1,\cdots,\lambda_m)^t\in\mathbf{R}^m$ and $\mu=(\mu_1,\cdots,\mu_p)^t\in\mathbf{R}^p$,

$$\begin{aligned}\partial\left(\lambda^t f+\mu^t g\right)(\bar{x}) &= \partial\left(\sum_{i=1}^m\lambda_i f_i+\sum_{j=1}^p\mu_j g_j\right)(\bar{x})\\ &\subseteq \partial\left(\sum_{i=1}^m\lambda_i f_i\right)(\bar{x})+\partial\left(\sum_{j=1}^p\mu_j g_j\right)(\bar{x})\\ &\subseteq \sum_{i=1}^m\lambda_i\partial f_i(\bar{x})+\sum_{j=1}^p\mu_j\partial g_j(\bar{x})\\ &= \left(\partial f(\bar{x})^t\lambda+\partial g(\bar{x})^t\mu\right).\end{aligned}$$

Thus,

$$\partial\left(\lambda^t f+\mu^t g\right)(\bar{x})\subseteq\left(\partial f(\bar{x})^t\lambda+\partial g(\bar{x})^t\mu\right). \tag{2}$$

Since a weak minimizer of order $k\geq 1$ for (NVOP) is a weak minimizer for (NVOP), the following nonsmooth Fritz John type necessary optimality conditions can be easily obtained from Craven [15].

Theorem 3.1. If a vector $\bar{x}\in S_0$ is a weak minimizer of order k with respect to ω for (NVOP) with $S=\mathbf{R}^n$, then there exist Lagrange multipliers $\bar{\lambda}\in K^*$ and $\bar{\mu}\in Q^*$ not both zero, such that

$$0\in\partial\left(\bar{\lambda}^t f+\bar{\mu}^t g\right)(\bar{x})$$

$$\bar{\mu}^t g(\bar{x})=0.$$

The necessary nonsmooth KKT type optimality conditions for (NVOP) can be given in the following form.

Theorem 3.2. If a vector $\bar{x}\in S_0$ is a weak minimizer of order k with respect to ω for (NVOP) with $S=\mathbf{R}^n$ and if Slater-type cone constraint qualification holds at $\bar{x}$, then there exist Lagrange multipliers $\bar{\lambda}\in K^*\setminus\{0\}$ and $\bar{\mu}\in Q^*$, such that

$$0\in\partial\left(\bar{\lambda}^t f+\bar{\mu}^t g\right)(\bar{x}) \tag{3}$$

$$\bar{\mu}^t g(\bar{x})=0. \tag{4}$$

Proof. Assume that $\bar{x}\in S_0$ is a weak minimizer of order k with respect to ω for (NVOP), then by Theorem 3.1 there exist $\bar{\lambda}\in K^*$ and $\bar{\mu}\in Q^*$, not both zero, such that (3) and (4) hold.

If possible, suppose $\bar{\lambda}=0$. Then, $\bar{\mu}\neq 0$ and (3) reduces to

$$0\in\partial\left(\bar{\mu}^t g\right)(\bar{x})\subseteq\partial g(\bar{x})^t\bar{\mu}.$$

So there exists $\bar{B}\in\partial g(\bar{x})$ such that

$$\bar{B}^t\bar{\mu}=0. \tag{5}$$

Now, since Slater-type cone constraint qualification holds at $\bar{x}$, we have for all $B \in \partial g(\bar{x})$, there exists a vector $\xi \in R^n$ such that $B\xi \in -\text{int}Q$. Since $\bar{\mu} \in Q^* \setminus \{0\}$, we get $\bar{\mu}^t B\xi < 0$. In particular, $\bar{\mu}^t \bar{B}\xi < 0$. On the contrary (5) implies $\xi^t \bar{B}^t \bar{\mu} = 0$. This contradiction justifies $\bar{\lambda} \neq 0$.

Now, we give sufficient optimality conditions for a feasible solution to be a higher-order (weak) minimizer for (NVOP).

Theorem 3.3. Let $\bar{x}$ be a feasible solution for (NVOP) and suppose there exist vectors $\bar{\lambda} \in K^*$, $\bar{\lambda} > 0$ and $\bar{\mu} \in Q^*$, $\bar{\mu} \geq 0$ such that

$$0 \in \left(\partial f(\bar{x})^t \bar{\lambda} + \partial g(\bar{x})^t \bar{\mu}\right) \tag{6}$$

$$\bar{\mu}^t g(\bar{x}) = 0. \tag{7}$$

Further, assume that *f* is *K*-nonsmooth (F,ρ)-convex of order *k* with respect to ω at $\bar{x}$ on S_0 and *g* is *Q*-nonsmooth (F,σ)-convex of order *k* with respect to the same ω at $\bar{x}$ on S_0. If $\rho \in \text{int}K$ and $\sigma \in Q$, then $\bar{x}$ is a weak minimizer of order *k* with respect to ω for (NVOP).

Proof. Assume on the contrary that $\bar{x}$ is not a weak minimizer of order *k* with respect to ω for (NVOP). Then, for any $\beta \in \text{int}K$, there exists a vector $\hat{x} \in S_0$ such that,

$$f(\hat{x}) - f(\bar{x}) - \beta\left\|\omega(\hat{x},\bar{x})\right\|^k \in -\text{int}K.$$

As $\rho \in \text{int}K$, the above relation holds in particular for $\beta = \rho$, so that we have

$$f(\hat{x}) - f(\bar{x}) - \rho\left\|\omega(\hat{x},\bar{x})\right\|^k \in -\text{int}K. \tag{8}$$

As (6) holds, there exist $\bar{A} \in \partial f(\bar{x})$ and $\bar{B} \in \partial g(\bar{x})$ such that

$$\bar{A}^t \bar{\lambda} + \bar{B}^t \bar{\mu} = 0. \tag{9}$$

Since *f* is *K*-nonsmooth (F,ρ)-convex of order *k* with respect to ω at $\bar{x}$ on S_0, we have

$$f(\hat{x}) - f(\bar{x}) - F(\hat{x},\bar{x};\bar{A}) - \rho\left\|\omega(\hat{x},\bar{x})\right\|^k \in K. \tag{10}$$

Adding (8) and (10), we get

$$-F(\hat{x},\bar{x};\bar{A}) \in \text{int}K.$$

As $\lambda \in K^* \setminus \{0\}$, we obtain

$$\bar{\lambda}^t F(\hat{x},\bar{x};\bar{A}) < 0. \tag{11}$$

Also, since *g* is *Q*-nonsmooth (F,σ) convex of order *k* with respect to ω at $\bar{x}$ on S_0 and $\bar{\mu} \in Q^*$, we have

$$\bar{\mu}^t\left[g(\hat{x}) - g(\bar{x}) - F(\hat{x},\bar{x};\bar{B}) - \sigma\left\|\omega(\hat{x},\bar{x})\right\|^k\right] \geq 0.$$

However, $\hat{x} \in S_0$, $\bar{\mu} \in Q^*$ and (7) together give

$$\bar{\mu}^t\left[F(\hat{x},\bar{x};\bar{B}) + \sigma\left\|\omega(\hat{x},\bar{x})\right\|^k\right] \leq 0. \tag{12}$$

Adding (11) and (12), we get

$$\bar{\lambda}^t F(\hat{x},\bar{x};\bar{A}) + \bar{\mu}^t F(\hat{x},\bar{x};\bar{B}) + \bar{\mu}^t \sigma\left\|\omega(\hat{x},\bar{x})\right\|^k < 0,$$

which implies that

$$\sum_i \bar{\lambda}_i F(\hat{x},\bar{x};\bar{A}_i) + \sum_j \bar{\mu}_j F(\hat{x},\bar{x};\bar{B}_j) + \bar{\mu}^t \sigma\left\|\omega(\hat{x},\bar{x})\right\| |^k < 0.$$

Using sublinearity of F under the assumption $\bar{\lambda} > 0$ and $\bar{\mu} \geq 0$, we obtain

$$F\left(\hat{x}, \bar{x}; \bar{\lambda}^t \bar{A} + \bar{\mu}^t \bar{B}\right) + \bar{\mu}^t \sigma \left\|\omega\left(\hat{x}, \bar{x}\right)\right\|^k < 0,$$

which on using (9) and (1), gives

$$\bar{\mu}^t \sigma \left\|\omega\left(\hat{x}, \bar{x}\right)\right\|^k < 0.$$

This is impossible as $\bar{\mu} \in Q^*$ and $\sigma \in Q$, so that $\bar{\mu}^t \sigma \geq 0$, and norm is a non-negative function. Hence $\bar{x}$ is a weak minimizer of order k with respect to ω for (NVOP).

Theorem 3.4. Suppose there exists a feasible solution $\bar{x}$ for (NVOP) and vectors $\bar{\lambda} \in K^*$, $\bar{\lambda} > 0$ and $\bar{\mu} \in Q^*$, $\bar{\mu} \geq 0$ such that (6) and (7) hold. Moreover, assume that f is K-nonsmooth (F,ρ)-pseudoconvex type I of order k with respect to ω at $\bar{x}$ on S_0 and g is Q-nonsmooth (F,σ)-quasiconvex type I of order k with respect to the same ω at $\bar{x}$ on S_0. If $\rho \in \operatorname{int}K$ and $\sigma \in Q$, then $\bar{x}$ is a weak minimizer of order k with respect to ω for (NVOP).

Proof: Let if possible, $\bar{x}$ be not a weak minimizer of order k with respect to ω for (NVOP). Then, for any $\beta \in \operatorname{int}K$, there exists $\hat{x} \in S_0$ such that,

$$f\left(\hat{x}\right) - f\left(\bar{x}\right) - \beta \left\|\omega\left(\hat{x}, \bar{x}\right)\right\|^k \in -\operatorname{int}K.$$

Since $\rho \in \operatorname{int}K$ taking, in particular, $\beta = \rho$ in the above relation, we obtain

$$f\left(\hat{x}\right) - f\left(\bar{x}\right) - \rho \left\|\omega\left(\hat{x}, \bar{x}\right)\right\|^k \in -\operatorname{int}K. \tag{13}$$

As (6) holds, there exist $\bar{A} \in \partial f\left(\bar{x}\right)$ and $\bar{B} \in \partial g\left(\bar{x}\right)$ such that (9) holds.

Since f is K-nonsmooth (F,ρ)-pseudoconvex type I of order k with respect to ω at $\bar{x}$ on S_0, (13) implies

$$F\left(\hat{x}, \bar{x}; \bar{A}\right) \in -\operatorname{int}K.$$

As $\lambda \in K^* \setminus \{0\}$, we have

$$\bar{\lambda}^t F\left(\hat{x}, \bar{x}; \bar{A}\right) < 0. \tag{14}$$

Now, $\hat{x} \in S_0$ means $-g\left(\hat{x}\right) \in Q$, so that $\bar{\mu}^t g\left(\hat{x}\right) \leq 0$. This along with (7) gives

$$\bar{\mu}^t \left\{g\left(\hat{x}\right) - g\left(\bar{x}\right)\right\} \leq 0. \tag{15}$$

If $\bar{\mu} \neq 0$, then (15) implies $g\left(\hat{x}\right) - g\left(\bar{x}\right) \notin \operatorname{int}Q$.

Since g is Q-nonsmooth (F,σ)-quasiconvex type I of order k with respect to ω at $\bar{x}$ on S_0, therefore

$$-\left[F\left(\hat{x}, \bar{x}; \bar{B}\right) + \sigma \left\|\omega\left(\hat{x}, \bar{x}\right)\right\|^k\right] \in Q,$$

so that

$$\bar{\mu}^t \left[F\left(\hat{x}, \bar{x}; \bar{B}\right) + \sigma \left\|\omega\left(\hat{x}, \bar{x}\right)\right\|^k\right] \leq 0. \tag{16}$$

If $\bar{\mu} = 0$, then also (16) holds.

Now, proceeding as in Theorem 3.3, we get a contradiction. Hence, $\bar{x}$ is a weak minimizer of order k with respect to ω for (NVOP).

Theorem 3.5. Assume that all the conditions of Theorem 3.3 (Theorem 3.4) hold with $\bar{\lambda} \in K^{s^*}$, $\bar{\lambda} > 0$. Then $\bar{x}$ is a minimizer of order k with respect to ω for (NVOP).

Proof: Let if possible, $\bar{x}$ be not a minimizer of order k with respect to ω for (NVOP), then for any $\beta \in \operatorname{int}K$ there exists $\hat{x} \in S_0$ such that

$$-\left[f\left(\hat{x}\right) - f\left(\bar{x}\right) - \beta \left\|\omega\left(\hat{x}, \bar{x}\right)\right\|^k\right] \in K \setminus \{0\}. \tag{17}$$

Proceeding on similar lines as in proof of Theorem 3.3 (Theorem3.4) and using (17) we have

$$-F\left(\hat{x},\bar{x};\bar{A}\right)\in K\setminus\{0\}.$$

As $\bar{\lambda}\in K^{s^*}$, we get

$$\bar{\lambda}^t F\left(\hat{x},\bar{x};\bar{A}\right)<0.$$

This leads to a contradiction as in Theorem 3.3 (Theorem 3.4). Hence, $\bar{x}$ is a minimizer of order *k* with respect to ω for (NVOP).

4. Unified Duality

On the lines of Cambini and Carosi [16], we associate with our primal problem (NVOP), the following unified dual problem (NVUD).

(NVUD) *K*-maximize $f(y)+\dfrac{l}{\lambda^t l}(1-\delta)\mu^t g(y)$

subject to $0\in\partial\left(\lambda^t f+\mu^t g\right)(y),$ (18)

$$\delta\mu^t g(y)\geq 0, \tag{19}$$

where $y\in S$, $l\in \text{int}K$, $\lambda\in K^*\setminus\{0\}$, $\mu\in Q^*$ and $\delta\in\{0,1\}$ is a 0 - 1 parameter.

Note that Wolfe dual and Mond-Weir dual can be obtained from (NVUD) on taking $\delta=0$ and $\delta=1$ respectively.

Definition 4.1. Given the problem (NVOP) and given a vector $l\in\text{int}K,$ we define the following Lagrange function:

$$\mathrm{L}(x,\lambda,\mu)=f(x)+\frac{l}{\lambda^t l}\mu^t g(x),\quad \forall x\in S,\ \lambda\in K^*,\ \mu\in Q^*.$$

Theorem 4.1. (Weak Duality) Let *x* be feasible for (NVOP) and (y,λ,μ) be feasible for (NVUD). If *f* is *K*-nonsmooth (F,ρ)-convex of order *k* with respect to ω at *y* on S_0 and *g* is *Q*-nonsmooth (F,σ)-convex of order *k* with respect to the same ω at *y* on S_0, with $\lambda>0,\ \mu\geq 0$ and

$$\lambda^t\rho+\mu^t\sigma\geq 0, \tag{20}$$

then,

$$f(y)+\frac{l}{\lambda^t l}(1-\delta)\mu^t g(y)-f(x)\notin\text{int}K.$$

Proof: Assume on the contrary that

$$f(y)+\frac{l}{\lambda^t l}(1-\delta)\mu^t g(y)-f(x)\in\text{int}K. \tag{21}$$

Since (y,λ,μ) is feasible for (NVUD), therefore by (2), there exist $\bar{A}\in\partial f(y)$ and $\bar{B}\in\partial g(y)$ such that

$$\bar{A}^t\lambda+\bar{B}^t\mu=0. \tag{22}$$

Since *f* is *K*-nonsmooth (F,ρ)-convex of order *k* with respect to ω at *y* on S_0, we have

$$f(x)-f(y)-F\left(x,y;\bar{A}\right)-\rho\left\|\omega(x,y)\right\|^k\in K. \tag{23}$$

Adding (21) and (23), we obtain

$$\frac{l}{\lambda^t l}(1-\delta)\mu^t g(y)-F\left(x,y;\bar{A}\right)-\rho\left\|\omega(x,y)\right\|^k\in\text{int}K.$$

As $\lambda \in K^* \setminus \{0\}$, we get

$$(1-\delta)\mu^t g(y) - \lambda^t F(x, y; \bar{A}) - \lambda^t \rho \|\omega(x, y)\|^k > 0. \tag{24}$$

Also, since g is Q-nonsmooth (F, σ)-convex of order k with respect to ω at y on S_0 and $\mu \in Q^*$, we have

$$\mu^t \left[g(x) - g(y) - F(x, y; \bar{B}) - \sigma \|\omega(x, y)\|^k \right] \geq 0. \tag{25}$$

Adding (24) and (25), we get

$$\mu^t g(x) - \delta\mu^t g(y) > \lambda^t F(x, y; \bar{A}) + \mu^t F(x, y; \bar{B}) + (\lambda^t \rho + \mu^t \sigma) \|\omega(x, y)\|^k$$

or,

$$\mu^t g(x) - \delta\mu^t g(y) > \sum_{i=1}^{m} \lambda_i F(x, y; \bar{A}_i) + \sum_{j=1}^{p} \mu_j F(x, y; \bar{B}_j) + (\lambda^t \rho + \mu' \sigma) \|\omega(x, y)\|^k.$$

Using sublinearity of F under the assumption that $\lambda > 0$ and $\mu \geq 0$, together with (22), (1) and (20), we obtain

$$\delta\mu^t g(y) < \mu^t g(x).$$

As $x \in S_0$, $-g(x) \in Q$ and $\mu \in Q^*$, so that $\mu^t g(x) \leq 0$ and we have $\delta\mu^t g(y) < 0$.

This contradicts the feasibility of (y, λ, μ), hence the result.

Theorem 4.2. (Weak Duality) Let x be feasible for (NVOP) and (y, λ, μ) be feasible for (NVUD) with $\lambda > 0$ and $\mu \geq 0$. Suppose the following conditions hold:

(i) If $\delta = 0$, $\rho \in K$, $\mathrm{L}(., \lambda, \mu)$ is K-nonsmooth (F, ρ)-pseudoconvex type II of order k with respect to ω at y on S_0, and

(ii) If $\delta = 1$, $\lambda^t \rho + \mu^t \sigma \geq 0$, f is K-nonsmooth (F, ρ)-pseudoconvex type II of order k with respect to ω at y on S_0 and g is Q-nonsmooth (F, σ)-quasiconvex type I of order k with respect to ω at y on S_0.

Then, we have

$$f(y) + \frac{l}{\lambda^t l}(1-\delta)\mu^t g(y) - f(x) \notin \mathrm{int}K.$$

Proof: Case (i): Let $\delta = 0$ and on the contrary assume that,

$$f(y) + \frac{l}{\lambda^t l}\mu^t g(y) - f(x) \in \mathrm{int}K. \tag{26}$$

Since x is feasible for (NVOP) and $\mu \in Q^*$, therefore $-\mu^t g(x) \geq 0$. Further, $l \in \mathrm{int}K$ so that

$$-\frac{l}{\lambda^t l}\mu^t g(x) \in K. \tag{27}$$

Adding (26) and (27), we get

$$\left[\left\{ f(y) + \frac{l}{\lambda^t l}\mu^t g(y) \right\} - \left\{ f(x) + \frac{l}{\lambda^t l}\mu^t g(x) \right\} \right] \in \mathrm{int}K.$$

That is,

$$-\left[\mathrm{L}(x, \lambda, \mu) - \mathrm{L}(y, \lambda, \mu) \right] \in \mathrm{int}K.$$

As $\mathrm{L}(., \lambda, \mu)$ is K-nonsmooth (F, ρ)-pseudoconvex type II of order k with respect to ω, we have for all $C = (C_1, \cdots, C_m)^t \in \partial \mathrm{L}(y, \lambda, \mu)$

$$F\left(x, y; C\right) + \rho \left\| \omega\left(x, y\right) \right\|^k \in -\mathrm{int}K .$$

Since, $\lambda \in K^* \setminus \{0\}$, we get

$$\lambda^t F\left(x, y; C\right) + \lambda^t \rho \left\| \omega\left(x, y\right) \right\|^k < 0 ,$$

or

$$\sum_{i=1}^{m} \lambda_i F\left(x, y; C_i\right) + \lambda^t \rho \left\| \omega\left(x, y\right) \right\|^k < 0 ,$$

so that

$$F\left(x, y; \lambda^t C\right) + \lambda^t \rho \left\| \omega\left(x, y\right) \right\|^k < 0 . \tag{28}$$

Now, since $\left(y, \lambda, \mu\right)$ is feasible for (NVUD),

$$\begin{aligned} 0 \in \partial\left(\lambda^t f + \mu^t g\right)\left(y\right) &= \partial\left(\lambda^t f + \frac{\lambda^t l}{\lambda^t l} \mu^t g\right)\left(y\right) \\ &= \partial\left(\sum_{i=1}^{m} \lambda_i f_i + \frac{1}{\lambda^t l} \sum_{i=1}^{m} \lambda_i l_i \mu^t g\right)\left(y\right) \\ &= \partial\left\{\sum_{i=1}^{m} \lambda_i \left(f_i + \frac{l_i}{\lambda^t l} \mu^t g\right)\right\}\left(y\right) \\ &\subseteq \sum_{i=1}^{m} \lambda_i \partial\left(f_i + \frac{l_i}{\lambda^t l} \mu^t g\right)\left(y\right) \\ &= \partial \mathrm{L}\left(y, \lambda, \mu\right)^t \lambda. \end{aligned}$$

Therefore, there exists $\hat{C} \in \partial \mathrm{L}\left(y, \lambda, \mu\right)$ such that $\lambda^t \hat{C} = 0$. Substituting in (28) and then using (1), we get

$$\lambda^t \rho \left\| \omega\left(x, y\right) \right\|^k < 0 ,$$

which is a contradiction, as $\lambda \in K^* \setminus \{0\}$, $\rho \in K$ and norm is a non-negative function.

Case (ii): Let $\delta = 1$, then we have to prove that

$$f\left(y\right) - f\left(x\right) \notin \mathrm{int}K .$$

Let if possible,

$$f\left(y\right) - f\left(x\right) \in \mathrm{int}K .$$

Since f is K-nonsmooth $\left(F, \rho\right)$-pseudoconvex type II of order k with respect to ω at y on S_0, we have

$$-\left\{F\left(x, y; \bar{A}\right) + \rho \left\| \omega\left(x, y\right) \right\|^k\right\} \in \mathrm{int}K .$$

As $\lambda \in K^* \setminus \{0\}$, we get

$$\lambda^t F\left(x, y; \bar{A}\right) + \lambda^t \rho \left\| \omega\left(x, y\right) \right\|^k < 0 . \tag{29}$$

Since x is feasible for (NVOP) and $\left(y, \lambda, \mu\right)$ is feasible for (NVUD), we have

$$\mu^t \left\{g\left(x\right) - g\left(y\right)\right\} \leq 0 . \tag{30}$$

If $\mu \neq 0$, (30) implies $g\left(x\right) - g\left(y\right) \notin \mathrm{int}Q$.

As g is Q-nonsmooth (F,σ)-quasiconvex type I of order k with respect to ω at y on S_0, we get

$$-\left\{F\left(x,y;\bar{B}\right)+\sigma\left\|\omega(x,y)\right\|^k\right\}\in Q .$$

Since $\mu\in Q^*$, we have

$$\mu^t F\left(x,y;\bar{B}\right)+\mu^t\sigma\left\|\omega(x,y)\right\|^k\leq 0 . \tag{31}$$

If $\mu=0$, then also (31) holds.

Since (y,λ,μ) is feasible for (NVUD), by Remark 3.1, there exist $\bar{A}\in\partial f(y)$ and $\bar{B}\in\partial g(y)$ such that (22) holds.

Adding (29) and (31), we get

$$\lambda^t F\left(x,y;\bar{A}\right)+\mu^t F\left(x,y;\bar{B}\right)+\left(\lambda^t\rho+\mu^t\sigma\right)\left\|\omega(x,y)\right\|^k<0 ,$$

or

$$\sum_{i=1}^{m}\lambda_i F\left(x,y;\bar{A}_i\right)+\sum_{j=1}^{p}\mu_j F\left(x,y;\bar{B}_j\right)+\left(\lambda^t\rho+\mu^t\sigma\right)\left\|\omega(x,y)\right\|^k<0 .$$

Using sublinearity of F with the fact that $\lambda>0$ and $\mu\geq 0$ and then using (22) and (1), we obtain

$$\left(\lambda^t\rho+\mu^t\sigma\right)\left\|\omega(x,y)\right\|^k<0 .$$

This contradicts the assumption that $\lambda^t\rho+\mu^t\sigma\geq 0$, hence the result.

Theorem 4.3. (Strong Duality) Let $\bar{x}$ be a weak minimizer of order k with respect to ω for (NVOP) with $S=\mathbf{R}^n$, at which Slater-type cone constraint qualification holds. Then there exist $\bar{\lambda}\in K^*\setminus\{0\}$, $\bar{\mu}\in Q^*$ such that $(\bar{x},\bar{\lambda},\bar{\mu})$ is feasible for (NVUD). Further, if the conditions of Weak Duality Theorem 4.1 (Theorem 4.2) hold for all feasible x for (NVOP) and all feasible (y,λ,μ) for (NVUD), then $\bar{x}$ is a weak maximizer of order k with respect to ω for (NVUD).

Proof: As $\bar{x}$ is a weak minimizer of order k with respect to ω for (NVOP), by Theorem 3.2 there exist $\bar{\lambda}\in K^*\setminus\{0\}$, $\bar{\mu}\in Q^*$ such that

$$0\in\partial\left(\bar{\lambda}^t f+\bar{\mu}^t g\right)(\bar{x}), \tag{32}$$

$$\bar{\mu}^t g(\bar{x})=0 . \tag{33}$$

Since $\delta\in\{0,1\}$, Equations (32) and (33) can be written as

$$0\in\partial\left(\bar{\lambda}^t f+\bar{\mu}^t g\right)(\bar{x}),$$

$$\delta\bar{\mu}^t g(\bar{x})=0 .$$

Thus, $(\bar{x},\bar{\lambda},\bar{\mu})$ is a feasible solution for (NVUD). Further, if $(\bar{x},\bar{\lambda},\bar{\mu})$ is not a weak maximizer of order k with respect to ω for (NVUD), then for any $\beta\in\operatorname{int}K$, there exists a feasible solution (y,λ,μ) of (NVUD) such that

$$\left\{f(y)+\frac{l}{\lambda^t l}(1-\delta)\mu^t g(y)\right\}-\left\{f(\bar{x})+\frac{l}{\bar{\lambda}^t l}(1-\delta)\bar{\mu}^t g(\bar{x})\right\}-\beta\left\|\omega(y,\bar{x})\right\|^k\in\operatorname{int}K,$$

or,

$$f(y)+\frac{l}{\lambda^t l}(1-\delta)\mu^t g(y)-f(\bar{x})-\beta\left\|\omega(y,\bar{x})\right\|^k\in\operatorname{int}K.$$

Since, $\beta \in \operatorname{int}K,\ \beta\left\|\omega\left(y,\bar{x}\right)\right\|^{k} \in \operatorname{int}K$, so that we have

$$f\left(y\right)+\frac{l}{\lambda^{t}l}\left(1-\delta\right)\mu^{t}g\left(y\right)-f\left(\bar{x}\right)\in \operatorname{int}K,$$

which contradicts Theorem 4.1 (Theorem 4.2). Hence $\left(\bar{x},\bar{\lambda},\bar{\mu}\right)$ is a weak maximizer of order k with respect to ω for (NVUD).

5. Conclusion

In this paper, we introduced the concept of a higher-order (weak) minimizer for a nonsmooth vector optimization problem over cones. Furthermore, to study the new solution concept, we defined new generalized classes of cone-nonsmooth (F, ρ)-convex functions and established several sufficient optimality and duality results using these classes. The results obtained in this paper will be helpful in studying the stability and convergence analysis of iterative procedures for various optimization problems.

References

[1] Bector, C.R., Chandra, S. and Bector, M.K. (1988) Sufficient Optimality Conditions and Duality for a Quasiconvex Programming Problem. *Journal of Optimization Theory and Applications*, **59**, 209-221.

[2] Mangasarian, O.L. (1969) Nonlinear Programming. McGraw-Hill, New York.

[3] Vial, J.P. (1983) Strong and Weak Convexity of Sets and Functions. *Mathematics of Operations Research*, **8**, 231-259. http://dx.doi.org/10.1287/moor.8.2.231

[4] Hanson, M.A. and Mond, B. (1982) Further Generalization of Convexity in Mathematical Programming. *Journal of Information and Optimization Sciences*, **3**, 25-32. http://dx.doi.org/10.1080/02522667.1982.10698716

[5] Preda, V. (1992) On Efficiency and Duality for Multiobjective Programs. *Journal of Mathematical Analysis and Applications*, **166**, 365-377. http://dx.doi.org/10.1016/0022-247X(92)90303-U

[6] Antczak, T. and Kisiel, K. (2006) Strict Minimizers of Order m in Nonsmooth Optimization Problems. *Commentationes Mathematicae Universitatis Carolinae*, **47**, 213-232.

[7] Antczak, T. (2011) Characterization of Vector Strict Global Minimizers of Order 2 in Differentiable Vector Optimization Problems under a New Approximation Method. *Journal of Computational and Applied Mathematics*, **235**, 4991-5000. http://dx.doi.org/10.1016/j.cam.2011.04.029

[8] Cromme, L. (1978) Strong Uniqueness: A Far Criterion for the Convergence Analysis of Iterative Procedures. *Numerische Mathematik*, **29**, 179-193. http://dx.doi.org/10.1007/BF01390337

[9] Studniarski, M. (1989) Sufficient Conditions for the Stability of Local Minimum Points in Nonsmooth Optimization. *Optimization*, **20**, 27-35. http://dx.doi.org/10.1080/02331938908843409

[10] Bhatia, G. and Sahay, R.R. (2013) Strict Global Minimizers and Higher-Order Generalized Strong Invexity in Multiobjective Optimization. *Journal of Inequalities and Applications*, **2013**, 31. http://dx.doi.org/10.1186/1029-242X-2013-31

[11] Clarke, F.H. (1983) Optimization and Nonsmooth Analysis. Wiley, New York.

[12] Studniarski, M. (1997) Characterizations of Strict Local Minima for Some Nonlinear Programming Problems. *Nonlinear Analysis*, *Theory*, *Methods & Applications*, **30**, 5363-5367. http://dx.doi.org/10.1016/S0362-546X(97)00352-0

[13] Ward, D.W. (1994) Characterizations of Strict Local Minima and Necessary Conditions for Weak Sharp Minima. *Journal of Optimization Theory and Applications*, **80**, 551-571. http://dx.doi.org/10.1007/BF02207780

[14] Nahak, C. and Mohapatra, R.N. (2012) Nonsmooth $\rho-\left(\eta,\theta\right)$-Invexity in Multiobjective Programming Problems. *Optimization Letters*, **6**, 253-260. http://dx.doi.org/10.1007/s11590-010-0239-1

[15] Craven, B.D. (1989) Nonsmooth Multiobjective Programming. *Numerical Functional Analysis and Optimization*, **10**, 49-64. http://dx.doi.org/10.1080/01630568908816290

[16] Cambini, R. and Carosi, L. (2010) Mixed Type Duality for Multiobjective Optimization Problems with Set Constraints. In: Jimėnez, M.A., Garzòn, G.R. and Lizana, A.R., Eds., *Optimality Conditions in Vector Optimization*, Bentham Science Publishers, Sharjah, 119-142.

Applied Mathematics, 2015, 6, 20-27
Published Online January 2015 in SciRes. http://www.scirp.org/journal/am
http://dx.doi.org/10.4236/am.2015.61003

Darboux Transformation and New Multi-Soliton Solutions of the Whitham-Broer-Kaup System

Tiantian Xu

College of Science, University of Shanghai for Science and Technology, Shanghai, China
Email: xutiantian0197@163.com

Received 4 November 2014; revised 2 December 2014; accepted 19 December 2014

Abstract

Through a variable transformation, the Whitham-Broer-Kaup system is transformed into a parameter Levi system. Based on the Lax pair of the parameter Levi system, the N-fold Darboux transformation with multi-parameters is constructed. Then some new explicit solutions for the Whitham-Broer-Kaup system are obtained via the given Darboux transformation.

Keywords

Whitham-Broer-Kaup Equation, Levi Parameter System, Lax Pair, Darboux Transformation, Soliton Solutions

1. Introduction

Studying of the nonlinear models in shallow water wave is very important, such as Korteweg-de Vries (KdV) equation [1] [2], Kadomtsev-Petviashvili (KP) equation [3] [4], Boussinesq equation [5] [6], etc. There are many methods to study these nonlinear models, such as the inverse scattering transformation [7], the Bäcklund transformation (BT) [8], the Hirota bilinear method [9], the Darboux transformation (DT) [10], and so on. Among those various approaches, the DT is a useful method to get explicit solutions.

In this paper, we investigate the Whitham-Broer-Kaup (WBK) system [11]-[13] for the dispersive long water in the shallow water

$$\begin{cases} u_t + uu_x + v_x + \beta u_{xx} = 0, \\ v_t + (uv)_x + \alpha u_{xxx} - \beta v_{xx} = 0, \end{cases} \tag{1}$$

where $u = u(x,t)$ is the field of the horizontal velocity, and $v = v(x,t)$ is the height that deviates from equi-

How to cite this paper: Xu, T.T. (2015) Darboux Transformation and New Multi-Soliton Solutions of the Whitham-Broer-Kaup System. *Applied Mathematics*, **6**, 20-27. http://dx.doi.org/10.4236/am.2015.61003

librium position of the liquid. The constants α and β represent different diffusion powers. If $\alpha=0$ and $\beta\neq 0$, the WBK system (1) reduces to the classical long-wave system that describes the shallow water wave with diffusion [14]. If $\alpha=1$ and $\beta=0$, the WBK system (1) becomes the modified Boussinesq-Burgers equation [7].

Many solutions have been obtained for the WBK system (1), such as the analytical solution, the soliton-like solution, the soliton solutions, the periodic solution, the rational solution, and so on [15]-[19].

In this paper, through a proper transformation

$$\begin{cases} u=c\left[\ln\left(r_x-q_x+q^2-r^2\right)\right]_x-2cr, \\ v=-c^2\left(r_x-q_x+q^2-r^2\right)-\dfrac{2\beta c-c^2}{2}\left[\ln\left(r_x-q_x+q^2-r^2\right)\right]_{xx}+\left(2\beta c-c^2\right)r_x, \end{cases} \tag{2}$$

the WBK system (1) is transformed into the parameter Levi system

$$\begin{cases} q_t-c\left(qr\right)_x-\dfrac{c}{2}r_{xx}=0, \\ r_t-\dfrac{c}{2}q_{xx}-3crr_x+cqq_x=0. \end{cases} \tag{3}$$

Based on the obtained Lax pair, we construct the N-fold DT of the parameter Levi system (3) and then get the N-fold DT of the WBK system (1). Resorting to the obtained DT, we get new multi-soliton solutions of the WBK system.

The paper is organized as follows. In Section 2, we construct the N-fold DT of the Levi system and the WBK system. In Section 3, DT will be applied to generate explicit solutions of the WBK system (1).

2. Darboux Transformation

In this section, we first construct the N-fold DT of the parameter Levi system, and then get explicit solutions of the WBK system.

We consider the following spectral problem corresponding to the Levi system (3)

$$\varphi_x=U\varphi,\quad \varphi=\left(\varphi_1,\varphi_2\right)^{\mathrm{T}},\quad U=\begin{pmatrix} \lambda+q & 2\lambda\left(r-q\right) \\ 1 & -\lambda-q \end{pmatrix} \tag{4}$$

and its auxiliary problem

$$\varphi_t=V\varphi,\quad V=\begin{pmatrix} -c\lambda^2+c\left(r-q\right)\lambda+\dfrac{c}{2}r_x+crq & -2c\left(r-q\right)\lambda^2+c\left(2r^2-2rq+q_x-r_x\right)\lambda \\ -c\lambda+cr & c\lambda^2-c\left(r-q\right)\lambda-\dfrac{c}{2}r_x-crq \end{pmatrix}, \tag{5}$$

where λ is a spectral parameter and $c^2=4\left(\alpha+\beta^2\right)$. The compatibility condition $\varphi_{xt}=\varphi_{tx}$ yields a zero curvature equation $U_t-V_x+UV-VU=0$ which leads to the Levi system (3) by a direct computation.

Now we introduce a transformation of (4) and (5)

$$\bar{\varphi}=T\varphi, \tag{6}$$

where T is defined by

$$T_x+TU=\bar{U}T,\quad T_t+TV=\bar{V}T. \tag{7}$$

Then the Lax pair (4) and (5) are transformed into

$$\bar{\varphi}_x=\bar{U}\bar{\varphi}, \tag{8}$$

$$\bar{\varphi}_t=\bar{V}\bar{\varphi}, \tag{9}$$

where $\bar{U}$, $\bar{V}$ have the same form as U, V, except replacing q, r, q_x, r_x with $\bar{q}$, $\bar{r}$, $\bar{q}_x$, $\bar{r}_x$, respectively.

In order to make the Lax pair (4) and (5) invariant under the transformation (6), it is necessary to find a matrix T.

Let the matrix T in (6) be in the form of

$$T = T(\lambda) = \alpha \begin{pmatrix} A(\lambda) & B(\lambda) \\ C(\lambda) & D(\lambda) \end{pmatrix} \tag{10}$$

with

$$A(\lambda) = \sum_{k=0}^{N-1} A_k \lambda^k + \lambda^N, \quad B(\lambda) = \sum_{k=0}^{N-1} B_k \lambda^{k+1}, \quad C(\lambda) = \sum_{k=0}^{N-1} C_k \lambda^k, \quad D(\lambda) = \sum_{k=0}^{N-1} D_k \lambda^k,$$

where $\alpha, A_k, B_k, C_k, D_k$ $(0 \le k \le N-1)$ are functions of x and t.

Let $\varphi(\lambda_j) = (\varphi_1(\lambda_j), \varphi_2(\lambda_j))^{\mathrm{T}}$, $\psi(\lambda_j) = (\psi_1(\lambda_j), \psi_2(\lambda_j))^{\mathrm{T}}$ be two basic solutions of the spectral problem (4) and use them to define a linear algebraic system

$$\begin{cases} \sum_{k=0}^{N-1} (A_k + B_k \delta_j \lambda_j) \lambda_j^k = -\lambda_j^N, \\ \sum_{k=0}^{N-1} (C_k + D_k \delta_j) \lambda_j^k = 0 \end{cases} \tag{11}$$

with

$$\delta_j = \frac{\varphi_2(\lambda_j) - r_j \psi_2(\lambda_j)}{\varphi_1(\lambda_j) - r_j \psi_1(\lambda_j)}, \quad 1 \le j \le 2N-1, \tag{12}$$

where the constants λ_j, $r_j\,(\lambda_k \ne \lambda_j, r_k \ne r_j, k \ne j)$ are suitably chosen such that the determinant of the coefficients of (11) are nonzero. If we take

$$B_{N-1} = r - q, \quad C_{N-1} = \frac{1}{2}, \tag{13}$$

then A_k, B_k, C_k, D_k $(0 \le k \le N-1)$ are uniquely determined by (11).

From (10), we have

$$\det T(\lambda_j) = \alpha^2 \left[A(\lambda_j) D(\lambda_j) - B(\lambda_j) C(\lambda_j) \right]. \tag{14}$$

We note that (11) can be written as a linear algebraic system

$$A(\lambda_j) = -\delta_j B(\lambda_j), \quad C(\lambda_j) = -\delta_j D(\lambda_j) \tag{15}$$

and

$$\det T(\lambda_j) = 0,$$

which implies that $\lambda_j\,(1 \le j \le 2N-1)$ are $2N-1$ roots of $\det T(\lambda) = 0$, that is

$$\det T(\lambda) = \gamma \prod_{j=1}^{2N-1} (\lambda - \lambda_j), \tag{16}$$

where γ is independent of λ. From the above facts, we can prove the following propositions.

Proposition 1. *Let* α *satisfy the following first-order differential equation*

$$\partial_x \ln \alpha = -\frac{r}{2} - \frac{q}{2} + (A_{N-1} - D_{N-1} - 2C_{N-2}) + \frac{1}{4D_{N-1} - 2r + 2q} \left[r_x - q_x + 2A_{N-1}(r-q) - 2B_{N-2} - r^2 + q^2 \right]. \tag{17}$$

Then the matrix $\bar{U}$ *determined by Equation* (7) *is the same form as* U :

$$\bar{U}=\begin{pmatrix}\lambda+\bar{q} & 2\lambda\left(\bar{r}-\bar{q}\right)\\ 1 & -\lambda-\bar{q}\end{pmatrix},$$

where the transformations from the old potentials q , r *to* $\bar{q}$, $\bar{r}$ *are given by*

$$\begin{cases}\bar{q}=\dfrac{r-q}{2}+\left(A_{N-1}-D_{N-1}-2C_{N-2}\right)-\dfrac{1}{4D_{N-1}-2r+2q}\left[r_x-q_x+2A_{N-1}\left(r-q\right)-2B_{N-2}-r^2+q^2\right],\\ \bar{r}=\dfrac{r-q}{2}+\left(A_{N-1}-D_{N-1}-2C_{N-2}\right)+\dfrac{1}{4D_{N-1}-2r+2q}\left[r_x-q_x+2A_{N-1}\left(r-q\right)-2B_{N-2}-r^2+q^2\right].\end{cases} \tag{18}$$

Proof: Let $T^{-1}=T^{*}/\det T$ and

$$\left(T_x+TU\right)T^{*}=\begin{pmatrix}f_{11}(\lambda) & f_{12}(\lambda)\\ f_{21}(\lambda) & f_{22}(\lambda)\end{pmatrix}, \tag{19}$$

where T^{*} denotes the adjoint matrix of T. It is easy to see that $f_{11}(\lambda)$ and $f_{22}(\lambda)$ are $2N$ th-order polynomials in λ, while $\lambda^{-1}f_{12}(\lambda)$, $f_{21}(\lambda)$ are (2N − 1)th-order polynomials in λ. From (4) and (12), we get

$$\delta_{jx}=1-2\left(\lambda_j+q\right)\delta_j-2\lambda_j\left(r-q\right)\delta_j^2. \tag{20}$$

By using (16) and (20), we can prove that $\lambda_j\left(1\le j\le 2N-1\right)$ are the roots of $f_{kj}(\lambda)\left(k,j=1,2\right)$. From (15), we have

$$\det T\,\big|\, f_{kj}(\lambda),\quad k,j=1,2.$$

Hence, together with (19), we have

$$\left(T_x+TU\right)T^{*}=\left(\det T\right)P(\lambda), \tag{21}$$

that is

$$T_x+TU=P(\lambda)T \tag{22}$$

with

$$P(\lambda)=\begin{pmatrix}p_{11}^{(1)}\lambda+p_{11}^{(0)} & p_{12}^{(1)}\lambda\\ p_{21}^{(1)}\lambda & p_{22}^{(1)}\lambda+p_{22}^{(0)}\end{pmatrix},$$

where $p_{kj}^{(l)}\left(k,j=1,2,l=0,1\right)$ are independent of λ. By comparing the coefficients of λ^{N+1}, λ^{N} and λ^{N-1} in (22), we find

$$p_{11}^{(1)}=-p_{22}^{(1)}=1,\quad p_{21}^{(0)}=1, \tag{23}$$

$$p_{12}^{(1)}=\frac{2}{2D_{N-1}-r+q}\left[r_x-q_x+2A_{N-1}\left(r-q\right)-2B_{N-2}-r^2+q^2\right], \tag{24}$$

$$p_{11}^{(0)}=\partial_x\ln\alpha+r-\frac{1}{2}p_{12}^{(1)}, \tag{25}$$

$$p_{22}^{(0)}=\partial_x\ln\alpha+4C_{N-2}+2D_{N-1}-2A_{N-1}+q. \tag{26}$$

Substituting (17) into (24)-(26) yields

$$p_{12}^{(1)}=2\left(\bar{r}-\bar{q}\right),\quad p_{11}^{(0)}=\bar{q},\quad p_{22}^{(0)}=-\bar{q}. \tag{27}$$

From (7) and (22), we find that $\bar{U} = P(\lambda)$. The proof is completed. □

Remark. When $N = 1$, assuming that $A_{-1} = B_{-1} = C_{-1} = D_{-1} = 0$, the DT can be rewritten as

$$\begin{aligned} \bar{q} &= \frac{r}{2} - \frac{q}{2} + (A_0 - D_0) - \frac{1}{4D_0 - 2r + 2q}\left[r_x - q_x + 2A_0(r-q) - r^2 + q^2\right], \\ \bar{r} &= \frac{r}{2} - \frac{q}{2} + (A_0 - D_0) + \frac{1}{4D_0 - 2r + 2q}\left[r_x - q_x + 2A_0(r-q) - r^2 + q^2\right]. \end{aligned} \tag{28}$$

Let the basic solution $\varphi(\lambda_j)$, $\psi(\lambda_j)$ of (4) satisfy (5) as well. Through a similar way as Proposition 1, we can prove that $\bar{V}$ has the same form as V under the transformation (6) and (18). We get the following proposition.

Proposition 2. *Suppose* α *satisfy the following equation*

$$\partial_t \ln\alpha = c\left[(\bar{r} - \bar{q})(A_{N-1} - 2C_{N-2}) + \frac{1}{2}(\bar{q}_x - \bar{r}_x) - A_{N-1}(r-q) + \bar{r}^2 - r^2 - \frac{1}{2}r_x + B_{N-2}\right]. \tag{29}$$

Then the matrix $\bar{V}$ *defined by* (9) *has the same form as* V, *that is*

$$\bar{V} = \begin{pmatrix} -c\lambda^2 + c(\bar{r} - \bar{q})\lambda + \frac{c}{2}\bar{r}_x + c\bar{r}\bar{q} & -2c(\bar{r} - \bar{q})\lambda^2 + c\left(2\bar{r}^2 - 2\bar{r}\bar{q} + \bar{q}_x - \bar{r}_x\right)\lambda \\ -c\lambda + c\bar{r} & c\lambda^2 - c(\bar{r} - \bar{q})\lambda - \frac{c}{2}\bar{r}_x - c\bar{r}\bar{q} \end{pmatrix},$$

where $\bar{q}$ *and* $\bar{r}$ *are given by* (18).

The proof of Proposition 2 is similar with Proposition 1, but it is much more tedious and then we omit the proof for brevity. For the similar proof we can also refer to [20] [21].

According to Proposition 1 and 2, the Lax pair (4) and (5) is transformed into the Lax pair (8) and (9), then the transformation (6) and (18): $(\varphi; q, r) \to (\bar{\varphi}; \bar{q}, \bar{r})$ is called the DT of the Lax pair (4) and (5). The Lax pair leads to the parameter Levi system (3) and then the transformation (6) and (18): $(\varphi; q, r) \to (\bar{\varphi}; \bar{q}, \bar{r})$ is also called DT of the parameter Levi system (3). On the other hand, together with the transformation (2), the parameter Levi system (3) is transformed into the WBK system (1), then we get the solutions of the WBK system (1).

Theorem 1. *If* (q, r) *is a solution of the parameter Levi system* (3), $(\bar{q}, \bar{r})$ *with*

$$\begin{cases} \bar{q} = \dfrac{r-q}{2} + (A_{N-1} - D_{N-1} - 2C_{N-2}) - \dfrac{1}{4D_{N-1} - 2r + 2q}\left[r_x - q_x + 2A_{N-1}(r-q) - 2B_{N-2} - r^2 + q^2\right], \\ \bar{r} = \dfrac{r-q}{2} + (A_{N-1} - D_{N-1} - 2C_{N-2}) + \dfrac{1}{4D_{N-1} - 2r + 2q}\left[r_x - q_x + 2A_{N-1}(r-q) - 2B_{N-2} - r^2 + q^2\right]. \end{cases} \tag{30}$$

is another solution of the parameter Levi system (3), *where* A_{N-1}, B_{N-2}, C_{N-2}, D_{N-1} *are determined by* (11) *and* (13).

From the transformation (2), we find that

Theorem 2. *If* (u, v) *is a solution of the WBK system* (1), $(\bar{u}, \bar{v})$ *with*

$$\begin{cases} \bar{u} = c\left[\ln\left(\bar{r}_x - \bar{q}_x + \bar{q}^2 - \bar{r}^2\right)\right]_x - 2c\bar{r}, \\ \bar{v} = -c^2\left(\bar{r}_x - \bar{q}_x + \bar{q}^2 - \bar{r}^2\right) - \dfrac{2\beta c - c^2}{2}\left[\ln\left(\bar{r}_x - \bar{q}_x + \bar{q}^2 - \bar{r}^2\right)\right]_{xx} + \left(2\beta c - c^2\right)\bar{r}_x, \end{cases} \tag{31}$$

is another solution of the WBK system (1), *where* $(\bar{q}, \bar{r})$ *is determined by* (30). *Then the transformation* $(\varphi; q, r) \to (\bar{\varphi}; \bar{q}, \bar{r})$ *is also called the DT of the WBK system* (1).

3. New Solutions

In this section, we take a trivial solution $(q, r) = (0, 1)$ as the "seed" solution, to obtain multi-soliton solutions of the WBK system (1).

Substituting $(q,r)=(0,1)$ into the Lax pair (4) and (5), the two basic solutions are

$$\varphi(\lambda_j)=\begin{pmatrix}\cosh\xi_j\\ -\frac{1}{2}\cosh\xi_j+\frac{k_j}{2\lambda_j}\sinh\xi_j\end{pmatrix},\quad \psi(\lambda_j)=\begin{pmatrix}\sinh\xi_j\\ -\frac{1}{2}\sinh\xi_j+\frac{k_j}{2\lambda_j}\cosh\xi_j\end{pmatrix} \tag{32}$$

with $\xi_j=k_j\left[x-c(\lambda_j-1)t\right]$, $k_j=\sqrt{\lambda_j^2+2\lambda_j}$ $(1\le j\le 2N-1)$.

According to (12), we get

$$\delta_j=-\frac{1}{2}+\frac{k_j}{2\lambda_j}\left(\frac{\tanh\xi_j-r_j}{1-r_j\tanh\xi_j}\right),\quad 1\le j\le 2N-1. \tag{33}$$

For simplicity, we discuss the following two cases, *i.e.* $N=1$ and $N=2$.

As $N=1$, let $\lambda=\lambda_1$, solving the linear algebraic system (11) and (13), we have

$$A_0=-\lambda_1-\delta_1\lambda_1,\quad D_0=-\frac{1}{2\delta_1}, \tag{34}$$

according to (28), we get

$$\bar{q}\triangleq\bar{q}[1]=\frac{1+2(1-\lambda_1)\delta_1-6\lambda_1\delta_1^2-4\lambda_1\delta_1^3}{2\delta_1(1+\delta_1)},\quad \bar{r}\triangleq\bar{r}[1]=\frac{1+2(1-\lambda_1)\delta_1+2(1-\lambda_1)\delta_1^2}{2\delta_1(1+\delta_1)}. \tag{35}$$

Substituting (35) into (31), we obtain the solution of the WBK system (1) as

$$\begin{cases}\bar{u}[1]=c\left[\ln\bar{w}[1]\right]_x-2c\bar{r}[1],\\ \bar{v}[1]=-c^2\left(\bar{w}[1]\right)-\dfrac{2\beta c-c^2}{2}\left[\ln\bar{w}[1]\right]_{xx}+\left(2\beta c-c^2\right)\bar{r}[1]_x\end{cases} \tag{36}$$

with $\bar{w}[1]=-\dfrac{2(1+\lambda_1)\delta_1+(1+2\lambda_1)\delta_1^2}{(1+\delta_1)^2}$.

By choosing proper parameters (such as $r_1=5$, $\lambda_1=7$, $c=1$, $\beta=1/15$), we find that $\bar{u}[1]$ is a bell-type-soliton and $\bar{v}[1]$ is a M-type-soliton.

As $N=2$, let $\lambda=\lambda_j\ (j=1,2,3)$, together with (11) and (13), we have

$$A_1=\frac{\Delta_{A_1}}{\Delta_1},\quad B_0=\frac{\Delta_{B_0}}{\Delta_1},\quad C_0=\frac{\Delta_{C_0}}{\Delta_2},\quad D_1=\frac{\Delta_{D_1}}{\Delta_2} \tag{37}$$

with

$$\Delta_1=\begin{vmatrix}1&\delta_1\lambda_1&\lambda_1\\1&\delta_2\lambda_2&\lambda_2\\1&\delta_3\lambda_3&\lambda_3\end{vmatrix},\quad \Delta_{A_1}=\begin{vmatrix}1&\delta_1\lambda_1&-\lambda_1^2-\delta_1\lambda_1^2\\1&\delta_2\lambda_2&-\lambda_2^2-\delta_2\lambda_2^2\\1&\delta_3\lambda_3&-\lambda_3^2-\delta_3\lambda_3^2\end{vmatrix},\quad \Delta_{B_0}=\begin{vmatrix}1&-\lambda_1^2-\delta_1\lambda_1^2&\lambda_1\\1&-\lambda_2^2-\delta_2\lambda_2^2&\lambda_2\\1&-\lambda_3^2-\delta_3\lambda_3^2&\lambda_3\end{vmatrix},$$

$$\Delta_2=\begin{vmatrix}1&\delta_1&\delta_1\lambda_1\\1&\delta_2&\delta_2\lambda_2\\1&\delta_3&\delta_3\lambda_3\end{vmatrix},\quad \Delta_{D_1}=\begin{vmatrix}1&\delta_1&-\frac{1}{2}\lambda_1\\1&\delta_2&-\frac{1}{2}\lambda_2\\1&\delta_3&-\frac{1}{2}\lambda_3\end{vmatrix},\quad \Delta_{C_0}=\begin{vmatrix}-\frac{1}{2}\lambda_1&\delta_1&\delta_1\lambda_1\\-\frac{1}{2}\lambda_2&\delta_2&\delta_2\lambda_2\\-\frac{1}{2}\lambda_3&\delta_3&\delta_3\lambda_3\end{vmatrix}.$$

With the help of (30), we get

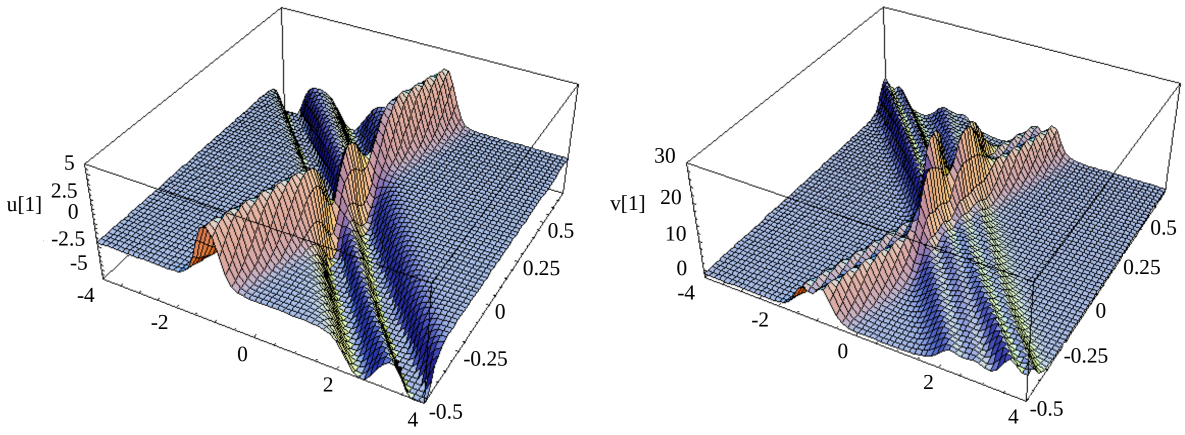

(*a*) (*b*)

Figure 1. Plots of the three-soliton solution (39).

$$\begin{aligned}\bar{q} &\triangleq \bar{q}[2] = \frac{1}{2} + A_1 - D_1 - 2C_0 - \frac{2A_1 - 2B_0 - 1}{4D_1 - 2},\\ \bar{r} &\triangleq \bar{r}[2] = \frac{1}{2} + A_1 - D_1 - 2C_0 + \frac{2A_1 - 2B_0 - 1}{4D_1 - 2}.\end{aligned} \tag{38}$$

Then we get another solution of the WBK system (1) by using of (31)

$$\begin{cases}\bar{u}[2] = c\left[\ln\bar{w}[2]\right]_x - 2c\bar{r}[2],\\ \bar{v}[2] = -c^2\bar{w}[2] - \left(\beta c - \dfrac{c^2}{2}\right)\left[\ln\bar{w}[2]\right]_{xx} + \left(2\beta c - c^2\right)\bar{r}[2]_x\end{cases} \tag{39}$$

with $\bar{w}[2] = \bar{r}[2]_x - \bar{q}[2]_x + \bar{q}[2]^2 - \bar{r}[2]^2$.

When we take $\lambda_1 = -5$, $\lambda_2 = -4$, $\lambda_3 = 3$, $c = 1$, $\beta = 1/20$, $r_1 = 3$, $r_2 = 1/2$, $r_3 = 2$, $\bar{u}[2]$ is a three-bell-type-soliton solution with two overtaking solitons and one head-on soliton (see **Figure 1(a)**) and $\bar{v}[2]$ is a three-*M*-type-soliton solution with two overtaking solitons and one head-on soliton (see **Figure 1(b)**). We note that by the obtained DT, we can get $(2N-1)$ soliton solutions which are different from those in [19] which are $2N$-soliton solutions.

Acknowledgements

This work is supported by Nurture Funds of National Project of University of Shanghai for Science and Technology (no. 14XPQ09).

References

[1] Zabusky, N.J. and Galvin, C.J. (1971) Shallow-Water Waves, the Korteweg-de Vries Equation and Solitons. *Journal of Fluid Mechanics*, **47**, 811-824. http://dx.doi.org/10.1017/S0022112071001393

[2] Dullin, H.R., Georg, A.G. and Holm, D.D. (2003) Camassa-Holm, Korteweg-de Vries-5 and Other Asymptotically Equivalent Equations for Shallow Water Waves. *Fluid Dynamics Research*, **33**, 73-95. http://dx.doi.org/10.1016/S0169-5983(03)00046-7

[3] Chakravarty, S. and Kodama, Y. (2009) Soliton Solutions of the KP Equation and Application to Shallow Water Waves. *Studies in Applied Mathematics*, **123**, 83-151. http://dx.doi.org/10.1111/j.1467-9590.2009.00448.x

[4] Kodama, Y. (2010) KP Solitons in Shallow Water. *Journal of Physical A*: *Mathematical and Theoretical*, **43**, Article ID: 434004. http://dx.doi.org/10.1088/1751-8113/43/43/434004

[5] Lambert, F., Musette, M. and Kesteloot, E. (1987) Soliton Resonances for the Good Boussinesq Equation. *Inverse Problems*, **3**, 275-288. http://dx.doi.org/10.1088/0266-5611/3/2/010

[6] Li, Y.S. and Zhang, J.E. (2001) Darboux Transformation of Classical Boussinesq System and Its Multi-Soliton Solu-

tions. *Physics Letters A*, **284**, 253-258. http://dx.doi.org/10.1016/S0375-9601(01)00331-0

[7] Ablowitz, M.J. and Clarkson, P.A. (1991) Solitons, Nonlinear Evolution Equations and Inverse Scattering. Cambridge University Press, Cambridge. http://dx.doi.org/10.1017/CBO9780511623998

[8] Rogers, C. and Schief, W.K. (2002) Bäcklund and Darboux Transformations Geometry and Modern Application in Soliton Theory. Cambridge University Press, Cambridge. http://dx.doi.org/10.1017/CBO9780511606359

[9] Hirota, R. (2004) The Direct Method in Soliton Theory. Cambridge University Press, Cambridge. http://dx.doi.org/10.1017/CBO9780511543043

[10] Gu, C.H., Hu, H.S. and Zhou, Z.X. (2005) Darboux Transformation in Soliton Theory and Its Geometric Applications. Shanghai Science Technology Publication House, Shanghai.

[11] Whitham, G.B. (1967) Variational Methods and Applications to Water Wave. *Proceedings of the Royal Society A*, **299**, 6-25. http://dx.doi.org/10.1098/rspa.1967.0119

[12] Broer, L.J. (1975) Approximate Equations for Long Water Waves. *Applied Scientific Research*, **31**, 377-395. http://dx.doi.org/10.1007/BF00418048

[13] Kaup, D.J. (1975) A Higher-Order Water Equation and Method for Solving It. *Progress of Theoretical Physics*, **54**, 396-408. http://dx.doi.org/10.1143/PTP.54.396

[14] Kupershmidt, B.A. (1985) Mathematics of Dispersive Water Waves. *Communications in Mathematical Physics*, **99**, 51-73. http://dx.doi.org/10.1007/BF01466593

[15] Xia, Z. (2004) Homogenous Balance Method and Exact Analytical Solutions for Whitham-Broer-Kaup Equations in the Shallow Water. *Chinese Quarterly Journal of Mathematics*, **19**, 240-246.

[16] Xie, F.D. and Gao, X.S. (2004) A Computational Approach to the New Type Solutions of Whitham-Broer-Kaup Equation in Shallow Water. *Communications in Theoretical Physics*, **41**, 179-182. http://dx.doi.org/10.1088/0253-6102/41/2/179

[17] Zhang, J.F., Guo, G.P. and Wu, F.M. (2002) New Multi-Soliton Solutions and Travelling Wave Solutions of the Dispersive Long-Wave Equations. *Chinese Physics*, **11**, 533-536. http://dx.doi.org/10.1088/1009-1963/11/6/303

[18] Lin, G.D., Gao, Y.T., Gai, X.L. and Meng, D.X. (2011) Extended Double Wronskian Solutions to the Whitham-Broer-Kaup Equations in Shallow Water. *Nonlinear Dynamics*, **64**, 197-206. http://dx.doi.org/10.1007/s11071-010-9857-5

[19] Wang, L., Gao, Y.T. and Gai, X.T. (2012) Gauge Transformation, Elastic and Inelastic Interactions for the Whitham-Broer-Kaup Shallow-Water Model. *Communications in Nonlinear Science and Numerical Simulation*, **17**, 2833-2844. http://dx.doi.org/10.1016/j.cnsns.2011.11.018

[20] Geng, X.G. and Tam, H.W. (1999) Darboux Transformation and Soliton Solutions for Generalized Nonlinear Schrödinger Equations. *Journal of Physical Society of Japan*, **68**, 1508-1512. http://dx.doi.org/10.1143/JPSJ.68.1508

[21] Huang, D.J. and Zhang, H.Q. (2008) Vandermonde-Like Determinants' Representations of Darboux Transformations and Explicit Solutions for the Modified Kadomtsev-Petviashvili Equation. *Physica A*, **387**, 4565-4580.

Applied Mathematics, 2015, 6, 28-36
Published Online January 2015 in SciRes. http://www.scirp.org/journal/am
http://dx.doi.org/10.4236/am.2015.61004

Scientific Research Publishing

Ground States for a Class of Nonlinear Schrodinger-Poisson Systems with Positive Potential

Guoqing Zhang*, **Xue Chen**

College of Sciences, University of Shanghai for Science and Technology, Shanghai, China
Email: *shzhangguoqing@126.com

Received 10 November 2014; revised 29 November 2014; accepted 15 December 2014

Abstract

Based on Nehari manifold, Schwarz symmetric methods and critical point theory, we prove the existence of positive radial ground states for a class of Schrodinger-Poisson systems in $\mathbb{R}^3$, which doesn't require any symmetry assumptions on all potentials. In particular, the positive potential is interesting in physical applications.

Keywords

Ground States, Schrodinger-Poisson Systems

1. Introduction

In this paper, we consider the following nonlinear Schrodinger-Poisson systems

$$\begin{cases} -\Delta u + V(x)u - \lambda\rho(x)\Phi u + Q(x)|u|^{p-2}u = 0, & x \in \mathbb{R}^3, \\ -\Delta\Phi = \rho(x)u^2, & x \in \mathbb{R}^3, \end{cases} \tag{1.1}$$

where $\lambda > 0$, $2 < p < 4$; $V(x)$, $\rho(x)$ and $Q(x)$ are positive potentials defined in $\mathbb{R}^3$.

In recent years, such systems have been paid great attention by many authors concerning existence, non-existence, multiplicity and qualitative behavior. The systems are to describe the interaction of nonlinear Schrodinger field with an electromagnetic field. When $\lambda = -1$, $V(x) = \rho(x) = 1$, $Q(x) = -1$, the existence of nontrivial solution for the problem (1.1) was proved as $p \in (4,6)$ in [1], and non-existence result for $p \in (0,2]$ or $p \in (6,+\infty)$ was proved in [2]. When $\lambda < 0$, $V(x) = \rho(x) = 1$, $Q(x) = -1$, using critical point theory,

*Corresponding author.

How to cite this paper: Zhang, G.Q. and Chen, X. (2015) Ground States for a Class of Nonlinear Schrodinger-Poisson Systems with Positive Potential. *Applied Mathematics*, **6**, 28-36. http://dx.doi.org/10.4236/am.2015.61004

Ruiz [3] obtained some multiplicity results for $p \in (2,3)$, and existence results for $p \in [3,6)$. Later, Ambrosetti and Ruiz [4], and Ambrosetti [5] generalized some existence results of Ruiz [3], and obtained the existence of infinitely solutions for the problem (1.1).

In particular, Sanchel and Soler [6] considered the following Schrodinger-Poisson-Slater systems

$$\begin{cases} -\Delta u + \omega u + \Phi u - |u|^{\frac{2}{3}} u = 0, & x \in \mathbb{R}^3, \\ -\Delta \Phi = u^2, & x \in \mathbb{R}^3, \end{cases} \tag{1.2}$$

where $\omega \in \mathbb{R}$. The problem (1.2) was introduced as the model of the Hartree-Foch theory for a one-component plasma. The solution is obtained by using the minimization argument and ω as a Lagrange multiplier. However, it is not known if the solution for the problem (1.2) is radial. Mugani [7] considered the following generalized Schrodinger-Poisson systems

$$\begin{cases} -\Delta u + \omega u - \lambda \Phi u + W_u(x,u) = 0, & x \in \mathbb{R}^3, \\ -\Delta \Phi = u^2, & x \in \mathbb{R}^3, \end{cases} \tag{1.3}$$

where $\omega \in \mathbb{R}$, $\lambda > 0$ and $W(x,s) = W(|x|,s)$, and proved the existence of radially symmetric solitary waves for the problem (1.3).

In this paper, without requiring any symmetry assumptions on $V(x)$, $\rho(x)$ and $Q(x)$, we obtain the existence of positive radial ground state solution for the problem (1.1). In particular, the positive potential $Q(x)$ implies that we are dealing with systems of particles having positive mass. It is interesting in physical applications.

The paper is organized as following. In Section 2, we collect some results and state our main result. In Section 3, we prove some lemmas and consider the problem (1.1) at infinity. Section 4 is devoted to our main theorem.

2. Preliminaries and Main Results

Let $L^s(\mathbb{R}^3)$, $1 \le s < +\infty$ denotes a Lebesgue space, the norm in $L^s(\mathbb{R}^3)$ is $|u|_s = \left(\int_{\mathbb{R}^3} |u|^s \mathrm{d}x \right)^{\left(\frac{1}{s}\right)}$, $D^{1,2}(\mathbb{R}^3)$ is the completion of $C_0^\infty(\mathbb{R}^3)$ with respect to the norm

$$\|u\|_{D^{1,2}} = \left(\int_{\mathbb{R}^3} |\nabla u|^2 \mathrm{d}x \right)^{\left(\frac{1}{2}\right)}$$

$H^1(\mathbb{R}^3)$ be the usual Sobolev space with the usual norm

$$\|u\|_{H^1} = \left(\int_{\mathbb{R}^3} \left(|\nabla u|^2 + |u|^2 \right) \mathrm{d}x \right)^{\left(\frac{1}{2}\right)}.$$

Assume that the potential $V(x)$ satisfies

H1) $V(x) \in C^1(\mathbb{R}^3, \mathbb{R})$, $\inf_{x \in \mathbb{R}^3} V(x) = 1$, $V(x) \le V_\infty = \lim_{|x| \to \infty} V(x) < \infty$.

Let $H_V^1(\mathbb{R}^3)$ be the Hilbert subspace of $u \in H^1(\mathbb{R}^3)$ such that

$$\|u\|_{H_V^1} = \left(\int_{\mathbb{R}^3} \left(|\nabla u|^2 + V(x)|u|^2 \right) \mathrm{d}x \right)^{\left(\frac{1}{2}\right)} \tag{2.1}$$

Then $H_V^1(\mathbb{R}^3) \subset H^1(\mathbb{R}^3) \subset L^s(\mathbb{R}^3)$, $2 \le s \le 6$ with the corresponding embeddings being continuous (see [8]). Furthermore, assume the potential $\rho(x)$ satisfies

H2) $\rho(x) > 0$, $\lim_{|x| \to +\infty} \rho(x) = \rho_\infty > 0$, $\rho_0(x) = \rho(x) - \rho_\infty \in L^2(\mathbb{R}^3)$.

It is easy to reduce the problem (1.1) to a single equation with a non-local term. Indeed, for every $v \in D^{1,2}(\mathbb{R}^3)$, we have

$$
\begin{aligned}
\left|\int_{\mathbb{R}^3} \rho(x) u^2 v \mathrm{d}x\right| &= \left|\int_{\mathbb{R}^3} (\rho(x)-\rho_\infty) u^2 v \mathrm{d}x + \int_{\mathbb{R}^3} \rho_\infty u^2 v \mathrm{d}x\right| \\
&\le \int_{\mathbb{R}^3} |\rho(x)-\rho_\infty| u^2 |v| \mathrm{d}x + \int_{\mathbb{R}^3} \rho_\infty u^2 |v| \mathrm{d}x \\
&\le \left(\int_{\mathbb{R}^3} \left(|\rho_0(x)| u^2\right)^{\left(\frac{6}{5}\right)} \mathrm{d}x\right)^{\left(\frac{6}{5}\right)} \left(\int_{\mathbb{R}^3} (v)^6 \mathrm{d}x\right)^{\left(\frac{1}{6}\right)} + \rho_\infty \left(\int_{\mathbb{R}^3} \left(u^2\right)^{\left(\frac{6}{5}\right)} \mathrm{d}x\right)^{\left(\frac{6}{5}\right)} \left(\int_{\mathbb{R}^3} (v)^6 \mathrm{d}x\right)^{\left(\frac{1}{6}\right)} \\
&\le |v|_6 \left[|\rho_0(x)|_2 \left(\int_{\mathbb{R}^3} \left(u^2\right)^3 \mathrm{d}x\right)^{\left(\frac{1}{3}\right)} + \rho_\infty \left(\int_{\mathbb{R}^3} \left(u^2\right)^{\left(\frac{6}{5}\right)} \mathrm{d}x\right)^{\left(\frac{6}{5}\right)} \right].
\end{aligned}
\tag{2.2}
$$

Since $\rho_0(x) = \rho(x) - \rho_\infty \in L^2(\mathbb{R}^3)$, $u \in H^1(\mathbb{R}^3)$ and (2.1), by the Lax-Milgram theorem, there exists a unique $\Phi[u]$ such that

$$
\int_{\mathbb{R}^3} \nabla \Phi[u] \nabla v \mathrm{d}x = \int_{\mathbb{R}^3} \rho(x) u^2 v \mathrm{d}x, \quad \forall v \in D^{1,2}(\mathbb{R}^3) \tag{2.3}
$$

It follows that $\Phi[u]$ satisfies the Poisson equation

$$
-\Delta \Phi[u] = \rho(x) u^2
$$

and there holds

$$
-\Phi[u] = \int_{\mathbb{R}^3} \frac{\rho(x) u^2(y)}{|x-y|} \mathrm{d}y = \frac{1}{|x|} * \rho(x) u^2
$$

Because $\rho(x) > 0$, we have $\Phi[u] > 0$ when $u \neq 0$, and $\|\Phi[u]\|_{D^{1,2}} = M \|u\|_{H^1}^2$, M is positive constant. Substituting $\Phi[u]$ in to the problem (1.1), we are lead to the equation with a non-local term

$$
-\Delta u + V(x) u - \lambda \rho(x) \Phi[u] u + Q(x) |u|^{p-2} u = 0. \tag{2.4}
$$

In the following, we collect some properties of the functional $\Phi[u]$, which are useful to study our problem.

Lemma 2.1. [9] For any $u \in H^1(\mathbb{R}^3)$, we have

1) $\Phi[u]: H^1(\mathbb{R}^3) \to D^{1,2}(\mathbb{R}^3)$ is continuous, and maps bounded sets into bounded sets;

2) if $u_n \to u$ weakly in $H^1(\mathbb{R}^3)$, then $\Phi[u_n] \to \Phi[u]$ weakly in $D^{1,2}(\mathbb{R}^3)$;

3) $\Phi[tu(x)] = t^2 \Phi[u(x)]$ for all $t \in \mathbb{R}$.

Now, we state our main theorem in this paper.

Theorem 2.2. Assume that $\lambda > 0$, $2 < p < 4$, the potential $V(x)$ satisfies condition $H1$), the potential $\rho(x)$ satisfies condition $H3$) and $\rho(x) \ge \rho_\infty$, the potential $Q(x)$ satisfies

$H3$) $Q(x) > 0$, $\lim_{|x| \to +\infty} Q(x) = Q_\infty > 0$, $Q_0(x) = Q(x) - Q_\infty \in L^{\frac{6}{6-p}}(\mathbb{R}^3)$

and $Q(x) \le Q_\infty$, $Q(x) - Q_\infty < 0$ on positive measure. Then there exists a positive radial ground state solution for the problem (1.1).

Remark 2.3. If $\lambda \le 0$, $V(x)$, $\rho(x)$ and $Q(x)$ are positive potentials defined in $\mathbb{R}^3$, and $2 < p < 6$, $(u, \Phi) \in H_V^1(\mathbb{R}^3) \times D^{1,2}(\mathbb{R}^3)$ be a solution for the problem (1.1). Then $(u, \Phi) = (0, 0)$, Indeed, we have

$$
\begin{aligned}
0 &= \int_{\mathbb{R}^3} \left(|\nabla u|^2 + V(x) u^2\right) \mathrm{d}x - \lambda \int_{\mathbb{R}^3} \rho(x) \Phi[u] u^2 \mathrm{d}x + \int_{\mathbb{R}^3} Q(x) |u|^p \mathrm{d}x \\
&\ge \int_{\mathbb{R}^3} \left(|\nabla u|^2 + V(x) u^2\right) \mathrm{d}x.
\end{aligned}
$$

Since $V(x)>0$, this implies $u=0$. By Lemma 2.1, we have $\Phi=0$.

3. Some Lemmas and the Problem (1.1) at Infinity

Now, we consider the functional $I_\lambda : H_V^1(\mathbb{R}^3)\to\mathbb{R}$ given by

$$\begin{aligned}I_\lambda(u)&=\frac{1}{2}\int_{\mathbb{R}^3}\left(|\nabla u|^2+V(x)u^2\right)\mathrm{d}x-\frac{\lambda}{4}\int_{\mathbb{R}^3}\rho(x)\Phi[u]u^2\mathrm{d}x+\frac{1}{p}\int_{\mathbb{R}^3}Q(x)|u|^p\mathrm{d}x\\&=\frac{1}{2}\|u\|_{H_V^1}^2-\frac{\lambda}{4}\int_{\mathbb{R}^3}\rho(x)\Phi[u]u^2\mathrm{d}x+\frac{1}{p}\int_{\mathbb{R}^3}Q(x)|u|^p\mathrm{d}x.\end{aligned}$$

Since $\rho(x)$ satisfies condition $H2$), by (2.2), the Holder inequality and Sobolev inequality, we have

$$\int_{\mathbb{R}^3}\rho(x)\Phi[u]u^2\mathrm{d}x\le\bar{S}^{-1}\left[S_6^{-2}|\rho|_2+\rho_\infty S_{\left(\frac{12}{5}\right)}^{-2}\right]\|u\|_{H_V^1}^2\|v\|_{D^{1,2}}, \tag{3.2}$$

where $\bar{S}=\inf_{u\in D^{1,2}(\mathbb{R}^3)\setminus\{0\}}\frac{\|u\|_{D^{1,2}}}{|u|_6}$ and $S=\inf_{u\in H_V^1(\mathbb{R}^3)\setminus\{0\}}\frac{\|u\|_{H_V^1}}{|u|_6}$. Since the potential $Q(x)$ satisfies condition Q, $2<p<4$, we have

$$\begin{aligned}\int_{\mathbb{R}^3}Q(x)|u|^p\mathrm{d}x&\le\left|\int_{\mathbb{R}^3}\left(Q(x)-Q_\infty\right)|u|^p\mathrm{d}x+\int_{\mathbb{R}^3}Q_\infty|u|^p\mathrm{d}x\right|\\&\le\int_{\mathbb{R}^3}|Q_0(x)||u|^p\mathrm{d}x+\int_{\mathbb{R}^3}Q_\infty|u|^p\mathrm{d}x\\&\le\left(\int_{\mathbb{R}^3}|Q_0(x)|^{\left(\frac{6}{6-p}\right)}\mathrm{d}x\right)^{\left(\frac{6-p}{6}\right)}\left(\int_{\mathbb{R}^3}(u)^6\mathrm{d}x\right)^{\left(\frac{p}{6}\right)}+Q_\infty\int_{\mathbb{R}^3}|u|^p\mathrm{d}x.\end{aligned}$$

By Sobolev inequality, we obtain that

$$\int_{\mathbb{R}^3}Q(x)|u|^p\mathrm{d}x\le M\|u\|_{H_V^1}^p \tag{3.3}$$

Combining (3.2) and (3.3), we obtain that the functional I_λ is a well defined C^1 functional, and if $u\in H_V^1(\mathbb{R}^3)$ is critical point of it, then the pair $(u,\Phi[u])$ is a weak solution of the problem (1.1).

Now, we define the Nehari manifold ([10]) of the functional I_λ

$$N_\lambda=\left\{u\in H_V^1(\mathbb{R}^3)\setminus\{0\}:H_\lambda(u)=0\right\},$$

where

$$H_\lambda(u)=I'_\lambda(u)[u]=\|u\|_{H_V^1}^2-\lambda\int_{\mathbb{R}^3}\rho(x)\Phi[u]u^2\mathrm{d}x+\int_{\mathbb{R}^3}Q(x)|u|^p\mathrm{d}x$$

Hence, we have

$$\begin{aligned}I'_\lambda(u)\big|_{N_\lambda}&=\frac{1}{4}\|u\|_{H_V^1}^2+\left(\frac{1}{p}-\frac{1}{4}\right)\int_{\mathbb{R}^3}Q(x)|u|^p\mathrm{d}x\\&=\left(\frac{1}{2}-\frac{1}{p}\right)\|u\|_{H_V^1}^2+\lambda\left(\frac{1}{p}-\frac{1}{4}\right)\int_{\mathbb{R}^3}\rho(x)\Phi[u]u^2\mathrm{d}x\\&=\left(\frac{1}{2}-\frac{1}{p}\right)\int_{\mathbb{R}^3}Q(x)|u|^p\mathrm{d}x-\frac{\lambda}{4}\int_{\mathbb{R}^3}\rho(x)\Phi[u]u^2\mathrm{d}x.\end{aligned} \tag{3.4}$$

Lemma 3.1. 1) For any $\lambda > 0$, $u \in H_V^1(\mathbb{R}^3)\setminus\{0\}$, there exists a unique $t(u) > 0$ such that $t(u)u \in N_\lambda$. Moreover, we have $I_\lambda(t(u)u) = \max_{t\ge 0} I_\lambda(tu)$.

2) $I_\lambda(u)$ is bounded from below on N_λ by a positive solution.

Proof. 1) Taking any $u \in H_V^1(\mathbb{R}^3)\setminus\{0\}$ and $\|u\|_{H_V^1} = 1$, we obtain that there exists a unique $t(u) > 0$ such that $t(u)u \in N_\lambda$. Indeed, we define the function $g(t) = I_\lambda(tu)$. We note that $g'(t) = (I'_\lambda(tu), v) = 0$ if only if $tu \in N_\lambda$. Since $g'(t) = 0$ is equivalent to

$$t^2\|u\|_{H_V^1}^2 - \lambda t^4 \int_{\mathbb{R}^3} \rho(x)\Phi[u]u^2 \mathrm{d}x + t^p \int_{\mathbb{R}^3} Q(x)|u|^p \mathrm{d}x = 0.$$

By $\rho(x)$, $Q(x) > 0$ and $\Phi[u] > 0$, we have

$$b = \int_{\mathbb{R}^3} \rho(x)\Phi[u]u^2 \mathrm{d}x > 0, \quad c = \int_{\mathbb{R}^3} Q(x)|u|^p \mathrm{d}x > 0.$$

By $\lambda > 0$, $2 < p < 4$, the equation $1 - \lambda bt^2 + ct^{p-2} = 0$ has a unique $t(u) > 0$ and the corresponding point $t(u)u \in N_\lambda$ and $I_\lambda(t(u)u) = \max_{t\ge 0} I_\lambda(tu)$.

2) Let $u \in N_\lambda$, by (3.4) and $2 < p < 4$, we have

$$\begin{aligned} I_\lambda(u) &= \left(\frac{1}{2} - \frac{1}{p}\right)\|u\|_{H_V^1}^2 + \lambda\left(\frac{1}{p} - \frac{1}{4}\right)\int_{\mathbb{R}^3} \rho(x)\Phi[u]u^2 \mathrm{d}x \\ &\ge \left(\frac{1}{2} - \frac{1}{p}\right)\|u\|_{H_V^1}^2 > C > 0. \end{aligned}$$

By the definition of Nehari manifold N_λ of the functional I_λ, we obtain that

u is a critical point of I_λ if and only if u is a critical point of I_λ constrained on N_λ. (3.5)

Now, we set

$$m_\lambda = \inf\{I_\lambda(u) : u \in N_\lambda\}$$

By 2) of Lemma 3.1, we have $m_\lambda > 0$.

Since $\lim_{|x|\to\infty} V(x) = V_\infty$, $\lim_{|x|\to+\infty} \rho(x) = \rho_\infty$, $\lim_{|x|\to+\infty} Q(x) = Q_\infty$, we consider the problem (1.1) at infinity

$$\begin{cases} -\Delta u + V_\infty u - \lambda\rho_\infty \Phi u + Q_\infty |u|^{p-2} u = 0, & x \in \mathbb{R}^3, \\ -\Delta\Phi = \rho_\infty u^2, & x \in \mathbb{R}^3. \end{cases} \tag{3.6}$$

Similar to (2.2), we obtain that there exists a unique $\tilde{\Phi}[u]$ such that

$$\int_{\mathbb{R}^3} \nabla\tilde{\Phi}[u]\nabla v \mathrm{d}x = \int_{\mathbb{R}^3} \rho_\infty u^2 v \mathrm{d}x, \quad \forall v \in D^{1,2}(\mathbb{R}^3).$$

It follows that $\tilde{\Phi}[u]$ satisfies the Poisson equation

$$-\Delta\tilde{\Phi}[u] = \rho_\infty u^2 \tag{3.7}$$

Hence substituting $\tilde{\Phi}[u]$ into the first equation of (3.6) we have to study the equivalent problem

$$-\Delta u + V_\infty u - \lambda\rho_\infty \tilde{\Phi}[u]u + Q_\infty |u|^{p-2} u = 0 \tag{3.8}$$

The weak solution of the problem (3.8) is the critical point of the functional

$$\begin{aligned} I_\lambda^\infty(u) &= \frac{1}{2}\int_{\mathbb{R}^3} \left(|\nabla u|^2 + V_\infty u^2\right) \mathrm{d}x - \frac{\lambda}{4}\int_{\mathbb{R}^3} \rho_\infty \tilde{\Phi}[u]u^2 \mathrm{d}x + \frac{1}{p}\int_{\mathbb{R}^3} Q_\infty |u|^p \mathrm{d}x \\ &= \frac{1}{2}\|u\|_{H_{V_\infty}^1}^2 - \frac{\lambda}{4}\int_{\mathbb{R}^3} \rho_\infty \tilde{\Phi}[u]u^2 \mathrm{d}x + \frac{1}{p}\int_{\mathbb{R}^3} Q_\infty |u|^p \mathrm{d}x, \end{aligned}$$

where $H^1_{V_\infty}(\mathbb{R}^3) = H^1(\mathbb{R}^3)$ is endowed with the norm

$$\|u\|_{H^1_{V_\infty}} = \left(\int_{\mathbb{R}^3} \left(|\nabla u|^2 + V_\infty u^2 \right) dx \right)^{\frac{1}{2}}$$

Define the Nehari manifold of the functional I_λ^∞

$$N_\lambda^\infty = \left\{ u \in H^1_{V_\infty}(\mathbb{R}^3) \setminus \{0\} : H_\lambda^\infty(u) = 0 \right\},$$

where

$$H_\lambda^\infty(u) = I_\lambda'^\infty(u)[u] = \|u\|^2_{H^1_{V_\infty}} - \lambda \int_{\mathbb{R}^3} \rho_\infty \tilde{\Phi}[u] u^2 dx + \int_{\mathbb{R}^3} Q_\infty |u|^p dx$$

and

$$m_\lambda^\infty = \inf \left\{ I_\lambda^\infty(u) : u \in N_\lambda^\infty \right\} > 0$$

The Nehari manifold N_λ^∞ has properties similar to those of N_λ.

Lemma 3.2. The problem (3.8) has a positive radial ground state solution $\omega_\infty \in N_\lambda^\infty$ such that

$$I_\lambda^\infty(\omega_\infty) = m_\lambda^\infty$$

For the proof of Lemma 3.2, we make use of Schwarz symmetric method. We begin by recalling some basic properties.

Let $f \in L^s(\mathbb{R}^3)$ such that $f \ge 0$, then there is a unique nonnegative function $f^* \in L^s(\mathbb{R}^3)$, called the Schwarz symmetric of f, such that it depends only on $|x|$, whose level sets

$$\left\{ x \in \mathbb{R}^3 : f(x) > t \right\} = \left\{ x \in \mathbb{R}^3 : f^*(x) > t \right\}.$$

We consider the following Poisson equation

$$-\Delta \phi = f \quad \text{and} \quad -\Delta v = f^*$$

From Theorem 1 of [11], we have

$$\int_{\mathbb{R}^3} |\nabla v|^s dx \ge \int_{\mathbb{R}^3} |\nabla \phi|^s dx, \quad \forall 0 < s \le 2.$$

Hence, let $\phi = \tilde{\Phi}[u]$, $f = \rho_\infty u^2$ and $v = \tilde{\Phi}[u^*]$, $f^* = \rho_\infty (u^*)^2$, we have

$$\int_{\mathbb{R}^3} \rho_\infty \tilde{\Phi}[u] u^2 dx \le \int_{\mathbb{R}^3} \rho_\infty \tilde{\Phi}[u^*] (u^*)^2 dx. \tag{3.9}$$

The Proof of Lemma 3.2. Let $u_n \in N_\lambda^\infty$ be such that $I_\lambda^\infty(u_n) \to m_\lambda^\infty$. Let $t_n > 0$ such that $t_n |u_n| \in N_\lambda^\infty$ then we have

$$\int_{\mathbb{R}^3} \left(|\nabla u_n|^2 + V_\infty (u_n)^2 \right) dx - \lambda \int_{\mathbb{R}^3} \rho_\infty \tilde{\Phi}[u_n] (u_n)^2 dx + \int_{\mathbb{R}^3} Q_\infty |u_n|^p dx = 0,$$

and

$$(t_n)^2 \int_{\mathbb{R}^3} \left(|\nabla u_n|^2 + V_\infty (u_n)^2 \right) dx - \lambda (t_n)^4 \int_{\mathbb{R}^3} \rho_\infty \tilde{\Phi}[u_n] (u_n)^2 dx + (t_n)^p \int_{\mathbb{R}^3} Q_\infty |u_n|^p dx = 0.$$

Hence, we obtain that

$$\left((t_n)^2 - (t_n)^4 \right) \int_{\mathbb{R}^3} \left(|\nabla u_n|^2 + V_\infty (u_n)^2 \right) dx + \left((t_n)^p - (t_n)^4 \right) \int_{\mathbb{R}^3} Q_\infty |u_n|^p dx = 0. \tag{3.10}$$

Since $t_n > 0$ and $2 < p < 4$, (3.10) implies that $t_n = 1$. Therefore, we can assume that $u_n \geq 0$. On the other hand, let $(u_n)^*$ be the Schwartz symmetric function associated to u_n, then we have

$$\int_{\mathbb{R}^3} |u_n|^p \mathrm{d}x = \int_{\mathbb{R}^3} \left|(u_n)^*\right|^p \mathrm{d}x, \quad \text{and} \quad \int_{\mathbb{R}^3} |\nabla u_n|^2 \mathrm{d}x \geq \int_{\mathbb{R}^3} \left|\nabla (u_n)^*\right|^2 \mathrm{d}x \tag{3.11}$$

Let $(t_n)^* > 0$ be such that $(t_n)^*(u_n)^* \in N_\lambda^\infty$, and $u_n \in N_\lambda^\infty$, by (3.9) and (3.11), we have

$$\begin{aligned}
0 &= \left[(t_n)^*\right]^2 \int_{\mathbb{R}^3} \left(\left|\nabla (u_n)^*\right|^2 + V_\infty \left[(u_n)^*\right]^2\right) \mathrm{d}x - \lambda \left[(t_n)^*\right]^4 \int_{\mathbb{R}^3} \rho_\infty \tilde{\Phi}\left[(u_n)^*\right]\left[(u_n)^*\right]^2 \mathrm{d}x + \left[(t_n)^*\right]^p \int_{\mathbb{R}^3} Q_\infty \left|(u_n)^*\right|^p \mathrm{d}x \\
&\leq \left[(t_n)^*\right]^2 \int_{\mathbb{R}^3} \left(|\nabla u_n|^2 + V_\infty (u_n)^2\right) \mathrm{d}x - \lambda \left[(t_n)^*\right]^4 \int_{\mathbb{R}^3} \rho_\infty \tilde{\Phi}[u_n](u_n)^2 \mathrm{d}x + \left[(t_n)^*\right]^p \int_{\mathbb{R}^3} Q_\infty |u_n|^p \mathrm{d}x \\
&= \left\{\left[(t_n)^*\right]^2 - \left[(t_n)^*\right]^4\right\} \int_{\mathbb{R}^3} \left(|\nabla u_n|^2 + V_\infty (u_n)^2\right) \mathrm{d}x + \left\{\left[(t_n)^*\right]^p - \left[(t_n)^*\right]^4\right\} \int_{\mathbb{R}^3} Q_\infty |u_n|^p \mathrm{d}x.
\end{aligned}$$

This implies that $(t_n)^* \leq 1$. Therefore, we have $I_\lambda^\infty\left([u_n]^*\right) \leq I_\lambda^\infty(u_n)$, and we can suppose that u_n is radial in $H_{V_\infty}^1(\mathbb{R}^3)$. Since $H_{V_\infty,r}^1(\mathbb{R}^3)$ is compactly embedded into $L^p(\mathbb{R}^3)$ for $2 < p < 4$, we obtain that m_λ^∞ is achieved at some $\omega_\infty \in N_\lambda^\infty$ which is positive and radial. Therefore, Lemma 3.2 is proved.

4. The Proof of Main Theorem

In this section, we prove Theorem 2.2. Firstly, we consider a compactness result and obtain the behavior of the (PS) sequence of the functional I_λ.

Lemma 4.1. Let u_n be a (PS)$_d$ sequence of the functional I_λ constrained on N_λ, that is

$$u_n \in N_\lambda, \quad I_\lambda(u_n) \to d \quad \text{and} \quad I_\lambda'(u_n)\big|_{N_\lambda} \to 0, \quad \text{as } n \to \infty \tag{4.1}$$

Then there exists a solution u of the problem (2.4), a number $k \in \mathbb{N} \cup \{0\}$, k functions $u^1, u^2, \cdots, u^k$ of $H_V^1(\mathbb{R}^3)$ and k sequences of points y_n^j, $0 \leq j \leq k$ such that

1) $\left|y_n^j\right| \to +\infty$, $\left|y_n^j - y_n^i\right| \to +\infty$, if $i \neq j$, $n \to \infty$;

2) $u_n - \sum_{j=1}^{k} u^j\left(\cdot - y_n^j\right) \to \bar{u}$;

3) $I_\lambda(u_n) \to I_\lambda(\bar{u}) + \sum_{j=1}^{k} I_\lambda^\infty\left(u^j\right)$;

4) u^j are non-trivial weak solution of the problem (3.8).

Proof. The proof is similar to that of Lemma 4.1 in [9].

By Lemma 4.1, taking into account that $I_\lambda^\infty\left(u^j\right) \geq m_\lambda$ for all j and $d \in (0, m_\lambda)$, we obtain that $k = 0$ and $u_n \to \bar{u}$ in $H_V^1(\mathbb{R}^3)$ (strongly), *i.e.* u_n is relatively compact for all $d \in (0, m_\lambda)$. Hence we only need to prove that the energy of a solution of the problem (2.4) cannot overcome the energy of a ground state solution of the problem (3.8).

The proof of Theorem 2.2. By Lemma 4.1, we only prove that $m_\lambda < m_\lambda^\infty$. Indeed, let $\omega_\infty \in N_\lambda^\infty$ such that $I_\lambda^\infty(\omega_\infty) = m_\lambda^\infty$, and let $t > 0$ such that $t\omega_\infty \in N_\lambda$. Since $V(x) \leq V_\infty$, $\rho(x) \geq \rho_\infty$ and $Q(x) \leq Q_\infty$, we have

$$\begin{aligned}
m_\lambda \leq I_\lambda(t\omega_\infty) &= \frac{t^2}{2} \int_{\mathbb{R}^3} \left(\left|\nabla \omega_\infty^2\right| + V(x)\omega_\infty^2\right) \mathrm{d}x - \frac{\lambda t^4}{4} \int_{\mathbb{R}^3} \rho(x) \Phi[\omega_\infty] \omega_\infty^2 \mathrm{d}x + \frac{t^p}{p} \int_{\mathbb{R}^3} Q(x) |\omega_\infty|^p \mathrm{d}x \\
&\leq \frac{t^2}{2} \int_{\mathbb{R}^3} \left(|\nabla \omega_\infty|^2 + V_\infty \omega_\infty^2\right) \mathrm{d}x - \frac{\lambda t^4}{4} \int_{\mathbb{R}^3} \rho_\infty \tilde{\Phi}[\omega_\infty] \omega_\infty^2 \mathrm{d}x + \frac{t^p}{p} \int_{\mathbb{R}^3} Q_\infty |\omega_\infty|^p \mathrm{d}x.
\end{aligned} \tag{4.2}$$

Since $\omega_\infty \in N_\lambda^\infty$ and $t\omega_\infty \in N_\lambda$, we have

$$\begin{aligned} t^4 \int_{\mathbb{R}^3} \left(|\nabla \omega_\infty|^2 + V_\infty \omega_\infty^2 \right) \mathrm{d}x + t^4 \int_{\mathbb{R}^3} Q_\infty |\omega_\infty|^p \mathrm{d}x &= \lambda t^4 \int_{\mathbb{R}^3} \rho_\infty \tilde{\Phi}[\omega_\infty] \omega_\infty^2 \mathrm{d}x \\ &\le \lambda t^4 \int_{\mathbb{R}^3} \rho(x) \Phi[\omega_\infty] \omega_\infty^2 \mathrm{d}x \\ &= t^2 \int_{\mathbb{R}^3} \left(|\nabla \omega_\infty^2| + V(x) \omega_\infty^2 \right) \mathrm{d}x + t^p \int_{\mathbb{R}^3} Q(x) |\omega_\infty|^p \mathrm{d}x \\ &\le t^2 \int_{\mathbb{R}^3} \left(|\nabla \omega_\infty|^2 + V_\infty \omega_\infty^2 \right) \mathrm{d}x + t^p \int_{\mathbb{R}^3} Q_\infty |\omega_\infty u|^p \mathrm{d}x. \end{aligned}$$

Therefore, we have

$$\left(t^4 - t^2\right) \int_{\mathbb{R}^3} \left(|\nabla \omega_\infty|^2 + V_\infty \omega_\infty^2 \right) \mathrm{d}x + \left(t^4 - t^p\right) \int_{\mathbb{R}^3} Q_\infty |\omega_\infty u|^p \mathrm{d}x \le 0$$

By $2 < p < 4$, we have $t \le 1$. If $t = 1$, we have $\omega_\infty \in N_\lambda^\infty$ and $\omega_\infty \in N_\lambda$. Hence, by $\omega_\infty \in N_\lambda^\infty$, we have

$$\int_{\mathbb{R}^3} \left(|\nabla \omega_\infty|^2 + V_\infty \omega_\infty^2 \right) \mathrm{d}x + \int_{\mathbb{R}^3} Q_\infty |\omega_\infty|^p \mathrm{d}x = \lambda \int_{\mathbb{R}^3} \rho_\infty \tilde{\Phi}[\omega_\infty] \omega_\infty^2 \mathrm{d}x \tag{4.3}$$

and by $\omega_\infty \in N_\lambda$, we have

$$\int_{\mathbb{R}^3} \left(|\nabla \omega_\infty|^2 + V(x) \omega_\infty^2 \right) \mathrm{d}x + \int_{\mathbb{R}^3} Q(x) |\omega_\infty|^p \mathrm{d}x = \lambda \int_{\mathbb{R}^3} \rho(x) \Phi[\omega_\infty] \omega_\infty^2 \mathrm{d}x. \tag{4.4}$$

Combining (4.3) and (4.4), we have

$$\int_{\mathbb{R}^3} \left(V_\infty - V(x)\right) \omega_\infty^2 \mathrm{d}x + \int_{\mathbb{R}^3} \left(Q_\infty - Q(x)\right) |\omega_\infty|^p \mathrm{d}x - \lambda \int_{\mathbb{R}^3} \rho_\infty \tilde{\Phi}[\omega_\infty] \omega_\infty^2 \mathrm{d}x + \lambda \int_{\mathbb{R}^3} \rho(x) \Phi[\omega_\infty] \omega_\infty^2 \mathrm{d}x = 0$$

Since $V(x) \le V_\infty$, $\rho(x) \ge \rho_\infty$, $Q(x) \le Q_\infty$, and $Q(x) - Q_\infty < 0$ on a positive measure, we have

$$\int_{\mathbb{R}^3} \left(Q_\infty - Q(x)\right) |\omega_\infty|^p \mathrm{d}x$$

which is not identically zero, and is contradiction. Hence, we have $t < 1$. By (4.2), we have

$$\begin{aligned} m_\lambda &< \frac{1}{2} \int_{\mathbb{R}^3} \left(|\nabla \omega_\infty|^2 + V_\infty \omega_\infty^2 \right) \mathrm{d}x - \frac{\lambda}{4} \int_{\mathbb{R}^3} \rho_\infty \tilde{\Phi}[\omega_\infty] \omega_\infty^2 \mathrm{d}x + \frac{1}{p} \int_{\mathbb{R}^3} Q_\infty |\omega_\infty|^p \mathrm{d}x \\ &= I_\lambda^\infty(\omega_\infty) = m_\lambda^\infty. \end{aligned}$$

Then there exists a positive radial ground state solution for the problem (1.1).

Acknowledgements

This research is supported by Shanghai Natural Science Foundation Project (No. 15ZR1429500), Shanghai Leading Academic Discipline Project (No. XTKX2012) and National Project Cultivate Foundation of USST (No. 13XGM05).

References

[1] D'Aprile, T. and Mugnai, D. (2004) Solitary Waves for Nonlinear Klein-Gordon-Maxwell and Schrodinger-Maxwell Equations. *Proceedings of the Royal Society of Edinburgh*: *Section A*, **134**, 1-14.

[2] D'Aprile, T. and Mugnai, D. (2004) Non-Existence Results for The coupled Klein-Gordon-Maxwell Equations. *Advanced Nonlinear Studies*, **4**, 307-322.

[3] Ruiz, D. (2006) The Schrodinger-Poisson Equation under the Effect of a Nonlinear Local Term. *Journal of Functional Analysis*, **237**, 655-674. http://dx.doi.org/10.1016/j.jfa.2006.04.005

[4] Ambrosetti, A. and Ruiz, D. (2008) Multiple Bound States for the Schrodinger-Poisson Problem. *Communications in*

Contemporary Mathematics, **10**, 391-404. http://dx.doi.org/10.1142/S021919970800282X

[5] Ambrosetti, A. (2008) On Schrodinger-Poisson Problem Systems. *Milan Journal of Mathematics*, **76**, 257-274. http://dx.doi.org/10.1007/s00032-008-0094-z

[6] Sanchez, O. and Soler, J. (2004) Long-Time Dynamics of the Schrodinger-Poisson-Slater System. *Journal of Statistical Physics*, **114**, 179-204. http://dx.doi.org/10.1023/B:JOSS.0000003109.97208.53

[7] Mugnai, D. (2011) The Schrodinger-Poisson System with Positive Potential. *Communications in Partial Differential Equations*, **36**, 1099-1117. http://dx.doi.org/10.1080/03605302.2011.558551

[8] Rabinowitz, P.H. (1992) On a Class of Nonlinear Schrodinger Equations. *Zeitschrift für angewandte Mathematik und Physik*, **43**, 270-291. http://dx.doi.org/10.1007/BF00946631

[9] Cerami, G. and Vaira, G. (2010) Positive Solutions for Some Non-Autonomous Schrodinger-Poisson Systems. *Journal of Differential Equations*, **248**, 521-543. http://dx.doi.org/10.1016/j.jde.2009.06.017

[10] Willem, M. (1996) Minimax Theorems, PNDEA Vol. 24. Birkhauser, Basel. http://dx.doi.org/10.1007/978-1-4612-4146-1

[11] Talenti, G. (1976) Elliptic Equations and Rearrangements. *Annali della Scuola Normale Superiore di Pisa*, **3**, 697-718.

Applied Mathematics, 2015, 6, 37-45
Published Online January 2015 in SciRes. http://www.scirp.org/journal/am
http://dx.doi.org/10.4236/am.2015.61005

Generalized Krein Parameters of a Strongly Regular Graph

Luís Almeida Vieira[1], Vasco Moço Mano[2]

[1]CMUP—Center of Research of Mathematics of University of Porto, Department of Civil Engineering, University of Porto, Porto, Portugal
[2]CIDMA—Center for Research and Development in Mathematics and Applications, Department of Mathematics, University of Aveiro, Aveiro, Portugal
Email: lvieira@fe.up.pt, vascomocomano@gmail.com

Received 11 November 2014; revised 8 December 2014; accepted 22 December 2014

Abstract

We consider the real three-dimensional Euclidean Jordan algebra associated to a strongly regular graph. Then, the Krein parameters of a strongly regular graph are generalized and some generalized Krein admissibility conditions are deduced. Furthermore, we establish some relations between the classical Krein parameters and the generalized Krein parameters.

Keywords

Algebraic Combinatorics, Association Schemes, Strongly Regular Graphs, Graphs and Linear Algebra

1. Introduction

In this paper we explore the close and interesting relationship of a three-dimensional Euclidean Jordan algebra $\mathcal{V}$ to the adjacency matrix of a strongly regular graph X. According to [1], the Jordan algebras were formally introduced in 1934 by Pascual Jordan, John von Neumann and Eugene Wigner in [2]. There, the authors attempted to deduce some of the Hermitian matrix properties and they came across a structure lately called a Jordan algebra. Euclidean Jordan algebras were born by adding an inner product with a certain property to a Jordan algebra. It is remarkable that Euclidean Jordan algebras turned out to have such a wide range of applications. For instance, we may cite the application of this theory to statistics [3], interior point methods [4] [5] and combinatorics [6]. More detailed literature on Euclidean Jordan algebras can be found in Koecher's lecture notes [7] and in the monograph by Faraut and Korányi [8].

Along this paper, we consider only simple graphs, *i.e.*, graphs without loops and parallel edges, herein called

How to cite this paper: Vieira, L.A. and Mano, V.M. (2015) Generalized Krein Parameters of a Strongly Regular Graph. *Applied Mathematics*, **6**, 37-45. http://dx.doi.org/10.4236/am.2015.61005

graphs. Considering a graph X, we denote its vertex set by $V(X)$ and its edge set by $E(X)$—an edge whose endpoints are the vertices x and y is denoted by xy. In such case, the vertices x and y are adjacent or neighbors. The number of vertices of X, $|V(X)|$, is called the order of X.

A graph in which all pairs of vertices are adjacent (non-adjacent) is called a complete (null) graph. The number of neighbors of a vertex v in $V(X)$ is called the degree of v. If all vertices of a graph X have degree k, for some natural number k, then X is k-regular.

We associate to X an n by n matrix $A=[a_{ij}]$, where each $a_{ij}=1$, if $v_iv_j \in E(X)$, otherwise $a_{ij}=0$, called the adjacency matrix of X. The eigenvalues of A are simply called the eigenvalues of X.

A non-null and not complete graph X is (n,k,a,c)-strongly regular; if it is k-regular, each pair of adjacent vertices has a common neighbors and each pair of non-adjacent vertices has c common neighbors. The parameters of a (n,k,a,c)-strongly regular graph are not independent and are related by the equality

$$k(k-a-1)=(n-k-1)c. \tag{1}$$

It is also well known (see, for instance, [9]) that the eigenvalues of a (n,k,a,c)-strongly regular graph X are k, θ and τ, where θ and τ are given by

$$\theta=\left(a-c+\sqrt{(a-c)^2+4(k-c)}\right)\Big/2, \tag{2}$$

$$\tau=\left(a-c-\sqrt{(a-c)^2+4(k-c)}\right)\Big/2. \tag{3}$$

Therefore, the usually called restricted eigenvalues θ and τ are such that the former is positive and the latter is negative. Their multiplicities can be obtained as follows (see, for instance, [10]):

$$\mu_1=\frac{1}{2}\left(n-1-\frac{(\theta+\tau)(n-1)+2k}{\theta-\tau}\right), \tag{4}$$

$$\mu_2=\frac{1}{2}\left(n-1+\frac{(\theta+\tau)(n-1)+2k}{\theta-\tau}\right). \tag{5}$$

Taking into account the above eigenvalues and their multiplicities, the following additional conditions are widely used as feasible conditions for parameters sets (n,k,a,c) of strongly regular graphs; that is, if (n,k,a,c) is a parameter set of a strongly regular graph, then the equality (1) and each one of the following inequalities holds:

- The nontrivial Krein conditions obtained in [11]:

$$(\theta+1)(k+\theta+2\theta\tau)\le(k+\theta)(\tau+1)^2, \tag{6}$$

$$(\tau+1)(k+\tau+2\theta\tau)\le(k+\tau)(\theta+1)^2. \tag{7}$$

- The Seidel's absolute bounds qre (see [12]):

$$n\le\frac{\mu_1(\mu_1+3)}{2} \quad \text{and} \quad n\le\frac{\mu_2(\mu_2+3)}{2}. \tag{8}$$

With these conditions, many of the parameter sets are discarded as possible parameters sets of strongly regular graphs. To decide whether a set of parameters is the parameter set of a strongly regular graph is one of the main problems on the study of strongly regular graphs. It is worth noticing that these Krein conditions and the Seidel's absolute bounds are special cases of general inequalities obtained for association schemes.

An association scheme with d classes is a finite set S together with $d+1$ relations R_i defined on S satisfying the following conditions.

1) The set of relations $\{R_0,R_1,\cdots,R_d\}$ is a partition of the Cartesian product of $S\times S$.

2) $R_0=\{(x,x):x\in S\}$.

3) If $(x,y)\in R_i$, then also $(y,x)\in R_i$, $\forall x,\ y\in S$ and for $i=0,\cdots,d$.

4) For each $(x,y) \in R_k$, the number p_{ij}^k of elements $z \in S$ such that $(x,z) \in R_i$ and $(z,y) \in R_j$ depends only from i, j and k.

The numbers p_{ij}^k are called the intersection numbers of the association scheme. Some authors call this type of association schemes symmetric association schemes. The relations R_i of the association scheme can be represented by their adjacency matrices A_i of order $n = |S|$ defined by $(A_i)_{xy} = \begin{cases} 1, & \text{if } (x,y) \in R_i, \\ 0, & \text{otherwise.} \end{cases}$ We may say that A_i is the adjacency matrix of the graph G_i, with $V(G_i) = S$ and $E(G_i) = R_i$. The Bose-Mesner algebra of the association scheme (introduced in [13]) is defined, using these matrices, by the following conditions, which are equivalent to the conditions 1) - 4) of the association scheme:

1) $\sum_{i=0}^{d} A_i = J_n$,
2) $A_0 = I_n$,
3) $A_i = A_i^{\mathrm{T}}, \quad \forall i \in \{0, \cdots, d\}$,
4) $A_i A_j = \sum_{k=0}^{d} p_{ij}^k A_k, \quad \forall i, j \in \{0, \cdots, d\}$,

where J_n is the matrix of order n whose entries are equal to one and I_n is the identity matrix of order n. From 1) we may conclude that the matrices A_i are linearly independent, and from 2) - 4) it follows that they generate a commutative $(d+1)$-dimensional algebra $\mathcal{A}$ of symmetric matrices with constant diagonal. The matrices A_i commute and then, they can be diagonalized simultaneously, *i.e.*, there exists a matrix B such that $\forall A \in \mathcal{A}$, $B^{-1}AB$ is a diagonal matrix. Thus, the algebra $\mathcal{A}$ is semisimple and has a unique complete system of orthogonal idempotents $E_0, \cdots, E_d$. Therefore, $\sum_{i=0}^{d} E_i = I_n$ and $E_i E_j = \delta_{ij} E_i$, where $\delta_{ij} = \begin{cases} 1, & \text{if } i = j, \\ 0, & \text{otherwise.} \end{cases}$

This paper is organized as follows. In Section 2, a short introduction on Euclidean Jordan algebras with the fundamental concepts is presented. In order to obtain new feasible conditions for the existence of a strongly regular graph, in Section 3, we define the generalized Krein parameters of a strongly regular graph. In Section 4, we establish some relations between the Krein parameters and the generalized Krein parameters, and present some properties of the generalized Krein parameters. Finally, since the generalized Krein parameters are nonnegative we establish new admissibility conditions, for the parameters of a strongly regular graph that give different information from that given by the Krein conditions 6) - 7).

2. Euclidean Jordan Algebras and Strongly Regular Graphs

In this section the main concepts of Euclidean Jordan Algebras that can be seen for instance in [8], are shortly surveyed.

Let $\mathcal{V}$ be a real vector space with finite dimension and a bilinear mapping $(u,v) \mapsto u \circ v$ from $\mathcal{V} \times \mathcal{V}$ to $\mathcal{V}$, that satisfies $(u \circ u) \circ u = u \circ (u \circ u)$, $\forall u \in \mathcal{V}$. Then, $\mathcal{V}$ is called a real power associative algebra. If $\mathcal{V}$ contains an element, *e*, such that for all *u* in $\mathcal{V}$, $e \circ u = u \circ e = u$, then *e* is called the *unit* element of $\mathcal{V}$. Considering a bilinear mapping $(u,v) \mapsto u \circ v$, if for all u and v in $\mathcal{V}$ we have $(J_1)] u \circ v = v \circ u$ and (J_2) $u \circ (u^2 \circ v) = u^2 \circ (u \circ v)$, with $u^2 = u \circ u$, then $\mathcal{V}$ is called a Jordan algebra. If $\mathcal{V}$ is a Jordan algebra with unit element, then $\mathcal{V}$ is power associative (cf. [8]). Given a Jordan algebra $\mathcal{V}$ with unit element e, if there is an inner product $\langle \cdot, \cdot \rangle$ that verifies the equality $\langle u \circ v, w \rangle = \langle v, u \circ w \rangle$, for any *u*, *v*, *w* in $\mathcal{V}$, then $\mathcal{V}$ is called an Euclidean Jordan algebra. An element c in an Euclidean Jordan algebra $\mathcal{V}$, with unit element e, is an idempotent if $c^2 = c$. Two idempotents c and d are orthogonal if $c \circ d = 0$. We call the set $\{c_1, c_2, \cdots, c_k\}$ a complete system of orthogonal idempotents if (i) $c_i^2 = c_i$, $\forall i \in \{1, \cdots, k\}$; (ii) $c_i \circ c_j = 0$, $\forall i \neq j$ and (iii) $c_1 + c_2 + \cdots + c_k = e$.

Let $\mathcal{V}$ be an Euclidean Jordan algebra with unit element *e*. Then, for every *u* in $\mathcal{V}$, there are unique distinct real numbers $\lambda_1, \lambda_2, \cdots, \lambda_k$, and an unique complete system of orthogonal idempotents $\{c_1, c_2, \cdots, c_k\}$ such that

$$u = \lambda_1 c_1 + \lambda_2 c_2 + \cdots + \lambda_k c_k, \tag{9}$$

with $c_j \in \mathbb{R}[u]$, $j = 1, \cdots, k$ (see [8], Theorem III 1.1). These λ_j's are the eigenvalues of *u* and (9) is called the first spectral decomposition of *u*.

The rank of an element *u* in $\mathcal{V}$ is the least natural number *k*, such that the set $\{e, u, \cdots, u^k\}$ is linear dependent (where $u^k = u \circ u^{k-1}$), and we write $\operatorname{rank}(u) = k$. This concept is expanded by defining the rank of the algebra $\mathcal{V}$ as the natural number $\operatorname{rank}(\mathcal{V}) = \max\{\operatorname{rank}(u) : u \in \mathcal{V}\}$. The elements of $\mathcal{V}$ with rank equal to the rank of $\mathcal{V}$ are the regular elements of $\mathcal{V}$. This set of regular elements is open and dense in $\mathcal{V}$. If *u* is a regular element of $\mathcal{V}$, with $r = \operatorname{rank}(u)$, then the set $\{e, u, u^2, \cdots, u^r\}$ is linearly dependent and the set $\{e, u, u^2, \cdots, u^{r-1}\}$ is linearly independent. Thus we may conclude that there exist unique real numbers $a_1(u), \cdots, a_r(u)$, such that $u^r - a_1(u)u^{r-1} + \cdots + (-1)^r a_r(u)e = 0$, where 0 is the null vector of $\mathcal{V}$. Therefore, with the necessary adjustments, we obtain the following polynomial in λ: $p(u, \lambda) = \lambda^r - a_1(u)\lambda^{r-1} + \cdots + (-1)^r a_r(u)$. This polynomial is called the characteristic polynomial of *u*, where each coefficient a_i is a homogeneous polynomial of degree i in the coordinates of u in a fixed basis of $\mathcal{V}$. Although we defined the characteristic polynomial for a regular element of $\mathcal{V}$, we can extend this definition to all the elements in $\mathcal{V}$, because each polynomial a_i is homogeneous and, as above referred, the set of regular elements of $\mathcal{V}$ is dense in $\mathcal{V}$. The roots of the characteristic polynomial of u, $\lambda_1, \lambda_2, \cdots, \lambda_r$ are called the eigenvalues of u. Furthermore, the coefficients $a_1(u)$ and $a_r(u)$ in the characteristic polynomial of *u*, are called the trace and the determinant of u, respectively.

From now on, we consider the Euclidean Jordan algebra of real symmetric matrices of order n, $\mathcal{V}$, such that $\forall A, B \in \mathcal{V}$, $A \circ B = (AB + BA)/2$, where AB is the usual product of matrices. Furthermore, the inner product of $\mathcal{V}$ is defined as $\langle A, B \rangle = \operatorname{tr}(AB)$, where tr is the classical trace of matrices, that is the sum of its eigenvalues.

Let X be a (n, k, a, c)-strongly regular graph such that $0 < c < k < n-1$, and let A be the adjacency matrix of X. Then A has three distinct eigenvalues, namely the degree of regularity k, and the restricted eigenvalues θ and τ, given in (2) and (3). Now we consider the Euclidean Jordan subalgebra of $\mathcal{V}$, $\mathcal{V}'$, spanned by the identity matrix of order n, I_n, and the powers of A. Since A has three distinct eigenvalues, then $\mathcal{V}'$ is a three dimensional Euclidean Jordan algebra with $\operatorname{rank}(\mathcal{V}') = 3$ and $B = \{I_n, A, A^2\}$ is a basis of $\mathcal{V}'$.

Let $S = \{E_0, E_1, E_2\}$ be the unique complete system of orthogonal idempotents of $\mathcal{V}'$ associated to A. Then

$$\begin{aligned} E_0 &= \frac{A^2 - (\theta+\tau)A + \theta\tau I_n}{(k-\theta)(k-\tau)} = \frac{J_n}{n}, \\ E_1 &= \frac{A^2 - (k+\tau)A + k\tau I_n}{(\theta-\tau)(\theta-k)}, \\ E_2 &= \frac{A^2 - (k+\theta)A + k\theta I_n}{(\tau-\theta)(\tau-k)}, \end{aligned} \tag{10}$$

where J_n is the matrix whose entries are all equal to 1. Since $\mathcal{V}'$ is an Euclidean Jordan algebra that is closed for the Hadamard product of matrices, denoted by $\bullet$ and S is a basis of $\mathcal{V}'$, then there exist real numbers $q^p_{\alpha 2}$ and $q^p_{\alpha\beta 11}$, $1 \le \alpha$, $\beta \le 3$, $\alpha \ne \beta$, such that

$$E_\alpha \bullet E_\alpha = \sum_{p=0}^{2} q^p_{\alpha 2} E_p, \quad E_\alpha \bullet E_\beta = \sum_{p=0}^{2} q^p_{\alpha\beta 11} E_p. \tag{11}$$

The real numbers, defined in (11), (whose notation will be clarified later) $q^p_{\alpha 2}$ and $q^p_{\alpha\beta 11}$, $1 \le \alpha$, $\beta \le 3$, $\alpha \ne \beta$, are called the "classical" Krein parameters of the graph X (cf. [10]). Since $q^1_{12} \ge 0$ and $q^2_{22} \ge 0$, the "classical" Krein admissibility conditions $\theta\tau^2 - 2\theta^2\tau - \theta^2 - k\theta + k\tau^2 + 2k\tau \ge 0$, and $\theta^2\tau - 2\theta\tau^2 - \tau^2 - k\tau + k\theta^2 + 2k\theta \ge 0$ (presented in [9], Theorem 21.3) can be deduced.

3. A Generalization of the Krein Parameters

Herein the generalized Krein parameters of a (n, k, a, c)-strongly regular graph are defined and then, necessary conditions for the existence of a (n, k, a, c)-strongly regular graph are deduced. These conditions are generalizations of the Krein conditions (see Theorem 21.3 in [9]). Throughout this paper we use a slight different notation from classical books like [9] [14], because, in this way, the connections between the "classical'' and the generalized parameters are better understood. Now we generalize the Krein parameters in order to obtain new generalized admissibility conditions on the parameters of strongly regular graphs. Firstly, considering $S = \{E_0, E_1, E_2\}$ defined like in (10) in the Basis B, and rewriting the idempotents under the new basis $\{I_n, A, J_n - A - I_n\}$ of

$\mathcal{V}'$ we obtain

$$E_0 = \frac{\theta-\tau}{n(\theta-\tau)} I_n + \frac{\theta-\tau}{n(\theta-\tau)} A + \frac{\theta-\tau}{n(\theta-\tau)} (J_n - A - I_n),$$
$$E_1 = \frac{|\tau| n+\tau-k}{n(\theta-\tau)} I_n + \frac{n+\tau-k}{n(\theta-\tau)} A + \frac{\tau-k}{n(\theta-\tau)} (J_n - A - I_n), \quad (12)$$
$$E_2 = \frac{\theta n+k-\theta}{n(\theta-\tau)} I_n + \frac{-n+k-\theta}{n(\theta-\tau)} A + \frac{k-\theta}{n(\theta-\tau)} (J_n - A - I_n).$$

Consider the natural number p and denote by $M_n(\mathbb{R})$ the set of square matrices of order n with real entries. Then for $B \in M_n(\mathbb{R})$, we denote by $B^{\bullet p}$ and $B^{\otimes p}$ the Hadamard power of order p of B and the Kronecker power of order p of B, respectively, with $B^{\bullet 1} = B$ and $B^{\otimes 1} = B$.

Now, we introduce the following compact notation for the Hadamard and the Kronecker powers of the elements of S. Let x, y, z, α, β and γ be natural numbers such that $1 \le \alpha, \beta, \gamma \le 3$, $x \ge 2$ and $\alpha < \beta$. Then we define

$$E_\alpha^{\bullet x} = (E_\alpha)^{\bullet x} \quad \text{and} \quad E_\alpha^{\otimes x} = (E_\alpha)^{\otimes x},$$
$$E_{\alpha\beta}^{\bullet yz} = (E_\alpha)^{\bullet y} \bullet (E_\beta)^{\bullet z} \quad \text{and} \quad E_{\alpha\beta}^{\otimes yz} = (E_\alpha)^{\otimes y} \otimes (E_\beta)^{\otimes z},$$

Again, since the Euclidean Jordan algebra $\mathcal{V}'$ is closed under the Hadamard product and S is a basis of $\mathcal{V}'$, then there exist real numbers $q_{\alpha x}^i$, $q_{\alpha\beta yz}^i$, $q_{(\alpha\oplus\beta)x}^i$ and $q_{\gamma(\alpha\oplus\beta)yz}^i$, such that

$$E_\alpha^{\bullet x} = \sum_{i=0}^{2} q_{\alpha x}^i E_i, \quad E_{\alpha\beta}^{\bullet yz} = \sum_{i=0}^{2} q_{\alpha\beta yz}^i E_i \quad (13)$$

We call the parameters $q_{\alpha x}^i$ and $q_{\alpha\beta yz}^i$ defined in (13) the generalized Krein parameters of the strongly regular graph X. Notice that $q_{\alpha 2}^i$ and $q_{\alpha\beta 11}^i$ are precisely the Krein parameters of X already presented. With this notation, the Greek letters are used as idempotent indices and the Latin letters are used as exponents of Hadamard (Kronecker) powers.

4. Relations between the Krein Parameters and the Generalized Krein Parameters

In this section we prove that the generalized Krein parameters can be expressed in function of the Krein parameters. Before that, it is worth to mention that the previously introduced generalizations are straightforward extended to the Krein parameters of symmetric association schemes with d $(d \ge 3)$ classes, see [9]. Notice that the algebra spanned by the matrices of a symmetric association scheme with d classes is an Euclidean Jordan Algebra with rank $d+1$ and with the Jordan product $A \circ B = \frac{AB+BA}{2}$ where AB is the usual product of matrices. Furthermore, the inner product of $\mathcal{V}$ is defined as $\langle A, B\rangle = \mathrm{tr}(AB)$ where $\mathrm{tr}(.)$ is the classical trace of matrices, that is, the sum of its eigenvalues. Let us consider the matrices P and Q of the Bose-Mesner algebra of an association scheme with d classes as defined in [14]. However, for convenience, we denote this matrix Q such as defined in [14] by Q^*. Therefore, we can say that $Q = \frac{1}{n} Q^*$, see [14]. Hence, we can say that the matrices P and Q satisfy,

$$Q_{ij} Q_{ik} = \sum_{l=0}^{2} q_{jk}^l Q_{il} \quad (14)$$

$$|Q_{ij}| \le \frac{\mu_j}{n} \quad (15)$$

$$|P_{ij}| \le n_j \quad (16)$$

$$\sum_{i=0}^{2} n_i Q_{ij} Q_{ik} \leq \frac{u_j}{n} \delta(j,k) \tag{17}$$

The matrices P and Q are usually called the eigenmatrix and the dual eigenmatrix of the association scheme, respectively.

Theorem 1. *Let* G *be a* (n,k,a,c)*-strongly regular graph such that* $0 < c \leq k < n-1$ *whose adjacency matrix is* A *and has the eigenvalues* k, θ *and* τ *and whose eigenmatrix and dual eigenmatrix matrix are respectively* P *and* Q *If* j, k *and* l *are natural numbers such that* $0 < j,\ k,\ l \leq 2$, *then*

$$q^{l}_{jk11} = \sum_{i=0}^{2} Q_{ij} Q_{ik} P_{li}. \tag{18}$$

Proof. Consider that $\{E_0, E_1, E_2\}$ is the of idempotents defined in (12) and the following notation $A_0 = I_n$, $A_1 = A$ and $A_2 = J_n - A - I_n$.

For $j,\ k,\ l \in \{0,1,2\}$ since $E_j = \sum_{i=0}^{2} Q_{ij} A_i$ and $E_k = \sum_{i=0}^{2} Q_{ik} A_i$, it follows that $E_j \bullet E_k = \sum_{i=0}^{2} Q_{ij} Q_{ik} A_i$. Therefore $E_j \bullet E_k E_l = \sum_{i=0}^{2} Q_{ij} Q_{ik} A_i E_l$ and since $A_j = \sum_{t=0}^{2} P_{tj} E_t$ implies $A_i E_l = P_{li} E_l$ we obtain

$$E_j \bullet E_k E_l = \sum_{i=0}^{2} Q_{ij} Q_{ik} P_{li} E_l. \tag{19}$$

Finally, from (19) the result follows.

Theorem 2. *Let* G *be a* (n,k,a,c)*-strongly regular graph such that* $0 < c \leq k < n-1$ *whose adjacency matrix is* A *and has the eigenvalues* k, θ *and* τ *and whose eigenmatrix and dual eigenmatrix matrix are respectively* P *and* Q. *Let* j, m *and* s *be natural numbers such that* $0 \leq j,\ s \leq 2$. *Then*

$$q^{s}_{jm} = \sum_{i=0}^{2} \left(Q_{ij}\right)^m P_{si}. \tag{20}$$

Proof. Taking into account that $Q_j^{\bullet m} = \sum_{i=0}^{2} q^{i}_{jm} E_i$ and by the equalities (21) and (22)

$$E_j = \sum_{i=0}^{2} Q_{ij} A_i, \tag{21}$$

$$A_i = \sum_{j=0}^{2} P_{ji} E_j, \tag{22}$$

we conclude that $E_j^{\bullet m} = \sum_{i=0}^{2} \left(Q_{ij}\right)^m A_i$ Therefore $q^{s}_{jm} E_s = E_j^{\bullet m} E_s = \sum_{i=0}^{2} \left(Q_{ij}\right)^m A_i E_s$ and since by (22) $A_i E_s = P_{si} E_s$ we obtain $q^{s}_{jm} E_s = \sum_{i=0}^{2} \left(Q_{ij}\right)^m P_{si} E_s$. Hence $q^{s}_{jm} = \sum_{i=0}^{2} \left(Q_{ij}\right)^m P_{si}$.

As an application of the Theorem 2 we may conclude that considering a strongly regular graph G the generalized Krein parameters q^{l}_{jm} can be expressed in function of the classical Krein parameters as follows:

$$q^{s}_{jm} = \sum_{l_1=0}^{2} \sum_{l_2=0}^{2} \cdots \sum_{l_{m-2}=0}^{2} q^{l_1}_{j2} q^{l_2}_{l_1 j11} \cdots q^{l_{m-2}}_{(m-3) j11} q^{s}_{l_{m-2} j11}. \tag{23}$$

The expression (23) is obtained using (14) and (20). Summarizing, we have the following corollary.

Corollary 1. *Let* G *be a* (n,k,a,c)*-strongly regular graph such that* $0 < c \leq k < n-1$. *Then for all natural numbers* j, m *and* s *such that* $0 \leq j,\ s \leq 2$

$$q^{s}_{j(2+m)} = \sum_{l_1=0}^{2} \sum_{l_2=0}^{2} \cdots \sum_{l_m=0}^{2} q^{l_1}_{j2} q^{l_2}_{l_1 j11} \cdots q^{l_m}_{l_{m-1} j11} q^{s}_{l_m j11}. \tag{24}$$

Theorem 3. *Let* G *be a* (n,k,a,c)*-strongly regular graph such that* $0 < c \leq k < n-1$. *Then for all natural numbers* i, j, m, n *and* s *such that* $0 \leq i,\ j,\ s \leq 2$,

$$q^{s}_{ijmn} = \sum_{l=0}^{2} \left(Q_{li}\right)^m \left(Q_{lj}\right)^n P_{sl}. \tag{25}$$

Proof. We have $E_i^{\bullet m} \bullet E_j^{\bullet n} = \sum_{l=0}^{2} q_{ijmn}^l E_l$. Since from (21) $E_i^{\bullet n} \bullet E_j^{m} = \sum_{l=0}^{2} (Q_{li})^n A_l \bullet \sum_{l=0}^{2} (Q_{li})^m A_l$ then $E_i^{\bullet n} \bullet E_j^{\bullet m} = \sum_{l=0}^{2} q_{ijmn}^l E_l$. Hence we obtain

$$E_i^{\bullet n} \bullet E_j^m E_s = \sum_{l=0}^{2} (Q_{li})^n (Q_{lj})^m P_{sl} E_s.$$

Therefore, the equality (25) follows. □

Recurring to (14) and (25), we may conclude the Corollary 2.

Corollary 2. *Let* G *be a* (n,k,a,c)*-strongly regular graph such that* $0 < c \le k < n-1$. *Then for all natural numbers* $i_1,\ i_2,\ m,\ n$ *and* s *such that* $0 \le i_1,\ i_2,\ s \le 2$,

$$q_{i_1 i_2 nm}^s = \sum_{l_1=0}^{2} \cdots \sum_{l_n=0}^{2} \sum_{l_{n+1}=0}^{2} \cdots \sum_{l_{n+m-2}=0}^{2} q_{i_1 2}^{l_1} q_{l_1 i_1 11}^{l_2} \cdots q_{l_{n-2} i_1 11}^{l_{n-1}} q_{l_{n-1} i_2 11}^{l_n} q_{l_n i_2 11}^{l_{n+1}} \cdots q_{l_{n+m-3} i_2 11}^{l_{n+m-2}} q_{l_{n+m-2} i_2 11}^{s}.$$

Theorem 4. *Let* G *be a* (n,k,a,c)*-strongly regular graph such that* $0 < c \le k < n-1$. *Then* $\forall n \in \mathbb{N}$ *and* $\forall i_1, \cdots, i_{n+1} \in \{0,1,2\}$,

$$\sum_{r=0}^{2} Q_{ri_1} \cdots Q_{ri_{n+1}} P_{sr} \ge 0. \tag{26}$$

Proof. We prove by induction on *n*. For $n = 1$ the inequality (26) holds, since the classical Krein parameters $q_{i_1 i_2 11}^s$ are nonnegative and $\sum_{r=0}^{2} Q_{ri_1} Q_{ri_2} P_{sr} = q_{i_1 i_2 11}^s$. Now assuming that the inequality (26) holds for $n = k \ge 1$, we prove that (26) also holds for $n = k+1$. Consider the sum $\sum_{r=0}^{2} Q_{ri_1} \cdots Q_{ri_{k+2}} P_{sr}$. Then from (14), we obtain

$$\begin{aligned}\sum_{r=0}^{2} Q_{ri_1} \cdots Q_{ri_{k+2}} P_{sr} &= \sum_{r=0}^{2} \sum_{l=0}^{2} q_{i_1 i_2 11}^l Q_{rl} Q_{ri_3} \cdots Q_{ri_{k+2}} P_{sr} \\ &= \sum_{l=0}^{2} q_{i_1 i_2 11}^l \sum_{r=0}^{2} Q_{rl} Q_{ri_3} \cdots Q_{ri_{k+2}} P_{sr}.\end{aligned}$$

Since for $n = k$ the inequality (26) is verified and the summands $\sum_{r=0}^{2} Q_{rl} Q_{ri_3} \cdots Q_{ri_{k+2}} P_{sr}$ are nonnegative, we may conclude that $\sum_{r=0}^{2} Q_{ri_1} \cdots Q_{ri_{n+1}} P_{sr} \ge 0$. □

Recurring to the Theorem 4 we are conducted to the Corollaries 3 and 4.

Corollary 3. *Let G be a* (n,k,a,c)*-strongly regular graph such that* $0 < c \le k < n-1$. *Then for all natural numbers* $i,\ m,\ s$ *and* s *such that* $0 \le i,\ s \le 2$ *the generalized Krein parameters* q_{im}^s *are nonnegative.*

Corollary 4. *Let* G *be a* (n,k,a,c)*-strongly regular graph such that* $0 < c \le k < n-1$. *Then for all natural numbers* $i,\ j,\ m,\ n$ *and s such that* $0 \le i,\ j,\ s \le 2$ *the generalized Krein parameters* q_{ijmn}^l *are nonnegative.*

Theorem 5. *Let G be a strongly regular graph and let i, s and m be natural numbers such that* $0 \le i,\ s \le 2$. *Then* $q_{im}^s \le 1$.

Proof. Recurring to the inequalities (14)-(17) we have:

$$\begin{aligned} q_{im}^s &= \sum_{t=0}^{2} (Q(t,i))^m P(s,t) = \left| \sum_{t=0}^{2} (Q(t,i))^{m-2} (Q(t,i))^2 P(s,t) \right| \\ &\le \sum_{t=0}^{2} \left| (Q(t,i))^{m-2} \right| \left| (Q(t,i))^2 \right| \left| P(s,t) \right| \le \sum_{t=0}^{2} \left(\frac{\mu_i}{n} \right)^{m-2} (Q(t,i))^2 n_t \\ &\le \sum_{t=0}^{2} 1^{m-2} (Q(t,i))^2 n_t \le \frac{\mu_i}{n} \le 1. \end{aligned}$$

Theorem 6. *Let G be a* (n,k,a,c)*-strongly regular graph such that* $0 < c \le k < n-1$. *Let* $i,\ j,\ m,\ n$ *and s be natural numbers such that* $0 \le i,\ j,\ s \le 2$ *and* $m + n \ge 3$. *Then the generalized Krein parameter* q_{ijmn}^s *satisfy* $q_{ijmn}^s \le 1$.

Proof. Similar to the Proof done in Theorem 5. □

Let G be a (n,k,a,c)-strongly regular graph such that $0 < c \le k < n-1$. Since the generalized Krein parameters $q_{i_1 i_2 mn}^s$ and $q_{i_1 m}^s$ are nonnegative then we can establish new admissibility conditions distinct from the Krein conditions (6) and (7). For instance, the generalized Krein condition $q_{13}^0 \ge 0$ allows us to establish a new theorem on strongly regular graphs after some algebraic manipulation of its expressions. Analyzing the generalized Krein parameter q_{13}^0 of a strongly regular graph with one in its spectra we deduce the following theorem (7).

Theorem 7. *Let* G *be a* (n,k,a,c)*-strongly regular graph such that* $0<c\le k<n-1$ *whose adjacency matrix is* A *and has the eigenvalues* k, $\theta=1$ *and* τ *If* $k\ge 9$ *then*

$$n\le \frac{3}{2}+\frac{53}{20}k. \tag{27}$$

Proof. Since $q_{13}^0\ge 0$ then we have

$$\left(\frac{\theta n+k-\theta}{n(\theta-\tau)}\right)^3+\left(\frac{-n+k-\theta}{n(\theta-\tau)}\right)^3 k+\left(\frac{k-\theta}{n(\theta-\tau)}\right)^3(n-k-1)\ge 0. \tag{28}$$

From the inequality (28) and after some simplifications we conclude that

$$n^2\left(\theta^3-k\right)+n\left(-3\theta^3+3k^2+3\theta^2k-3k\theta\right)+\left(2\theta^3-2k^3+6\theta k^2-6\theta^2k\right)\ge 0.$$

Therefore if $\theta=1$ then

$$n^2(1-k)+n\left(-3+3k^2+3k-3k\right)+\left(2-2k^3+6k^2-6k\right)\ge 0$$

Finally we have

$$n^2(1-k)+n\left(-3+3k^2\right)+2\left(1-k^3+3k^2-3k\right)\ge 0 \tag{29}$$

Dividing both members of (29) by $1-k$ we are supposing that $k>1$ we obtain

$$n^2-3n(1+k)+2\left(k^2-2k+1\right)\le 0. \tag{30}$$

Now from the inequality (30) we conclude that if G is a (n,p,a,c)-strongly regular graph with one in his spectra[1] then $k\ge 9$ implies that $n\le \frac{3}{2}+\frac{53}{20}k.$

We now present in **Table 1** some examples of parameter sets (n,k,a,c) that do not verify the inequality (27) of Theorem 7. We consider the parameter sets $P_1=(28,9,0,4)$, $P_2=(64,21,0,10)$, $P_3=(1225,456,39,247)$, $P_4=(1296,481.0,40.0,260)$ and $P_5=(1024,385,36,210)$. For each example we present the respective eigenvalues θ, τ and the value of q_{kn} defined by $q_{kn}=\frac{53}{20}k+\frac{3}{2}-n.$

5. Some Conclusions

In this paper, we have generalized the Krein parameters of a strongly regular graph and obtained some relations

Table 1. Numerical results when $k\ge 9$.

	P_1	P_2	P_3	P_4	P_5
θ	1	1	1	1	1
τ	−5	−11	−209	−221	−175
$q^1_{\theta\tau kn}$	−2.65	−6.85	−15.1	−19.85	−2.5

[1]We must note that the equation $x^2-3x(1+k)+2(1-2k+k^2)=0$ as the roots $x_1=\frac{3(k+1)-\sqrt{k^2+34k+1}}{2}$ and the root $x_2=\frac{3(k+1)+\sqrt{k^2+34k+1}}{2}$. Since $k>8$ implies that $k^2+34k+1\le 5k^2$ and finally this implies that $x_2\le\frac{3(k+1)+\sqrt{5}k}{2}$ therefore $x_2\le\frac{3}{2}+\frac{53k}{20}$.

between the classical Krein parameters and the generalized Krein parameters (see Corollaries 1 and 2). We also establish that these generalize Krein parameters are always positive and less than one (see Corollaries 3 and 4, and Theorems 5 and 6). Let i, j, m, n and s be natural numbers such that $0 \le i, j, s \le 2$. The generalized Krein admissibility conditions $q_{ijmn}^{s} \ge 0$ with $m+n \ge 3$ and $q_{im}^{s} \ge 0$ with $m \ge 3$ allow us to establish new admissibility conditions; they permit us to establish new inequalities on the parameters of a strongly regular graph. For instance the generalized Krein parameter condition $q_{23}^{0} \ge 0$ after some algebraic manipulation allows us to establish the inequality (27) in Theorem 7. Finally, we conclude that we can extend the definition of generalized Krein parameters to a symmetric association scheme with d classes.

Acknowledgements

1) Luís Almeida Vieira was supported by the European Regional Development Fund through the program COMPETE and by the Portuguese Government through the FCT—Fundação para a Ciência e a Tecnologia under the project PEst—C/MAT/UI0144/2013.

2) Vasco Moço Mano was partially supported by Portuguese Funds trough CIDMA—Center for Research and development in Mathematics and Applications, Department of Mathematics, University of Aveiro, 3810-193, Aveiro, Portugal and the Portuguese Foundation for Science and Technology (FCT-Fundação para a Ciência e Tecnologia), within Project PEst-OE/MAT/UI4106/2014.

3) The authors would like to thank the anonymous referee for his/her careful revision and relevant comments that improved our paper.

References

[1] McCrimmon, K. (1978) Jordan Algebras and Their Applications. *Bulletin of the American Mathematical Society*, **84**, 612-627. http://dx.doi.org/10.1090/S0002-9904-1978-14503-0

[2] Jordan, P., Neuman, J.V. and Wigner, E. (1934) On an Algebraic Generalization of the Quantum Mechanical Formalism. *Annals of Mathematics*, **35**, 29-64. http://dx.doi.org/10.2307/1968117

[3] Massan, H. and Neher, E. (1998) Estimation and Testing for Lattice Conditional Independence Models on Euclidean Jordan Algebras. *Annals of Statistics*, **26**, 1051-1082. http://dx.doi.org/10.1214/aos/1024691088

[4] Faybusovich, L. (1997) Euclidean Jordan Algebras and Interior-Point Algorithms. *Positivity*, **1**, 331-357. http://dx.doi.org/10.1023/A:1009701824047

[5] Faybusovich, L. (2007) Linear Systems in Jordan Algebras and Primal-Dual Interior-Point Algorithms. *Journal of Computational and Applied Mathematics*, **86**, 149-175. http://dx.doi.org/10.1016/S0377-0427(97)00153-2

[6] Cardoso, D.M. and Vieira, L.A. (2004) Euclidean Jordan Algebras with Strongly Regular Graphs. *Journal of Mathematical Sciences*, **120**, 881-894. http://dx.doi.org/10.1023/B:JOTH.0000013553.99598.cb

[7] Koecher, M. (1999) The Minnesota Notes on Jordan Algebras and Their Applications. Krieg, A. and Walcher, S., Eds., Springer, Berlin.

[8] Faraut, J. and Korányi, A. (1994) Analysis on Symmetric Cones. Oxford Science Publications, Oxford.

[9] Godsil, C. and Royle, G. (2001) Algebraic Graph Theory. Springer, Berlin. http://dx.doi.org/10.1007/978-1-4613-0163-9

[10] van Lint, J.H. and Wilson, R.M. (2004) A Course in Combinatorics. Cambridge University Press, Cambridge.

[11] Scott Jr., L.L. (1973) A Condition on Higman's Parameters. *Notices of the American Mathematical Society*, **20**, A-97.

[12] Delsarte, Ph., Goethals, J.M. and Seidel, J.J. (1975) Bounds for Systems of Lines and Jacobi Polynomials. *Philips Research Reports*, **30**, 91-105.

[13] Bose, R.C. and Mesner, D.M. (1952) On Linear Associative Algebras Corresponding to Association Schemes of Partially Balanced Designs. *The Annals of Mathematical Statistics*, **47**, 151-184.

[14] Brower, A.E. and Haemers, W.H. (1995) Association Schemes. In: Grahm, R., Grotsel, M. and Lovász. L., Eds., *Handbook of Combinatorics*, Elsevier, Amsterdam, 745-771.

Applied Mathematics, 2015, 6, 46-56
Published Online January 2015 in SciRes. http://www.scirp.org/journal/am
http://dx.doi.org/10.4236/am.2015.61006

Associative Space-Time Sedenions and Their Application in Relativistic Quantum Mechanics and Field Theory

Victor L. Mironov[1,2], Sergey V. Mironov[1]

[1]Institute for Physics of Microstructures RAS, Nizhny Novgorod, Russia
[2]Lobachevsky State University of Nizhny Novgorod, Nizhny Novgorod, Russia
Email: mironov@ipmras.ru

Received 24 October 2014; revised 20 November 2014; accepted 15 December 2014

Abstract

We present an alternative sixteen-component hypercomplex scalar-vector values named "space-time sedenions", generating associative noncommutative space-time Clifford algebra. The generalization of relativistic quantum mechanics and field theory equations based on sedenionic wave function and space-time operators is discussed.

Keywords

Clifford Algebra, Space-Time Sedenions, Relativistic Quantum Mechanics, Sedenionic Klein-Gordon Equation, Sedenionic Dirac Equation, Sedenionic Maxwell Equiations

1. Introduction

The multicomponent hypercomplex numbers such as quaternions and octonions are widely used for the reformulation of quantum mechanics and field theory equations. The first generalization of quantum mechanics and electrodynamics was made on the basis of four-component quaternions, which were interpreted as scalar-vector structures [1]-[5]. The next step was taken on the basis of eight-component octonions, which were interpreted as the sum of scalar, pseudoscalar, polar vector and axial vector [6]-[11]. Scalars and axial vectors are not transformed under spatial inversion, while pseudoscalars and polar vectors change their sign under spatial inversion. Therefore, this interpretation takes only the symmetry with respect to the spatial inversion into account. However, a consistent relativistic approach requires taking full time and space symmetries into consideration that leads to the sixteen-component space-time algebras.

The well-known sixteen-component hypercomplex numbers, sedenions, are obtained from octonions by the

How to cite this paper: Mironov, V.L. and Mironov, S.V. (2015) Associative Space-Time Sedenions and Their Application in Relativistic Quantum Mechanics and Field Theory. *Applied Mathematics*, **6**, 46-56.
http://dx.doi.org/10.4236/am.2015.61006

Cayley-Dickson extension procedure [12] [13]. In this case the sedenion is defined as

$$S = O_1 + O_2 \boldsymbol{e}, \tag{1}$$

where O_i is an octonion and the parameter of duplication $\boldsymbol{e}$ is similar to imaginary unit $\boldsymbol{e}^2 = -1$. The algebra of sedenions has the specific rules of multiplication. The product of two sedenions

$$S_1 = O_{11} + O_{12} \boldsymbol{e},$$

$$S_2 = O_{21} + O_{22} \boldsymbol{e},$$

is defined as

$$S_1 S_2 = \left(O_{11} + O_{12}\boldsymbol{e}\right)\left(O_{21} + O_{22}\boldsymbol{e}\right) = \left(O_{11}O_{21} - \bar{O}_{22}O_{12}\right) + \left(O_{22}O_{11} + O_{12}\bar{O}_{21}\right)\boldsymbol{e}, \tag{2}$$

where $\bar{O}_{ij}$ is conjugated octonion. The sedenionic multiplication (2) allows one to introduce a well-defined norm of sedenion. However, such procedure of constructing the higher hypercomplex numbers leads to the fact that the sedenions as well as octonions generate normed but nonassociative algebra [14]-[16]. It complicates the use of the Cayley-Dickson sedenions in the physical applications.

Recently we have developed an alternative approach to constructing the multicomponent values based on our scalar-vector conception realized in associative eight-component octons [17]-[19] and sixteen-component sedeons [20]-[24]. In particular, we have demonstrated the method, which allows one to reformulate the equations of relativistic quantum mechanics and field theory on the basis of sedeonic space-time operators and scalar-vector wave functions. In this paper we present an alternative version of the sixteen-component associative space-time hypercomplex algebra and demonstrate some of its application to the generalization of relativistic quantum mechanics and field theory equations.

2. Sedenionic Space-Time Algebra

It is known, the quaternion is a four-component object

$$\hat{q} = q_0 \mathbf{a_0} + q_1 \mathbf{a_1} + q_2 \mathbf{a_2} + q_3 \mathbf{a_3}, \tag{3}$$

where components q_ν (Greek indexes $\nu = 0,1,2,3$) are numbers (complex in general), $\mathbf{a_0} \equiv 1$ is scalar units and values $\mathbf{a_m}$ (Latin indexes m = 1, 2, 3) are quaternionic units, which are interpreted as unit vectors. The rules of multiplication and commutation for $\mathbf{a_m}$ are presented in **Table 1**. We introduce also the space-time basis $\mathbf{e_t}$, $\mathbf{e_r}$, $\mathbf{e_{tr}}$, which is responsible for the space-time inversions. The indexes **t** and **r** indicate the transformations (**t** for time inversion and **r** for spatial inversion), which change the corresponding values. The value $\mathbf{e_0} \equiv 1$ is a scalar unit. For convenience we introduce numerical designations $\mathbf{e_1} \equiv \mathbf{e_t}$ (time scalar unit); $\mathbf{e_2} \equiv \mathbf{e_r}$ (space scalar unit) and $\mathbf{e_3} \equiv \mathbf{e_{tr}}$ (space-time scalar unit). The rules of multiplication and commutation for this basis we choose similar to the rules for quaternionic units (see **Table 2**).

Table 1. Multiplication rules for unit vectors $\mathbf{a_m}$.

	$\mathbf{a_1}$	$\mathbf{a_2}$	$\mathbf{a_3}$
$\mathbf{a_1}$	-1	$\mathbf{a_3}$	$-\mathbf{a_2}$
$\mathbf{a_2}$	$-\mathbf{a_2}$	-1	$\mathbf{a_1}$
$\mathbf{a_3}$	$\mathbf{a_2}$	$-\mathbf{a_1}$	-1

Table 2. Multiplication rules for space-time units.

	$\mathbf{e_1}$	$\mathbf{e_2}$	$\mathbf{e_3}$
$\mathbf{e_1}$	-1	$\mathbf{e_3}$	$-\mathbf{e_2}$
$\mathbf{e_2}$	$-\mathbf{e_2}$	-1	$\mathbf{e_1}$
$\mathbf{e_3}$	$\mathbf{e_2}$	$-\mathbf{e_1}$	-1

Note that the unit vectors $\mathbf{a}_1$, $\mathbf{a}_2$, $\mathbf{a}_3$ and the space-time units $\mathbf{e}_1$, $\mathbf{e}_2$, $\mathbf{e}_3$ generate the anticommutative algebras:

$$\begin{aligned}\mathbf{a_n a_m} &= -\mathbf{a_m a_n},\\ \mathbf{e_n e_m} &= -\mathbf{e_m e_n},\end{aligned} \tag{4}$$

for $\mathbf{n} \neq \mathbf{m}$, but $\mathbf{e}_1$, $\mathbf{e}_2$, $\mathbf{e}_3$ commute with $\mathbf{a}_1$, $\mathbf{a}_2$, $\mathbf{a}_3$:

$$\mathbf{e_n a_m} = \mathbf{a_m e_n}, \tag{5}$$

for any $\mathbf{n}$ and $\mathbf{m}$. Besides, we assume the associativity of $\mathbf{e}_1$, $\mathbf{e}_2$, $\mathbf{e}_3$, $\mathbf{a}_1$, $\mathbf{a}_2$, $\mathbf{a}_3$ multiplication.

Then we can introduce the sixteen-component space-time sedenion $\tilde{\boldsymbol{V}}$ in the following form:

$$\begin{aligned}\tilde{\boldsymbol{V}} &= \mathbf{e_0}\left(V_{00}\mathbf{a_0} + V_{01}\mathbf{a_1} + V_{02}\mathbf{a_2} + V_{03}\mathbf{a_3}\right) + \mathbf{e_1}\left(V_{10}\mathbf{a_0} + V_{11}\mathbf{a_1} + V_{12}\mathbf{a_2} + V_{13}\mathbf{a_3}\right)\\ &+ \mathbf{e_2}\left(V_{20}\mathbf{a_0} + V_{21}\mathbf{a_1} + V_{22}\mathbf{a_2} + V_{23}\mathbf{a_3}\right) + \mathbf{e_3}\left(V_{30}\mathbf{a_0} + V_{31}\mathbf{a_1} + V_{32}\mathbf{a_2} + V_{33}\mathbf{a_3}\right).\end{aligned} \tag{6}$$

The sedenionic components $V_{\nu\mu}$ are numbers (complex in general). Introducing designation of scalar and vector values in accordance with the following relations

$$\begin{aligned}V &= \mathbf{e_0} V_{00}\mathbf{a_0},\\ \vec{V} &= \mathbf{e_0}\left(V_{01}\mathbf{a_1} + V_{02}\mathbf{a_2} + V_{03}\mathbf{a_3}\right),\\ V_\mathbf{t} \equiv V_\mathbf{1} &= \mathbf{e_1} V_{10}\mathbf{a_0},\\ \vec{V}_\mathbf{t} \equiv \vec{V}_\mathbf{1} &= \mathbf{e_1}\left(V_{11}\mathbf{a_1} + V_{12}\mathbf{a_2} + V_{13}\mathbf{a_3}\right),\\ V_\mathbf{r} \equiv V_\mathbf{2} &= \mathbf{e_2} V_{20}\mathbf{a_0},\\ \vec{V}_\mathbf{r} \equiv \vec{V}_\mathbf{2} &= \mathbf{e_2}\left(V_{21}\mathbf{a_1} + V_{22}\mathbf{a_2} + V_{23}\mathbf{a_3}\right),\\ V_\mathbf{tr} \equiv V_\mathbf{3} &= \mathbf{e_3} V_{30}\mathbf{a_0},\\ \vec{V}_\mathbf{tr} \equiv \vec{V}_\mathbf{3} &= \mathbf{e_3}\left(V_{31}\mathbf{a_1} + V_{32}\mathbf{a_2} + V_{33}\mathbf{a_3}\right).\end{aligned} \tag{7}$$

we can represent the sedenion in the following scalar-vector form:

$$\tilde{\boldsymbol{V}} = V + \vec{V} + V_\mathbf{t} + \vec{V}_\mathbf{t} + V_\mathbf{r} + \vec{V}_\mathbf{r} + V_\mathbf{tr} + \vec{V}_\mathbf{tr}. \tag{8}$$

Thus, the sedenionic algebra encloses four groups of values, which are differed with respect to spatial and time inversion.

1) Absolute scalars (V) and absolute vectors $(\vec{V})$ are not transformed under spatial and time inversion.

2) Time scalars $(V_\mathbf{t})$ and time vectors $(\vec{V}_\mathbf{t})$ are changed (in sign) under time inversion and are not transformed under spatial inversion.

3) Space scalars $(V_\mathbf{r})$ and space vectors $(\vec{V}_\mathbf{r})$ are changed under spatial inversion and are not transformed under time inversion.

4) Space-time scalars $(V_\mathbf{tr})$ and space-time vectors $(\vec{V}_\mathbf{tr})$ are changed under spatial and time inversion.

Further we will use the symbol 1 instead units $\mathbf{a_0}$ and $\mathbf{e_0}$ for simplicity. Introducing the designations of scalar-vector values

$$\begin{aligned}\bar{\boldsymbol{V}}_0 &= V_{00} + V_{01}\mathbf{a_1} + V_{02}\mathbf{a_2} + V_{03}\mathbf{a_3},\\ \bar{\boldsymbol{V}}_1 &= V_{10} + V_{11}\mathbf{a_1} + V_{12}\mathbf{a_2} + V_{13}\mathbf{a_3},\\ \bar{\boldsymbol{V}}_2 &= V_{20} + V_{21}\mathbf{a_1} + V_{22}\mathbf{a_2} + V_{23}\mathbf{a_3},\\ \bar{\boldsymbol{V}}_3 &= V_{30} + V_{31}\mathbf{a_1} + V_{32}\mathbf{a_2} + V_{33}\mathbf{a_3}.\end{aligned} \tag{9}$$

we can write the sedenion (6) in the following compact form:

$$\tilde{\boldsymbol{V}} = \bar{\boldsymbol{V}}_0 + \mathbf{e_1}\bar{\boldsymbol{V}}_1 + \mathbf{e_2}\bar{\boldsymbol{V}}_2 + \mathbf{e_3}\bar{\boldsymbol{V}}_3. \tag{10}$$

On the other hand, introducing designations of space-time sedenion-scalars

$$\begin{aligned}\boldsymbol{V}_0 &= \left(V_{00} + \mathbf{e_1}V_{10} + \mathbf{e_2}V_{20} + \mathbf{e_3}V_{30}\right),\\ \boldsymbol{V}_1 &= \left(V_{01} + \mathbf{e_1}V_{11} + \mathbf{e_2}V_{21} + \mathbf{e_3}V_{31}\right),\\ \boldsymbol{V}_2 &= \left(V_{02} + \mathbf{e_1}V_{12} + \mathbf{e_2}V_{22} + \mathbf{e_3}V_{32}\right),\\ \boldsymbol{V}_3 &= \left(V_{03} + \mathbf{e_1}V_{13} + \mathbf{e_2}V_{23} + \mathbf{e_3}V_{33}\right).\end{aligned} \tag{11}$$

we can write the sedenion (6) as

$$\tilde{\boldsymbol{V}} = \boldsymbol{V}_0 + \boldsymbol{V}_1\mathbf{a_1} + \boldsymbol{V}_2\mathbf{a_2} + \boldsymbol{V}_3\mathbf{a_3}, \tag{12}$$

or introducing the sedenion-vector

$$\vec{\boldsymbol{V}} = \vec{V} + \vec{V}_{\mathbf{t}} + \vec{V}_{\mathbf{r}} + \vec{V}_{\mathbf{tr}} = \boldsymbol{V}_1\mathbf{a_1} + \boldsymbol{V}_2\mathbf{a_2} + \boldsymbol{V}_3\mathbf{a_3}, \tag{13}$$

we can rewrite the sedenion in following compact form:

$$\tilde{\boldsymbol{V}} = \boldsymbol{V}_0 + \vec{\boldsymbol{V}}. \tag{14}$$

Further we will indicate sedenion-scalars and sedenion-vectors with the bold capital letters.

Let us consider the sedenionic multiplication in detail. The sedenionic product of two sedenions $\tilde{\boldsymbol{A}}$ and $\tilde{\boldsymbol{B}}$ can be represented in the following form

$$\tilde{\boldsymbol{A}}\tilde{\boldsymbol{B}} = \left(\boldsymbol{A}_0 + \vec{\boldsymbol{A}}\right)\left(\boldsymbol{B}_0 + \vec{\boldsymbol{B}}\right) = \boldsymbol{A}_0\boldsymbol{B}_0 + \boldsymbol{A}_0\vec{\boldsymbol{B}} + \vec{\boldsymbol{A}}\boldsymbol{B}_0 + \left(\vec{\boldsymbol{A}}\cdot\vec{\boldsymbol{B}}\right) + \left[\vec{\boldsymbol{A}}\times\vec{\boldsymbol{B}}\right]. \tag{15}$$

Here we denoted the sedenionic scalar multiplication of two sedenion-vectors (internal product) by symbol "·" and round brackets

$$\left(\vec{\boldsymbol{A}}\cdot\vec{\boldsymbol{B}}\right) = -\boldsymbol{A}_1\boldsymbol{B}_1 - \boldsymbol{A}_2\boldsymbol{B}_2 - \boldsymbol{A}_3\boldsymbol{B}_3, \tag{16}$$

and sedenionic vector multiplication (external product) by symbol "×" and square brackets,

$$\left[\vec{\boldsymbol{A}}\times\vec{\boldsymbol{B}}\right] = \left(\boldsymbol{A}_2\boldsymbol{B}_3 - \boldsymbol{A}_3\boldsymbol{B}_2\right)\mathbf{a_1} + \left(\boldsymbol{A}_3\boldsymbol{B}_1 - \boldsymbol{A}_1\boldsymbol{B}_3\right)\mathbf{a_2} + \left(\boldsymbol{A}_1\boldsymbol{B}_2 - \boldsymbol{A}_2\boldsymbol{B}_1\right)\mathbf{a_3}. \tag{17}$$

In (16) and (17) the multiplication of sedenionic components is performed in accordance with (11) and **Table 2**. Thus the sedenionic product

$$\tilde{\boldsymbol{F}} = \tilde{\boldsymbol{A}}\tilde{\boldsymbol{B}} = \boldsymbol{F}_0 + \vec{\boldsymbol{F}}, \tag{18}$$

has the following components:

$$\begin{aligned} \boldsymbol{F}_0 &= \boldsymbol{A}_0\boldsymbol{B}_0 - \boldsymbol{A}_1\boldsymbol{B}_1 - \boldsymbol{A}_2\boldsymbol{B}_2 - \boldsymbol{A}_3\boldsymbol{B}_3, \\ \boldsymbol{F}_1 &= \boldsymbol{A}_1\boldsymbol{B}_0 + \boldsymbol{A}_0\boldsymbol{B}_1 + \left(\boldsymbol{A}_2\boldsymbol{B}_3 - \boldsymbol{A}_3\boldsymbol{B}_2\right), \\ \boldsymbol{F}_2 &= \boldsymbol{A}_2\boldsymbol{B}_0 + \boldsymbol{A}_0\boldsymbol{B}_2 + \left(\boldsymbol{A}_3\boldsymbol{B}_1 - \boldsymbol{A}_1\boldsymbol{B}_3\right), \\ \boldsymbol{F}_3 &= \boldsymbol{A}_3\boldsymbol{B}_0 + \boldsymbol{A}_0\boldsymbol{B}_3 + \left(\boldsymbol{A}_1\boldsymbol{B}_2 - \boldsymbol{A}_2\boldsymbol{B}_1\right). \end{aligned} \tag{19}$$

Note that in the sedenionic algebra the square of vector is defined as

$$\vec{A}^2 = \left(\vec{A}\cdot\vec{A}\right) = -A_1^2 - A_2^2 - A_3^2, \tag{20}$$

and the square of modulus of vector is

$$\left|\vec{A}\right|^2 = -\left(\vec{A}\cdot\vec{A}\right) = A_1^2 + A_2^2 + A_3^2. \tag{21}$$

3. Spatial Rotation and Space-Time Inversion

The rotation of sedenion $\tilde{\boldsymbol{V}}$ on the angle θ around the absolute unit vector $\vec{n}$ is realized by sedenion

$$\tilde{\boldsymbol{U}} = \cos(\theta/2) + \vec{n}\sin(\theta/2), \tag{22}$$

and by conjugated sedenion $\tilde{\boldsymbol{U}}^*$:

$$\tilde{\boldsymbol{U}}^* = \cos(\theta/2) - \vec{n}\sin(\theta/2), \tag{23}$$

with

$$\tilde{\boldsymbol{U}}\tilde{\boldsymbol{U}}^* = \tilde{\boldsymbol{U}}^*\tilde{\boldsymbol{U}} = 1. \tag{24}$$

The transformed sedenion $\tilde{\boldsymbol{V}}'$ is defined as sedenionic product

$$\tilde{\boldsymbol{V}}' = \tilde{\boldsymbol{U}}^*\tilde{\boldsymbol{V}}\tilde{\boldsymbol{U}}, \tag{25}$$

Thus, the transformed sedenion $\tilde{\boldsymbol{V}}'$ can be written as

$$\begin{aligned}\tilde{\boldsymbol{V}}' &= \left[\cos(\theta/2) - \vec{n}\sin(\theta/2)\right]\left(\boldsymbol{V}_0 + \vec{\boldsymbol{V}}\right)\left[\cos(\theta/2) + \vec{n}\sin(\theta/2)\right] \\ &= \boldsymbol{V}_0 + \vec{\boldsymbol{V}}\cos\theta - \vec{n}\left(\vec{n}\cdot\vec{\boldsymbol{V}}\right)(1-\cos\theta) - \left[\vec{n}\times\vec{\boldsymbol{V}}\right]\sin\theta.\end{aligned} \tag{26}$$

It is clearly seen that rotation does not transform the sedenion-scalar part, but the sedenionic vector $\vec{V}$ is rotated on the angle θ around $\vec{n}$.

The operations of time inversion $(\hat{R}_{\mathbf{t}})$, space inversion $(\hat{R}_{\mathbf{r}})$ and space-time inversion $(\hat{R}_{\mathbf{tr}})$ are connected with transformations in $\mathbf{e}_1$, $\mathbf{e}_2$, $\mathbf{e}_3$ basis and can be presented as

$$\begin{aligned}\hat{R}_{\mathbf{t}}\tilde{\boldsymbol{V}} &= -\mathbf{e}_2\tilde{\boldsymbol{V}}\mathbf{e}_2 = \overline{\boldsymbol{V}}_0 - \mathbf{e}_1\overline{\boldsymbol{V}}_1 + \mathbf{e}_2\overline{\boldsymbol{V}}_2 - \mathbf{e}_3\overline{\boldsymbol{V}}_3,\\ \hat{R}_{\mathbf{r}}\tilde{\boldsymbol{V}} &= -\mathbf{e}_1\tilde{\boldsymbol{V}}\mathbf{e}_1 = \overline{\boldsymbol{V}}_0 + \mathbf{e}_1\overline{\boldsymbol{V}}_1 - \mathbf{e}_2\overline{\boldsymbol{V}}_2 - \mathbf{e}_3\overline{\boldsymbol{V}}_3,\\ \hat{R}_{\mathbf{tr}}\tilde{\boldsymbol{V}} &= -\mathbf{e}_3\tilde{\boldsymbol{V}}\mathbf{e}_3 = \overline{\boldsymbol{V}}_0 - \mathbf{e}_1\overline{\boldsymbol{V}}_1 - \mathbf{e}_2\overline{\boldsymbol{V}}_2 + \mathbf{e}_3\overline{\boldsymbol{V}}_3.\end{aligned} \tag{27}$$

4. Sedenionic Lorentz Transformations

The relativistic event four-vector can be represented in the follow sedenionic form:

$$\tilde{\boldsymbol{S}} = \mathbf{e}_1 ct + \mathbf{e}_2\vec{r}\,. \tag{28}$$

The square of this valueis the Lorentzinvariant

$$\tilde{\boldsymbol{S}}\tilde{\boldsymbol{S}} = -c^2t^2 + x^2 + y^2 + z^2\,. \tag{29}$$

The Lorentz transformation of event four-vector is realized by sedenions

$$\begin{aligned}\tilde{\boldsymbol{L}} &= \operatorname{ch}\vartheta + \mathbf{e}_3\vec{m}\operatorname{sh}\vartheta,\\ \tilde{\boldsymbol{L}}^* &= \operatorname{ch}\vartheta - \mathbf{e}_3\vec{m}\operatorname{sh}\vartheta,\end{aligned} \tag{30}$$

where $\operatorname{th}2\vartheta = v/c$, v is velocity of motion along the absolute unit vector $\vec{m}$. Note that

$$\tilde{\boldsymbol{L}}^*\tilde{\boldsymbol{L}} = \tilde{\boldsymbol{L}}\tilde{\boldsymbol{L}}^* = 1\,. \tag{31}$$

The transformed event four-vector $\tilde{\boldsymbol{S}}'$ is written as

$$\begin{aligned}\tilde{\boldsymbol{S}}' &= \tilde{\boldsymbol{L}}^*\,\tilde{\boldsymbol{S}}\,\tilde{\boldsymbol{L}} = \left(\operatorname{ch}\vartheta - \mathbf{e}_3\operatorname{sh}\vartheta\vec{m}\right)\left(\mathbf{e}_1 ct + \mathbf{e}_2\vec{r}\right)\left(\operatorname{ch}\vartheta + \mathbf{e}_3\operatorname{sh}\vartheta\vec{m}\right)\\ &= \mathbf{e}_1 ct\operatorname{ch}2\vartheta + \mathbf{e}_1\left(\vec{m}\cdot\vec{r}\right)\operatorname{sh}2\vartheta + \mathbf{e}_2\vec{r} - \mathbf{e}_2 ct\vec{m}\operatorname{sh}2\vartheta + \mathbf{e}_2\left(\vec{m}\cdot\vec{r}\right)\vec{m}\left(1-\operatorname{ch}2\vartheta\right).\end{aligned} \tag{32}$$

Separating the values with $\mathbf{e}_1$ and $\mathbf{e}_2$ we get the well known formulas for time and coordinates transformation [25]:

$$t' = \frac{t - xv/c^2}{\sqrt{1-v^2/c^2}},\quad x' = \frac{x - tv}{\sqrt{1-v^2/c^2}},\quad y' = y,\quad z' = z\,, \tag{33}$$

where x is the coordinate along the $\vec{m}$ vector.

Let us also consider the Lorentz transformation of the full sedenion $\tilde{\boldsymbol{V}}$. The transformed sedenion $\tilde{\boldsymbol{V}}'$ can be written as sedenionic product

$$\tilde{\boldsymbol{V}}' = \tilde{\boldsymbol{L}}^*\,\tilde{\boldsymbol{V}}\tilde{\boldsymbol{L}}\,. \tag{34}$$

$$\begin{aligned}\tilde{\boldsymbol{V}}' &= \left(\operatorname{ch}\vartheta - \mathbf{e}_{\mathbf{tr}}\operatorname{sh}\vartheta\vec{m}\right)\left(\boldsymbol{V}_0 + \vec{\boldsymbol{V}}\right)\left(\operatorname{ch}\vartheta + \mathbf{e}_{\mathbf{tr}}\operatorname{sh}\vartheta\vec{m}\right)\\ &= \boldsymbol{V}_0\operatorname{ch}^2\vartheta + \mathbf{e}_{\mathbf{tr}}\boldsymbol{V}_0\mathbf{e}_{\mathbf{rt}}\operatorname{sh}^2\vartheta - \left(\mathbf{e}_{\mathbf{tr}}\boldsymbol{V}_0 - \boldsymbol{V}_0\mathbf{e}_{\mathbf{tr}}\right)\vec{m}\operatorname{ch}\vartheta\operatorname{sh}\vartheta + \vec{\boldsymbol{V}}\operatorname{ch}^2\vartheta\\ &\quad - \mathbf{e}_{\mathbf{tr}}\vec{m}\vec{\boldsymbol{V}}\vec{m}\mathbf{e}_{\mathbf{tr}}\operatorname{sh}^2\vartheta - \left(\mathbf{e}_{\mathbf{tr}}\vec{m}\vec{\boldsymbol{V}} - \vec{\boldsymbol{V}}\vec{m}\mathbf{e}_{\mathbf{tr}}\right)\operatorname{ch}\vartheta\operatorname{sh}\vartheta.\end{aligned} \tag{35}$$

Rewriting the expression (35) with scalar (16) and vector (17) products we get

$$\begin{aligned}\tilde{\boldsymbol{V}}' &= \boldsymbol{V}_0\operatorname{ch}^2\vartheta + \mathbf{e}_{\mathbf{tr}}\boldsymbol{V}_0\mathbf{e}_{\mathbf{tr}}\operatorname{sh}^2\vartheta - \left(\mathbf{e}_{\mathbf{tr}}\boldsymbol{V}_0 - \boldsymbol{V}_0\mathbf{e}_{\mathbf{tr}}\right)\vec{m}\operatorname{ch}\vartheta\operatorname{sh}\vartheta + \vec{\boldsymbol{V}}\operatorname{ch}^2\vartheta - \mathbf{e}_{\mathbf{tr}}\vec{\boldsymbol{V}}\mathbf{e}_{\mathbf{tr}}\operatorname{sh}^2\vartheta - 2\mathbf{e}_{\mathbf{tr}}\left(\vec{m}\cdot\vec{\boldsymbol{V}}\right)\mathbf{e}_{\mathbf{tr}}\vec{m}\operatorname{sh}^2\vartheta\\ &\quad - \left(\mathbf{e}_{\mathbf{tr}}\left(\vec{m}\cdot\vec{\boldsymbol{V}}\right) - \left(\vec{\boldsymbol{V}}\cdot\vec{m}\right)\mathbf{e}_{\mathbf{tr}}\right)\operatorname{ch}\vartheta\operatorname{sh}\vartheta - \left(\mathbf{e}_{\mathbf{tr}}\left[\vec{m}\times\vec{\boldsymbol{V}}\right] - \left[\vec{\boldsymbol{V}}\times\vec{m}\right]\mathbf{e}_{\mathbf{tr}}\right)\operatorname{ch}\vartheta\operatorname{sh}\vartheta.\end{aligned} \tag{36}$$

Thus, the transformed sedenion has the following components:

$$
\begin{aligned}
&V' = V, \\
&V'_{\mathbf{tr}} = V_{\mathbf{tr}}, \\
&V'_{\mathbf{r}} = V_{\mathbf{r}} \operatorname{ch} 2\vartheta - \mathbf{e}_{\mathbf{tr}} \left(\vec{m} \cdot \vec{V}_{\mathbf{t}}\right) \operatorname{sh} 2\vartheta, \\
&V'_{\mathbf{t}} = V_{\mathbf{t}} \operatorname{ch} 2\vartheta - \mathbf{e}_{\mathbf{tr}} \left(\vec{m} \cdot \vec{V}_{\mathbf{r}}\right) \operatorname{sh} 2\vartheta, \\
&\vec{V}' = \vec{V} \operatorname{ch} 2\vartheta - \left(\vec{m} \cdot \vec{V}\right) \vec{m} \left(1 - \operatorname{ch} 2\vartheta\right) - \mathbf{e}_{\mathbf{tr}} \left[\vec{m} \times \vec{V}_{\mathbf{rt}}\right] \operatorname{sh} 2\vartheta, \\
&\vec{V}'_{\mathbf{tr}} = \vec{V}_{\mathbf{tr}} \operatorname{ch} 2\vartheta - \left(\vec{m} \cdot \vec{V}_{\mathbf{tr}}\right) \vec{m} \left(1 - \operatorname{ch} 2\vartheta\right) - \mathbf{e}_{\mathbf{tr}} \left[\vec{m} \times \vec{V}\right] \operatorname{sh} 2\vartheta, \\
&\vec{V}'_{\mathbf{r}} = \vec{V}_{\mathbf{r}} + \left(\vec{m} \cdot \vec{V}_{\mathbf{r}}\right) \vec{m} \left(1 - \operatorname{ch} 2\vartheta\right) - \mathbf{e}_{\mathbf{tr}} V_{\mathbf{t}} \vec{m} \operatorname{sh} 2\vartheta, \\
&\vec{V}'_{\mathbf{t}} = \vec{V}_{\mathbf{t}} + \left(\vec{m} \cdot \vec{V}_{\mathbf{t}}\right) \vec{m} \left(1 - \operatorname{ch} 2\vartheta\right) - \mathbf{e}_{\mathbf{tr}} V_{\mathbf{r}} \vec{m} \operatorname{sh} 2\vartheta.
\end{aligned}
\tag{37}
$$

5. Subalgebras of Space-Time Complex Numbers, Quaternions and Octonions

The sedenionic basis introduced above enables constructing different types of low-dimensional hypercomplex numbers. For example, one can introduce space-time complex numbers

$$
\begin{aligned}
&Z_{\mathbf{t}} = z_1 + \mathbf{e}_{\mathbf{t}} z_2, \\
&Z_{\mathbf{r}} = z_1 + \mathbf{e}_{\mathbf{r}} z_2, \\
&Z_{\mathbf{tr}} = z_1 + \mathbf{e}_{\mathbf{tr}} z_2,
\end{aligned}
\tag{38}
$$

where z_1 and z_2 real numbers. These values are transformed under space and time conjugation and Lorentz transformations. Moreover, we can consider the space-time quaternions, which differ in their properties with respect to the operations of the spatial and time inversion and Lorentz transformations:

$$\hat{q} = q_0 \mathbf{a_0} + \mathbf{e_0} \left(q_1 \mathbf{a_1} + q_2 \mathbf{a_2} + q_3 \mathbf{a_3}\right), \tag{39}$$

$$\hat{q}_{\mathbf{t}} = q_0 \mathbf{a_0} + \mathbf{e}_{\mathbf{t}} \left(q_1 \mathbf{a_1} + q_2 \mathbf{a_2} + q_3 \mathbf{a_3}\right), \tag{40}$$

$$\hat{q}_{\mathbf{r}} = q_0 \mathbf{a_0} + \mathbf{e}_{\mathbf{r}} \left(q_1 \mathbf{a_1} + q_2 \mathbf{a_2} + q_3 \mathbf{a_3}\right), \tag{41}$$

$$\hat{q}_{\mathbf{tr}} = q_0 \mathbf{a_0} + \mathbf{e}_{\mathbf{tr}} \left(q_1 \mathbf{a_1} + q_2 \mathbf{a_2} + q_3 \mathbf{a_3}\right). \tag{42}$$

The absolute quaternion (39) is the sum of the absolute scalar and absolute vector. It remains constant under the transformations of space and time inversion (27). Time quaternion $\hat{q}_{\mathbf{t}}$, space quaternion $\hat{q}_{\mathbf{r}}$ and space-time quaternion $\hat{q}_{\mathbf{tr}}$ are transformed under inversions in accordance with the commutation rules for the basis elements $\mathbf{e_t}$, $\mathbf{e_r}$, $\mathbf{e_{tr}}$. For example, performing the operation of time inversion (see (27)) with the quaternion $\hat{q}_{\mathbf{t}}$ we obtain the conjugated quaternion

$$\hat{R}_{\mathbf{t}} \hat{q}_{\mathbf{t}} = -\mathbf{e}_{\mathbf{r}} \hat{q}_{\mathbf{t}} \mathbf{e}_{\mathbf{r}} = q_0 \mathbf{a_0} - \mathbf{e}_{\mathbf{t}} \left(q_1 \mathbf{a_1} + q_2 \mathbf{a_2} + q_3 \mathbf{a_3}\right). \tag{43}$$

In addition, the sedenionic basis allows one to construct various types of space-time eight-component octonions:

$$\breve{G}_{\mathbf{t}} = G_{00} + G_{01} \mathbf{a_1} + G_{02} \mathbf{a_2} + G_{03} \mathbf{a_3} + \mathbf{e}_{\mathbf{t}} G_{10} + \mathbf{e}_{\mathbf{t}} \left(G_{11} \mathbf{a_1} + G_{12} \mathbf{a_2} + G_{13} \mathbf{a_3}\right), \tag{44}$$

$$\breve{G}_{\mathbf{r}} = G_{00} + G_{01} \mathbf{a_1} + G_{02} \mathbf{a_2} + G_{03} \mathbf{a_3} + \mathbf{e}_{\mathbf{r}} G_{20} + \mathbf{e}_{\mathbf{r}} \left(G_{21} \mathbf{a_1} + G_{22} \mathbf{a_2} + G_{23} \mathbf{a_3}\right), \tag{45}$$

$$\breve{G}_{\mathbf{tr}} = G_{00} + G_{01} \mathbf{a_1} + G_{02} \mathbf{a_2} + G_{03} \mathbf{a_3} + \mathbf{e}_{\mathbf{tr}} G_{30} + \mathbf{e}_{\mathbf{tr}} \left(G_{31} \mathbf{a_1} + G_{32} \mathbf{a_2} + G_{33} \mathbf{a_3}\right). \tag{46}$$

6. Generalized Sedenionic Equations of Relativistic Quantum Mechanics

The wave function of free quantum particle should satisfy an equation, which is obtained from the Einstein relation for energy and momentum

$$E^2 - c^2 p^2 = m_0^2 c^4, \tag{47}$$

by means of changing classical energy E and momentum $\vec{p}$ on corresponding quantum-mechanical operators:

$$\hat{E} = i\hbar\frac{\partial}{\partial t} \text{ and } \hat{\vec{p}} = -i\hbar\vec{\nabla} . \tag{48}$$

Here c is the speed of light, m_0 is the particle rest mass, $\hbar$ is the Planck constant. In sedenion algebra the Einstein relation (47) can be written as

$$\left(\mathbf{e}_\mathbf{t}E + \mathbf{e}_\mathbf{r}c\vec{p} + i\mathbf{e}_\mathbf{tr}m_0c^2\right)\left(\mathbf{e}_\mathbf{t}E + \mathbf{e}_\mathbf{r}c\vec{p} + i\mathbf{e}_\mathbf{tr}m_0c^2\right) = 0 . \tag{49}$$

Let us consider the wave function in the form of space-time sedenion

$$\tilde{\boldsymbol{W}}(t,\vec{r}) = \boldsymbol{W}_0(t,\vec{r}) + \vec{\boldsymbol{W}}(t,\vec{r}) . \tag{50}$$

Then the generalized sedenionic wave equation for free particle can be written in the following symmetric form:

$$\left(\mathbf{e}_\mathbf{t}\frac{1}{c}\frac{\partial}{\partial t} - \mathbf{e}_\mathbf{r}\vec{\nabla} + \mathbf{e}_\mathbf{tr}\frac{m_0c}{\hbar}\right)\left(\mathbf{e}_\mathbf{t}\frac{1}{c}\frac{\partial}{\partial t} - \mathbf{e}_\mathbf{r}\vec{\nabla} + \mathbf{e}_\mathbf{tr}\frac{m_0c}{\hbar}\right)\tilde{\boldsymbol{W}} = 0 . \tag{51}$$

Note that for electrically charged particle in an external electromagnetic field we have the following sedenionic wave equation:

$$\left(\mathbf{e}_\mathbf{t}\frac{1}{c}\frac{\partial}{\partial t} + \mathbf{e}_\mathbf{t}\frac{ie}{\hbar c}\varphi - \mathbf{e}_\mathbf{r}\vec{\nabla} + \mathbf{e}_\mathbf{r}\frac{ie}{\hbar c}\vec{A} + \mathbf{e}_\mathbf{tr}\frac{m_0c}{\hbar}\right)\left(\mathbf{e}_\mathbf{t}\frac{1}{c}\frac{\partial}{\partial t} + \mathbf{e}_\mathbf{t}\frac{ie}{\hbar c}\varphi - \mathbf{e}_\mathbf{r}\vec{\nabla} + \mathbf{e}_\mathbf{r}\frac{ie}{\hbar c}\vec{A} + \mathbf{e}_\mathbf{tr}\frac{m_0c}{\hbar}\right)\tilde{\boldsymbol{W}} = 0 . \tag{52}$$

This equation describes the particles with spin 1/2 in an external electromagnetic field [18] [21].

There is a special class of particles described by the first-order wave equation [26]. For these particles the sedenionic Dirac-like wave equation has the following form:

$$\left(\mathbf{e}_\mathbf{t}\frac{1}{c}\frac{\partial}{\partial t} - \mathbf{e}_\mathbf{r}\vec{\nabla} + \mathbf{e}_\mathbf{tr}\frac{m_0c}{\hbar}\right)\tilde{\boldsymbol{W}} = 0 . \tag{53}$$

In fact, this equation describes the special quantum field with zero field strengths [19]. Analogously the electrically charged particle interacting with external electromagnetic field is described by the following sedenionic first-order wave equation:

$$\left(\mathbf{e}_\mathbf{t}\frac{1}{c}\frac{\partial}{\partial t} + \mathbf{e}_\mathbf{t}\frac{ie}{\hbar c}\varphi - \mathbf{e}_\mathbf{r}\vec{\nabla} + \mathbf{e}_\mathbf{r}\frac{ie}{\hbar c}\vec{A} + \mathbf{e}_\mathbf{tr}\frac{m_0c}{\hbar}\right)\tilde{\boldsymbol{W}} = 0 . \tag{54}$$

This equation also describes particles with spin 1/2 in an external electromagnetic field [19].

7. Generalized Sedenionic Equations for Massive Field

The generalized sedenionic wave equation

$$\left(\mathbf{e}_\mathbf{t}\frac{1}{c}\frac{\partial}{\partial t} - \mathbf{e}_\mathbf{r}\vec{\nabla} + \mathbf{e}_\mathbf{tr}\frac{m_0c}{\hbar}\right)\left(\mathbf{e}_\mathbf{t}\frac{1}{c}\frac{\partial}{\partial t} - \mathbf{e}_\mathbf{r}\vec{\nabla} + \mathbf{e}_\mathbf{tr}\frac{m_0c}{\hbar}\right)\tilde{\boldsymbol{W}} = 0 , \tag{55}$$

enables another interpretation. It can be considered as the equation for the force massive field [27]. In this case the parameter m_0 is the mass of quantum of field and $\tilde{\boldsymbol{W}}$ is field potential. Considering the phenomenological source of field $\tilde{\boldsymbol{J}}$ we can propose the following nonhomogeneous wave equation for the field potential:

$$\left(\mathbf{e}_\mathbf{t}\frac{1}{c}\frac{\partial}{\partial t} - \mathbf{e}_\mathbf{r}\vec{\nabla} + \mathbf{e}_\mathbf{tr}\frac{m_0c}{\hbar}\right)\left(\mathbf{e}_\mathbf{t}\frac{1}{c}\frac{\partial}{\partial t} - \mathbf{e}_\mathbf{r}\vec{\nabla} + \mathbf{e}_\mathbf{tr}\frac{m_0c}{\hbar}\right)\tilde{\boldsymbol{W}} = \tilde{\boldsymbol{J}} . \tag{56}$$

Seemingly this equation describes the baryon (strong) field [23] [24] and $\tilde{\boldsymbol{J}}$ is baryon current. On the other hand, corresponding nonhomogeneous first-order equation

$$\left(\mathbf{e}_\mathbf{t}\frac{1}{c}\frac{\partial}{\partial t} - \mathbf{e}_\mathbf{r}\vec{\nabla} + \mathbf{e}_\mathbf{tr}\frac{m_0c}{\hbar}\right)\tilde{\boldsymbol{W}} = \tilde{\boldsymbol{I}} , \tag{57}$$

describes the lepton (weak) field, where $\tilde{\boldsymbol{I}}$ is a lepton current [23] [24].

8. Generalized Sedenionic Equations for Massless Field

In the special case, when the mass of quantum m_0 is equal to zero, the Equation (56) coincides with the equation for electromagnetic field. Indeed, choosing the potential as

$$\tilde{\boldsymbol{W}} = \mathbf{e}_t \varphi + \mathbf{e}_r \vec{A}, \tag{58}$$

and the source of field as

$$\tilde{\boldsymbol{J}} = -\mathbf{e}_t 4\pi\rho - \mathbf{e}_r \frac{4\pi}{c}\vec{j}, \tag{59}$$

we obtain the following wave equation:

$$\left(\mathbf{e}_t \frac{1}{c}\frac{\partial}{\partial t} - \mathbf{e}_r \vec{\nabla}\right)\left(\mathbf{e}_t \frac{1}{c}\frac{\partial}{\partial t} - \mathbf{e}_r \vec{\nabla}\right)\left(\mathbf{e}_t \varphi + \mathbf{e}_r \vec{A}\right) = -\mathbf{e}_t 4\pi\rho - \mathbf{e}_r \frac{4\pi}{c}\vec{j}. \tag{60}$$

After the action of the first operator in the left-hand side of Equation (60) we obtain

$$\left(\mathbf{e}_t \frac{1}{c}\frac{\partial}{\partial t} - \mathbf{e}_r \vec{\nabla}\right)\left(\mathbf{e}_t \varphi + \mathbf{e}_r \vec{A}\right) = -\frac{1}{c}\frac{\partial \varphi}{\partial t} + \mathbf{e}_{tr}\frac{1}{c}\frac{\partial \vec{A}}{\partial t} + \mathbf{e}_{tr}\vec{\nabla}\varphi + \left(\vec{\nabla}\cdot\vec{A}\right) + \left[\vec{\nabla}\times\vec{A}\right]. \tag{61}$$

In sedenionic algebra the electric and magnetic fields are defined as

$$\begin{aligned} \vec{E} &= -\frac{1}{c}\frac{\partial \vec{A}}{\partial t} - \vec{\nabla}\varphi, \\ \vec{H} &= \left[\vec{\nabla}\times\vec{A}\right]. \end{aligned} \tag{62}$$

Besides we can define the scalar field

$$f = -\frac{1}{c}\frac{\partial \varphi}{\partial t} + \left(\vec{\nabla}\cdot\vec{A}\right). \tag{63}$$

Assuming electric charge conservation the scalar field f can be chosen equal to zero, that coincides with Lorentz gauge condition [22]. In Lorentz gauge we can rewrite the expression (61) as

$$\left(\mathbf{e}_t \frac{1}{c}\frac{\partial}{\partial t} - \mathbf{e}_r \vec{\nabla}\right)\left(\mathbf{e}_t \varphi + \mathbf{e}_r \vec{A}\right) = -\mathbf{e}_{tr}\vec{E} + \vec{H}. \tag{64}$$

Then the wave Equation (60) can be represented in the following form:

$$\left(\mathbf{e}_t \frac{1}{c}\frac{\partial}{\partial t} - \mathbf{e}_r \vec{\nabla}\right)\left(-\mathbf{e}_{tr}\vec{E} + \vec{H}\right) = -\mathbf{e}_t 4\pi\rho - \mathbf{e}_r \frac{4\pi}{c}\vec{j}. \tag{65}$$

Performing sedenionic multiplication in the left-hand side of Equation (65) we get

$$\mathbf{e}_r \frac{1}{c}\frac{\partial \vec{E}}{\partial t} + \mathbf{e}_t\left(\vec{\nabla}\cdot\vec{E}\right) + \mathbf{e}_t\left[\vec{\nabla}\times\vec{E}\right] + \mathbf{e}_t \frac{1}{c}\frac{\partial \vec{H}}{\partial t} - \mathbf{e}_r\left(\vec{\nabla}\cdot\vec{H}\right) - \mathbf{e}_r\left[\vec{\nabla}\times\vec{H}\right] = -\mathbf{e}_t 4\pi\rho - \mathbf{e}_r \frac{4\pi}{c}\vec{j}. \tag{66}$$

Separating space-time values we obtain the system of equations in the following form:

$$\begin{aligned} &\mathbf{e}_t\left(\vec{\nabla}\cdot\vec{E}\right) = -\mathbf{e}_t 4\pi\rho, && (\text{time scalar part}) \\ &\mathbf{e}_r\left[\vec{\nabla}\times\vec{E}\right] = \mathbf{e}_r \frac{1}{c}\frac{\partial \vec{E}}{\partial t} + \mathbf{e}_r \frac{4\pi}{c}\vec{j}, && (\text{space vector part}) \\ &\mathbf{e}_t\left[\vec{\nabla}\times\vec{E}\right] = -\mathbf{e}_t \frac{1}{c}\frac{\partial \vec{H}}{\partial t}, && (\text{time vector part}) \\ &\mathbf{e}_r\left(\vec{\nabla}\cdot\vec{H}\right) = 0. && (\text{space scalar part}) \end{aligned} \tag{67}$$

The system (67) coincides with the Maxwell equations.

Among the solutions of the homogeneous sedeonic wave equation of electromagnetic field (60) there is a special class that satisfies the sedeonic first-order equation of the following form [22]:

$$\left(\mathbf{e}_t \frac{1}{c}\frac{\partial}{\partial t} - \mathbf{e}_r \vec{\nabla}\right)\tilde{\boldsymbol{W}}_\nu = 0. \tag{68}$$

This equation describes the free neutrino field. On the other hand, let us consider the nonhomogeneous equation of neutrino field

$$\left(\mathbf{e}_{\mathrm{t}}\frac{1}{c}\frac{\partial}{\partial t}-\mathbf{e}_{\mathrm{r}}\vec{\nabla}\right)\tilde{\boldsymbol{W}}_{\nu}=\tilde{\boldsymbol{I}}_{\nu}, \tag{69}$$

where $\tilde{\boldsymbol{I}}_{\nu}$ is phenomenological source. We choose the scalar source in the form

$$\tilde{\boldsymbol{I}}_{\nu}=4\pi\sigma_{\nu}, \tag{70}$$

where σ_{ν} is the density of neutrino charge. Choosing the potential $\tilde{\boldsymbol{W}}_{\nu}$ in the form (58):

$$\tilde{\boldsymbol{W}}_{\nu}=i\mathbf{e}_{\mathrm{t}}\varphi_{\nu}+\mathbf{e}_{\mathrm{r}}\vec{A}_{\nu}, \tag{71}$$

we obtain following nonhomogeneous equation for the neutrino field:

$$\left(\mathbf{e}_{\mathrm{t}}\frac{1}{c}\frac{\partial}{\partial t}-\mathbf{e}_{\mathrm{r}}\vec{\nabla}\right)\left(\mathbf{e}_{\mathrm{t}}\varphi_{\nu}+\mathbf{e}_{\mathrm{r}}\vec{A}_{\nu}\right)=4\pi\sigma_{\nu}. \tag{72}$$

It follows that in this case only scalar field strength f_{ν} (see (63)) is nonzero:

$$f_{\nu}=4\pi\sigma_{\nu}. \tag{73}$$

The density of neutrino charge for point source is equal

$$\sigma_{\nu}=q_{\nu}\delta\left(\vec{r}\right), \tag{74}$$

where q_{ν} is point neutrino charge. Then the interaction energy of two point neutrino charges can be represented as follows:

$$W_{\nu1\nu2}=\frac{1}{8\pi}\int f_{\nu1}f_{\nu2}\mathrm{d}V. \tag{75}$$

Substituting (73) and (74), we obtain

$$W_{\nu1\nu2}=2\pi q_{\nu1}q_{\nu2}\delta\left(\vec{R}\right), \tag{76}$$

where $\vec{R}$ is the vector of distance between first and second charges.

9. Discussion

The algebra of sedenions proposed in this article is the anticommutative associative space-time Clifford algebra. The sedenionic basis elements $\mathbf{a_n}$ are responsible for the spatial rotation, while the elements $\mathbf{e_n}$ are responsible for the space-time inversions. Mathematically, these two bases are equivalent, and the different physical properties attributed to them are an important physical essence of our sedenionic hypothesis.

In contrast to the previously discussed sedeonic algebra [20]-[23], which uses the multiplication rules of basic elements $\mathbf{a}'_{\mathbf{n}}$ and $\mathbf{e}'_{\mathbf{n}}$ proposed by A. Macfarlane [28], the multiplication rules for sedenionic basis elements $\mathbf{a_n}$ and $\mathbf{e_n}$ coincide with the rules for quaternion units introduced by W. R. Hamilton [29]. There is a close connection between these two basses. The transition from the sedeonic basis to sedenionic basis is performed by following replacement:

$$\mathbf{a}'_{\mathbf{n}}=i\mathbf{a_n},$$

$$\mathbf{e}'_{\mathbf{n}}=i\mathbf{e_n}.$$

There is one disadvantage of sedenions connected with the fact that the square of the vector is a negative value. However, on the other side the sedenionic rules of cross-multiplying do not contain the imaginary unit and this leads to the some simplifications in the calculations. But of course, the physical results do not depend on the choice of algebra, so these two algebras are equivalent.

10. Conclusion

Thus, in this paper we presented the sixteen-component hypercomplex values sedenions, generating associative noncommutative space-time algebra. We considered the generalization of the relativistic quantum mechanics and theory of massive and massless fields based on hypercomplex scalar-vector wave functions and sedenionic space-time operators.

Acknowledgements

The authors are very thankful to G. V. Mironova for kind assistance and moral support.

References

[1] Adler, S.L. (1995) Quaternionic Quantum Mechanics and Quantum Fields. Oxford University Press, New York.

[2] Imaeda, K. (1976) A New Formulation of Classical Electrodynamics. *Nuovocimento*, **32**, 138-162. http://dx.doi.org/10.1007/BF02726749

[3] Majernik, V. (1999) Quaternionic Formulation of the Classical Fields. *Advances in Applied Clifford Algebras*, **9**, 119-130. http://dx.doi.org/10.1007/BF03041944

[4] Davies, A.J. (1990) Quaternionic Dirac Equation. *Physical Review D*, **41**, 2628-2630. http://dx.doi.org/10.1103/PhysRevD.41.2628

[5] Schwartz, C. (2006) Relativistic Quaternionic Wave Equation. *Journal of Mathematical Physics*, **47**, Article ID: 122301. http://dx.doi.org/10.1063/1.2397555

[6] Liu, Y.-F. (2002) Triality, Biquaternion and Vector Representation of the Dirac Equation. *Advances in Applied Clifford Algebras*, **12**, 109-124. http://dx.doi.org/10.1007/BF03161242

[7] Gogberashvili, M. (2006) Octonionic Electrodynamics. *Journal of Physics A*: *Mathematics in General*, **39**, 7099-7104. http://dx.doi.org/10.1088/0305-4470/39/22/020

[8] Gamba, A. (1998) Maxwell's Equations in Octonion Form. *NuovoCimento A*, **111**, 293-302.

[9] Tolan, T., Özdas, K. and Tanisli, M. (2006) Reformulation of Electromagnetism with Octonions. *Nuovo Cimento B*, **121**, 43-55. http://dx.doi.org/10.1393/ncb/i2005-10189-9

[10] Gogberashvili, M. (2006) Octonionic Version of Dirac Equations. *International Journal of Modern Physics A*, **21**, 3513-3523. http://dx.doi.org/10.1142/S0217751X06028436

[11] De Leo, S. and Abdel-Khalek, K. (1996) Octonionic Dirac Equation. *Progress in Theoretical Physics*, **96**, 833-846. http://dx.doi.org/10.1143/PTP.96.833

[12] Dickson, L.E. (1919) On Quaternions and Their Generalization and the History of the Eight Square Theorem. *Annals of Mathematics*, **20**, 155-171. http://dx.doi.org/10.2307/1967865

[13] Imaeda, K. and Imaeda, M. (2000) Sedenions: Algebra and Analysis. *Applied Mathematics and Computations*, **115**, 77-88. http://dx.doi.org/10.1016/S0096-3003(99)00140-X

[14] Carmody, K. (1988) Circular and Hyperbolic Quaternions, Octonions, and Sedenions. *Applied Mathematics and Computations*, **28**, 47-72. http://dx.doi.org/10.1016/0096-3003(88)90133-6

[15] Carmody, K. (1997) Circular and Hyperbolic Quaternions, Octonions, and Sedenions—Further Results. *Applied Mathematics and Computations*, **84**, 27-47. http://dx.doi.org/10.1016/S0096-3003(96)00051-3

[16] Köplinger, J. (2006) Dirac Equation on Hyperbolic Octonions. *Applied Mathematics and Computations*, **182**, 443-446. http://dx.doi.org/10.1016/j.amc.2006.04.005

[17] Mironov, V.L. and Mironov, S.V. (2009) Octonic Representation of Electromagnetic Field Equations. *Journal of Mathematical Physics*, **50**, Article ID: 012901. http://dx.doi.org/10.1063/1.3041499

[18] Mironov, V.L. and Mironov, S.V. (2009) Octonic Second-Order Equations of Relativistic Quantum Mechanics. *Journal of Mathematical Physics*, **50**, Article ID: 012302. http://dx.doi.org/10.1142/S0217751X09045480

[19] Mironov, V.L. and Mironov, S.V. (2009) Octonic First-Order Equations of Relativistic Quantum Mechanics. *International Journal of Modern Physics A*, **24**, 4157-4167. http://dx.doi.org/10.1142/S0217751X09045480

[20] Mironov, V.L. and Mironov, S.V. (2011) Noncommutative Sedeons and Their Application in Field Theory. e-Print. http://arxiv.org/abs/1111.4035

[21] Mironov, V.L. and Mironov, S.V. (2013) Reformulation of Relativistic Quantum Mechanics Equations with Non-Commutative Sedeons. *Applied Mathematics*, **4**, 53-60. http://dx.doi.org/10.4236/am.2013.410A3007

[22] Mironov, V.L. and Mironov, S.V. (2014) Sedeonic Equations of Gravitoelectromagnetism. *Journal of Modern Physics*, **5**, 917-927. http://dx.doi.org/10.4236/jmp.2014.510095

[23] Mironov, S.V. and Mironov, V.L. (2014) Sedeonic Equations of Massive Fields. *International Journal of Theoretical*

Physics, e-Print. http://vixra.org/abs/1311.0005

[24] Mironov, S.V. and Mironov, V.L. (2014) Space-Time Sedeons and Their Application in Relativistic Quantum Mechanics and Field Theory. Institute for Physics of Microstructures RAS, Nizhny Novgorod. http://vixra.org/abs/1407.0068

[25] Landau, L.D. and Lifshits, E.M. (1975) Classical Theory of Fields. 4th Edition, Pergamon Press, New York.

[26] Dirac, P.A.M. (1958) The Principles of Quantum Mechanics. Clarendon Press, Oxford.

[27] Cafaro, C. and Ali, S.A. (2006) The Spacetime Algebra Approach to Massive Classical Electrodynamics with Magnetic Monopoles. *Advances in Applied Clifford Algebras*, **17**, 23-36. http://dx.doi.org/10.1007/s00006-006-0014-7

[28] Macfarlane, A. (1900) Hyperbolic Quaternions. *Proceedings of the Royal Society at Edinburgh*, **1899-1900 Session**, 169-181.

[29] Hamilton, W.R. (1853) Lectures on Quaternions. Royal Irish Academy, Dublin.

Applied Mathematics, **2015**, **6**, **57-70**
Published Online January 2015 in SciRes. http://www.scirp.org/journal/am
http://dx.doi.org/10.4236/am.2015.61007

The Distribution of the Concentration Ratio for Samples from a Uniform Population

Giovanni Girone, Antonella Nannavecchia

Faculty of Economics, University of Bari, Bari, Italy
Email: giovanni.girone@uniba.it, nannavecchia@lum.it

Received 24 October 2014; revised 20 November 2014; accepted 16 December 2014

Abstract

In the present paper we derived, with direct method, the exact expressions for the sampling probability density function of the Gini concentration ratio for samples from a uniform population of size *n* = 6, 7, 8, 9 and 10. Moreover, we found some regularities of such distributions valid for any sample size.

Keywords

Gini Concentration Ratio, Uniform Distribution, Order Statistics, Probability Density Function

1. Introduction

In 1914 Corrado Gini [1] introduced the concentration ratio R for the measure of inequality among values of a frequency distribution. The Gini index is widely used in fields as diverse as sociology, health science, engineering, and in particular, economics to measure the inequality of income distribution.

Various aspects of the Gini index have been taken into account. One of the most interesting topics regards the estimation of the concentration ratio (Hoeffding, 1948 [2]; Glasser, 1962 [3]; Cucconi, 1965 [4]; Dall'Aglio, 1965 [5]). More recently, Deltas (2003) [6] discussed the sources of bias of the Gini coefficient for small samples. This has implications for the comparison of inequality among subsamples, some of which may be small, and the use of the Gini index in measuring firm size inequality in markets with a small number of firms. Barret and Donald (2009) [7] considered statistical inference for consistent estimators of generalized Gini indices. The empirical indices are shown to be asymptotically normally distributed using functional limit theory. Moreover, asymptotic variance expressions are obtained using influence functions. Davidson (2009) [8] derived an approximation for the estimator of the Gini index by which it is expressed as a sum of IID random variables. This approximation allows developing a reliable standard error that is simple to compute. Fakoor, Ghalibaf and Azarnoosh (2011) [9] considered nonparametric estimators of the Gini index based on a sample from length-bi-

How to cite this paper: Girone, G. and Nannavecchia, A. (2015) The Distribution of the Concentration Ratio for Samples from a Uniform Population. *Applied Mathematics*, **6**, 57-70. http://dx.doi.org/10.4236/am.2015.61007

ased distributions. They showed that these estimators are strongly consistent for the Gini index. Also, they obtained an asymptotic normality for the corresponding Gini index.

Girone (1968) [10] focused on the study of the sampling distribution of the Gini index and in 1971 [11] derived the exact expression for samples drawn from an exponential population. In 1971 Girone [12] obtained, with direct method, the sampling distribution function of the Gini ratio for samples of size $n \leq 5$ drawn from a uniform population.

In the present note (Section 2), we calculate the joint probability density function (p.d.f.) of the random sample of size *n* and, then, the joint p.d.f. of the *n* order statistics. Hence, we transform one of the order statistics in their average and the remaining $n - 1$ order statistics are divided by the same average. We calculate the joint p.d.f. of the new *n* variables and integrating with respect to the average we obtain the joint p.d.f. of the other $n - 1$ variables. One of these variables is transformed in the concentration ratio. We calculate the joint p.d.f. of the concentration ratio and of the other $n - 2$ variables and at last we integrate this p.d.f. with respect to the $n - 2$ variables obtaining the marginal p.d.f. of the concentration ratio. The main difficulty of this procedure consists in the identification of the region of integration of the $n - 2$ variables, for two reasons: firstly the need to decompose this region into subregions which allow identifying directly the limits of integration and secondly the growing number of such subregions that makes the derivation heavy.

In Sections 3-7, using the software Mathematica, we derive the exact distributions of the concentration ratio for samples from a uniform distribution of size $n = 6, 7, 8, 9$ and 10. Moreover (Section 8), we find some regularities of such distributions valid for any sample size.

2. The Procedure to Derive the Distribution of the Concentration Ratio

Let random variables $X_1, X_2, \cdots, X_n$ from a uniform population have p.d.f.

$$f(x) = \begin{cases} 1, & 0 < x < 1, \\ 0, & \text{elsewhere.} \end{cases} \tag{1}$$

The joint p.d.f. of the variables is

$$h(x_1, x_2, \cdots, x_n) = \begin{cases} 1, & 0 < x_i < 1, \ \text{for } i = 1, 2, \cdots, n, \\ 0, & \text{elsewhere.} \end{cases} \tag{2}$$

The joint p.d.f. of the order statistics $X_{(1)}, X_{(2)}, \cdots, X_{(n)}$ is

$$h\left(x_{(1)}, x_{(2)}, \cdots, x_{(n)}\right) = \begin{cases} n!, & 0 < x_{(1)} < x_{(2)} < \cdots < x_{(n)} < 1, \\ 0, & \text{elsewhere.} \end{cases} \tag{3}$$

By transforming the variables

$$S = X_{(1)} + X_{(2)} + \cdots + X_{(n)},$$

$$D_{(i)} = \frac{X_{(i)}}{S}, \quad \text{for } i = 1, 2, \cdots, n-1,$$

whose Jacobian is

$$J = S^{n-1},$$

we obtain the joint p.d.f. of the variables *S* and $D_{(1)}, D_{(2)}, \cdots, D_{(n-1)}$ that can be written as

$$g\left(s, d_{(1)}, d_{(2)}, \cdots, d_{(n-1)}\right) = (n-1)! s^{n-1}, \tag{4}$$

$$\text{for } 0 < sd_{(1)} < sd_{(2)} < \cdots < sd_{(n-1)} < s\left(1 - d_{(1)} - d_{(2)} - \cdots - d_{(n-1)}\right) < 1.$$

We integrate expression [4] with respect to the variable *S* and obtain the joint p.d.f. of the variables $D_{(1)}, D_{(2)}, \cdots, D_{(n-1)}$ that can be written as

$$f\left(d_{(1)},d_{(2)},\cdots,d_{(n-1)}\right)=\frac{(n-1)!}{\left(1-d_{(1)}-d_{(2)}-\cdots-d_{(n-1)}\right)^{n}},\tag{5}$$

for $0<d_{(1)}<d_{(2)}<\cdots<d_{(n-1)}<1-d_{(1)}-d_{(2)}-\cdots-d_{(n-1)}$.

By transforming the variable $D_{(n-1)}$ in the variable R *i.e.* the concentration ratio

$$R=1-\frac{2}{n-1}\sum_{i=1}^{n-1}(n-i)D_{(i)},$$

from which we get

$$D_{(n-1)}=\frac{(n-1)(1-R)}{2}-\sum_{i=1}^{n-2}(n-i)D_{(i)},$$

the Jacobian of the transformation is

$$J=\frac{n-1}{2}$$

and the joint p.d.f. of the variable R and $D_{(1)},D_{(2)},\cdots,D_{(n-2)}$ is

$$h\left(d_{(1)},d_{(2)},\cdots,d_{(n-2)},R\right)=\frac{2^{n}(n-1)!}{\left(2-(n-1)(1-R)+2\sum_{i=1}^{n-2}(n-i-1)d_{(i)}\right)^{n}},\tag{6}$$

for

$$0<d_{(1)}<d_{(2)}<\cdots<d_{(n-2)}<\frac{(n-1)(1-R)}{2}-\sum_{i=1}^{n-2}(n-i)d_{(i)}<1-\frac{(n-1)(1-R)}{2}+\sum_{i=1}^{n-2}(n-i-1)d_{(i)}.\tag{7}$$

By integrating expression [6] with respect to the variables $D_{(1)},D_{(2)},\cdots,D_{(n-2)}$ over the regions determined by inequalities [7], we get the marginal p.d.f. of the concentration ratio R.

3. The Distribution of the Concentration Ratio for *n* = 6

The procedure indicated in Section 2 is used to obtain the following p.d.f. (**Figure 1**) of the concentration ratio R for random samples of size $n = 6$:

$$g(R)=\frac{27}{50\left(\frac{1}{5}+R\right)^{2}}-\frac{1728}{25\left(\frac{2}{5}+R\right)^{2}}+\frac{19683}{25\left(\frac{3}{5}+R\right)^{2}}-\frac{55296}{25\left(\frac{4}{5}+R\right)^{2}}+\frac{3375}{2(1+R)^{2}},\ \text{for } 0<R<\frac{1}{5},$$

$$g(R)=-\frac{125}{144R^{2}}+\frac{7853}{75\left(\frac{1}{5}+R\right)^{2}}-\frac{449523}{400\left(\frac{2}{5}+R\right)^{2}}+\frac{677147}{225\left(\frac{3}{5}+R\right)^{2}}-\frac{55296}{25\left(\frac{4}{5}+R\right)^{2}},\ \text{for } \frac{1}{5}<R<\frac{2}{5},$$

$$g(R)=\frac{32}{75\left(-\frac{1}{5}+R\right)^{2}}-\frac{11131}{240R^{2}}+\frac{33773}{75\left(\frac{1}{5}+R\right)^{2}}-\frac{449523}{400\left(\frac{2}{5}+R\right)^{2}}+\frac{19683}{25\left(\frac{3}{5}+R\right)^{2}},\ \text{for } \frac{2}{5}<R<\frac{3}{5},$$

$$g(R)=-\frac{27}{400\left(-\frac{2}{5}+R\right)^{2}}+\frac{437}{75\left(-\frac{1}{5}+R\right)^{2}}-\frac{11131}{240R^{2}}+\frac{7853}{75\left(\frac{1}{5}+R\right)^{2}}-\frac{1728}{25\left(\frac{2}{5}+R\right)^{2}},\ \text{for } \frac{3}{5}<R<\frac{4}{5},$$

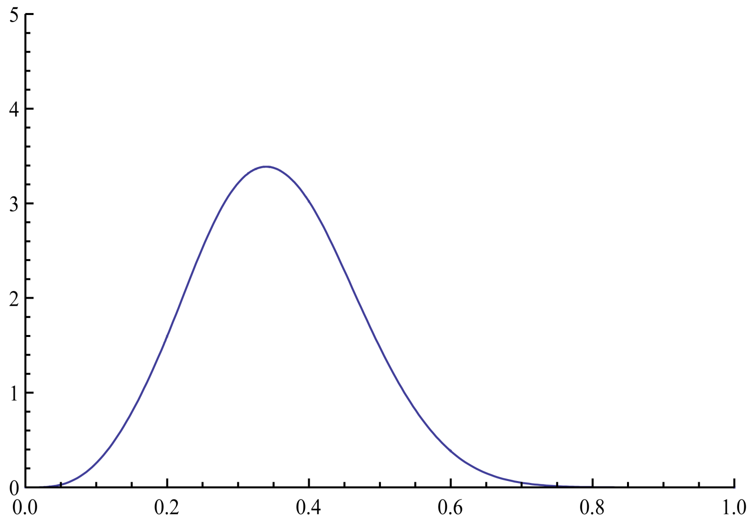

Figure 1. Probability density function of the concentration ratio R for random samples of size n = 6 from a uniform population.

$$g(R)=\frac{1}{450\left(-\frac{3}{5}+R\right)^2}-\frac{27}{400\left(-\frac{2}{5}+R\right)^2}+\frac{32}{75\left(-\frac{1}{5}+R\right)^2}-\frac{125}{144R^2}+\frac{27}{50\left(\frac{1}{5}+R\right)^2},\ \text{for } \frac{4}{5}<R<1.$$

Characteristic values of the distribution are:

mean $E(R)=-3+\frac{11696\log 2}{15}+\frac{243\log 3}{2}-\frac{1250\log 5}{3}=0.35222,$

second moment $E\left(R^2\right)=16-\frac{69056\log 2}{25}-\frac{24219\log 3}{50}+\frac{18125\log 5}{12}=0.13716,$

third moment $E\left(R^3\right)=-\frac{1368}{25}+\frac{678688\log 2}{125}+\frac{156006\log 3}{125}-\frac{12625\log 5}{4}=0.05785,$

fourth moment $E\left(R^4\right)=\frac{89237}{625}-\frac{25434496\log 2}{3125}-\frac{7691436\log 3}{3125}+\frac{15290\log 5}{3}=0.02606,$

standard deviation $\sigma(R)=0.11444,$

index of skewness $\gamma_1(R)=0.20793,$

index of kurtosis $\gamma_2(R)=-0.16767.$

The distribution of the concentration ratio R for samples of size n = 6 from a uniform population shows a slight positive skewness and platykurtosis.

4. The Distribution of the Concentration Ratio for n = 7

The procedure indicated in Section 2 is used to obtain the following p.d.f. (**Figure 2**) of the concentration ratio R for random samples of size n = 7:

$$g(R)=-\frac{117649}{518400\left(\frac{1}{6}+R\right)^2}+\frac{117649}{1620\left(\frac{2}{6}+R\right)^2}-\frac{1058841}{640\left(\frac{3}{6}+R\right)^2}+\frac{3764768}{405\left(\frac{4}{6}+R\right)^2}$$
$$-\frac{367653125}{20736\left(\frac{5}{6}+R\right)^2}+\frac{1058841}{100(1+R)^2},\quad \text{for } 0<R<\frac{1}{6},$$

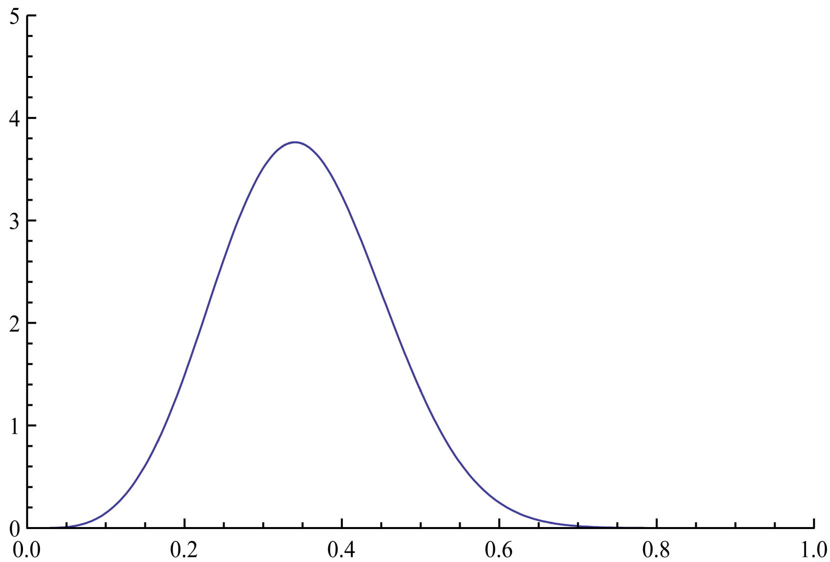

Figure 2. Probability density function of the concentration ratio R for random samples of size $n = 7$ from a uniform population.

$$g(R)=\frac{9}{20R^2}-\frac{14356253}{103680\left(\frac{1}{6}+R\right)^2}+\frac{2450309}{810\left(\frac{2}{6}+R\right)^2}-\frac{2099205}{128\left(\frac{3}{6}+R\right)^2}+\frac{49230947}{1620\left(\frac{4}{6}+R\right)^2}-\frac{367653125}{20736\left(\frac{5}{6}+R\right)^2},\quad \text{for } \frac{1}{6}<R<\frac{2}{6},$$

$$g(R)=-\frac{3125}{10368\left(-\frac{1}{6}+R\right)^2}+\frac{7853}{90R^2}-\frac{46303907}{25920\left(\frac{1}{6}+R\right)^2}+\frac{7450309}{810\left(\frac{2}{6}+R\right)^2}-\frac{2099205}{128\left(\frac{3}{6}+R\right)^2}+\frac{3764768}{405\left(\frac{4}{6}+R\right)^2},\quad \text{for } \frac{2}{6}<R<\frac{3}{6},$$

$$g(R)=\frac{32}{405\left(-\frac{2}{6}+R\right)^2}-\frac{1064201}{51840\left(-\frac{1}{6}+R\right)^2}+\frac{33773}{90R^2}-\frac{46303907}{25920\left(\frac{1}{6}+R\right)^2}+\frac{2450309}{810\left(\frac{2}{6}+R\right)^2}-\frac{1058841}{640\left(\frac{3}{6}+R\right)^2},\quad \text{for } \frac{3}{6}<R<\frac{4}{6},$$

$$g(R)=-\frac{9}{1280\left(-\frac{3}{6}+R\right)^2}+\frac{463}{324\left(-\frac{2}{6}+R\right)^2}-\frac{1064201}{51840\left(-\frac{1}{6}+R\right)^2}+\frac{7853}{90R^2}-\frac{14356253}{103680\left(\frac{1}{6}+R\right)^2}+\frac{117649}{1620\left(\frac{2}{6}+R\right)^2},\quad \text{for } \frac{4}{6}<R<\frac{5}{6},$$

$$g(R)=\frac{1}{8100\left(-\frac{4}{6}+R\right)^2}-\frac{9}{1280\left(-\frac{3}{6}+R\right)^2}+\frac{32}{405\left(-\frac{2}{6}+R\right)^2}-\frac{3125}{10368\left(-\frac{1}{6}+R\right)^2}+\frac{9}{20R^2}-\frac{117649}{518400\left(\frac{1}{6}+R\right)^2},\quad \text{for } \frac{5}{6}<R<1.$$

Characteristic values of the distribution are:

mean $E(R)=-\frac{7}{2}+\frac{35072\log 2}{15}-\frac{21797\log 3}{160}+\frac{359375\log 5}{288}+\frac{823543\log 7}{1440}=0.34951,$

second moment $E(R^2)=\frac{763}{36}+\frac{3806128\log 2}{405}+\frac{451251\log 3}{80}-\frac{359375\log 5}{72}-\frac{15647317\log 7}{6480}=0.13291,$

third moment

$$E(R^3)=-\frac{18179}{216}-\frac{2771144\log 2}{135}-\frac{4266351\log 3}{320}+\frac{18546875\log 5}{1728}+\frac{5764801\log 7}{960}=0.05417,$$

fourth moment

$$E(R^4)=\frac{165193}{648}+\frac{40601588\log 2}{1215}+\frac{7638867\log 3}{320}+\frac{263234375\log 5}{15552}-\frac{895191241\log 7}{77760}=0.02342,$$

standard deviation $\sigma(R)=0.10367,$

index of skewness $\gamma_1(R)=0.18545,$

index of kurtosis $\gamma_2(R)=-0.14535.$

The distribution of the concentration ratio R for samples of size $n = 7$ from a uniform population shows slight positive skewness and platykurtosis, both lower than those obtained for samples of size $n = 6$.

5. The Distribution of the Concentration Ratio for $n = 8$

The procedure indicated in Section 2 is used to obtain the following p.d.f. (Figure 3) of the concentration ratio R for random samples of size $n = 8$:

$$g(R)=\frac{8192}{99225\left(\frac{1}{7}+R\right)^2}-\frac{2097152}{33075\left(\frac{2}{7}+R\right)^2}+\frac{663552}{245\left(\frac{3}{7}+R\right)^2}-\frac{536870912}{19845\left(\frac{4}{7}+R\right)^2}+\frac{128000000}{1323\left(\frac{5}{7}+R\right)^2}-\frac{169869312}{1225\left(\frac{6}{7}+R\right)^2}+\frac{137682944}{2025(1+R)^2},\quad \text{for } 0<R<\frac{1}{7},$$

$$g(R)=-\frac{16807}{86400R^2}+\frac{9613463}{66150\left(\frac{1}{7}+R\right)^2}-\frac{2548367503}{423360\left(\frac{2}{7}+R\right)^2}+\frac{386863168}{6615\left(\frac{3}{7}+R\right)^2}-\frac{173031518287}{846720\left(\frac{4}{7}+R\right)^2}+\frac{19007619787}{66150\left(\frac{5}{7}+R\right)^2}-\frac{169869312}{1225\left(\frac{6}{7}+R\right)^2},\quad \text{for } \frac{1}{7}<R<\frac{2}{7},$$

$$g(R)=\frac{81}{490\left(-\frac{1}{7}+R\right)^2}-\frac{14356253}{120960R^2}+\frac{31094051}{6615\left(\frac{1}{7}+R\right)^2}-\frac{18601017487}{423360\left(\frac{2}{7}+R\right)^2}+\frac{1969741961}{13230\left(\frac{3}{7}+R\right)^2}-\frac{173031518287}{846720\left(\frac{4}{7}+R\right)^2}+\frac{128000000}{1323\left(\frac{5}{7}+R\right)^2},\quad \text{for } \frac{2}{7}<R<\frac{3}{7},$$

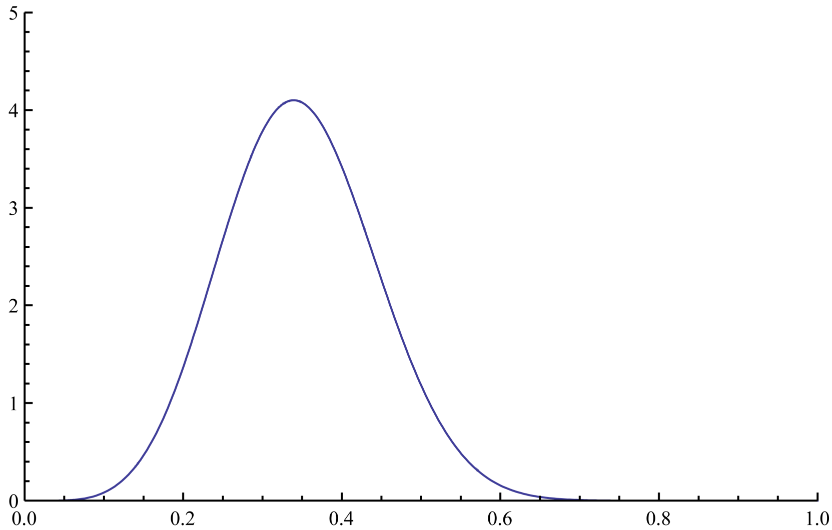

Figure 3. Probability density function of the concentration ratio R for random samples of size $n = 8$ from a uniform population.

$$g(R) = -\frac{15625}{254016\left(-\frac{2}{7}+R\right)^2} + \frac{274531}{6615\left(-\frac{1}{7}+R\right)^2} - \frac{46303907}{30240R^2} + \frac{268282153}{19845\left(\frac{1}{7}+R\right)^2}$$
$$-\frac{18601017487}{423360\left(\frac{2}{7}+R\right)^2} + \frac{386863168}{6615\left(\frac{3}{7}+R\right)^2} - \frac{536870912}{19845\left(\frac{4}{7}+R\right)^2}, \quad \text{for } \frac{3}{7} < R < \frac{4}{7},$$

$$g(R) = \frac{64}{6615\left(-\frac{3}{7}+R\right)^2} - \frac{2472719}{423360\left(-\frac{2}{7}+R\right)^2} + \frac{1254307}{6615\left(-\frac{1}{7}+R\right)^2} - \frac{46303907}{30240R^2}$$
$$+\frac{31094051}{6615\left(\frac{1}{7}+R\right)^2} - \frac{2548367503}{423360\left(\frac{2}{7}+R\right)^2} + \frac{663552}{245\left(\frac{3}{7}+R\right)^2}, \quad \text{for } \frac{4}{7} < R < \frac{5}{7},$$

$$g(R) = -\frac{81}{156800\left(-\frac{4}{7}+R\right)^2} + \frac{15949}{66150\left(-\frac{3}{7}+R\right)^2} - \frac{2472719}{423360\left(-\frac{2}{7}+R\right)^2} + \frac{274531}{6615\left(-\frac{1}{7}+R\right)^2}$$
$$-\frac{14356253}{120960R^2} + \frac{9613463}{66150\left(\frac{1}{7}+R\right)^2} - \frac{2097152}{33075\left(\frac{2}{7}+R\right)^2}, \quad \text{for } \frac{5}{7} < R < \frac{6}{7},$$

$$g(R) = \frac{1}{198450\left(-\frac{5}{7}+R\right)^2} - \frac{81}{156800\left(-\frac{4}{7}+R\right)^2} + \frac{64}{6615\left(-\frac{3}{7}+R\right)^2} - \frac{15625}{254016\left(-\frac{2}{7}+R\right)^2}$$
$$+\frac{81}{490\left(-\frac{1}{7}+R\right)^2} - \frac{16807}{86400R^2} + \frac{8192}{99225\left(\frac{1}{7}+R\right)^2}, \quad \text{for } \frac{6}{7} < R < 1.$$

Characteristic values of the distribution are:

mean $E(R) = -4 + \frac{3475456\log 2}{315} + \frac{2775303\log 3}{560} - \frac{2421875\log 5}{1008} - \frac{3411821\log 7}{720} = 0.34747,$

second moment $E(R^2) = \frac{190}{7} - \frac{3184576\log 2}{63} - \frac{8776431\log 3}{392} + \frac{4140625\log 5}{392} + \frac{7882483\log 7}{360} = 0.12985,$

third moment

$$E(R^3) = -\frac{6016}{49} + \frac{658405376\log 2}{5145} + \frac{1492752159\log 3}{27440} - \frac{129921875\log 5}{5488} - \frac{13596863\log 7}{240} = 0.05160,$$

fourth moment

$$E(R^4) = \frac{145475}{343} - \frac{3729880384\log 2}{15435} - \frac{2307400911\log 3}{24010} + \frac{533984375\log 5}{14406} + \frac{9851303\log 7}{90} = 0.02162,$$

standard deviation $\sigma(R) = 0.09544,$
index of skewness $\gamma_1(R) = 0.16867,$
index of kurtosis $\gamma_2(R) = -0.12824.$

The distribution of the concentration ratio R for samples of size $n = 8$ from a uniform population shows slight positive skewness and platykurtosis, both lower than those obtained for samples of size $n = 6$ and 7.

6. The Distribution of the Concentration Ratio for *n* = 9

The procedure indicated in Section 2 is used to obtain the following p.d.f. (**Figure 4**) of the concentration ratio R for random samples of size $n = 9$:

$$g(R) = -\frac{531441}{20070400\left(\frac{1}{8}+R\right)^2} + \frac{531441}{11200\left(\frac{2}{8}+R\right)^2} - \frac{10460353203}{2867200\left(\frac{3}{8}+R\right)^2} + \frac{2125764}{35\left(\frac{4}{8}+R\right)^2}$$
$$-\frac{41518828125}{114688\left(\frac{5}{8}+R\right)^2} + \frac{10460353203}{11200\left(\frac{6}{8}+R\right)^2} - \frac{437664515463}{409600\left(\frac{7}{8}+R\right)^2} + \frac{544195584}{1225(1+R)^2}, \quad \text{for } 0 < R < \frac{1}{8},$$

$$g(R) = \frac{1024}{14175R^2} - \frac{9819117949}{77414400\left(\frac{1}{8}+R\right)^2} + \frac{15242823}{1600\left(\frac{2}{8}+R\right)^2} - \frac{1441266427931}{9289728\left(\frac{3}{8}+R\right)^2} + \frac{857395628}{945\left(\frac{4}{8}+R\right)^2}$$
$$-\frac{6604248318741}{2867200\left(\frac{5}{8}+R\right)^2} + \frac{2358496602787}{907200\left(\frac{6}{8}+R\right)^2} - \frac{437664515463}{409600\left(\frac{7}{8}+R\right)^2}, \quad \text{for } \frac{1}{8} < R < \frac{2}{8},$$

$$g(R) = -\frac{823543}{11059200\left(-\frac{1}{8}+R\right)^2} + \frac{9613463}{75600R^2} - \frac{715845826021}{77414400\left(\frac{1}{8}+R\right)^2} + \frac{1262942489}{8640\left(\frac{2}{8}+R\right)^2}$$
$$-\frac{2582172507227}{3096576\left(\frac{3}{8}+R\right)^2} + \frac{156844988749}{75600\left(\frac{4}{8}+R\right)^2} - \frac{6604248318741}{2867200\left(\frac{5}{8}+R\right)^2} + \frac{10460353203}{11200\left(\frac{6}{8}+R\right)^2}, \quad \text{for } \frac{2}{8} < R < \frac{3}{8},$$

$$g(R) = \frac{81}{2240\left(-\frac{1}{8}+R\right)^2} - \frac{183689449}{3096576\left(-\frac{2}{8}+R\right)^2} + \frac{31094051}{7560R^2} - \frac{193012968877}{3096576\left(\frac{1}{8}+R\right)^2}$$
$$+\frac{2971536239}{8640\left(\frac{2}{8}+R\right)^2} - \frac{2582172507227}{3096576\left(\frac{3}{8}+R\right)^2} + \frac{857395628}{945\left(\frac{4}{8}+R\right)^2} - \frac{41518828125}{114688\left(\frac{5}{8}+R\right)^2}, \quad \text{for } \frac{3}{8} < R < \frac{4}{8},$$

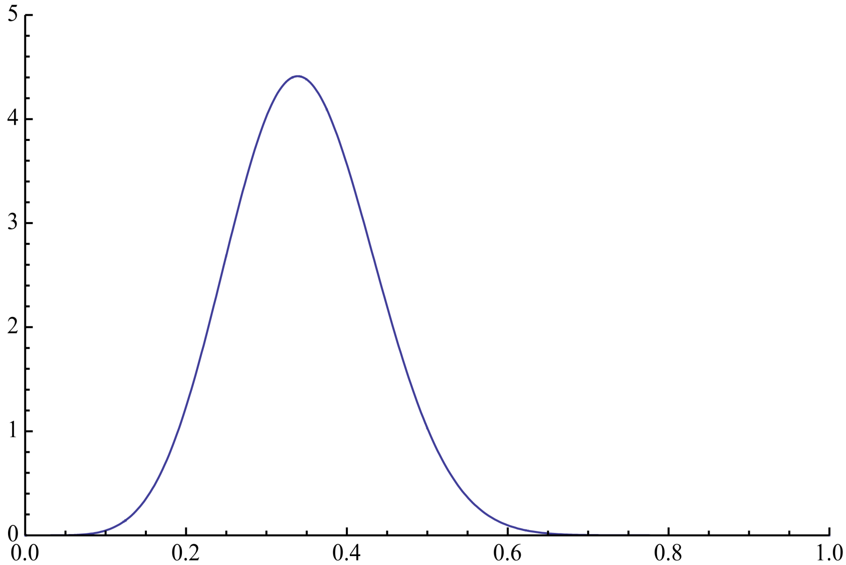

Figure 4. Probability density function of the concentration ratio R for random samples of size $n = 9$ from a uniform population.

$$g(R) = -\frac{78125}{9289728\left(-\frac{3}{8}+R\right)^2} + \frac{783437}{60480\left(-\frac{2}{8}+R\right)^2} - \frac{2575720699}{3096576\left(-\frac{1}{8}+R\right)^2} + \frac{268282153}{22680R^2} - \frac{193012968877}{3096576\left(\frac{1}{8}+R\right)^2} + \frac{1262942489}{8640\left(\frac{2}{8}+R\right)^2} - \frac{1441266427931}{9289728\left(\frac{3}{8}+R\right)^2} + \frac{2125764}{35\left(\frac{4}{8}+R\right)^2}, \quad \text{for } \frac{4}{8} < R < \frac{5}{8},$$

$$g(R) = \frac{4}{4725\left(-\frac{4}{8}+R\right)^2} - \frac{90129527}{77414400\left(-\frac{3}{8}+R\right)^2} + \frac{19593601}{302400\left(-\frac{2}{8}+R\right)^2} - \frac{2575720699}{3096576\left(-\frac{1}{8}+R\right)^2} + \frac{31094051}{7560R^2} - \frac{715845826021}{77414400\left(\frac{1}{8}+R\right)^2} + \frac{15242823}{1600\left(\frac{2}{8}+R\right)^2} - \frac{10460353203}{2867200\left(\frac{3}{8}+R\right)^2}, \quad \text{for } \frac{5}{8} < R < \frac{6}{8},$$

$$g(R) = -\frac{81}{2867200\left(-\frac{5}{8}+R\right)^2} + \frac{2251}{75600\left(-\frac{4}{8}+R\right)^2} - \frac{90129527}{77414400\left(-\frac{3}{8}+R\right)^2} + \frac{783437}{60480\left(-\frac{2}{8}+R\right)^2} - \frac{183689449}{3096576\left(-\frac{1}{8}+R\right)^2} + \frac{9613463}{75600R^2} - \frac{9819117949}{77414400\left(\frac{1}{8}+R\right)^2} + \frac{531441}{11200\left(\frac{2}{8}+R\right)^2}, \quad \text{for } \frac{6}{8} < R < \frac{7}{8},$$

$$g(R) = \frac{1}{6350400\left(-\frac{6}{8}+R\right)^2} - \frac{81}{2867200\left(-\frac{5}{8}+R\right)^2} + \frac{4}{4725\left(-\frac{4}{8}+R\right)^2} - \frac{78125}{9289728\left(-\frac{3}{8}+R\right)^2} + \frac{81}{2240\left(-\frac{2}{8}+R\right)^2} - \frac{823543}{11059200\left(-\frac{1}{8}+R\right)^2} + \frac{1024}{14175R^2} - \frac{531441}{20070400\left(\frac{1}{8}+R\right)^2}, \quad \text{for } \frac{7}{8} < R < 1.$$

Characteristic values of the distribution are:

mean $E(R) = -\frac{9}{2} - \frac{18425272\log 2}{315} - \frac{1948617\log 3}{1120} + \frac{1953125\log 5}{576} + \frac{109531219\log 7}{5760} = 0.34589,$

second moment

$$E(R^2) = \frac{1083}{32} + \frac{31176874\log 2}{105} + \frac{209048769\log 3}{35840} - \frac{150390625\log 5}{9216} - \frac{1101076991\log 7}{11520} = 0.12754,$$

third moment

$$E(R^3) = -\frac{43983}{256} - \frac{69161579\log 2}{84} + \frac{394860663\log 3}{57344} + \frac{947265625\log 5}{24576} + \frac{31654522291\log 7}{122880} = 0.04969,$$

fourth moment

$$E(R^4) = \frac{2732815}{4096} + \frac{58613649\log 2}{35} - \frac{36660941253\log 3}{458752} - \frac{36018359375\log 5}{589824} - \frac{739122430613\log 7}{1474560} = 0.02032,$$

standard deviation $\sigma(R) = 0.08889,$

index of skewness $\gamma_1(R) = 0.15559,$

index of kurtosis $\gamma_2(R) = -0.11467.$

The distribution of the concentration ratio R for samples of size $n = 9$ from a uniform population shows slight positive skewness and platykurtosis, both lower than those obtained for samples of size $n = 6$, 7 and 8.

7. The Distribution of the Concentration Ratio for $n = 10$

The procedure indicated in Section 2 is used to obtain the following p.d.f. (Figure 5) of the concentration ratio R for random samples of size $n = 10$:

$$g(R) = \frac{78125}{10287648\left(\frac{1}{9}+R\right)^2} - \frac{10000000}{321489\left(\frac{2}{9}+R\right)^2} + \frac{234375}{56\left(\frac{3}{9}+R\right)^2} - \frac{5120000000}{45927\left(\frac{4}{9}+R\right)^2} + \frac{762939453125}{734832\left(\frac{5}{9}+R\right)^2}$$

$$- \frac{30000000}{7\left(\frac{6}{9}+R\right)^2} + \frac{450375078125}{52488\left(\frac{7}{9}+R\right)^2} - \frac{2621440000000}{321489\left(\frac{8}{9}+R\right)^2} + \frac{4613203125}{1568(1+R)^2}, \quad \text{for } 0 < R < \frac{1}{9},$$

$$g(R) = -\frac{59049}{2508800R^2} + \frac{6102360983}{64297800\left(\frac{1}{9}+R\right)^2} - \frac{29486161727807}{2351462400\left(\frac{2}{9}+R\right)^2} + \frac{91871139}{280\left(\frac{3}{9}+R\right)^2} - \frac{282890791328125}{94058496\left(\frac{4}{9}+R\right)^2}$$

$$+ \frac{112482309211387}{9185400\left(\frac{5}{9}+R\right)^2} - \frac{78160683773061}{793800\left(\frac{6}{9}+R\right)^2} + \frac{1465749080718869}{64297800\left(\frac{7}{9}+R\right)^2} - \frac{2621440000000}{321489\left(\frac{8}{9}+R\right)^2}, \quad \text{for } \frac{1}{9} < R < \frac{2}{9},$$

$$g(R) = \frac{32768}{1148175\left(-\frac{1}{9}+R\right)^2} - \frac{9819117949}{87091200R^2} + \frac{133551832049}{9185400\left(\frac{1}{9}+R\right)^2}$$

$$- \frac{34956443674391}{1161216\left(\frac{2}{9}+R\right)^2} + \frac{227124686777}{68040\left(\frac{3}{9}+R\right)^2} - \frac{4488452581986787}{335923200\left(\frac{4}{9}+R\right)^2}$$

$$+ \frac{239423780652283}{9185400\left(\frac{5}{9}+R\right)^2} - \frac{8684520419229}{358400\left(\frac{6}{9}+R\right)^2} + \frac{450375078125}{52488\left(\frac{7}{9}+R\right)^2}, \quad \text{for } \frac{2}{9} < R < \frac{3}{9},$$

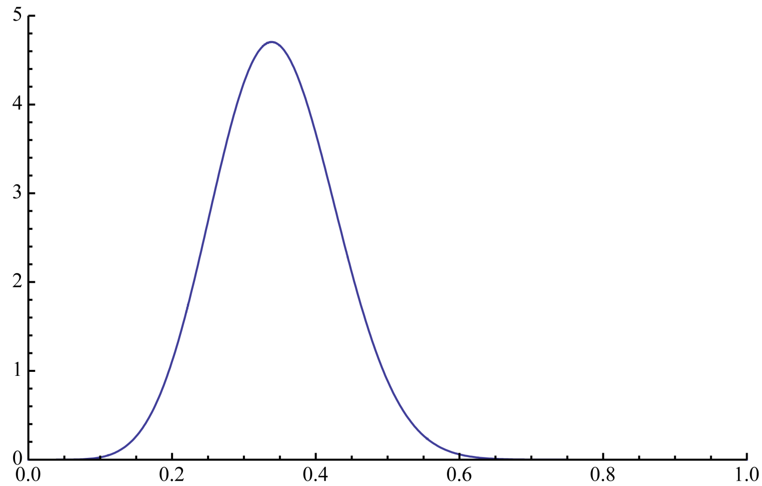

Figure 5. Probability density function of the concentration ratio R for random samples of size $n = 10$ from a uniform population.

$$
\begin{aligned}
g(R) = {} & -\frac{5764801}{335923200\left(-\frac{2}{9}+R\right)^2}+\frac{605566249}{9185400\left(-\frac{1}{9}+R\right)^2}-\frac{715845826021}{87091200R^2} \\
& +\frac{373815952381}{1837080\left(\frac{1}{9}+R\right)^2}-\frac{167366716643141}{94058496\left(\frac{2}{9}+R\right)^2}+\frac{2371170173011}{340200\left(\frac{3}{9}+R\right)^2} \\
& -\frac{4488452581986787}{335923200\left(\frac{4}{9}+R\right)^2}+\frac{112482309211387}{9185400\left(\frac{5}{9}+R\right)^2}-\frac{30000000}{7\left(\frac{6}{9}+R\right)^2}, \quad \text{for } \frac{3}{9}<R<\frac{4}{9},
\end{aligned}
$$

$$
\begin{aligned}
g(R) = {} & \frac{3}{560\left(-\frac{3}{9}+R\right)^2}-\frac{1859135071}{94058496\left(-\frac{2}{9}+R\right)^2}+\frac{4305254531}{1837080\left(-\frac{1}{9}+R\right)^2} \\
& -\frac{193012968877}{3483648R^2}+\frac{429101140253}{918540\left(\frac{1}{9}+R\right)^2}-\frac{167366716643141}{94058496\left(\frac{2}{9}+R\right)^2} \\
& +\frac{227124686777}{68040\left(\frac{3}{9}+R\right)^2}-\frac{282890791328125}{94058496\left(\frac{4}{9}+R\right)^2}+\frac{762939453125}{734832\left(\frac{5}{9}+R\right)^2}, \quad \text{for } \frac{4}{9}<R<\frac{5}{9},
\end{aligned}
$$

$$
\begin{aligned}
g(R) = {} & -\frac{78125}{94058496\left(-\frac{4}{9}+R\right)^2}+\frac{195677}{68040\left(-\frac{3}{9}+R\right)^2}-\frac{29538353821}{94058496\left(-\frac{2}{9}+R\right)^2} \\
& +\frac{12705254531}{1837080\left(-\frac{1}{9}+R\right)^2}-\frac{193012968877}{3483648R^2}+\frac{373815952381}{1837080\left(\frac{1}{9}+R\right)^2} \\
& -\frac{34956443674391}{94058496\left(\frac{2}{9}+R\right)^2}+\frac{91871139}{280\left(\frac{3}{9}+R\right)^2}-\frac{5120000000}{45927\left(\frac{4}{9}+R\right)^2}, \quad \text{for } \frac{5}{9}<R<\frac{6}{9},
\end{aligned}
$$

$$g(R)=\frac{64}{1148175\left(-\frac{5}{9}+R\right)^2}-\frac{404606309}{2351462400\left(-\frac{4}{9}+R\right)^2}+\frac{779623}{48600\left(-\frac{3}{9}+R\right)^2}$$
$$-\frac{29538353821}{94058496\left(-\frac{2}{9}+R\right)^2}+\frac{4305254531}{1837080\left(-\frac{1}{9}+R\right)^2}-\frac{715845826021}{87091200R^2}$$
$$+\frac{133551832049}{9185400\left(\frac{1}{9}+R\right)^2}-\frac{29486161727807}{2351462400\left(\frac{2}{9}+R\right)^2}+\frac{234375}{56\left(\frac{3}{9}+R\right)^2},\quad \text{for } \frac{6}{9}<R<\frac{7}{9},$$

$$g(R)=-\frac{3}{2508800\left(-\frac{6}{9}+R\right)^2}+\frac{180731}{64297800\left(-\frac{5}{9}+R\right)^2}-\frac{404606309}{2351462400\left(-\frac{4}{9}+R\right)^2}$$
$$+\frac{195677}{68040\left(-\frac{3}{9}+R\right)^2}-\frac{1859135071}{94058496\left(-\frac{2}{9}+R\right)^2}+\frac{605566249}{9185400\left(-\frac{1}{9}+R\right)^2}$$
$$-\frac{9819117949}{87091200R^2}+\frac{6102360983}{64297800\left(\frac{1}{9}+R\right)^2}-\frac{10000000}{321489\left(\frac{2}{9}+R\right)^2},\quad \text{for } \frac{7}{9}<R<\frac{8}{9},$$

$$g(R)=\frac{1}{257191200\left(-\frac{7}{9}+R\right)^2}-\frac{3}{2508800\left(-\frac{6}{9}+R\right)^2}+\frac{64}{1148175\left(-\frac{5}{9}+R\right)^2}$$
$$-\frac{78125}{94058496\left(-\frac{4}{9}+R\right)^2}+\frac{3}{560\left(-\frac{3}{9}+R\right)^2}-\frac{5764801}{335923200\left(-\frac{2}{9}+R\right)^2}$$
$$+\frac{32768}{1148175\left(-\frac{1}{9}+R\right)^2}-\frac{59049}{2508800R^2}+\frac{78125}{10287648\left(\frac{1}{9}+R\right)^2},\quad \text{for } \frac{8}{9}<R<1.$$

Characteristic values of the distribution are:

mean $E(R)=-5+\frac{686419424\log 2}{2835}-\frac{88683579\log 3}{1120}+\frac{60546875\log 5}{6048}-\frac{40353607\log 7}{810}=0.34462,$

second moment

$$E\left(R^2\right)=-\frac{4977475650505}{1666598976}+\frac{5506009449897293\log 2}{57868020}-\frac{3870789417061723\log 3}{115736040}$$
$$+\frac{23520914453125\log 5}{5143824}-\frac{155338805614063\log 7}{8266860}=0.12574,$$

third moment

$$E\left(R^3\right)=-\frac{56500}{243}+\frac{302665066912\log 2}{76545}-\frac{1609375311\log 3}{1120}$$
$$+\frac{99482421875\log 5}{489888}-\frac{133852914419\log 7}{174960}=0.04823,$$

fourth moment

$$E\left(R^4\right)=\frac{6581554}{6561}-\frac{10398297681152\log 2}{1240029}+\frac{1892901777\log 3}{560}-\frac{10382748828125\log 5}{19840464}$$
$$+\frac{1189583980753\log 7}{787320}=0.01933,$$

standard deviation $\sigma(R)=0.08352,$
index of skewness $\gamma_1(R)=0.14505,$
index of kurtosis $\gamma_2(R)=-0.10366.$

The distribution of the concentration ratio *R* for samples of size *n* = 10 from a uniform population shows slight positive skewness and platykurtosis, both lower than those obtained for samples of size $n=6,7,8$ and 9.

8. Some Regularities of the Distributions

The analysis of the p.d.f. for $n=2,3,\cdots,10$ shows some regularities:

- The p.d.f. of the concentration ratio *R*, for $0<R<1/n$ and for samples of size *n*, can be expressed by

$$g(R)=\sum_{i=1}^{n-1}\frac{(-1)^{1+i}\left[n(n-1)\right]^{n-1}\binom{n-2}{i-1}}{\left[(n-1)!\right]^2\left(\frac{n-i}{n-1}+R\right)^2};$$

- Furthermore, the p.d.f. of the concentration ratio *R*, for $(n-1)/n<R<1$ and for samples of size *n*, can be expressed by

$$g(R)=\sum_{i=1}^{n-1}\frac{(-1)^{n+1-i}(n+1-i)^{n-1}\binom{n-2}{i-1}}{\left[(n-1)!\right]^2\left(\frac{2-i}{n-1}+R\right)^2};$$

- The density of the concentration ratio *R*, for $0<R<1/n$ and for samples of size *n*, is given by

$$\int_0^{\frac{1}{n}}g(R)\mathrm{d}R=\frac{n^{n-2}}{\left[(n-1)!\right]^2};$$

- The density of the concentration ratio *R*, for $(n-1)/n<R<1$ and for samples of size *n*, is given by

$$\int_{\frac{n-1}{n}}^{1}g(R)\mathrm{d}R=\frac{1}{\left[(n-1)!\right]^2};$$

- The *j*th term of the density of the concentration ratio *R*, denoted as $a_{i,j}$, verifies the following symmetry

$$a_{i,j}=a_{j,i}.$$

The coefficients of the $a_{i,i}$ terms of the p.d.f. of the concentration ratio *R* for samples of size $n-1$ multiplied by $(n-1)/n$ become the coefficients of the $a_{i+1,i+1}$ terms of the same p.d.f. for sample of size *n*.

These results are valid for every sample size and may allow reducing the heavy calculation to determine the p.d.f. of the concentration ratio *R*.

9. Concluding Remarks

In the present paper we obtain the distributions of the Gini concentration ratio *R* for samples of size $n=6,7,8,9$ and 10 drawn from a uniform population. We use the same method used by Girone [12] to derive the same distributions for samples of size $n\le 5$. We obtain the p.d.f. of the concentration ratio *R* calculating a multiple integral in $n-1$ dimensions for each region from $(k-1)/(n-1)$ to $k/(n-1)$ for $k=1,2,\cdots,n-1$. The limits of integration are defined by solving the inequalities of the order statistics divided by the sample mean and expressed in terms of the concentration ratio R for the values assumed in each of such regions. The calculation of the limits of integration is particularly heavy and requires a very long processing time.

The obtained results show that the p.d.f. of the concentration ratio R is given by hyperbolic splines with degree 2 and with nodes in $k/(n-1)$ for $k=1,2,\cdots,n-1$. Such distributions are unimodal with mean tending to $1/3$, which is the value of the concentration ratio R for the population, and have decreasing standard deviation. Moreover, the distributions show a slight positive skewness and platykurtosis that tend to decrease as n increases.

Beyond the possibility to obtain similar results for samples of larger size, open problems are the derivation of the exact expression for the mean and the other features of the distribution of the concentration ratio R for random samples of size n drawn from a uniform population.

References

[1] Gini, C. (1914) L'ammontare e la composizionedellaricchezzadellenazioni. Bocca, Torino.

[2] Hoeffding, W. (1948) A Class of Statistics with Asymptotically Normal Distribution. *Annals of Mathematical Statistics*, **19**, 293-325.

[3] Glasser, G.J. (1962) Variance Formulas for the Mean Difference and the Coefficient of Concentration. *Journal of the American Statistical Association*, **57**, 648-654. http://dx.doi.org/10.1080/01621459.1962.10500553

[4] Cucconi, O. (1965) Sulla distribuzionecampionaria del rapporto R di concentrazione. *Statistica*, **25**, 119.

[5] Dall'Aglio, G. (1965) Comportamentoasintoticodellestimedelladifferenza media e del rapporto di concentrazione. *Metron*, **24**, 379-414.

[6] Deltas, G. (2003) The Small-Sample Bias of the Gini Coefficient: Results and Implications for Empirical Research. *Review of Economics and Statistics*, **85**, 226-234. http://dx.doi.org/10.1162/rest.2003.85.1.226

[7] Barrett, G.F. and Donald, S.G. (2009) Statistical Inference with Generalized Gini Indices of Inequality, Poverty, and Welfare. *Journal of Business & Economic Statistics*, **27**, 1-17. http://dx.doi.org/10.1198/jbes.2009.0001

[8] Davidson, R. (2009) Reliable Inference for the Gini Index. *Journal of Econometrics*, **150**, 30-40. http://dx.doi.org/10.1016/j.jeconom.2008.11.004

[9] Fakoor, V., Ghalibaf, M.B. and Azarnoosh, H.A. (2011) Asymptotic Behaviors of the Lorenz Curve and Gini Index in Sampling from a Length-Biased Distribution. *Statistics and Probability Letters*, **81**, 1425-1435. http://dx.doi.org/10.1016/j.spl.2011.04.013

[10] Girone, G. (1968) Sulcomportamentocampionariosimulato del rapporto di concentrazione. *Annalidella Facoltà di Economia e Commerciodell'Universitàdegli Studi di Bari*, **23**, 5-11.

[11] Girone, G. (1971) La distribuzione del rapporto di concentrazione per campionicasuali di variabiliesponenziali. *Studi di Probabilità*, *Statistica e Ricercaoperativa in onore di Giuseppe Pompilj*, Oderisi, Gubbio.

[12] Girone, G. (1971) La distribuzione del rapporto di concentrazione per piccolicampioniestratti da unapopolazioneuniforme. *Annalidell'Istituto di Statisticadell'Universitàdegli Studi di Bari*, **36**, 31-52.

Applied Mathematics, 2015, 6, 71-77
Published Online January 2015 in SciRes. http://www.scirp.org/journal/am
http://dx.doi.org/10.4236/am.2015.61008

On Asymptotic Stability of Linear Control Systems

Şerife Yılmaz*, Taner Büyükköroğlu, Vakif Dzhafarov

Department of Mathematics, Faculty of Science, Anadolu University, Eskisehir, Turkey
Email: *serifeyilmaz@anadolu.edu.tr, tbuyukkoroglu@anadolu.edu.tr, vcaferov@anadolu.edu.tr

Received 10 November 2014; revised 6 December 2014; accepted 25 December 2014

Abstract

Asymptotic stability of linear systems is closely related to Hurwitz stability of the system matrices. For uncertain linear systems we consider stability problem through common quadratic Lyapunov functions (CQLF) and problem of stabilization by linear feedback.

Keywords

Common Quadratic Lyapunov Functions, Uncertain System, Gradient Method, Bendixson Theorem

1. Introduction

Let linear uncertain system

$$\dot{x} = Ax, \quad A \in \operatorname{conv}\{A_1, A_2, \cdots, A_N\} \tag{1}$$

be given where $x = x(t) \in \mathbb{R}^n$, A_i $(i = 1, 2, \cdots, N)$ are $n \times n$ real matrices. Consider the following matrix inequalities

$$A_i^{\mathrm{T}} P + PA_i < 0 \quad (i = 1, 2, \cdots, N) \tag{2}$$

where $P > 0$ and the symbol "$>$" stands for positive definiteness. The matrix P is called a common solution to (2).

If the system (2) has a common $P > 0$ solution, then this system is uniformly asymptotically stable [1].

The problem of existence of common positive definite solution P of (2) has been studied in a lot of works (see [1]-[7] and references therein). Numerical solution for common P via nondifferentiable convex optimization has been discussed in [8].

*Corresponding author.

How to cite this paper: Yılmaz, Ş., Büyükköroğlu, T. and Dzhafarov, V. (2015) On Asymptotic Stability of Linear Control Systems. *Applied Mathematics*, **6**, 71-77. http://dx.doi.org/10.4236/am.2015.61008

In the first part of the paper we treat the problem (2) as a nonconvex optimization problem (minimization of a convex function under nonconvex constraints) and apply a modified gradient method. The comparison with [8] shows that our approach gives better result in some cases.

In the second part we consider the stabilization problem, *i.e.* the following question: for the affine family

$$\{A(q): q \in R\}$$

where $R \subset \mathbb{R}^l$ is a box, is there a stable member? We consider a sufficient condition which follows from the Bendixson theorem [9].

2. Gradient Method

According to [2], let $\mathcal{S}$ be the set (subspace) of $(n \cdot N) \times (n \cdot N)$ dimensional symmetric block-diagonal matrices of the form $R \oplus R \oplus \cdots \oplus R$ where R is symmetric.

Let $Z_1, Z_2, \cdots, Z_r$ be a basis of $\mathcal{S}$, $r = n(n+1)/2$,

$$Q_i = (-Z_i) \oplus \left(A_1^{\mathrm{T}} Z_i + Z_i A_1\right) \oplus \cdots \oplus \left(A_N^{\mathrm{T}} Z_i + Z_i A_N\right)$$

$$\phi(x) = \phi(x_1, x_2, \cdots, x_r) = \lambda_{\max}\left(\sum_{i=1}^{r} x_i Q_i\right) \tag{3}$$

Then $\{A_1, A_2, \cdots, A_N\}$ has CQLF $\Leftrightarrow$ there exists $x_* \in \mathbb{R}^r$ such that $\phi(x_*) < 0$. In this case the matrix $P(x_*)$ is a common solution to (2) where

$$P(x) = \begin{pmatrix} x_1 & x_2 & \cdots & x_n \\ x_2 & x_{n+1} & \cdots & x_{2n-1} \\ \vdots & \vdots & \ddots & \vdots \\ x_n & x_{2n-1} & \cdots & x_r \end{pmatrix}.$$

The function $\phi(x)$ is positive homogenous $(\phi(\alpha x) = \alpha\phi(x)$ for all $\alpha \geq 0)$. Therefore the vector x can be restricted to the condition $\|x\| = 1$. The advantage of the restriction $\|x\| = 1$ shows the following proposition.

Proposition 1. Let $S = \{x \in \mathbb{R}^r : x = 1\}$ be the unit sphere, let the function $f : \mathbb{R}^r \to \mathbb{R}$ be positive homogeneous $(f(\lambda x) = \lambda f(x)$ for all $\lambda > 0)$ and be differentiable at $a \in S$. Assume that $f(a) > 0$. Then $\langle g, a\rangle < 0$ where $g = -\nabla f(x)\big|_{x=a}$, ∇ denotes the gradient and $\langle \cdot, \cdot \rangle$ denotes the scalar product.

Proof: Since f is positive homogeneous, it increases in the direction of the vector *a*: for $\lambda > 1$,

$$f(\lambda a) = \lambda f(a) > f(a).$$

Therefore the directional derivative of *f* at *a* in the direction of *a* is positive $D_a f(a) > 0$.

On the other hand

$$D_a f(a) = \langle \nabla f, a \rangle$$

and

$$\langle \nabla f, a \rangle > 0 \quad \text{or} \quad \langle -\nabla f, a \rangle < 0 \quad \text{or} \quad \langle g, a \rangle < 0. \qquad \square$$

Proposition 1 shows that under its assumption the minus gradient vector at the point *a* is directed into the unit ball (**Figure 1**).

Consider the following optimization problem

$$\begin{gathered} \phi(x) \to \text{minimize} \\ \text{subject to } x = 1. \end{gathered}$$

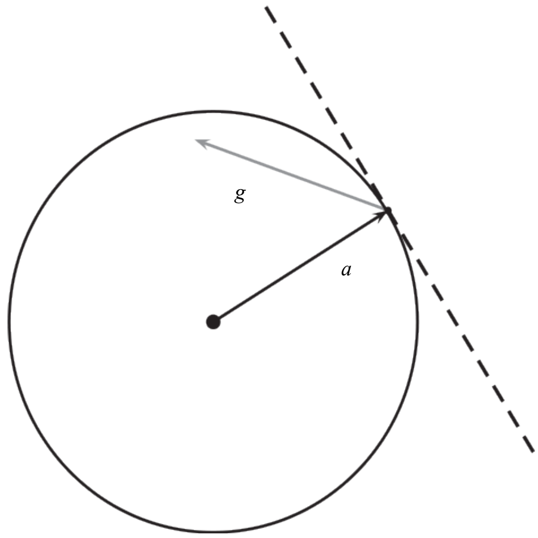

Figure 1. The direction (g) of the minus gradient.

Since the matrix $\sum_{i=1}^{r} x_i Q_i$ is symmetric, the function $\phi(x)$ (3) can be written as

$$\phi(x) = \max_{\|u\|=1} u^{\mathrm{T}} \left(\sum_{i=1}^{r} x_i Q_i \right) u.$$

The gradient vector of $\phi(x)$ at a point a is:

$$\nabla \phi(x)\big|_{x=a} = \left(u^{\mathrm{T}} Q_1 u, u^{\mathrm{T}} Q_2 u, \cdots, u^{\mathrm{T}} Q_r u \right) \tag{4}$$

where u is the unit eigenvector of $\sum_{i=1}^{r} a_i Q_i$ corresponding to the simple maximum eigenvalue [2].

Well-known gradient algorithm in combination with Proposition 1 gives the following.

Algorithm 1.

Step 1. Take an initial point $x^0 = S$. Compute $\phi(x^0)$. If $\phi(x^0) \geq 0$, find t such that the line

$$l(t) = x^0 - t \cdot \nabla \phi(x)\big|_{x=x^0}$$

intersects the unit sphere S (**Figure 2**).

Step 2. Take $x^1 = x^0 - t_* \cdot \nabla \phi(x)\big|_{x=x^0}$ where t_* satisfies the condition $\|l(t_*)\| = 1$. If $\phi(x^1) < 0$, x^1 is required point. Otherwise find t such that the line $l(t) = x^1 - t \cdot \nabla \phi(x)\big|_{x=x^1}$ intersects the unit sphere and repeat the procedure.

Example 1. Consider the switched system

$$\dot{x} \in \{A_1, A_2\} x$$

where

$$A_1 = \begin{pmatrix} -4 & -1 & 3 \\ -3 & -2 & 2 \\ 3 & 0 & -3 \end{pmatrix}, \quad A_2 = \begin{pmatrix} -8 & -3 & 1 \\ 9 & 2 & 0 \\ 6 & 3 & -6 \end{pmatrix}$$

are Hurwitz stable matrices. Let

$$Z_1 = \begin{pmatrix} 1 & 0 & 0 \\ 0 & 0 & 0 \\ 0 & 0 & 0 \end{pmatrix}, \quad Z_2 = \begin{pmatrix} 0 & 1 & 0 \\ 1 & 0 & 0 \\ 0 & 0 & 0 \end{pmatrix}, \quad Z_3 = \begin{pmatrix} 0 & 0 & 1 \\ 0 & 0 & 0 \\ 1 & 0 & 0 \end{pmatrix},$$

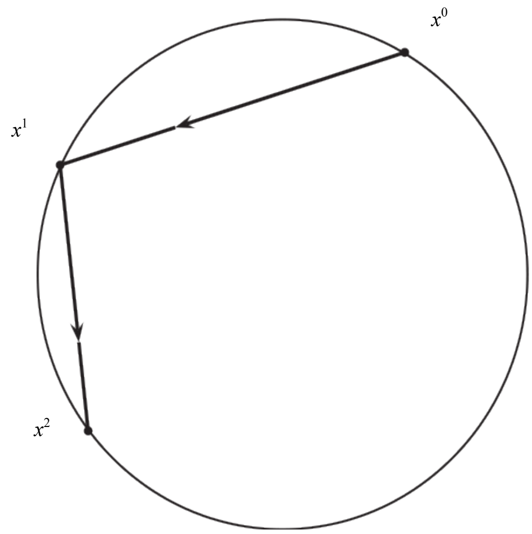

Figure 2. Searching on the unit sphere.

$$Z_4 = \begin{pmatrix} 0 & 0 & 0 \\ 0 & 1 & 0 \\ 0 & 0 & 0 \end{pmatrix}, \quad Z_5 = \begin{pmatrix} 0 & 0 & 0 \\ 0 & 0 & 1 \\ 0 & 1 & 0 \end{pmatrix} \text{ and } Z_6 = \begin{pmatrix} 0 & 0 & 0 \\ 0 & 0 & 0 \\ 0 & 0 & 1 \end{pmatrix}.$$

For $i = 1, 2, \cdots, 6$

$$Q_i = (-Z_i) \oplus \left(A_1^{\mathrm{T}} Z_i + Z_i A_1\right) \oplus \left(A_2^{\mathrm{T}} Z_i + Z_i A_2\right).$$

Take the initial point $x^0 = \left(1/\sqrt{3}, 0, 0, 1/\sqrt{3}, 0, 1/\sqrt{3}\right)^{\mathrm{T}}$, then

$$P\left(x^0\right) = \begin{pmatrix} 1/\sqrt{3} & 0 & 0 \\ 0 & 1/\sqrt{3} & 0 \\ 0 & 0 & 1/\sqrt{3} \end{pmatrix}$$

is positive definite. Eigenvalues of the matrix

$$\sum_{i=1}^{6} x_i^0 Q_i = \frac{1}{\sqrt{3}} \cdot Q_1 + 0 \cdot Q_2 + 0 \cdot Q_3 + \frac{1}{\sqrt{3}} \cdot Q_4 + 0 \cdot Q_5 + \frac{1}{\sqrt{3}} \cdot Q_6$$

are -12.507, -5.364, 4.015, -0.224, -0.577, -8.566, -1.601.

Maximum eigenvalue 4.015 is simple and the corresponding unit eigenvector is

$$v = (0, 0, 0, 0, 0, 0, -0.317, -0.911, -0.261)^{\mathrm{T}}.$$

Gradient of the function ϕ at x^0 is

$$\nabla \phi(x)\big|_{x=x^0} = (3.189, 6.162, 0.671, -8.537, -8.049, -1.607)^{\mathrm{T}}.$$

The vector $x^1 = x^0 - t \cdot \nabla \phi(x)\big|_{x=x^0}$ should be on the six dimensional unit sphere. Therefore $t = 0.0425$ and

$$x^1 = (0.7129, 0.2620, 0.0285, 0.2143, -0.3422, 0.5090)^{\mathrm{T}}.$$

After 9 steps, we get $\phi\left(x^9\right) < 0$ where

$$x^9 = (0.7950, 0.2183, -0.0623, 0.2185, -0.1254, 0.5028)^{\mathrm{T}},$$

$$P(x^9) = \begin{pmatrix} 0.7950 & 0.2183 & -0.0623 \\ 0.2183 & 0.2185 & -0.1254 \\ -0.0623 & -0.1254 & 0.5028 \end{pmatrix}.$$

$P(x^9)$ is a common positive definite solution for $A_1^{\mathrm{T}} P(x^9) + P(x^9) A_1 < 0$ and $A_2^{\mathrm{T}} P(x^9) + P(x^9) A_2 < 0$.

The same problem solved by the algorithm from [8] gives answer only after 70 steps. We have solved a number of examples using the above gradient algorithm and by the algorithm from [8]. These examples show that this algorithm is faster than the algorithm from [8] in some cases.

As the comparison with the algorithm from [8] is concerned, the algorithm from [8] at each step uses the gradient only one maximum eigenvalue function, *i.e.* at 1 step it uses the gradient of $P \to \lambda_{\max}\left(A_1^{\mathrm{T}} P + P A_1\right)$, at 2 step the gradient of $P \to \lambda_{\max}\left(A_2^{\mathrm{T}} P + P A_2\right)$ and so on. This procedure delays the convergence. In our algorithm we use the function $P \to \max_i\left(\lambda_{\max}\left(A_i^{\mathrm{T}} P + P A_i\right)\right)$ and the corresponding gradient direction decreases the greates maximum eigenvalue.

On the other hand an obviously advantage of the method from [8] is the choose of the step size, which is given by an exact formula, whereas our step size is determined by the intersection of the corresponding rays with the unit sphere.

3. Sufficient Condition for a Stable Member

In this section we consider a sufficient condition for a stable member which is obtained by using Bendixson's theorem.

If a matrix is symmetric then it is stable if and only if it is negative definite. Therefore if a family consists of symmetric matrices then searching for stable element is equivalent to the searching for negative definite one.

On the other hand every real $n \times n$ matrix A can be decomposed

$$A = B + C,$$
$$B = \frac{1}{2}\left(A + A^{\mathrm{T}}\right),$$
$$C = \frac{1}{2}\left(A + A^{\mathrm{T}}\right).$$

where B is symmetric and C is skew-symmetric. Bendixson's theorem gives important inequalities for the eigenvalues of A, B and C.

Theorem 1. ([9], p. 40) If A is an $n \times n$ matrix, $B = \frac{1}{2}\left(A + A^{\mathrm{T}}\right)$ and $\lambda_1, \lambda_2, \cdots, \lambda_n$ $\left(|\lambda_1| \ge |\lambda_2| \ge \cdots \ge |\lambda_n|\right)$, $\mu_1 \ge \mu_2 \ge \cdots \ge \mu_n$ are the eigenvalues of A, B then

$$\mu_n \le \mathrm{Re}(\lambda_i) \le \mu_1 \quad (i = 1, 2, \cdots, n).$$

Bendixson's theorem leads to the following.

Proposition 2. Let the family $\{A(q) : q \in R\}$ be given and $B(q)$ is the symmetric part of $A(q)$. Then

1) If there exists $q_* \in R$ such that $B(q_*)$ is Hurwitz stable then $A(q_*)$ is also Hurwitz stable,

2) If there exists $q_* \in R$ such that $B(q_*)$ is positive stable (all eigenvalues lie in the open right half plane) then $A(q_*)$ is also positive stable.

Proposition 2 gives a sufficient condition for the existence of a stable element.

In the case of affine family

$$A(q) = A_0 + q_1 A_1 + q_2 A_2 + \cdots + q_l A_l$$

where $q = (q_1, q_2, \cdots, q_l)^{\mathrm{T}} \in R$, R is a box or $R = \mathbb{R}^l$, the searching procedure for stable element in $B(q)$ can be effectively solved by powerful tools of Linear Matrix Inequalities (Matlab's LMI Toolbox).

In the non-affine case of the family $A(q)$ the gradient algorithm for a stable element in $B(q)$ is applicable.

Example 2. Consider affine family

$$A(q)=\begin{pmatrix} 6-3q_1-q_2-q_3 & 2+q_1-4q_3 & -2-5q_1-q_2-q_3 \\ 5+q_1+3q_2-q_3 & 8-2q_1-2q_2+2q_3 & 3+q_1-3q_3 \\ 5+5q_1-q_2+2q_3 & -4q_1-5q_2+q_3 & -2q_1-q_2 \end{pmatrix}$$

$q_i \in [-10,10]$ $(i=1,2,3)$. Then

$$B(q)=\begin{pmatrix} 6-3q_1-q_2-q_3 & (7+2q_1+3q_2-5q_3)/2 & (3-2q_2+q_3)/2 \\ (7+2q_1+3q_2-5q_3)/2 & 8-2q_1-2q_2+2q_3 & (3-3q_1-5q_2-2q_3)/2 \\ (3-2q_2+q_3)/2 & (3-3q_1-5q_2-2q_3)/2 & -2q_1-q_2 \end{pmatrix}.$$

LMI method applied to the matrix inequality problem $B(q)<0$ gives the value within a few seconds

$$q_* = (9.4591, -3.5180, -0.0354)^{\mathrm{T}}$$

and $B(q_*)$, and consequently $A(q_*)$ is stable.

LMI method applied to the inequality $B(q)>0$ gives also

$$\tilde{q} = (-2.6549, 1.3609, 0.9393)^{\mathrm{T}}$$

so the family $A(q)$ contains positive stable matrix $A(\tilde{q})$.

We have investigated Example 2 by the algorithm from [10] and positive answer is obtained after about 100 seconds.

Example 3. Consider non-affine family

$$A(q)=\begin{pmatrix} q_1q_2+q_2-2 & -q_1q_3+q_1-q_3-9 & -3q_2q_3+3q_2+3q_3-10 \\ -17-q_1+q_3 & -q_1-4 & q_2-4 \\ q_1+5 & q_1+11 & q_2-6 \end{pmatrix}$$

$q_i \in [-10,10]$ $(i=1,2,3)$. Here

$$B(q)=\begin{pmatrix} q_1q_2+q_2-2 & -\frac{q_1q_3}{2}-13 & \frac{q_1-3q_2(q_3-1)+3q_3-5}{2} \\ -\frac{q_1q_3}{2}-13 & -q_1-4 & \frac{q_1+q_2+7}{2} \\ \frac{q_1-3q_2(q_3-1)+3q_3-5}{2} & \frac{q_1+q_2+7}{2} & q_2-6 \end{pmatrix}.$$

Consider the function

$$G(q)=\lambda_{\max}(B(q))=\max_{\|v\|=1} v^{\mathrm{T}}B(q)v.$$

We are looking for q satisfying $G(q)<0$. If for some q the maximal eigenvalue $\lambda_{\max}(B(q))$ is simple then $G(q)$ is differentiable at q and its gradient can be easily calculated (by the analogy with (4)).

For this example, gradient method gives solution after 7 steps:

$$q^0=(0,0,0)^{\mathrm{T}},\ \cdots,\ q^7=(5.270,-6.252,0.959)^{\mathrm{T}}$$

(see **Table 1**). The step size *t* is chosen from the decreasing condition of the function $G(q)$: *t* must be chosen such that

$$G(q^{k+1})=G\left(q^k-t\nabla G|_{q^k}\right)<G(q^k).$$

This example has been solved by the algorithm from [10] as well. Positive answer has been obtained only after

Table 1. Gradient algorithm for example 3.

k	q^k	$\lambda_{\max}$	multiplicity	$\nabla G\|_{q^k}$
0	$(0,0,0)$	11.079	1	$(-0.452, 0.208, -0.508)$
1	$(0.411, -0.189, 0.462)$	10.632	1	$(-0.332, 0.655, -0.355)$
2	$(0.714, -0.785, 0.786)$	9.910	1	$(-0.482, 0.930, -0.383)$
3	$(1.153, -1.632, 1.135)$	8.634	1	$(-0.719, 1.173, -0.184)$
4	$(1.808, -2.700, 1.303)$	6.712	1	$(-1.061, 1.303, 0.291)$
5	$(2.774, -3.886, 1.038)$	3.840	1	$(-1.391, 1.360, 0.060)$
6	$(4.040, -5.123, 0.983)$	0.444	1	$(-1.352, 1.240, 0.267)$
7	$(5.270, -6.252, 0.959)$	-2.404		

55 steps. We start with $q^0 = (0,0,0)$ and the algorithm from [10] gives another stabilizing point

$$q^{55} = (3.2721, -2.3853, 2.3818)^{\mathrm{T}}.$$

The eigenvalues of $A(q^{55})$ are $\lambda_1 = -27.8402$, $\lambda_{2,3} = -0.004 \pm j0.2326$.

4. Conclusion

In the first part of the paper, we consider the stability problem of a matrix polytope through common quadratic Lyapunov functions. We suggest a modified gradient algorithm. In the second part by using Bendixson's theorem a sufficient condition for a stable member is given.

References

[1] Liberzon, D. (2003) Switching in System and Control. Birkhäuser, Boston. http://dx.doi.org/10.1007/978-1-4612-0017-8

[2] Boyd, S. and Yang, Q. (1989) Structured and Simultaneous Lyapunov Functions for System Stability Problems. *International Journal of Control*, **49**, 2215-2240. http://dx.doi.org/10.1080/00207178908559769

[3] Büyükköroğlu, T., Esen, Ö. and Dzhafarov, V. (2011) Common Lyapunov Functions for Some Special Classes of Stable Systems. *IEEE Transactions on Automatic Control*, **56**, 1963-1967. http://dx.doi.org/10.1109/TAC.2011.2137510

[4] Cheng, D., Guo, L. and Huang, J. (2003) On Quadratic Lyapunov Functions. *IEEE Transactions on Automatic Control*, **48**, 885-890. http://dx.doi.org/10.1109/TAC.2003.811274

[5] Mason, O. and Shorten, R. (2006) On the Simultaneous Diagonal Stability of a Pair of Positive Linear Systems. *Linear Algebra and Its Applications*, **413**, 13-23. http://dx.doi.org/10.1016/j.laa.2005.07.019

[6] Narendra, K.S. and Balakrishnan, J. (1994) A Common Lyapunov Function for Stable LTI Systems with Commuting A-Matrices. *IEEE Transactions on Automatic Control*, **39**, 2469-2471. http://dx.doi.org/10.1109/9.362846

[7] Shorten, R.N. and Narendra, K.S. (2002) Necessary and Sufficient Conditions for the Existence of a Common Quadratic Lyapunov Function for a Finite Number of Stable Second Order Linear Time-Invariant Systems. *International Journal of Adaptive Control and Signal Processing*, **16**, 709-728. http://dx.doi.org/10.1002/acs.719

[8] Liberzon, D. and Tempo, R. (2004) Common Lyapunov Functions and Gradient Algorithms. *IEEE Transactions on Automatic Control*, **49**, 990-994. http://dx.doi.org/10.1109/TAC.2004.829632

[9] Marcus, M. and Minc, H.A. (1992) Survey of Matrix Theory and Matrix Inequalities. Dover, New York.

[10] Polyak, B.T. and Shcherbakov, P.S. (1999) Numerical Search of Stable or Unstable Element in Matrix or Polynomial Families: A Unified Approach to Robustness Analysis and Stabilization. *Robustness in Identification and Control Lecture Notes in Control and Information Sciences*, **254**, 344-358. http://dx.doi.org/10.1007/BFb0109879

Applied Mathematics, 2015, 6, 78-94
Published Online January 2015 in SciRes. http://www.scirp.org/journal/am
http://dx.doi.org/10.4236/am.2015.61009

Symmetry Analysis for MHD Viscous Flow and Heat Transfer over a Stretching Sheet

Hossam S. Hassan

Department of Basic and Applied Science, Arab Academy for Science, Technology and Maritime Transport, Alexandria, Egypt
Email: hossams@aast.edu

Received 26 October 2014; revised 22 November 2014; accepted 10 December 2014

Abstract

This work deals with the boundary layer flow and heat transfer of an electrically conducting viscous fluid over a stretching sheet. Lie-group method is applied for determining the symmetry reductions for the governing equations by reducing the number of independent variables in the given system of partial differential equations by one, leading to a system of non-linear ordinary differential equation. The resulting system is then solved numerically using shooting method coupled with Runge-Kutta scheme. Effects of various values of physical parameters on the horizontal and vertical velocities, temperature profiles, wall heat transfer and the wall shear stress (skin friction), have been studied and the results are plotted. Furthermore, a comparison between the present results with existing numerical and homotopy methods has been reported and we found that they are in a good agreement.

Keywords

MHD Flow, Viscous Flow, Stretching Sheet, Lie-Group, Similarity Solution

1. Introduction

The boundary layer flow and heat transfer of an incompressible viscous fluid over a stretching sheet appear in several manufacturing processes of industry such as the aerodynamic extrusion of plastic sheets, the extrusion of polymers, hot rolling, the cooling of metallic plates, glass-fiber production, etc., [1].

Sakiadis [2] presented the pioneering work in this field. He investigated the flow induced by a semi-infinite horizontally moving wall in an ambient fluid.

Crane [3] studied the flow over a linearly stretching sheet in an ambient fluid and gave a similarity solution in closed analytical form for the steady two-dimensional problem. He presented a closed form exponential solution

How to cite this paper: Hassan, H.S. (2015) Symmetry Analysis for MHD Viscous Flow and Heat Transfer over a Stretching Sheet. *Applied Mathematics*, **6**, 78-94. http://dx.doi.org/10.4236/am.2015.61009

for the planar viscous flow of linear stretching case.

Gupta and Gupta [4] investigated the effect of mass transfer on the Crane flow. They analyzed the viscous flow and heat transfer by an isothermal stretching sheet with suction/injection.

Chiam [5] studied the boundary layer flow due to a plate stretching with a power-low velocity distribution in presence of a magnetic field. To yield similarity equations, a special form of the magnetic field is chosen. He presented linearized solutions for the case of large magnetic parameters and derived an expression for the skin friction coefficient using Crocco's transformation and compared it numerically using Runge-Kutta shooting algorithm with Newton iteration.

Vajravelu [6] studied flow and heat transfer in a viscous fluid over a non-linear stretching sheet. In his study, the heat transfer is analyzed when the sheet is maintained at a constant temperature and the viscous dissipation is neglected. He used a fourth-order Runge-Kutta integration scheme to solve the resulting nonlinear differential equations.

Cortell [7] presented a numerical analysis for the flow and heat transfer in a viscous fluid over a nonlinear stretching sheet by employing a novel numerical procedure. In his work, he studied two cases for the nonlinear stretching sheet, with constant surface temperature and with prescribed surface temperature. The resulting nonlinear ordinary differential equations after converting the governing partial differential equations by a similarity transformation are solved using Runge-Kutta scheme.

Abbas and Hayat [8] studied the radiation effects on the magnetohydrodynamic (MHD) flow of an incompressible viscous fluid in a porous space. In their study, they extended the analysis of Cortell [7] by considering a MHD flow, analyzed the flow in a porous medium, included the radiation effects and provided analytic solution namely homotopy analysis method (HAM) instead of numerical technique applied in [7]. Hayat *et al*. [9] investigated the magnetohydrodynamic (MHD) boundary layer flow by employing the modified Adomian decomposition method and the Padé approximation and developed the series solution of the governing non-linear problem.

Ghotbi [10] considered the problem of the boundary layer flow of an incompressible viscous fluid over a nonlinear stretching sheet. In order to obtain analytical solution of the governing nonlinear differential equations, HAM is applied.

Mehmood *et al*. [11] reported the corrections to HAM results presented in [10]. A comparison between their HAM solution and the exact solution obtained by Pavlov [12] was made and it was in a good agreement.

Javed *et al*. [13] investigated the boundary layer flow and heat transfer analysis of electrically conducting viscous fluid over a nonlinearly shrinking sheet. They used a similarity transformation to reduce the governing partial differential equations to a set of nonlinear ordinary differential equations. The resulting system of equations is then solved numerically using an implicit finite difference scheme known as Keller-box method.

Fathizadeh *et al*. [14] employed the modification of the homotopy perturbation method to solve the MHD boundary-layer equations. In their work, the viscous fluid is electrically conducting in the presence of a uniform applied magnetic field and the induced magnetic field is neglected for small magnetic Reynolds number. They obtained the similarity solutions of ordinary differential equation resulting from the momentum equation. Some numerical comparisons among the new modified homotopy perturbation method, the standard homotopy perturbation, the exact solution and the shooting method are obtained.

In this paper, we shall investigate the solution of the MHD boundary layer flow for an incompressible viscous fluid over a sheet stretching according to a power-law velocity. Lie-group theory is applied to the equations of motion for determining symmetry reductions of partial differential equations [15]-[30]. The resulting system of nonlinear differential equations is then solved numerically using shooting method coupled with Runge-Kutta scheme. Our results are compared with the work of [5]-[14].

2. Mathematical Formulation of the Problem

We consider the MHD flow over a flat plate coinciding with the plane $\bar{y}=0$, of an incompressible viscous fluid with heat transfer. The wall is stretched horizontally by applying on both sides two equal and opposite forces along the $\bar{x}$-axis to keep the origin fixed. The fluid is electrically conducting under the influence of an applied magnetic field $B(\bar{x})$ in the $\bar{y}$-direction normally to the stretching sheet, **Figure 1**.

The induced magnetic field is neglected. Under these assumptions, the continuity, momentum and energy equations become

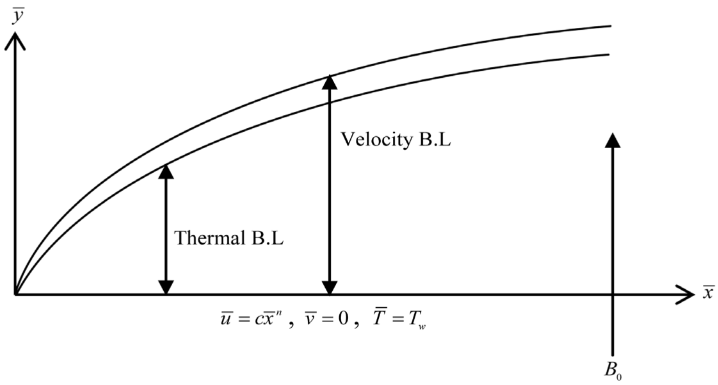

Figure 1. Physical model and coordinate system.

$$\text{The continuity equation}: \frac{\partial \bar{u}}{\partial \bar{x}} + \frac{\partial \bar{v}}{\partial \bar{y}} = 0, \tag{2.1}$$

$$\text{The momentum equation}: \bar{u}\frac{\partial \bar{u}}{\partial \bar{x}} + \bar{v}\frac{\partial \bar{u}}{\partial \bar{y}} = \nu \frac{\partial^2 \bar{u}}{\partial \bar{y}^2} - \frac{\sigma B^2(\bar{x})}{\rho}\bar{u}, \tag{2.2}$$

$$\text{The energy equation}: \rho c_p\left(\bar{u}\frac{\partial \bar{T}}{\partial \bar{x}} + \bar{v}\frac{\partial \bar{T}}{\partial \bar{y}}\right) = \alpha \frac{\partial^2 \bar{T}}{\partial \bar{y}^2}, \tag{2.3}$$

where $\bar{u}$ and $\bar{v}$, are the velocity components in the $\bar{x}$ and $\bar{y}$ directions, respectively, ν is the kinematic viscosity, ρ is the fluid density, σ is the electrical conductivity of the fluid, c_p is the specific heat of the fluid at constant pressure, α is the thermal conductivity of the fluid, and $\bar{T}$ is the temperature.

The magnetic field is defined by

$$B(\bar{x}) = B_0 \bar{x}^{\frac{n-1}{2}}, \tag{2.4}$$

where B_0 and n are constants.

The boundary conditions are

$$\begin{aligned}&(\text{i})\ \ \bar{u} = c\bar{x}^n,\ \ \bar{v} = 0,\ \ \bar{T} = T_w \ \text{ at } \bar{y} = 0,\\ &(\text{ii})\ \ \bar{u} \to 0,\ \ \bar{T} \to T_\infty \ \text{ as } \bar{y} \to \infty,\end{aligned} \tag{2.5}$$

where c is a constant, T_w is the uniform temperature of the stretching sheet and T_∞ is the temperature at large distance from the wall, where $T_w > T_\infty$.

The variables in Equations (2.1)-(2.5) are dimensionless according to

$$x = \frac{c\bar{x}}{U_1},\quad y = \sqrt{\frac{(n+1)c}{2\nu}}\bar{y},\quad u = \frac{\bar{u}}{U_1},\quad v = \sqrt{\frac{(n+1)}{2c\nu}}\bar{v},\quad T = \frac{\bar{T} - T_\infty}{T_w - T_\infty}, \tag{2.6}$$

where U_1 is the characteristic velocity.

Substitution from Equation (2.6) into Equations (2.1)-(2.3) gives

$$\frac{\partial u}{\partial x} + \frac{\partial v}{\partial y} = 0, \tag{2.7}$$

$$u\frac{\partial u}{\partial x} + v\frac{\partial u}{\partial y} = \left(\frac{n+1}{2}\right)\frac{\partial^2 u}{\partial y^2} - Kx^{n-1}u, \tag{2.8}$$

$$u\frac{\partial T}{\partial x} + v\frac{\partial T}{\partial y} = \left(\frac{n+1}{2}\right)\frac{1}{\Pr}\frac{\partial^2 T}{\partial y^2}, \tag{2.9}$$

where, $K=\dfrac{\sigma B_0^2}{\rho c}$ is a constant, $\Pr=\dfrac{\mu c_p}{\alpha}$ is the Prandtl number, and $\mu=\nu\rho$ is the dynamic viscosity. Without losing of generality, let, $\left(\dfrac{U_1}{c}\right)^{n-1}=1$.

The boundary conditions Equation (2.5) will be

$$\begin{aligned}&(\mathrm{i})\ \ u=x^n,\ \ v=0,\ \ T=1\ \text{ at }\ y=0,\\&(\mathrm{ii})\ \ u\to 0,\ \ T\to 0\ \text{ as }\ y\to\infty.\end{aligned}\tag{2.10}$$

From the continuity Equation (2.7) there exist stream function $\Psi(x,y)$ such that,

$$u(x,y)=\frac{\partial\Psi}{\partial y},\quad v(x,y)=-\frac{\partial\Psi}{\partial x},\tag{2.11}$$

which satisfies Equation (2.7) identically.

Substituting from Equation (2.11) into Equations (2.8)-(2.9), yields

$$\Psi_y\Psi_{xy}-\Psi_x\Psi_{yy}=\left(\frac{n+1}{2}\right)\Psi_{yyy}-Kx^{n-1}\Psi_y,\tag{2.12}$$

$$\Psi_yT_x-\Psi_xT_y=\left(\frac{n+1}{2}\right)\frac{1}{\Pr}T_{yy},\tag{2.13}$$

where subscripts denote partial derivatives.

The boundary conditions Equation (2.8) will be

$$\begin{aligned}&(\mathrm{i})\ \ \Psi_y=x^n,\ \ \Psi_x=0,\ \ T=1\ \text{ at }\ y=0,\\&(\mathrm{ii})\ \ \Psi_y\to 0,\ \ T\to 0\ \text{ as }\ y\to\infty.\end{aligned}\tag{2.14}$$

3. Solution of the Problem

Firstly, we derive the similarity solutions using Lie-group method under which Equations (2.12)-(2.13) and the boundary conditions Equation (2.14) are invariant, and then we use these symmetries to determine the similarity variables.

Consider the one-parameter (ε) Lie group of infinitesimal transformations in $(x,y;\Psi,T)$ given by

$$\begin{aligned}x^*&=x+\varepsilon X(x,y;\Psi,T)+O(\varepsilon^2),\\y^*&=y+\varepsilon Y(x,y;\Psi,T)+O(\varepsilon^2),\\\Psi^*&=\Psi+\varepsilon\eta(x,y;\Psi,T)+O(\varepsilon^2),\\T^*&=T+\varepsilon\zeta(x,y;\Psi,T)+O(\varepsilon^2),\end{aligned}\tag{3.1}$$

where "ε" is the group parameter.

A system of partial differential Equations (2.12)-(2.13) is said to admit a symmetry generated by the vector field

$$\Gamma\equiv X\frac{\partial}{\partial x}+Y\frac{\partial}{\partial y}+\eta\frac{\partial}{\partial\Psi}+\zeta\frac{\partial}{\partial T},\tag{3.2}$$

if it is left invariant by the transformation $(x,y;\Psi,T)\to(x^*,y^*;\Psi^*,T^*)$.

The solutions $\Psi=\Psi(x,y)$ and $T=T(x,y)$, are invariant under the symmetry Equation (3.2) if

$$\Phi_\Psi=\Gamma\left(\Psi-\Psi(x,y)\right)=0,\quad\text{when}\quad\Psi=\Psi(x,y),\tag{3.3}$$

and

$$\Phi_T = \Gamma\left(T - T\left(x, y\right)\right) = 0, \quad \text{when} \quad T = T\left(x, y\right). \tag{3.4}$$

Assume,

$$\Delta_1 = \Psi_y \Psi_{xy} - \Psi_x \Psi_{yy} - \left(\frac{n+1}{2}\right)\Psi_{yyy} + Kx^{n-1}\Psi_y, \tag{3.5}$$

$$\Delta_2 = \Psi_y T_x - \Psi_x T_y - \left(\frac{n+1}{2}\right)\frac{1}{\Pr}T_{yy}. \tag{3.6}$$

A vector Γ given by Equation (3.2), is said to be a Lie point symmetry vector field for Equations (2.12)-(2.13) if

$$\Gamma^{[3]}\left(\Delta_j\right)\Big|_{\Delta_j = 0} = 0, \quad j = 1, 2, \tag{3.7}$$

where,

$$\begin{aligned}\Gamma^{[3]} \equiv{}& X\frac{\partial}{\partial x} + Y\frac{\partial}{\partial y} + \eta\frac{\partial}{\partial \Psi} + \zeta\frac{\partial}{\partial T} + \eta^x\frac{\partial}{\partial \Psi_x} + \eta^y\frac{\partial}{\partial \Psi_y} + \zeta^x\frac{\partial}{\partial T_x} + \zeta^y\frac{\partial}{\partial T_y}\\ &+ \eta^{xy}\frac{\partial}{\partial \Psi_{xy}} + \eta^{yy}\frac{\partial}{\partial \Psi_{yy}} + \zeta^{yy}\frac{\partial}{\partial T_{yy}} + \eta^{yyy}\frac{\partial}{\partial \Psi_{yyy}},\end{aligned} \tag{3.8}$$

is the third prolongation of Γ.

To calculate the prolongation of the given transformation, we need to differentiate Equation (3.1) with respect to each of the variables, x and y. To do this, we introduce the following total derivatives

$$\begin{aligned}D_x &\equiv \partial_x + \Psi_x\partial_\Psi + T_x\partial_T + \Psi_{xx}\partial_{\Psi_x} + T_{xx}\partial_{T_x} + \Psi_{xy}\partial_{\Psi_y} + \cdots,\\ D_y &\equiv \partial_y + \Psi_y\partial_\Psi + T_y\partial_T + \Psi_{yy}\partial_{\Psi_y} + T_{yy}\partial_{T_y} + \Psi_{xy}\partial_{\Psi_x} + \cdots,\end{aligned} \tag{3.9}$$

Equation (3.7) gives the following linear partial differential equation

$$\left(n-1\right)KXx^{n-2}\Psi_y - \eta^x\Psi_{yy} + \eta^y\left[\Psi_{xy} + Kx^{n-1}\right] + \eta^{xy}\Psi_y - \eta^{yy}\Psi_x - \left(\frac{n+1}{2}\right)\eta^{yyy} = 0, \tag{3.10}$$

$$-\eta^x T_y + \eta^y T_x + \zeta^x\Psi_y - \zeta^y\Psi_x - \left(\frac{n+1}{2}\right)\frac{1}{\Pr}\zeta^{yy} = 0. \tag{3.11}$$

The components η^x, η^y, ζ^x, ζ^y, η^{xy}, η^{yy}, ζ^{yy}, η^{yyy} can be determined from the following expressions

$$\begin{aligned}\eta^S &= D_S\eta - \Psi_x D_S X - \Psi_y D_S Y,\\ \zeta^S &= D_S\zeta - T_x D_S X - T_y D_S Y,\\ \eta^{JS} &= D_S\eta^J - \Psi_{Jx}D_S\phi - \Psi_{Jy}D_S\zeta,\\ \zeta^{JS} &= D_S\zeta^J - T_{Jx}D_S X - T_{Jy}D_S Y,\end{aligned} \tag{3.12}$$

where S and J are stand for x and y.

Invariance of the boundary conditions Equation (2.14i), yields

$$\zeta = 0. \tag{3.13}$$

Substitution from Equations (3.12)-(3.13) into Equation (3.11) will lead to a large expression, then, equating to zero the coefficients of T_{xy}, $\Psi_y T_{xy}$, $T_y T_{xy}$, $\Psi_y T_x T_y$, $\Psi_x \Psi_y T_y$ and T_x, gives

$$X_y = X_\Psi = X_T = Y_T = Y_\Psi = \eta_y = 0. \tag{3.14}$$

Substitution from Equation (3.14) into Equation (3.11) will remove many terms. Then, equating to zero the coefficients of T_y and $\Psi_x T_y$, leads to the following system of determining equations:

$$\eta_x - \left(\frac{n+1}{2}\right)\frac{1}{\mathrm{Pr}} Y_{yy} = 0, \tag{3.15}$$

$$X_x - Y_y - \eta_\Psi = 0. \tag{3.16}$$

Again, substitution from Equations (3.12)-(3.16) into Equation (3.10) will remove many terms. Then, equating to zero the coefficients of T_y, $\Psi_x \Psi_y$, Ψ_{yy}, $\left(\Psi_y\right)^2$, $\Psi_x \left(\Psi_y\right)^2$ and Ψ_y, gives

$$\eta_T = Y_{yy} = \eta_x = Y_{xy} = \eta_{\Psi\Psi} = 0, \tag{3.17}$$

and

$$X - \left(\frac{2}{1-n}\right) x Y_y = 0. \tag{3.18}$$

Solving the system of Equations (3.14)-(3.18) in view of the invariance of the boundary conditions Equation (2.14), yields

$$X = \frac{2c_1 x}{1-n}, \quad Y = c_1 y + c_2, \quad \eta = \left(\frac{1+n}{1-n}\right) c_1 \Psi + c_3, \quad \zeta = 0. \tag{3.19}$$

The system of nonlinear Equations (2.12)-(2.13) has the three-parameter Lie group of point symmetries generated by

$$\Gamma_1 \equiv \frac{2x}{1-n}\frac{\partial}{\partial x} + y\frac{\partial}{\partial y} + \frac{1+n}{1-n}\Psi\frac{\partial}{\partial \Psi}, \quad \Gamma_2 \equiv \frac{\partial}{\partial y} \quad \text{and} \quad \Gamma_3 \equiv \frac{\partial}{\partial \Psi}. \tag{3.20}$$

The one-parameter group generated by Γ_1 consists of scaling, whereas Γ_2 and Γ_3 consists of translation. The commutator table of the symmetries is given in **Table 1**, where the entry in the *i*-th row and *j*-th column is defined as $\left[\Gamma_i, \Gamma_j\right] = \Gamma_i \Gamma_j - \Gamma_j \Gamma_i$.

The finite transformations corresponding to the symmetries Γ_1, Γ_2 and Γ_3 are respectively

$$\left.\begin{array}{llll} \Gamma_1 : x^* = \mathrm{e}^{\frac{2}{1-n}\varepsilon_1} x, & y^* = \mathrm{e}^{\varepsilon_1} y, & \Psi^* = \mathrm{e}^{\frac{1+n}{1-n}\varepsilon_1} \Psi, & T^* = T \\ \Gamma_2 : x^* = x, & y^* = y + \varepsilon_2, & \Psi^* = \Psi, & T^* = T \\ \Gamma_3 : x^* = x, & y^* = y, & \Psi^* = \Psi + \varepsilon_3, & T^* = T \end{array}\right\}, \tag{3.21}$$

where ε_1, ε_2 and ε_3 are the group parameters.

We look for solutions that invariant under the linear combination of the operators given by Equation (3.20). By determine the one-dimensional optimal system of subalgebras of the given partial differential equation, all of these solutions can be obtained. Olver's approach given in [17] starts out by computing the commutators of the

Table 1. Table of commutators of the basis operators.

	Γ_1	Γ_2	Γ_3
Γ_1	0	$-\Gamma_2$	$-\frac{1+n}{1-n}\Gamma_3$
Γ_2	Γ_2	0	0
Γ_3	$\frac{1+n}{1-n}\Gamma_3$	0	0

symmetry Lie algebra Equation (3.20) and then obtaining the adjoint representations. The adjoint action on Lie algebras is defined by the adjoint operator given by

$$\mathrm{Ad}_{\exp(a\Gamma_i)}\left\langle \Gamma_j \right\rangle = \mathrm{e}^{-a\Gamma_i}\Gamma_j \mathrm{e}^{a\Gamma_i}, \tag{3.22}$$

where, a is a small parameter.

In terms of Lie brackets using Campbell-Baker-Hausdorff theorem [31], this operator can be rewritten as

$$\mathrm{Ad}_{\exp(a\Gamma_i)}\left\langle \Gamma_j \right\rangle = \Gamma_j - a\left[\Gamma_i,\Gamma_j\right] + \frac{a^2}{2!}\left[\Gamma_i,\left[\Gamma_i,\Gamma_j\right]\right] - \cdots. \tag{3.23}$$

In our problem, $\Omega = \left\langle \Gamma_1,\Gamma_2,\Gamma_3 \right\rangle$ is the Lie algebra associated with the symmetry group. The calculations of the adjoint action are summarized in **Table 2**.

To construct the one-dimensional optimal system of Ω, consider a general element of Ω given by

$$G = a_1\Gamma_1 + a_2\Gamma_2 + a_3\Gamma_3, \tag{3.24}$$

for some constants a_1, a_2 and a_3, and probe whether G can be transformed to a new element G' under the general adjoint action, where G' takes a simpler form than G, [32].

Let,

$$G' = \mathrm{Ad}_{\exp(a\Gamma_i)}\left\langle G \right\rangle = a_1'\Gamma_1 + a_2'\Gamma_2 + a_3'\Gamma_3. \tag{3.25}$$

We make appropriate choice of a such that the a_i' 's can be made 0 or 1. We end up with simpler forms of G that will constitute the one-dimensional optimal system.

By substitution $\Gamma_i = \Gamma_2$ in Equation (3.25) and dropping the primes, we get

$$G' = a_1\Gamma_1 + \left(a_2 - aa_1\right)\Gamma_2 + a_3\Gamma_3. \tag{3.26}$$

Now, Equation (3.26) prompts the consideration of the cases $a_1 \neq 0$ and $a_1 = 0$.

Case (1): $a_1 \neq 0$

By choosing $\left(a = a_2/a_1\right)$ and scaling the resulting operator by a_1, Equation (3.26) will be

$$G' = \Gamma_1 + a_3\Gamma_3. \tag{3.27}$$

We can further consider the subcases $a_3 \neq 0$ and $a_3 = 0$. Therefore, an optimal system of one-dimensional subalgebra for this case is given by $\left\{\Gamma_1, \Gamma_1 + \delta\Gamma_3\right\}$, where, $\delta \in R$.

Case (2): $a_1 = 0$

Using repeatedly the adjoint operation to simplify G, an optimal system of one-dimensional subalgebra for this case is given by $\left\{\Gamma_2, \Gamma_2 + \gamma\Gamma_3\right\}$, where, $\gamma \in R$.

In summary, the optimal system of one-dimensional subalgebras of the symmetry Lie algebra is

$$\Theta = \left\{\Gamma_1, \Gamma_2, \Gamma_1 + \delta\Gamma_3, \Gamma_2 + \gamma\Gamma_3\right\}. \tag{3.28}$$

Table 3 shows the solution of the invariant surface conditions associated with the optimal system.

(*i*) *Solutions invariant under* $\boldsymbol{\Gamma_1}$:

The characteristic

Table 2. Table of adjoint representations.

Ad	Γ_1	Γ_2	Γ_3
Γ_1	Γ_1	$\mathrm{e}^{a}\Gamma_2$	$\mathrm{e}^{\frac{1+n}{1-n}a}\Gamma_3$
Γ_2	$\Gamma_1 - a\Gamma_2$	Γ_2	Γ_3
Γ_3	$\Gamma_1 - \frac{1+n}{1-n}a\Gamma_3$	Γ_2	Γ_3

Table 3. Solutions of the invariant surface conditions associated with the optimal system.

Generator	Characteristic $\Phi=(\Phi_\Psi,\Phi_T)$	Solutions of the invariant surface conditions
Γ_1	$\Phi_\Psi=\frac{1+n}{1-n}\Psi-\frac{2x}{1-n}\Psi_x-y\Psi_y,\ \Phi_T=-\frac{2x}{1-n}T_x-yT_y$	$\Psi=x^{\frac{n+1}{2}}F(\lambda),\ T=\theta(\lambda),\ \lambda=yx^{\frac{n-1}{2}}$
Γ_2	$\Phi_\Psi=-\Psi_y,\ \Phi_T=-T_y$	$\Psi=\Psi(x),\ T=T(x)$
$\Gamma_1+\delta\Gamma_3$	$\Phi_\Psi=\frac{1+n}{1-n}\Psi+\delta-\frac{2x}{1-n}\Psi_x-y\Psi_y,\ \Phi_T=-\frac{2x}{1-n}T_x-yT_y$	$\Psi=x^{\frac{n+1}{2}}F(\lambda)-\frac{1-n}{1+n}\delta,\ T=\theta(\lambda),\ \lambda=yx^{\frac{n-1}{2}}$
$\Gamma_2+\gamma\Gamma_3$	$\Phi_\Psi=\gamma-\Psi_y,\ \Phi_T=-T_y$	$\Psi=\gamma y+g(x),\ T=T(x)$

$$\Phi=(\Phi_\Psi,\Phi_T), \tag{3.29}$$

has the components

$$\Phi_\Psi=\frac{1+n}{1-n}\Psi-\frac{2x}{1-n}\Psi_x-y\Psi_y,\quad \Phi_T=-\frac{2x}{1-n}T_x-yT_y. \tag{3.30}$$

Therefore, the general solutions of the invariant surface conditions Equations (3.3)-(3.4) are

$$\Psi=x^{\frac{n+1}{2}}F(\lambda),\quad T=\theta(\lambda), \tag{3.31}$$

where $\lambda=yx^{\frac{n-1}{2}}$ is the similarity variable.

Substitution from Equation (3.31) into Equations (2.12)-(2.13), yields

$$\frac{d^3F}{d\lambda^3}+F\frac{d^2F}{d\lambda^2}-\beta\left(\frac{dF}{d\lambda}\right)^2-M\frac{dF}{d\lambda}=0, \tag{3.32}$$

$$\frac{d^2\theta}{d\lambda^2}+\mathrm{Pr}F\frac{d\theta}{d\lambda}=0, \tag{3.33}$$

where, $\beta=\frac{2n}{n+1}$ and $M=\frac{2K}{n+1}$ is the magnetic parameter, where $\sqrt{M}$ is the Hartmann number.

The boundary conditions Equation (2.14) will be

$$\begin{aligned}&(\mathrm{i})\ \frac{dF}{d\lambda}=1,\ F=0,\ \theta=1\ \text{at}\ \lambda=0,\\&(\mathrm{ii})\ \frac{dF}{d\lambda}\to 0,\ \theta\to 0\ \text{as}\ \lambda\to\infty.\end{aligned} \tag{3.34}$$

(ii) Solutions invariant under $\boldsymbol{\Gamma_2}$ **:**

The characteristic Equation (3.29) has the components

$$\Phi_\Psi=-\Psi_y,\quad \Phi_T=-T_y. \tag{3.35}$$

Therefore, the general solutions of the invariant surface conditions Equations (3.3)-(3.4) are

$$\Psi=\Psi(x),\quad T=T(x). \tag{3.36}$$

Practically, Equation (3.36) is a solution of Equations (2.12)-(2.13), even though it is not a particularly interesting one which contradicts the boundary conditions Equation (2.14). So, no solutions are invariant under the group generated by Γ_2.

(iii) Solutions invariant under $\boldsymbol{\Gamma_1+\delta\Gamma_3}$ **:**

The characteristic Equation (3.29) has the components

$$\Phi_{\Psi} = \frac{1+n}{1-n}\Psi + \delta - \frac{2x}{1-n}\Psi_x - y\Psi_y, \quad \Phi_T = -\frac{2x}{1-n}T_x - yT_y. \tag{3.37}$$

Therefore, the general solutions of the invariant surface conditions Equations (3.3)-(3.4) are

$$\Psi = x^{\frac{n+1}{2}} F(\lambda) - \frac{1-n}{1+n}\delta, \quad T = \theta(\lambda), \tag{3.38}$$

where $\lambda = yx^{\frac{n-1}{2}}$ is the similarity variable, which gives the same solutions invariant under Γ_1.

(*iv*) *Solutions invariant under* $\boldsymbol{\Gamma_2 + \gamma\Gamma_3}$:

The characteristic Equation (3.29) has the components

$$\Phi_{\Psi} = \gamma - \Psi_y, \quad \Phi_T = -T_y. \tag{3.39}$$

Therefore, the general solutions of the invariant surface conditions Equations (3.3)-(3.4) are

$$\Psi = \gamma y + g(x), \quad T = T(x). \tag{3.40}$$

This contradicts the boundary conditions Equation (2.14). So, no solutions are invariant under the group generated by $\Gamma_2 + \gamma\Gamma_3$.

4. Results and Discussion

The system of non-linear differential Equations (3.32)-(3.33) with the boundary conditions Equation (3.34) is solved numerically using the shooting method, coupled with Runge-Kutta scheme. From Equations (2.11) and (3.31), we get

$$U = \frac{u}{x^n} = \frac{\mathrm{d}F}{\mathrm{d}\lambda}, \quad V = \frac{v}{x^{\frac{n-1}{2}}} = -\frac{n+1}{2}\left[F + \left(\frac{n-1}{n+1}\right)\lambda\frac{\mathrm{d}F}{\mathrm{d}\lambda}\right]. \tag{4.1}$$

The effects of the parameter β which is a function of the power-index n, the Hartmann number $\sqrt{M}$, and the Prandtl number $\Pr$ on the horizontal and vertical velocities, and temperature profiles are illustrated in **Figures 2-8**. Moreover, the numerical values of the skin friction $f''(0)$ (wall shear stress) and rate of heat transfer $-\theta'(0)$ are tabulated in **Tables 4-11**, for different values of parameters of interest.

4.1. The Horizontal Velocity

Figure 2 illustrates the effect of β on the profile of the horizontal velocity U. It is noted that, the horizontal velocity decreases as β increases both for $M = 0$ (hydrodynamic fluid) and $M = 1$ (hydromagnetic fluid) but this decreasing is smaller with $M = 1$ compared with the case $M = 0$, that is because the magnetic force acts as a resistance to the flow, [13]. Also, the boundary layer thickness decreases by increasing β and the flow makes the stretching surface rougher.

Figure 3 describes the effect of M on the behavior of the horizontal velocity U. As seen, by increasing the magnetic field, the horizontal velocity and the thickness of the boundary layer decrease. From **Figure 3(a)** we can conclude that, for $\beta = -1.5$ with small values of M less than 0.4 near the surface, the behavior of the horizontal velocity is differ from the well-known cases, that is because the horizontal velocity increases to a maximum values before it starts to decrease.

4.2. The Vertical Velocity

Figure 4 shows the behaviour of the vertical velocity V for $\beta = 1.5$, over a range of the magnetic parameter M. As seen, the absolute value of the vertical velocity increases with the decrease of M.

Figure 5 illustrates the behaviour of the vertical velocity V for $M = 1$ over a range of the parameter β. As seen, the absolute value of the vertical velocity increases with the increase of β.

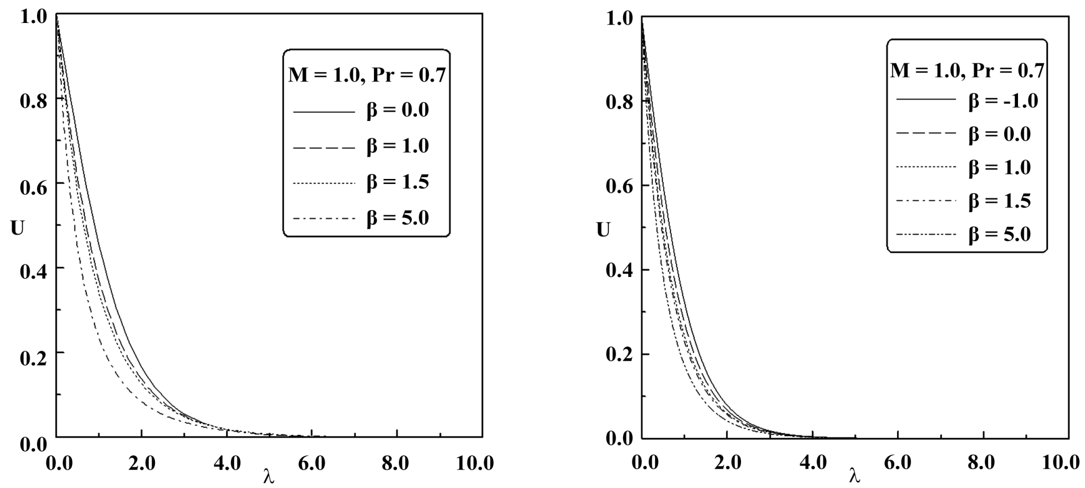

(a) (b)

Figure 2. Horizontal velocity profiles over a range of β with $\Pr = 0.7$ for: (a) $M = 0$; (b) $M = 1$.

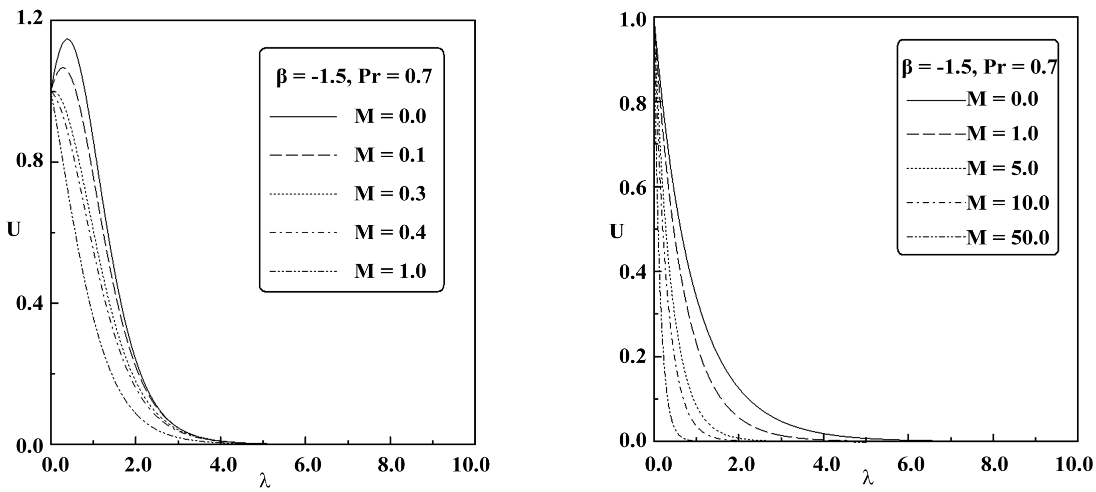

(a) (b)

Figure 3. Horizontal velocity profiles over a range of M with $\Pr = 0.7$ for: (a) $\beta = -1.5$; (b) $\beta = 1.5$.

4.3. The Temperature

Figure 6 illustrates the variation of the temperature profiles θ for $\beta = 1.5$ with Prandtl number $\Pr = 0.7$, over a range of M. We notice that, the temperature profiles increases as M increases.

Figure 7 describes the distribution of the temperature θ for $M = 0$ with $\Pr = 1.0$, over a range of the nonlinear stretching parameter n. As seen, with an increase in n, the temperature increases.

Figure 8 shows the variation of the temperature profiles θ for $\beta = 1.5$ with $M = 0.0$, over a range of the Prandtl number $\Pr$. As seen, the temperature decreases as the Prandtl number increases which consistent with the fact that the thermal boundary layer thickness decreases as the Prandtl number $\Pr$ increases.

4.4. Wall Shear Stress

The dimensionless wall shear stress $F''(0)$ (skin friction) is computed for different values of the Hartmann number $\sqrt{M}$ and the parameter β. **Table 4** shows the numerical values of the skin friction $F''(0)$ for different values of the nonlinear stretching parameter n with $M = 0.0$. As seen, the absolute value of the dimensionless wall shear stress $|F''(0)|$ increases with increasing n, that is because by increasing the values of n

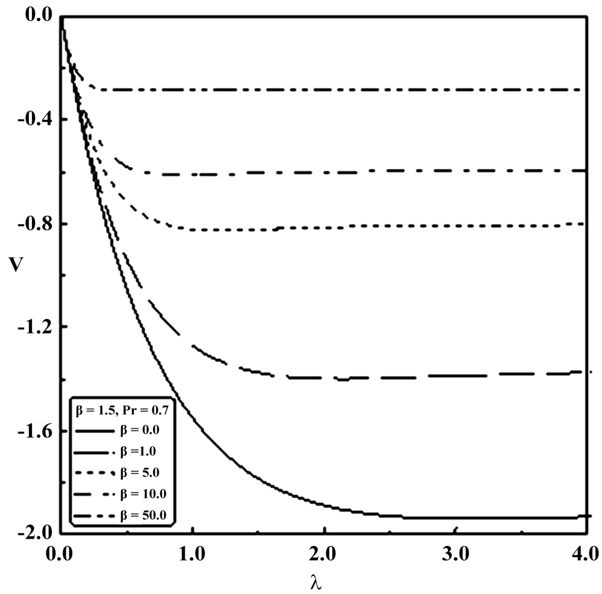

Figure 4. Vertical velocity profiles over a range of M with $\beta = 1.5$ and $\Pr = 0.7$.

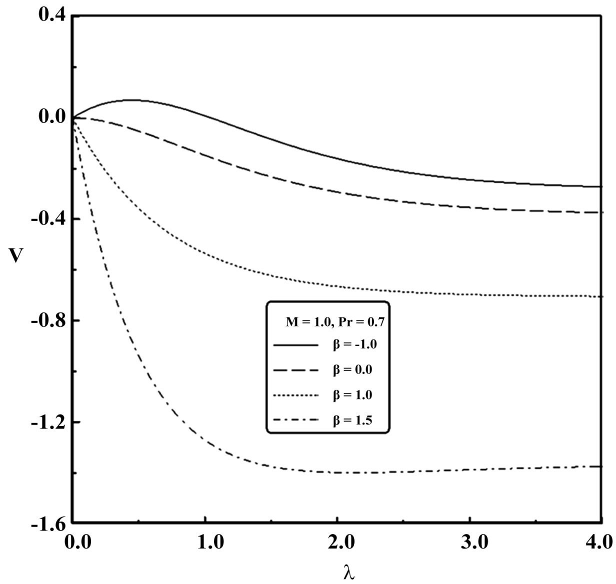

Figure 5. Vertical velocity profiles over a range of β with $M = 1$ and $\Pr = 0.7$.

the layer thickness decreases with an increase in the skin friction at the wall which may cause to lose the smoothness of the stretching wall. So, by increasing the value of n, the flow makes the stretching surface rougher. An excellent agreement between our work and other works is absorbed.

Tables 5-8 show the numerical values of $F''(0)$ over a range of M with at $\beta = 1$, 1.5, 5, -1 and $\beta = -1.5$, respectively. As M increases, the absolute value of the dimensionless wall shear stress $|F''(0)|$ increases and the thickness of the boundary layer decreases. From **Table 8**, we noticed that, for small values of M less than 0.4, $|F''(0)|$ decreases as M increases which is consistent with **Figure 3(a)**. Again, an excellent agreement is achieved between our work and other works. No convergent value for $F''(0)$ is obtained by Hayat *et al*. [9] when $\beta = -1.5$ at $M = 0.0$, see **Table 8**.

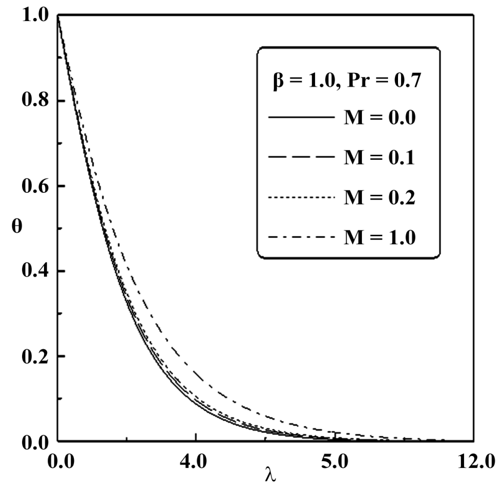

Figure 6. Temperature profiles over a range of M with $\beta = 1.5$ and $\Pr = 0.7$.

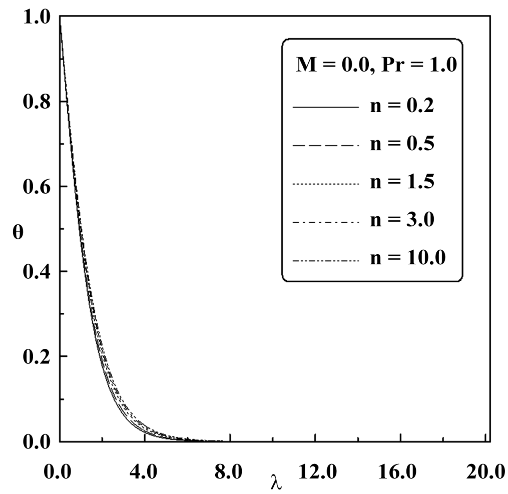

Figure 7. Temperature profiles over a range of n with $M = 0.0$ and $\Pr = 1.0$.

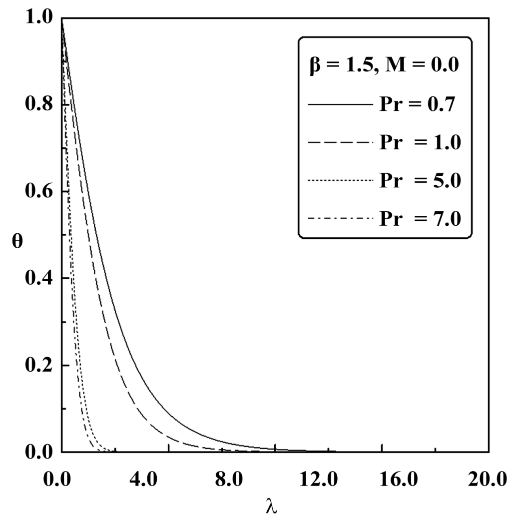

Figure 8. Temperature profiles over a range of $\Pr$ with $\beta = 1.5$ and $M = 0.0$.

Table 4. Comparison between the values of $F''(0)$ for different n with $M = 0.0$.

n	Vajravelu [6]	Cortell [7]	Abbas & Hayat [8]	Javed *et al.* [13]	Present work
0.00	−1.0000	−0.627547	−0.627547	−0.627554	−0.6275556
0.20		−0.766758	−0.766837	−0.766837	−0.7668370
0.50		−0.889477	−0.889544	−0.889543	−0.8895435
0.75		−0.953786	−0.953956	−0.953956	−0.9539564
1.00		−1.000000	−1.000000	−1.000000	−1.0000000
1.50		−1.061587	−1.061601	−1.061601	−1.0616011
3.00		−1.148588	−1.148593	−1.148593	−1.1485931
5.00	−1.1945				−1.1944906
7.00		−1.216847	−1.216851	−1.216850	−1.2168503
10.00	−1.2348	−1.234875	−1.234874	−1.234875	−1.2348750
20.00		−1.257418	−1.257423	−1.257423	−1.2574230
100.00		−1.276768	−1.276773	−1.276773	−1.2767731

Table 5. Comparison between the values of $F''(0)$ for different M at $\beta = 1.0$.

M	Pavlov [12]	Ghotbi [10]	Mehmood *et al.* [11]	Hayat *et al.* [9]	Fathizadeh *et al.* [14]	Present work
0	−1.00000			−1.00000	−1.00000	−1.0000000
1	−1.41421	−1.41421	−1.41421	−1.41421	−1.41421	−1.4142136
2	−1.73205		−1.73205			−1.7320508
3	−2.00000		−2.00000			−2.0000000
4	−2.23607		−2.23607			−2.2360680
5	−2.44948	−2.44948	−2.44948	−2.44948	−2.44948	−2.4494897
10	−3.31662	−3.31662	−3.31606	−3.31662	−3.31662	−3.3166248
15	−4.00000		−4.00100			−4.0000000
50	−7.14142			−7.14142	−7.14142	−7.1414284
100	−10.04987			−10.04987	−10.0499	−10.0498756
500	−22.38302			−22.38302	−22.383	−22.3830293
1000	−31.63858			−31.63858	−31.6386	−31.6385840

Table 6. Comparison between the values of $F''(0)$ for different M at $\beta = 1.5$.

M	Chiam [5]	Ghotbi [10]	Hayat *et al.* [9]	Fathizadeh *et al.* [14]	Present work
0	−1.14860		−1.1547	−1.1547	−1.1486025
1	−1.52527	−1.5252	−1.5252	−1.5252	−1.5252751
5	−2.51615	−2.5161	−2.5161	−2.5161	−2.5161550
10	−3.36631	−3.3663	−3.3663	−3.3663	−3.3663151
50	−7.16471		−7.1647	−7.1647	−7.1647100
100	−10.0664		−10.0776	−10.0776	−10.0664392
500			−22.3904	−22.3904	−22.3904733
1000			−31.6438	−31.6438	−31.6438511

Table 7. Comparison between the values of $F''(0)$ for different M at $\beta = 5$.

M	Chiam [5]	Hayat *et al.* [9]	Fathizadeh *et al.* [14]	Present work
0	−1.90253	−1.9098	−1.9098	−1.9025302
1	−2.15290	−2.1528	−2.1528	−2.1529005
5	−2.94144	−2.9414	−2.9414	−2.9414400
10	−3.69566	−3.6956	−3.6956	−3.6956600
50	−7.32561	−7.3256	−7.3256	−7.3256104
100	−10.1816	−10.1816	−10.1816	−10.1816304
500		−22.4425	−22.4425	−22.4425144
1000		−31.6806	−31.6806	−31.6806970

Table 8. Comparison between the values of $F''(0)$ for different M at $\beta = -1.0$ and $\beta = -1.5$.

M	$\beta = -1.0$			$\beta = -1.5$		
	Chiam [5]	Hayat *et al.* [9]	Present work	Chiam [5]	Hayat *et al.* [9]	Present work
0	0	0	−0.0000010	0.72725		0.7272522
0.1	−0.13215		−0.1321503	0.45107		0.4510704
0.2	−0.24783		−0.2478346	0.23038		0.2303800
0.3	−0.35006		−0.3500590	0.05203		0.0520301
0.4	−0.44140		−0.4414001	−0.09506		−0.0950601
0.5	−0.52395		−0.5239522	−0.21922		−0.2192231
1	−0.85111	−0.8511	−0.8511102	−0.65298	−0.6532	−0.6529817
5	−2.16287	−2.1628	−2.1628674	−2.08524	−2.0852	−2.0852400
10	−3.11003	−3.1100	−3.1100280	−3.05623	−3.0562	−3.0562320
50		−7.0475	−7.0475366		−7.0238	−7.0238680
100	−9.98335	−9.9833	−9.9833469	−9.96665	−9.9666	−9.9666500
500		−22.3532	−22.3532277		−22.3457	−22.3457703
1000		−31.6175	−31.6175069		−31.6122	−31.6122354

Table 9. Comparison between the values of $(-\theta'(0))$ for different values of $\Pr$ and n with $M = 0.0$.

n	$\Pr = 1.0$				$\Pr = 5.0$			
	Cortell [7]	Abbas & Hayat [8]	Javed *et al.* [13]	Present work	Cortell [7]	Abbas & Hayat [8]	Javed *et al.* [13]	Present work
0.2	0.610262	0.610217	0.610202	0.6102172	1.607175	1.607925	1.607788	1.6077882
0.5	0.595277	0.595201	0.595201	0.5952010	1.586744	1.586833	1.586783	1.5867823
1.5	0.574537	0.574729	0.574730	0.5747321	1.557463	1.557672	1.557696	1.5576960
3	0.564472	0.564661	0.564662	0.5646656	1.542337	1.542145	1.543182	1.5431820
10	0.554960	0.554878	0.554879	0.5548930	1.528573	1.528857	1.528930	1.5289301

Table 10. Comparison between the values of $\left(-\theta'(0)\right)$ at $M = 0.0$ for different values of $\Pr$ and n.

n	$\Pr = 0.71$		$\Pr = 7.0$	
	Vajravelu [6]	Present work	Vajravelu [6]	Present work
1.00	0.4590	0.4590330	1.8953	1.8953002
5.00	0.4394	0.4394328	1.8610	1.8610243
10.00	0.4357	0.4357003	1.8541	1.8541054

Table 11. Numerical values of $\left(-\theta'(0)\right)$ for different M at $\beta = -1.0$ and $\Pr = 0.7$.

M	$-\theta'(0)$
0.0	0.5644206
0.1	0.5454137
0.2	0.5280396
0.3	0.5124372
0.4	0.4983892
0.5	0.4856431
1.0	0.4416029
5.0	0.4039894

4.5. Wall Shear Stress

Table 9 illustrates the numerical values of the surface heat flux $\left(-\theta'(0)\right)$ for different values of the Prandtl number $\Pr$ and nonlinear stretching parameter n with $M = 0.0$. The thickness of thermal boundary layer becomes thinner when $\Pr$ increases and this causes an increase in the gradient of the temperature, so, the surface heat flux $\left(-\theta'(0)\right)$ increases as $\Pr$ increases. As seen, the results of the present work are in very good agreement with other works, **Table 9**.

Also, from **Table 9**, it is noticed that, for fixed value of $\Pr$, the surface heat flux $\left(-\theta'(0)\right)$ decreases as nonlinear stretching parameter n increases. Also, the value of $\left(-\theta'(0)\right)$ is positive which is consistent with the fact that the heat flows from the sheet surface to the fluid as long as $T_w > T_\infty$.

Another comparison between the present work with the work of Vajravelu [6] is made, see **Table 10**.

Table 11 illustrates the numerical values of the surface heat flux $\left(-\theta'(0)\right)$ for different values of the M with $\beta = -1.0$ and $\Pr = 0.7$. As seen, the surface heat flux $\left(-\theta'(0)\right)$ decreases as M increases.

5. Conclusion

We have used Lie-group method to obtain the similarity reductions of the MHD boundary-layer equations. By determining the transformation group under which the given system of partial differential equations and its boundary conditions are invariant, we obtained the invariants and the symmetries of these equations. In turn, we used these invariants and symmetries to determine the similarity variables that reduced the number of independent variables. The resulting system of ordinary differential equations was solved numerically using shooting method coupled with Runge-Kutta scheme and the results were plotted. The numerical values of the wall shear stress (skin friction) and surface heat flux were compared with those obtained by other works and they were found in a good agreement.

Acknowledgements

The author would like to express his appreciations for the potential reviewers for their valuable comments that

improved the paper and enhanced the results.

References

[1] Pop, S.R., Grosan, T. and Pop, I. (2004) Radiation Effects on the Flow near the Stagnation Point of a Stretching Sheet. *Technische Mechanik*, **25**, 100-106.

[2] Sakiadis, B.C. (1961) Boundary Layer Behaviour on Continuous Solid Surfaces, II. The Boundary Layer on a Continuous Flat Surface. *AIChE Journal*, **7**, 221-225. http://dx.doi.org/10.1002/aic.690070211

[3] Crane, L.J. (1970) Flow past a Stretching Plate. *Journal of Applied Mathematics and Physics* (*ZAMP*), **21**, 645-647. http://dx.doi.org/10.1007/BF01587695

[4] Gupta, P.S. and Gupta, A.S. (1977) Heat and Mass Transfer on a Stretching Sheet with Suction or Blowing. *Canadian Journal of Chemical Engineering*, **55**, 744-746. http://dx.doi.org/10.1002/cjce.5450550619

[5] Chaim, T.C. (1995) Hydromagnetic Flow over a Surface Stretching with a Power-Law Velocity. *International Journal of Engineering Science*, **33**, 429-435. http://dx.doi.org/10.1016/0020-7225(94)00066-S

[6] Vajravelu, K. (2001) Viscous Flow over a Nonlinearly Stretching Sheet. *Applied Mathematics and Computation*, **124**, 281-288. http://dx.doi.org/10.1016/S0096-3003(00)00062-X

[7] Cortell, R. (2007) Viscous Flow and Heat Transfer over a Nonlinearly Stretching Sheet. *Applied Mathematics and Computation*, **184**, 864-873. http://dx.doi.org/10.1016/j.amc.2006.06.077

[8] Abbas, Z. and Hayat, T. (2008) Radiation Effects on MHD Flow in a Porous Space. *International Journal of Heat and Mass Transfer*, **51**, 1024-1033. http://dx.doi.org/10.1016/j.ijheatmasstransfer.2007.05.031

[9] Hayat, T., Hussain, Q. and Javed, T. (2009) The Modified Decomposition Method and Padé Approximants for the MHD Flow over a Non-Linear Stretching Sheet. *Nonlinear Analysis: Real World Applications*, **10**, 966-973. http://dx.doi.org/10.1016/j.nonrwa.2007.11.020

[10] Ghotbi, A.R. (2009) Homotopy Analysis Method for Solving the MHD Flow over a Non-Linear Stretching Sheet. *Communications in Nonlinear Science and Numerical Simulation*, **14**, 2653-2663.

[11] Mehmood, A., Munawar, S. and Ali, A. (2010) Comments to: ‘‘Homotopy Analysis Method for Solving the MHD Flow over a Non-Linear Stretching Sheet (Commun. Nonlinear Sci. Numer. Simul. 14 (2009) (2653-2663)”. *Communications in Nonlinear Science and Numerical Simulation*, **15**, 4233-4240. http://dx.doi.org/10.1016/j.cnsns.2009.12.039

[12] Pavlov, K.B. (1974) Magnetohydrodynamic Flow of an Incompressible Viscous Fluid Caused by Deformation of a Surface. *Magnitnaya Gidrodinamika*, **4**, 146-147.

[13] Javed, T., Abbas, Z., Sajid, M. and Ali, N. (2011) Heat Transfer Analysis for a Hydromagnetic Viscous Fluid over a Non-Linear Shrinking Sheet. *International Journal of Heat and Mass Transfer*, **54**, 2034-2042. http://dx.doi.org/10.1016/j.ijheatmasstransfer.2010.12.025

[14] Fathizadah, M., Madani, M., Khan, Y., Faraz, N., Yıldırım, A. and Tutkun, S. (2013) An Effective Modification of the Homotopy Perturbation Method for MHD Viscous Flow over a Stretching Sheet. *Journal of King Saud University-Science*, **25**, 107-113. http://dx.doi.org/10.1016/j.jksus.2011.08.003

[15] Hill, J.M. (1982) Solution of Differential Equations by Means of One-Parameter Groups. Pitman Publishing Company, Boston.

[16] Seshadri, R. and Na, T.Y. (1985) Group Invariance in Engineering Boundary Value Problems. Springer-Verlag, New York. http://dx.doi.org/10.1007/978-1-4612-5102-6

[17] Olver, P.J. (1986) Applications of Lie Groups to Differential Equations. Springer-Verlag, New York.

[18] Ibragimov, N.H. (1999) Elementary Lie Group Analysis and Ordinary Differential Equations. Wiley, New York.

[19] Boutros, Y.Z., Abd-el-Malek, M.B., Badran, N.A. and Hassan, H.S. (2006) Lie-Group Method for Unsteady Flows in a Semi-Infinite Expanding or Contracting Pipe with Injection or Suction through a Porous Wall. *Journal of Computational and Applied Mathematics*, **197**, 465-494. http://dx.doi.org/10.1016/j.cam.2005.11.031

[20] Boutros, Y.Z., Abd-el-Malek, M.B., Badran, N.A. and Hassan, H.S. (2007) Lie-Group Method of Solution for Steady Two-Dimensional Boundary-Layer Stagnation-Point Flow towards a Heated Stretching Sheet Placed in a Porous Medium. *Meccanica*, **41**, 681-691. http://dx.doi.org/10.1007/s11012-006-9014-x

[21] Boutros, Y.Z., Abd-el-Malek, M.B., Badran, N.A. and Hassan, H.S. (2007) Lie-Group Method Solution for Two-Dimensional Viscous Flow between Slowly Expanding or Contracting Walls with Weak Permeability. *Applied Mathematical Modelling*, **31**, 1092-1108. http://dx.doi.org/10.1016/j.apm.2006.03.026

[22] Abd-el-Malek, M.B., Badran, N.A. and Hassan, H.S. (2007) Lie-Group Method for Predicting Water Content for Immiscible Flow of Two Fluids in a Porous Medium. *Applied Mathematical Sciences*, **1**, 1169-1180.

[23] Abd-el-Malek, M.B. and Hassan, H.S. (2010) Symmetry Analysis for Steady Boundary-Layer Stagnation-Point Flow of Rivlin-Ericksen Fluid of Second Grade Subject to Suction. *Nonlinear Analysis*: *Modelling and Control*, **15**, 379-396.

[24] Abd-el-Malek, M.B. and Hassan, H.S. (2010) Solution of Burgers' Equation with Time-Dependent Kinematic Viscosity via Lie-Group Analysis. *Proceedings of the* 5*th International Workshop* "*Group Analysis of Differential Equations & Integrable Systems*", Protaras-Cyprus, 6-10 June 2010, 6-14.

[25] Abd-el-Malek, M.B., Badran, N.A., Hassan, H.S. and Abbas, H.H. (2013) New Solutions for Solving the Problem of Particle Trajectories in Linear Deep-Water Waves via Lie-Group Method. *Applied Mathematics and Computation*, **219**, 11365-11375. http://dx.doi.org/10.1016/j.amc.2013.05.059

[26] Abd-el-Malek, M.B. and Hassan, H.S. (2014) Lie Group Method for Solving the Problem of Fission Product Behavior in Nuclear Fuel. *Mathematical Methods in the Applied Sciences*, **37**, 420-427. http://dx.doi.org/10.1002/mma.2802

[27] Hassan, H.S., Mahrous, S.A., Sharara, A. and Hassan, A. (2014) A Study for MHD Boundary Layer Flow of Variable Viscosity over a Heated Stretching Sheet via Lie-Group Method. *Applied Mathematics & Information Sciences*, in Press.

[28] Abd-el-Malek, M.B., Badran, N.A., Hassan, H.S. and Abbas, H.H. (2015) New Solutions for Solving Boussinesq Equation via Potential Symmetries Method. *Applied Mathematics and Computation*, **251**, 225-232. http://dx.doi.org/10.1016/j.amc.2014.11.055

[29] Abd-el-Malek, M.B., Badran, N.A., Hassan, H.S. and Abbas, H.H. (2014) Lie Group Method for Studying the Thermophoresis and Heat Generation Effect on Free-Convection Laminar Boundary-Layer Flow over a Vertical Flat Plate. Submitted for Publication.

[30] Abd-el-Malek, M.B. and Hassan, H.S. (2014) Solution of N-Dimensional Radially Symmetric Non-Linear Diffusion Equation via Symmetry Analysis. Submitted for Publication.

[31] Jacobson, N. (1979) Lie Algebras. Dover, New York.

[32] WafoSoh, C. (2005) Invariant Solutions of the Unidirectional Flow of an Electrically Charged Power-Law Non-Newtonian Fluid over a Flat Plate in Presence of a Transverse Magnetic Field. *Communications in Nonlinear Science and Numerical Simulation*, **10**, 537-548. http://dx.doi.org/10.1016/j.cnsns.2003.12.008

Applied Mathematics, 2015, 6, 95-105
Published Online January 2015 in SciRes. http://www.scirp.org/journal/am
http://dx.doi.org/10.4236/am.2015.61010

On the Inverse MEG Problem with a 1-D Current Distribution

George Dassios, Konstantia Satrazemi

Department of Chemical Engineering, University of Patras and ICE/HT-FORTH, Patras, Greece
Email: gdassios@otenet.gr

Received 29 October 2014; revised 20 November 2014; accepted 8 December 2014

Abstract

The inverse problem of magnetoencephalography (MEG) seeks the neuronal current within the conductive brain that generates a measured magnetic flux in the exterior of the brain-head system. This problem does not have a unique solution, and in particular, it is not even possible to identify the support of the current if it extends over a three-dimensional set. However, a localized current supported on a zero-, one- or two-dimensional set can in principle be identified. In the present work, we demonstrate an analytic algorithm that is able to recover a one-dimensional distribution of current from the knowledge of the exterior magnetic flux field. In particular, we consider a neuronal current that is supported on a small line segment of arbitrary location and orientation in space, and we reduce the identification of its characteristics to a nonlinear algebraic system. A series of numerical tests show that this system has a unique real solution. A special case is easily solved via the use of trivial algebraic operations.

Keywords

Magnetoencephalography, Current Identification

1. Introduction

The brain is a conducting material and therefore, every generated neuronal current is accompanied by an induction current. Consequently, when we measure the magnetic flux density outside the head we actually measure the effects of both the neuronal as well as the induction current. This is the main problem with the inverse problem of magnetoencephalography, the fact that the induction current "hides" somehow the primary neuronal excitation. An excellent review of the electromagnetic activity of the human brain can be found in [1], as well as in the book by Malmivuo and Plonsey [2].

Exactly a hundred and sixty years ago Helmholtz [3] showed that it is not possible to recover an electric current within a conductor from knowledge of the magnetic flux generated outside the conductor. However, a complete quantitative characterization of what part of the current is possible to be identified was a topic of intense investigation during the last two decades and the main results can be found in [4]. Fokas proved that, independently of the geometry of the conductor, we cannot recover more than one out of the three functions that define the current, in the case of electroencephalography, and no more than two such functions in the case of magnetoencephalography. Even in the case that we have complete data from both modalities, still one out of the three functions is not recoverable. Another related question concerns localized neuronal currents. If the current is restricted to a small subset of the conducting brain tissue, is it possible to identify the characteristics of this current and especially its extent and its location? Albanese and Monk [5] proved that such localization is not possible. More precisely they showed that it is impossible to find the support of the current if the current occupies a three-dimensional subset of the brain. However, if the current is distributed over a surface, which is a two-dimensional subset, a curve, which is a one-dimension subset, or on isolated points, which form zero-dimensional subsets, then it is possible to identify it. It is the purpose of the present work to demonstrate that this is true for a one-dimensional current distribution. In particular, we consider a dipolar current distribution over a small line segment, and we develop an algorithm that reduces the identification of the position, the length and the orientation of the line segment, as well as the average dipolar moment of the current, to the solution of a nonlinear algebraic system. The solution of this system can be handled numerically.

2. The MEG Problem for a Single Dipole

Within the Quasi-Static Theory of Electromagnetism Magnetoencephalography [6]-[8] the magnetic field, generated by a dipolar current at the point $\boldsymbol{r}_0$ having the moment $\boldsymbol{Q}$, is given by the Geselowitz formula [9]

$$\boldsymbol{B}(\boldsymbol{r};\boldsymbol{r}_0)=\frac{\mu_0}{4\pi}\boldsymbol{Q}\times\frac{\boldsymbol{r}-\boldsymbol{r}_0}{|\boldsymbol{r}-\boldsymbol{r}_0|^3}-\frac{\mu_0\sigma}{4\pi}\oint_S u(\boldsymbol{r}';\boldsymbol{r}_0)\hat{\boldsymbol{n}}(\boldsymbol{r}')\times\frac{\boldsymbol{r}-\boldsymbol{r}'}{|\boldsymbol{r}-\boldsymbol{r}'|^3}\mathrm{d}s(\boldsymbol{r}'),\quad \boldsymbol{r}\in\Omega^c \tag{1}$$

where u is the electric potential on the boundary S of the conducting medium Ω representing the brain-head system. In Formula (1), Ω^C denotes the exterior domain, σ is the constant conductivity of the brain tissue, μ_0 is the magnetic permeability both inside and outside Ω and $\boldsymbol{n}$ stands for the outward unit normal on the boundary S.

When Ω is a sphere of radius a we know from the solution of the corresponding electroencephalography problem that the electric potential on the boundary of the sphere is given by [10] [11]

$$u(\boldsymbol{r}';\boldsymbol{r}_0)=\frac{1}{4\pi\sigma}(\boldsymbol{Q}\cdot\nabla_{r_0})\sum_{n=1}^{\infty}\frac{2n+1}{n}\frac{r_0^n}{\alpha^{n+1}}P_n(\hat{\boldsymbol{r}}'\cdot\hat{\boldsymbol{r}}_0)=\frac{1}{\sigma}(\boldsymbol{Q}\cdot\nabla_{r_0})\sum_{n=1}^{\infty}\sum_{m=-n}^{n}\frac{1}{n}\frac{r_0^n}{\alpha^{n+1}}Y_n^m(\hat{\boldsymbol{r}}')Y_n^m(\hat{\boldsymbol{r}}_0)^*. \tag{2}$$

where Y_n^m stands for the normalized complex spherical harmonics

$$Y_n^m(\boldsymbol{r})=\sqrt{\frac{2n+1}{4\pi}\frac{(n-|m|)!}{(n+|m|)!}}P_n^{|m|}(\cos\vartheta)\mathrm{e}^{im\phi} \tag{3}$$

and P_n^m denotes the Legendre functions of the first kind.

Inserting expression (2) in the Formula (1) and performing the indicated integration we can obtain the magnetic field outside the sphere. However, since the magnetic field $\boldsymbol{B}$ in the exterior to the sphere is both solenoidal and irrotational it follows that there exists a scalar magnetic potential U, which is also harmonic, such that [8]

$$\boldsymbol{B}(\boldsymbol{r};\boldsymbol{r}_0)=\nabla U(\boldsymbol{r};\boldsymbol{r}_0),\quad r>a \tag{4}$$

Then, a series of calculations lead to the following expression for the magnetic potential [10] [11],

$$\begin{aligned}U(\boldsymbol{r};\boldsymbol{r}_0)&=\mu_0(\boldsymbol{Q}\times\boldsymbol{r}_0\cdot\nabla_{r_0})\sum_{n=1}^{\infty}\sum_{m=-n}^{n}\frac{1}{(n+1)(2n+1)}\frac{r_0^n}{r^{n+1}}Y_n^m(\hat{\boldsymbol{r}}_0)Y_n^m(\hat{\boldsymbol{r}})^*\\&=\frac{\mu_0}{4\pi}(\boldsymbol{Q}\times\boldsymbol{r}_0\cdot\nabla_{r_0})\sum_{n=1}^{\infty}\frac{1}{n+1}\frac{r_0^n}{r^{n+1}}P_n(\hat{\boldsymbol{r}}\cdot\hat{\boldsymbol{r}}_0).\end{aligned} \tag{5}$$

The above expression provides the magnetic potential in the exterior of the sphere due to a single current dipole $\{\boldsymbol{r}_0, \boldsymbol{Q}\}$. Therefore, it can be considered as the fundamental solution of the MEG problem for the spherical geometry [12]. Consequently, any discrete, or continuous, current distribution can be obtained through summation, or integration, respectively, of the above fundamental solution [13].

3. The Field of a Linearly Distributed Current

We consider here the special case where the neuronal current is supported on a small segment of a smooth curve which is parametrically centered at the point $\boldsymbol{r}_0$. Let this curve be represented by the equation

$$\boldsymbol{r} = \boldsymbol{r}(t), \quad t \in [-L, L], \quad \boldsymbol{r}(0) = \boldsymbol{r}_0 \tag{6}$$

The neuronal current is then described by the function $\boldsymbol{J}^p(\boldsymbol{r}(t))$, $t \in [-L, L]$. Since the support curve is taken to be small we can approximate the current $\boldsymbol{J}^p(\boldsymbol{r}(t))$ by the linear part of its Taylor expansion, that is

$$\boldsymbol{J}^p(\boldsymbol{r}(t)) = \boldsymbol{J}^p(\boldsymbol{r}_0) + t\frac{\mathrm{d}\boldsymbol{r}(0)}{\mathrm{d}t} \cdot \left[\nabla \otimes \boldsymbol{J}^p(\boldsymbol{r}_0)\right] + O(t^2) \tag{7}$$

where the symbol $\otimes$ denotes tensor product.

In particular, if the curve is a small line segment of length $2L$, centered at $\boldsymbol{r}_0$ and oriented along the direction $\hat{\boldsymbol{\alpha}} = (\alpha_1, \alpha_2, \alpha_3)$, that is

$$\boldsymbol{r}(t) = \boldsymbol{r}_0 + t\hat{\boldsymbol{\alpha}}, \quad t \in [-L, L] \tag{8}$$

then representation (7) is written as

$$\boldsymbol{J}^p(\boldsymbol{r}(t)) \approx \boldsymbol{Q} + t\boldsymbol{l} \tag{9}$$

where $\boldsymbol{Q} = (Q_1, Q_2, Q_3) = \boldsymbol{J}^p(\boldsymbol{r}_0)$ provides an average moment, and $\boldsymbol{l} = (l_1, l_2, l_3) = \hat{\boldsymbol{\alpha}} \cdot \nabla \otimes \boldsymbol{J}^p(\boldsymbol{r}_0)$ provides an average directional derivative of the current along the direction $\hat{\boldsymbol{\alpha}}$.

Next we calculate the total potential which is generated by the approximate current (9). We recall that our ultimate goal is to invert the MEG data in order to identify the quantities $\boldsymbol{Q}$, $\boldsymbol{r}_0$, $\hat{\boldsymbol{\alpha}}$ and L, which are nine particular numbers, considering that the direction $\hat{\boldsymbol{\alpha}}$ has two independent components. Therefore, we should be able to obtain these nine numbers from a few initial terms of the expansion (5).

Formula (5), for the excitation dipole $\{\boldsymbol{r}', \boldsymbol{J}(\boldsymbol{r}')\}$, is written as

$$U(\boldsymbol{r};\boldsymbol{r}') = \frac{\mu_0}{4\pi}\left(\boldsymbol{J}^p(\boldsymbol{r}') \times \boldsymbol{r}'\right) \cdot \left[\frac{1}{2r^2}\nabla_{r'}\left(r'P_1(\hat{\boldsymbol{r}} \cdot \hat{\boldsymbol{r}}')\right) + \frac{1}{3r^3}\nabla_{r'}\left(r'^2P_2(\hat{\boldsymbol{r}} \cdot \hat{\boldsymbol{r}}')\right) + \frac{1}{4r^4}\nabla_{r'}\left(r'^3P_3(\hat{\boldsymbol{r}} \cdot \hat{\boldsymbol{r}}')\right)\right] + O(r^{-5}) \tag{10}$$

Using the standard expressions of the Legendre polynomials [14] and performing the indicated calculation we obtain the following relations, which are written in dyadic form [15] in order to isolate the factors that are going to be integrated

$$\nabla_{r'}\left(r'P_1(\hat{\boldsymbol{r}} \cdot \hat{\boldsymbol{r}}')\right) = \hat{\boldsymbol{r}} \tag{11}$$

$$\nabla_{r'}\left(r'^2P_2(\hat{\boldsymbol{r}} \cdot \hat{\boldsymbol{r}}')\right) = \left(3\hat{\boldsymbol{r}} \otimes \hat{\boldsymbol{r}} - \tilde{\boldsymbol{I}}\right) \cdot \boldsymbol{r}' = \left(3\hat{\boldsymbol{r}} \otimes \hat{\boldsymbol{r}} - \tilde{\boldsymbol{I}}\right).\left(\boldsymbol{r}_0 + t\hat{\boldsymbol{\alpha}}\right), \tag{12}$$

$$\begin{aligned}\nabla_{r'}\left(r'^3P_3(\hat{\boldsymbol{r}} \cdot \hat{\boldsymbol{r}}')\right) &= \frac{3}{2}\left(5\hat{\boldsymbol{r}} \otimes \hat{\boldsymbol{r}} \otimes \hat{\boldsymbol{r}} - 2\tilde{\boldsymbol{I}} \otimes \hat{\boldsymbol{r}} - \hat{\boldsymbol{r}} \otimes \tilde{\boldsymbol{I}}\right) : \boldsymbol{r}' \otimes \boldsymbol{r}' \\ &= \frac{3}{2}\left(5\hat{\boldsymbol{r}} \otimes \hat{\boldsymbol{r}} \otimes \hat{\boldsymbol{r}} - 2\tilde{\boldsymbol{I}} \otimes \hat{\boldsymbol{r}} - \hat{\boldsymbol{r}} \otimes \tilde{\boldsymbol{I}}\right) : \left(\boldsymbol{r}_0 + t\hat{\boldsymbol{\alpha}}\right) \otimes \left(\boldsymbol{r}_0 + t\hat{\boldsymbol{\alpha}}\right).\end{aligned} \tag{13}$$

The symbol $\tilde{\boldsymbol{I}}$ denotes the identity dyadic, ":" defines the double contraction [15]

$$(\boldsymbol{a} \otimes \boldsymbol{b}) : (\boldsymbol{c} \otimes \boldsymbol{d}) = (\boldsymbol{b} \cdot \boldsymbol{c})(\boldsymbol{a} \cdot \boldsymbol{d}) \tag{14}$$

and similarly the triple contraction is defined as

$$\left(\boldsymbol{a}\otimes\boldsymbol{b}\otimes\boldsymbol{c}\right)\vdots\left(\boldsymbol{d}\otimes\boldsymbol{e}\otimes\boldsymbol{f}\right)=\left(\boldsymbol{c}\cdot\boldsymbol{d}\right)\left(\boldsymbol{b}\cdot\boldsymbol{e}\right)\left(\boldsymbol{a}\cdot\boldsymbol{f}\right) \tag{15}$$

The exterior potential, given in (10), can be written in its Cartesian form [11] [13] as follows

$$U\left(\boldsymbol{r};\boldsymbol{r}'\right)=\frac{\mu_0}{4\pi}\left[\frac{H_1\left(\boldsymbol{r}\right)}{r^3}+\frac{H_2\left(\boldsymbol{r}\right)}{r^5}+\frac{H_3\left(\boldsymbol{r}\right)}{r^7}\right]+O\left(r^{-5}\right) \tag{16}$$

where the coefficients

$$H_1\left(\boldsymbol{r}\right)=\frac{1}{2}\boldsymbol{r}\cdot\left(\boldsymbol{J}^p\left(\boldsymbol{r}'\right)\times\boldsymbol{r}'\right) \tag{17}$$

$$H_2\left(\boldsymbol{r}\right)=\boldsymbol{r}\otimes\boldsymbol{r}:\boldsymbol{r}'\otimes\left(\boldsymbol{J}^p\left(\boldsymbol{r}'\right)\times\boldsymbol{r}'\right) \tag{18}$$

$$H_3\left(\boldsymbol{r}\right)=\frac{3}{8}\left(5\boldsymbol{r}\otimes\boldsymbol{r}\otimes\boldsymbol{r}-r^2\boldsymbol{r}\otimes\tilde{\boldsymbol{I}}\right)\vdots\boldsymbol{r}'\otimes\boldsymbol{r}'\otimes\left(\boldsymbol{J}^p\left(\boldsymbol{r}'\right)\times\boldsymbol{r}'\right) \tag{19}$$

are homogeneous harmonic functions [13].

In what follows we insert the expressions (8) and (9) in (17), (18) and (19) and integrate the resulting equations with respect to t from $-L$ to L. Performing these calculations we arrive at the expressions

$$H_1\left(\boldsymbol{r}\right)=\frac{1}{2}\boldsymbol{r}\cdot\int_{-L}^{L}\left(\boldsymbol{Q}+t\boldsymbol{l}\right)\times\left(\boldsymbol{r}_0+t\hat{\boldsymbol{\alpha}}\right)\mathrm{d}t=L\boldsymbol{r}\cdot\left(\boldsymbol{Q}\times\boldsymbol{r}_0\right)+\frac{1}{3}L^3\boldsymbol{r}\cdot\left(\boldsymbol{l}\times\hat{\boldsymbol{\alpha}}\right), \tag{20}$$

$$\begin{aligned}H_2\left(\boldsymbol{r}\right)&=\boldsymbol{r}\otimes\boldsymbol{r}:\int_{-L}^{L}\left(\boldsymbol{r}_0+t\hat{\boldsymbol{\alpha}}\right)\otimes\left(\boldsymbol{Q}+t\boldsymbol{l}\right)\times\left(\boldsymbol{r}_0+t\hat{\boldsymbol{\alpha}}\right)\mathrm{d}t\\&=\frac{2}{3}L\boldsymbol{r}\otimes\boldsymbol{r}:\left[3\boldsymbol{r}_0\otimes\left(\boldsymbol{Q}\times\boldsymbol{r}_0\right)+L^2\boldsymbol{r}_0\otimes\left(\boldsymbol{l}\times\hat{\boldsymbol{\alpha}}\right)+L^2\hat{\boldsymbol{\alpha}}\otimes\left(\boldsymbol{Q}\times\hat{\boldsymbol{\alpha}}\right)+L^2\hat{\boldsymbol{\alpha}}\otimes\left(\boldsymbol{l}\times\boldsymbol{r}_0\right)\right],\end{aligned} \tag{21}$$

$$\begin{aligned}H_3\left(\boldsymbol{r}\right)&=\frac{3}{8}\left(5\boldsymbol{r}\otimes\boldsymbol{r}\otimes\boldsymbol{r}-r^2\boldsymbol{r}\otimes\tilde{\boldsymbol{I}}\right)\vdots\int_{-L}^{L}\left(\boldsymbol{r}_0+t\hat{\boldsymbol{\alpha}}\right)\otimes\left(\boldsymbol{r}_0+t\hat{\boldsymbol{\alpha}}\right)\otimes\left(\boldsymbol{Q}+t\boldsymbol{l}\right)\times\left(\boldsymbol{r}_0+t\hat{\boldsymbol{\alpha}}\right)\mathrm{d}t\\&=\frac{L}{20}\left(5\boldsymbol{r}\otimes\boldsymbol{r}\otimes\boldsymbol{r}-r^2\boldsymbol{r}\otimes\tilde{\boldsymbol{I}}\right)\vdots\left[5\boldsymbol{r}_0\otimes\boldsymbol{r}_0\otimes\left(3\boldsymbol{Q}\times\boldsymbol{r}_0+L^2\boldsymbol{l}\times\hat{\boldsymbol{\alpha}}\right)\right.\\&\quad\left.+5L^2\left(\boldsymbol{r}_0\otimes\hat{\boldsymbol{\alpha}}+\hat{\boldsymbol{\alpha}}\otimes\boldsymbol{r}_0\right)\otimes\left(\boldsymbol{Q}\times\hat{\boldsymbol{\alpha}}+\boldsymbol{l}\times\boldsymbol{r}_0\right)+\hat{\boldsymbol{\alpha}}\otimes\hat{\boldsymbol{\alpha}}\otimes\left(5L^2\boldsymbol{Q}\times\boldsymbol{r}_0+3L^4\boldsymbol{l}\times\hat{\boldsymbol{\alpha}}\right)\right].\end{aligned} \tag{22}$$

Finally, we replace the above expressions of the harmonic functions H_1, H_2, H_3 in the expansion (16) and obtain the Cartesian representation of the exterior potential U up to the terms of order r^{-5}. That solves the relative forward MEG problem for a neuronal excitation that is supported on a small line segment.

4. Determination of the Current

The harmonic functions H_1, H_2 and H_3 are homogeneous polynomials of degrees 1, 2 and 3, respectively, that is

$$H_1\left(\boldsymbol{r}\right)=A_1x_1+A_2x_2+A_3x_3 \tag{23}$$

$$H_2\left(\boldsymbol{r}\right)=B_1x_1^2+B_2x_2^2+B_3x_3^2+B_{12}x_1x_2+B_{23}x_2x_3+B_{31}x_3x_1 \tag{24}$$

where, because of harmonicity, we should have the constrain

$$B_1+B_2+B_3=0 \tag{25}$$

and

$$H_3\left(\boldsymbol{r}\right)=C_1x_1^3+C_2x_2^3+C_3x_3^3+C_{12}x_1^2x_2+C_{21}x_2^2x_1+C_{23}x_2^2x_3+C_{32}x_3^2x_2+C_{31}x_3^2x_1+C_{13}x_1^2x_3+C_{123}x_1x_2x_3 \tag{26}$$

together with the constrains

$$3C_1+C_{21}+C_{31}=0 \tag{27}$$

$$C_{12} + 3C_2 + C_{32} = 0 \tag{28}$$

$$C_{13} + C_{23} + 3C_3 = 0 \tag{29}$$

In the idealized case where the exterior magnetic potential U is known, the expansion (16) is known and therefore the coefficients A, B and C are also known. Hence, if we rewrite the polynomials H_1, H_2 and H_3 in terms of the Cartesian monomials that appear in (23), (24) and (26), then we can utilize their linear independence to equate each monomial with the corresponding known coefficients A, B or C.

Equations (20) and (23) imply immediately that

$$\boldsymbol{A} = (A_1, A_2, A_3) = L(\boldsymbol{Q} \times \boldsymbol{r}_0) + \frac{1}{3}L^3(\boldsymbol{l} \times \hat{\boldsymbol{\alpha}}) \tag{30}$$

Then, from Equations (30) and (33) we obtain the six relations

$$B_1 = \frac{2}{3}L^3\left[x_{01}(l_2\alpha_3 - l_3\alpha_2) + \alpha_1(l_2x_{03} - l_3x_{02}) + \alpha_1(Q_2\alpha_3 - Q_3\alpha_2)\right] + 2Lx_{01}(Q_2x_{03} - Q_3x_{02}) \tag{31}$$

$$B_2 = \frac{2}{3}L^3\left[x_{02}(l_3\alpha_1 - l_1\alpha_3) + \alpha_2(l_3x_{01} - l_1x_{03}) + \alpha_2(Q_3\alpha_1 - Q_1\alpha_3)\right] + 2Lx_{02}(Q_3x_{01} - Q_1x_{03}) \tag{32}$$

$$B_3 = \frac{2}{3}L^3\left[x_{03}(l_1\alpha_2 - l_2\alpha_1) + \alpha_3(l_1x_{02} - l_2x_{01}) + \alpha_3(Q_1\alpha_2 - Q_2\alpha_1)\right] + 2Lx_{03}(Q_1x_{02} - Q_2x_{01}) \tag{33}$$

$$\begin{aligned} B_{12} = {} & \frac{2}{3}L^3\left[x_{01}(l_3\alpha_1 - l_1\alpha_3) + \alpha_1(l_3x_{01} - l_1x_{03}) + \alpha_1(Q_3\alpha_1 - Q_1\alpha_3)\right] \\ & + \frac{2}{3}L^3\left[x_{02}(l_2\alpha_3 - l_3\alpha_2) + \alpha_2(l_2x_{03} - l_3x_{02}) + \alpha_2(Q_2\alpha_3 - Q_3\alpha_2)\right] \\ & + 2Lx_{01}(Q_3x_{01} - Q_1x_{03}) + 2Lx_{02}(Q_2x_{03} - Q_3x_{02}), \end{aligned} \tag{34}$$

$$\begin{aligned} B_{23} = {} & \frac{2}{3}L^3\left[x_{02}(l_1\alpha_2 - l_2\alpha_1) + \alpha_2(l_1x_{02} - l_2x_{01}) + \alpha_2(Q_1\alpha_2 - Q_2\alpha_1)\right] \\ & + \frac{2}{3}L^3\left[x_{03}(l_3\alpha_1 - l_1\alpha_3) + \alpha_3(l_3x_{01} - l_1x_{03}) + \alpha_3(Q_3\alpha_1 - Q_1\alpha_3)\right] \\ & + 2Lx_{02}(Q_1x_{02} - Q_2x_{01}) + 2Lx_{03}(Q_3x_{01} - Q_1x_{03}), \end{aligned} \tag{35}$$

$$\begin{aligned} B_{31} = {} & \frac{2}{3}L^3\left[x_{03}(l_2\alpha_3 - l_3\alpha_2) + \alpha_3(l_2x_{03} - l_3x_{02}) + \alpha_3(Q_2\alpha_3 - Q_3\alpha_2)\right] \\ & + \frac{2}{3}L^3\left[x_{01}(l_1\alpha_2 - l_2\alpha_1) + \alpha_1(l_1x_{02} - l_2x_{01}) + \alpha_1(Q_1\alpha_2 - Q_2\alpha_1)\right] \\ & + 2Lx_{03}(Q_2x_{03} - Q_3x_{02}) + 2Lx_{01}(Q_1x_{02} - Q_2x_{01}). \end{aligned} \tag{36}$$

where it is easily shown that condition (25) holds.

Similarly, from Equations (22) and (26) we obtain

$$\begin{aligned} C_1 = {} & \frac{1}{4}\left[3L\left(5x_{01}^2 - r_0^2\right) + L^3\left(5\alpha_1^2 - 1\right)\right](Q_2x_{03} - Q_3x_{02}) + \frac{1}{20}\left[5L^3\left(5x_{01}^2 - r_0^2\right) + 3L^5\left(5\alpha_1^2 - 1\right)\right](l_2\alpha_3 - l_3\alpha_2) \\ & + \frac{1}{2}L^3\left[5x_{01}\alpha_1 - (\boldsymbol{r}_0 \cdot \hat{\boldsymbol{a}})\right](Q_2\alpha_3 - Q_3\alpha_2 + l_2x_{03} - l_3x_{02}), \end{aligned} \tag{37}$$

$$\begin{aligned} C_2 = {} & \frac{1}{4}\left[3L\left(5x_{02}^2 - r_0^2\right) + L^3\left(5\alpha_2^2 - 1\right)\right](Q_3x_{01} - Q_1x_{03}) + \frac{1}{20}\left[5L^3\left(5x_{02}^2 - r_0^2\right) + 3L^5\left(5\alpha_2^2 - 1\right)\right](l_3\alpha_1 - l_1\alpha_3) \\ & + \frac{1}{2}L^3\left[5x_{02}\alpha_2 - (\boldsymbol{r}_0 \cdot \hat{\boldsymbol{a}})\right](Q_3\alpha_1 - Q_1\alpha_3 + l_3x_{01} - l_1x_{03}), \end{aligned} \tag{38}$$

$$C_3 = \frac{1}{4}\left[3L\left(5x_{03}^2 - r_0^2\right) + L^3\left(5\alpha_3^2 - 1\right)\right]\left(Q_1 x_{02} - Q_2 x_{01}\right) + \frac{1}{20}\left[5L^3\left(5x_{03}^2 - r_0^2\right) + 3L^5\left(5\alpha_3^2 - 1\right)\right]\left(l_1\alpha_2 - l_2\alpha_1\right)$$
$$+\frac{1}{2}L^3\left[5x_{03}\alpha_3 - \left(\boldsymbol{r}_0 \cdot \hat{\boldsymbol{a}}\right)\right]\left(Q_1\alpha_2 - Q_2\alpha_1 + l_1 x_{02} - l_2 x_{01}\right). \tag{39}$$

for the cubic terms x_1^3, x_2^3 and x_3^3, respectively. For the cross-terms $x_1^2 x_2$ and $x_1 x_2^2$ we obtain the expressions

$$C_{12} = \frac{1}{4}\left[3L\left(5x_{01}^2 - r_0^2\right) + L^3\left(5\alpha_1^2 - 1\right)\right]\left(Q_3 x_{01} - Q_1 x_{03}\right) + \frac{1}{20}\left[5L^3\left(5x_{01}^2 - r_0^2\right) + 3L^5\left(5\alpha_1^2 - 1\right)\right]\left(l_3\alpha_1 - l_1\alpha_3\right)$$
$$+\frac{5}{2}\left(3Lx_{01}x_{02} + L^3\alpha_1\alpha_2\right)\left(Q_2 x_{03} - Q_3 x_{02}\right) + \frac{1}{2}\left(5L^3 x_{01}x_{02} + 3L^5\alpha_1\alpha_2\right)\left(l_2\alpha_3 - l_3\alpha_2\right) \tag{40}$$
$$+\frac{5}{2}L^3\left(\alpha_1 x_{02} + \alpha_2 x_{01}\right)\left(Q_2\alpha_3 - Q_3\alpha_2 + l_2 x_{03} - l_3 x_{02}\right) + \frac{1}{2}L^3\left(5\alpha_1 x_{01} - \boldsymbol{r}_0 \cdot \hat{\boldsymbol{a}}\right)\left(Q_3\alpha_1 - Q_1\alpha_3 + l_3 x_{01} - l_1 x_{03}\right),$$

and

$$C_{21} = \frac{1}{4}\left[3L\left(5x_{02}^2 - r_0^2\right) + L^3\left(5\alpha_2^2 - 1\right)\right]\left(Q_2 x_{03} - Q_3 x_{02}\right) + \frac{1}{20}\left[5L^3\left(5x_{02}^2 - r_0^2\right) + 3L^5\left(5\alpha_2^2 - 1\right)\right]\left(l_2\alpha_3 - l_3\alpha_2\right)$$
$$+\frac{5}{2}\left(3Lx_{01}x_{02} + L^3\alpha_1\alpha_2\right)\left(Q_3 x_{01} - Q_1 x_{03}\right) + \frac{1}{2}\left(5L^3 x_{01}x_{02} + 3L^5\alpha_1\alpha_2\right)\left(l_3\alpha_1 - l_1\alpha_3\right) \tag{41}$$
$$+\frac{5}{2}L^3\left(\alpha_1 x_{02} + \alpha_2 x_{01}\right)\left(Q_3\alpha_1 - Q_1\alpha_3 + l_3 x_{01} - l_1 x_{03}\right) + \frac{1}{2}L^3\left(5\alpha_2 x_{02} - \boldsymbol{r}_0 \cdot \hat{\boldsymbol{a}}\right)\left(Q_2\alpha_3 - Q_3\alpha_2 + l_2 x_{03} - l_3 x_{02}\right),$$

Similarly, for the cross-terms $x_2^2 x_3$ and $x_2 x_3^2$ we obtain

$$C_{23} = \frac{1}{4}\left[3L\left(5x_{02}^2 - r_0^2\right) + L^3\left(5\alpha_2^2 - 1\right)\right]\left(Q_1 x_{02} - Q_2 x_{01}\right) + \frac{1}{20}\left[5L^3\left(5x_{02}^2 - r_0^2\right) + 3L^5\left(5\alpha_2^2 - 1\right)\right]\left(l_1\alpha_2 - l_2\alpha_1\right)$$
$$+\frac{5}{2}\left(3Lx_{02}x_{03} + L^3\alpha_2\alpha_3\right)\left(Q_3 x_{01} - Q_1 x_{03}\right) + \frac{1}{2}\left(5L^3 x_{02}x_{03} + 3L^5\alpha_2\alpha_3\right)\left(l_3\alpha_1 - l_1\alpha_3\right) \tag{42}$$
$$+\frac{5}{2}L^3\left(\alpha_3 x_{02} + \alpha_2 x_{03}\right)\left(Q_3\alpha_1 - Q_1\alpha_3 + l_3 x_{01} - l_1 x_{03}\right) + \frac{1}{2}L^3\left(5\alpha_2 x_{02} - \boldsymbol{r}_0 \cdot \hat{\boldsymbol{a}}\right)\left(Q_1\alpha_2 - Q_2\alpha_1 + l_1 x_{02} - l_2 x_{01}\right),$$

and

$$C_{32} = \frac{1}{4}\left[3L\left(5x_{03}^2 - r_0^2\right) + L^3\left(5\alpha_3^2 - 1\right)\right]\left(Q_3 x_{01} - Q_1 x_{03}\right) + \frac{1}{20}\left[5L^3\left(5x_{03}^2 - r_0^2\right) + 3L^5\left(5\alpha_3^2 - 1\right)\right]\left(l_3\alpha_1 - l_1\alpha_3\right)$$
$$+\frac{5}{2}\left(3Lx_{02}x_{03} + L^3\alpha_2\alpha_3\right)\left(Q_1 x_{02} - Q_2 x_{01}\right) + \frac{1}{2}\left(5L^3 x_{02}x_{03} + 3L^5\alpha_2\alpha_3\right)\left(l_1\alpha_2 - l_2\alpha_1\right) \tag{43}$$
$$+\frac{5}{2}L^3\left(\alpha_3 x_{02} + \alpha_2 x_{03}\right)\left(Q_1\alpha_2 - Q_2\alpha_1 + l_1 x_{02} - l_2 x_{01}\right) + \frac{1}{2}L^3\left(5\alpha_3 x_{03} - \boldsymbol{r}_0 \cdot \hat{\boldsymbol{a}}\right)\left(Q_3\alpha_1 - Q_1\alpha_3 + l_3 x_{01} - l_1 x_{03}\right),$$

while, for the cross-terms $x_3^2 x_1$ and $x_3 x_1^2$ we obtain

$$C_{31} = \frac{1}{4}\left[3L\left(5x_{03}^2 - r_0^2\right) + L^3\left(5\alpha_3^2 - 1\right)\right]\left(Q_2 x_{03} - Q_3 x_{02}\right) + \frac{1}{20}\left[5L^3\left(5x_{03}^2 - r_0^2\right) + 3L^5\left(5\alpha_3^2 - 1\right)\right]\left(l_2\alpha_3 - l_3\alpha_2\right)$$
$$+\frac{5}{2}\left(3Lx_{01}x_{03} + L^3\alpha_1\alpha_3\right)\left(Q_1 x_{02} - Q_2 x_{01}\right) + \frac{1}{2}\left(5L^3 x_{01}x_{03} + 3L^5\alpha_1\alpha_3\right)\left(l_1\alpha_2 - l_2\alpha_1\right) \tag{44}$$
$$+\frac{5}{2}L^3\left(\alpha_1 x_{03} + \alpha_3 x_{01}\right)\left(Q_1\alpha_2 - Q_2\alpha_1 + l_1 x_{02} - l_2 x_{01}\right) + \frac{1}{2}L^3\left(5\alpha_3 x_{03} - \boldsymbol{r}_0 \cdot \hat{\boldsymbol{a}}\right)\left(Q_2\alpha_3 - Q_3\alpha_2 + l_2 x_{03} - l_3 x_{02}\right),$$

and

$$C_{13}=\frac{1}{4}\left[3L\left(5x_{01}^2-r_0^2\right)+L^3\left(5\alpha_1^2-1\right)\right]\left(Q_1x_{02}-Q_2x_{01}\right)+\frac{1}{20}\left[5L^3\left(5x_{01}^2-r_0^2\right)+3L^5\left(5\alpha_1^2-1\right)\right]\left(l_1\alpha_2-l_2\alpha_1\right)$$
$$+\frac{5}{2}\left(3Lx_{01}x_{03}+L^3\alpha_1\alpha_3\right)\left(Q_2x_{03}-Q_3x_{02}\right)+\frac{1}{2}\left(5L^3x_{01}x_{03}+3L^5\alpha_1\alpha_3\right)\left(l_2\alpha_3-l_3\alpha_2\right) \tag{45}$$
$$+\frac{5}{2}L^3\left(\alpha_1x_{03}+\alpha_3x_{01}\right)\left(Q_2\alpha_3-Q_3\alpha_2+l_2x_{03}-l_3x_{02}\right)+\frac{1}{2}L^3\left(5\alpha_1x_{01}-\boldsymbol{r}_0\cdot\hat{\boldsymbol{a}}\right)\left(Q_1\alpha_2-Q_2\alpha_1+l_1x_{02}-l_2x_{01}\right),$$

Finally for the product term $x_1x_2x_3$ we obtain

$$\begin{aligned}C_{123}=&\frac{5}{2}\left(3Lx_{02}x_{03}+L^3\alpha_2\alpha_3\right)\left(Q_2x_{03}-Q_3x_{02}\right)+\frac{5}{2}\left(3Lx_{01}x_{03}+L^3\alpha_1\alpha_3\right)\left(Q_3x_{01}-Q_1x_{03}\right)\\&+\frac{5}{2}\left(3Lx_{01}x_{02}+L^3\alpha_1\alpha_2\right)\left(Q_1x_{02}-Q_2x_{01}\right)+\frac{1}{2}\left(5L^3x_{02}x_{03}+3L^5\alpha_2\alpha_3\right)\left(l_2\alpha_3-l_3\alpha_2\right)\\&+\frac{1}{2}\left(5L^3x_{01}x_{03}+3L^5\alpha_1\alpha_3\right)\left(l_3\alpha_1-l_1\alpha_3\right)+\frac{1}{2}\left(5L^3x_{01}x_{02}+3L^5\alpha_1\alpha_2\right)\left(l_1\alpha_2-l_2\alpha_1\right)\\&+\frac{5}{2}L^3\left(\alpha_2x_{03}+\alpha_3x_{02}\right)\left(Q_2\alpha_3-Q_3\alpha_2+l_2x_{03}-l_3x_{02}\right)\\&+\frac{5}{2}L^3\left(\alpha_1x_{03}+\alpha_3x_{01}\right)\left(Q_3\alpha_1-Q_1\alpha_3+l_3x_{01}-l_1x_{03}\right)\\&+\frac{5}{2}L^3\left(\alpha_1x_{02}+\alpha_2x_{01}\right)\left(Q_1\alpha_2-Q_2\alpha_1+l_1x_{02}-l_2x_{01}\right).\end{aligned} \tag{46}$$

It is straightforward to verify that the three constrains (27)-(29) are satisfied.

The set of the 16 equations, which are the 20 scalar equations appearing in (30)-(46) minus the four constrains (25) and (27)-(29), defines a nonlinear system for the determination of the 12 independent variables $\boldsymbol{r}_0$, $\hat{\boldsymbol{a}}$, $\boldsymbol{l}$, $\boldsymbol{Q}$ and L, three components for each one of the vectors $\boldsymbol{r}_0$, $\boldsymbol{l}$, $\boldsymbol{Q}$, two components for the direction vector $\hat{\boldsymbol{a}}$ and one for the length L. In fact, we can simplify this system as follows. In view of Equation (30) the three components of the exterior product $\boldsymbol{Q}\times\boldsymbol{r}_0$ provide the relations

$$Q_2x_{03}-Q_3x_{02}=\frac{A_1}{L}-\frac{L^2}{3}\left(l_2\alpha_3-l_3\alpha_2\right) \tag{47}$$

$$Q_3x_{01}-Q_1x_{03}=\frac{A_2}{L}-\frac{L^2}{3}\left(l_3\alpha_1-l_1\alpha_3\right) \tag{48}$$

$$Q_1x_{02}-Q_2x_{01}=\frac{A_3}{L}-\frac{L^2}{3}\left(l_1\alpha_2-l_2\alpha_1\right) \tag{49}$$

and these relations reduce the Equations (31)-(36) to

$$B_1=2A_1x_{01}+\frac{2}{3}L^3\alpha_1\left(l_2x_{03}-l_3x_{02}+Q_2\alpha_3-Q_3\alpha_2\right) \tag{50}$$

$$B_2=2A_2x_{02}+\frac{2}{3}L^3\alpha_2\left(l_3x_{01}-l_1x_{03}+Q_3\alpha_1-Q_1\alpha_3\right) \tag{51}$$

$$B_3=2A_3x_{03}+\frac{2}{3}L^3\alpha_3\left(l_1x_{02}-l_2x_{01}+Q_1\alpha_2-Q_2\alpha_1\right) \tag{52}$$

$$B_{12}=2\left(A_1x_{02}+A_2x_{01}\right)+\frac{2}{3}L^3\alpha_1\left(l_3x_{01}-l_1x_{03}+Q_3\alpha_1-Q_1\alpha_3\right)+\frac{2}{3}L^3\alpha_2\left(l_2x_{03}-l_3x_{02}+Q_2\alpha_3-Q_3\alpha_2\right) \tag{53}$$

$$B_{23}=2\left(A_2x_{03}+A_3x_{02}\right)+\frac{2}{3}L^3\alpha_3\left(l_3x_{01}-l_1x_{03}+Q_3\alpha_1-Q_1\alpha_3\right)+\frac{2}{3}L^3\alpha_2\left(l_1x_{02}-l_2x_{01}+Q_1\alpha_2-Q_2\alpha_1\right) \tag{54}$$

$$B_{31}=2\left(A_3x_{01}+A_1x_{03}\right)+\frac{2}{3}L^3\alpha_1\left(l_1x_{02}-l_2x_{01}+Q_1\alpha_2-Q_2\alpha_1\right)+\frac{2}{3}L^3\alpha_3\left(l_2x_{03}-l_3x_{02}+Q_2\alpha_3-Q_3\alpha_2\right) \tag{55}$$

Furthermore, utilizing the Equations (50)-(52) we arrive at the relations

$$2\left(\frac{x_{01}}{\alpha_1}-\frac{x_{02}}{\alpha_2}\right)\left(\alpha_1A_2-\alpha_2A_1\right)=B_{12}-\frac{\alpha_2}{\alpha_1}B_1-\frac{\alpha_1}{\alpha_2}B_2 \tag{56}$$

$$2\left(\frac{x_{02}}{\alpha_2}-\frac{x_{03}}{\alpha_3}\right)\left(\alpha_2A_3-\alpha_3A_2\right)=B_{23}-\frac{\alpha_2}{\alpha_3}B_3-\frac{\alpha_3}{\alpha_2}B_2 \tag{57}$$

$$2\left(\frac{x_{03}}{\alpha_3}-\frac{x_{01}}{\alpha_1}\right)\left(\alpha_3A_1-\alpha_1A_3\right)=B_{31}-\frac{\alpha_1}{\alpha_3}B_3-\frac{\alpha_3}{\alpha_1}B_1 \tag{58}$$

which allow rewriting Equations (37)-(46) as follows

$$C_1=\frac{3B_1}{4\alpha_1}\left(5x_{01}\alpha_1-\boldsymbol{r}_0\cdot\hat{\boldsymbol{a}}\right)+\frac{L^5}{15}\left(5\alpha_1^2-1\right)\left(l_2\alpha_3-l_3\alpha_2\right)+\frac{3A_1}{4}\left[\frac{L^2}{3}\left(5\alpha_1^2-1\right)-\left(5x_{01}^2+r_0^2\right)+2\frac{x_{01}}{\alpha_1}\left(\boldsymbol{r}_0\cdot\hat{\boldsymbol{a}}\right)\right] \tag{59}$$

$$C_2=\frac{3B_2}{4\alpha_2}\left(5x_{02}\alpha_2-\boldsymbol{r}_0\cdot\hat{\boldsymbol{a}}\right)+\frac{L^5}{15}\left(5\alpha_2^2-1\right)\left(l_3\alpha_1-l_1\alpha_3\right)+\frac{3A_2}{4}\left[\frac{L^2}{3}\left(5\alpha_2^2-1\right)-\left(5x_{02}^2+r_0^2\right)+2\frac{x_{02}}{\alpha_2}\left(\boldsymbol{r}_0\cdot\hat{\boldsymbol{a}}\right)\right] \tag{60}$$

$$C_3=\frac{3B_3}{4\alpha_3}\left(5x_{03}\alpha_3-\boldsymbol{r}_0\cdot\hat{\boldsymbol{a}}\right)+\frac{L^5}{15}\left(5\alpha_3^2-1\right)\left(l_1\alpha_2-l_2\alpha_1\right)+\frac{3A_3}{4}\left[\frac{L^2}{3}\left(5\alpha_3^2-1\right)-\left(5x_{03}^2+r_0^2\right)+2\frac{x_{03}}{\alpha_3}\left(\boldsymbol{r}_0\cdot\hat{\boldsymbol{a}}\right)\right] \tag{61}$$

$$\begin{aligned}C_{12}=&\frac{5}{2}A_1\left(3x_{01}x_{02}+L^2\alpha_1\alpha_2\right)+\frac{1}{4}A_2\left[3\left(5x_{01}^2-r_0^2\right)+L^2\left(5\alpha_1^2-1\right)\right]+\frac{15}{4\alpha_1}\left(B_1-2A_1x_{01}\right)\left(\alpha_1x_{02}+\alpha_2x_{01}\right)\\&+\frac{3}{4\alpha_2}\left(B_2-2A_2x_{02}\right)\left(5\alpha_1x_{01}-\boldsymbol{r}_0\cdot\hat{\boldsymbol{a}}\right)+\frac{2}{3}L^5\alpha_1\alpha_2\left(l_2\alpha_3-l_3\alpha_2\right)+\frac{1}{15}L^5\left(5\alpha_1^2-1\right)\left(l_3\alpha_1-l_1\alpha_3\right),\end{aligned} \tag{62}$$

$$\begin{aligned}C_{21}=&\frac{5}{2}A_2\left(3x_{01}x_{02}+L^2\alpha_1\alpha_2\right)+\frac{1}{4}A_1\left[3\left(5x_{02}^2-r_0^2\right)+L^2\left(5\alpha_2^2-1\right)\right]+\frac{15}{4\alpha_2}\left(B_2-2A_2x_{02}\right)\left(\alpha_1x_{02}+\alpha_2x_{01}\right)\\&+\frac{3}{4\alpha_1}\left(B_1-2A_1x_{01}\right)\left(5\alpha_2x_{02}-\boldsymbol{r}_0\cdot\hat{\boldsymbol{a}}\right)+\frac{2}{3}L^5\alpha_1\alpha_2\left(l_3\alpha_1-l_1\alpha_3\right)+\frac{1}{15}L^5\left(5\alpha_2^2-1\right)\left(l_2\alpha_3-l_3\alpha_2\right),\end{aligned} \tag{63}$$

$$\begin{aligned}C_{23}=&\frac{5}{2}A_2\left(3x_{02}x_{03}+L^2\alpha_2\alpha_3\right)+\frac{1}{4}A_3\left[3\left(5x_{02}^2-r_0^2\right)+L^2\left(5\alpha_2^2-1\right)\right]+\frac{15}{4\alpha_2}\left(B_2-2A_2x_{02}\right)\left(\alpha_2x_{03}+\alpha_3x_{02}\right)\\&+\frac{3}{4\alpha_3}\left(B_3-2A_3x_{03}\right)\left(5\alpha_2x_{02}-\boldsymbol{r}_0\cdot\hat{\boldsymbol{a}}\right)+\frac{2}{3}L^5\alpha_2\alpha_3\left(l_3\alpha_1-l_1\alpha_3\right)+\frac{1}{15}L^5\left(5\alpha_2^2-1\right)\left(l_1\alpha_2-l_2\alpha_1\right),\end{aligned} \tag{64}$$

$$\begin{aligned}C_{32}=&\frac{5}{2}A_3\left(3x_{02}x_{03}+L^2\alpha_2\alpha_3\right)+\frac{1}{4}A_2\left[3\left(5x_{03}^2-r_0^2\right)+L^2\left(5\alpha_3^2-1\right)\right]+\frac{15}{4\alpha_3}\left(B_3-2A_3x_{03}\right)\left(\alpha_2x_{03}+\alpha_3x_{02}\right)\\&+\frac{3}{4\alpha_2}\left(B_2-2A_2x_{02}\right)\left(5\alpha_3x_{03}-\boldsymbol{r}_0\cdot\hat{\boldsymbol{a}}\right)+\frac{2}{3}L^5\alpha_2\alpha_3\left(l_1\alpha_2-l_2\alpha_1\right)+\frac{1}{15}L^5\left(5\alpha_3^2-1\right)\left(l_3\alpha_1-l_1\alpha_3\right),\end{aligned} \tag{65}$$

$$\begin{aligned}C_{31}=&\frac{5}{2}A_3\left(3x_{01}x_{03}+L^2\alpha_1\alpha_3\right)+\frac{1}{4}A_1\left[3\left(5x_{03}^2-r_0^2\right)+L^2\left(5\alpha_3^2-1\right)\right]+\frac{15}{4\alpha_3}\left(B_3-2A_3x_{03}\right)\left(\alpha_1x_{03}+\alpha_3x_{01}\right)\\&+\frac{3}{4\alpha_1}\left(B_1-2A_1x_{01}\right)\left(5\alpha_3x_{03}-\boldsymbol{r}_0\cdot\hat{\boldsymbol{a}}\right)+\frac{2}{3}L^5\alpha_1\alpha_3\left(l_1\alpha_2-l_2\alpha_1\right)+\frac{1}{15}L^5\left(5\alpha_3^2-1\right)\left(l_2\alpha_3-l_3\alpha_2\right),\end{aligned} \tag{66}$$

$$C_{13}=\frac{5}{2}A_1\left(3x_{01}x_{03}+L^2\alpha_1\alpha_3\right)+\frac{1}{4}A_3\left[3\left(5x_{01}^2-r_0^2\right)+L^2\left(5\alpha_1^2-1\right)\right]+\frac{15}{4\alpha_1}\left(B_1-2A_1x_{01}\right)\left(\alpha_1x_{03}+\alpha_3x_{01}\right)$$
$$+\frac{3}{4\alpha_3}\left(B_3-2A_3x_{03}\right)\left(5\alpha_1x_{01}-\boldsymbol{r}_0\cdot\hat{\boldsymbol{a}}\right)+\frac{2}{3}L^5\alpha_1\alpha_3\left(l_2\alpha_3-l_3\alpha_2\right)+\frac{1}{15}L^5\left(5\alpha_1^2-1\right)\left(l_1\alpha_2-l_2\alpha_1\right). \tag{67}$$

and

$$C_{123}=\frac{5}{2}A_1\left(3x_{02}x_{03}+L^2\alpha_2\alpha_3\right)+\frac{5}{2}A_2\left(3x_{01}x_{03}+L^2\alpha_1\alpha_3\right)+\frac{5}{2}A_3\left(3x_{01}x_{02}+L^2\alpha_1\alpha_2\right)+\frac{2}{3}L^5\alpha_2\alpha_3\left(l_2\alpha_3-l_3\alpha_2\right)$$
$$+\frac{2}{3}L^5\alpha_1\alpha_3\left(l_3\alpha_1-l_1\alpha_3\right)+\frac{2}{3}L^5\alpha_1\alpha_2\left(l_1\alpha_2-l_2\alpha_1\right)+\frac{15}{4\alpha_1}\left(B_1-2A_1x_{01}\right)\left(\alpha_2x_{03}+\alpha_3x_{02}\right)$$
$$+\frac{15}{4\alpha_2}\left(B_2-2A_2x_{02}\right)\left(\alpha_1x_{03}+\alpha_3x_{01}\right)+\frac{15}{4\alpha_3}\left(B_3-2A_3x_{03}\right)\left(\alpha_1x_{02}+\alpha_2x_{01}\right). \tag{68}$$

Because of the constrains (27)-(29), only 7 out of the 10 equations (59)-(68) are independent. Then, the reduced set of these 7 independent equations, plus the 6 equations (47)-(49) and (53)-(55) provides a nonlinear system for the determination of the unknown quantities $\boldsymbol{r}_0$, $\hat{\boldsymbol{a}}$, $\boldsymbol{Q}$, $\boldsymbol{l}$ and L. However, since some of these quantities enter the system through the components of exterior products, it follows that the above quantities cannot be completely specified. For example, from Equations (47)-(49) it follows that it is not possible to identify the three components of $\boldsymbol{Q}$ from the exterior product of $\boldsymbol{Q}$ with the position vector $\boldsymbol{r}_0$, since the component of $\boldsymbol{Q}$ that is parallel to $\boldsymbol{r}_0$ gives a vanishing term. Hence, this component of $\boldsymbol{Q}$ forms a "silent" source [8]. The solution of this system can easily be obtained with the use of classical computational methods.

To illustrate the inversion algorithm we consider the following special case.

Special Case. Let us assume that we have the a-priori information that the line segment is oriented along the x_1-axis and that its middle point is $\boldsymbol{r}_0=\left(0,0,r_0\right)$. This choice leads to

$$A_1=LQ_2r_0 \tag{69}$$

$$A_3=-\frac{1}{3}L^3l_2 \tag{70}$$

$$C_1=Q_2r_0\left(L^3-\frac{3}{4}Lr_0^2\right) \tag{71}$$

$$C_2=\frac{1}{4}Q_1r_0\left(L^3+3Lr_0^2\right)-\frac{1}{4}l_3\left(L^3r_0^2+\frac{3}{5}L^5\right) \tag{72}$$

$$C_{12}=Q_1\left(\frac{3}{4}Lr_0^3-L^3r_0\right)+l_3\left(\frac{3}{5}L^5-\frac{1}{4}L^3r_0^2\right) \tag{73}$$

$$C_{31}=\frac{1}{4}Q_2r_0\left(12Lr_0^2-11L^3\right) \tag{74}$$

Inserting the expression of A_1 in the equations for C_1 and C_{31} we obtain the following 2×2 system for the determination of L^2 and r_0^2

$$4A_1L^2-3A_1r_0^2=4C_1 \tag{75}$$

$$-11A_1L^2+12A_1r_0^2=4C_{31} \tag{76}$$

which immediately gives the values of L and r_0

$$L=2\sqrt{\frac{4C_1+C_{31}}{5A_1}} \tag{77}$$

$$r_0 = 2\sqrt{\frac{11C_1 + 4C_{31}}{15A_1}} \tag{78}$$

Then from (69) we obtain

$$Q_2 = \frac{A_1}{Lr_0} \tag{79}$$

and from (70) we obtain

$$l_2 = -\frac{3}{8}A_3\left(\frac{5A_1}{4C_1 + C_{31}}\right)^{3/2} \tag{80}$$

Finally, from (72) and (73) we obtain a 2×2 system for the unknowns Q_1 and l_3, from which we obtain

$$Q_1 = \frac{\left(12L^2 - 5r_0^2\right)C_2 + \left(3L^2 + 5r_0^2\right)C_{12}}{5L^3 r_0^3} \tag{81}$$

$$l_3 = \frac{\left(4L^2 - 3r_0^2\right)C_2 + \left(L^2 + 3r_0^2\right)C_{12}}{L^5 r_0^2} \tag{82}$$

with L and r_0 given by (77) and (78), respectively. Note that the only constants that remain unspecified are l_1 and Q_3, but the constant l_1 is not needed, and the constant Q_3 can not be determined since the component $Q_3\hat{\boldsymbol{x}}_3$ is parallel to the position vector $\boldsymbol{r}_0$, and therefore their exterior product vanishes.

Acknowledgements

The present work is part of the project "Functional Brain", which is implemented within the "ARISTEIA" Action of the "OPERATIONAL PROGRAMME EDUCATION AND LIFELONG LEARNING" and is co-funded by the European Social Fund (ESF) and National Resources.

References

[1] Hamalainen, M., Hari, R., Ilmoniemi, R.J., Knuutila, J. and Lounasmaa, O. (1993) Magnetoencephalography—Theory, Instrumentation, and Applications to Noninvasive Studies of the Working Human Brain. *Reviews of Modern Physics*, **65**, 413. http://dx.doi.org/10.1103/RevModPhys.65.413

[2] Malmivuo, J. and Plonsey, R. (1995) Bioelectromagnetism. Oxford University Press, New York.

[3] Helmholtz, H. (1853) Ueber einige Gesetze der Vertheilung elektrischer Str ome in k orperlichen Leitern mit Anwendung auf die thierisch-elektrischen Versuche. *Annalen der Physik und Chemie*, **89**, 211-233, 353-377.

[4] Dassios, G. and Fokas, A.S. (2013) The Definitive Non Uniqueness Results for Deterministic EEG and MEG Data. *Inverse Problems*, **29**, 1-10. http://dx.doi.org/10.1088/0266-5611/29/6/065012

[5] Albanese, R. and Monk, P.B. (2006) The Inverse Source Problem for Maxwell's Equations. *Inverse Problems*, **22**, 1023-1035. http://dx.doi.org/10.1088/0266-5611/22/3/018

[6] Landau, L.D. and Lifshitz, E.M. (1960) Electrodynamics of Continuous Media. Pergamon Press, London.

[7] Plonsey, R. and Heppner, D.B. (1967) Considerations of Quasi-Stationarity in Electrophysiological Systems. *Bulletin of Mathematical Biophysics*, **29**, 657-664. http://dx.doi.org/10.1007/BF02476917

[8] Sarvas, J. (1987) Basic Mathematical and Electromagnetic Concepts of the Biomagnetic Inverse Problems. *Physics in Medicine and Biology*, **32**, 11-22. http://dx.doi.org/10.1088/0031-9155/32/1/004

[9] Geselowitz, D.B. (1970) On the Magnetic Field Generated outside an Inhomogeneous Volume Conductor by Internal Current Sources. *IEEE Transactions in Biomagnetism*, **6**, 346-347. http://dx.doi.org/10.1109/TMAG.1970.1066765

[10] Dassios, G. (2009) Electric and Magnetic Activity of the Brain in Spherical and Ellipsoidal Geometry. *Mathematical Modeling in Biomedical Imaging I Lecture Notes in Mathematics*, 133-202.

[11] Dassios, G. (2012) Ellipsoidal Harmonics. Theory and Applications. Cambridge University Press, Cambridge. http://dx.doi.org/10.1017/CBO9781139017749

[12] Dassios, G. and Fokas, A.S. (2009) Electro-Magneto-Encephalography and Fundamental Solutions. *Quarterly of Applied Mathematics*, **67**, 771-780.

[13] Dassios, G. and Fokas, A.S. (2009) Electro-Magneto-Encephalography for the Three-Shell Model: Dipoles and Beyond for the Spherical Geometry. *Inverse Problems*, **25**, Article ID: 035001. http://dx.doi.org/10.1088/0266-5611/25/3/035001

[14] Morse, P.M. and Feshbach, H. (1953) Methods of Theoretical Physics, Volume I. McGraw-Hill, New York.

[15] Brand, L. (1947) Vector and Tensor Analysis. John Wiley and Sons, New York.

Applied Mathematics, 2015, 6, 106-115
Published Online January 2015 in SciRes. http://www.scirp.org/journal/am
http://dx.doi.org/10.4236/am.2015.61011

Scientific Research Publishing

Unsteady Incompressible Flow of a Generalized Oldroyd-B Fluid between Two Oscillating Infinite Parallel Plates in Presence of a Transverse Magnetic Field

Dhiman Bose, Uma Basu

Department of Applied Mathematics, University of Calcutta, Calcutta, India
Email: dhimanbose09@gmail.com

Received 27 November 2014; revised 18 December 2014; accepted 30 December 2014

Abstract

In this paper an attempt has been made to study the unsteady incompressible flow of a generalized Oldroyd-B fluid between two oscillating parallel plates in presence of a transverse magnetic field. An exact solution for the velocity field has been obtained by means of Laplace and finite Fourier sine transformations in series form in terms of Mittage-Leffler function. The dependence of the velocity field on fractional as well as material parameters has been illustrated graphically. The velocity fields for the classical Newtonian, generalized Maxwell, generalized second grade and ordinary Oldroyd-B fluids are recovered as limiting cases of the flow considered for the generalized Oldroyd-B fluid.

Keywords

Oldroyd-B Fluid, Exact Solution, Mittage-Lefller Function, Fractional Derivative, Transverse Magnetic Field

1. Introduction

The magneto hydrodynamic flow problem between two parallel plates has shown immense attention during the last several decades. The study has significant applications in the field of hydrodynamical machines and apparatus, magnetic storage devices, computer storage devices, lubrication, crystal growth processes, radial diffusers, MHD pumps, MHD power generators, purification of crude oil, petroleum industries etc. Bandelli *et al.* [1] discussed start-up flows of second grade fluids in domains with one finite dimension. Fetecau *et al.* [2] investigated

How to cite this paper: Bose, D. and Basu, U. (2015) Unsteady Incompressible Flow of a Generalized Oldroyd-B Fluid between Two Oscillating Infinite Parallel Plates in Presence of a Transverse Magnetic Field. *Applied Mathematics*, **6**, 106-115. http://dx.doi.org/10.4236/am.2015.61011

exact solutions for the flow of a generalized Oldroyd-B fluid induced by a constantly accelerating plate between two side walls perpendicular to the plate. Hayat *et al.* [3] made homotopy analysis of MHD boundary layer flow of an upper-convected Maxwell fluid. Jamil and Khan [4] studied slip effects on fractional viscoelastic fluids. Shen *et al.* [5] studied the Rayleigh-Stokes problem for a heated generalized second grade fluid with fractional derivative model. Vieru *et al.* [6] discussed the flow of a generalized Oldroyd-B fluid due to a constantly accelerating plate. Wenchang *et al.* [7] investigated unsteady flows of a viscoelastic fluid with the fractional Maxwell model between two parallel plates. Vieru *et al.* [8] studied the unsteady flow of a generalized Oldroyd-B fluid due to an infinite plate subject to a time-dependent shear stress.

In the present paper we consider the flow of a generalized Oldroyd-B fluid between two oscillating infinite parallel plates in presence of transverse magnetic field. We have formulated the expression for the velocity field for the said flow in terms of Mittage-Leffler function. In the constitutive equation of the fluid model, the time derivative of integral order has been replaced by Riemann-Liouville fractional calculus operator. The exact solution for the velocity field is obtained by using the method of integral transformations and the dependence of the said field on the material as well as fractional calculus parameters is illustrated graphically.

2. Mathematical Formulation and Basic Equation

Let us consider an incompressible generalized Oldroyd-B fluid bounded by two infinite parallel plates as shown in **Figure 1**. The plates are initially at rest and at $t \to 0^{+}$ the plates start to oscillate in its plane with the velocity $V\cos(\omega_1 t)$ and $V\cos(\omega_2 t)$ where V is the fluid velocity. Due to the shear, the fluid is moved gradually. We have taken Cartesian coordinate system. *x*- and *y*-coordinates are taken along and perpendicular to the parallel plates respectively. Accordingly, the initial condition is given by $u(y,0)=0$, $0 \le y \le 1$ and the boundary conditions are given by $u(0,t)=V\cos(\omega_1 t)$, $u(d,t)=V\cos(\omega_2 t)$.

We take the velocity and stress of the form

$$V = u(y,t)\hat{\mathbf{i}}, \quad S = S(y,t) \tag{1}$$

where $u(y,t)$ is the velocity component in the *x*-direction.

The constitutive relationship for the fluid associated with the present problem is given by,

$$\left(1+\lambda^{\alpha} D_t^{\alpha}\right) S_{xy} = \mu\left(1+\lambda_r^{\beta} D_t^{\beta}\right)\frac{\partial u(y,t)}{\partial t} \tag{2}$$

In the relation (2), D_t^{α} and D_t^{β} are Caputo operators defined by

$$D_t^{p} g(t) = \frac{1}{\Gamma(1-p)}\int_0^t (t-\tau)^{-p} g'(\tau)\,\mathrm{d}\tau, \quad 0 \le p < 1 \tag{3}$$

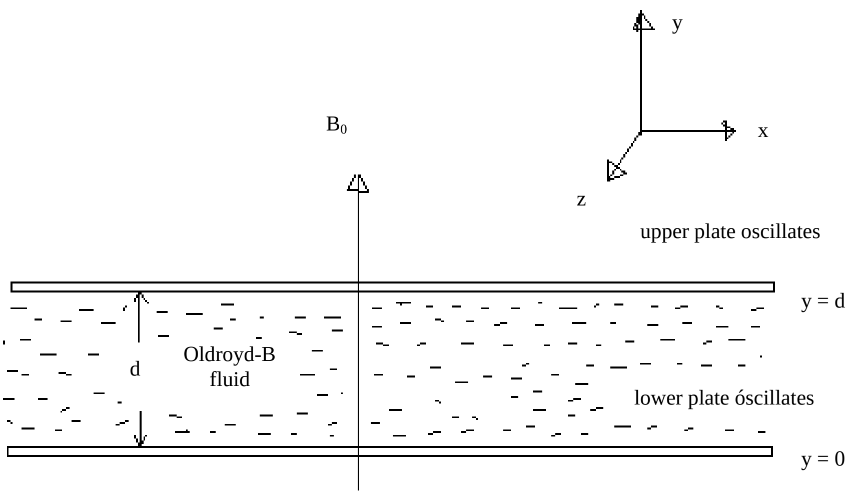

Figure 1. Geometry of the problem.

According to our problem,

$$S_{xx}=S_{yy}=S_{zz}=S_{xz}=S_{yz}=0,\quad S_{xy}=S_{yx}$$

We consider a generalized Oldroyd-B fluid between two infinite parallel disks in presence of an imposed magnetic field B_0 that acts in the direction of the positive y-axis. Then in the presence of the body force $\sigma B_0^2 u$, the momentum equation is given by

$$\rho\frac{\partial u}{\partial t}=\frac{\partial}{\partial y}S_{xy}-\sigma B_0^2 u \tag{4}$$

where "σ" is constant and "ρ" is the density of the fluid.

Eliminating S_{xy} between the Equations (2) and (4) we have the governing equation

$$\left(1+\lambda^{\alpha}D_t^{\alpha}\right)\frac{\partial u(y,t)}{\partial t}=\nu\left(1+\lambda_r^{\beta}D_t^{\beta}\right)\frac{\partial^2 u(y,t)}{\partial y^2}-M\left(1+\lambda^{\alpha}D_t^{\alpha}\right)u(y,t) \tag{5}$$

where $\nu=\dfrac{\mu}{\rho}$ is the kinematic viscosity and $M=\dfrac{\sigma B_0^2}{\rho}$.

Introducing the non-dimensional quantities,

$$u^*=\frac{u}{V},\quad y^*=\frac{y}{d},\quad t^*=\frac{\mu t}{\rho d^2},\quad \lambda^{*\alpha}=\lambda^{\alpha}\left(\frac{\nu}{d^2}\right)^{\alpha}$$

$$\lambda_r^{*\beta}=\lambda_r^{\beta}\left(\frac{\nu}{d^2}\right)^{\alpha},\quad \nu=\frac{\mu}{\rho},\quad M^*=M\frac{d^2}{\nu}$$

we get the governing equation in non-dimensional quantities as

$$\left(1+\lambda^{\alpha}D_t^{\alpha}\right)\frac{\partial u(y,t)}{\partial t}=\left(1+\lambda_r^{\beta}D_t^{\beta}\right)\frac{\partial^2 u(y,t)}{\partial y^2}-M\left(1+\lambda^{\alpha}D_t^{\alpha}\right)u(y,t) \tag{6}$$

(Omitting the dimensionless mark "*")

$$\text{subject to initial condition } u(y,0)=0 \tag{7}$$

and the boundary conditions $u(0,t)=\cos(\omega_1 t)$, for $t>0$

$$u(1,t)=\cos(\omega_2 t)\quad\text{for } t>0 \tag{8}$$

Taking finite Fourier sine transformation we get from Equation (6)

$$\left(1+\lambda^{\alpha}D_t^{\alpha}\right)\frac{\mathrm{d}}{\mathrm{d}t}U_s(n,t)=\left(1+\lambda_r^{\beta}D_t^{\beta}\right)\int_0^1\frac{\partial^2 u}{\partial y^2}\sin(n\pi y)\,\mathrm{d}y-M\left(1+\lambda^{\alpha}D_t^{\alpha}\right)U_s(n,t) \tag{9}$$

where $U_s(n,t)=\int_0^1 u(y,t)\sin(n\pi y)\,\mathrm{d}y$ is the finite Fourier sine transformation of $u(y,t)$.

Using the boundary conditions (8) the Equation (9) can be rewritten as

$$\begin{aligned}\left(1+\lambda^{\alpha}D_t^{\alpha}\right)\frac{\mathrm{d}}{\mathrm{d}t}U_s(n,t)&=\left(1+\lambda_r^{\beta}D_t^{\beta}\right)\left[n\pi\left\{(-1)^{n+1}\cos(\omega_2 t)+\cos(\omega_1 t)\right\}-(n\pi)^2U_s(n,t)\right]\\&\quad-M\left(1+\lambda^{\alpha}D_t^{\alpha}\right)U_s(n,t)\end{aligned} \tag{10}$$

Taking Laplace transformation and using $U_s(n,0)=0$ we get from the above equation

$$\bar{U}_s(n,p)=(-1)^{n+1}\frac{n\pi p}{p^2+\omega_2^2}\frac{1+\lambda_r^\beta p^\beta}{(p+M)(1+\lambda^\alpha p^\alpha)+(n\pi)^2(1+\lambda_r^\beta p^\beta)}$$
$$+\frac{n\pi p}{p^2+\omega_1^2}\frac{1+\lambda_r^\beta p^\beta}{(p+M)(1+\lambda^\alpha p^\alpha)+(n\pi)^2(1+\lambda_r^\beta p^\beta)} \tag{11}$$
$$-\frac{n\pi\lambda_r^\beta\left[(-1)^{n+1}+1\right]}{(p+M)(1+\lambda^\alpha p^\alpha)+(n\pi)^2(1+\lambda_r^\beta p^\beta)}$$

Now in order to avoid the lengthy procedure of residues and contour integrals, we rewrite the Equation (11) into series form as

$$\bar{U}_s(n,p)=\frac{(-1)^{n+1}}{n\pi}\frac{p}{p^2+\omega_2^2}\left[1-\sum_{k=0}^{\infty}\frac{(-1)^k}{(n\pi)^{2(k+1)}}\sum_{m,l\geq 0}^{m+l=k+1}\frac{(k+1)!}{m!l!}M^m\sum_{n_1,w\geq 0}^{n_1+w=k}\frac{k!}{n_1!w!}\frac{\lambda^{\alpha n_1}p^{\alpha n_1+l}}{\lambda_r^{\beta(k+1)}}\frac{1+\lambda^\alpha p^\alpha}{\left(\lambda_r^{-\beta}+p^\beta\right)^{k+1}}\right]$$
$$+\frac{1}{n\pi}\frac{p}{p^2+\omega_1^2}\left[1-\sum_{k=0}^{\infty}\frac{(-1)^k}{(n\pi)^{2(k+1)}}\sum_{m,l\geq 0}^{m+l=k+1}\frac{(k+1)!}{m!l!}M^m\sum_{n_1,w\geq 0}^{n_1+w=k}\frac{k!}{n_1!w!}\frac{\lambda^{\alpha n_1}p^{\alpha n_1+l}}{\lambda_r^{\beta(k+1)}}\frac{1+\lambda^\alpha p^\alpha}{\left(\lambda_r^{-\beta}+p^\beta\right)^{k+1}}\right] \tag{12}$$
$$-\frac{\lambda_r^\beta}{n\pi}\left[(-1)^{n+1}+1\right]\sum_{k=0}^{\infty}\frac{(-1)^k}{(n\pi)^{2k}\lambda_r^{\beta(k+1)}}\sum_{m,l\geq 0}^{m+l=k}\frac{k!}{m!l!}M^m\sum_{n_1,w\geq 0}^{n_1+w=k}\frac{k!}{n_1!w!}\frac{\lambda^{\alpha k}p^{\alpha(k+1)-m}}{\left(\lambda_r^{-\beta}+p^\beta\right)^{k+1}}$$

Now we have an important Laplace transformation of the nth order derivative of Mittage-Leffler function $E_{\alpha,\lambda}(z)$ given by

$$\int_0^\infty e^{-pt}t^{\alpha n+\lambda-1}E_{\alpha,\lambda}^{(n)}\left(-at^\alpha\right)dt=\frac{n!\,p^{\alpha-\lambda}}{\left(p^\alpha+a\right)^{n+1}} \tag{13}$$

where

$$E_{\alpha,\lambda}^{(n)}(z)=\frac{d^n}{dz^n}E_{\alpha,\lambda}(z)=\sum_{j=0}^{\infty}\frac{(j+n)!z^j}{j!\Gamma(\alpha j+\alpha n+\lambda)} \tag{14}$$

Taking Laplace Inverse transformation we get from the Equation (12)

$$U_s(n,t)=\frac{(-1)^{n+1}}{n\pi}\cos(\omega_2 t)-\frac{(-1)^{n+1}}{n\pi}\sum_{k=0}^{\infty}\frac{(-1)^k}{(n\pi)^{2(k+1)}}\sum_{m,l\geq 0}^{m+l=k+1}\frac{(k+1)!}{m!l!}M^m\sum_{n_1,w\geq 0}^{n_1+w=k}\frac{1}{n_1!w!}\frac{\lambda^{\alpha n_1}}{\lambda_r^{\beta(k+1)}}$$
$$\times\int_0^t\cos(\omega_2(t-\tau))\left[\tau^{\beta(k+1)-\alpha n_1-l-1}E_{\beta,\beta-\alpha n_1-l}^{(k)}\left(-\lambda_r^{-\beta}\tau^\beta\right)+\tau^{\beta(k+1)-\alpha(n_1+1)-l-1}E_{\beta,\beta-\alpha(n_1+1)-l}^{(k)}\left(-\lambda_r^{-\beta}\tau^\beta\right)\right]d\tau$$
$$+\frac{1}{n\pi}\cos(\omega_1 t)-\frac{1}{n\pi}\sum_{k=0}^{\infty}\frac{(-1)^k}{(n\pi)^{2(k+1)}}\sum_{m,l\geq 0}^{m+l=k+1}\frac{(k+1)!}{m!l!}M^m\sum_{n_1,w\geq 0}^{n_1+w=k}\frac{1}{n_1!w!}\frac{\lambda^{\alpha n_1}}{\lambda_r^{\beta(k+1)}} \tag{15}$$
$$\times\int_0^t\cos(\omega_1(t-\tau))\left[\tau^{\beta(k+1)-\alpha n_1-l-1}E_{\beta,\beta-\alpha n_1-l}^{(k)}\left(-\lambda_r^{-\beta}\tau^\beta\right)+\lambda^\alpha\tau^{\beta(k+1)-\alpha(n_1+1)-l-1}E_{\beta,\beta-\alpha(n_1+1)-l}^{(k)}\left(-\lambda_r^{-\beta}\tau^\beta\right)\right]d\tau$$
$$-\frac{\lambda_r^\beta}{n\pi}\left[(-1)^{n+1}+1\right]\sum_{k=0}^{\infty}\frac{(-1)^k}{(n\pi)^{2k}\lambda_r^{\beta(k+1)}}\sum_{m,l\geq 0}^{m+l=k}\frac{k!}{m!l!}M^m\sum_{n_1,w\geq 0}^{n_1+w=k}\frac{1}{n_1!w!}\lambda^{\alpha k}t^{\beta(k+1)-\alpha(k+1)+m-1}E_{\beta,\beta-\alpha(k+1)+m}^{(k)}\left(-\lambda_r^{-\beta}t^\beta\right)$$

Taking inverse finite Fourier sine transformation we get the velocity profile from the Equation (18) as

$$u(y,t)=y\cos(\omega_2 t)+(1-y)\cos(\omega_1 t)+2\sum_{n=1}^{\infty}\frac{(-1)^n}{n\pi}\sin(n\pi y)\sum_{k=0}^{\infty}\frac{(-1)^k}{(n\pi)^{2(k+1)}}\sum_{m,l\geq 0}^{m+l=k+1}\frac{(k+1)!}{m!l!}M^m\sum_{n_1,w\geq 0}^{n_1+w=k}\frac{1}{n_1!w!}\frac{\lambda^{\alpha n_1}}{\lambda_r^{\beta(k+1)}}$$

$$\times\int_0^t\cos(\omega_2(t-\tau))\Big[\tau^{\beta(k+1)-\alpha n_1-l-1}\times E^{(k)}_{\beta,\beta-\alpha n_1-l}\left(-\lambda_r^{-\beta}\tau^{\beta}\right)+\lambda^{\alpha}\tau^{\beta(k+1)-\alpha(n_1+1)-l-1}E^{(k)}_{\beta,\beta-\alpha(n_1+1)-l}\left(-\lambda_r^{-\beta}\tau^{\beta}\right)\Big]\mathrm{d}\tau$$

$$-2\sum_{n=1}^{\infty}\frac{1}{n\pi}\sin(n\pi y)\sum_{k=0}^{\infty}\frac{(-1)^k}{(n\pi)^{2(k+1)}}E^{(k)}_{\beta,\beta-\alpha(n_1+1)-l}\left(-\lambda_r^{-\beta}\tau^{\beta}\right)\Big]\mathrm{d}\tau$$

$$-2\sum_{n=1}^{\infty}\frac{1}{n\pi}\sin(n\pi y)\sum_{k=0}^{\infty}\frac{(-1)^k}{(n\pi)^{2(k+1)}}\sum_{m,l\geq 0}^{m+l=k+1}\frac{(k+1)!}{m!l!}M^m\sum_{n_1,w\geq 0}^{n_1+w=k}\frac{1}{n_1!w!}\frac{\lambda^{\alpha n_1}}{\lambda_r^{\beta(k+1)}}$$

$$\times\int_0^t\cos(\omega_1(t-\tau))\Big[\tau^{\beta(k+1)-\alpha n_1-l-1}E^{(k)}_{\beta,\beta-\alpha n_1-l}\left(-\lambda_r^{-\beta}\tau^{\beta}\right)+\lambda^{\alpha}\tau^{\beta(k+1)-\alpha(n_1+1)-l-1}E^{(k)}_{\beta,\beta-\alpha(n_1+1)-l}\left(-\lambda_r^{-\beta}\tau^{\beta}\right)\Big]\mathrm{d}\tau$$

$$-2\sum_{n=1}^{\infty}\lambda_r^{\beta}\left[(-1)^{n+1}+1\right]\frac{\sin(n\pi y)}{n\pi}$$

$$\times\sum_{k=0}^{\infty}\frac{(-1)^k}{(n\pi)^{2k}\lambda_r^{\beta(k+1)}}\sum_{m,l\geq 0}^{m+l=k}\frac{k!}{m!l!}M^m\sum_{n_1,w\geq 0}^{n_1+w=k}\frac{1}{n_1!w!}\lambda^{\alpha k}t^{\beta(k+1)-\alpha(k+1)+m-1}E^{(k)}_{\beta,\beta-\alpha(k+1)+m}\left(-\lambda_r^{-\beta}t^{\beta}\right).\tag{16}$$

3. Limiting Cases

Case-I If $\alpha\to 0.0$, $\lambda_r\to 0.0$ then the equation of motion is given by

$$\left(1+\lambda^{\alpha}\right)\frac{\partial u(y,t)}{\partial t}=\frac{\partial^2 u(y,t)}{\partial y^2}-M\left(1+\lambda^{\alpha}\right)u(y,t)\tag{17}$$

subject to the initial and boundary conditions given by the Equations (7) and (8) respectively.

The Equation (17) represents the governing equation of a classical Newtonian fluid and the corresponding velocity field is given by

$$u=y\cos(\omega_2 t)+(1-y)\cos(\omega_1 t)$$
$$+2\sum_{n=1}^{\infty}\frac{(-1)^n}{n\pi}\sin(n\pi y)\sum_{k=0}^{\infty}\frac{(-1)^k}{(n\pi)^{2(k+1)}}\sum_{m,l\geq 0}^{m+l=k+1}\frac{(k+1)!}{m!l!}M^l\sum_{s,i\geq 0}^{s+i=k+1}\frac{(k+1)!}{s!i!}\lambda^{\alpha s}t^{-m}E^{(0)}_{2,1-m}\left(-\omega_2^2t^2\right)\tag{18}$$
$$-2\sum_{n=1}^{\infty}\frac{1}{n\pi}\sin(n\pi y)\sum_{k=0}^{\infty}\frac{(-1)^k}{(n\pi)^{2(k+1)}}\sum_{m,l\geq 0}^{m+l=k+1}\frac{(k+1)!}{m!l!}M^l\sum_{s,i\geq 0}^{s+i=k+1}\frac{(k+1)!}{s!i!}\lambda^{\alpha s}t^{-m}E^{(0)}_{2,1-m}\left(-\omega_1^2t^2\right).$$

Case-II If $\beta\neq 0.0$, $\lambda_r\to 0.0$ then the equation is given by

$$\left(1+\lambda^{\alpha}D_t^{\alpha}\right)\frac{\partial u(y,t)}{\partial t}=\frac{\partial^2 u(y,t)}{\partial y^2}-M\left(1+\lambda^{\alpha}D_t^{\alpha}\right)u(y,t)\tag{19}$$

subject to the initial and boundary conditions given by the Equations (7) and (8).

The Equation (19) represents the governing equation of a generalized Maxwell fluid and the corresponding velocity field is given by

$$u=y\cos(\omega_2 t)+(1-y)\cos(\omega_1 t)$$
$$+2\sum_{n=1}^{\infty}\frac{(-1)^n}{n\pi}\sin(n\pi y)\sum_{k=0}^{\infty}\frac{(-1)^k}{(n\pi)^{2(k+1)}}\sum_{m,l\geq 0}^{m+l=k+1}\frac{(k+1)!}{m!l!}M^l\sum_{s,i\geq 0}^{s+i=k+1}\frac{(k+1)!}{s!i!}\lambda^{\alpha s}t^{-(\alpha s+m)}E^{(0)}_{2,1-\alpha s-m}\left(-\omega_2^2t^2\right)\tag{20}$$
$$-2\sum_{n=1}^{\infty}\frac{1}{n\pi}\sin(n\pi y)\sum_{k=0}^{\infty}\frac{(-1)^k}{(n\pi)^{2(k+1)}}\sum_{m,l\geq 0}^{m+l=k+1}\frac{(k+1)!}{m!l!}M^l\sum_{s,i\geq 0}^{s+i=k+1}\frac{(k+1)!}{s!i!}\lambda^{\alpha s}t^{-(\alpha s+m)}E^{(0)}_{2,1-\alpha s-m}\left(-\omega_1^2t^2\right).$$

Case-III If $\alpha \neq 0.0$, $\lambda \to 0.0$ then the equation of motion is given by

$$\frac{\partial u(y,t)}{\partial t} = \left(1+\lambda_r^\beta D_t^\beta\right)\frac{\partial^2 u(y,t)}{\partial y^2} - Mu(y,t) \tag{21}$$

subject to the initial and boundary conditions given by the Equations (7) and (8) respectively.

The Equation (21) is the governing equation for a generalized second grade fluid and the velocity field is given by

$$\begin{aligned} u &= y\cos(\omega_2 t) + (1-y)\cos(\omega_1 t) \\ &+2\sum_{n=1}^{\infty}\frac{(-1)^n}{n\pi}\sin(n\pi y)\sum_{k=0}^{\infty}\frac{(-1)^k}{(n\pi)^{2(k+1)}}\sum_{m,l\ge 0}^{m+l=k+1}\frac{(k+1)!}{m!l!}\frac{M^m}{\lambda_r^{\beta(k+1)}}\int_0^t \cos(\omega_2(t-\tau))\tau^{\beta(k+1)+m-k-2}E^{(k)}_{\beta,\beta+m-k-1}\left(-\lambda_r^{-\beta}\tau^\beta\right)\mathrm{d}\tau \\ &-2\sum_{n=1}^{\infty}\frac{1}{n\pi}\sin(n\pi y)\sum_{k=0}^{\infty}\frac{(-1)^k}{(n\pi)^{2(k+1)}}\sum_{m,l\ge 0}^{m+l=k+1}\frac{(k+1)!}{m!l!}\frac{M^m}{\lambda_r^{\beta(k+1)}}\int_0^t \cos(\omega_1(t-\tau))\tau^{\beta(k+1)+m-k-2}E^{(k)}_{\beta,\beta+m-k-1}\left(-\lambda_r^{-\beta}\tau^\beta\right)\mathrm{d}\tau \\ &-2\sum_{n=1}^{\infty}\lambda_r^\beta\left[(-1)^{n+1}+1\right]\frac{\sin(n\pi y)}{n\pi}\sum_{k=0}^{\infty}\frac{(-1)^k}{(n\pi)^{2k}\lambda_r^{\beta(k+1)}}\sum_{m,l\ge 0}^{m+l=k}\frac{M^m}{m!l!}t^{\beta(k+1)+m-k-1}E^{(k)}_{\beta,\beta+m-k}\left(-\lambda_r^{-\beta}t^\beta\right). \end{aligned} \tag{22}$$

Case-IV If $\alpha \to 1.0$, $\lambda_r \to 0.0$ then the equation of motion is given by

$$\left(1+\lambda^\alpha\frac{\partial}{\partial t}\right)\frac{\partial u(y,t)}{\partial t} = \frac{\partial^2 u(y,t)}{\partial y^2} - M\left(1+\lambda^\alpha\frac{\partial}{\partial t}\right)u(y,t) \tag{23}$$

subject to the initial and boundary conditions given by the Equations (7) and (8) respectively.

The Equation (23) represents the governing equation of an ordinary Oldroyd-B fluid and the corresponding velocity field is given by

$$\begin{aligned} u &= y\cos(\omega_2 t) + (1-y)\cos(\omega_1 t) \\ &+2\sum_{n=1}^{\infty}\frac{(-1)^n}{n\pi}\sin(n\pi y)\sum_{k=0}^{\infty}\frac{(-1)^k}{(n\pi)^{2(k+1)}}\sum_{m,l\ge 0}^{m+l=k+1}\frac{(k+1)!}{m!l!}M^m\sum_{l,w\ge 0}^{l+w=k+1}\frac{(k+1)!}{l!w!}\lambda^{\alpha l}t^{m-k-l}E^{(0)}_{2,1+m-k-l}\left(-\omega_2^2 t^2\right) \\ &-2\sum_{n=1}^{\infty}\frac{1}{n\pi}\sin(n\pi y)\sum_{k=0}^{\infty}\frac{(-1)^k}{(n\pi)^{2(k+1)}}\sum_{m,l\ge 0}^{m+l=k+1}\frac{(k+1)!}{m!l!}M^m\sum_{l,w\ge 0}^{l+w=k+1}\frac{(k+1)!}{l!w!}\lambda^{\alpha l}t^{m-k-l}E^{(0)}_{2,1+m-k-l}\left(-\omega_2^2 t^2\right). \end{aligned} \tag{27}$$

4. Conclusions and Numerical Results

In this paper we have presented the flow of a generalized Oldroyd-B fluid between two oscillating infinite parallel plates. The velocity field has been determined by means of Laplace and finite Fourier sine transformations in series form in terms of Mittage-Leffler function. The dependence of the velocity field on the fractional calculus parameters and material parameters has been illustrated graphically. The solutions for the four limiting cases have been discussed from the solution of the flow problems of a generalized Oldroyd-B fluid.

In **Figure 2** the velocity is depicted against the distance from the lower plate for different values of the fractional calculus parameter α. As α increases, the fluid velocity increases and there are points of local minimum and local maximum in the velocity curves which are oscillatory in nature. Negative velocity can be observed near the upper plate for values of α near zero in **Figure 2**. The velocity is depicted against the distance from the lower plate for different values of fractional calculus parameter β in **Figure 3**. As β increases, the fluid velocity decreases, which is opposite to the case in **Figure 2** and the points of local minimum and maximum can be observed in the velocity curves. The flow patterns are oscillatory in nature. In **Figure 4** the velocity is plotted against the distance from the lower plate for different values of the parameter *M*. As the parameter *M* takes increasing values, the fluid velocity increases and the velocity curves are oscillatory in nature. The velocity profile is plotted against the distance from the lower plate for different values of the frequency of oscillation ω_1 of the lower plate in **Figure 5**. It is evident from the figure that the fluid velocity decreases for higher values of the parameter ω_1. The initial points of the velocity curves near the lower plate are different in domain of spatial

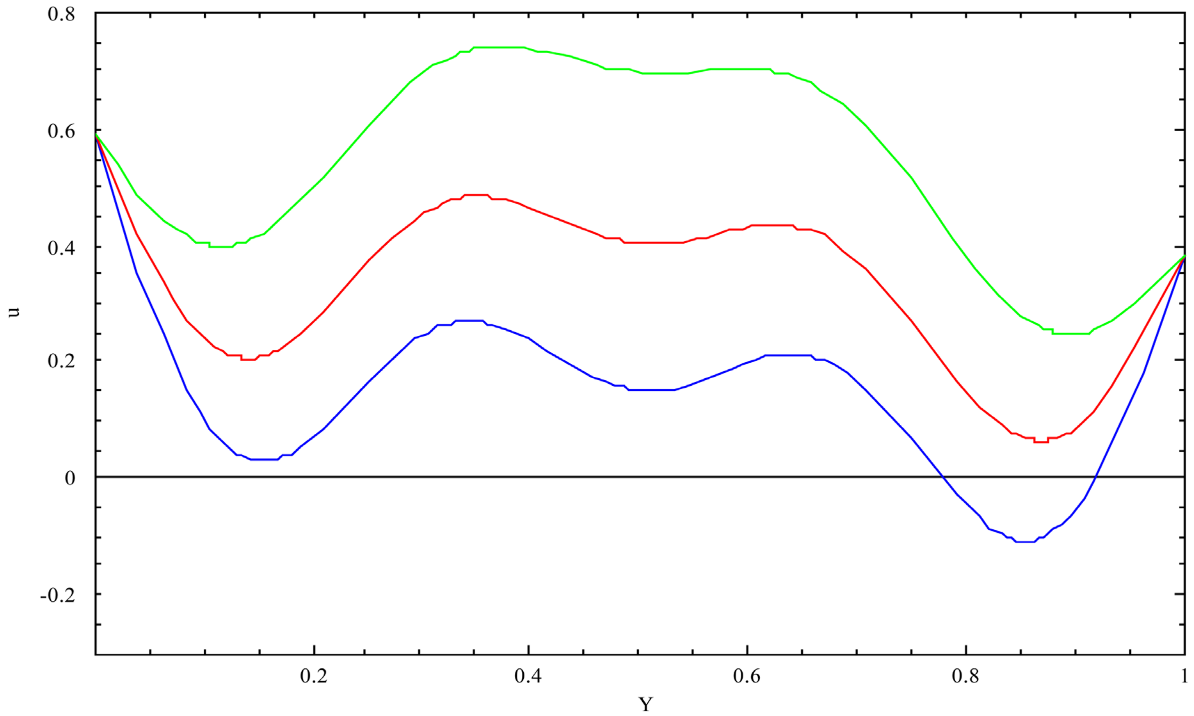

Figure 2. The velocity profile is depicted against the distance from the lower plate for different values of the fractional calculus parameter α. $\omega_1 = 1.2$, $\omega_2 = 1.5$, $M = 10$, $\lambda = 6$, $\lambda_r = 3$, $\beta = 0.8$, $t = \pi/4$, $\alpha = 0.1$ ________, $\alpha = 0.2$ ________, $\alpha = 0.3$ ________.

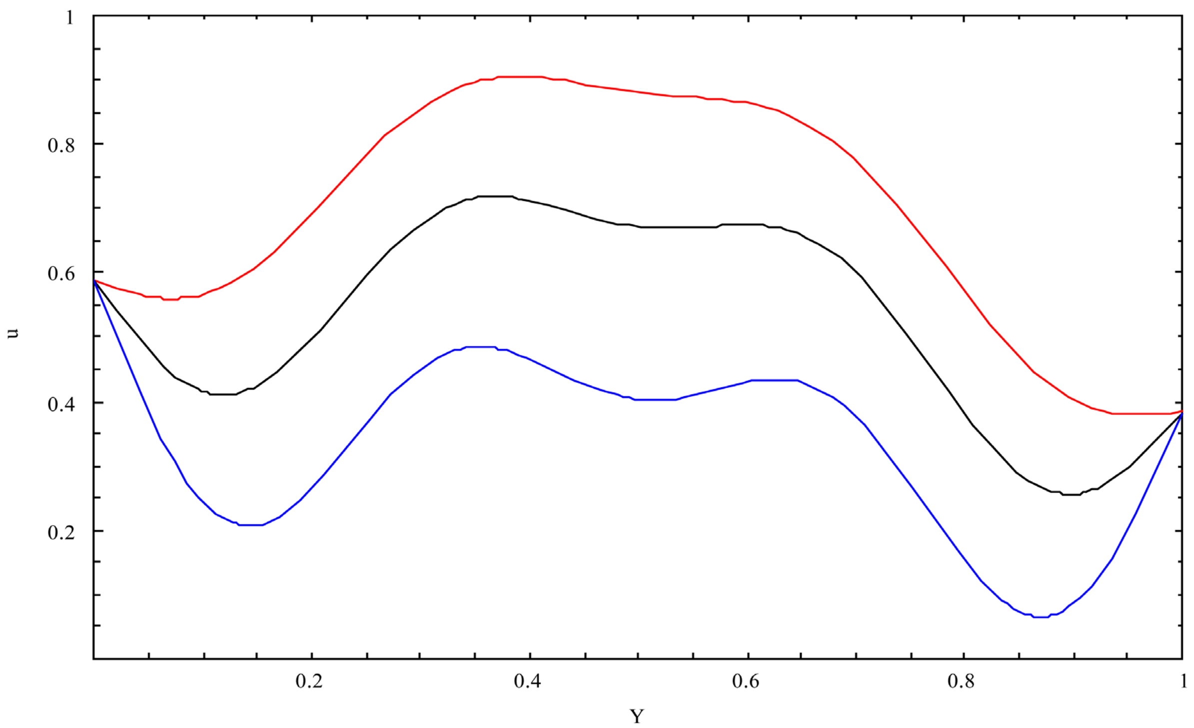

Figure 3. The velocity profile is depicted against the distance from the lower plate for different values of the fractional calculus parameter β. $\omega_1 = 1.2$, $\omega_2 = 1.5$, $M = 10$, $\lambda = 6$, $\lambda_r = 3$, $\alpha = 0.2$, $t = \pi/4$, $\beta = 0.6$ ________, $\beta = 0.7$ ________, $\beta = 0.8$ ________.

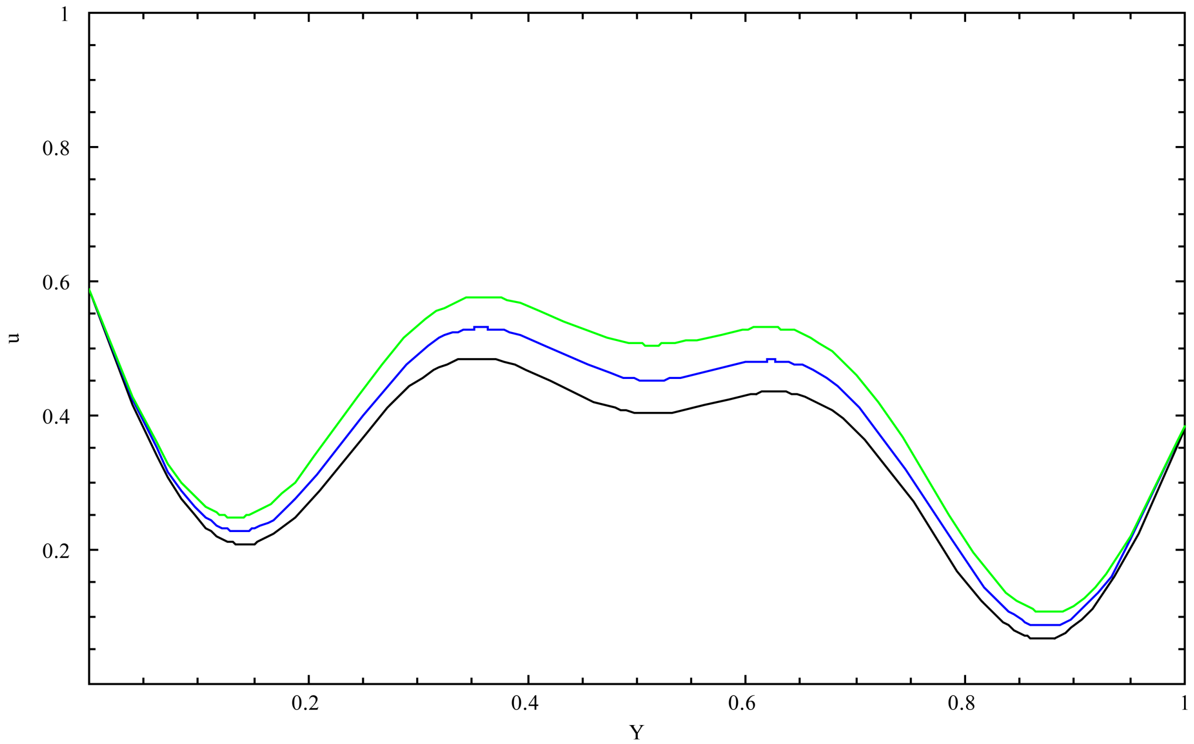

Figure 4. The velocity is depicted against the distance from the lower plate for different values of parameter M. $\omega_1 = 1.2$, $\omega_2 = 1.5$, $\lambda = 6$, $\lambda_r = 3$, $\alpha = 0.2$, $\beta = 0.8$, $t = \pi/4$, $M = 10$ ________, $M = 11$ ________, $M = 12$ ________.

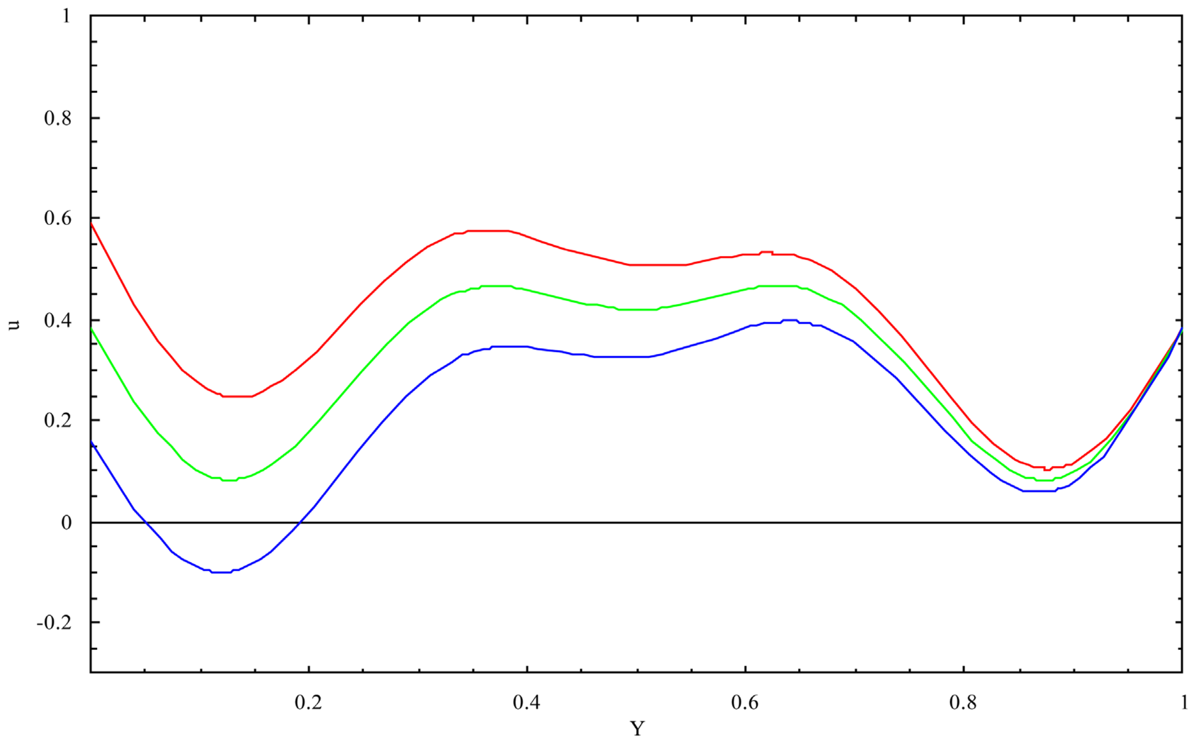

Figure 5. The velocity is depicted against the distance from the lower plate for different values of the parameter ω_1. $\omega_2 = 1.5$, $M = 10$, $\lambda = 6$, $\lambda_r = 3$, $\alpha = 0.2$, $\beta = 0.8$, $t = \pi/4$, $\omega_1 = 1.2$ ________, $\omega_1 = 1.5$ ________, $\omega_1 = 1.8$ ________.

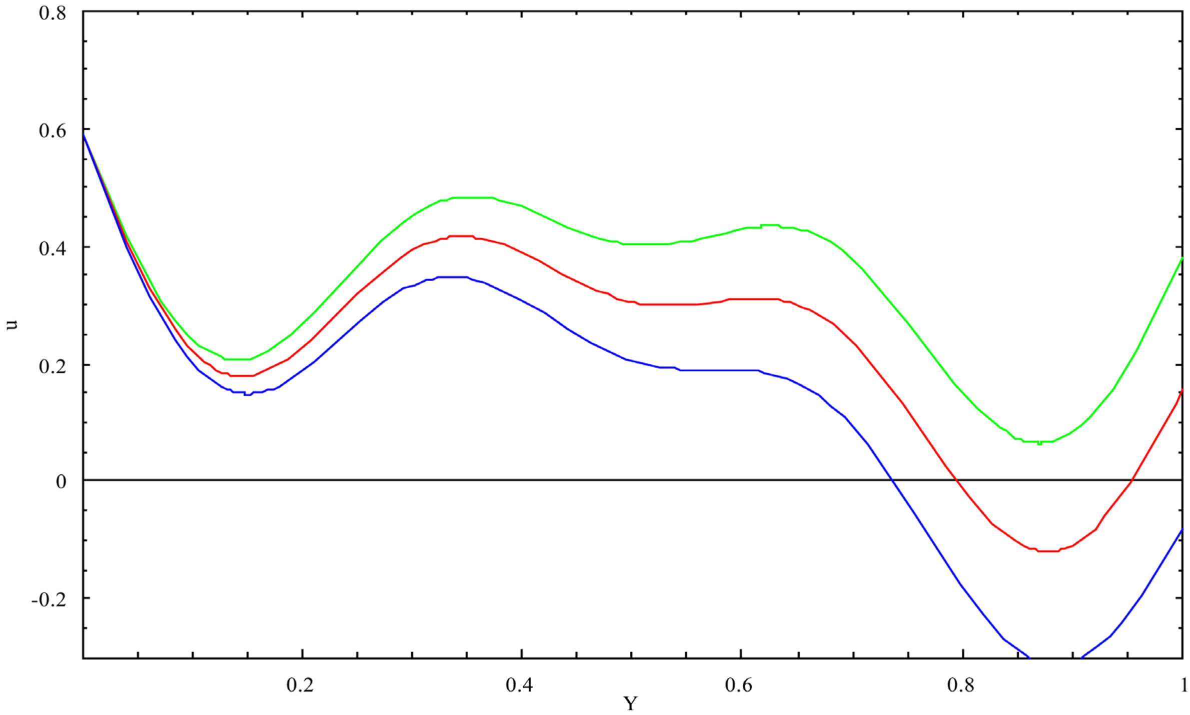

Figure 6. The velocity profile is depicted against the distance from the lower plate for different values of the parameter ω_2. $\omega_1 = 1.2$, $M = 10$, $\lambda = 6$, $\lambda_r = 3$, $\alpha = 0.2$, $\beta = 0.8$, $t = \pi/4$, $\omega_2 = 1.5$ ________, $\omega_2 = 1.8$ ________, $\omega_2 = 2.1$ ________.

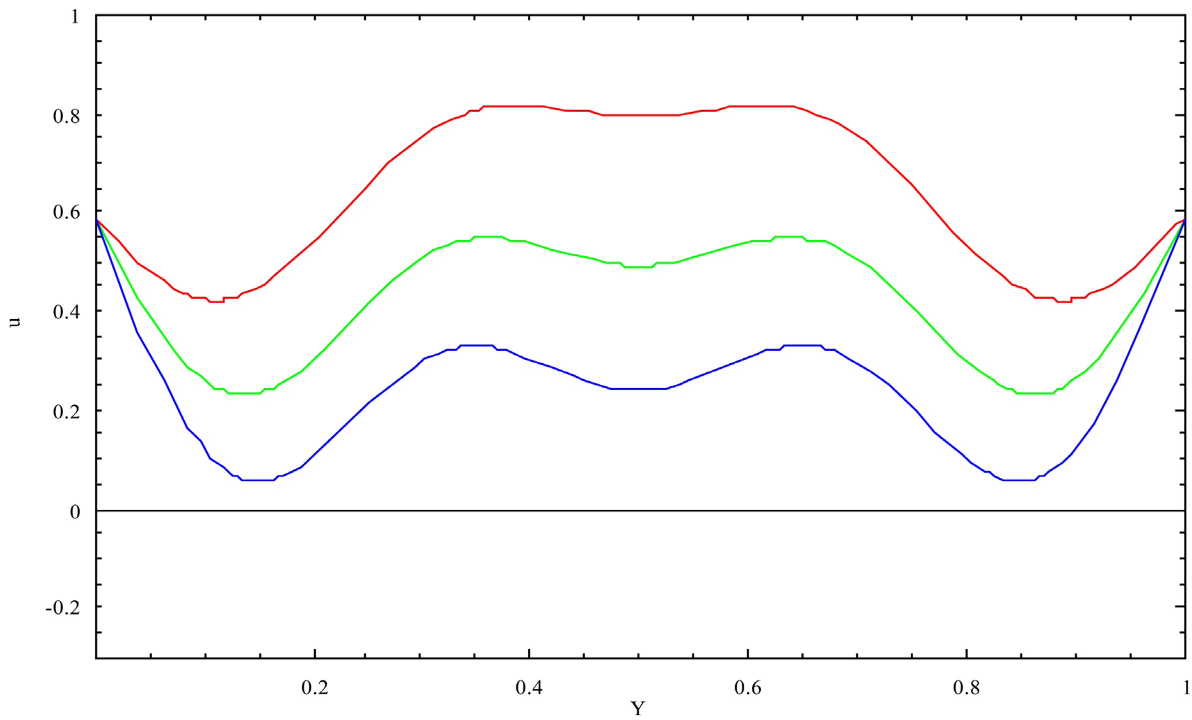

Figure 7. The velocity profile is depicted against the distance from the lower plate for different values of the fractional calculus parameter α and for equal values of ω_1 and ω_2, $\omega_1 = \omega_2 = 1.2$, $M = 10$, $\lambda = 6$, $\lambda_r = 3$, $\beta = 0.8$, $t = \pi/4$, $\alpha = 0.1$ ________, $\alpha = 0.2$ ________, $\alpha = 0.3$ ________.

variable Y for different values of frequency of oscillation ω_1 of the lower plate. There is negative velocity in **Figure 5** near the lower plate for values for higher frequency of oscillation of the lower plate. In **Figure 6** as the frequency of the oscillation ω_2 of the upper plate changes, the terminal points of the velocity curves near the upper plate differ. The fluid velocity decreases with the increase of the frequency of oscillation ω_2 of the upper plate near that one. It can be noticed that there are points of local minimum and maximum for velocity curves for all the three cases. Negative velocity can be observed near the upper plate in **Figure 6** for higher values of the frequency of oscillation of the upper plate. In **Figure 7** the velocity profile is depicted against the distance from the lower plate for different values of the parameter α in which the frequencies of oscillations of the plates are equal *i.e.* $\omega_1 = \omega_2$. The fluid velocity increases with increasing values of α and the velocity curves are oscillatory in nature. It can be noticed that for equal frequency of oscillations of the two plates, the heights of the initial and terminal points on the velocity curve in the domain of spatial variable are equal.

References

[1] Bandeli, R. and Rajagopal, K.R. (1995) Start-Up Flows of Second Grade Fluids in Domains with One Finite Dimension. *International Journal of Non-Linear Mechanics*, **30**, 817-839. http://dx.doi.org/10.1016/0020-7462(95)00035-6

[2] Fetecau, C., Fetecau, C., Karman, M. and Vieru, D. (2009) Exact Solutions for the Flow of a Generalized Oldroyd-B Fluid Induced by a Constantly Accelerating Plate between Two Side Walls Perpendicular to the Plate. *Journal of Non-Newtonian Fluid Mechanics*, **156**, 189-201. http://dx.doi.org/10.1016/j.jnnfm.2008.06.005

[3] Hayat, T. and Sajid, M. (2007) Homotopy Analysis of MHD Boundary Layer Flow of an Upper-Convected Maxwell Fluid. *International Journal of Engineering Science*, **45**, 393-401. http://dx.doi.org/10.1016/j.ijengsci.2007.04.009

[4] Jamil, M. and Khan, N.A. (2011) Slip Effects on Fractional Viscoelastic Fluids. *International Journal of Differential Equations*, **2011**, Article ID 193813. http://dx.doi.org/10.1155/2011/193813

[5] Shen, F., Tan, W., Zhao, Y. and Masuoka, T. (2006) The Rayleigh-Stokes Problem for a Heated Generalised Second Grade Fluid with Fractional Derivative Model. *Nonlinear Analysis*: *Real World Application*, **7**, 1072-1080. http://dx.doi.org/10.1016/j.nonrwa.2005.09.007

[6] Vieru, D., Fetecau, C. and Fetecau, C. (2008) Flow of a Generalized Oldroyd-B Fluid Due to a Constantly Accelerating Plate. *Applied Mathematics and Computation*, **201**, 834-842. http://dx.doi.org/10.1016/j.amc.2007.12.045

[7] Wenchang, T., Wenxiao, P. and Mingyu, X. (2003) A Note on Unsteady Flows of a Viscoelastic Fluid with the Fractional Maxwell Model between Two Parallel Plates. *International Journal of Non-Linear Mechanics*, **38**, 645-650. http://dx.doi.org/10.1016/S0020-7462(01)00121-4

[8] Vieru, D., Fetecau, C. and Fetecau, C. (2010) Unsteady Flow of a Generalized Oldroyd-B Fluid Due to an Infinite Plate Subject to a Time-Dependent Shear Stress. *Canadian Journal of Physics*, **88**, 675-687. http://dx.doi.org/10.1139/P10-055

Applied Mathematics, 2015, 6, 116-127
Published Online January 2015 in SciRes. http://www.scirp.org/journal/am
http://dx.doi.org/10.4236/am.2015.61012

Neutrosophic Soft Expert Sets

Mehmet Şahin[1], Shawkat Alkhazaleh[2], Vakkas Uluçay[1]

[1]Department of Mathematics, Gaziantep University, Gaziantep, Turkey
[2]Department of Mathematics, Faculty of Science and Art, Shaqra University, Shaqra, KSA
Email: mesahin@gantep.edu.tr, shmk79@gmail.com, vulucay27@gmail.com

Received 14 November 2014; revised 6 December 2014; accepted 24 December 2014

Abstract

In this paper we introduce the concept of neutrosophic soft expert set (NSES). We also define its basic operations, namely complement, union, intersection, AND and OR, and study some of their properties. We give examples for these concepts. We give an application of this concept in a decision-making problem.

Keywords

Soft Expert Set, Neutrosophic Soft Set, Neutrosophic Soft Expert Set

1. Introduction

In some real-life problems in expert system, belief system, information fusion and so on, we must consider the truth-membership as well as the falsity-membership for proper description of an object in uncertain, ambiguous environment. Intuitionistic fuzzy sets were introduced by Atanassov [1]. After Atanassov's work, Smarandache [2] [3] introduced the concept of neutrosophic set which is a mathematical tool for handling problems involving imprecise, indeterminacy and inconsistent data. In 1999, Molodtsov [4] initiated a novel concept of soft set theory as a new mathematical tool for dealing with uncertainties. After Molodtsov's work, some different operations and applications of soft sets were studied by Chen *et al*. [5] and Maji *et al*. [6]. Later, Maji [7] firstly proposed neutrosophic soft sets with operations. Alkhazaleh *et al*. generalized the concept of fuzzy soft expert sets which include that possibility of each element in the universe is attached with the parameterization of fuzzy sets while defining a fuzzy soft expert set [8]. Alkhazaleh *et al.* [9] generalized the concept of parameterized interval-valued fuzzy soft sets, where the mapping in which the approximate function are defined from fuzzy parameters set, and they gave an application of this concept in decision making. In the other study, Alkhazaleh and Salleh [10] introduced the concept soft expert sets where user can know the opinion of all expert sets. Alkhazaleh and Salleh [11] generalized the concept of a soft expert set to fuzzy soft expert set, which is a more effective and useful. They also defined its basic operations, namely complement, union, intersection, AND and OR, and gave

How to cite this paper: Şahin, M., Alkhazaleh, S. and Uluçay, V. (2015) Neutrosophic Soft Expert Sets. *Applied Mathematics*, **6**, 116-127. http://dx.doi.org/10.4236/am.2015.61012

an application of this concept in decision-making problem. They also studied a mapping on fuzzy soft expert classes and its properties. Our objective is to introduce the concept of neutrosophic soft expert set. In Section 1, we introduce from intuitionistic fuzzy sets to soft expert sets. In Section 2, preliminaries are given. In Section 3, we also define the concept of neutrosophic soft expert set and its basic operations, namely complement, union, intersection AND and OR. In Section 4, we give an application of this concept in a decision-making problem. In Section 5 conclusions are given.

2. Preliminaries

In this section we recall some related definitions.

2.1. Definition: [3] Let U be a space of points (objects), with a generic element in U denoted by u. A neutrosophic set (N-sets) A in U is characterized by a truth-membership function T_A, a indeterminacy-membership function I_A and a falsity-membership function F_A. $T_A(u)$; $I_A(u)$ and $F_A(u)$ are real standard or nonstandard subsets of $[0,1]$. It can be written as

$$A=\left\{\left\langle u,\left(T_A(u),I_A(u),F_A(u)\right)\right\rangle : u\in U, T_A(u), I_A(u), F_A(u)\in[0,1]\right\}.$$

There is no restriction on the sum of $T_A(u)$; $I_A(u)$ and $F_A(u)$, so

$$0\le \sup T_A(u)+\sup I_A(u)+\sup F_A(u)\le 3.$$

2.2. Definition: [7] Let U be an initial universe set and E be a set of parameters. Consider $A\subseteq E$. Let $P(U)$ denotes the set of all neutrosophic sets of U. The collection (F,A) is termed to be the soft neutrosophic set over U, where F is a mapping given by $F:A\to P(U)$.

2.3. Definition: [6] A neutrosophic set A is contained in another neutrosophic set B *i.e.* $A\subseteq B$ if $\forall x\in X$, $T_A(x)\le T_B(x)$, $I_A(x)\le I_B(x)$, $F_A(x)\ge F_B(x)$.

Let U be a universe, E a set of parameters, and X a soft experts (agents). Let O be a set of opinion, $Z=E\times X\times O$ and $A\subseteq Z$.

2.4. Definition: [9] A pair (F, A) is called a soft expert set over U, where F is mapping given by $F:A\to P(U)$ where $P(U)$ denotes the power set of U.

2.5. Definition: [11] A pair (F,A) is called a fuzzy soft expert set over U, where F is mapping given by $F:A\to I^U$ where I^U denotes the set of all fuzzy subsets of U.

2.6. Definition: [11] For two fuzzy soft expert sets (F,A) and (G,B) over U, (F,A) is called a fuzzy soft expert subset of (G,B) if

1) $B\subseteq A$,

2) $\forall\varepsilon\in A$, $F(\varepsilon)$ is fuzzy subset of $G(\varepsilon)$.

This relationship is denoted by $(F,A)\subseteq(G,B)$. In this case (G,B) is called a fuzzy soft expert superset of (F,A).

2.7. Definition: [11] Two fuzzy soft expert sets (F,A) and (G,B) over U are said to be equal.

If (F,A) is a fuzzy soft expert subset of (G,B) and (G,B) is a fuzzy soft expert subset of (F,A).

2.8. Definition: [11] An agree-fuzzy soft expert set $(F,A)_1$ over U is a fuzzy soft expert subset of (F,A) defined as follow

$$(F,A)_1=\{F_1(\alpha):\alpha\in E\times X\times\{1\}\}.$$

2.9. Definition: [11] A disagree-fuzzy soft expert set $(F,A)_0$ over U is a fuzzy soft expert subset of (F,A) defined as follow

$$(F,A)_0=\{F_0(\alpha):\alpha\in E\times X\times\{0\}\}.$$

2.10. Definition: [11] Complement of a fuzzy soft expert set. The complement of a fuzzy soft expert set (F,A) denoted by $(F,A)^c$ and is defined as $(F,A)^c=(F^c,\neg A)$ where $F^c=\neg A\to I^U$ is mapping given by

$$F^c(\alpha)=c(F(\alpha))\quad\forall\alpha\in A,$$

where c is a fuzzy complement.

2.11. Definition: [11] The intersection of fuzzy soft expert sets (F,A) and (G,B) over U, denoted by $(F,A)\tilde{\cap}(G,B)$, is the fuzzy soft expert set (H,C) where $C = A\cup B$ and $\forall\varepsilon\in C$,

$$H(\varepsilon)=\begin{cases}F(\varepsilon), & \text{if } \varepsilon\in A-B\\ G(\varepsilon), & \text{if } \varepsilon\in B-A\\ t(F(\varepsilon),G(\varepsilon)), & \text{if } \varepsilon\in A\cap B\end{cases}$$

where t is a t-norm.

2.12. Definition: [11] The intersection of fuzzy soft expert sets (F,A) and (G,B) over U, denoted by $(F,A)\tilde{\cup}(G,B)$, is the fuzzy soft expert set (H,C) where $C = A\cup B$ and $\forall\varepsilon\in C$,

$$H(\varepsilon)=\begin{cases}F(\varepsilon), & \text{if } \varepsilon\in A-B\\ G(\varepsilon), & \text{if } \varepsilon\in B-A\\ s(F(\varepsilon),G(\varepsilon)), & \text{if } \varepsilon\in A\cap B\end{cases}$$

where s is an s-norm.

2.13. Definition: [11] If (F,A) and (G,B) are two fuzzy soft expert sets over U then "(F,A) AND (G,B)" denoted by $(F,A)\wedge(G,B)$ is defined by

$$(F,A)\wedge(G,B)=(H,A\times B)$$

such that $H(\alpha,\beta)=t(F(\alpha),G(\beta))$, $\forall(\alpha,\beta)\in A\times B$ where t is a t-norm.

2.14. Definition: [11] If (F,A) and (G,B) are two fuzzy soft expert sets over U then "(F,A) OR (G,B)" denoted by $(F,A)\vee(G,B)$ is defined by

$$(F,A)\vee(G,B)=(H,A\times B)$$

such that $H(\alpha,\beta)=s(F(\alpha),G(\beta))$, $\forall(\alpha,\beta)\in A\times B$ where s is an s-norm.

Using the concept of neutrosophic set now we introduce the concept of neutrosophic soft expert set.

3. Neutrosophic Soft Expert Set

In this section, we introduce the definition of a neutrosophic soft expert set and give basic properties of this concept.

Let U be a universe, E a set of parameters, X a set of experts (agents), and $O=\{1=\text{agree},0=\text{disagree}\}$ a set of opinions. Let $Z=E\times X\times O$ and $A\subseteq Z$.

3.1. Definition: A pair (F,A) is called a neutrosophic soft expert set over U, where F is mapping given by

$$F: A\to P(U)$$

where $P(U)$ denotes the power neutrosophic set of U. For definition we consider an example.

3.1. Example: Suppose the following U is the set of car under consideration E is the set of parameters. Each parameter is a neutrosophic word or sentence involving neutrosophic words.

$$U=\{u_1,u_2,u_3\}$$

$$E=\{\text{easy to use; quality}\}=\{e_1,e_2\}$$

$$X=\{p,q,r\}$$

be a set of experts. Suppose that

$$F(e_1,p,1)=\{\langle u_1,0.3,0.5,0.7\rangle,\langle u_3,0.5,0.6,0.3\rangle\}$$

$$F(e_1,q,1)=\{\langle u_2,0.8,0.2,0.3\rangle,\langle u_3,0.9,0.5,0.7\rangle\}$$

$$F(e_1, r, 1) = \{\langle u_1, 0.4, 0.7, 0.6\rangle\}$$

$$F(e_2, p, 1) = \{\langle u_1, 0.4, 0.2, 0.3\rangle, \langle u_2, 0.7, 0.1, 0.3\rangle\}$$

$$F(e_2, q, 1) = \{\langle u_3, 0.3, 0.4, 0.2\rangle\}$$

$$F(e_2, r, 1) = \{\langle u_2, 0.3, 0.4, 0.9\rangle\}$$

$$F(e_1, p, 0) = \{\langle u_2, 0.5, 0.2, 0.3\rangle\}$$

$$F(e_1, q, 0) = \{\langle u_1, 0.6, 0.3, 0.5\rangle\}$$

$$F(e_1, r, 0) = \{\langle u_2, 0.7, 0.6, 0.4\rangle, \langle u_3, 0.9, 0.5, 0.7\rangle\}$$

$$F(e_2, p, 0) = \{\langle u_3, 0.7, 0.9, 0.6\rangle\}$$

$$F(e_2, q, 0) = \{\langle u_1, 0.7, 0.3, 0.6\rangle, \langle u_2, 0.6, 0.2, 0.5\rangle\}$$

$$F(e_2, r, 0) = \{\langle u_1, 0.6, 0.2, 0.5\rangle, \langle u_3, 0.7, 0.2, 0.8\rangle\}$$

The neutrosophic soft expert set (F, Z) is a parameterized family $\{F(e_i), i = 1, 2, 3, \cdots\}$ of all neutrosophic sets of U and describes a collection of approximation of an object.

3.1. Definition: Let (F, A) and (G, B) be two neutrosophic soft expert sets over the common universe U. (F, A) is said to be neutrosophic soft expert subset of (G, B), if $A \tilde{\subseteq} B$ and $T_{F(e)}(x) \tilde{\leq} T_{G(e)}(x)$, $I_{F(e)}(x) \tilde{\leq} I_{G(e)}(x)$, $F_{F(e)}(x) \tilde{\geq} F_{G(e)}(x)$ $\forall e \in A$, $x \in U$. We denote it by $(F, A) \tilde{\subseteq} (G, B)$.

(F, A) is said to be neutrosophic soft expert superset of (G, B) if (G, B) is a neutrosophic soft expert subset of (F, A). We denote by $(F, A) \tilde{\supseteq} (G, B)$.

3.2. Example: Suppose that a company produced new types of its products and wishes to take the opinion of some experts about concerning these products. Let $U = \{u_1, u_2, u_3\}$ be a set of product, $E = \{e_1, e_2\}$ a set of decision parameters where $e_i(i = 1, 2)$ denotes the decision "easy to use", "quality" respectively and let $X = \{p, q, r\}$ be a set of experts. Suppose

$$A = \{(e_1, p, 1), (e_2, p, 0), (e_1, q, 1), (e_1, r, 0), (e_2, r, 1)\}$$

$$B = \{(e_1, p, 1), (e_2, p, 0), (e_1, q, 1)\}$$

Clearly $B \tilde{\subseteq} A$. Let (F, A) and (G, B) be defined as follows:

$$\begin{aligned}(F, A) = \{&[(e_1, p, 1), \langle u_1, 0.3, 0.5, 0.7\rangle, \langle u_2, 0.5, 0.2, 0.3\rangle], [(e_2, p, 0), \langle u_2, 0.2, 0.4, 0.7\rangle], \\ &[(e_1, q, 1), \langle u_1, 0.6, 0.3, 0.5\rangle, \langle u_2, 0.6, 0.2, 0.3\rangle], [(e_1, r, 0), \langle u_1, 0.2, 0.7, 0.3\rangle], \\ &[(e_2, r, 1), \langle u_2, 0.3, 0.4, 0.9\rangle, \langle u_3, 0.7, 0.2, 0.8\rangle]\}, \\ (G, B) = \{&[(e_1, p, 1), \langle u_1, 0.3, 0.5, 0.7\rangle, \langle u_2, 0.5, 0.2, 0.3\rangle], [(e_2, p, 0), \langle u_2, 0.2, 0.4, 0.7\rangle], \\ &[(e_1, q, 1), \langle u_1, 0.6, 0.3, 0.5\rangle, \langle u_2, 0.6, 0.2, 0.3\rangle]\}.\end{aligned}$$

Therefore

$$(F, A) \tilde{\supseteq} (G, B).$$

3.3. Definition: Equality of two neutrosophic soft expert sets. Two (NSES), (F, A) and (G, B) over the common universe U are said to be equal if (F, A) is neutrosophic soft expert subset of (G, B) and (G, B) is neutrosophic soft expert subset of (F, A).We denote it by

$$(F,A)=(G,B).$$

3.4. Definition: NOT set of set parameters. Let $E=\{e_1,e_2,\cdots,e_n\}$ be a set of parameters. The NOT set of E is denoted by $\neg E=\{\neg e_1,\neg e_2,\cdots,\neg e_n\}$ where $\neg e_i=$ not e_i, $\forall i$.

3.3. Example: Consider 3.2.example. Here $\neg E=\{\text{not easy to use, not quality}\}$.

3.5. Definition: Complement of a neutrosophic soft expert set. The complement of a neutrosophic soft expert set (F,A) denoted by $(F,A)^c$ and is defined as $(F,A)^c=(F^c,\neg \mathrm{A})$ where $F^c=\neg A\to P(U)$ is mapping given by $F^c(x)$ =neutrosophic soft expert complement with $T_{F^c(x)}=F_{F(x)}$, $I_{F^c(x)}=I_{F(x)}$, $F_{F^c(x)}=T_{F(x)}$.

3.4. Example: Consider the 3.1 Example. Then $(F,Z)^c$ describes the "not easy to use of the car" we have

$$\begin{aligned}(F,Z)^c=\{&(\neg e_1,p,1),[\langle u_2,0.3,0.2,0.5\rangle][(\neg e_1,q,1),\langle u_1,0.5,0.3,0.6\rangle],\\
&[(\neg e_1,r,1),\langle u_2,0.4,0.6,0.7\rangle,\langle u_3,0.7,0.5,0.9\rangle],\\
&[(\neg e_2,p,1),\langle u_3,0.6,0.9,0.7\rangle],\\
&[(\neg e_2,q,1),\langle u_1,0.6,0.3,0.7\rangle,\langle u_2,0.5,0.2,0.6\rangle],\\
&[(\neg e_2,r,1),\langle u_1,0.5,0.2,0.6\rangle,\langle u_3,0.8,0.2,0.7\rangle],\\
&[(\neg e_1,p,0),\langle u_1,0.7,0.5,0.3\rangle,\langle u_3,0.3,0.6,0.5\rangle],\\
&[(\neg e_1,q,0),\langle u_2,03,0.2,0.8\rangle,\langle u_3,0.9,0.5,0.7\rangle],\\
&[(\neg e_1,r,0),\langle u_1,0.6,0.7,0.4\rangle],\\
&[(\neg e_2,p,0),\langle u_1,0.3,0.2,0.4\rangle,\langle u_2,0.3,0.1,0.7\rangle],\\
&[(\neg e_2,q,0),\langle u_3,0.2,0.4,0.3\rangle],\\
&[(\neg e_2,r,0),\langle u_2,0.9,0.4,0.3\rangle]\}.\end{aligned}$$

3.6. Definition: Empty or null neutrosophic soft expert set with respect to parameter. A neutrosophic soft expert set (H,A) over the universe U is termed to be empty or null neutrosophic soft expert set with respect to the parameter A if

$$T_{H(e)}(m)=0,\quad F_{H(e)}(m)=0,\quad I_{H(e)}(m)=0,\quad \forall m\in U,\quad \forall e\in A.$$

In this case the null neutrosophic soft expert set (NNSES) is denoted by $\Phi_{\underset{A}{\vee}}$.

3.5. Example: Let $U=\{u_1,u_2,u_3\}$ the set of three cars be considered as universal set $E=\{\text{good}\}=\{e_1\}$ be the set of parameters that characterizes the car and let $X=\{p,q\}$ be a set of experts.

$$\begin{aligned}\Phi_{\underset{A}{\vee}}&=(\text{NNSES})\\
&=\{[(e_1,p,1),\langle u_1,0,0,0\rangle,\langle u_2,0,0,0\rangle],[(e_1,q,1),\langle u_1,0,0,0\rangle,\langle u_2,0,0,0\rangle],[(e_1,p,0),\langle u_3,0,0,0\rangle],\\
&\quad[(e_1,q,0),\langle u_3,0,0,0\rangle]\}.\end{aligned}$$

Here the (NNSES) (H,A) is the null neutrosophic soft expert sets.

3.7. Definition: An agree-neutrosophic soft expert set $(F,A)_1$ over U is a neutrosophic soft expert subset of (F,A) defined as follow

$$(F,A)_1=\{F_1(m): m\in E\times X\times\{1\}\}.$$

3.6. Example: Consider 3.1. Example. Then the agree-neutrosophic soft expert set $(F,A)_1$ over U is

$$\begin{aligned}(F,A)_1=\{&[(e_1,p,1),\langle u_1,0.3,0.5,0.7\rangle,\langle u_3,0.5,0.6,0.3\rangle],[(e_1,q,1),\langle u_2,0.8,0.2,0.3\rangle,\langle u_3,0.9,0.5,0.7\rangle],\\&[(e_1,r,1),\langle u_1,0.4,0.7,0.6\rangle],[(e_2,p,1),\langle u_1,0.4,0.2,0.3\rangle,\langle u_2,0.7,0.1,0.3\rangle],\\&[(e_2,q,1),\langle u_3,0.3,0.4,0.2\rangle],[(e_2,r,1),\langle u_2,0.3,0.4,0.9\rangle]\}.\end{aligned}$$

3.8. Definition: A disagree-neutrosophic soft expert set $(F,A)_0$ over U is a neutrosophic soft expert subset of (F,A) defined as follow

$$(F,A)_0=\{F_0(m):m\in E\times X\times\{0\}\}.$$

3.7. Example: Consider 3.1. Example. Then the disagree-neutrosophic soft expert set $(F,A)_0$ over U is

$$\begin{aligned}(F,A)_0=\{&[(e_1,p,0),\langle u_2,0.5,0.2,0.3\rangle],[(e_1,q,0),\langle u_1,0.6,0.3,0.5\rangle],\\&[(e_1,r,0),\langle u_2,0.7,0.6,0.4\rangle,\langle u_3,0.9,0.5,0.7\rangle],[(e_2,p,0),\langle u_3,0.7,0.9,0.6\rangle],\\&[(e_2,q,0),\langle u_1,0.7,0.3,0.6\rangle,\langle u_2,0.6,0.2,0.5\rangle],[(e_2,r,0),\langle u_1,0.6,0.2,0.5\rangle,\langle u_3,0.7,0.2,0.8\rangle]\}.\end{aligned}$$

3.9. Definition: Union of two neutrosophic soft expert sets.

Let (H,A) and (G,B) be two NSESs over the common universe U. Then the union of (H,A) and (G,B) is denoted by "$(H,A)\tilde{\cup}(G,B)$" and is defined by $(H,A)\tilde{\cup}(G,B)=(K,C)$, where $C=A\cup B$ and the truth-membership, indeterminacy-membership and falsity-membership of (K,C) are as follows:

$$T_{H(e)}(m)=\begin{cases}T_{H(e)}(m), & \text{if } e\in A-B,\\ T_{G(e)}(m), & \text{if } e\in B-A,\\ \max\left(T_{H(e)}(m),T_{G(e)}(m)\right), & \text{if } e\in A\cap B.\end{cases}$$

$$I_{K(e)}(m)=\begin{cases}I_{H(e)}(m), & \text{if } e\in A-B,\\ I_{G(e)}(m), & \text{if } e\in B-A,\\ \dfrac{\left(I_{H(e)}(m),I_{G(e)}(m)\right),}{2} & \text{if } e\in A\cap B.\end{cases}$$

$$F_{H(e)}(m)=\begin{cases}F_{H(e)}(m), & \text{if } e\in A-B,\\ F_{G(e)}(m), & \text{if } e\in B-A,\\ \min\left(F_{H(e)}(m),F_{G(e)}(m)\right), & \text{if } e\in A\cap B.\end{cases}$$

3.8. Example: Let (H,A) and (G,B) be two NSESs over the common universe U

$$(H,A)=\{[(e_1,p,1),\langle u_1,0.3,0.5,0.7\rangle,\langle u_3,0.5,0.6,0.2\rangle],[(e_1,q,1),\langle u_1,0.6,0.3,0.5\rangle,\langle u_2,0.8,0.2,0.3\rangle]\},$$

$$(G,B)=\{(e_1,p,1),\langle u_1,0.4,0.6,0.2\rangle,\langle u_2,0.7,0.5,0.8\rangle\}.$$

Therefore $(H,A)\tilde{\cup}(G,B)=(K,C)$

$$\begin{aligned}(K,C)=\{&[(e_1,p,1),\langle u_1,0.4,0.55,0.2\rangle,\langle u_2,0.7,0.5,0.8\rangle,\langle u_3,0.5,0.6,0.2\rangle],\\&[(e_1,q,1),\langle u_1,0.6,0.3,0.5\rangle,\langle u_2,0.8,0.2,0.3\rangle]\}.\end{aligned}$$

3.10. Definition: Intersection of two neutrosophic soft expert sets. Let (H,A) and (G,B) be two NSESs over the common universe *U*. Then the intersection of (H,A) and (G,B) is denoted by "$(H,A)\tilde{\cap}(G,B)$" and is defined by $(H,A)\tilde{\cap}(G,B)=(K,C)$, where $C=A\cap B$ and the truth-membership, indeterminacy-membership and falsity-membership of (K,C) are as follows:

$$T_{H(e)}(m)=\min\left(T_{H(e)}(m),T_{G(e)}(m)\right),$$

$$I_{K(e)}(m)=\frac{I_{H(e)}(m)+I_{G(e)}(m)}{2},$$

$$F_{H(e)}(m)=\max\left(F_{H(e)}(m),F_{G(e)}(m)\right),\quad \text{if } e\in A\cap B.$$

3.9. Example: Let (H,A) and (G,B) be two NSESs over the common universe *U*

$$(H,A)=\left\{\left[(e_1,p,1),\langle u_1,0.3,0.5,0.7\rangle,\langle u_3,0.5,0.6,0.2\rangle\right],\left[(e_1,q,1),\langle u_1,0.6,0.3,0.5\rangle,\langle u_2,0.8,0.2,0.3\rangle\right]\right\},$$

$$(G,B)=\left\{(e_1,p,1),\langle u_1,0.4,0.6,0.2\rangle,\langle u_2,0.7,0.5,0.8\rangle\right\}.$$

Therefore $(H,A)\tilde{\cap}(G,B)=(K,C)$

$$(K,C)=\left\{(e_1,p,1),\langle u_1,0.3,0.55,0.7\rangle\right\}.$$

3.1. Proposition: If (H,A) and (G,B) are neutrosophic soft expert sets over *U*. Then

1) $(H,A)\tilde{\cup}(G,B)=(G,B)\tilde{\cup}(H,A)$
2) $(H,A)\tilde{\cap}(G,B)=(G,B)\tilde{\cap}(H,A)$
3) $\left((H,A)^c\right)^c=(H,A)$
4) $(H,A)\tilde{\cup}\Phi=(H,A)$
5) $(H,A)\tilde{\cap}\Phi=\Phi$

Proof: 1) We want to prove that $(H,A)\tilde{\cup}(G,B)=(G,B)\tilde{\cup}(H,A)$ by using 3.9 definition and we consider the case when if $e\in A\cap B$ as the other cases are trivial, then we have

$$\begin{aligned}(H,A)\tilde{\cup}(G,B)&=\left\{\left\langle u,\max\left(T_{H(e)}(m),T_{G(e)}(m)\right),\frac{I_{H(e)}(m)+I_{G(e)}(m)}{2},\min\left(F_{H(e)}(m),F_{G(e)}(m)\right)\right\rangle:u\in U\right\}\\&=\left\{\left\langle u,\max\left(T_{G(e)}(m),T_{H(e)}(m)\right),\frac{I_{G(e)}(m)+I_{H(e)}(m)}{2},\min\left(F_{G(e)}(m),F_{H(e)}(m)\right)\right\rangle:u\in U\right\}\\&=(G,B)\tilde{\cup}(H,A).\end{aligned}$$

The proof of the propositions 2) to 5) are obvious.

3.2. Proposition: If (H,A), (G,B) and (K,D) are three neutrosophic soft expert sets over *U*. Then

1) $\left((H,A)\tilde{\cup}(G,B)\right)\tilde{\cup}(M,D)=(H,A)\tilde{\cup}\left((G,B)\tilde{\cup}(M,D)\right)$
2) $\left((H,A)\tilde{\cap}(G,B)\right)\tilde{\cap}(M,D)=(H,A)\tilde{\cap}\left((G,B)\tilde{\cap}(M,D)\right)$

Proof: 1) We want to prove that $\left((H,A)\tilde{\cup}(G,B)\right)\tilde{\cup}(M,D)=(H,A)\tilde{\cup}\left((G,B)\tilde{\cup}(M,D)\right)$ by using 3.9 definition and we consider the case when if $e\in A\cap B$ as the other cases are trivial, then we have

$$(H,A)\tilde{\cup}(G,B)=\left\{\left\langle u,\max\left(T_{H(e)}(m),T_{G(e)}(m)\right),\frac{I_{H(e)}(m)+I_{G(e)}(m)}{2},\min\left(F_{H(e)}(m),F_{G(e)}(m)\right)\right\rangle:u\in U\right\}$$

We also consider her the case when $e\in D$ as the other cases are trivial, then we have

$$\left((H,A)\tilde{\cup}(G,B)\right)\tilde{\cup}(M,D)$$

$$=\left\{\left(\left\langle u,\max\left(T_{H(e)}(m),T_{G(e)}(m)\right),\frac{I_{H(e)}(m)+I_{G(e)}(m)}{2},\min\left(F_{H(e)}(m),F_{G(e)}(m)\right)\right\rangle\right),\right.$$

$$\left.\left(T_{M(e)}(m),I_{M(e)}(m),F_{M(e)}(m)\right):u\in U\right\}$$

$$=\left\{\left(T_{H(e)}(m),I_{H(e)}(m),F_{H(e)}(m)\right),\right.$$

$$\left.\left(\left\langle u,\max\left(T_{G(e)}(m),T_{M(e)}(m)\right),\frac{I_{G(e)}(m)+I_{M(e)}(m)}{2},\min\left(F_{G(e)}(m),F_{M(e)}(m)\right)\right\rangle\right),:u\in U\right\}$$

$$=(H,A)\tilde{\cup}\left((G,B)\tilde{\cup}(M,D)\right).$$

2) The proof is straightforward.

3.3. Proposition: If (H,A), (G,B) and (M,D) are three neutrosophic soft expert sets over *U*. Then

1) $\left((H,A)\tilde{\cup}(G,B)\right)\tilde{\cap}(M,D)=\left((H,A)\tilde{\cap}(M,D)\right)\tilde{\cup}\left((G,B)\tilde{\cap}(M,D)\right)$

2) $\left((H,A)\tilde{\cap}(G,B)\right)\tilde{\cup}(M,D)=\left((H,A)\tilde{\cup}(M,D)\right)\tilde{\cap}\left((G,B)\tilde{\cup}(M,D)\right)$

Proof: We use the same method as in the previous proof.

3.11. Definition: AND operation on two neutrosophic soft expert sets. Let (H,A) and (G,B) be two NSESs over the common universe *U*. Then "AND" operation on them is denoted by "$(H,A)\tilde{\wedge}(G,B)$" and is defined by $(H,A)\tilde{\wedge}(G,B)=(K,A\times B)$ where the truth-membership, indeterminacy-membership and falsity-membership of $(K,A\times B)$ are as follows:

$$T_{H(\alpha,\beta)}(m)=\min\left(T_{H(\alpha)}(m),T_{G(\beta)}(m)\right),$$

$$I_{K(\alpha,\beta)}(m)=\frac{I_{H(\alpha)}(m)+I_{G(\beta)}(m)}{2},$$

$$F_{H(\alpha,\beta)}(m)=\max\left(F_{H(\alpha)}(m),F_{G(\beta)}(m)\right),\quad \text{if } \forall\alpha\in A,\ \forall\beta\in B.$$

3.10. Example: Let (H,A) and (G,B) be two NSESs over the common universe *U*. Then (H,A) and (G,B) is a follows:

$$(H,A)=\left\{\left[(e_1,p,1),\langle u_1,0.3,0.5,0.7\rangle,\langle u_3,0.5,0.6,0.2\rangle\right],\left[(e_1,q,1),\langle u_1,0.6,0.3,0.5\rangle,\langle u_2,0.8,0.2,0.3\rangle\right]\right\},$$

$$(G,B)=\left\{(e_1,p,1),\langle u_1,0.4,0.6,0.2\rangle,\langle u_2,0.7,0.5,0.8\rangle\right\}.$$

Therefore $(H,A)\tilde{\wedge}(G,B)=(K,A\times B)$

$$(K,A\times B)=\left\{\left[(e_1,p,1),(e_1,p,1)\langle u_1,0.3,0.55,0.7\rangle,\langle u_2,0.7,0.5,0.8\rangle,\langle u_3,0.5,0.6,0.2\rangle\right],\right.$$

$$\left.\left[(e_1,q,1),(e_1,p,1)\langle u_1,0.4,0.45,0.5\rangle,\langle u_2,0.7,0.35,0.8\rangle\right]\right\},$$

3.12. Definition: OR operation on two neutrosophic soft expert sets. Let (H,A) and (G,B) be two NSESs over the common universe *U*. Then "OR" operation on them is denoted by "$(H,A)\tilde{\vee}(G,B)$" and is defined by $(H,A)\tilde{\vee}(G,B)=(O,A\times B)$ where the truth-membership, indeterminacy-membership and falsity-membership of $(O,A\times B)$ are as follows:

$$T_{O(\alpha,\beta)}(m) = \max\left(T_{H(\alpha)}(m), T_{G(\beta)}(m)\right),$$
$$I_{O(\alpha,\beta)}(m) = \frac{I_{H(\alpha)}(m) + I_{G(\beta)}(m)}{2},$$
$$F_{O(\alpha,\beta)}(m) = \min\left(F_{H(\alpha)}(m), F_{G(\beta)}(m)\right), \quad \text{if} \quad \forall\alpha \in A,\ \forall\beta \in B.$$

3.11. Example: Let (H,A) and (G,B) be two NSESs over the common universe U. Then (H,A) OR (G,B) is a follows:

$$(H,A) = \left\{\left[(e_1,p,1),\langle u_1,0.3,0.5,0.7\rangle,\langle u_3,0.5,0.6,0.2\rangle\right],\left[(e_1,q,1),\langle u_1,0.6,0.3,0.5\rangle\langle u_2,0.8,0.2,0.3\rangle\right]\right\},$$
$$(G,B) = \left\{(e_1,p,1),\langle u_1,0.4,0.6,0.2\rangle,\langle u_2,0.7,0.5,0.8\rangle\right\}.$$

Therefore $(H,A)\tilde{\vee}(G,B) = (O, A\times B)$

$$(O,A\times B) = \left\{\left[(e_1,p,1),(e_1,p,1)\langle u_1,0.4,0.55,0.2\rangle,\langle u_2,0.8,0.2,0.3\rangle,\langle u_3,0.5,0.6,0.2\rangle\right],\right.$$
$$\left.\left[(e_1,q,1),(e_1,p,1)\langle u_1,0.6,0.45,0.2\rangle,\langle u_2,0.8,0.35,0.2\rangle,\langle u_3,0.5,0.6,0.2\rangle\right]\right\}.$$

3.4. Proposition: If (H,A) and (G,B) are neutrosophic soft expert sets over U. Then

1) $\left((H,A)\tilde{\wedge}(G,B)\right)^c = (H,A)^c\,\tilde{\vee}\,(G,B)^c$

2) $\left((H,A)\tilde{\vee}(G,B)\right)^c = (H,A)^c\,\tilde{\wedge}\,(G,B)^c$

Proof: 1) Let $(H,A) = \left\{\left\langle u, T_{H(x)}(m), I_{H(x)}(m), F_{H(x)}(m)\right\rangle : u \in U\right\}$ and

$$(G,B) = \left\{\left\langle u, T_{G(x)}(m), I_{G(x)}(m), F_{G(x)}(m)\right\rangle : u \in U\right\}$$

be two NSESs over the common universe U. Also let $(H,A)\tilde{\wedge}(G,B) = (K, A\times B)$, where

$$(K,A\times B) = \left\{\left\langle u, \min\left(T_{H(\alpha)}(m), T_{G(\beta)}(m)\right), \frac{I_{H(\alpha)}(m) + I_{G(\beta)}(m)}{2}, \max\left(F_{H(\alpha)}(m), F_{G(\beta)}(m)\right)\right\rangle : u \in U\right\}$$

Therefore

$$\left((H,A)\tilde{\wedge}(G,B)\right)^c = (K,A\times B)^c$$
$$= \left\{\left\langle u, \max\left(F_{H(\alpha)}(m), F_{G(\beta)}(m)\right), \frac{I_{H(\alpha)}(m) + I_{G(\beta)}(m)}{2}, \min\left(T_{H(\alpha)}(m), T_{G(\beta)}(m)\right)\right\rangle : u \in U\right\},$$

Again

$$(H,A)^c\,\tilde{\vee}\,(G,B)^c$$
$$= \left\{\left\langle u, \max\left(F_{H^c(\alpha)}(m), F_{G^c(\beta)}(m)\right), \frac{I_{H^c(\alpha)}(m) + I_{G^c(\beta)}(m)}{2}, \min\left(T_{H^c(\alpha)}(m), T_{G^c(\beta)}(m)\right)\right\rangle : u \in U\right\}$$
$$= \left\{\left\langle u, \min\left(T_{H(\alpha)}(m), T_{G(\beta)}(m)\right), \frac{I_{H(\alpha)}(m) + I_{G(\beta)}(m)}{2}, \max\left(F_{H(\alpha)}(m), F_{G(\beta)}(m)\right)\right\rangle : u \in U\right\}^c$$
$$= \left\{\left\langle u, \max\left(F_{H(\alpha)}(m), F_{G(\beta)}(m)\right), \frac{I_{H(\alpha)}(m) + I_{G(\beta)}(m)}{2}, \min\left(T_{H(\alpha)}(m), T_{G(\beta)}(m)\right)\right\rangle : u \in U\right\}.$$

Hence the result is proved.

3.5. Proposition: If (H,A), (G,B) and (M,D) are three neutrosophic soft expert sets over *U*. Then

1) $((H,A)\tilde{\vee}(G,B))\tilde{\vee}(M,D)=(H,A)\tilde{\vee}((G,B)\tilde{\vee}(M,D))$

2) $((H,A)\tilde{\wedge}(G,B))\tilde{\wedge}(M,D)=(H,A)\tilde{\wedge}((G,B)\tilde{\wedge}(M,D))$

3) $((H,A)\tilde{\vee}(G,B))\tilde{\wedge}(M,D)=((H,A)\tilde{\wedge}(M,D))\tilde{\vee}((G,B)\tilde{\wedge}(M,D))$

4) $((H,A)\tilde{\wedge}(G,B))\tilde{\vee}(M,D)=((H,A)\tilde{\vee}(M,D))\tilde{\wedge}((G,B)\tilde{\vee}(M,D))$

Proof: We use the same method as in the previous proof.

4. An Application of Neutrosophic Soft Expert Set

In this section, we present an application of neutrosophic soft expert set theory in a decision-making problem. The problem we consider is as below:

Suppose that a hospital to buy abed. Seven alternatives are as follows:

$$U=\{u_1,u_2,u_3,u_4,u_5,u_6,u_7\},$$

suppose there are five parameters $E=\{e_1,e_2,e_3,e_4,e_5\}$ where the parameters $e_i\ (i=1,2,3,4,5)$ stand for "medical bed", "soft bed", "orthopedic bed", "moving bed", "air bed", respectively. Let $X=\{p,q,r\}$ be a set of experts. Suppose:

$$\begin{aligned}(F,Z)=\{&((e_1,p,1),\{u_1,u_3,u_6\}),((e_1,q,1),\{u_1,u_3,u_4,u_7\}),\\
&((e_1,r,1),\{u_1,u_2,u_4,u_5,u_7\}),((e_2,p,1),\{u_3,u_5,u_6,u_7\}),\\
&((e_2,q,1),\{u_1,u_3,u_4,u_6\}),((e_2,r,1),\{u_1,u_3,u_4,u_5\}),\\
&((e_3,p,1),\{u_1,u_2,u_6,u_7\}),((e_3,q,1),\{u_1,u_2,u_4,u_5,u_7\}),\\
&((e_3,r,1),\{u_1,u_2,u_3,u_4,u_6,u_7\}),((e_4,p,1),\{u_1,u_2,u_5,u_6\}),\\
&((e_4,q,1),\{u_2,u_3,u_4,u_6,u_7\}),((e_4,r,1),\{u_1,u_2,u_3,u_5,u_6\}),\\
&((e_5,p,1),\{u_1,u_3,u_4,u_5,u_6,u_7\}),((e_5,q,1),\{u_3,u_4,u_5\}),\\
&((e_5,r,1),\{u_1,u_3,u_4,u_7\}),((e_1,p,0),\{u_2,u_4,u_5,u_7\}),\\
&((e_1,q,0),\{u_2,u_5,u_6\}),((e_1,r,0),\{u_3,u_6\}),\\
&((e_2,p,0),\{u_1,u_2,u_4\}),((e_2,q,0),\{u_2,u_5,u_7\}),\\
&((e_2,r,0),\{u_2,u_6,u_7\}),((e_3,p,0),\{u_3,u_4,u_5\}),((e_3,q,0),\{u_3,u_6\}),\\
&((e_3,r,0),\{u_5\}),((e_4,p,0),\{u_3,u_4,u_7\}),\\
&((e_4,q,0),\{u_1,u_5\}),((e_4,r,0),\{u_4,u_7\}),((e_5,p,0),\{u_2\}),\\
&((e_5,q,0),\{u_1,u_2,u_6,u_7\}),((e_5,r,0),\{u_2,u_5,u_6\})\}.\end{aligned}$$

In **Table 1** and **Table 2** we present the agree-neutrosophic soft expert set and disagree-neutrosophic soft expert set, respectively, such that if $u_{ij}\in F_1(\varepsilon)$ then $u_{ij}=1$ otherwise $u_{ij}=0$, and if $u_{ij}\in F_0(\varepsilon)$ then $u_{ij}=1$ otherwise $u_{ij}=0$ where u_{ij} are the entries in **Table 1** and **Table 2**.

The following algorithm may be followed by the hospital wants to buy a bed.

1) input the neutrosophic soft expert set (F,Z),

2) find an agree-neutrosophic soft expert set and a disagree-soft expert set,

3) find $c_j=\sum_i u_{ij}$ for agree-neutrosophic soft expert set,

4) find $k_j=\sum_i u_{ij}$ for disagree-neutrosophic soft expert set,

5) find $s_j=c_j-k_j$,

6) find *m*, for which $s_m=\max s_j$.

Table 1. Agree-neutrosophic soft expert set.

U	u_1	u_2	u_3	u_4	u_5	u_6	u_7
(e_1, p)	1	0	1	0	0	1	0
(e_2, p)	0	0	1	0	1	1	1
(e_3, p)	1	1	0	0	0	1	1
(e_4, p)	1	1	0	0	1	1	0
(e_5, p)	1	0	1	1	1	1	1
(e_1, q)	1	0	1	1	0	0	1
(e_2, q)	1	0	1	1	0	1	0
(e_3, q)	1	1	0	1	1	0	1
(e_4, q)	0	1	1	1	0	1	1
(e_5, q)	0	0	1	1	1	0	0
(e_1, r)	1	1	0	1	1	0	1
(e_2, r)	1	0	1	1	1	0	0
(e_3, r)	1	1	1	1	0	1	1
(e_4, r)	1	1	1	0	1	1	0
(e_5, r)	1	0	1	1	0	0	1
$c_j = \sum_i u_{ij}$	$c_1 = 12$	$c_2 = 7$	$c_3 = 11$	$c_4 = 10$	$c_5 = 7$	$c_6 = 9$	$c_7 = 9$

Table 2. Disagree-neutrosophic soft expert set.

U	u_1	u_2	u_3	u_4	u_5	u_6	u_7
(e_1, p)	0	1	0	1	1	0	1
(e_2, p)	1	1	0	1	0	0	0
(e_3, p)	0	0	1	1	1	0	0
(e_4, p)	0	0	1	1	0	0	1
(e_5, p)	0	1	0	0	0	0	0
(e_1, q)	0	1	0	0	1	1	0
(e_2, q)	0	1	0	0	1	0	1
(e_3, q)	0	0	1	0	0	1	0
(e_4, q)	1	0	0	0	1	0	0
(e_5, q)	1	1	0	0	0	1	1
(e_1, r)	0	0	1	0	0	1	0
(e_2, r)	0	1	0	0	0	1	1
(e_3, r)	0	0	0	0	1	0	0
(e_4, r)	0	0	0	1	0	0	1
(e_5, r)	0	1	0	0	1	1	0
$k_j = \sum_i u_{ij}$	$k_1 = 3$	$k_2 = 8$	$k_3 = 4$	$k_4 = 5$	$k_5 = 7$	$k_6 = 6$	$k_7 = 6$

Table 3. $s_j = c_j - k_j$.

$c_j = \sum_i u_{ij}$	$k_j = \sum_i u_{ij}$	$s_j = c_j - k_j$
$c_1 = 12$	$k_1 = 3$	$s_1 = 9$
$c_2 = 7$	$k_2 = 8$	$s_2 = -1$
$c_3 = 11$	$k_3 = 4$	$s_3 = 7$
$c_4 = 10$	$k_4 = 5$	$s_4 = 5$
$c_5 = 7$	$k_5 = 7$	$s_5 = 0$
$c_6 = 9$	$k_6 = 6$	$s_6 = 3$
$c_7 = 9$	$k_7 = 6$	$s_7 = 3$

Then s_m is the optimal choice object. If m has more than one value, then any one of them could be chosen by hospital using its option. Now we use this algorithm to find the best choices for to get to the hospital bed. From **Table 1** and **Table 2** we have **Table 3**.

Then $\max s_j = s_1$, so the hospital will select the bed u_1. In any case if they do not want to choose u_1 due to some reasons they second choice will be u_3.

5. Conclusion

In this paper, we have introduced the concept of neutrosophic soft expert set which is more effective and useful and studied some of its properties. Also the basic operations on neutrosophic soft expert set namely complement, union, intersection, AND and OR have been defined. Finally, we have presented an application of NSES in a decision-making problem.

References

[1] Atanassov, K. (1986) Intuitionistic Fuzzy Sets. *Fuzzy Sets and Systems*, **20**, 87-96. http://dx.doi.org/10.1016/S0165-0114(86)80034-3

[2] Smarandache, F. (2005) Neutrosophic Set, a Generalization of the Intuitionistic Fuzzy Sets. *International Journal of Pure and Applied Mathematics*, **24**, 287-297.

[3] Smarandache, F. (1998) A Unifying Field in Logics. Neutrosophy: Neutrosophic Probability, Set and Logic. American Research Press, Rehoboth.

[4] Molodtsov, D.A. (1999) Soft Set Theory-First Results. *Computers and Mathematics with Applications*, **37**, 19-31. http://dx.doi.org/10.1016/S0898-1221(99)00056-5

[5] Chen, D., Tsang, E.C.C., Yeung, D.S. and Wang, X. (2005) The Parameterization Reduction of Soft Sets and Its Application. *Computers and Mathematics with Applications*, **49**, 757-763. http://dx.doi.org/10.1016/j.camwa.2004.10.036

[6] Maji, P.K., Roy, A.R. and Biswas, R. (2003) Soft Set Theory. *Computers and Mathematics with Applications*, **45**, 555-562. http://dx.doi.org/10.1016/S0898-1221(03)00016-6

[7] Maji, P.K. (2013) Neutrosophic Soft Set. *Computers and Mathematics with Applications*, **45**, 555-562. http://dx.doi.org/10.1016/S0898-1221(03)00016-6

[8] Alkhazaleh, S., Salleh, A.R. and Hassan, N. (2011) Possibility Fuzzy Soft Set. *Advances in Decision Sciences*, **2011**, Article ID: 479756. http://dx.doi.org/10.1155/2011/479756

[9] Alkhazaleh, S., Salleh, A.R. and Hassan, N. (2011) Fuzzy Parameterized Interval-Valued Fuzzy Soft Set. *Applied Mathematical Sciences*, **5**, 3335-3346.

[10] Alkhazaleh, S. and Salleh, A.R. (2011) Soft Expert Sets. *Advances in Decision Sciences*, **2011**, Article ID: 757868. http://dx.doi.org/10.1155/2011/757868

[11] Alkhazaleh, S. and Salleh, A.R. (2014) Fuzzy Soft Expert Set and Its Application. *Applied Mathematics*, **5**, 1349-1368. http://dx.doi.org/10.4236/am.2014.59127

Applied Mathematics, 2015, 6, 128-135
Published Online January 2015 in SciRes. http://www.scirp.org/journal/am
http://dx.doi.org/10.4236/am.2015.61013

Evaluation of Kinetic Properties of Dendritic Potassium Current in Ghostbursting Model of Electrosensory Neurons

Takaaki Shirahata

Kagawa School of Pharmaceutical Sciences, Tokushima Bunri University, Sanuki, Japan
Email: tshi@kph.bunri-u.ac.jp

Received 25 October 2014; revised 20 November 2014; accepted 10 December 2014

Abstract

A ghostbursting model is a mathematical model (a system of coupled nonlinear ordinary differential equations) that is based on the Hodgkin-Huxley formalism. The ghostbursting model describes bursting similar to the *in vitro* bursting of electrosensory neurons of weakly electric fish. Doiron and coworkers have focused on two system parameters of the model: maximal conductance of the dendritic potassium current $(g_{Dr,d})$ and the current injected into the somatic compartment (I_s). They performed bifurcation analysis and revealed that the $(g_{Dr,d}, I_s)$-parameter space was divided into three dynamical states: quiescence, periodic tonic spiking, and bursting. The present study focused on a third system parameter: the time constant of dendritic potassium current inactivation (τ_{pd}). A computer simulation of the model revealed how the dynamical states of the $(g_{Dr,d}, I_s)$-parameter space changed in response to variations of τ_{pd}.

Keywords

Mathematical Model, Bifurcation, Ghostbursting, Time Constant

1. Introduction

Hodgkin and Huxley [1] proposed a mathematical model that is composed of a system of four-coupled nonlinear ordinary differential equations (page 518 in [1]) and that describes the action potential regeneration of the squid giant axon and the biophysical mechanisms underlying the action potential generation. Various types of mathematical models describing the electrical excitability of neurons and endocrine cells have been developed on the

How to cite this paper: Shirahata, T. (2015) Evaluation of Kinetic Properties of Dendritic Potassium Current in Ghostbursting Model of Electrosensory Neurons. *Applied Mathematics*, **6**, 128-135. http://dx.doi.org/10.4236/am.2015.61013

basis of the concepts proposed by Hodgkin and Huxley [1], and analyses of these models, including the RPeD1 neuron model in [2], various bursting models in Chapter 5 of [3], and pituitary lactotroph bursting model in [4], are important research areas in the field of applied mathematics. The concepts proposed by Hodgkin and Huxley [1] are also important in the fields of theoretical physics [5] and mathematical physics [6]. The Hodgkin-Huxley model is also used in drug-disease modeling (see Chapter 5.2.2 in [7]).

A ghostbursting model [8], which is a mathematical model based on the concepts proposed by Hodgkin and Huxley [1], describes a system of six-coupled nonlinear ordinary differential equations [see Equations (1) to (6) in Section 2]. This model exhibits bursting similar to that observed in *in vitro* recordings of pyramidal cells in the electrosensory lateral line lobe (ELL) of the weakly electric fish *Apteronotus leptorhynchus*. This model consists of two compartments: the somatic compartment [see Equations (1) and (2) in Section 2] and the dendritic compartment [see Equations (3) to (6) in Section 2]. Doiron *et al*. have focused on two system parameters of the model: maximal conductance of the delayed-rectifying potassium current in the dendritic compartment $\left(g_{Dr,d}\right)$ [see Equation (3)] and the current injected into the somatic compartment $\left(I_s\right)$ [see Equation (1)]. They performed $\left(g_{Dr,d}, I_s\right)$-parameter bifurcation analysis of the model (see Figure 6 in [8]). This figure indicates that the organizing center of the $\left(g_{Dr,d}, I_s\right)$-parameter bifurcation diagram is a codimension-two bifurcation point and that unfolding the codimension-two bifurcation point yields two types of bifurcation manifolds: a curve for a saddle-node bifurcation of fixed points (SNFP curve) and a curve for a saddle-node bifurcation of limit cycles (SNLC curve). The SNFP and SNLC curves divide the $\left(g_{Dr,d}, I_s\right)$-parameter space into three dynamical states: quiescence, periodic tonic spiking, and bursting. When crossing the SNFP curve with an increase in I_s under a condition in which $g_{Dr,d}$ is fixed to a certain value smaller than the $g_{Dr,d}$ value at the codimension-two bifurcation point, the dynamical state changes from quiescence to bursting. When crossing the SNFP curve with an increase in I_s under a condition in which $g_{Dr,d}$ is fixed to a certain value larger than the $g_{Dr,d}$ value at the codimension-two bifurcation point, the dynamical state changes from quiescence to periodic tonic spiking. The periodic tonic spiking further changes into bursting when the SNLC curve is crossed with an increase in I_s. In addition, various bursting patterns are shown in Figure 13 in [8] and Figure 3 in [9].

Vo *et al*. have indicated that it is important to investigate the kinetic properties of ionic conductance for understanding the dynamics of pituitary cell models [10]. In other words, variations in the time constant values of ionic conductance can change the dynamical states of the cell model (Figure 4 in [10]). Doiron *et al*. have also suggested that the appropriate setting of the time constant value in dendritic potassium current inactivation is important for bursting dynamics (see the last paragraph of Section 3.3 in [8]). However, how variations in the time constant values affect the $\left(g_{Dr,d}, I_s\right)$-parameter space was not revealed in their study. Therefore, to contribute to an in-depth understanding of the kinetic properties of dendritic potassium current inactivation, in the present study, we performed numerical analysis and clarified the influence of time constant variations on the $\left(g_{Dr,d}, I_s\right)$-parameter space.

2. Materials and Methods

The ghostbursting model [Equations (1)-(6)] contains the following six state variables: the somatic membrane potential $\left[V_s\left(\text{mV}\right)\right]$, activating variable of the somatic delayed-rectifying potassium current $\left(n_s\right)$, dendritic membrane potential $\left[V_d\left(\text{mV}\right)\right]$, inactivating variable of the dendritic sodium current $\left(h_d\right)$, activating variable of the dendritic delayed-rectifying potassium current $\left(n_d\right)$, and inactivating variable of the dendritic delayed-rectifying potassium current $\left(p_d\right)$. The time evolution of these variables is described with the following equations:

$$C_m \frac{\mathrm{d}V_s}{\mathrm{d}t} = I_s - g_{Na,s}\left(\frac{1}{1+\mathrm{e}^{-(V_s-V_{ms})/k_{ms}}}\right)^2\left(1-n_s\right)\left(V_s-E_{Na}\right) - g_{Dr,s}n_s^2\left(V_s-E_K\right) - g_L\left(V_s-E_L\right) - \frac{g_c}{\kappa}\left(V_s-V_d\right) \quad (1)$$

$$\frac{\mathrm{d}n_s}{\mathrm{d}t} = \frac{1}{\tau_{ns}}\left(\frac{1}{1+\mathrm{e}^{-(V_s-V_{ns})/k_{ns}}} - n_s\right) \quad (2)$$

$$C_m \frac{\mathrm{d}V_d}{\mathrm{d}t} = -g_{Na,d}\left(\frac{1}{1+\mathrm{e}^{-(V_d-V_{md})/k_{md}}}\right)^2 h_d\left(V_d-E_{Na}\right) - g_{Dr,d}n_d^2 p_d\left(V_d-E_K\right) - g_L\left(V_d-E_L\right) - \frac{g_c}{1-\kappa}\left(V_d-V_s\right) \quad (3)$$

$$\frac{\mathrm{d}h_d}{\mathrm{d}t} = \frac{1}{\tau_{hd}}\left(\frac{1}{1+\mathrm{e}^{-(V_d - V_{hd})/k_{hd}}} - h_d\right) \tag{4}$$

$$\frac{\mathrm{d}n_d}{\mathrm{d}t} = \frac{1}{\tau_{nd}}\left(\frac{1}{1+\mathrm{e}^{-(V_d - V_{nd})/k_{nd}}} - n_d\right) \tag{5}$$

$$\frac{\mathrm{d}p_d}{\mathrm{d}t} = \frac{1}{\tau_{pd}}\left(\frac{1}{1+\mathrm{e}^{-(V_d - V_{pd})/k_{pd}}} - p_d\right) \tag{6}$$

where the definitions and values of the above-mentioned parameters are listed in **Table 1**. Equation (1) indicates that the time evolution of the somatic membrane potential (V_s) is regulated by the fast inward sodium current

Table 1. Values of the parameters in Equations (1)-(6) from [8].

Parameter	Value	Unit	Definition
C_m	1	μF/cm^2	Membrane capacitance
I_s	5.6 - 6.6	mA/cm^2	Current injected into somatic compartment
$g_{Na,s}$	55	mS/cm^2	Maximal conductance of the somatic sodium current
$g_{Dr,s}$	20	mS/cm^2	Maximal conductance of the somatic potassium current
$g_{Na,d}$	5	mS/cm^2	Maximal conductance of the dendritic sodium current
$g_{Dr,d}$	11.2 - 14.0	mS/cm^2	Maximal conductance of the dendritic potassium current
g_L	0.18	mS/cm^2	Leak conductance
g_c	1	mS/cm^2	Coupling coefficient
κ	0.4		Ratio of the somatic-to-total surface area
E_{Na}	40	mV	Reversal potential for the sodium ion
E_K	−88.5	mV	Reversal potential for the potassium ion
E_L	−70	mV	Reversal potential of the leak current
V_{ms}	−40	mV	Voltage at the midpoint of the steady-state function of the somatic sodium current activating variable
k_{ms}	3	mV	Slope factor of the steady-state function of the somatic sodium current activating variable
V_{md}	−40	mV	Voltage at the midpoint of the steady-state function of the dendritic sodium current activating variable
k_{md}	5	mV	Slope factor of the steady-state function of the dendritic sodium current activating variable
V_{ns}	−40	mV	Voltage at the midpoint of the steady-state function of n_s
k_{ns}	3	mV	Slope factor of the steady-state function of n_s
V_{hd}	−52	mV	Voltage at the midpoint of the steady-state function of h_d
k_{hd}	−5	mV	Slope factor of the steady-state function of h_d
V_{nd}	−40	mV	Voltage at the midpoint of the steady-state function of n_d
k_{nd}	5	mV	Slope factor of the steady-state function of n_d
V_{pd}	−65	mV	Voltage at the midpoint of the steady-state function of p_d
k_{pd}	−6	mV	Slope factor of the steady-state function of p_d
τ_{ns}	0.39	ms	Time constant of n_s
τ_{hd}	1	ms	Time constant of h_d
τ_{nd}	0.9	ms	Time constant of n_d
τ_{pd}	4.2, 5.0, 5.8	ms	Time constant of p_d

(the 2nd term), outward delayed-rectifying potassium current (the 3rd term), leak current (the 4th term), and electrotonic diffusive current between the somatic and dendritic compartments (the 5th term). Similarly, Equation (3) indicates that the time evolution of the dendritic membrane potential (V_d) is regulated by the fast inward sodium current (the 1st term), outward delayed-rectifying potassium current (the 2nd term), leak current (the 3rd term), and electrotonic diffusive current between the somatic and dendritic compartments (the 4th term). Equations (2), (4), (5), and (6) indicate that the activating or inactivating variables approach the steady-state function $\frac{1}{1+\mathrm{e}^{-(V_x-V_y)/k_y}}$ $(x = s, d.y = ns, hd, nd, pd.)$ at a rate that depends on the time constant τ_y $(y = ns, hd, nd, pd.)$. For detailed explanations of the model, see [8].

The free and open source software Scilab (http://www.scilab.org/) was used to numerically solve equations (1)-(6) under the following initial conditions: $V_s = -70$ mV, $n_s = 0.00005$, $V_d = -70$ mV, $h_d = 0.973$, $n_d = 0.002$, and $p_d = 0.697$. The response of the model to various $(g_{Dr,d}, I_s)$ values was investigated under different values of τ_{pd}. The total simulation time was 1.2 s, and the constant depolarizing current pulse (I_s) was injected between 0.1 s and 1.1 s. Otherwise, the injected current was zero.

3. Results

3.1. Reproduction of Previous Results

The ghostbursting model can show the three dynamical states: quiescence (**Figure 1(a)**), periodic tonic spiking (**Figure 1(b)**), and bursting (**Figure 1(c)**). The present study shows that the regions of these dynamical states in the $(g_{Dr,d}, I_s)$-parameter space change in response to τ_{pd} variations (**Figure 2**). The results at low τ_{pd} are shown in **Figure 2(a)**, those at intermediate τ_{pd} are shown in **Figure 2(b)**, and those at high τ_{pd} are shown in **Figure 2(c)**. First, in the present study, we performed a simulation of the model with $(g_{Dr,d}, I_s)$ variable values set at $\tau_{pd} = 5.0$ ms (**Figure 2(b)**), which was the same condition as that used in Figure 6 in [8]. At a low I_s value (5.6 μA/cm^2), the dynamical state of the model was that of quiescence, irrespective of the $g_{Dr,d}$ value (× in **Figure 2(b)**). An example of the time course of the somatic membrane potential during the quiescent state is shown in **Figure 1(a)**. At high I_s values (≥5.8 μA/cm^2), the dynamical state was that of periodic tonic spiking (○ in **Figure 2(b)**) or bursting (● in **Figure 2(b)**). In other words, when the $g_{Dr,d}$ value was small (≤12.0 mS/cm^2), the dynamical state was that of bursting. In contrast, when the $g_{Dr,d}$ value was large (≥12.2 mS/cm^2), the dynamical state was that of periodic tonic spiking at smaller I_s values and that of bursting at larger I_s values, and the I_s threshold between periodic tonic spiking and bursting increased as the $g_{Dr,d}$ value was increased. Examples of the time courses of the somatic membrane potential during periodic tonic spiking and bursting are shown in **Figure 1(b)** and **Figure 1(c)**, respectively. When the above-mentioned results were compared with previous findings (Figure 6 in [8]), the present numerical analysis could reproduce the previous results.

Based on the previous results (Figure 6 in [8]), SNFP was thought to occur at certain I_s values between × and ● in **Figure 2(b)**. In addition, SNFP was thought to occur at certain I_s values between × and ○ in **Figure 2(b)**. SNLC was thought to occur at certain I_s values between ○ and ● in **Figure 2(b)**. Codimension-two bifurcation was thought to occur at a certain $(g_{Dr,d}, I_s)$ value that is surrounded by ×, ○, and ● in **Figure 2(b)**.

3.2. Effects of Changes in τ_{pd} on the $(g_{Dr,d}, I_s)$-Parameter Space

The simulation results under conditions in which the τ_{pd} value was decreased and increased are shown in **Figure 2(a)** and **Figure 2(c)**, respectively. At a low I_s value (5.6 μA/cm^2), the dynamical state was that of quiescence, irrespective of the $g_{Dr,d}$ value (× in **Figure 2(a)** or **Figure 2(c)**), which is the same as that shown in **Figure 2(b)**. The I_s threshold between quiescence and bursting, which is the boundary between × and ● in **Figure 2(a)** and **Figure 2(c)**, is the same as that shown in **Figure 2(b)**. The I_s threshold between quiescence and periodic tonic spiking, which is the boundary between × and ○ in **Figure 2(a)** and **Figure 2(c)**, is also the same as that shown in **Figure 2(b)**. These results suggested that changes in the τ_{pd} values did not affect SNFP.

At high I_s values (≥5.8 μA/cm^2), patterns similar to **Figure 2(b)** were observed. In other words, when the $g_{Dr,d}$ value was small (≤12.8 mS/cm^2 in **Figure 2(a)** and ≤11.6 mS/cm^2 in **Figure 2(c)**), the dynamical state was that of bursting only (● in **Figure 2(a)** and **Figure 2(c)**). In contrast, when the $g_{Dr,d}$ value was large (≥13.0 mS/cm^2 in **Figure 2(a)** and ≥11.8 mS/cm^2 in **Figure 2(c)**), the dynamical state was that of periodic tonic

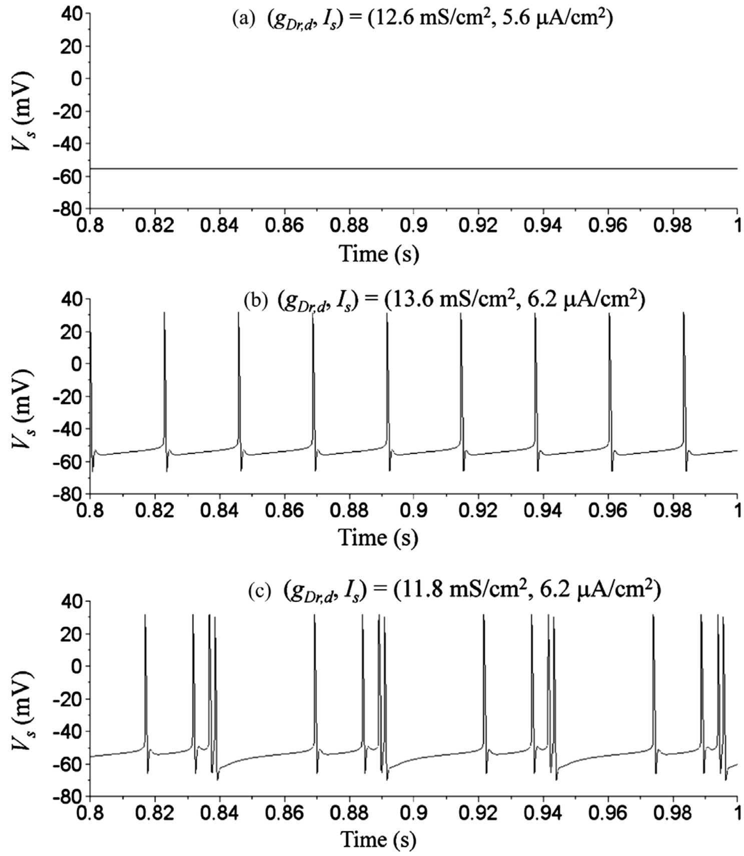

Figure 1. Examples of the time courses of the simulated somatic membrane potential (V_s) at different $g_{Dr,d}$ and I_s values at $\tau_{pd} = 5.0$ ms. (a) Quiescent state at $(g_{Dr,d}, I_s) = (12.6, 5.6)$; (b) Periodic tonic spiking state at $(g_{Dr,d}, I_s) = (13.6, 6.2)$; (c) Bursting state at $(g_{Dr,d}, I_s) = (11.8, 6.2)$.

spiking (○ in **Figure 2(a)** and **Figure 2(c)**) at smaller I_s values and that of bursting at larger I_s values. The I_s threshold between periodic tonic spiking and bursting increased as the $g_{Dr,d}$ value increased, as illustrated in **Figure 2(a)** and **Figure 2(c)**. However, the I_s threshold between periodic tonic spiking and bursting differed among **Figure 2(a)**, **Figure 2(b)**, and **Figure 2(c)**. In other words, an increase in the τ_{pd} value with fixed $g_{Dr,d}$ values increased the I_s threshold between periodic tonic spiking and bursting. These results suggested that changes in the τ_{pd} values had a great impact on SNLC and changes in the τ_{pd} values had no influence on the I_s value of the codimension-two bifurcation point but had a great impact on the $g_{Dr,d}$ value of the codimension-two bifurcation point.

4. Discussion

In the field of dynamical systems, it is important to investigate the dependence of the solutions of ordinary differential equations on system parameters. The present study illustrates the dependence of the qualitative nature of the solutions of ordinary differential equations on the following system parameters: $g_{Dr,d}$, I_s, and τ_{pd}. In the ghost bursting model, there were three qualitatively different dynamical states: quiescence, spiking, and bursting. In particular, the present results revealed how the dynamical states of the two-dimensional $(g_{Dr,d}, I_s)$-parameter space changed in response to variations in the third parameter τ_{pd}. These results are important in that they imply a relationship between τ_{pd} and bifurcation manifolds in the $(g_{Dr,d}, I_s)$-parameter space. In other words, these findings suggested that an increase in the τ_{pd} value did not shift the SNFP curve in the $(g_{Dr,d}, I_s)$-parameter space but rather shifted the SNLC curve upward. A very interesting finding in the present

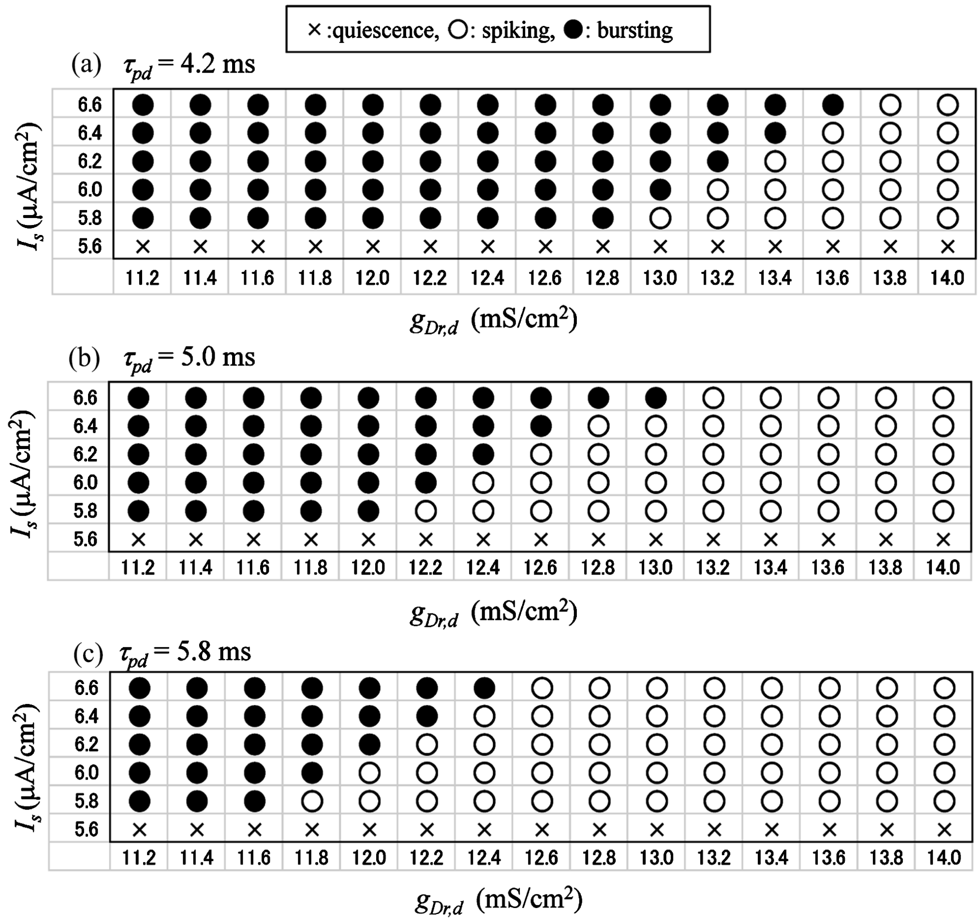

Figure 2. The effects of variations in the τ_{pd} value on the dynamical states in the two-dimensional $(g_{Dr,d}, I_s)$-parameter space (a) $\tau_{pd} = 4.2$ ms; (b) $\tau_{pd} = 5.0$ ms; (c) $\tau_{pd} = 5.8$ ms. The symbols are ×: quiescence, ○: periodic tonic spiking, and ●: bursting.

study, which was not reported in the previous study [8], is that there was a nonlinear relationship between τ_{pd} and the area of the bursting state. In other words, although the amount of τ_{pd} decrease was the same (−0.8 ms) between the changes from **Figure 2(c)** to **Figure 2(b)** and the changes from **Figure 2(b)** to **Figure 2(a)**, the amount of increase in the area of the bursting state in the latter case was much larger than that in the former case.

Other examples that illustrate how the dynamical states of two-dimensional parameter space change in response to variations in the third parameter are (1) a model of CA1 pyramidal neuron spiking dynamics (Figure 12 in [11]) and (2) a compartmental model of Cheyne-Stokes respiration (Figure 5 in [12]). In analysis of the CA1 model, Bianchi *et al*. have focused on the following three parameters: the injected current (I_{inj}), half-activation voltage of the transient sodium current $(V_{1/2(\mathrm{mNaT})})$, and half-activation voltage of the delay-rectifier potassium current $(V_{1/2(\mathrm{mKDR})})$. Their findings revealed that the dynamical states of the two-dimensional $(V_{1/2(\mathrm{mNaT})}, I_{inj})$-parameter space hardly changed in response to variations in $V_{1/2(\mathrm{mKDR})}$, while the dynamical states of the two-dimensional $(V_{1/2(\mathrm{mKDR})}, I_{inj})$-parameter space drastically changed in response to variations in $V_{1/2(\mathrm{mNaT})}$. In analysis of the Cheyne-Stokes respiration model, Atamanyk and Langford focused on the following three parameters: the partial pressure of CO_2 in the inspired air (x_I), ventilation-perfusion ratio (V_A/F), and slope of the Hill function (μ). Their findings revealed that the two-dimensional $(V_A/F, \mu)$-parameter space was divided into stable equilibria and unstable equilibria regions by a Hopf bifurcation curve and that an increase in x_I shifted the Hopf bifurcation curve upward, resulting in an expansion of the stable equilibria region.

Study [13] proposed an algorithm for the visualization of the bifurcation manifolds in the three-dimensional parameter space. In the three-dimensional parameter space, the parameter sets at which codimension one-bifurcation occurs are visualized as bifurcation surfaces. Higher codimension bifurcations are located at intersections of the bifurcation surfaces. For example, analyses of a socioeconomic model have revealed codimension-one bifurcation surfaces: a Hopf bifurcation surface and a saddle-node bifurcation surface (Figure 5 in [13]). In addition, the following codimension-two bifurcation curves were visualized: a Gavrilov-Guckenheimer bifurcation curve and a Takens-Bogdanov bifurcation curve. In contrast to the findings of the previous study [13], in the present study, we did not visualize bifurcation manifolds in the three-dimensional $\left(g_{Dr,d}, I_s, \tau_{pd}\right)$-parameter space. However, when considering the changes in the dynamical states of the two-dimensional $\left(g_{Dr,d}, I_s\right)$-parameter space in response to variations in τ_{pd} (**Figure 2**), one can roughly imagine the bifurcation manifold in the three-dimensional $\left(g_{Dr,d}, I_s, \tau_{pd}\right)$-parameter space. In other words, in the three-dimensional parameter space that is defined as a three-dimensional orthogonal coordinate system with axis lines $g_{Dr,d}$, I_s and τ_{pd}, the parameter sets at which SNFP occurs are thought to form the surface of SNFP that is orthogonal to the $\left(g_{Dr,d}, I_s\right)$ plane, while the parameter sets at which SNLC occurs are thought to form the surface of SNLC that is not orthogonal to the $\left(g_{Dr,d}, I_s\right)$ plane. The parameter sets at which codimension-two bifurcation occurs are thought to form a bifurcation curve at the intersection of the surfaces of SNFP and SNLC.

5. Conclusion

In conclusion, the novelty of this paper is that it reveals in detail the influence of τ_{pd} variations on the dynamical states in the $\left(g_{Dr,d}, I_s\right)$-parameter space of the ghostbursting model.

Acknowledgements

The author would like to thank Enago (www.enago.jp) for the English language review.

References

[1] Hodgkin, A.L. and Huxley, A.F. (1952) A Quantitative Description of Membrane Current and Its Application to Conduction and Excitation in Nerve. *Journal of Physiology*, **117**, 500-544. http://dx.doi.org/10.1113/jphysiol.1952.sp004764

[2] Bungay, S.D. and Campbell, S.A. (2009) Modelling a Respiratory Central Pattern Generator Neuron in *Lymnaea stagnalis*. *Canadian Applied Mathematics Quarterly*, **17**, 283-291.

[3] Ermentrout, G.B. and Terman, D. (2010) Mathematical Foundations of Neuroscience. Springer, New York. http://dx.doi.org/10.1007/978-0-387-87708-2

[4] Teka, W., Tabak, J., Vo, T., Wechselberger, M. and Bertram, R. (2011) The Dynamics Underlying Pseudo-Plateau Bursting in a Pituitary Cell Model. *Journal of Mathematical Neuroscience*, **1**, 12. http://dx.doi.org/10.1186/2190-8567-1-12

[5] Blagoev, K.B., Shukla, K. and Levine, H. (2013) We Need Theoretical Physics Approaches to Study Living Systems. *Physical Biology*, **10**, Article ID: 040201. http://dx.doi.org/10.1088/1478-3975/10/4/040201

[6] Holmes, P., Eckhoff, P., Wong-Lin, K.F., Bogacz, R., Zacksenhouse, M. and Cohen, J.D. (2010) The Physics of Decision Making: Stochastic Differential Equations as Models for Neural Dynamics and Evidence Accumulation in Cortical Circuits. Exner, P., Ed., *XVIth International Congress on Mathematical Physics*: Prague, 3-8 August 2009, 123-142. http://dx.doi.org/10.1142/9789814304634_0006

[7] Gieschke, R. and Serafin, D. (2014) Development of Innovative Drugs via Modeling with MATLAB: A Practical Guide. Springer, Heidelberg. http://dx.doi.org/10.1007/978-3-642-39765-3

[8] Doiron, B., Laing, C., Longtin, A. and Maler, L. (2002) Ghostbursting: A Novel Neuronal Burst Mechanism. *Journal of Computational Neuroscience*, **12**, 5-25. http://dx.doi.org/10.1023/A:1014921628797

[9] Shirahata, T. (2012) Analysis of the Electrosensory Pyramidal Cell Bursting Model for Weakly Electric Fish: Model Prediction under Low Levels of Dendritic Potassium Conductance. *Acta Biologica Hungarica*, **63**, 313-320. http://dx.doi.org/10.1556/ABiol.63.2012.3.1

[10] Vo, T., Tabak, J., Bertram, R. and Wechselberger, M. (2014) A Geometric Understanding of How Fast Activating Potassium Channels Promote Bursting in Pituitary Cells. *Journal of Computational Neuroscience*, **36**, 259-278. http://dx.doi.org/10.1007/s10827-013-0470-8

[11] Bianchi, D., Marasco, A., Limongiello, A., Marchetti, C., Marie, H., Tirozzi, B. and Migliore, M. (2012) On the Me-

chanisms Underlying the Depolarization Block in the Spiking Dynamics of CA1 Pyramidal Neurons. *Journal of Computational Neuroscience*, **33**, 20-225. http://dx.doi.org/10.1007/s10827-012-0383-y

[12] Atamanyk, J. and Langford, W.F. (2003) A Compartmental Model of Cheyne-Stokes Respiration. In: Ruan, S., Wolkowicz, G.S.K. and Wu, J., Eds., *Dynamical Systems and Their Applications in Biology* (*Fields Institute Communications Volume* 36), American Mathematical Society, Providence, 1-16.

[13] Stiefs, D., Gross, T., Steuer, R. and Feudel, U. (2008) Computation and Visualization of Bifurcation Surfaces. *International Journal of Bifurcation and Chaos*, **18**, 2191-2206. http://dx.doi.org/10.1142/S0218127408021658

Applied Mathematics, 2015, 6, 136-148
Published Online January 2015 in SciRes. http://www.scirp.org/journal/am
http://dx.doi.org/10.4236/am.2015.61014

Implementation of the Homotopy Perturbation Sumudu Transform Method for Solving Klein-Gordon Equation

Amr M. S. Mahdy[1], Adel S. Mohamed[1], Ahmad A. H. Mtawa[2]

[1]Department of Mathematics, Faculty of Science, Zagazig University, Zagazig, Egypt
[2]Department of Mathematics, Faculty of Science, University of Benghazi, Benghazi, Libya
Email: amr-mahdy85@yahoo.com, 3adel@live.nl, hussanahmad65@yahoo.com

Received 20 November 2014; accepted 3 December 2014; published 13 January 2015

Abstract

In this paper, the homotopy perturbation Sumudu transform method (HPSTM) is extended to solve linear and nonlinear fractional Klein-Gordon equations. To illustrate the reliability of the method, some examples are presented. The convergence of the HPSTM solutions to the exact solutions is shown. As a novel application of homotopy perturbation Sumudu transform method, the presented work shows some essential differences with existing similar application, and also four classical examples highlight the significance of this work.

Keywords

Mittag-Leffler Functions, Caputo Derivative, Sumudu Transform, Homotopy Perturbation Method, Klein-Gordon Equation

1. Introduction

Nonlinear phenomena that appear in many areas of scientific fields such as solid state physics, plasma physics, fluid dynamics, mathematical biology and chemical kinetics are modeled in terms of nonlinear partial differential equations and in many scientific and engineering applications; one of the corner stones of modeling is partial differential equations. For example, the Klein-Gordon equation of the form

$$w_{tt}(x,t)+bw(x,t)+g(w(x,t))=f(x,t), \tag{1}$$

with initial conditions

How to cite this paper: Mahdy, A.M.S., Mohamed, A.S. and Mtawa, A.A.H. (2015) Implementation of the Homotopy Perturbation Sumudu Transform Method for Solving Klein-Gordon Equation. *Applied Mathematics*, **6**, 136-148.
http://dx.doi.org/10.4236/am.2015.61014

$$w(x,0)=h(x),\ \ w_t(x,0)=k(x), \tag{2}$$

appears in modeling of problems in quantum field theory, relativistic physics, dispersive wave phenomena, plasma physic, nonlinear optics and applied physical sciences. The complexity of the equations though requires the use of numerical and analytical methods in most cases. Numerous analytical and numerical methods have been presented in recent years. Some of these analytical methods are the Fourier transform method [1], the fractional Green function method [2], the popular Laplace transform method [3] [4], the Sumudu transform method [5], the iteration method [4], the Mellin transform method and the method of orthogonal polynomials [3].

Some numerical methods are also popular, such as the homotopy perturbation method (HPM) [6]-[8], the modified homotopy perturbation method (MHPM) [9], the differential transform method (DTM) [10], the variational iteration method (VIM) [11] [12], the homotopy analysis method (HAM) [13] [14], the Sumudu decomposition method [15] and the Adomian decomposition method [16] [17].

Among these methods, the HPM is a universal approach which can be used to solve FODEs and FPDEs; on the other hand, various methods are combined with the homotopy perturbation method, such as the variational homotopy perturbation method, which is a combination of the variational iteration method and the homotopy perturbation method [18]. Another such combination is the homotopy perturbation transformation method which is constructed by combining two powerful methods, namely, the homotopy perturbation method and the Laplace transform method [19].

The Sumudu transformation method is one of the most important transform methods introduced in the early 1990s by Gamage K. Watugala. It is a powerful tool for solving many kinds of PDEs in various fields of science and engineering [20] [21]. And also various methods are combined with the Sumudu transformation method, such as the homotopy analysis Sumudu transform method (HASTD) [22], which is a combination of the homotopy analysis method and the Sumudu transformation method. Another example is the Sumudu decomposition method (SDM) [23], which is a combination of the Sumudu transform method and the Adomian decomposition method.

In this paper, an efficient approach is proposed to use the homotopy perturbation Sumudu transform method (HPSTM) to derive the exact solution of various types, which is a combination of the homotopy perturbation method and the Sumudu transform method. However, Singh [24] used the homotopy perturbation Sumudu transform method to obtain the exact solution of linear and nonlinear equations which are PDEs of integer order. In this paper we consider the fractional Klein-Gordon equation

$$\frac{\partial^\alpha}{\partial t^\alpha}w(x,t)+bw(x,t)+g\left(w(x,t)\right)=f(x,t), \tag{3}$$

and try to show the convergence of the homotopy perturbation Sumudu transform method in solving this equation.

The paper is structured in six sections. In Section 2, we begin with an introduction to some necessary definitions of fractional calculus theory. In Section 3, we describe the basic ideal of the homotopy perturbation method. In Section 4, we describe the homotopy perturbation Sumudu transform method. In Section 5, we present four examples to show the efficiency of using HPSTM to solve FPDEs and also to compare our results with those obtained by other existing methods. Finally, relevant conclusions are drawn in Section 6.

2. Basic Definitions of Fractional Calculus

In this section, we present the basic definitions and properties of the fractional calculus theory, which are used further in this paper.

Definition 1. A real function $f(t), t>0$, is said to be in the space $C_\sigma, \sigma\in\mathbb{R}$, if there exists a real number $p>\sigma$ such that $f(t)=t^p f_1(t)$ where $f_1(t)\in C[0,\infty)$, and it is said to be in the space C_σ^m if $f^{(m)}\in C_\sigma$, $m\in\mathbb{N}$.

Definition 2. The left sided Riemann-Liouville fractional integral of order $\alpha\ge 0$, of a function $f\in C_\sigma$, $\sigma\ge -1$ is defined as:

$$J^\alpha f(t)=\frac{1}{\Gamma(\alpha)}\int_0^t (t-\zeta)^{\alpha-1} f(\zeta)\mathrm{d}\zeta, \tag{4}$$

where $\alpha>0$, $t>0$ and $\Gamma(\alpha)$ is the Gamma function.

Definition 3. Let $f \in C_\mu^n$, $n \in \mathbb{N} \cup \{0\}$. The Caputo fractional derivative of f is defined in [18] as follows:

$$D_t^\alpha f(t) = \begin{cases} \dfrac{1}{\Gamma(n-\alpha)} \int_0^t (t-\zeta)^{n-\alpha-1} f^{(n)}(\zeta) \mathrm{d}\zeta, & n-1 < \alpha \le n, \\ D_t^n f(t), & \alpha = n. \end{cases} \tag{5}$$

Note that according to [13], Equations (4) and (5) become

$$J_t^\alpha f(x,t) = \frac{1}{\Gamma(\alpha)} \int_0^t (t-\zeta)^{\alpha-1} f(x,\zeta) \mathrm{d}\zeta, \text{ for } \alpha > 0, t > 0, \tag{6}$$

and

$$D_t^\alpha f(x,t) = \frac{1}{\Gamma(n-\alpha)} \int_0^t (t-\zeta)^{n-\alpha-1} f^{(n)}(\zeta) \mathrm{d}\zeta, \quad n-1 < \alpha \le n. \tag{7}$$

Definition 4. The single parameter and the two parameters variants of the Mittag-Leffler functions are denoted by $E_\alpha(t)$ and $E_{\alpha,\beta}(t)$, respectively, which are relevant for their connection with fractional calculus, and are defined as:

$$E_\alpha(t) = \sum_{j=0}^{\infty} \frac{t^j}{\Gamma(\alpha j + 1)}, \quad \alpha > 0, \ t \in \mathbb{C}, \tag{8}$$

$$E_{\alpha,\beta}(t) = \sum_{j=0}^{\infty} \frac{t^j}{\Gamma(\alpha j + \beta)}, \quad \alpha, \beta > 0, \ t \in \mathbb{C}. \tag{9}$$

Some special cases of the Mittag-Leffler function are as follows:

1) $E_1(t) = \mathrm{e}^t$;

2) $E_{\alpha,1}(t) = E_\alpha(t)$;

3) $\dfrac{\mathrm{d}^k}{\mathrm{d}t^k}\left[t^{\beta-1} E_{\alpha,\beta}(at^\alpha)\right] = t^{\beta-k-1} E_{\alpha,\beta-k}(at^\alpha)$.

Other properties of the Mittag-Leffler functions can be found in [25]. These functions are generalizations of the exponential function, because, most linear differential equations of fractional order have solutions that are expressed in terms of these functions.

Definition 5. Sumudu transform over the following set of functions,

$$A = \left\{ f(t) \middle| \exists M, \tau_1, \tau_2 > 0, \left| f(t) \right| < M\mathrm{e}^{\frac{|t|}{\tau_j}} \text{ if } t \in (-1)^j \times [0, \infty) \right\}, \tag{10}$$

is defined by

$$\mathbf{S}[f(t)] = G(u) = \int_0^\infty f(ut) \mathrm{e}^{-t} \mathrm{d}t, \tag{11}$$

where $u \in (\tau_1, \tau_2)$.

Some special properties of the Sumudu transform are as follows:

1) $S[1] = 1$;

2) $S\left[\dfrac{t^m}{\Gamma(m+1)}\right] = u^m, \ m > 0$;

3) $S\left[\mathrm{e}^{at}\right] = \dfrac{1}{1-au}$;

4) $S\left[\alpha f(t)+\beta g(t)\right]=\alpha S\left[f(t)\right]+\beta S\left[g(t)\right]$.

Other properties of the Sumudu transform can be found in [26].

Definition 6. $G(u)$ is the Sumudu transform of $f(t)$. And according to ref. [26] we have:

1) $G(1/s)/s$, is a meromorphic function, with singularities having $\operatorname{Re}(s)<\gamma$, and

2) there exists a circular region Γ with radius R and positive constants, M and k, with

$$\left|\frac{G(1/s)}{s}\right|<MR^{-k},$$

then the function $f(t)$ is given by

$$\mathbf{S}^{-1}\left[G(s)\right]=\frac{1}{2\pi i}\int_{\gamma-i\infty}^{\gamma+i\infty}\mathrm{e}^{st}G\left(\frac{1}{s}\right)\frac{\mathrm{d}s}{s}=\sum\text{residuse}\left[\mathrm{e}^{st}\frac{G(1/s)}{s}\right] \tag{12}$$

Definition 7. The Sumudu transform, $S\left[f(t)\right]$, of the Caputo fractional integral is defined as [5]

$$\mathbf{S}\left[D_t^{\alpha}f(t)\right]=\frac{G(u)}{u^{\alpha}}-\sum_{k=0}^{n-1}\frac{f^{(k)}(0)}{u^{\alpha-k}}, \tag{13}$$

then it can be easily understood that

$$\mathbf{S}\left[D_t^{\alpha}f(x,t)\right]=\frac{\mathbf{S}\left[f(x,t)\right]}{u^{\alpha}}-\sum_{k=0}^{n-1}\frac{f^{(k)}(x,0)}{u^{\alpha-k}},\quad n-1<\alpha\le n. \tag{14}$$

3. The Basic Idea of the Homotopy Perturbation Method

In this section, we will briefly present the algorithm of this method. At first, the following nonlinear differential equation is considered:

$$A(u)-f(x)=0,\quad x\in\Omega, \tag{15}$$

with the boundary conditions

$$B(u,\partial u/\partial n)=0,\quad x\in\Gamma, \tag{16}$$

where A, B, $f(x)$ and Γ are a general differential function operator, a boundary operator, a known an analytical function and the boundary of the domain Ω, respectively.

The operator A can be decomposed into a linear operator, denoted by $\mathbf{L}$, and a nonlinear operator, denoted by $\mathbf{N}$. Therefore, Equation (15) can be written as follows

$$\mathbf{L}(u)+\mathbf{N}(u)-f(x)=0. \tag{17}$$

Now we construct a homotopy $v(x,p):\Omega\times[0,1]\to\mathbb{R}$ with satisfies:

$$\mathbf{H}(v,p)=(1-p)\left[\mathbf{L}(v)-\mathbf{L}(u_0)\right]+p\left[A(u)-f(x)\right]=0,\quad 0\le p\le 1, \tag{18}$$

which is equivalent to

$$\mathbf{H}(v,p)=\mathbf{L}(v)-\mathbf{L}(u_0)+p\mathbf{L}(u_0)+p\left[\mathbf{N}(v)-f(x)\right]=0,\quad 0\le p\le 1, \tag{19}$$

where u_0 is the initial approximation of Equation (15) that satisfies the boundary condition and p is an embedding parameter.

When the value of p is changed from zero to unity, we can easily see that

$$\mathbf{H}(v,0)=\mathbf{L}(v)-\mathbf{L}(u_0)=0, \tag{20}$$

$$\mathbf{H}(v,1)=\mathbf{L}(v)-\mathbf{N}(v)-f(x)=A(u)-f(x)=0, \tag{21}$$

in topology, this changing process is called deformation, and Equations (20) and (21) are called homotopic.

If the p-parameter is considered as small, then the solution of Equations (17) and (18) can be expressed as a power series in p as follows

$$v = v_0 + pv_1 + p^2 v_2 + p^3 v_3 + \cdots \tag{22}$$

The best approximation for the solution of Equation (15) is

$$u = \lim_{p \to 1} v = v_0 + v_1 + v_2 + v_3 + \cdots. \tag{23}$$

4. The Homotopy Perturbation Sumudu Transform Method

In order to elucidate the solution procedure of this method, we consider a general fractional nonlinear partial differential equation of the form:

$$D_t^{\alpha} w(x,t) = \mathbf{L}w(x,t) + \mathbf{N}w(x,t) + q(x,t), \tag{24}$$

with $n-1 < \alpha \le n,$ and subject to the initial condition

$$\frac{\partial^{(r)} w(x,0)}{\partial t^r} = w^{(r)}(x,0) = f_r(x), \quad r = 0,1,\cdots,n-1, \tag{25}$$

where $D_t^{\alpha} w(x,t)$ is the Caputo fractional derivative, $q(x,t)$ is the source term, $\mathbf{L}$ is the linear operator and $\mathbf{N}$ is the general nonlinear operator.

Taking the Sumudu transform (denoted throughout this paper by $\mathbf{S}$) on both sides of Equation (24), we have

$$\mathbf{S}\left[D_t^{\alpha} w(x,t)\right] = \mathbf{S}\left[\mathbf{L}w(x,t) + \mathbf{N}w(x,t) + q(x,t)\right]. \tag{26}$$

Using the property of the Sumudu transform and the initial conditions in Equation (25), we have

$$u^{-\alpha}\mathbf{S}\left[w(x,t)\right] - \sum_{k=0}^{n-1} u^{-(\alpha-k)} w^k(x,0) = \mathbf{S}\left[\mathbf{L}w(x,t) + \mathbf{N}w(x,t) + q(x,t)\right], \tag{27}$$

and

$$\mathbf{S}\left[w(x,t)\right] = \sum_{k=0}^{n-1} u^k f_k(x) + u^{\alpha}\mathbf{S}\left[\mathbf{L}w(x,t) + \mathbf{N}w(x,t) + q(x,t)\right]. \tag{28}$$

Operating with the Sumudu inverse on both sides of Equation (28) we get

$$w(x,t) = \mathbf{S}^{-1}\left[\sum_{k=0}^{n-1} u^k f_k(x)\right] + \mathbf{S}^{-1}\left[u^{\alpha}\mathbf{S}\left[\mathbf{L}w(x,t) + \mathbf{N}w(x,t) + q(x,t)\right]\right]. \tag{29}$$

Now, pplying the classical perturbation technique. And assuming that the solution of Equation (29) is in the form

$$w(x,t) = \sum_{n=0}^{\infty} p^n w_n(x,t), \tag{30}$$

where $p \in [0,1]$ is the homotopy parameter. The nonlinear term of Equation (29) can be decomposed as

$$\mathbf{N}w(x,t) = \sum_{n=0}^{\infty} p^n H_n(w), \tag{31}$$

where H_i are He's polynomials, which can be calculated with the formula [27]

$$H_n(w_0, w_1, w_2, \cdots, w_n) = \frac{1}{n!}\frac{\partial^n}{\partial p^n}\left[\mathbf{N}\left(\sum_{i=0}^{\infty} p^i w_i\right)\right]_{p=0}, \; n = 0,1,2,\cdots \tag{32}$$

Substituting Equation (30) and (31) in Equation (29), we get

$$\sum_{n=0}^{\infty} p^n w_n(x,t) = \mathbf{S}^{-1}\left[\sum_{k=0}^{n-1} u^k f_k(x)\right] + p\mathbf{S}^{-1}\left[u^{\alpha}\mathbf{S}\left[\mathbf{L}\left(\sum_{n=0}^{\infty} p^n w_m(x,t)\right) + \sum_{n=0}^{\infty} p^n H_n(w) + q(x,t)\right]\right]. \tag{33}$$

Equating the terms with identical powers of p, we can obtain a series of equations as the follows:

$$\begin{aligned} p^0 &: w_0(x,t) = \mathbf{S}^{-1}\left[\sum_{k=0}^{n-1} u^k f_k(x)\right], \\ &\vdots \\ p^n &: w_n(x,t) = \mathbf{S}^{-1}\left[u^{\alpha}\mathbf{S}\left[\mathbf{L}\left(\sum_{n=0}^{\infty} p^n w_n(x,t)\right) + \sum_{n=0}^{\infty} p^n H_n(w) + q(x,t)\right]\right]. \end{aligned} \tag{34}$$

By utilizing the results in Equation (34), and substituting them into Equation (30) then the solution of Equation (24) can be expressed as a power series in p. The best approximation for the solution of Equation (24) is:

$$w(x,t) = \lim_{p\to 1}\sum_{n=0}^{\infty} p^n w_n(x,t) = w_0 + w_1 + w_2 + \cdots. \tag{35}$$

5. Applications

In this section, in order to assess the applicability and the accuracy of the fractional homotopy Sumudu transform method the following four examples.

Example 1. Consider the time-fractional partial differential Klein-Gordon equation

$$D_t^{\alpha} w(x,t) = \frac{\partial^2 w(x,t)}{\partial x^2} - w(x,t),\ 1 < \alpha \le 2 \tag{36}$$

subject to the initial conditions

$$w(x,0) = 0, \quad w_t(x,0) = x. \tag{37}$$

Taking the Sumudu transform on both sides of Equation (36), thus we get

$$\mathbf{S}\left[D_t^{\alpha} w(x,t)\right] = \mathbf{S}\left[D_x^2 w(x,t) - w(x,t)\right],$$

and

$$u^{-\alpha}\mathbf{S}\left[w(x,t)\right] - \left(u^{-\alpha} w(x,0) + u^{1-\alpha}\frac{\partial w(x,0)}{\partial t}\right) = \mathbf{S}\left[D_x^2 w(x,t) - w(x,t)\right].$$

Using the property of the Sumudu transform and the initial condition in Equation (37), we have

$$\mathbf{S}\left[w(x,t)\right] = xt + u^{\alpha}\mathbf{S}\left[D_x^2 w(x,t) - w(x,t)\right]. \tag{38}$$

Operating with the Sumudu inverse on both sides of Equation (38) we get

$$\left[w(x,t)\right] = xt + \mathbf{S}^{-1}\left[u^{\alpha}\mathbf{S}\left[D_x^2 w(x,t) - w(x,t)\right]\right]. \tag{39}$$

By applying the homotopy perturbation method, and substituting Equation (30) in Equation(39) we have

$$\sum_{n=0}^{\infty} p^n w_n(x,t) = xt + p\mathbf{S}^{-1}\left[u^{\alpha}\mathbf{S}\left[\left(D_x^2 - 1\right)\left(\sum_{n=0}^{\infty} p^n w_m(x,t)\right)\right]\right]. \tag{40}$$

Equating the terms with identical powers of p, we get

$$p^0 : w_0(x,t) = xt,$$

$$p^1 : w_1(x,t) = \frac{-xt^{\alpha+1}}{\Gamma(\alpha+2)},$$

$$p^2 : w_2(x,t) = \frac{xt^{2\alpha+1}}{\Gamma(2\alpha+2)},$$

$$p^3 : w_3(x,t) = \frac{-xt^{3\alpha+1}}{\Gamma(3\alpha+2)},$$

$$\vdots$$

$$p^n : w_n(x,t) = \frac{(-1)^n xt^{n\alpha+1}}{\Gamma(n\alpha+2)}.$$

Thus the solution of Equation (36) is given by

$$\begin{aligned} w(x,t) &= \lim_{p\to 1}\sum_{n=0}^{\infty} p^n w_n(x,t) \\ &= x\left(t - \frac{t^{\alpha+1}}{\Gamma(\alpha+2)} + \frac{t^{2\alpha+1}}{\Gamma(2\alpha+2)} - \frac{t^{3\alpha+1}}{\Gamma(3\alpha+2)} + \cdots\right) \\ &= x\sum_{n=0}^{\infty}\frac{(-1)^n xt^{n\alpha+1}}{\Gamma(n\alpha+2)} = xtE_{\alpha,2}\left(-t^{\alpha}\right) \end{aligned} \tag{41}$$

If we put $\alpha \to 2$ in Equation (41) or solve Equation (36) and (37) with $\alpha = 2$, we obtain the exact solution

$$w(x,t) = x\sum_{n=0}^{\infty}\frac{(-1)^n xt^{n\alpha+1}}{\Gamma(n\alpha+2)} = x\sin t.$$

which is in full agreement with the result in Ref. [28].

Example 2. Consider the inhomogeneous linear time-fractional partial differential Klein-Gordon equation

$$D_t^{\alpha} w(x,t) = \frac{\partial^2 w(x,t)}{\partial x^2} - w(x,t) + 2\sin x,\ 1 < \alpha \le 2 \tag{42}$$

subject to the initial conditions

$$w(x,0) = \sin(x), \quad w_t(x,0) = 1. \tag{43}$$

Taking the Sumudu transform on both sides of Equation (42), thus we get

$$\mathbf{S}\left[D_t^{\alpha} w(x,t)\right] = \mathbf{S}\left[D_x^2 w(x,t) - w(x,t) + 2\sin(x)\right],$$

and

$$u^{-\alpha}\mathbf{S}\left[w(x,t)\right] - \left(u^{-\alpha} w(x,0) + u^{1-\alpha}\frac{\partial w(x,0)}{\partial t}\right) = \mathbf{S}\left[D_x^2 w(x,t) - w(x,t) + 2\sin(x)\right].$$

Using the property of the Sumudu transform and the initial condition in Equation (43), we have

$$\mathbf{S}\left[w(x,t)\right] = \sin(x) + t + u^{\alpha}\mathbf{S}\left[D_x^2 w(x,t) - w(x,t) + 2\sin(x)\right]. \tag{44}$$

Operating with the Sumudu inverse on both sides of Equation (44) we get

$$\left[w(x,t)\right] = \sin(x) + t + \mathbf{S}^{-1}\left[u^{\alpha}\mathbf{S}\left[D_x^2 w(x,t) - w(x,t) + 2\sin(x)\right]\right]. \tag{45}$$

By applying the homotopy perturbation method, and substituting Equation (30) in Equation (45) we have

$$\sum_{n=0}^{\infty} p^n w_n(x,t) = \sin(x) + t + p\mathbf{S}^{-1}\left[u^{\alpha}\mathbf{S}\left[\left(D_x^2 - 1\right)\left(\sum_{n=0}^{\infty} p^n w_m(x,t)\right) + 2\sin(x)\right]\right]. \tag{46}$$

Equating the terms with identical powers of p, we get

$$p^0 : w_0(x,t) = \sin(x) + t,$$

$$p^1 : w_1(x,t) = \frac{-t^{\alpha+1}}{\Gamma(\alpha+2)},$$

$$p^2 : w_2(x,t) = \frac{t^{2\alpha+1}}{\Gamma(2\alpha+2)},$$

$$p^3 : w_3(x,t) = \frac{-t^{3\alpha+1}}{\Gamma(3\alpha+2)},$$

$$\vdots$$

$$p^n : w_n(x,t) = \frac{(-1)^n t^{n\alpha+1}}{\Gamma(n\alpha+2)}.$$

Thus the solution of Equation (42) is given by

$$\begin{aligned} w(x,t) &= \lim_{p\to 1}\sum_{n=0}^{\infty} p^n w_n(x,t) \\ &= \sin(x) + t - \frac{t^{\alpha+1}}{\Gamma(\alpha+2)} + \frac{t^{2\alpha+1}}{\Gamma(2\alpha+2)} - \frac{t^{3\alpha+1}}{\Gamma(3\alpha+2)} + \cdots \\ &= \sin(x) + \sum_{n=0}^{\infty}\frac{(-1)^n x t^{n\alpha+1}}{\Gamma(n\alpha+2)} = \sin(x) + tE_{\alpha,2}\left(-t^{\alpha}\right) \end{aligned} \tag{47}$$

If we put $\alpha \to 2$ in Equation (47) or solve Equation (42) and (43) with $\alpha = 2$, we obtain the exact solution

$$w(x,t) = \sin(x) + \sum_{n=0}^{\infty}\frac{(-1)^n x t^{n\alpha+1}}{\Gamma(n\alpha+2)} = \sin(x) + \sin t.$$

which is in full agreement with the result in Ref. [28].

Example 3. Consider the non-linear time-fractional partial differential Klein-Gordon equation

$$D_t^{\alpha} w(x,t) = \frac{\partial^2 w(x,t)}{\partial x^2} - w^2(x,t) + 2x^2 - 2t^2 + x^4t^4,\ 1 < \alpha \le 2 \tag{48}$$

subject to the initial conditions

$$w(x,0) = 0, \quad w_t(x,0) = 0. \tag{49}$$

Taking the Sumudu transform on both sides of Equation (48), thus we get

$$\mathbf{S}\left[D_t^{\alpha} w(x,t)\right] = \mathbf{S}\left[D_x^2 w(x,t) - w^2(x,t) + 2x^2 - 2t^2 + x^4t^4\right],$$

and

$$u^{-\alpha}\mathbf{S}\left[w(x,t)\right] - \left(u^{-\alpha} w(x,0) + u^{1-\alpha}\frac{\partial w(x,0)}{\partial t}\right) = \mathbf{S}\left[D_x^2 w(x,t) - w^2(x,t) + 2x^2 - 2t^2 + x^4t^4\right].$$

Using the property of the Sumudu transform and the initial condition in Equation (49), we have

$$\mathbf{S}\left[w(x,t)\right]=u^{\alpha}\mathbf{S}\left[D_x^2 w(x,t)-w^2(x,t)+2x^2-2t^2+x^4t^4\right]. \tag{50}$$

Operating with the Sumudu inverse on both sides of Equation (50) we get

$$\left[w(x,t)\right]=\mathbf{S}^{-1}\left[u^{\alpha}\mathbf{S}\left[D_x^2 w(x,t)-w^2(x,t)+2x^2-2t^2+x^4t^4\right]\right]. \tag{51}$$

By applying the homotopy perturbation method, and substituting Equation (30) in Equation (51) we have

$$\sum_{n=0}^{\infty}p^n w_n(x,t)=p\mathbf{S}^{-1}\left[u^{\alpha}\mathbf{S}\left[D_x^2\left(\sum_{n=0}^{\infty}p^n w_m(x,t)\right)-\left(\sum_{n=0}^{\infty}p^n w_m(x,t)\right)^2+2x^2-2t^2+x^4t^4\right]\right]. \tag{52}$$

Equating the terms with identical powers of p, we get

$$p^0: w_0(x,t)=0,$$

$$p^1: w_1(x,t)=\frac{2x^2t^{\alpha}}{\Gamma(\alpha+1)},$$

$$p^2: w_2(x,t)=\left[\frac{4t^{2\alpha}}{\Gamma^2(\alpha+1)}-\frac{4x^4t^{3\alpha}}{\Gamma^3(\alpha+1)}-\frac{2t^{\alpha+2}}{\Gamma(\alpha+1)}+\frac{x^4t^{\alpha+4}}{\Gamma(\alpha+1)}\right],$$

$$\vdots$$

Thus the solution of Equation (48) is given by

$$w(x,t)=\lim_{p\to 1}\sum_{n=0}^{\infty}p^n w_n(x,t)=\frac{2x^2t^{\alpha}}{\Gamma(\alpha+1)}+\frac{4t^{2\alpha}}{\Gamma^2(\alpha+1)}-\frac{4x^4t^{3\alpha}}{\Gamma^3(\alpha+1)}-\frac{2t^{\alpha+2}}{\Gamma(\alpha+1)}+\frac{x^4t^{\alpha+4}}{\Gamma(\alpha+1)}+\cdots \tag{53}$$

If we put $\alpha\to 2$ in Equation (53) or solve Equation (48) and (49) with $\alpha=2,$ and so on, we can find that

$$w_n(x,t)=0,\quad n>1,$$

we obtain the exact solution

$$w(x,t)=x^2t^2.$$

which is in full agreement with the result in Ref. [28].

Example 4. Consider the one-dimensional linear inhomogeneous fractional Klein-Gordon equation

$$D_t^{\alpha}w(x,t)=\frac{\partial^2 w(x,t)}{\partial x^2}-w(x,t)+6x^3t+6\left(x^3-6x\right)t^3,,t>0,\ x\in\mathbb{R},1<\alpha\le 2 \tag{54}$$

subject to the initial conditions

$$w(x,0)=0,\quad w_t(x,0)=0. \tag{55}$$

Taking the Sumudu transform on both sides of Equation (54), thus we get

$$\mathbf{S}\left[D_t^{\alpha}w(x,t)\right]=\mathbf{S}\left[D_x^2 w(x,t)-w(x,t)+6x^3t+6\left(x^3-6x\right)t^3\right],$$

and

$$u^{-\alpha}\mathbf{S}\left[w(x,t)\right]-\left(u^{-\alpha}w(x,0)+u^{1-\alpha}\frac{\partial w(x,0)}{\partial t}\right)=\mathbf{S}\left[D_x^2 w(x,t)-w\left(x,t+6x^3t+6\left(x^3-6x\right)t^3\right)\right].$$

Using the property of the Sumudu transform and the initial condition in Equation (55), we have

$$\mathbf{S}\left[w(x,t)\right]=u^{\alpha}\mathbf{S}\left[D_x^2 w(x,t)-w(x,t)+6x^3t+6\left(x^3-6x\right)t^3\right]. \tag{56}$$

Operating with the Sumudu inverse on both sides of Equation (56) we get

$$\left[w(x,t)\right]=\mathbf{S}^{-1}\left[u^{\alpha}\mathbf{S}\left[D_x^2 w(x,t)-w(x,t)+6x^3t+6\left(x^3-6x\right)t^3\right]\right]. \tag{57}$$

By applying the homotopy perturbation method, and substituting Equation (30) in Equation (57) we have

$$\sum_{n=0}^{\infty}p^n w_n(x,t)=p\mathbf{S}^{-1}\left[u^{\alpha}\mathbf{S}\left[\left(D_x^2-1\right)\left(\sum_{n=0}^{\infty}p^n w_m(x,t)\right)+6x^3t+6\left(x^3-6x\right)t^3\right]\right]. \tag{58}$$

Equating the terms with identical powers of p, we get

$$\begin{aligned}
&p^0: w_0(x,t)=0,\\
&p^1: w_1(x,t)=\frac{6x^3t^{\alpha+1}}{\Gamma(\alpha+2)}+\frac{6\left(x^3-6x\right)t^{\alpha+3}}{\Gamma(\alpha+4)},\\
&p^2: w_2(x,t)=-\left[\frac{6\left(x^3-6x\right)t^{2\alpha+1}}{\Gamma(2\alpha+2)}+\frac{6\left(x^3-12x\right)t^{2\alpha+3}}{\Gamma(2\alpha+4)}\right]\\
&\quad\vdots
\end{aligned}$$

Thus the solution of Equation (54) is given by

$$w(x,t)=\lim_{p\to 1}\sum_{n=0}^{\infty}p^n w_n(x,t)=\frac{6x^3t^{\alpha+1}}{\Gamma(\alpha+2)}+\frac{6\left(x^3-6x\right)t^{\alpha+3}}{\Gamma(\alpha+4)}-\left[\frac{6\left(x^3-6x\right)t^{2\alpha+1}}{\Gamma(2\alpha+2)}+\frac{6\left(x^3-12x\right)t^{2\alpha+3}}{\Gamma(2\alpha+4)}\right]+\cdots \tag{59}$$

If we put $\alpha\to 2$ in Equation (59) or solve Equation (54) and (55) with $\alpha=2$, we obtain the exact solution

$$w(x,t)=x^3t^3-0.0019047619x^3t^7+0.01428571429xt^7+\cdots.$$

which is in full agreement with the result in Ref. [29].

As it is presented above in Example 4 we obtained homotopy perturbation Sumudu transform solution of Equation (54) for values of $\alpha=2$, $\alpha=1.5$, $\alpha=1.75$. **Figures 1-4** show the approximate solutions for Equation (54) obtained for the three different values of α using the homotopy perturbation Sumudu transform method

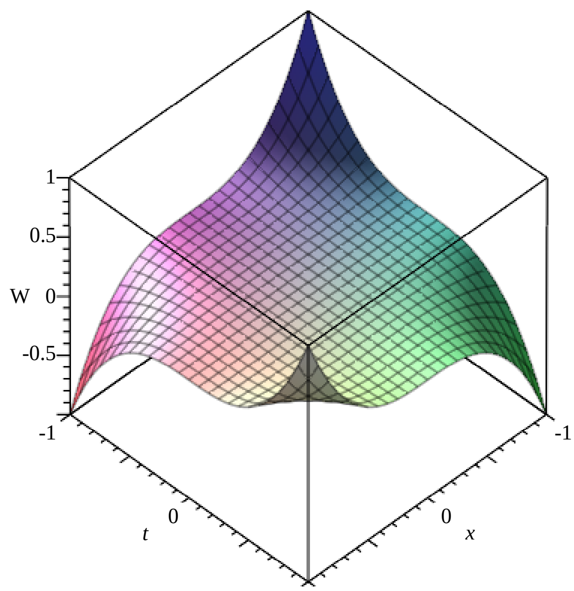

Figure 1. Profiles of $w(x, t)$ when $\alpha = 2$: exact solution of (54).

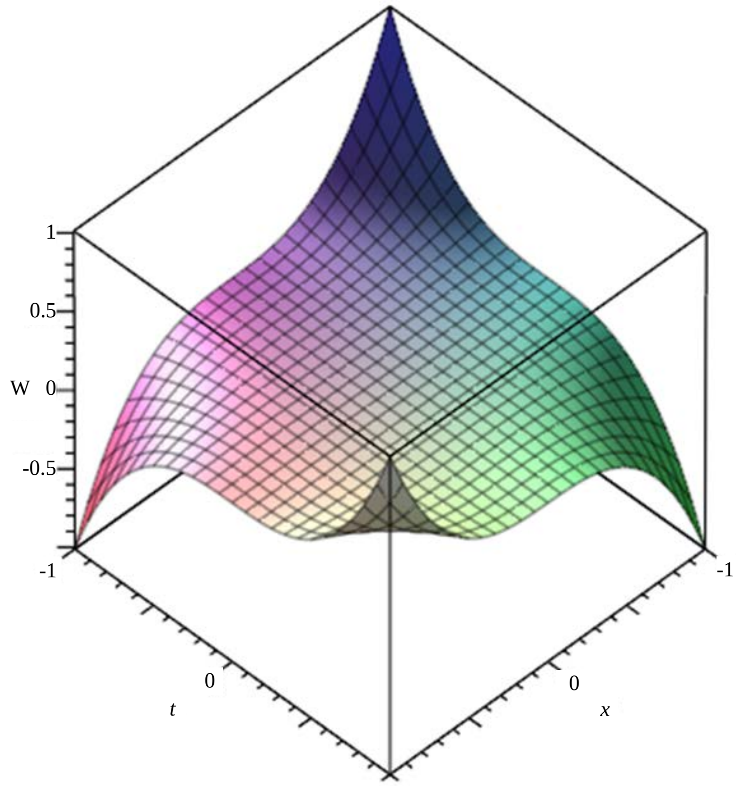

Figure 2. Profiles of $w(x, t)$ when $\alpha = 2$: approximate solution of (54).

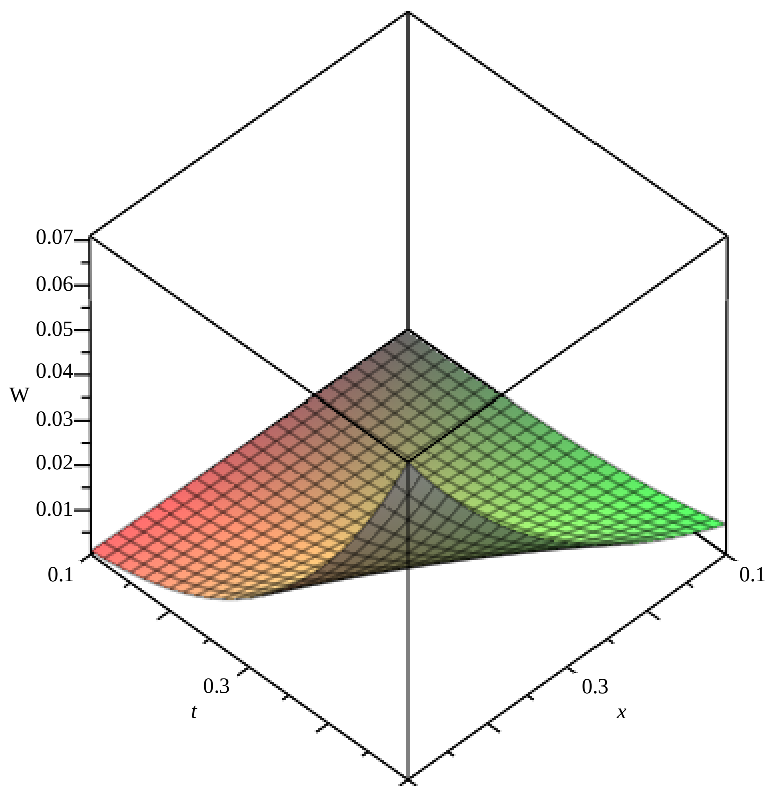

Figure 3. Profiles of $w(x, t)$ when $\alpha = 1.5$: approximate solution of (54).

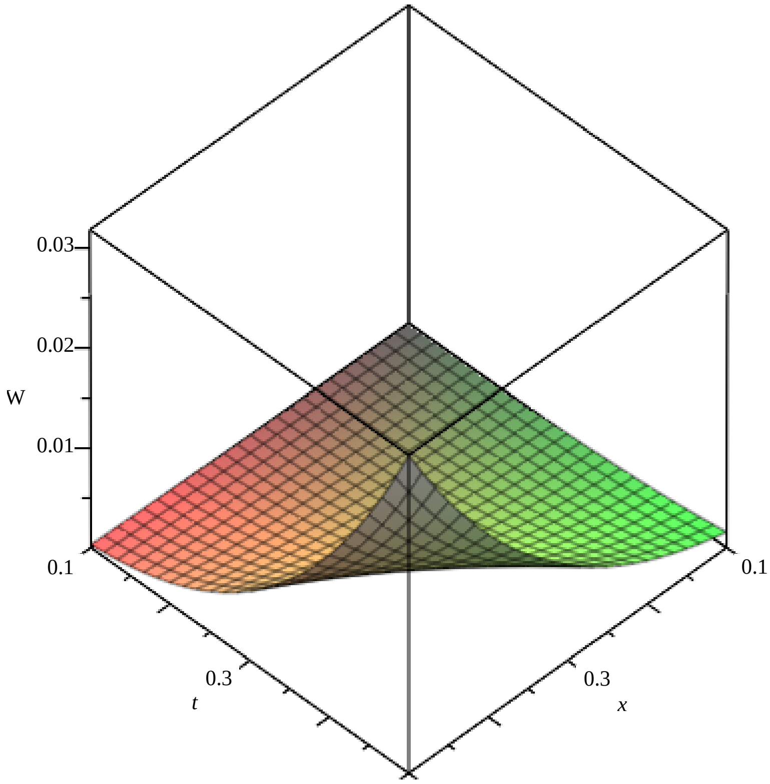

Figure 4. Profiles of $w(x, t)$ when $\alpha = 1.75$: approximate solution of (54).

(HPSTM). The values of $\alpha = 2$ is the only case for which we know the exact solution $w(x,t) = x^3t^3$ and the results of (HPSTM) are in excellent agreement with the exact solution.

6. Conclusion

In this paper, we have introduced a combination of the homotopy perturbation method and the Sumudu transform method for time fractional problems. This combination builds a strong method called the HPSTD. This method has been successfully applied to one-dimensional fractional equations and also for problems of linear and nonlinear partial differential equations. The HPSTD is an analytical method and runs by using the initial conditions only. Thus, it can be used to solve equations with fractional and integer order with respect to time. An important advantage of the new approach is its low computational load.

References

[1] Magin, R.L. and Ovadia, M. (2008) Modeling the Cardiac Tissue Electrode Interface Using Fractional Calculus. *Journal of Vibration and Control*, **14**, 1431-1442. http://dx.doi.org/10.1177/1077546307087439

[2] Mainardi, F. (1995) Fractional Diffusive Waves in Viscoelastic Solids. In: Wegner, J.L. and Norwood, F.R., Eds., *Nonlinear Waves in Solids*, ASME Book No. AMR 137, Fairfield, 93-97.

[3] Odibat, Z. and Momani, S. (2007) A Reliable Treatment of Homotopy Perturbation Method for Klein-Gordon Equations. *Physics Letters A*, **365**, 351-357. http://dx.doi.org/10.1016/j.physleta.2007.01.064

[4] Podlubny, I. (1999) Fractional Differential Equations: An Introduction to Fractional Derivatives, Fractional Equations, to Methods of Their Solution and Same of Their Applications. Science and Engineering, Academic Press, New York.

[5] Gupta, V.G. and Sharma, B. (2010) Application of Sumudu Transform in Reaction-Diffusion Systems and Nonlinear Waves. *Applied Mathematical Sciences*, **4**, 435-446.

[6] He, J.H. (1998) Approximate Analytical Solution for Seepage Flow with Fractional Derivatives in Porous Media. *Computer Methods in Applied Mechanics and Engineering*, **167**, 57-68. http://dx.doi.org/10.1016/S0045-7825(98)00108-X

[7] He, J.H. (2005) Limit Cycle and Bifurcation of Nonlinear Problems. *Chaos*, *Solutions and Fractals*, **24**, 827-833. http://dx.doi.org/10.1016/j.chaos.2005.03.007

[8] He, J.H. (1997) A New Approach to Nonlinear Partial Differential Equations. *Communications in Nonlinear Science and Numerical Simulation*, **2**, 230-235. http://dx.doi.org/10.1016/S1007-5704(97)90007-1

[9] Hesameddini, E. and Latifzadeh, H. (2011) An Optimal Choice of Initial Solutions in the Homotopy Perturbation Method. *International Journal of Nonlinear Sciences and Numerical Simulation*, **10**, 1389-1398.

[10] Miller, K.S. and Ross, B. (1993) An Introduction to the Fractional Calculus and Fractional Differential Equations. John Wiley and Sons, New York.

[11] Bhalekar, S. and Daftardar-Gejji, V. (2008) New Iterative Method: Application to Partial Differential Equations. *Applied Mathematics and Computer*, **203**, 778-783. http://dx.doi.org/10.1016/j.amc.2008.05.071

[12] Daftardar-Gejji, V. and Bhalekar, S. (2010) Solving Fractional Boundary Value Problems with Dirichlet Boundary Conditions Using a New Iterative Method. *Computers and Mathematics with Applications*, **59**, 1801-1809. http://dx.doi.org/10.1016/j.camwa.2009.08.018

[13] Arafa, A.A.M., Rida, S.Z. and Mohamed, H. (2011) Homotopy Analysis Method for Solving Biological Population Model. *Communications in Theoretical Physics*, **56**, 797-800.

[14] Hilfe, R., Ed. (2000) Applications of Fractional Calculus in Physics. World Scientific, Singapore.

[15] Eltayeb, H. and Kilicman, A. (2012) Application of Sumudu Decomposition Method to Solve Nonlinear System of Partial Differential Equations. *Abstract and Applied Analysis*, **2012**, Article ID: 412948. http://dx.doi.org/10.1155/2012/412948

[16] Adomian, G. (1994) Solving Frontier Problems of Physics: Decomposition Method. Kluwer Academic Publishers, Boston and London. http://dx.doi.org/10.1007/978-94-015-8289-6

[17] Cheng, J.F. and Chu, Y.M. (2011) Solution to the Linear Fractional Differential Equation Using Adomian Decomposition Method. *Mathematical Problems in Engineering*, **2011**, 1-14. http://dx.doi.org/10.1155/2011/587068

[18] Noor, M.A. and Mohyud-Din, S.T. (2008) Variational Homotopy Perturbation Method for Solving Higher Dimensional Initial Boundary Value Problems. *Mathematical Problems in Engineering*, **2008**, 1-11. http://dx.doi.org/10.1155/2008/696734

[19] Kumar, S., Yildirin, A. and Wei, L. (2012) A Fractional Model of the Diffusion Equation and Its Analytical Solution Using Laplace Transform. *Scientia Iranica*, **19**, 1117-1123. http://dx.doi.org/10.1016/j.scient.2012.06.016

[20] Moustafa, O.L. (2003) On the Cauchy Problem for Some Fractional Order Partial Differential Equations. *Chaos Solutions Fractals*, **18**, 135-140. http://dx.doi.org/10.1016/S0960-0779(02)00586-6

[21] Rafei, M. and Ganji, D.D. (2006) Explicit Solutions of Helmboltz Equation and Fifth-Order KdV Equation Using Homotopy Perturbation Method. *International Journal of Nonlinear Sciences and Numerical Simulation*, **73**, 321-329.

[22] Rathore, S., Kumar, D., Singh, J. and Gupta, S. (2012) Homotopy Analysis Sumudu Transform Method for Nonlinear Equations. *International Journal of Industrial Mathematics*, **4**, 301-314.

[23] Kumar, D., Singh, J. and Rathore, S. (2012) Sumudu Decomposition Method for Nonlinear Equations. *International Mathematical Forum*, **7**, 515-521.

[24] Singh, J., Kumar, D. and Sushila (2011) Homotopy Perturbation Sumudu Transform Method for Nonlinear Equations. *Advances in Theoretical and Applied Mechanics*, **4**, 165-175.

[25] Kilbas, A.A., Saigo, M. and Saxena, R.K. (2004) Generalized Mittag-Leffler Function and Generalized Fractional Calculus Operators. *Integral Transforms and Special Functions*, **15**, 31-49. http://dx.doi.org/10.1080/10652460310001600717

[26] Belgacem, F.B.M. and Karaballi, A.A. (2006) Sumudu Transform Fundamental Properties Investigations and Applications. *Journal of Applied Mathematics and Stochastic Analysis*, **2006**, 1-23. http://dx.doi.org/10.1155/JAMSA/2006/91083

[27] Ghorbani, A. (2009) Beyond Adomian Polynomials: He Polynomials. *Chaos*, *Solitons and Fractals*, **39**, 1486-1492. http://dx.doi.org/10.1016/j.chaos.2007.06.034

[28] Marasi, H.R. and Karimi, S. (2014) Convergence of the Variational Iteration Method for Solving Fractional Klein-Gordon Equation. *Journal of Mathematical and Computational Science*, **4**, 257-266.

[29] Turut, V. and Güzel, N. (2013) On Solving Partial Differential Equations of Fractional Order by Using the Variational Iteration Method and Multivariate Padé Approximations. *European Journal of Pure and Applied Mathematics*, **6**, 147-171.

Applied Mathematics, 2015, 6, 149-162
Published Online January 2015 in SciRes. http://www.scirp.org/journal/am
http://dx.doi.org/10.4236/am.2015.61015

Element Free Gelerkin Method for 2-D Potential Problems

Ali Rahmani Firoozjaee*, Ehsan Hendi, Farzad Farvizi

Faculty of Civil Engineering Department, Babol University of Technology, Babol, Iran
Email: *Rahmani@nit.ac.ir

Received 20 November 2014; accepted 2 December 2014; published 16 January 2015

Abstract

A meshfree method namely, element free Gelerkin (EFG) method, is presented in this paper for the solution of governing equations of 2-D potential problems. The EFG method is a numerical method which uses nodal points in order to discretize the computational domain, but where the use of connectivity is absent. The unknowns in the problems are approximated by means of connectivity-free technique known as moving least squares (MLS) approximation. The effect of irregular distribution of nodal points on the accuracy of the EFG method is the main goal of this paper as a complement to the precedent researches investigated by proposing an irregularity index (II) in order to analyze some 2-D benchmark examples and the results of sensitivity analysis on the parameters of the method are presented.

Keywords

Element Free Galerkin (EFG) Method, Potential Problems, Moving Least Squares Approximation, Irregular Distribution of Nodal Points, Irregularity Index

1. Introduction

Partial differential equations arise in connection with various physical and geometrical problems in which the functions involved depend on two or more independent variables, usually on time t and on one or several space variables [1]. A potential problem is one of the most important partial differential equations in engineering mathematics, because it occurs in connection with gravitational fields, electrostatics fields, steady-state heat conduction, incompressible fluid flow, and other areas [1].

Mesh based numerical methods, such as finite element method (FEM) and boundary element method (BEM), have been the primary numerical techniques in engineering computations. In spite of the positive points of the

*Corresponding author.

How to cite this paper: Firoozjaee, A.R., Hendi, E. and Farvizi, F. (2015) Element Free Gelerkin Method for 2-D Potential Problems. *Applied Mathematics*, **6**, 149-162. http://dx.doi.org/10.4236/am.2015.61015

finite element method, it still suffers from high preprocessing time, low accuracy of stresses, difficulty in incorporating adaptivity and it is also not an ideal tool for certain classes of problems, e.g. large deformations, material damage, crack growth, and moving boundaries [2] [3]. Therefore, meshless or meshfree methods are an ideal choice for these problems, because only a set of nodes is required for the problem domain discretization.

In the past few decades, a variety of new meshless methods have been developed, including the smoothed particle hydrodynamics (SPH) method [4], the finite point method (FPM) [5], the diffuse element method (DEM) [6], the element free Galerkin (EFG) method [7], the point interpolation method (PIM) [8], the hp clouds method [9], the partition of unity method (PUM) [10], the meshless local Petrov-Galerkin (MLPG) method [11], the local point interpolation method (LPIM) [12], the discrete least squares meshless (DLSM) method [13], the boundary point interpolation method (BPIM) [14], and the meshless method with boundary integral equations [15]-[18].

Recently several meshless methods are proposed in order to solve potential problems. The improved EFG method [19] based on the improved MLS approximation is used to solve 2-D potential problems. The method of fundamental solution (MFS), in which the desingularization technique is used to regularize the singularity and hyper singularity of the kernel functions, is applied to solve potential problems [20]. The discrete least squares meshless method with extra Gauss points is suggested for the solution of elliptic partial differential equations [21]. Singh and Singh used EFG method to solve 2-D potential flow problems [22] with regular distribution of nodal points.

The element free Galerkin (EFG) method that was developed by Belytschko *et al*. [7], is one of the most commonly used meshless methods and is based on the earlier version of diffuse element method [6]. In the EFG method, moving least squares (MLS) shape functions are used for the approximation of the field variables [23]; a background cell is used for numerical integration and Lagrange multipliers or penalty method is used for the imposition of essential boundary conditions.

The element free Galerkin method is presented in this paper to solve potential problems, and the effect of irregularity distribution of nodal points by using a proposed irregularity index (II) that was not considered in the previous researches for the EFG method, is investigated. In what follows, the construction of MLS shape functions is first explained. EFG method for discretization of the governing differential equation is then explained. Several 2-D potential problems are solved using the proposed method; sensitivity analysis on the parameters of the proposed method is also carried out, and the results are presented.

2. MLS Approximation

2.1. MLS Interpolants Function

MLS is a very important component of the element free Galerkin (EFG) method for the approximation of the field variables. The MLS approximation u^h of a scalar function u at point $\mathbf{x}$ is given as

$$u^h(\mathbf{x}) = \sum_{i=1}^{m} p_i(\mathbf{x}) a_i(\mathbf{x}) = P^{\mathrm{T}}(\mathbf{x}) a(\mathbf{x}) \tag{1}$$

where $P(\mathbf{x})$ is a polynomial basis function of the spatial coordinates, m is the number of monomial terms in the basis function, and $a(\mathbf{x})$ is a vector of coefficients given by

$$a^{\mathrm{T}}(\mathbf{x}) = \left(a_1(\mathbf{x}), a_2(\mathbf{x}), \cdots, a_m(\mathbf{x})\right) \tag{2}$$

The polynomial basis function $P(\mathbf{x})$ is built from Pascal's triangle and pyramid for 2- and 3-D problems, respectively. In 2-D problems, linear and quadratic basis functions are given as

$$P^{\mathrm{T}}(\mathbf{x}) = (1, x, y) \quad (m = 3 \ \text{ linear basis}) \tag{3}$$

$$P^{\mathrm{T}}(\mathbf{x}) = \left(1, x, y, xy, x^2, y^2\right) \quad (m = 6 \ \text{ quadratic basis}) \tag{4}$$

The unknown coefficients in Equation (1) can be found by minimizing the following weighted least squares method.

$$J=\sum_{i=1}^{n}W\left(\mathbf{x}-\mathbf{x}_I\right)\left[u^h\left(\mathbf{x}\right)-u\left(\mathbf{x}_I\right)\right]^2=\sum_{i=1}^{n}W\left(\mathbf{x}-\mathbf{x}_I\right)\left[\sum_{i=1}^{m}p_i\left(\mathbf{x}_i\right)\cdot a_i\left(\mathbf{x}\right)-u\left(\mathbf{x}_I\right)\right]^2 \tag{5}$$

where $W\left(\mathbf{x}-\mathbf{x}_I\right)$ is the weight function of node $\mathbf{x}_I$ at a point $\mathbf{x}$ which for simplicity it will be stated as $W_I\left(x\right)$.

Equation (5) using vector notation can be written as:

$$J=\left(pa-u\right)^{\mathrm{T}}W\left(\mathbf{x}\right)\left(pa-u\right) \tag{6}$$

The minimum of J with respect to $a\left(\mathbf{x}\right)$ is found by

$$\frac{\partial J}{\partial a}=0 \tag{7}$$

This leads to the following system of linear equations

$$A\left(\mathbf{x}\right)a\left(\mathbf{x}\right)=B\left(\mathbf{x}\right)U \tag{8}$$

Here $A\left(\mathbf{x}\right)$ and $B\left(\mathbf{x}\right)$ are $\left(m\times m\right)$ and $\left(m\times n\right)$ matrices, respectively, and are given as

$$A\left(\mathbf{x}\right)=\sum_{i=1}^{n}W_i\left(\mathbf{x}\right)p\left(\mathbf{x}_i\right)p^{\mathrm{T}}\left(\mathbf{x}_i\right) \tag{9}$$

$$B\left(\mathbf{x}\right)=\left[W_1\left(\mathbf{x}\right)P\left(\mathbf{x}_1\right),W_2(\mathbf{x})P\left(\mathbf{x}_2\right),W_3\left(\mathbf{x}\right)P\left(\mathbf{x}_3\right),\cdots,W_n\left(\mathbf{x}\right)P\left(\mathbf{x}_n\right)\right] \tag{10}$$

And U is $\left(n\times 1\right)$ vector and is given as

$$U=\left[u_1,u_2,u_3,\cdots,u_n\right]^{\mathrm{T}} \tag{11}$$

$a\left(\mathbf{x}\right)$ can be found using Equation (8);

$$a\left(\mathbf{x}\right)=A^{-1}\left(\mathbf{x}\right)B\left(\mathbf{x}\right)U \tag{12}$$

Putting $a\left(\mathbf{x}\right)$ from Equation (12) into Equation (1) leads to

$$u^h\left(\mathbf{x}\right)=P^{\mathrm{T}}\left(\mathbf{x}\right)A^{-1}\left(\mathbf{x}\right)B\left(\mathbf{x}\right)U=\phi\left(\mathbf{x}\right)U=\sum_{i=1}^{n}\varphi_i\left(\mathbf{x}\right)u_i \tag{13}$$

where $\phi\left(\mathbf{x}\right)$ is a vector of shape functions. The first derivative of the shape functions with respect to the spatial coordinates is also required for the numerical implementation and is given as

$$\phi_{,i}=P_{,i}^{\mathrm{T}}A^{-1}B+P^{\mathrm{T}}\left(A_{,i}^{-1}B+A^{-1}B_{,i}\right) \tag{14}$$

where

$$A_{,i}=-A^{-1}A_{,i}\,A^{-1} \tag{15}$$

and the index after the comma is a spatial derivative.

2.2. Weight Function

Weight function is an important part of the MLS approximation. There are no predefined rules to select the weight function for a particular application, but the weight function that could be used for meshless methods should have the following properties:

1) Its value should be maximized at the node and decrease with the distance from the node.

2) Smooth and non-negative.

3) It should have a compact support, *i.e.* non-zero over a small neighborhood of a node. This compact support is known as the influence domain of a node (nodal point).

Influence domain of a nodal point is a very important concept in meshless methods, as it determines the region in which it has influence. The size of influence domain for a node *i* is $d_w = d_{\max} c_i$, where $d_{\max}$ is a scaling parameter and c_i is determined by searching for enough neighbor nodes such that matrix *A* in Equation (8) is invertible. In regular distribution of nodal points c_i can be chosen as the distance between two neighboring nodes. In this paper, the cubic spline weight function is used;

$$W(\bar{d}) = \begin{cases} \frac{2}{3} - 4\bar{d}^2 + 4\bar{d}^3 & \text{for } \bar{d} \le \frac{1}{2} \\ \frac{4}{3} - 4\bar{d} + 4\bar{d}^2 - \frac{4}{3}\bar{d}^3 & \text{for } \frac{1}{2} < \bar{d} \le 1 \\ 0 & \text{for } \bar{d} > 1 \end{cases} \tag{16}$$

where $\bar{d} = (\|\mathbf{x} - \mathbf{x}_i\|)/d_w$ is the distance between node $\mathbf{x}_i$ and point of interest $\mathbf{x}$. Weight function derivatives with respect to the spatial coordinates are also required for the shape function derivatives as given in Equation (14) and are given as follows [2]:

$$\frac{\mathrm{d}W}{\mathrm{d}\bar{d}} = \begin{cases} -8\bar{d} + 12\bar{d}^2 & \text{for } \bar{d} \le \frac{1}{2} \\ -4 + 8\bar{d} - 4\bar{d}^2 & \text{for } \frac{1}{2} < \bar{d} \le 1 \\ 0 & \text{for } \bar{d} > 1 \end{cases} \tag{17}$$

3. EFG Method for Potential Problems

3.1. 2-D Potential Formulation

Consider a Poisson's partial differential equation in a two dimensional domain Ω bounded by Γ;

$$\nabla^2 u + g(x, y) = 0, \quad \text{in } \Omega \tag{18}$$

where $g(x, y)$ is a source term. On one part of the boundary, Γ_u is the Dirichlet boundary condition, and on the other part, Γ_q is the Neumann boundary condition.

$$u = \bar{u}, \quad \text{on } \Gamma_u \tag{19}$$

$$\frac{\partial u}{\partial n} = \bar{q}, \quad \text{on } \Gamma_q \tag{20}$$

where *n* is the outward normal vector to the boundary.

3.2. Enforcement of Essential Boundary Condition

The MLS shape functions do not satisfy the Kronecker delta property, *i.e.* $\phi_i(\mathbf{x}_j) \ne \delta_{ij}$, and are termed as approximants instead of interpolants. The values obtained from the MLS approximation are therefore, not the same as the nodal values, *i.e.* $u^h(\mathbf{x}_i) \ne u_i$, and are known as nodal parameters. This leads to some difficulties in imposition essential boundary condition in contrast to conventional FEM [2].

In this paper, the penalty method is used to enforce the essential boundary condition. The use of penalty method produces system of equations of the same dimension that FEM produces for the same number of nodes, and the modified stiffness matrix is still positively defined; moreover, the symmetry and the bandedness of the system matrix are preserved [2].

In the EFG method, the essential boundary condition has the form

$$\sum_i^n \phi_i(\mathbf{x}) u_i = \bar{u}, \quad \text{on } \Gamma_u \tag{21}$$

where $\bar{u}(\mathbf{x})$ is the prescribed potential on the boundary.

Consider the problem stated in Equation (18), a penalty factor is applied to penalize the difference between the potential of the MLS approximation and the prescribed potential on the essential boundary [2]. The constrained Galerkin weak form uses the penalty method and with substituting the expression of MLS approximation of Equation (13) can then be posed as

$$-\iint_{\Omega}\left[\frac{\partial\phi_i}{\partial x}\frac{\partial u}{\partial x}+\frac{\partial\phi_i}{\partial y}\frac{\partial u}{\partial y}\right]\mathrm{d}\Omega+\int_{\Gamma_q}\phi_i\bar{q}\mathrm{d}\Gamma_q+\alpha\int_{\Gamma_u}\phi_i u\mathrm{d}\Gamma_u-\alpha\int_{\Gamma_u}\phi_i\bar{u}d\Gamma_u+\iint_{\Omega}\phi_i g\mathrm{d}\Omega=0 \tag{22}$$

where $\alpha=(\alpha_1,\alpha_2,\cdots,\alpha_k)$ is a diagonal matrix of the penalty factor that $k=2$ for 2-D case. The penalty factor $\alpha_i(1,\cdots,\alpha_k)$ can be a function of the coordinates, and it can be different from one another. Although in practice the identical constant of a large positive number is assigned for penalty factor, which can be chosen by following method [2]

$$\alpha=1.0\times10^{4\,-13}\times\max\ (\text{diagonal element in the stiffness matrix}) \tag{23}$$

The final system of equation of the EFG formulation with penalty method is

$$\left[K+K^{\alpha}\right]u=F+F^{\alpha} \tag{24}$$

where

$$K_{ij}=\iint_{\Omega}\left[\frac{\partial\phi_i}{\partial x}\frac{\partial\phi_j}{\partial x}+\frac{\partial\phi_i}{\partial y}\frac{\partial\phi_j}{\partial y}\right]\mathrm{d}\Omega \tag{25}$$

$$F_i=\int_{\Gamma_q}\bar{q}\phi_i\mathrm{d}\Gamma_q+\iint_{\Omega}\phi_i g\mathrm{d}\Omega \tag{26}$$

The additional matrix K^{α} is the global penalty matrix assembled using the nodal matrix defined by

$$K_{ij}^{\alpha}=\alpha\int_{\Gamma_u}\phi_i\phi_j\mathrm{d}\Gamma_u \tag{27}$$

And the vector F^{α} is caused by the essential boundary condition that its nodal vector has the form

$$F_i^{\alpha}=\alpha\int_{\Gamma_u}\phi_i\bar{u}\mathrm{d}\Gamma_u \tag{28}$$

4. Irregularity Index (II)

To demonstrate the efficiency and accuracy of the EFG method in dealing with irregular distribution of nodal points, following irregularity index (II) is proposed in this paper

$$\mathrm{II}=\frac{r_{\min}}{r_{\max}} \tag{29}$$

where $r_{\max}$ and $r_{\min}$ are the maximum and minimum distances between nodal points, respectively, that are located in circular local domain such that each local domain includes at least 5 nodal points. The interval of the proposed index is $0\le\mathrm{II}\le0.5$, in which 0 indicates fully irregular and 0.5 indicates fully regular distribution of nodal points.

5. Numerical Examples

In this section, three 2-D numerical examples are solved to demonstrate the efficiency and accuracy of the proposed method. The effect of irregularity in distribution of nodal points is investigated by using of a proposed irregularity index (II) and the results are compared with the existing analytical solutions.

5.1. 2-D Poisson's Equation with Mixed Boundary Conditions

Consider the following 2-D Poisson's equation

$$\frac{\partial^2 u}{\partial x^2}+\frac{\partial^2 u}{\partial y^2}=\cos(\pi x)\cos(\pi y), \quad 0\le x\le 1,\ 0\le y\le 1 \tag{30}$$

with the following Dirichlet and Neumann boundary conditions

$$u(x,0)=-\frac{1}{2\pi^2}\cos(\pi x), \quad u(0,y)=-\frac{1}{2\pi^2}\cos(\pi y) \tag{31}$$

$$\frac{\partial u}{\partial x}(1,y)=0, \quad \frac{\partial u}{\partial y}(x,1)=0 \tag{32}$$

the analytical solution of the aforementioned Poisson's equation is

$$u^{exact}=-\frac{1}{2\pi^2}\cos(\pi x)\cos(\pi y) \tag{33}$$

The above-mentioned problem is solved using two different sets of 81 distributed nodes. In all of these cases, the polynomial basis function is considered as $P^{\mathrm{T}}=[1 \quad x \quad y]$ and the ratio of influence domain is considered 3. The regular and irregular distribution of 81 nodal points for this problem is shown in **Figure 1** and **Figure 2**. The analytical and EFG solution on a mesh of 81 nodal points with 96 and 1152 Gauss points along x axis are shown in **Figure 3** and **Figure 4**, respectively, to assess the effect of number of Gauss points on the solution accuracy.

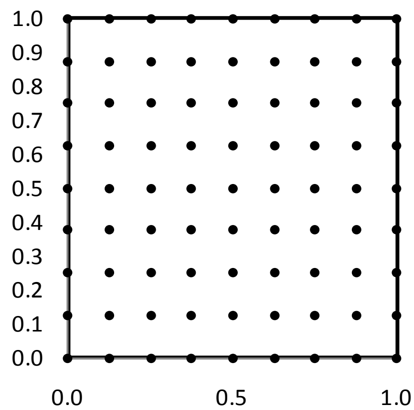

Figure 1. Nodal distribution on a rectangular domain with II = 0.5.

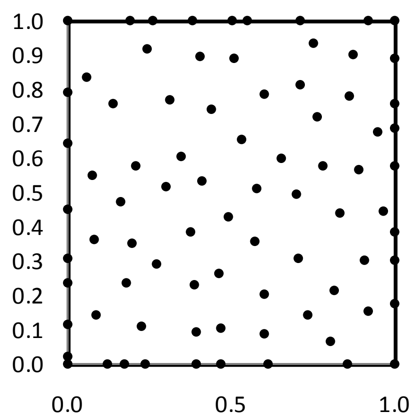

Figure 2. Nodal distribution on a rectangular domain with II = 0.0727.

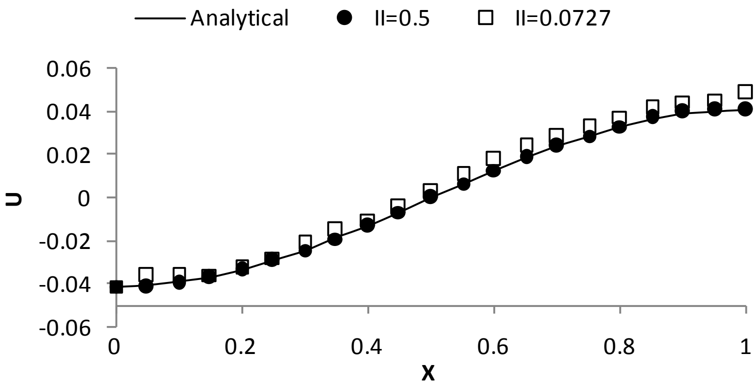

Figure 3. Results obtained by analytical and EFG method at $y = 0.2$ with 96 Gauss points.

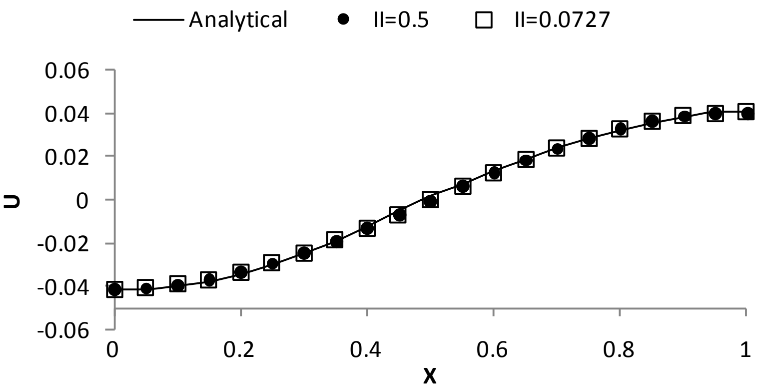

Figure 4. Results obtained by analytical and EFG methodat $y = 0.2$ with 1152 Gauss points.

There are different parameters in the EFG method that affect the obtained results. In this paper a sensitivity analysis is carried out on these parameters. Number of nodal points, number of Gauss points, ratio of influence domain, number of monomial terms in the basis function, and the type of weight function, are the parameters that are analyzed. For the sensitivity analysis the following error norm has been used

$$e_0 = \frac{\sum_{i=1}^{n} \left| u_i^{exact} - u_i^{num} \right|}{\sum_{i=1}^{n} \left| u_i^{exact} \right|} \tag{34}$$

where u_i^{exact} and u_i^{num} is the quantity of analytical solution and numerical solution, respectively. For the sensitivity analysis, one of the parameters is changed while the others are constant. The result of this analysis is shown in **Tables 1-10**, and the computational time is presented.

The results of **Table 1** indicate that the errors are dramatically reduced with increasing the number of nodal points while they get nearly constant when more nodal points are added. These results are also used to evaluate the convergence rate of the method with respect to nodal points and the results are shown in **Figure 5**.

The results of **Table 2** and **Table 3** quantitatively emphasize the rule of Gauss points on the accuracy of the EFG method and demonstrate high accuracy and low sensitivity of the proposed method in dealing with irregular distribution of nodal points.

This problem is solved here with different values of irregularity index to present the effect of irregularity distribution of nodal points. This analysis is done by using a proposed index that is shown in **Table 4** and a convergence rate is also demonstrates the obtained results in **Figure 6**. These results indicate the convergent behavior of the method as expected.

Table 1. The effect of number of nodal points on the error norm with 480 regular Gauss points.

Number of nodal points	25	36	64	81
Δx	0.250	0.200	0.143	0.125
e_0	0.3944	0.0730	0.0031	0.0029
CPU TIME (Sec)	0.6708	0.7800	0.8580	0.9572

Table 2. The effect of number of Gauss points on the error norm with 81 regular nodal points.

Number of Gauss points	96	320	480	1152
e_0	0.0153	0.0032	0.0029	0.0022
CPU TIME (Sec)	0.6084	0.7800	0.9672	1.6848

Table 3. The effect of number of Gauss points on the error norm with 81 irregular nodal points.

Number of Gauss points	96	320	480	1152
e_0	0.3273	0.2289	0.1323	0.0577
CPU TIME (Sec)	1.3193	2.2932	2.3868	4.5396

Table 4. The effect of irregularity of nodal points on the error norm with 81 irregular nodal points.

Irregularity Index (II)	0.5	0.0727	0.0143	0.0012
e_0	0.0002	0.0577	0.0991	0.1907
CPU TIME (Sec)	1.6848	4.5396	0.9984	1.6068

Table 5. The effect of ratio of influence domain on the error norm with 81 regular nodal points.

Ratio of influence domain	1.12	2	3	4.8	6.4
e_0	0.0112	0.0026	0.0007	0.1156	0.6371
CPU TIME (Sec)	0.3276	0.7176	1.5912	4.4928	7.5660

Table 6. The effect of ratio of influence domain on the error norm with 81 irregular nodal points.

Ratio of influence domain	1.12	2	3	4.8	6.4
e_0	0.7114	0.1583	0.0577	0.0134	0.0025
CPU TIME (Sec)	1.2168	1.5756	4.5396	13.3536	22.3237

Table 7. The effect of number of monomial terms in basis function on the error norm (regular).

The number of monomial terms in the basis function	0	1	2
e_0	0.0029	0.0007	0.0006
CPU time (Sec)	1.2792	1.5912	2.3868

Table 8. The effect of number of monomial terms in basis function on the error norm (ırregular).

The number of monomial terms in the basis function	0	1	2
e_0	0.0267	0.0577	0.1645
CPU time (Sec)	3.7284	4.5396	6.2400

Table 9. The effect of the type of weight function on the error norm with 81 regular nodal points.

Type of weight functions	Cubic spline	Quartic spline	Exponential
e_0	0.0006	0.0016	0.0070
CPU time (Sec)	2.3868	2.4180	2.3556

Table 10. The effect of the type of weight function on the error norm with 81 irregular nodal points.

Type of weight functions	Cubic spline	Quartic spline	Exponential
e_0	0.0577	0.1428	0.2116
CPU time (Sec)	4.5396	3.2136	4.1340

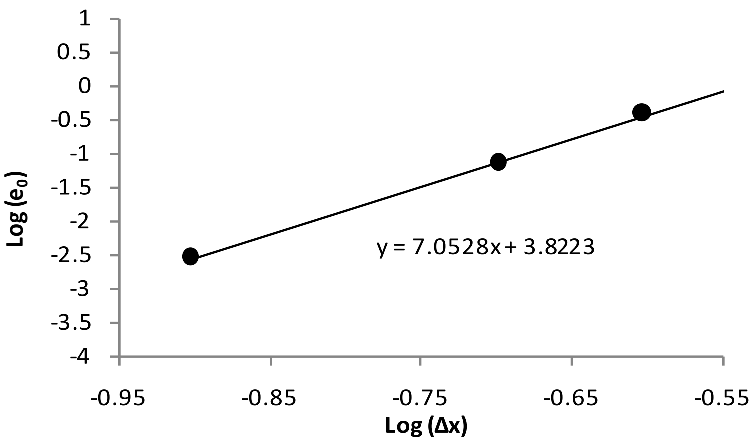

Figure 5. Convergence rate of the method with respect to nodal points.

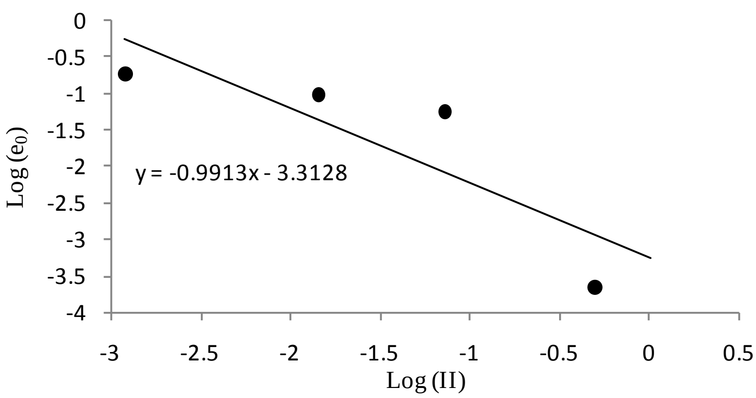

Figure 6. Convergence rate of the method with respect to irregularity index.

The problem is solved again on a mesh of 81 regularly and irregularly distributed of nodal points with different ratio of influence domain and 1152 Gauss points. The effect of this parameter is investigated in **Table 5** and **Table 6**. The values of this ratio in **Table 6** vary in the same way as **Table 5** to have a better comparison between them. The results of **Table 5** demonstrate that the appropriate interval of ratio of influence domain in regular distribution of nodal points is 2 - 3, while it is obvious from **Table 6** that the errors are decreased by increasing this ratio.

The number of monomial terms in basis function is the other parameter that can affect the performance of the EFG method. In this case, the problem domain is discretized with 81 regular and irregular nodal points with 1152 Gauss points. The ratio of influence domain in **Table 7** and **Table 8** is considered 3 to have a better comparison between them.

According to the results of **Table 7** and **Table 8**, the errors are diminished by increasing the number of monomial terms in basis function in regular distribution of nodal points, however, this effect is opposite in irregular distribution of nodal points because the higher number of monomial terms, the more nodal points are acquired in a favorable influence domain.

The other parameter that affects the solution's accuracy of the EFG method is the type weight function. In order to investigate this effect, the problem domain is discretized again with 81 regular and irregular meshes of nodes with 1152 Gauss points and three types of weight functions that are considered. It is also notable that the ratio of influence domain in both cases is considered 3.

It can be concluded from **Table 9** and **Table 10** in both cases, the solution's accuracy obtained by cubic spline is more desirable than the other weigh functions.

5.2. Poisson's Equation with Dirichlet Boundary Conditions on a Torus [19]

The second example is a 2-D Poisson's equation with Dirichlet boundary conditions on the torus. The equation is

$$\frac{\mathrm{d}^2u}{\mathrm{d}x^2}+\frac{\mathrm{d}^2u}{\mathrm{d}y^2}-4=0 \qquad a<r<b,\ \ 0<\theta<2\pi \tag{35}$$

with the following boundary conditions

$$u(a,\theta)=0 \tag{36}$$

$$u(b,\theta)=0 \tag{37}$$

and the analyticalsolutionofthisproblemis

$$u(r,\theta)=\left(r^2-a^2\right)-\left(a^2-b^2\right)\left(\frac{\log r-\log a}{\log a-\log b}\right) \tag{38}$$

here, $a=1$ and $b=2$ are assumed. The regular distribution of nodal points is shown in **Figure 7**. The above-mentioned problem is solved using two different sets of 460 distributed nodes that are shown in **Figure 7** and **Figure 8**. The analytical and numerical solutions along r direction at any angle with 460 nodal points are plotted in **Figure 9** and the ratio of influence domain is considered 3 for this problem again.

5.3. Flow over a Circular Cylinder

In this section, flow over a circular cylinder is considered. Such a flow can be generated by adding a uniform flow, in the positive x direction to a doublet at the origin directed in the negative x direction. The geometry of the example is shown in **Figure 10** and the governing equation of that is as follows:

$$\nabla^2\phi=\frac{\partial^2\phi}{\partial x^2}+\frac{\partial^2\phi}{\partial y^2}=0, \quad \text{in } \Omega \tag{39}$$

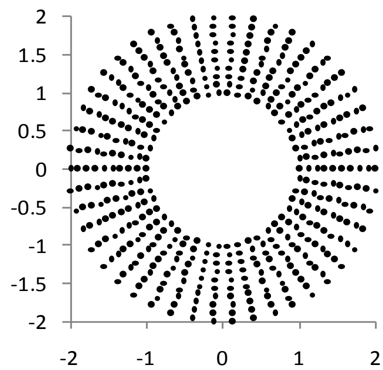

Figure 7. Nodal distribution on a tours domain with II = 0.3862.

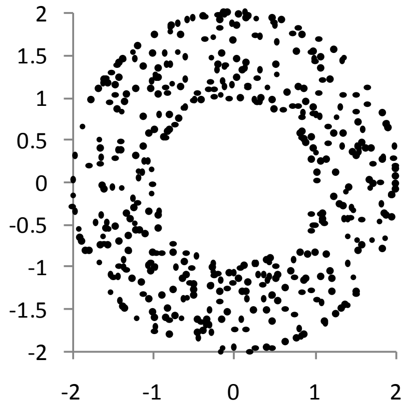

Figure 8. Nodal distribution on a tours domain with II = 0.0114.

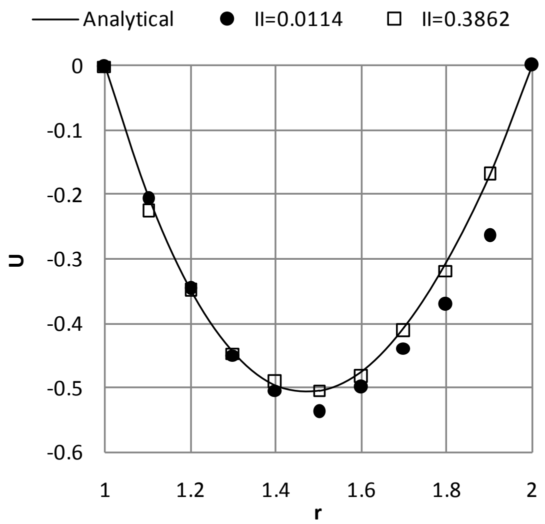

Figure 9. Results obtained by analytical and EFG method alongr direction at any angle.

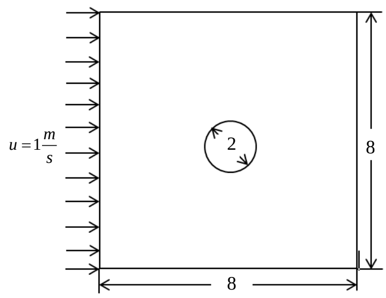

Figure 10. Flow over acircular cylinder.

and the exact solution is

$$\phi = x\left(u + \frac{1}{\left(x^2 + y^2\right)}\right) \tag{40}$$

where u is the fluid's velocity. Due to the symmetry, only the one-quarter of the problem domain is considered. This domain with its boundary condition is shown in **Figure 11**.

The above-mentioned problem is solved using three different sets of 241 distributions of nodal points with 962 Gauss points. It is notable that the ratio of influence domain in all cases is considered 3 and the distribution of nodal points with different values of irregular index is shown in **Figure 12-14**. The analytical and the EFG solutions along *y* axis are shown in **Figure 15**.

6. Conclusion

A meshless method namely element free Galerkin (EFG) method is presented in this paper. In order to investigate the performance and accuracy of the method, some 2-D potential problems on regular and irregular distribution

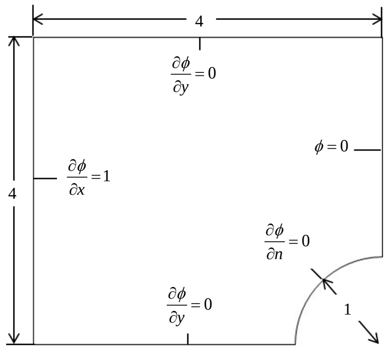

Figure 11. Boundary condition of the flow over a circular cylinder.

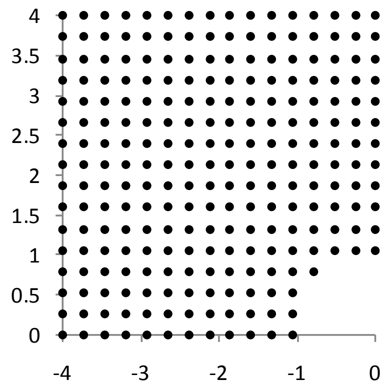

Figure 12. Nodal distribution of flow over a circular cylinder with II = 0.49999.

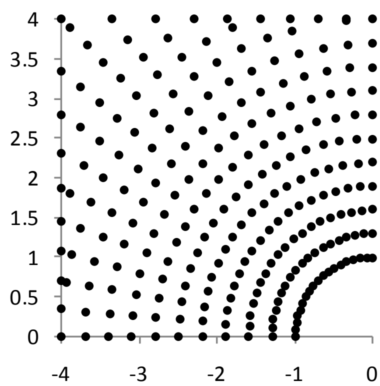

Figure 13. Nodal distribution of flow over a circular cylinder with II = 0.02323.

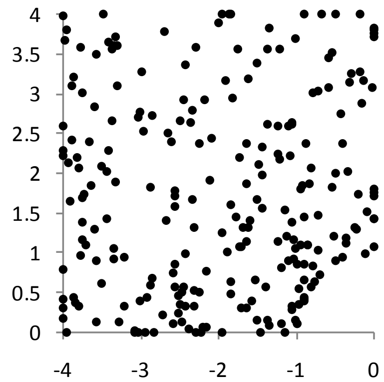

Figure 14. Nodal distribution of flow over a circular cylinder with II = 0.00289.

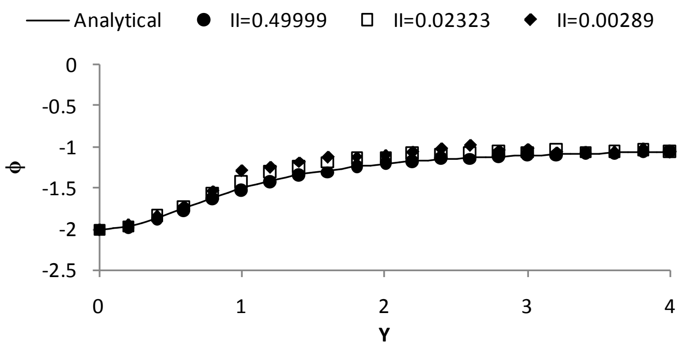

Figure 15. Results obtained by analytical and EFG method at $x = -1.0$.

of nodal points by using a proposed irregularity index (II) are analyzed and compared with the exact solution. A sensitivity analysis on the parameters of the EFG method is also carried out. From above analysis, it can be inferred that the errors are dramatically reduced by increasing the number of nodal points and Gauss points while they get nearly constant when more of them are added. It is also notable that the appropriate ratio of influence domain has been found to be 2 - 3 for regular mesh of nodal points, and in irregular mesh of nodal points, the errors are converged by increasing this ratio. Increasing the number of monomial terms in basis function is another factor that can improve the accuracy of the EFG method in regular distribution of nodal points while this effect is contradictory in comparison with irregular distribution of nodal points. The effect of using different type of weight functions is another parameter considered and the results indicate better performance of the method in using cubic spline weight function. Finally, it can be concluded that EFG method can be used to solve problems on irregular mesh of nodes with admissible performance.

References

[1] Kreyszig, E. (2010) Advanced Engineering Mathematics. Wiley, Hoboken.

[2] Liu, G.R. and Gu, Y. (2005) An Introduction to Meshfree Methods and Their Programming, Vol. 1. Springer, Berlin.

[3] Zhuang, X. (2010) Meshless Methods: Theory and Application in 3D Fracture Modelling with Level Sets. Durham University, Durham.

[4] Monaghan, J.J. (1988) An Introduction to SPH. *Computer Physics Communications*, **48**, 89-96. http://dx.doi.org/10.1016/0010-4655(88)90026-4

[5] Onate, E., *et al*. (1996) A Finite Point Method in Computational Mechanics. Applications to Convective Transport and Fluid Flow. *International Journal for Numerical Methods in Engineering*, **39**, 3839-3866. http://dx.doi.org/10.1002/(SICI)1097-0207(19961130)39:22<3839::AID-NME27>3.0.CO;2-R

[6] Nayroles, B., Touzot, G. and Villon, P. (1992) Generalizing the Finite Element Method: Diffuse Approximation and Diffuse Elements. *Computational Mechanics*, **10**, 307-318. http://dx.doi.org/10.1007/BF00364252

[7] Belytschko, T., Lu, Y.Y. and Gu, L. (1994) Element-Free Galerkin Methods. *International Journal for Numerical Methods in Engineering*, **37**, 229-256. http://dx.doi.org/10.1002/nme.1620370205

[8] Liu, G.R. and Gu, Y. (2001) A Point Interpolation Method for Two-Dimensional Solids. *International Journal for Numerical Methods in Engineering*, **50**, 937-951. http://dx.doi.org/10.1002/1097-0207(20010210)50:4<937::AID-NME62>3.0.CO;2-X

[9] Liszka, T.J., Duarte, C.A.M. and Tworzydlo, W.W. (1996) hp-Meshless Cloud Method. *Computer Methods in Applied Mechanics and Engineering*, **139**, 263-288. http://dx.doi.org/10.1016/S0045-7825(96)01086-9

[10] Babuška, I. and Melenk, J.M. (1997) The Partition of Unity Method. *International Journal for Numerical Methods in Engineering*, **40**, 727-758. http://dx.doi.org/10.1002/(SICI)1097-0207(19970228)40:4<727::AID-NME86>3.0.CO;2-N

[11] Atluri, S. and Zhu, T. (1998) A New Meshless Local Petrov-Galerkin (MLPG) Approach in Computational Mechanics. *Computational Mechanics*, **22**, 117-127. http://dx.doi.org/10.1007/s004660050346

[12] Gu, Y. and Liu, G.R. (2001) A Local Point Interpolation Method for Static and Dynamic Analysis of Thin Beams. *Computer Methods in Applied Mechanics and Engineering*, **190**, 5515-5528. http://dx.doi.org/10.1016/S0045-7825(01)00180-3

[13] Rahmani Firoozjaee, A. and Afshar, M.H. (2011) Discrete Least Squares Meshless (DLSM) Method for Simulation of Steady State Shallow Water Flows. *Scientia Iranica*, **18**, 835-845. http://dx.doi.org/10.1016/j.scient.2011.07.016

[14] Gu, Y. and Liu, G. (2002) A Boundary Point Interpolation Method for Stress Analysis of Solids. *Computational Mechanics*, **28**, 47-54. http://dx.doi.org/10.1007/s00466-001-0268-9

[15] Liew, K., Cheng, Y. and Kitipornchai, S. (2007) Analyzing the 2D Fracture Problems via the Enriched Boundary Element-Free Method. *International Journal of Solids and Structures*, **44**, 4220-4233. http://dx.doi.org/10.1016/j.ijsolstr.2006.11.018

[16] Liew, K., Cheng, Y. and Kitipornchai, S. (2005) Boundary Element-Free Method (BEFM) for Two-Dimensional Elastodynamic Analysis Using Laplace Transform. *International Journal for Numerical Methods in Engineering*, **64**, 1610-1627. http://dx.doi.org/10.1002/nme.1417

[17] Liew, K., Cheng, Y. and Kitipornchai, S. (2006) Boundary Element-Free Method (BEFM) and Its Application to Two-Dimensional Elasticity Problems. *International Journal for Numerical Methods in Engineering*, **65**, 1310-1332. http://dx.doi.org/10.1002/nme.1489

[18] Liew, K., Sun, Y. and Kitipornchai, S. (2007) Boundary Element-Free Method for Fracture Analysis of 2-D Anisotropic Piezoelectric Solids. *International Journal for Numerical Methods in Engineering*, **69**, 729-749. http://dx.doi.org/10.1002/nme.1786

[19] Zhang, Z., Zhao, P. and Liew, K. (2009) Improved Element-Free Galerkin Method for Two-Dimensional Potential Problems. *Engineering Analysis with Boundary Elements*, **33**, 547-554. http://dx.doi.org/10.1016/j.enganabound.2008.08.004

[20] Young, D., Chen, K. and Lee, C. (2005) Novel Meshless Method for Solving the Potential Problems with Arbitrary Domain. *Journal of Computational Physics*, **209**, 290-321. http://dx.doi.org/10.1016/j.jcp.2005.03.007

[21] Firoozjaee, A.R. and Afshar, M.H. (2009) Discrete Least Squares Meshless Method with Sampling Points for the Solution of Elliptic Partial Differential Equations. *Engineering Analysis with Boundary Elements*, **33**, 83-92. http://dx.doi.org/10.1016/j.enganabound.2008.03.004

[22] Singh, I. and Singh, A. (2009) A Meshfree Solution of Tow-Dimensional Potential Flow Problems. *World Academy of Science*, *Engineering and Technology*, *International Science Index*, **27**, 587-597.

[23] Lancaster, P. and Salkauskas, K. (1981) Surfaces Generated by Moving Least Squares Methods. *Mathematics of Computation*, **37**, 141-158. http://dx.doi.org/10.1090/S0025-5718-1981-0616367-1

Applied Mathematics, 2015, 6, 163-172
Published Online January 2015 in SciRes. http://www.scirp.org/journal/am
http://dx.doi.org/10.4236/am.2015.61016

Travelling Wave Solutions of Kaup-Kupershmidt Equation Which Describes Pseudo Spherical Surfaces

G. M. Gharib

Mathematics Department, College of Science and Information Technology, Zarqa University, Zarqa, Jordan
Email: Gharibmusa@gmail.com

Received 1 December 2014; accepted 16 December 2014; published 19 January 2015

Abstract

In this paper I introduce the geometric notion of a differential system describing surfaces of a constant negative curvature and describe a family of pseudo-spherical surface for Kaup-Kupershmidt Equation with constant Gaussian curvature −1. I obtained new soliton solutions for Kaup-Kupershmidt Equation by using the modified sine-cosine method.

Keywords

Soliton Solutions, Pseudo Spherical Surfaces, Nonlinear Evolution Equations

1. Introduction

Many partial differential equations which continue to be investigated due to their role in mathematics and physics exhibit interrelationships with the geometry of surfaces, or submanifolds, immersed in a three-dimensional space [1]. In particular, it has been known for a while that there is a relationship between surfaces of a constant negative Gaussian curvature in Euclidean three-space, the Sine-Gordon Equation and Bäcklund transformations which are relevant to the given equation [2]. Moreover, the original Bäcklund transformation for the Sine-Gordon Equation is also a simple geometric construction for pseudospherical surfaces [3]-[5]. It is well known that nonlinear complex physical phenomena are related to nonlinear partial differential equations (NLPDEs) which are involved in many fields from physics to biology, chemistry, mechanics, etc.

As mathematical models of the phenomena, the investigation of exact solutions to the NLPDEs reveals to be very important for the understanding of these physical problems. Many mathematicians and physicists have well understood this importance when they decided to pay special attention to the development of sophisticated methods for constructing exact solutions to the NLPDEs. Thus, a number of powerful methods have been presented.

We can cite the inverse scattering transform [6], the Bäcklund and Darboux transform [7]-[10], Hirota's bilinear method [11], the homogeneous balance method [12], Jacobi elliptic function method [13], the tanh method and extended tanh-function method [14]-[20], F-expansion method [21]-[23] and so on. The notion of conservation laws is important in the study of nonlinear evolution equations (NLEEs) appearing in mathematical physics [24].

Consider Kaup-Kupershmidt Equation,

$$u_t = u_{5x} + 5uu_{3x} + \frac{25}{2}u_x u_{2x} + 5u^2 u_x \tag{1}$$

where $u = u(x,t)$ is a function of two independent variables t and x.

2. Kaup-Kupershmidt Equation Which Describes Pseudo Spherical Surfaces

I recall the definition [25]-[28] of a differential equation (DE) that describes a pss. Let M^2 be a two dimensional differentiable manifold with coordinates (x,t). A DE for a real function $u(x,t)$ describes a pss if it is a necessary and sufficient condition for the existence of differentiable functions

$$f_{ij},\quad 1 \le i \le 3,\quad 1 \le j \le 2, \tag{2}$$

depending on u and its derivatives such that the one-forms

$$\omega_1 = f_{11}dx + f_{12}dt,\quad \omega_2 = f_{21}dx + f_{22}dt,\quad \omega_3 = f_{31}dx + f_{32}dt, \tag{3}$$

satisfy the structure equations of a pss, *i.e.*,

$$d\omega_1 = \omega_3 \wedge \omega_2,\quad d\omega_2 = \omega_1 \wedge \omega_3,\quad d\omega_3 = \omega_1 \wedge \omega_2. \tag{4}$$

I obtain that the Kaup-Kupershmidt Equation (1) describes pseudospherical surfaces, with associated one forms $\omega_i = f_{i1}dx + f_{i2}dt \quad 1 \le i \le 3$ given by

$$\begin{aligned}
f_{11} &= -\frac{1}{2}\left(u + \eta^2 - 1\right),\\
f_{21} &= \eta,\\
f_{31} &= -\frac{1}{2}\left(u + \eta^2 + 1\right),\\
f_{12} &= -\frac{1}{2}\left(u_{4x} + \eta u_{3x}\right) + \frac{1}{4}\left(-9u - \eta^2 + 1\right)u_{2x} - 2u_x^2 + 2\eta u u_x - \frac{1}{2}u^3 + \frac{1}{2}u^2\left(1 - \eta^2\right),\\
f_{22} &= -\frac{1}{2}u_{3x} - 2uu_x - \frac{\eta}{2}\left(-u_{2x} - 2u^2\right),\\
f_{32} &= f_{12} - \frac{1}{2}u_{2x} - u^2.
\end{aligned} \tag{5}$$

As a consequence, each solution of the DE provides a local metric on M^2, whose Gaussian curvature is constant, equal to −1. Moreover, the above definition is equivalent to saying that DE for u is the integrability condition for the problem [19] [29]:

$$d\phi = \Omega\phi,\quad \phi = \begin{pmatrix}\phi_1\\ \phi_2\end{pmatrix}, \tag{6}$$

where d denotes exterior differentiation, ϕ is a column vector and the 2×2 matrix $\Omega\left(\Omega_{ij}, i, j = 1,2\right)$ is traceless

$$\Omega = \frac{1}{2}\begin{pmatrix}\omega_2 & \omega_1 - \omega_3\\ \omega_1 + \omega_3 & -\omega_2\end{pmatrix}. \tag{7}$$

3. Exact Solution for Kaup-Kupershmidt Equation

With the rapid development of science and technology, the study kernel of modern science is changed from linear to nonlinear step by step. Many nonlinear science problems can simply and exactly be described by using the mathematical model of nonlinear equation. Up to now, many important physical nonlinear evolution equations are found, such as Sine-Gordon Equation, KdV Equations, Schrodinger Equation all possess solitary wave solutions. There exist many methods to seek for the solitary wave solutions, such as inverse scattering method, Hopf-Cole transformation, Miura transformations, Darboux transformation and Bäcklund transformation [7]-[10], but solving nonlinear equations is still an important task [27]-[30]. In this paper, with the aid of Mathematica, a traveling wave solution for a class of Kaup-Kupershmidt Equation,

$$u_t = u_{5x} + 5uu_{3x} + \frac{25}{2}u_x u_{2x} + 5u^2 u_x.$$

In order to obtain the soliton solution of (1), I will use the modified sine-cosine to develop traveling wave solutions to this equation. The modified sine-cosine method admits the use of solutions [30]

$$u(x,t) = a\cos^n \rho, \quad \rho = \mu(x - ct + b_0), \tag{8}$$

and

$$u(x,t) = a\sin^n \rho, \quad \rho = \mu(x - ct + b_0), \tag{9}$$

where a is the soliton amplitude, μ is the width of the soliton, c is the soliton velocity and b_0 is constant to be determined later, the unknown index n will be determined during the course of derivation of the solution of Equation (8). From Equation (8), I obtain

$$\begin{aligned}
&u^2(x,t) = a^2\cos^{2n}\rho,\\
&u_t = ac\mu n\cos^{n-1}\rho\sin\rho,\\
&u_x = -a\mu n\cos^{n-1}\rho\sin\rho,\\
&u_{2x} = -a\mu^2 n(n-2)\cos^n\rho + a\mu^2 n(n-1)\cos^{n-2}\rho,\\
&u_{3x} = -a\mu^3 n(n-1)(n-2)\cos^{n-3}\rho\sin\rho + a\mu^3 n^2(n-2)\cos^{n-1}\rho\sin\rho,\\
&u_{5x} = -a\mu^5 n(n-1)(n-2)(n-3)(n-4)\cos^{n-5}\rho\sin\rho + 2a\mu^5 n(n-1)(n-2)\left(n^2-2n+2\right)\cos^{n-3}\rho\sin\rho\\
&\qquad - a\mu^5 n^5\cos^{n-1}\rho\sin\rho.
\end{aligned} \tag{10}$$

From Equation (9), I obtain

$$\begin{aligned}
&u^2(x,t) = a^2\sin^{2n}\rho,\\
&u_t = -ac\mu n\sin^{n-1}\rho\cos\rho,\\
&u_x = a\mu n\sin^{n-1}\rho\cos\rho,\\
&u_{2x} = -a\mu^2 n(n-2)\sin^n\rho + a\mu^2 n(n-1)\sin^{n-2}\rho,\\
&u_{3x} = a\mu^3 n(n-1)(n-2)\sin^{n-3}\rho\cos\rho - a\mu^3 n^2(n-2)\sin^{n-1}\rho\cos\rho,\\
&u_{5x} = a\mu^5 n(n-1)(n-2)(n-3)(n-4)\sin^{n-5}\rho\cos\rho - 2a\mu^5 n(n-1)(n-2)\left(n^2-2n+2\right)\sin^{n-3}\rho\cos\rho\\
&\qquad + a\mu^5 n^5\sin^{n-1}\rho\cos\rho.
\end{aligned} \tag{11}$$

With the aid of Mathematica or Maple, from (8) and (10), we can get

$$\begin{aligned}
&u_t - u_{5x} - 5uu_{3x} - \frac{25}{2}u_x u_{2x} - 5u^2 u_x = ac\mu n\cos^{n-1}\rho\sin\rho + a\mu^5 n(n-1)(n-2)(n-3)(n-4)\cos^{n-5}\rho\sin\rho\\
&-2a\mu^5 n(n-1)(n-2)\left(n^2-2n+2\right)\cos^{n-3}\rho\sin\rho + a\mu^5 n^5\cos^{n-1}\rho\sin\rho + 5a^2\mu^3 n(n-1)(n-2)\cos^{2n-3}\rho\sin\rho\\
&-5a^2\mu^3 n^2(n-2)\cos^{2n-1}\rho\sin\rho - \frac{25}{2}a^2\mu^3 n^2(n-2)\cos^{2n-1}\rho\sin\rho + \frac{25}{2}a^2\mu^3 n^2(n-1)\cos^{2n-3}\rho\sin\rho\\
&+5a^3\mu n\cos^{3n-1}\rho\sin\rho = 0
\end{aligned} \tag{12}$$

Now, from Equation (12) equating the exponents $n-5$ and $2n-3$ leads $n-5=2n-3$, which gives $n=-2$, such that $n(n-1)(n-2)(n-3)(n-4)\neq 0$.

Also from Equation (12) equating the coefficients of like powers of $\cos^{-3}\rho\sin\rho$, $\cos^{-5}\rho\sin\rho$ and $\cos^{-7}\rho\sin\rho$ to zero, I get

$$ac\mu n + a\mu^5 n^5 = 0, \tag{13}$$

$$-2a\mu^5 n(n-1)(n-2)\left(n^2-2n+2\right) - 5a^2\mu^3 n^2(n-2) - \frac{25}{2}a^2\mu^3 n^2(n-2) = 0, \tag{14}$$

$$a\mu^5 n(n-1)(n-2)(n-3)(n-4) + 5a^2\mu^3 n(n-1)(n-2) + \frac{25}{2}a^2\mu^3 n^2(n-1) + 5a^3\mu n = 0. \tag{15}$$

Solving the above system by the aid of Wu elimination method [31], I obtain the three solutions

$$a = -\frac{12}{7}\mu^2, \quad c = -16\mu^4, \tag{16}$$

and

$$a = -3\mu^2, \quad c = -16\mu^4, \tag{17}$$

and

$$a = -24\mu^2, \quad c = -16\mu^4. \tag{18}$$

Then the soliton solutions of the Kaup-Kupershmidt Equation is given by

$$u_1(x,t) = -\frac{12}{7}\mu^2\sec^2\mu\left(x+16\mu^4 t + b_0\right), \text{ see **Figure 1** and **Figure 2**} \tag{19}$$

and

$$u_2(x,t) = -3\mu^2\sec^2\mu\left(x+16\mu^4 t + b_0\right), \text{ see **Figure 3** and **Figure 4**} \tag{20}$$

and

$$u_3(x,t) = -24\mu^2\sec^2\mu\left(x+16\mu^4 t + b_0\right). \text{ see **Figure 5** and **Figure 6**} \tag{21}$$

If setting $\mu = i\sigma$, then the solutions (19) and (21) are given by

$$u_4(x,t) = \frac{12}{7}\sigma^2\operatorname{sech}^2\sigma\left(x+16\sigma^4 t + b_0\right), \text{ see **Figure 7** and **Figure 8**} \tag{22}$$

and

$$u_5(x,t) = 3\sigma^2\operatorname{sech}^2\sigma\left(x+16\sigma^4 t + b_0\right), \text{ see **Figure 9** and **Figure 10**} \tag{23}$$

and

$$u_6(x,t) = 24\sigma^2\operatorname{sech}^2\sigma\left(x+16\sigma^4 t + b_0\right). \text{ see **Figure 11** and **Figure 12**} \tag{24}$$

The double-kink solutions (19), (20), and (21) are characterized by the eigenvalue $\mu=1$ (see **Figures 1-6**). The solutions (22), (23) and (24) are the single-soliton solutions (see **Figures 7-12**) corresponding to the eigenvalue $\sigma=1$.

4. Conclusions

The new types of exact traveling wave solution obtained in this paper for the Kaup-Kupershmidt Equation will

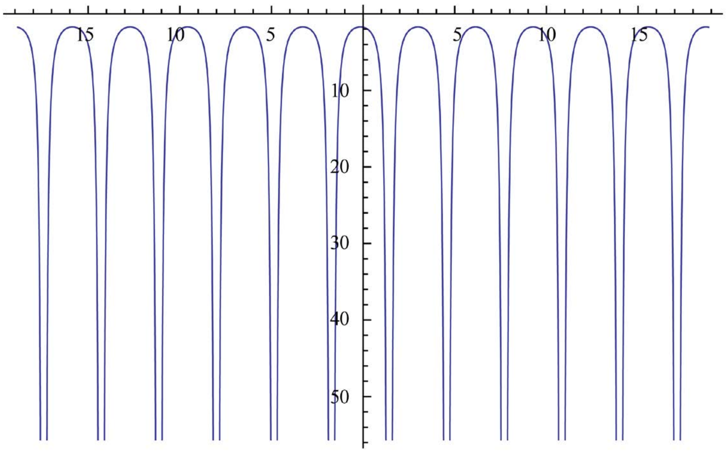

Figure 1. See [6]: solution u_1 is shown at $t = 1$, $\mu = 1$ and $b_0 = 3$.

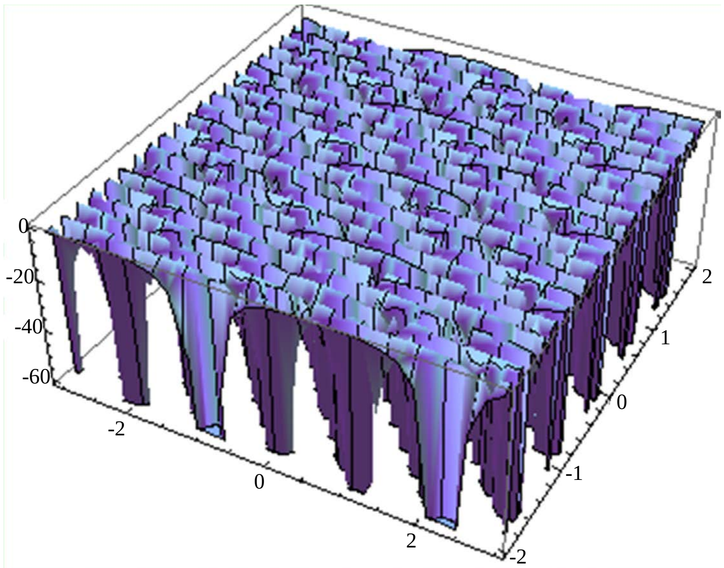

Figure 2. See [20]: solution u_1 is shown at $\mu = 1$ and $b_0 = 3$.

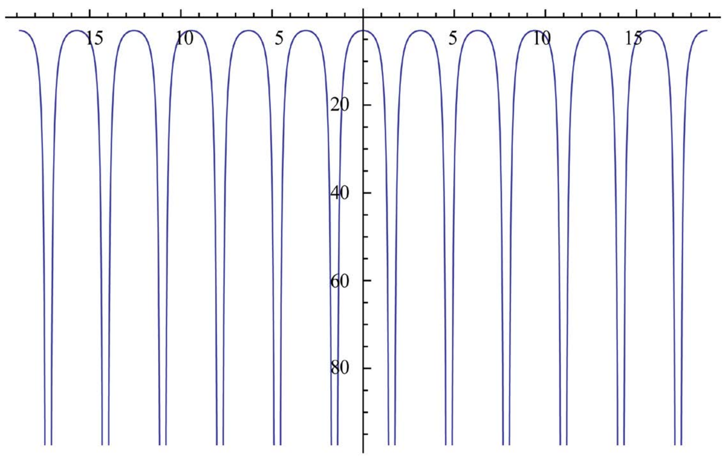

Figure 3. See [6]: solution u_2 is shown at $t = 0$, $\mu = 1$ and $b_0 = 0$.

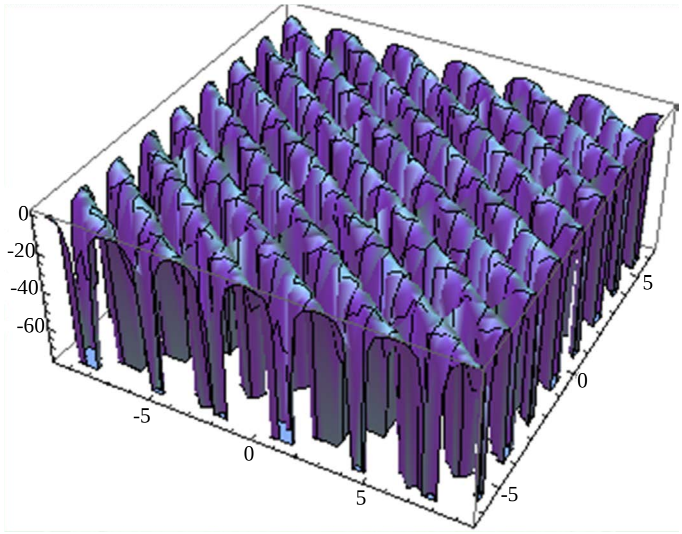

Figure 4. See [20]: solution u_2 is shown at $\mu = 1$ and $b_0 = -3$.

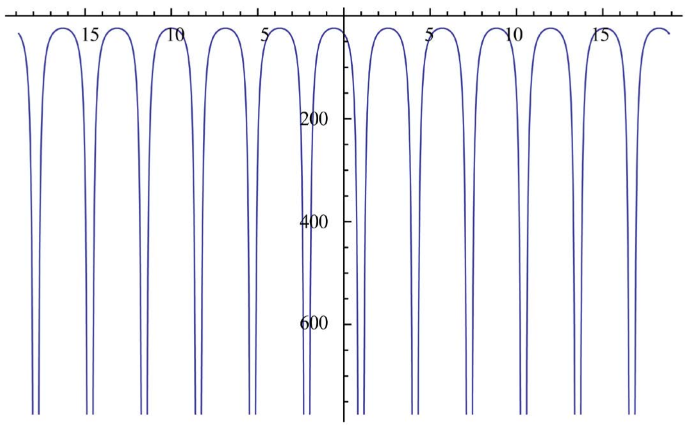

Figure 5. See [6]: solution u_3 is shown at $t = 2$, $\mu = 1$ and $b_0 = 0$.

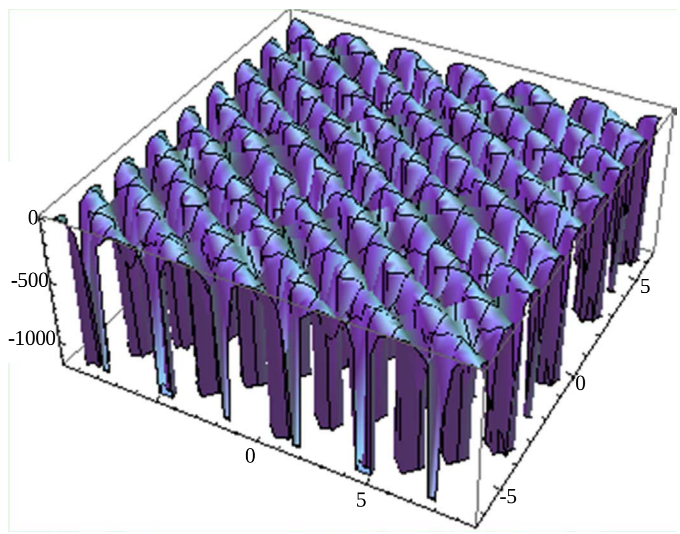

Figure 6. See [20]: solution u_3 is shown at $\mu = 1$ and $b_0 = 0$.

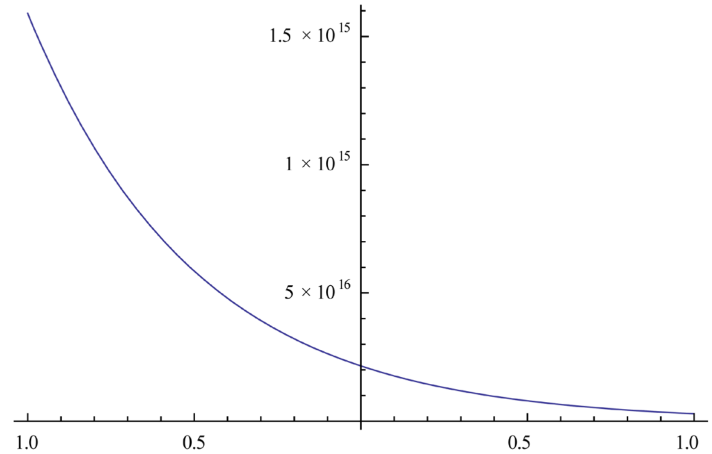

Figure 7. See [6]: solution u_4 is shown at $t=1$, $\sigma=1$ and $b_0=3$.

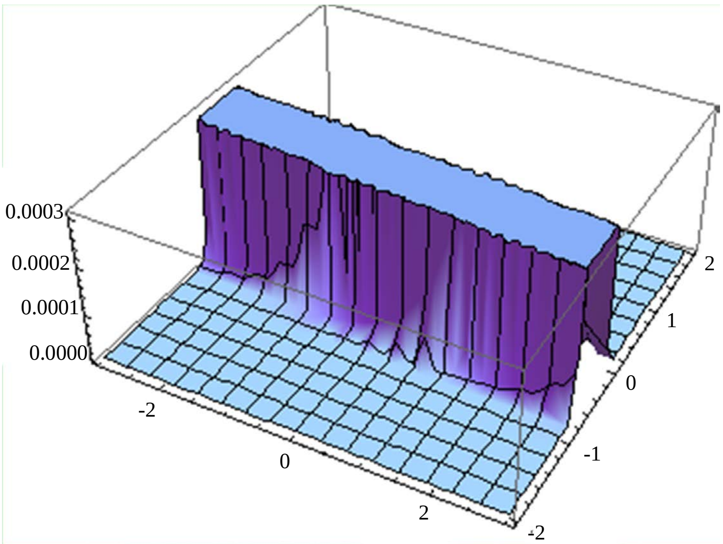

Figure 8. See [20]: solution u_4 is shown at $\sigma=1$ and $b_0=3$.

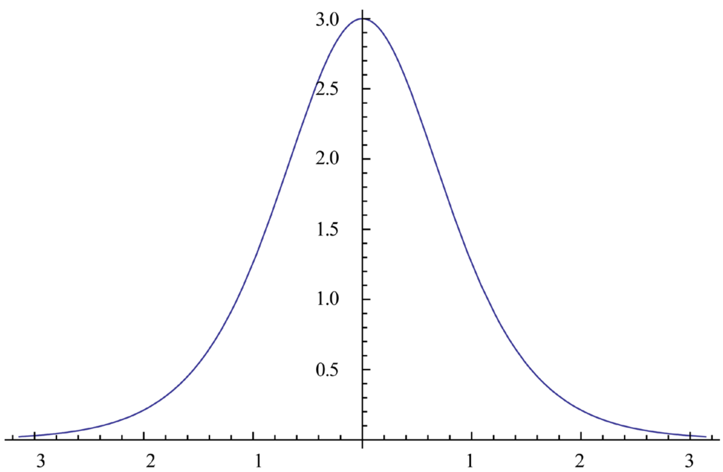

Figure 9. See [6]: solution u_5 is shown at $t=0$, $\sigma=1$ and $b_0=0$.

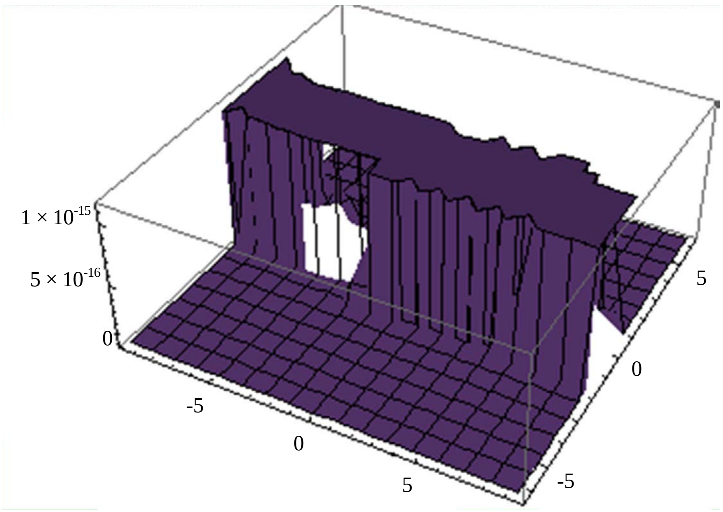

Figure 10. See [20]: solution u_5 is shown at $\sigma = 1$ and $b_0 = -3$.

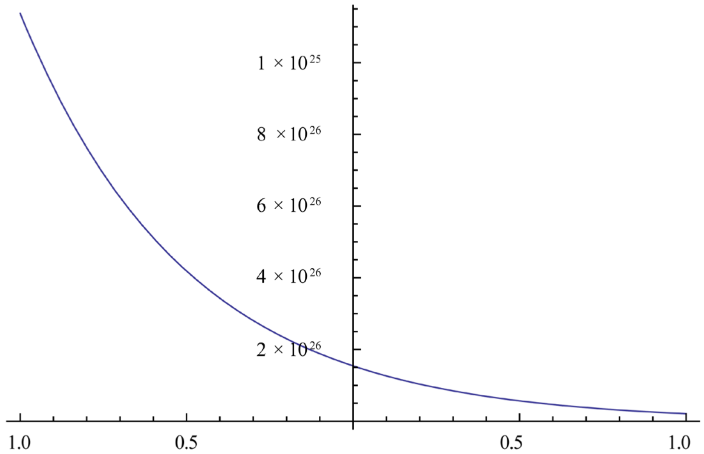

Figure 11. See [6]: solution u_6 is shown at $t = 2$, $\sigma = 1$ and $b_0 = 0$.

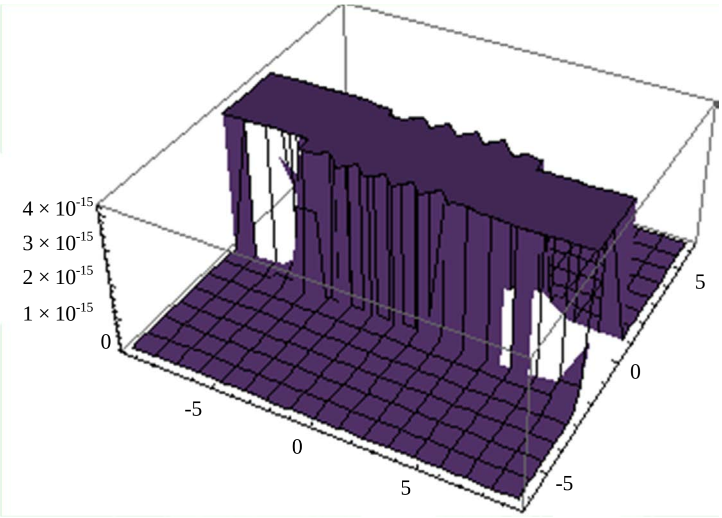

Figure 12. See [20]: solution u_6 is shown at $\sigma = 1$ and $b_0 = 0$.

be of benefit to future studies.

The Soliton Equations play a central role in the field of integrable systems and also play a fundamental role in several other areas of mathematics and physics.

A soliton is a localized pulse-like nonlinear wave that possesses remarkable stability properties. Typically, problems that admit soliton solutions are in the form of evolution equations that describe how some variable or a set of variables evolves in time from a given state. The equations may take a variety of forms, for example, PDEs, differential difference equations, partial difference equations, integro-differential equations, as well as coupled ODEs of finite order.

In this paper, we considered the construction of exact solutions to Kaup-Kupershmidt Equation. I obtain travelling wave solutions for the above equation by using the modified sine-cosine method with the aid of Mathematica.

A travelling wave of permanent form has already been met; this is the solitary wave solution of the nonlinear evolution equation itself. Such a wave is a special solution of the governing equation which does not change its shape and propagates at constant speed.

The soliton phenomena of nonlinear evolution equations represent an important and well-established field of modern physics, mathematical physics and applied mathematics. Solitons are found in various areas of physics from hydrodynamics and plasma physics, nonlinear optics and solid state physics, to field theory and gravitation. NLEEs which describe soliton phenomena have a universal character.

Funding

This research is funded by the Deanship of Research and Graduate Studies in Zarqa University/Jordan.

References

[1] Rogers, C. and Schief, W.F. (2002) Bäcklund and Darboux Transformations, Geometry and Modern Applications in Soliton Theory. In: Ablowitz, M.J., Eds., *Cambridge Texts in Applied Mathematics*, Cambridge University Press, Cambridge.

[2] Matveev, V.A. and Salle, M.A. (1991) Darboux Transformation and Solitons. Springer-Verlag, Berlin. http://dx.doi.org/10.1007/978-3-662-00922-2

[3] Sayed, S.M. and Gharib, G.M. (2009) Canonical Reduction of Self-Dual Yang-Mills Equations to Fitzhugh-Nagumo Equation and Exact Solutions. *Chaos, Solitons & Fractals*, **39**, 492-498. http://dx.doi.org/10.1016/j.chaos.2007.01.076

[4] Klingenberg, W. (1982) Riemannian Geometry. Walter de Gruyter, Berlin, New York.

[5] Bracken, P. (2010) Surfaces Specified by Integrable Systems of Partial Differential Equations Determined by Structure Equations and Lax Pair. *Journal of Geometry and Physics*, **60**, 562-569. http://dx.doi.org/10.1016/j.geomphys.2009.12.004

[6] Abolwitz, M.J. and Clarkson, P.A. (1991) Solitons, Nonlinear Evolution Equation and Inverse Scattering. Cambridge University Press, Cambridge. http://dx.doi.org/10.1017/CBO9780511623998

[7] Rogers, C. and Wong, P. (1984) On Reciprocal Bäcklund Transformations of Inverse Scattering Schemes. *Physica Scripta*, **30**, 10-14. http://dx.doi.org/10.1088/0031-8949/30/1/003

[8] Wazwaz, A.M. (2006) Two Reliable Methods for Solving Variants of the KdV Equation with Compact and Noncompact Structures. *Chaos, Solitons & Fractals*, **28**, 454-462. http://dx.doi.org/10.1016/j.chaos.2005.06.004

[9] Geng, X.G. and Wang, H. (2013) Coupled Camassa-Holm Equations—Peakons and Infinitely Many Conservation Laws. *Journal of Mathematical Analysis and Applications*, **403**, 262-271. http://dx.doi.org/10.1016/j.jmaa.2013.02.030

[10] Khater, A.H., Callebaut, D.K. and Sayed, S.M. (2004) Conservation Laws for Some Nonlinear Evolution Equations Which Describe Pseudo-Spherical Surfaces. *Journal of Geometry and Physics*, **51**, 332-352. http://dx.doi.org/10.1016/j.geomphys.2003.11.009

[11] Cavalcante, J.A. and Tenenblat, K. (1988) Conservation Laws for Nonlinear Evolution Equations. *Journal of Mathematical Physics*, **29**, 1044-1059. http://dx.doi.org/10.1063/1.528020

[12] Beals, R., Rabelo, M. and Tenenblat, K. (1989) Bӑcklund Transformations and Inverse Scattering Solutions for Some Pseudo-Spherical Surfaces. *Studies in Applied Mathematics*, **81**, 125-134.

[13] Reyes, E.G. (2000) Conservation Laws and Calapso-Guichard Deformations of Equations Describing Pseudo-Spherical Surfaces. *Journal of Mathematical Physics*, **41**, 2968-2979. http://dx.doi.org/10.1063/1.533284

[14] Reyes, E.G. (2001) On Geometrically Integrable Equations and Hierarchies of Pseudo-Spherical Type. *Contemporary*

Mathematics, **285**, 145-156.

[15] Chern, S.S. and Tenenblat, K. (1986) Pseudospherical Surfaces and Evolution Equations. *Studies in Applied Mathematics*, **74**, 55-83.

[16] Khater, A.H., Callebaut, D.K., Abdalla, A.A., Shehata, A.R. and Sayed, S.M. (1999) Bäcklund Transformations and Exact Solutions for Self-Dual *SU*(3) Yang-Mills Equations. *IL Nuovo Cimento B*, **114**, 1-10.

[17] Qu, C., Si, Y. and Liu, R. (2003) On Affine Sawada-Kotera Equation. *Chaos*, *Solitons & Fractals*, **15**, 131-139. http://dx.doi.org/10.1016/S0960-0779(02)00121-2

[18] Wright, O.C. (2003) The Darboux Transformation of Some Manakov Systems. *Applied Mathematics Letters*, **16**, 647-652. http://dx.doi.org/10.1016/S0893-9659(03)00061-2

[19] Hirota, R. (2004) The Direct Method in Soliton Theory. Cambridge University Press, Cambridge. http://dx.doi.org/10.1017/CBO9780511543043

[20] Khater, A.H., Callebaut, D.K. and Sayed, S.M. (2006) Exact Solutions for Some Nonlinear Evolution Equations Which Describe Pseudo-Spherical Surfaces. *Journal of Computational and Applied Mathematics*, **189**, 387-411. http://dx.doi.org/10.1016/j.cam.2005.10.007

[21] Liu, S.K., Fu, Z.T., Liu, S.D. and Zhao, Q. (2001) Jacobi Elliptic Function Expansion Method and Periodic Wave Solutions of Nonlinear Wave Equations. *Physics Letters A*, **289**, 69-74. http://dx.doi.org/10.1016/S0375-9601(01)00580-1

[22] Fan, E. (2000) Extended Tanh-Function Method and Its Applications to Nonlinear Equations. *Physics Letters A*, **277**, 212-218. http://dx.doi.org/10.1016/S0375-9601(00)00725-8

[23] Malfliet, W. and Hereman, W. (1996) The Tanh Method: I. Exact Solutions of Nonlinear Evolution and Wave Equations. *Physica Scripta*, **54**, 569-575.

[24] Chadan, K. and Sabatier, P.C. (1977) Inverse Problems in Quantum Scattering Theory. Springer, New York. http://dx.doi.org/10.1007/978-3-662-12125-2

[25] Ablowitz, M.J., Chakravarty, S. and Halburd, R. (1998) On Painlevé and Darboux-Halphen Type Equations. In: Conte, R., Ed., *The Painlevé Property*: *One Century Later*, CRM Series in Mathematical Physics, Springer, Berlin.

[26] Al-Ali, E.M. (2013) Traveling Wave Solutions for a Generalized Kawahara and Hunter-Saxton Equations. *International Journal of Mathematical Analysis*, **7**, 1647-1666.

[27] Sayed, S.M. (2013) The Bäcklund Transformations, Exact Solutions, and Conservation Laws for the Compound Modified Korteweg-de Vries-Sine-Gordon Equations Which Describe Pseudospherical Surfaces. *Journal of Applied Mathematics*, **2013**, Article ID: 613065. http://dx.doi.org/10.1155/2013/613065

[28] Matveev, V.B. and Salle, M.A. (1991) Darboux Transformations and Solitons. Springer-Verlag, Berlin.

[29] Tenenblat, K. (1998) Transformations of Manifolds and Applications to Differential Equations. Pitman Monographs and Surveys in Pure and Applied Mathematics 93, Addison Wesley Longman, England.

[30] Wazwaz, A.M. (2004) New Compactons, Solitons and Periodic Solutions for Nonlinear Variants of the KdV and the KP Equations. *Chaos*, *Solitons & Fractals*, **22**, 249-260. http://dx.doi.org/10.1016/j.chaos.2004.01.005

[31] Wu, W.T. (1994) Polynomial Equations-Solving and Its Applications. In: *Algorithms and Computation*, *Lecture Notes in Computer Science* 834, Springer-Verlag, Berlin, 1-9.

Applied Mathematics, 2015, 6, 173-181
Published Online January 2015 in SciRes. http://www.scirp.org/journal/am
http://dx.doi.org/10.4236/am.2015.61017

Necessary Conditions for the Application of Moving Average Process of Order Three

O. E. Okereke[1], I. S. Iwueze[2], J. Ohakwe[3]

[1]Department of Statistics, Michael Okpara University of Agriculture, Umudike, Nigeria
[2]Department of Statistics, Federal University of Technology, Owerri, Nigeria
[3]Department of Mathematical, Computer and Physical Sciences, Federal University, Otueke, Nigeria
Email: emmastat5000@yahoo.co.uk

Received 26 November 2014; accepted 12 December 2014; published 19 January 2015

Abstract

Invertibility is one of the desirable properties of moving average processes. This study derives consequences of the invertibility condition on the parameters of a moving average process of order three. The study also establishes the intervals for the first three autocorrelation coefficients of the moving average process of order three for the purpose of distinguishing between the process and any other process (linear or nonlinear) with similar autocorrelation structure. For an invertible moving average process of order three, the intervals obtained are $\frac{-1-\sqrt{5}}{4} < \rho_1 < \frac{1-\sqrt{5}}{4}$**,** $-0.5 < \rho_2 < 0.5$ **and** $-0.5 < \rho_1 < 0.5$**.**

Keywords

Moving Average Process of Order Three, Characteristic Equation, Invertibility Condition, Autocorrelation Coefficient, Second Derivative Test

1. Introduction

Moving average processes (models) constitute a special class of linear time series models. A moving average process of order q ($\mathrm{MA}(q)$ process) is of the form:

$$X_t = \theta_1 e_{t-1} + \theta_2 e_{t-2} + \cdots + \theta_q e_{t-q} + e_q \tag{1.1}$$

where $\theta_1, \theta_2, \cdots, \theta_q$ are real constants and e_t, $t \in Z$ is a sequence of independent and identically distributed random variables with zero mean and constant variance. These processes have been widely used to model

How to cite this paper: Okereke, O.E., Iwueze, I.S. and Ohakwe, J. (2015) Necessary Conditions for the Application of Moving Average Process of Order Three. *Applied Mathematics*, **6**, 173-181. http://dx.doi.org/10.4236/am.2015.61017

time series data from many fields [1]-[3]. The model in (1.1) is always stationary. Hence, a required condition for the use of the moving average process is that it is invertible. Let $B^m e_t = e_{t-m}$, then the model in (1.1) is invertible if the roots of the characteristic equation

$$1+\theta_1 B+\theta_2 B^2+\cdots+\theta_q B^q=0 \tag{1.2}$$

lie outside the unit circle. The invertibility conditions of the first order and second order moving average models have been derived [4] [5].

Ref. [6] used a moving average process of order three (MA (3) process) in his simulation study. Though, higher order moving average processes have been used to model time series data, not much has been said about the properties of their autocorrelation functions. This study focuses on the invertibility condition of an MA (3) process. Consideration is also given to the properties of its autocorrelation coefficients of an invertible moving average process of order three.

2. Consequence of Invertibility Condition on the Parameters of an MA (3) Process

For $q=3$, the following moving average process of order 3 is obtained from (1.1):

$$X_t=\theta_1 e_{t-1}+\theta_2 e_{t-2}+\theta_3 e_{t-3}+e_t \tag{2.1}$$

The characteristic equation corresponding to (2.1) is given by

$$1+\theta_1 B+\theta_2 B^2+\theta_3 B^3=0 \tag{2.2}$$

Dividing (2.2) by θ_3 yields

$$B^3+\frac{\theta_2}{\theta_3}B^2+\frac{\theta_1}{\theta_3}B+\frac{1}{\theta_3}=0 \tag{2.3}$$

It is important to know that (2.2) is a cubic equation. Detailed information on how to solve cubic equations can be found in [7] [8] among others. It has been a common tradition to consider the nature of the roots of a characteristic equation while determining the invertibility condition of a time series model [9]. As a cubic equation, (2.2) may have three distinct real roots, one real root and two complex roots, two real equal roots or three real equal roots. The nature of the roots of (2.2) is determined with the help of the discriminant [8]

$$D=D_1^2-D_2^3 \tag{2.4}$$

where

$$D_1=\frac{2\left(\frac{\theta_2}{\theta_3}\right)^3-9\left(\frac{\theta_2}{\theta_3}\right)\left(\frac{\theta_1}{\theta_3}\right)+27\left(\frac{1}{\theta_3}\right)}{54} \tag{2.5}$$

and

$$D_2=\frac{\left(\frac{\theta_2}{\theta_3}\right)^2-3\left(\frac{\theta_1}{\theta_3}\right)}{9} \tag{2.6}$$

If $D<0$, (2.2) has the following distinct roots [7]

$$x_1=-2\sqrt{D_2}\cos\left(\frac{\theta}{3}\right)-\frac{\theta_2}{3}, \tag{2.7}$$

$$x_2=-2\sqrt{D_2}\cos\left(\frac{\theta+2\pi}{3}\right)-\frac{\theta_2}{3}, \tag{2.8}$$

and

$$x_3 = -2\sqrt{D_2}\cos\left(\frac{\theta - 2\pi}{3}\right) - \frac{\theta_2}{3}. \tag{2.9}$$

where θ is measured in radians and $\theta = \cos^{-1}\left(\frac{D_1}{\sqrt{D_2^3}}\right)$.

When $D > 0$, (2.2) has only real root given by [1] as

$$x_1 = \sqrt[3]{-D_1 + \sqrt{D}} + \sqrt[3]{-D_1 - \sqrt{D}} - \frac{\theta_2}{3} \tag{2.10}$$

The other roots are [8]

$$x_2,\ x_3 = \frac{-(ax_1 + b) \pm \sqrt{(ax_1 + b)^2 - 4a(ax_1^2 + bx_1 + c)}}{2a} \tag{2.11}$$

If $D_1 \neq 0$, $D_2 \neq 0$ and $D_1^2 = D_2^3$, then $D = 0$ and (2.2) has two equal roots. The roots of (2.2) in this case, are the same as (2.7), (2.8) and (2.9). For $D = 0$ and $D_1 = D_2 = 0$, (2.2) has three real equal roots. Each of these roots is given by [8] as

$$x = \frac{-\theta_2}{3\theta_3} \tag{2.12}$$

For (2.1) to be invertible, the roots of (2.2) are all expected to lie outside the unit circle and $|\theta_3| < 1$. In the following theorem, the invertibility conditions of an MA (3) process are given subject to the condition that the corresponding characteristic equation has three real equal roots.

Theorem 1. If the characteristic equation $1 + \theta_1 B + \theta_2 B^2 + \theta_3 B^3 = 0$ has three real equal roots, then the moving average process of order three $X_t = \theta_1 e_{t-1} + \theta_2 e_{t-2} + \theta_3 e_{t-3} + e_t$ is invertible if

$$\theta_2 - 3\theta_3 > 0,\ \ \theta_2 + 3\theta_3 < 0 \ \text{ and } \ |\theta_3| < 1.$$

Proof

For invertibility, we expect each of the three real equal roots to lie outside the unit circle. Thus,

$$\left|\frac{-\theta_2}{3\theta_3}\right| > 1 \Rightarrow \frac{-\theta_2}{3\theta_3} < -1 \ \text{ or } \ \frac{-\theta_2}{3\theta_3} > 1$$

Solving the inequality $\frac{-\theta_2}{3\theta_3} < -1$, we obtain

$$\theta_2 - 3\theta_3 > 0$$

For $\frac{-\theta_2}{3\theta_3} > 1$, we have

$$\theta_2 + 3\theta_3 < 0$$

Since each of the roots lie outside the unit circle, the absolute value of their product must therefore be greater than one. Hence,

$$|\theta_3| < 1$$

This completes the proof.

The invertibility region of a moving average of order three with equal roots of the characteristic Equation (2.2) is enclosed by triangle OAB in **Figure 1**.

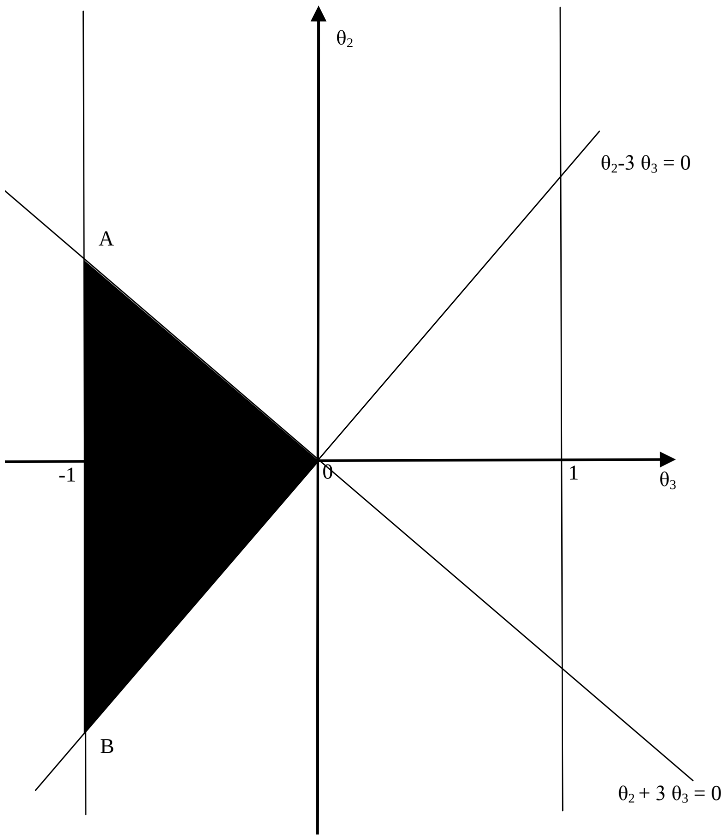

Figure 1. Invertibility region of an MA (3) process when the characteristic equation has three real equal roots.

3. Identification of Moving Average Process

Model identification is a crucial aspect of time series analysis. A common practice is to examine the structures of the autocorrelation function (ACF) and partial autocorrelation function (PACF) of a given time series. In this regard, a time series is said to follow a moving average process of order q if its associated autocorrelation function cut off after lag q and the corresponding partial autocorrelation function decays exponentially [10]. Authors using this method, believe that each process has unique ACF representation. However, the existence of similar autocorrelation structures between moving average process and pure diagonal bilinear time series process of the same order makes it difficult to identify a moving average process based on the pattern of its ACF. Furthermore, a careful look at the autocorrelation function of the square of a time series can help one determine if the series follows a moving average process. If the series can be generated by a moving average process, then its square follows a moving average process of the same order [11] [12]. The conditions under which we use the autocorrelation function to distinguish among processes behaving like moving average processes of order one and two have been determined by [13] [14] respectively. These conditions are all defined in terms of the extreme values of autocorrelation coefficients of the processes.

4. Intervals for Autocorrelation Coefficients of a Moving Average Process of Order Three

As stated in Section 3, knowledge of the extreme values of the autocorrelation coefficient of a moving average process of a particular order can enable us ensure proper identification of the process. It has been observed that for a moving average process of order one, $-0.5 \le \rho_1 \le 0.5$ [15] while for a moving average process of order two $-\frac{\sqrt{2}}{2} \le \rho_1 \le \frac{\sqrt{2}}{2}$ and $-0.5 \le \rho_2 \le 0.5$ [5]. In order to generalize about the range of values of ρ_q for a moving average process of order q, it is worthwhile to determine the range values of ρ_3 for a moving average process of order three. The model in (2.1) has the following autocorrelation function [10]:

$$\rho_k = \begin{cases} 1, & k = 0 \\ \dfrac{\theta_1 + \theta_1\theta_2 + \theta_2\theta_3}{1 + \theta_1^2 + \theta_2^2 + \theta_3^2}, & k = \pm 1 \\ \dfrac{\theta_2 + \theta_1\theta_3}{1 + \theta_1^2 + \theta_2^2 + \theta_3^2}, & k = \pm 2 \\ \dfrac{\theta_3}{1 + \theta_1^2 + \theta_2^2 + \theta_3^2}, & k = \pm 3 \\ 0, & k \neq \pm 1, \pm 2, \pm 3 \end{cases} \tag{4.1}$$

We can deduce from (4.1) that the autocorrelation function at lag one of the MA (3) process is

$$\rho_1 = \frac{\theta_1 + \theta_1\theta_2 + \theta_2\theta_3}{1 + \theta_1^2 + \theta_2^2 + \theta_3^2} \tag{4.2}$$

Using the Scientific Note Book, the minimum and maximum values of ρ_1 are found to be $\dfrac{-1-\sqrt{5}}{4}$ and $\dfrac{1-\sqrt{5}}{4}$ respectively. For the autocorrelation function at lag two, we have

$$\rho_2 = \frac{\theta_2 + \theta_1\theta_3}{1 + \theta_1^2 + \theta_2^2 + \theta_3^2} \tag{4.3}$$

The extreme values of ρ_2 are equally obtained with the help of the Scientific Note Book. To this effect, ρ_2 has a minimum value of −0.5 and a maximum value of 0.5.

From (4.1), we obtain

$$\rho_3 = \frac{\theta_3}{1 + \theta_1^2 + \theta_2^2 + \theta_3^2} \tag{4.4}$$

Based on the result obtained from the Scientific Notebook, ρ_3 has a minimum value of −0.5 and a maximum value of 0.5. However, the intervals for ρ_3 can easily be obtained analytically and this result is generalized in Theorem 2 for ρ_q of the MA (q) process.

The partial derivatives of ρ_3 with respect to θ_1, θ_2 and θ_3 are

$$\frac{\partial \rho_3}{\partial \theta_1} = \frac{-2\theta_1\theta_3}{\left(1 + \theta_1^2 + \theta_2^2 + \theta_3^2\right)^2} \tag{4.5}$$

$$\frac{\partial \rho_3}{\partial \theta_2} = \frac{-2\theta_2\theta_3}{\left(1 + \theta_1^2 + \theta_2^2 + \theta_3^2\right)^2} \tag{4.6}$$

$$\frac{\partial \rho_3}{\partial \theta_3} = \frac{1 + \theta_1^2 + \theta_2^2 - \theta_3^2}{\left(1 + \theta_1^2 + \theta_2^2 + \theta_3^2\right)^2} \tag{4.7}$$

The critical points of ρ_3 occurs when $\dfrac{\partial \rho_3}{\partial \theta_i} =$, $i = 1,2,3$. Equating each of the partial derivatives in (4.5), (4.6) and (4.7) to zero, we obtain

$$\theta_1\theta_3 = 0 \tag{4.8}$$

$$\theta_2\theta_3 = 0 \tag{4.9}$$

$$1+\theta_1^2+\theta_2^2-\theta_3^2 = 0 \tag{4.10}$$

From (4.10), we have

$$\theta_3 = \pm\sqrt{1+\theta_1^2+\theta_2^2} \tag{4.11}$$

Using (4.8), we obtain

$$\theta_1 = 0 \tag{4.12}$$

or

$$\theta_3 = 0 \tag{4.13}$$

Substituting $\theta_1 = 0$ into (4.11) yields

$$\theta_3 = \pm\sqrt{1+\theta_2^2} \tag{4.14}$$

For $\theta_3 = -\sqrt{1+\theta_2^2}$, (4.9) becomes

$$\theta_2\left(\sqrt{1+\theta_2^2}\right) = 0$$

$$\theta_2^2\left(1+\theta_2^2\right) = 0$$

$$\theta_2 = 0 \quad \text{or} \quad \theta_2 = \pm\sqrt{-1} \tag{4.15}$$

If we also substitute $\theta_3 = \sqrt{1+\theta_2^2}$ into (4.9), we obtain

$$\theta_2 = 0 \quad \text{or} \quad \theta_2 = \pm\sqrt{-1} \tag{4.16}$$

When we substitute $\theta_1 = 0$ and $\theta_2 = 0$ into (4.11), we have $\theta_3 = \pm 1$. It is also clear that if $\theta_1 = 0$ and $\theta_2 = -\sqrt{-1}$, then $\theta_3 = 0$. Similar result is obtained when $\theta_1 = 0$ and $\theta_2 = \sqrt{-1}$.

Hence, the critical points of ρ_3 are $(0,0,-1)$, $(0,0,1)$, $\left(0,-\sqrt{-1},0\right)$ and $\left(0,\sqrt{-1},0\right)$.

The minimum and maximum values of a function occur at it critical points. To determine which of the critical points is a local minimum, local maximum or a saddle point, we shall apply the second derivative test. The second derivative test for critical points of a function of three variables $\rho_3 = f(x,y,z)$ focuses on the Hessian matrix:

$$H = \begin{bmatrix} f_{xx} & f_{xy} & f_{xz} \\ f_{xy} & f_{yy} & f_{yz} \\ f_{xz} & f_{yz} & f_{zz} \end{bmatrix} \tag{4.17}$$

where

$$f_{xx} = \frac{\partial^2\rho_3}{\partial\theta_1^2} = \frac{-2\theta_3\left(1+\theta_1^2+\theta_2^2+\theta_3^2\right)+8\theta_1\theta_3^2}{\left(1+\theta_1^2\theta_2^2\theta_3^2\right)^3} \tag{4.18}$$

$$f_{xy} = \frac{\partial^2\rho_3}{\partial\theta_1\partial\theta_2} = \frac{-8\theta_1\theta_2\theta_3}{\left(1+\theta_1^2\theta_2^2\theta_3^2\right)^3} \tag{4.19}$$

$$f_{xz} = \frac{\partial^2\rho_3}{\partial\theta_1\partial\theta_3} = \frac{-2\theta_1\left(1+\theta_1^2+\theta_2^2+\theta_3^2\right)+8\theta_1\theta_3^2}{\left(1+\theta_1^2\theta_2^2\theta_3^2\right)^3} \tag{4.20}$$

$$f_{yy} = \frac{-2\theta_3\left(1+\theta_1^2+\theta_2^2+\theta_3^2\right)+8\theta_2^2\theta_3}{\left(1+\theta_1^2\theta_2^2\theta_3^2\right)^3} \tag{4.21}$$

$$f_{yz} = \frac{-2\theta_2\left(1+\theta_1^2+\theta_2^2+\theta_3^2\right)+8\theta_2\theta_3^2}{\left(1+\theta_1^2\theta_2^2\theta_3^2\right)^3} \tag{4.22}$$

$$f_{zz} = \frac{-2\theta_3\left(1+\theta_1^2\theta_2^2\theta_3^2\right)-4\theta_3\left(1+\theta_1^2+\theta_2^2-\theta_3^2\right)}{\left(1+\theta_1^2\theta_2^2\theta_3^2\right)^3} \tag{4.23}$$

Let (a,b,c) be a critical point of $\rho_3 = f(x,y,z)$. Then (a,b,c) is called a local minimum point if at (a,b,c), $\Delta_1 = f_{xx} > 0$, $\Delta_2 = \begin{vmatrix} f_{xx} & f_{xy} \\ f_{xy} & f_{yy} \end{vmatrix} > 0$ and $\Delta_3 = |H| > 0$ [16]. If $f_{xx} < 0$, $\Delta_2 > 0$ and $\Delta_3 < 0$ at (a,b,c), then (a,b,c) represents a local maximum.

A critical point that is neither a local minimum nor a local maximum is called a saddle point.

Though ρ_3 has four critical points, it is not defined at $\left(0,-\sqrt{-1},0\right)$ and $\left(0,\sqrt{-1},0\right)$. We then focus on the classification of the two remaining critical points.

At $(0,0,-1)$

$$H = \begin{bmatrix} \frac{1}{2} & 0 & 0 \\ 0 & \frac{1}{2} & 0 \\ 0 & 0 & \frac{1}{2} \end{bmatrix}$$

Hence, $\Delta_1 = \frac{1}{2} > 0$, $\Delta_2 = \begin{vmatrix} \frac{1}{2} & 0 \\ 0 & \frac{1}{2} \end{vmatrix} = \frac{1}{4} > 0$ and $\Delta_3 = \begin{vmatrix} \frac{1}{2} & 0 & 0 \\ 0 & \frac{1}{2} & 0 \\ 0 & 0 & \frac{1}{2} \end{vmatrix} = \frac{1}{8} > 0$.

Therefore, $(0,0,-1)$ is a local minimum. The value of ρ_3 at this point is -0.5.

For the critical points $(0,0,1)$, we have

$$H = \begin{bmatrix} -\frac{1}{2} & 0 & 0 \\ 0 & -\frac{1}{2} & 0 \\ 0 & 0 & -\frac{1}{2} \end{bmatrix}$$

Consequently,

$$\Delta_1 = -\frac{1}{2} < 0,$$

$$\Delta_2 = \begin{vmatrix} -\frac{1}{2} & 0 \\ 0 & -\frac{1}{2} \end{vmatrix} = \frac{1}{4} > 0$$

and

$$\Delta_3 = \begin{vmatrix} -\frac{1}{2} & 0 & 0 \\ 0 & -\frac{1}{2} & 0 \\ 0 & 0 & -\frac{1}{2} \end{vmatrix} = -\frac{1}{8} < 0.$$

We therefore conclude that $(0,0,1)$ is a local maximum. The maximum value of ρ_3 obtained at $(0,0,1)$ is 0.5.

We can deduce from the result in this section and other previous works that for MA (1) process $|\rho_1| \le 0.5$, while for MA (2) process and MA (3) process $|\rho_2| \le 0.5$ and $|\rho_3| \le 0.5$ respectively.

In what follows, we establish the bounds for ρ_q, where q is order of the moving average process.

Theorem 2.

Let $X_t = \theta_1 e_{t-1} + \theta_2 e_{t-2} + \cdots + \theta_q e_{t-q} + e_q$ be an MA (q) process. Then, $|\rho_q| \le 0.5$.

Proof

It is easily seen that for the MA (q) process,

$$\rho_q = \frac{\theta_q}{1+\theta_1^2+\theta_2^2+\cdots+\theta_q^2}$$

Partial derivatives of ρ_q with respect to $\rho_q = \theta_1, \theta_2, \cdots, \theta_q$ are as follows

$$\frac{\partial \rho_q}{\partial \theta_1} = \frac{-2\theta_1\theta_q}{\left(1+\theta_1^2+\theta_2^2+\cdots+\theta_q^2\right)^2},$$

$$\frac{\partial \rho_q}{\partial \theta_2} = \frac{-2\theta_2\theta_q}{\left(1+\theta_1^2+\theta_2^2+\cdots+\theta_q^2\right)^2},$$

$$\vdots$$

$$\frac{\partial \rho_q}{\partial \theta_{q-1}} = \frac{-2\theta_{q-1}\theta_q}{\left(1+\theta_1^2+\theta_2^2+\cdots+\theta_q^2\right)^2},$$

$$\frac{\partial \rho_q}{\partial \theta_q} = \frac{1+\theta_1^2+\theta_2^2+\cdots+\theta_{q-1}^2-\theta_q^2}{\left(1+\theta_1^2+\theta_2^2+\cdots+\theta_q^2\right)^2}.$$

Equating each of the partial derivatives to zero yields

$$\begin{aligned} &-2\theta_1\theta_q = 0, \\ &-2\theta_2\theta_q = 0, \\ &\quad\vdots \\ &-2\theta_{q-1}\theta_q = 0, \\ &1+\theta_1^2+\theta_2^2+\cdots+\theta_{q-1}^2-\theta_q^2 = 0. \end{aligned} \tag{4.24}$$

From (4.24), we obtain

$$\theta_q = \pm\sqrt{1+\theta_1^2+\theta_2^2+\cdots-\theta_{q-1}^2} \tag{4.25}$$

Since $\theta_q \ne 0$ for an MA (q) process, it is obvious that the $q-1$ equations preceding (4.24) are only satisfied if $\theta_1 = \theta_2 = \cdots = \theta_{q-1} = 0$. Substituting $\theta_1 = \theta_2 = \cdots = \theta_{q-1} = 0$ into (4.25) leads to $\theta_q = \pm 1$. The two critical points of ρ_q are then $(0,0,0,\cdots,-1)$ and $(0,0,0,\cdots,1)$.

At $(0,0,0,\cdots,-1)$, $\rho_q = -0.5$ while at $(0,0,0,\cdots,1)$, $\rho_q = 0.5$. It then follows that $|\rho_q| \le 0.5$.

Remark: For an invertible MA (3) process, $|\theta_3| < 1$. Hence, $\frac{-1-\sqrt{5}}{4} < \rho_1 < \frac{1-\sqrt{5}}{4}$, $-0.5 < \rho_2 < 0.5$ and $-0.5 < \rho_1 < 0.5$.

5. Conclusion

We have established necessary conditions for the parameters of an invertible MA (3) process. When the characteristic equation has three real equal roots, the conditions are $\theta_2 - 3\theta_3 > 0$, $\theta_2 + 3\theta_3 < 0$ and $|\theta_3| < 1$. Also the intervals for the autocorrelation coefficients of an invertible moving average process of order three are established. These are $\frac{-1-\sqrt{5}}{4} < \rho_1 < \frac{1-\sqrt{5}}{4}$, $-0.5 < \rho_2 < 0.5$ and $-0.5 < \rho_1 < 0.5$. It is also noteworthy that the condition on ρ_3 for an invertible MA (3) process is generalized for ρ_q of the invertible MA (q) process. That is for the invertible MA (q) process, $|\rho_q| < 0.5$. These results can now be used to compare other linear and nonlinear processes that have similar autocorrelation structures with the MA (3) process.

References

[1] Moses, R.L. and Liu, D. (1991) Optimal Nonnegative Definite Approximation of Estimated Moving Average Covariance Sequences. *IEEE Transactions on Signal Processing*, **39**, 2007-2015. http://dx.doi.org/10.1109/78.134433

[2] Qian, G. and Zhao, X. (2007) On Time Series Model Selection Involving Many Candidate ARMA Models. *Computational Statistics and Data Analysis*, **51**, 6180-6196. http://dx.doi.org/10.1016/j.csda.2006.12.044

[3] Li, Z.Y. and Li, D.G. (2008) Strong Approximation for Moving Average Processes under Dependence Assumptions. *Acta Mathematica Scientia*, **28**, 217-224. http://dx.doi.org/10.1016/S0252-9602(08)60023-5

[4] Box, G.E.P., Jenkins, G.M. and Reinsel, G.C. (1994) Time Series Analysis: Forecasting and Control. 3rd Edition, Prentice-Hall, Englewood Cliffs.

[5] Okereke, O.E., Iwueze, I.S. and Johnson, O. (2013) Extrema of Autocorrelation Coefficients for Moving Average Processes of Order Two. *Far East Journal of Theoretical Statistics*, **42**, 137-150.

[6] Al-Marshadi, A.H. (2012) Improving the Order Selection of Moving Average Time Series Model. *African Journal of Mathematics and Computer Science Research*, **5**, 102-106.

[7] Adewumi, M. (2014) Solution Techniques for Cubic Expressions and Root Finding. Courseware Module, Pennsylvania State University, Pennsylvania.

[8] Okereke, O.E., Iwueze, I.S. and Johnson, O. (2014) Some Contributions to the Solution of Cubic Equations. *British Journal of Mathematics and Computer Science*, **4**, 2929-2941. http://dx.doi.org/10.9734/BJMCS/2014/10934

[9] Wei, W.W.S. (2006) Time Series Analysis, Univariate and Multivariate Methods. 2nd Edition, Pearson Addision Wesley, New York.

[10] Chatfield, C. (1995) The Analysis of Time Series. 5th Edition, Chapman and Hall, London.

[11] Palma, W. and Zevallos, M. (2004) Analysis of the Correlation Structure of Square of Time Series. *Journal of Time Series Analysis*, **25**, 529-550. http://dx.doi.org/10.1111/j.1467-9892.2004.01797.x

[12] Iwueze, I.S. and Ohakwe, J. (2011) Covariance Analysis of the Squares of the Purely Diagonal Bilinear Time Series Models. *Brazilian Journal of Probability and Statistics*, **25**, 90-98. http://dx.doi.org/10.1214/09-BJPS111

[13] Iwueze, I.S. and Ohakwe, J. (2009) Penalties for Misclassification of First Order Bilinear and Linear Moving Average Time Series Processes. http://interstatjournals.net/Year/2009/articles/0906003.pdf

[14] Okereke, O.E. and Iwueze, I.S. (2013) Region of Comparison for Second Order Moving Average and Pure Diagonal Bilinear Processes. *International Journal of Applied Mathematics and Statistical Sciences*, **2**, 17-26.

[15] Montgomery, D.C., Jennings, C.L. and Kaluchi, M. (2008) Introduction to Time Series Analysis and Forecasting. John Wiley and Sons, New Jersey.

[16] Sittinger, B.D. (2010) The Second Derivative Test. www.faculty.csuci.edu/brian.sittinger/2nd_Derivtest.pdf

Applied Mathematics, 2015, 6, 182-194
Published Online January 2015 in SciRes. http://www.scirp.org/journal/am
http://dx.doi.org/10.4236/am.2015.61018

Novel Bounds for Solutions of Nonlinear Differential Equations

A. A. Martynyuk

S.P. Timoshenko Institute of Mechanics of NAS of Ukraine, Kyiv, Ukraine
Email: center@inmech.kiev.ua

Received 14 November 2014; accepted 1 December 2014; published 19 January 2015

Abstract

In this paper the estimates for norms of solutions to nonlinear systems are obtained via an integral inequality. As an application we considered affine control systems and systems of equations for synchronization of motions.

Keywords

Nonlinear Systems, Novel Bounds for Solutions, Stability, Synchronization

1. Introduction

The problem of estimating the norms of solutions to nonlinear systems of ordinary differential equations remains urgent due to extensive application of the latter in the description of real processes in many mechanical, physical and other nature systems. Usually, to obtain the estimates of norms of solutions to linear and weakly nonlinear equations, the Gronwall-Bellman lemma is applied (see, for example, [1]-[3] and bibliography therein). The development of the theory of nonlinear inequalities has substantially widened the possibilities for obtaining the estimates of norms of solutions to nonlinear systems and has given an impetus to their application in the qualitative theory of equations (see, for example, [4]-[6]).

Both linear and nonlinear integral inequalities are efficiently used for the development of the direct Lyapunov method, in particular, for the investigation of motion boundedness and stability of nonlinear weakly connected systems [7].

The present paper is aimed at obtaining new estimates of norms of solutions for some classes of nonlinear equations of perturbed motion. The paper is arranged as follows.

In Section 2 the statement of the problem is given in view of some results of papers [1] [3].

Section 3 presents main results on obtaining the estimates of norms of solutions for some classes of nonlinear systems of differential equations. In this regard, several results from [8] are taken into account.

How to cite this paper: Martynyuk, A.A. (2015) Novel Bounds for Solutions of Nonlinear Differential Equations. *Applied Mathematics*, **6**, 182-194. http://dx.doi.org/10.4236/am.2015.61018

In Section 4 two application problems are considered: a problem on stabilization of solutions to affine system (cf. [8]) and a problem on estimation of divergence of solutions at synchronization (cf. [9]).

In Section 5 the possibilities of application of this approach for solution of modern problems of nonlinear dynamics and systems theory are discussed.

2. Statement of the Problem

Consider a nonlinear system of ordinary differential equations of perturbed motion

$$\frac{\mathrm{d}x}{\mathrm{d}t} = A(t)x + f(t,x), \quad x(t_0) = x_0, \tag{1}$$

where $x \in \mathbb{R}^n$; $f \in C(\mathbb{R}_+ \times \mathbb{R}^n, \mathbb{R}^n)$, $A(t)$ is an $n \times n$-matrix with the elements continuous on any finite interval. It is assumed that solution $x(t) = x(t,t_0,x_0)$ of problem (1) exists and is unique for all $0 \le t < \infty$ and $(t_0, x_0) \in \mathbb{R}_+ \times \mathbb{R}^n$.

Equations of type (1) are found in many problems of mechanics (see, for example, [1] [10] and bibliography therein). Moreover, these equations may be treated as the ones describing the perturbation of the system of linear equations

$$\frac{\mathrm{d}x}{\mathrm{d}t} = A(t)x, \quad x(t_0) = x_0, \tag{2}$$

In order to establish boundedness and stability conditions for solutions of system (1) it is necessary to estimate the norms of solutions under various types of restrictions on system (2) and vector-function of nonlinearities in system (1).

The purpose of this paper is to obtain estimates of norms of solutions to some classes of nonlinear ordinary differential Equations (1) in terms of nonlinear and pseudo-linear integral inequalities.

3. Main Results

First,we shall determine the estimate of the norm of solutions $x(t)$ of system (1) under the following assumptions:

A_1. For all $t \ge 0$ there exists a nonnegative integrable function $b(t)$ such that

$$\|A(t)\| \le b(t) \quad \text{for all} \quad t \ge 0;$$

A_2. For all $t \ge t_0$ and $u \ge 0$ there exists a continuous nonnegative integrable function $w(t,u)$, $w(t,0) = 0$, such that (cf. [11])

$$\|f(t,x)\| \le w(t,\|x\|)$$

for all $(t,x) \in \mathbb{R}_+ \times \mathbb{R}^n$.

Here and elsewhere an Euclidian norm of the vector x and a spectral norm of the matrix consistent with it are used.

Theorem 1. *For system* (1) *let conditions of assumptions* A_1 *and* A_2 *be satisfied, then for any solution* $x(t) = x(t,t_0,x_0)$ *with the initial values* $x_0 : \|x\| \le c$, $0 < c < +\infty$ *the inequality*

$$\|x(t)\| \le c + \int_{t_0}^{t} \left[b(s)\|x(s)\| + w(s,\|x(s)\|) \right] \mathrm{d}s \tag{3}$$

holds for all $t \ge t_0 \ge 0$.

If there exist:

(a) *a continuous and nonnegative function* $v(t)$ *for all* $t \ge t_0$ *and*

(b) *a continuous, nonnegative and nondecreasing function* $g(u)$ *for* $u \ge 0$ *such that*

$$w\left(t, z\exp\left(\int_{t_0}^{t} b(s)\,\mathrm{d}s\right)\right)\exp\left(-\int_{t_0}^{t} b(s)\,\mathrm{d}s\right) \le v(t)g(z), \quad t \ge t_0, \quad z \ge 0,$$

then for all $t \in [t_0, \beta)$ *the inequality*

$$\|x(t)\| \le G^{-1}\left[G(c) + \int_{t_0}^{t} v(s)\,\mathrm{d}s\right] \exp\left(\int_{t_0}^{t} b(s)\,\mathrm{d}s\right), \tag{4}$$

holds true, where G^{-1} *is a function converse with respect to the function* $G(u)$:

$$G(u) - G(u_0) = \int_{u_0}^{u} \frac{\mathrm{d}s}{g(s)}, \quad 0 < u_0 \le c \le u \le \infty,$$

and the value β *is determined by the correlation*

$$\beta = \sup\left\{t \ge t_0 : G(c) + \int_{t_0}^{t} v(s)\,\mathrm{d}s \in \mathrm{dom}G^{-1}\right\}.$$

(c) *If, additionally, there exists a constant* $a^0 > 0$ *such that*

$$\int_{t_0}^{\infty} v(t)\,\mathrm{d}t \le \int_{a^0}^{\infty} \frac{\mathrm{d}s}{g(s)},$$

then inequality (4) *is satisfied for all* $t \ge t_0$, *i.e.* $\beta = \infty$ *for the values* $c \in (0, a^0)$.

Proof. Let the right-hand part of inequality (3) be equal $p(t)\exp\left(\int_{t_0}^{t} b(s)\,\mathrm{d}s\right)$. Using inequality (3) and condition (b) of Theorem 1 we get

$$\left[\frac{\mathrm{d}p}{\mathrm{d}t} + b(t)\,p(t)\right]\exp\left(\int_{t_0}^{t} b(s)\,\mathrm{d}s\right) = b(t)\|x(t)\| + w(t, \|x(t)\|)$$
$$\le \left[b(t)\,p(t) + v(t)\,g\left(\|x(t)\|\exp\left(-\int_{t_0}^{t} b(s)\,\mathrm{d}s\right)\right)\right]\exp\left(\int_{t_0}^{t} b(s)\,\mathrm{d}s\right).$$

Since the function g is nondecreasing and

$$\|x(t)\| \le p(t)\exp\left(\int_{t_0}^{t} b(s)\,\mathrm{d}s\right),$$

we get the inequality

$$\frac{\mathrm{d}p}{\mathrm{d}t} \le v(t)\,g(p(t)), \quad p(t_0) = c.$$

Hence, by the Bihari lemma (see [10], p. 110) we have

$$p(t) \le G^{-1}\left[G(c) + \int_{t_0}^{t} v(s)\,\mathrm{d}s\right],$$

for all $t \in (t_0, \beta)$. This implies estimate (4).

To prove the second assertion of Theorem 1 we note that the continuability condition for function $p(t)$ is the inequality

$$G(c) + \int_{t_0}^{\infty} v(s)\,\mathrm{d}s \le \int_{u_0}^{\infty} \frac{\mathrm{d}s}{g(s)}$$

or

$$\int_{t_0}^{\infty} v(s)\,\mathrm{d}s \le -\int_{u_0}^{c} \frac{\mathrm{d}s}{g(s)} + \int_{u_0}^{\infty} \frac{\mathrm{d}s}{g(s)} = \int_{c}^{\infty} \frac{\mathrm{d}s}{g(s)}.$$

This inequality is satisfied for any $c \in (0, a^0)$ for which condition (c) of Theorem 1 holds true. Since $c < a^0$, we have

$$\int_{t_0}^{\infty} v(s)\,\mathrm{d}s \le \int_{a_0}^{\infty} \frac{\mathrm{d}s}{g(s)} < \int_{c}^{\infty} \frac{\mathrm{d}s}{g(s)}.$$

Hence it follows that for $c \in (0, a^0)$ the value $\beta = \infty$. This proves Theorem 1.

Further we shall consider system (1) under the following assumption.

A_3. There exist a nonnegative integrable function $c(t)$ for all $t \ge t_0 \ge 0$ and a constant $\alpha > 1$ such that

$$\| f(t,x)\| \le c(t)\|x\|^{\alpha}$$

for all $(t,x) \in \mathbb{R}_+ \times \mathbb{R}^n$.

Theorem 2. *For the system of Equations* (1) *let conditions of Assumptions* A_1 *and* A_3 *be satisfied. Then for the norm of solutions* $x(t) = x(t, t_0, x_0)$ *the estimate*

$$\|x(t)\| \le \frac{\|x_0\| \exp \int_{t_0}^{t} b(s)\,\mathrm{d}s}{\left[1 - (\alpha-1)\|x_0\|^{\alpha-1} \int_{t_0}^{t} c(s) \exp\left((\alpha-1)\int_{s}^{t} b(\tau)\,\mathrm{d}\tau\right)\mathrm{d}s\right]^{\frac{1}{\alpha-1}}} \tag{5}$$

holds true for all $t \ge t_0 \ge 0$ *whenever*

$$(\alpha-1)\|x_0\|^{\alpha-1} \int_{t_0}^{t} c(s) \exp\left((\alpha-1)\int_{s}^{t} b(\tau)\,\mathrm{d}\tau\right)\mathrm{d}s < 1. \tag{6}$$

Proof. Let $x(t)$ be the solution of system of Equations (1) with the initial conditions $x(t_0) = x_0$, $t_0 \ge 0$. Under conditions A_1 and A_3 Equation (1) yields the estimate of the norm of solution $x(t)$ in the form

$$\|x(t)\| \le \|x_0\| + \int_{t_0}^{t} b(s)\|x(s)\|\,\mathrm{d}s + \int_{t_0}^{t} c(s)\|x(s)\|^{\alpha}\,\mathrm{d}s. \tag{7}$$

We transform inequality (7) to the pseudo-linear form

$$\|x(t)\| \le \|x_0\| + \int_{t_0}^{t} \left(b(s) + c(s)\|x(s)\|^{\alpha-1}\right)\|x(s)\|\,\mathrm{d}s, \tag{8}$$

and applying the Gronwall-Bellman lemma [1] arrive at the estimate

$$\|x(t)\| \le \|x_0\| \exp\left(\int_{t_0}^{t} \left(b(s) + c(s)\|x(s)\|^{\alpha-1}\right)\mathrm{d}s\right) \tag{9}$$

for all $t \ge t_0 \ge 0$.

Further, for estimation of the expression

$$\exp\left(\int_{t_0}^{t} c(s)\|x(s)\|^{\alpha-1}\,\mathrm{d}s\right)$$

the following approach is applied (cf. [8]).

Designate $\|x(t)\| = \psi(t)$ for all $t \ge t_0$ and from inequality (9) obtain

$$\psi^{\alpha-1}(t) \le \|x_0\|^{\alpha-1} \exp\left[(\alpha-1)\int_{t_0}^{t}\left(b(s)+c(s)\psi^{\alpha-1}(s)\right)\mathrm{d}s\right]. \tag{10}$$

Multiplying both parts of inequality (10) by the expression

$$-(\alpha-1)c(t)\exp\left(-(\alpha-1)\int_{t_0}^{t}c(s)\psi^{\alpha-1}(s)\mathrm{d}s\right),$$

we get

$$-(\alpha-1)c(t)\psi^{\alpha-1}(t)\exp\left[-(\alpha-1)\int_{t_0}^{t}c(s)\psi^{\alpha-1}(s)\mathrm{d}s\right] \ge -(\alpha-1)\|x_0\|^{\alpha-1}c(t)\exp\left[(\alpha-1)\int_{t_0}^{t}b(s)\mathrm{d}s\right].$$

This implies that

$$-(\alpha-1)\|x_0\|^{\alpha-1}c(t)\exp\left[(\alpha-1)\int_{t_0}^{t}b(s)\mathrm{d}s\right] \le \frac{\mathrm{d}}{\mathrm{d}t}\left[\exp\left(-(\alpha-1)\int_{t_0}^{t}c(s)\psi^{\alpha-1}(s)\mathrm{d}s\right)\right].$$

Integrating the obtained inequality between the limits t_0 and t we arrive at

$$1-(\alpha-1)\|x_0\|^{\alpha-1}\int_{t_0}^{t}c(s)\exp\left[(\alpha-1)\int_{t_0}^{s}b(\tau)\mathrm{d}\tau\right]\mathrm{d}s \le \exp\left[-(\alpha-1)\int_{t_0}^{t}c(s)\psi^{\alpha-1}(s)\mathrm{d}s\right].$$

Under condition (6) this estimate implies

$$\exp\left[(\alpha-1)\int_{t_0}^{t}c(s)\psi^{\alpha-1}(s)\mathrm{d}s\right] \le \frac{1}{1-(\alpha-1)\|x_0\|^{\alpha-1}\int_{t_0}^{t}c(s)\exp\left((\alpha-1)\int_{s}^{t}b(\tau)\mathrm{d}\tau\right)\mathrm{d}s}.$$

Moreover, inequality (10) becomes

$$\psi^{\alpha-1}(t) \le \|x_0\|^{\alpha-1}\frac{\exp\left[(\alpha-1)\int_{t_0}^{t}b(s)\mathrm{d}s\right]}{1-(\alpha-1)\|x_0\|^{\alpha-1}\int_{t_0}^{t}c(s)\exp\left((\alpha-1)\int_{s}^{t}b(\tau)\mathrm{d}\tau\right)\mathrm{d}s}.$$

This inequality yields estimate (5) for all $t \ge t_0 \ge 0$ for which condition (6) is satisfied.

This completes the proof of Theorem 2.

Inequality (7) is a partial case of inequality (3) and its representation in pseudo-linear form (8) allows us to simplify the procedure of obtaining the estimate of norm of solutions to system (1).

Theorem 2 has a series of corollaries as applied to some classes of systems of ordinary differential equations.

Corollary 1. Consider system (1) for $A(t) \equiv 0$ for all $t \ge t_0 \ge 0$

$$\frac{\mathrm{d}x}{\mathrm{d}t} = f(t,x), \quad x(t_0) = x_0. \tag{11}$$

This is an essentially nonlinear system, *i.e.* a system without linear approximation. Such systems are found in the consideration of systems with dry friction, electroacoustic waveguides and in other problems. Systems with sector nonlinearity (see [12]) are close to this type of systems.

If condition A_3 is fulfilled with the function $c(t)$ such that

$$\int_{t_k}^{t_{k+1}} c(s)\mathrm{d}s > 0,$$

for any $(t_k, t_{k+1}) \in \mathbb{R}_+$, $t_k < t_{k+1}$, $k = 0,1,2,\cdots$, then

$$\|x(t)\| \le \|x_0\| + \int_{t_0}^{t} c(s)\|x(s)\|^{\alpha}\,\mathrm{d}s.$$

Applying to this inequality the same procedure as in the proof of Theorem 2 it is easy to show that if

$$1-(\alpha-1)\|x_0\|^{\alpha-1}\int_{t_0}^{t} c(s)\,\mathrm{d}s > 0$$

for all $t \ge t_0 \ge 0$, then

$$\|x(t)\| \le \frac{\|x_0\|}{\left(1-(\alpha-1)\|x_0\|^{\alpha-1}\int_{t_0}^{t} c(s)\,\mathrm{d}s\right)^{\frac{1}{\alpha-1}}} \tag{12}$$

for all $t \ge t_0 \ge 0$.

Comment 1. Estimate (12) is obtained as well by an immediate application of the Bihari lemma (see [10]) to the inequality

$$\|x(t)\| \le \|x_0\| + \int_{t_0}^{t} c(s)\|x(s)\|^{\alpha}\,\mathrm{d}s$$

with the function $\Phi(u) = \|x\|^{\alpha}$, $\alpha > 0$, $\alpha \ne 1$.

Corollary 2. In system (1) let $f(t,x) \equiv B(t,x)x$, where $B: \mathbb{R}_+ \times \mathbb{R}^n \to \mathbb{R}^{n\times n}$ is an $n\times n$-matrix continuous with respect to $(t,x) \in \mathbb{R}_+ \times \mathbb{R}^n$.

Consider a system of non-autonomous linear equations with pseudo-linear perturbation

$$\frac{\mathrm{d}x}{\mathrm{d}t} = \big(A(t) + B(t,x)\big)x, \quad x(t_0) = x_0. \tag{13}$$

Assume that condition A_1 is satisfied and there exists a nonnegative integrable function $h(t)$ such that

$$\|B(t,x)\| \le h(t)\|x\|, \tag{14}$$

for all $(t,x) \in \mathbb{R}_+ \times \mathbb{R}^n$.

Equation (13) implies that

$$\|x(t)\| \le \|x_0\| + \int_0^t \left(b(s)\|x(s)\| + h((s)\|x(s)\|^2\right)\mathrm{d}s. \tag{15}$$

Applying to inequality (15) the same procedure as in the proof of Theorem 2 we get the estimate

$$\|x(t)\| \le \frac{\|x_0\|\exp\int_0^t b(s)\,\mathrm{d}s}{1-\|x_0\|\int_0^t h(s)\exp\int_0^s b(\tau)\,\mathrm{d}\tau\,\mathrm{d}s} \tag{16}$$

which holds true for the values of $(t) \in [0,\infty)$ for which

$$1-\|x_0\|\int_0^t h(s)\exp\int_0^s b(\tau)\,\mathrm{d}\tau\,\mathrm{d}s > 0. \tag{17}$$

Comment 2. If in inequality (15) functions $b(t) = h(t) = 1$ for all $t \ge t_0 \ge 0$, then Theorem 1 yields the estimate (see [4])

$$\|x(t)\| \le \frac{\|x_0\|\exp(t-t_0)}{1+\|x_0\|(1-\exp(t-t_0))}$$

for all $t \in [t_0, \tau)$, where τ is determined by the formula $\tau = t_0 + \ln \dfrac{1+\|x_0\|}{\|x_0\|}$.

Corollary 3. In system (1) let $f(t,x) = A_2(t)x^2 + \cdots + A_n x^n$, where $x^i = \mathrm{col}(x_1^i, x_2^i, \cdots, x_n^i)$ for all $i = 2,3,\cdots,n$. Further we shall consider the system of nonlinear equations

$$\frac{dx}{dt} = \sum_{k=1}^{n} A_k(t)x^k, \quad x(t_0) = x_0, \tag{18}$$

where $A_i \in C(\mathbb{R}_+, \mathbb{R}^{n\times n})$ are $(n\times n)$-matrices with the elements continuous on any finite interval and $A_1(t) \equiv A(t)$.

Assume that there exist nonnegative integrable on $[0,\infty)$ functions $b_k(t)$, $k = 1,2,\cdots,n$, such that

$$\|A_k(t)\| \le b_k(t), \quad k = 1,2,\cdots,n \tag{19}$$

In view of (19) we get from (18) the inequality

$$\|x(t)\| \le \|x_0\| + \int_0^t \sum_{k=1}^{n} \|A_k(s)\| \|x(s)\|^k \, ds \le \|x_0\| + \int_0^t \sum_{k=1}^{n} b_k(s) \|x(s)\|^k \, ds. \tag{20}$$

Inequality (20) is presented in pseudo-linear form

$$\|x(t)\| \le \|x_0\| + \int_0^t \left(b_1(s) + \sum_{k=2}^{n} b_k(s) \|x(s)\|^{k-1} \right) \|x(s)\| ds.$$

Hence

$$\|x(t)\| \le \|x_0\| \exp\left(\int_0^t \left(b_1(s) + \sum_{k=2}^{n} b_k(s) \|x(s)\|^{k-1} \right) ds \right). \tag{21}$$

We shall find the estimate of the expression $\exp\left(\int_0^t \sum_{k=2}^{n} b_k(s) \|x(s)\|^{k-1} \, ds \right)$.

Inequality (21) implies that the estimate

$$\begin{aligned} \|x(t)\|^{k-1} &\le \|x_0\|^{k-1} \exp\left[(k-1) \int_0^t \left(b_1(s) + \sum_{r=2}^{n} b_r(s) \|x(s)\| \right)^{r-1} ds \right] \\ &\le \|x_0\|^{k-1} \exp\left[\int_0^t \left((k-1) b_1(s) + (n-1) \sum_{r=2}^{n} b_r(s) \|x(s)\|^{r-1} \right) ds \right]. \end{aligned}$$

is true.

Multiplying both parts of this inequality by the negative expression

$$-(n-1) b_k(t) \exp\left[-(n-1) \int_0^t \sum_{r=2}^{n} b_r(s) \|x(s)\|^{r-1} \, ds \right]$$

we get

$$-(n-1) b_k(t) \|x(t)\|^{k-1} \exp\left[-(n-1) \int_0^t \sum_{r=2}^{n} b_r(s) \|x(s)\|^{r-1} \, ds \right] \ge -(n-1) b_k(t) \|x_0\|^{k-1} \exp\left[(k-1) \int_0^t b_1(s) ds \right].$$

Summing up both parts of this inequality from $k = 2$ to n we find

$$-(n-1)\sum_{k=2}^{n}b_k(t)\|x(t)\|^{k-1}\exp\left[-(n-1)\int_0^t\sum_{r=2}^{n}b_r(s)\|x(s)\|^{r-1}\,\mathrm{d}s\right]\geq -(n-1)\sum_{k=2}^{n}b_k(t)\|x_0\|^{k-1}\exp\left[(k-1)\int_0^t b_1(s)\,\mathrm{d}s\right].$$

Integration of this inequality between 0 and t results in the following inequality

$$\exp\left[-(n-1)\int_0^t\sum_{k=2}^{n}b_k(s)\|x(s)\|^{k-1}\,\mathrm{d}s\right]\geq 1-(n-1)\int_0^t\sum_{k=2}^{n}b_k(s)\|x_0\|^{k-1}\exp\left[(k-1)\int_0^t b_1(\tau)\,\mathrm{d}\tau\right]\mathrm{d}s$$

From this inequality we find that

$$\exp\left[\int_0^t\sum_{k=2}^{n}b_k(s)\|x(s)\|^{k-1}\,\mathrm{d}s\right]\leq\frac{1}{\left\{1-(n-1)\int_0^t\sum_{k=2}^{n}b_k(s)\|x_0\|^{k-1}\exp\left[(k-1)\int_0^t b_1(\tau)\,\mathrm{d}\tau\right]\mathrm{d}s\right\}^{\frac{1}{n-1}}}$$

Hence follows the estimate

$$\|x(t)\|\leq\frac{\|x_0\|\exp\left(\int_0^t b_1(s)\,\mathrm{d}s\right)}{\left\{1-(n-1)\int_0^t\sum_{k=2}^{n}b_k(s)\|x_0\|^{k-1}\exp\left[(k-1)\int_0^t b_1(\tau)\,\mathrm{d}\tau\right]\mathrm{d}s\right\}^{\frac{1}{n-1}}}\tag{22}$$

which is valid for all $t\in[0,\infty)$ such that

$$1-(n-1)\int_0^t\sum_{k=2}^{n}\|x_0\|^{k-1}b_k(s)\exp\left((k-1)\int_0^s b_1(\tau)\,\mathrm{d}\tau\right)\mathrm{d}s>0$$

Estimate (5) allows boundedness and stability conditions for solution of system (1) to be established in the following form.

Theorem 3. *If conditions* A_1 *and* A_3 *of Theorem* 2 *are satisfied for all* $(t,x)\in\mathbb{R}_+\times\mathbb{R}^n$ *and there exists a constant* $\beta>0$ *such that* $\|x(t)\|_{(5)}<\beta$ *for all* $t\geq t_0$, *where* β *may depend on each solution, then the solution* $x(t,t_0,x_0)$ *of system* (1) *is bounded.*

Theorem 4. *If conditions* A_1 *and* A_3 *of Theorem* 2 *are satisfied for all* $(t,x)\in\mathbb{R}_+\times\mathbb{R}^n$ *and* $f(t,x)=0$ *for* $x=0$, *and for any* $\varepsilon>0$ *and* $t_0\geq 0$ t_0? 0 *there exists a* $\delta(t_0,\varepsilon)>0$ *such that if* $\|x_0\|<\delta(t_0,\varepsilon)$, *then the estimate* $\|x(t)\|_{(5)}<\varepsilon$ *is satisfied for all* $t\geq t_0$, *then the zero solution of system* (1) *is stable.*

The proofs of Theorems 3 and 4 follow immediately from the estimate of norm of solutions $x(t)$ in the form of (5). The notations $\|x(t)\|_{(5)}<\beta$ and $\|x(t)\|_{(5)}<\varepsilon$ mean that the right hand part of inequality (5) must satisfy these inequalities under appropriate initial conditions.

Similar assertions are valid for the systems of Equations (11), (13) and (18) in terms of estimates (12), (16) and (22).

4. Applications

4.1. Stabilization of Motions of Affine System

Consider an affine system with many controlling bodies

$$\frac{\mathrm{d}x}{\mathrm{d}t}=A(t)x(t)+\sum_{i=1}^{l}G_i(t,x(t))u_i(t)+Bu_0(t),\tag{23}$$

$$y(t)=Cx(t),\tag{24}$$

$$x(t_0)=x_0,\tag{25}$$

where $x \in \mathbb{R}^n$, $A(t)$ is an $n \times n$-matrix with continuous elements on any finite interval, $G_i(t,x)$ is an $n \times m$-matrix, the control vectors $u_i(t) \in \mathbb{R}^m$ for all $i = 1,2,\cdots,l$, B is an $n \times m$-matrix and the control $u_0(t) \in \mathbb{R}^m$, C is a constant $n \times n$-matrix, x_0 is a vector of the initial states of system (23). With regard to system (23) the following assumptions are made:

A_4. Functions $G_i(t,0) = 0$, $i = 1,2,\cdots,l$, for all $t \ge 0$.

A_5. There exists a constant $n \times m$-matrix K_0 such that for the system

$$\frac{\mathrm{d}y}{\mathrm{d}t} = \left(A(t) - BK_0C\right)y$$

the fundamental matrix $\Phi(t)$ satisfies the estimate

$$\left\|\Phi(t)\Phi^{-1}(s)\right\| \le M\mathrm{e}^{-\alpha(t-s)},$$

for $t \ge s \ge t_0$, where M and α are some positive constants.

A_6. There exist constants $\gamma_i > 0$ and $q > 1$ such that

$$\left\|G_i(t,x)\right\| \le \gamma_i \|x\|^q,$$

for all $i = 1,2,\cdots,l$.

The following assertion takes place.

Theorem 5. *Let conditions of assumptions* A_4 - A_6 *be satisfied and, moreover,*

$$1 - \gamma q M^{q+1} \sum_{i=1}^{l} \left(\|K_iC\|\right)\|x_0\|_l^q \int_0^t \mathrm{e}^{-\alpha q s}\mathrm{d}s > 0,$$

where $\gamma = \sum_{i=1}^{l} \gamma_i$.

Then the controls

$$u_i(t) = -K_i y(t), \quad i = 1,2,\cdots,l, \quad u_0(t) = -K_0 y(t)$$

stabilize the motion of system (23) *to the exponentially stable one.*

Proof. Let the controls $u_i(t) = -K_i y(t)$ and $u_0(t) = -K_0 y(t)$ be used to stabilize the motions of system (23). Besides, we have

$$\frac{\mathrm{d}x}{\mathrm{d}t} = \left(A(t) - BK_0C\right)x(t) - \sum_{i=1}^{l} G_i\left(t, x(t)\right)\left(K_iCx(t)\right).$$

and

$$x(t) = \Phi(t)\Phi^{-1}(t_0)x_0 - \int_{t_0}^{t} \Phi(t)\Phi^{-1}(s)\sum_{i=1}^{l} G_i\left(s, x(s)\right)\left(K_iCx(s)\right)\mathrm{d}s. \tag{26}$$

In view of conditions of Theorem 5 we get from (26) the estimate of norm of solution of system (23) in the form

$$\left\|x(t)\right\| \le \left\|x_0\right\| M\mathrm{e}^{-\alpha t} + \int_0^t \gamma M\mathrm{e}^{-\alpha(t-s)} \sum_{i=1}^{l} \left\|K_iC\right\| \left\|x(s)\right\|^{q+1} \mathrm{d}s. \tag{27}$$

We transform inequality (27) to the form

$$\left\|x(t)\mathrm{e}^{\alpha t}\right\| \le \left\|x_0\right\| M + \int_0^t \gamma M\mathrm{e}^{-\alpha q s} \sum_{i=1}^{l} \left\|K_iC\right\| \left\|x(s)\mathrm{e}^{\alpha s}\right\|^{q+1} \mathrm{d}s. \tag{28}$$

Applying Corollary 3 to inequality (28) we get

$$\left\|x(t)e^{\alpha t}\right\| \le \frac{M\left\|x_0\right\|}{\left(1-\gamma q M^{q+1}\sum_{i=1}^{l}\left(\left\|K_i C\right\|\right)\left\|x_0\right\|_I^q \int_0^t e^{-\alpha q s}ds\right)^{\frac{1}{q}}}$$

$$= \frac{M\left\|x_0\right\|}{\left(1+\frac{\gamma M^{q+1}\sum_{i=1}^{l}\left(\left\|K_i C\right\|\right)\left\|x_0\right\|_I^q}{\alpha}\left(e^{-\alpha q t}-1\right)\right)^{\frac{1}{q}}}$$

$$\le \frac{M\left\|x_0\right\|}{\left(1-\frac{\gamma M^{q+1}\sum_{i=1}^{l}\left(\left\|K_i C\right\|\right)\left\|x_0\right\|^q}{\alpha}\right)^{\frac{1}{q}}}.$$

for all $t \ge 0$.

If condition

$$1-\gamma q M^{q+1}\sum_{i=1}^{l}\left(\left\|K_i C\right\|\right)\left\|x_0\right\|_I^q \int_0^t e^{-\alpha q s}ds > 0,$$

of Theorem 5 is satisfied, then

$$1-\frac{\gamma M^{q+1}\sum_{i=1}^{l}\left(\left\|K_i C\right\|\right)\left\|x_0\right\|^q}{\alpha} > 0$$

and for the norm of solution $x(t)$ we have the estimate

$$\left\|x(t)\right\| \le M_0\left\|x_0\right\|e^{-\alpha t}$$

for all $t \ge 0$, where

$$M_0 = \frac{M}{\left(1-\frac{\gamma M^{q+1}\sum_{i=1}^{l}\left(\left\|K_i C\right\|\right)\left\|x_0\right\|^q}{\alpha}\right)^{\frac{1}{q}}}.$$

This completes the proof of Theorem 5.

4.2. Syncronization of Motions

The theory of motion synchronizations studies the systems of differential equations of the form (see [9] and bibliography therein)

$$\frac{dx}{dt} = \mu f(t,x,\mu), \quad x(t_0) = x_0, \tag{29}$$

where $f(t,x,\mu): \mathbb{R}_+ \times \mathbb{R}^n \times [0,1] \to \mathbb{R}^n$, f is a function continuous with respect to t, x, μ and periodic with respect to t with the period T, and μ is a small parameter. Alongside system (29) we shall consider an adjoint system of equations

$$\frac{\mathrm{d}\overline{x}}{\mathrm{d}t} = \mu g(\overline{x}), \quad \overline{x}(t_0) = x_0, \tag{30}$$

where

$$g(x) = \frac{1}{T}\int_0^T f(s, x, 0)\,\mathrm{d}s.$$

Assume that in the neighborhood of point x_0 for sufficiently small value of μ for any $t \in [0, T]$ the vector-function f and its partial derivatives are continuous. Designate

$$M = \max_{t\in[0,T],\|x-x_0\|\le d,\mu\le\mu^*}\left\{\|f(t,x,\mu)\|, \left\|\frac{\partial f}{\partial \mu}\right\|, \left\|\frac{\partial f_i}{\partial v_j}\right\|\right\}.$$

It is clear that the solutions of Equations (29) and (30) remain in the neighborhood $\|x - x_0\| \le d$ for $|\mu t| < dM^{-1}$.

With allowance for

$$x(t,\mu) = x_0 + \mu\int_0^t f(s, x(s,\mu), \mu)\,\mathrm{d}s$$

and

$$\overline{x}(t,\mu) = x_0 + \mu\int_0^t g(\overline{x}(s,\mu))\,\mathrm{d}s,$$

we compile the correlation

$$\begin{aligned} x(x,\mu) - \overline{x}(t,\mu) &= \mu\int_0^t \left[f(s, x(s,\mu), \mu) - f(s, x(s,\mu), 0)\right]\mathrm{d}s + \mu\int_0^t \left[f(s, x(s,\mu), 0) - f(s, \overline{x}(s,\mu), 0)\right]\mathrm{d}s \\ &\quad + \mu\int_0^t \left[f(s, \overline{x}(s,\mu), 0) - g(\overline{x}(s,\mu))\right]\mathrm{d}s. \end{aligned} \tag{31}$$

As it is shown in monograph [9] for the first and third summands in correlation (31) the following estimates hold true

$$\left\|\int_0^t \left[f(s, x(s,\mu), \mu) - f(s, x(s,\mu), 0)\right]\mathrm{d}s\right\| \le M\mu t, \tag{32}$$

$$\left\|\int_0^t \left[f(s, \overline{x}(s,\mu), 0) - g(\overline{x}(s,\mu))\right]\mathrm{d}s\right\| \le 2MT + 4M^2T\mu t. \tag{33}$$

To estimate the second summand we assume that there exist an integrable function $N(t): \mathbb{R}_+ \to \mathbb{R}_+$ such that for any $t_1, t_2 \in [0, T]$ $(0 \le t_1 < t_2)$

$$\int_{t_1}^{t_2} N(s)\,\mathrm{d}s > 0$$

and $\alpha > 1$ such that

$$\|f(t, x, 0) - f(t, \overline{x}, 0)\| \le N(t)\|x - \overline{x}\|^\alpha \tag{34}$$

in the domain of values $t \in [0, T]$ and $x, \overline{x} \in D$.

In view of estimates (32)-(34) we find from (31)

$$\left\|x(s,\mu)-\bar{x}(s,\mu)\right\| \le \mu\left(2MT+\left(4M^2T+M\right)\mu t\right)+\mu\int_0^s N(\tau)\left\|x(\tau,\mu)-\bar{x}(\tau,\mu)\right\|^{\alpha}\,\mathrm{d}\tau \tag{35}$$

for all $s \le t$.

Let there exist $\mu^* \in [0,1]$ such that

$$1-(\alpha-1)\left[\mu\left(2MT+\left(4M^2T+M\right)\mu t\right)\right]^{\alpha-1}\mu\int_0^T N(s)\,\mathrm{d}s > 0 \tag{36}$$

for all $\mu < \mu^*$. Then the norm of divergence of solutions $x(t,\mu)$ and $\bar{x}(t,\mu)$ under the same initial conditions is estimated as follows

$$\left\|x(t,\mu)-\bar{x}(t,\mu)\right\| \le \frac{\mu\left[2MT+\left(4M^2T+M\right)\mu t\right]}{\left\{1-(\alpha-1)\left[\mu\left(2MT+\left(4M^2T+M\right)\mu t\right)\right]^{\alpha-1}\mu\int_0^T N(s)\,\mathrm{d}s\right\}^{\frac{1}{\alpha-1}}} \tag{37}$$

for all $t \in [0,T]$ and for $\mu < \mu^*$.

Estimate (37) is obtained from inequality (35) by the application of Corollary 1.

Comment 3. If in estimate (34) $\alpha = 1$ and $N(t) = M$, then the application of the Gronwall-Bellman lemma to inequality (35) yields the estimate of divergence between solutions in the form [9]

$$\left\|x(t,\mu)-\bar{x}(t,\mu)\right\| \le \mu\left[2MT+\left(4M^2T+M\right)\mu t\right]\exp(\mu MT)$$

for all $t \in [0,T]$.

5. Concluding Remarks

In this paper the estimates of norms of solutions to differential equations of form (1), (11) and (13) are obtained in terms of nonlinear and pseudo-linear integral inequalities. This approach facilitates establishing the estimates of norms of solutions for some classes of systems of equations of perturbed motion found in various applied problems (see [11] [13]). Efficiency of the obtained results is illustrated by two problems of nonlinear dynamics.

It is of interest to develop the obtained results in the investigation of solutions to dynamic equations on time scale (see [14] [15]). In monograph [16] the integral inequalities on time scale form a basis of one of the methods of analysis of solutions to dynamic equations.

References

[1] Bellman, R. (1953) Stability Theory of Differential Equations. Dover Publications, New York, 166 p.

[2] Martynyuk, A.A., Lakshmikantham, V. and Leela, S. (1979) Stability of Motion: Method of Integral Inequalities. Naukova Dumka, Kiev. (In Russian)

[3] Ahmad, S. and Rao, M.R.M. (1980) Ordinary Differential Equations. Affiliated East-West Press Pvt Ltd., New Delhi-Madras, 266 p.

[4] Gutowski, R. and Radziszewski, B. (1970) Asymptotic Behaviour and Properties of Solutions of a System of Non Linear Second Order Ordinary Differential Equations Describing Motion of Mechanical Systems. *Archiwum Mechaniki Stosowanej*, **6**, 675-694.

[5] Martynyuk, A.A. and Gutowski, R. (1979) Integral Inequalities and Stability of Motion. Naukova Dumka, Kiev. (In Russian)

[6] Pachpatte, B.G. (1998) Inequalities for Differential and Integral Equations. Academic Press, San Diego.

[7] Martynyuk, A., Chernetskaya, L. and Martynyuk, V. (2013) Weakly Connected Nonlinear Systems: Boundedness and Stability of Motion. CRC Press, Boca Raton.

[8] Louartassi, Y., Mazoudi, E.H.E. and Elalami, N. (2012) A New Generalization of Lemma Gronwall-Bellman. *Applied Mathematical Sciences*, **6**, 621-628.

[9] Rozo, M. (1971) Nonlinear Oscillations and Stability Theory. Nauka, Moscow. (In Russian)

[10] Demidovich, B.P. (1967) Lectures on Mathematical Stability Theory. Nauka, Moscow. (In Russian)

[11] Brauer, F. (1963) Bounds for Solutions of Ordinary Differential Equations. *Proceedings of the American Mathematical Society*, **14**, 36-43. http://dx.doi.org/10.1090/S0002-9939-1963-0142829-0

[12] Aleksandrov, A.Yu., Aleksandrova, E.B. and Zhabko, A.P. (2013) Stability Analysis of a Class of Nonlinear Nonstationary Systems via Averaging. *Nonlinear Dynamics and Systems Theory*, **13**, 332-343.

[13] N'Doye, I., Zasadzinski, M., Darouach, M., Radhy, N.-E. and Bouaziz, A. (2011) Exponential Stabilization of a Class of Nonlinear Systems: A Generalized Gronwall-Bellman Lemma Approach. *Nonlinear Analysis*, **74**, 7333-7341. http://dx.doi.org/10.1016/j.na.2011.07.051

[14] Babenko, S.V. and Martynyuk, A.A. (2013) Nonlinear Dynamic Inequalities and Stability of Quasi-Linear Systems on Time Scales. *Nonlinear Dynamics and Systems Theory*, **13**, 13-24.

[15] Bohner, M. and Martynyuk, A.A. (2007) Elements of Stability Theory of A. M. Lyapunov for Dynamic Equations on Time Scales. *Nonlinear Dynamics and Systems Theory*, **7**, 225-251.

[16] Martynyuk, A.A. (2012) Stability Theory of Solutions of Dynamic Equations on Time Scales. Phoenix, Kiev. (In Russian)

Applied Mathematics, 2015, 6, 195-205
Published Online January 2015 in SciRes. http://www.scirp.org/journal/am
http://dx.doi.org/10.4236/am.2015.61019

Some Sequence of Wrapped Δ-Labellings for the Complete Bipartite Graph

Tomoko Adachi, Daigo Kikuchi

Department of Information Sciences, Toho University, Funabashi, Japan
Email: adachi@is.sci.toho-u.ac.jp

Received 2 January 2015; accepted 17 January 2015; published 20 January 2015

Abstract

The design of large disk array architectures leads to interesting combinatorial problems. Minimizing the number of disk operations when writing to consecutive disks leads to the concept of "cluttered orderings" which were introduced for the complete graph by Cohen *et al.* (2001). Mueller *et al.* (2005) adapted the concept of wrapped Δ-labellings to the complete bipartite case. In this paper, we give some sequence in order to generate wrapped Δ-labellings as cluttered orderings for the complete bipartite graph. New sequence we give is different from the sequences Mueller *et al.* gave, though the same graphs in which these sequences are labeled.

Keywords

Cluttered Ordering, RAID, Disk Arrays, Label for a Graph

1. Introduction

The desire to speed up secondary storage systems has lead to the development of disk arrays which achieve performance through disk parallelism. While performance improves with increasing numbers of disks, the chance of data loss coming from catastrophic failures, such as head crashes and failures of the disk controller electronics, also increases. To avoid high rates of data loss in large disk arrays, one includes redundant information stored on additional disks—also called check disks—which allows the reconstruction of the original data—stored on the so-called information disks—even in the presence of disk failures. These disk array architectures are known as redundant arrays of independent disks (RAID) (see [1] [2]).

Optimal erasure-correcting codes using combinatorial framework in disk arrays are discussed in [1] [3]. For an optimal ordering, there are [4] [5]. Cohen *et al*. [6] gave a cyclic construction for a cluttered ordering of the complete graph. In the case of a complete graph, there are [7] [8]. Furthermore, in the case of a complete bipartite graph, Mueller *et al*. [9] gave a cyclic construction for a cluttered ordering of the complete bipartite graph by

How to cite this paper: Adachi, T. and Kikuchi, D. (2015) Some Sequence of Wrapped Δ-Labellings for the Complete Bipartite Graph. *Applied Mathematics*, **6**, 195-205. http://dx.doi.org/10.4236/am.2015.61019

utilizing the notion of a wrapped **Δ**-labelling. In the case of a complete tripartite graph, we refer to [10].

As **Figure 1**, we present the case $\ell = 2$. For example, information disk 1 is associated to the check disks *a* and *c*. A 2-dimensional parity code can be modeled by the complete bipartite graph $K_{\ell,\ell} = (U,V,E)$ in the following way. The point set of $K_{\ell,\ell}$ is partitioned into the two sets—*U* and *V* both having cardinality ℓ. Assign the points of *U* to the ℓ check bits corresponding to the rows and the points of *V* to the ℓ check bits corresponding to the columns. By definition, in $K_{\ell,\ell}$ any point of *U* is connected with any point of *V* exactly on edge constituting the edge set *E*, *i.e.*, $|E| = \ell^2$ (see **Figure 2**).

In this paper, we make label to the vertex of a bipartite graph. For example, we make label 1, 3, 0 and −1, respectively, to four vertices *a*, *b*, *c* and *d* of a bipartite graph in **Figure 2**. By such labelling, we get that the label of the edge $\{a,c\}$ is $1-0=1$; the label of the edge $\{a,d\}$ is $1-(-1)=2$; the label of the edge $\{b,c\}$ is $3-0=3$ and the label of the edge $\{b,d\}$ is $3-(-1)=4$. The labellings $[1,3]$ of the upper vertices $[a,b]$ and the labellings $[0,-1]$ of the lower vertices $[c,d]$ are sequences. The goal of this paper is to find new sequence in order to generate wrapped **Δ**-labellings as cluttered orderings for the complete bipartite graph. In Section 5, we give new sequence which we want. The new sequence we give is different from the sequences Mueller *et al*. [9] gave, though the same graphs in which these sequences are labeled.

2. A Cluttered Ordering

In a RAID system disk writes are expensive operations and should therefore be minimized. In many applications there are writes on a small fraction of consecutive disks—say *d* disks—where *d* is small in comparison to *k*, the number of information disks. Therefore, to minimize the number of operations when writing to *d* consecutive information disks one has to minimize the number of check disks—say *f*—associated to the *d* information disks.

Let $G = (V,E)$ be a graph with $n = |V|$ vertices and edge set $E = \{e_0, e_1, \cdots, e_{m-1}\}$. Let $d \le m$ be a positive integer, called a *window* of *G*, and π a permutation on $\{0,1,\cdots,m-1\}$, called an *edge ordering* of *G*. Then, given a graph *G* with edge ordering π and window *d*, we define $V_i^{\pi,d}$ to be the set of vertices which are connected by an edge of $\{e_{\pi(i)}, e_{\pi(i+1)}, \cdots, e_{\pi(i+d-1)}\}$, $0 \le i \le m-1$, where indices are considered modulo *m*. The cost of accessing a subgraph of *d* consecutive edges is measured by the number of its vertices. An upper bound of this cost is given by the *d-maximum access cost* of *G* defined as $\max_i |V_i^{\pi,d}|$. An ordering π is a (*d*, *f*)-*cluttered ordering*, if it has *d*-maximum access cost equal to *f*. We are interested in minimizing the parameter *f*.

Let ℓ be a positive integer and let $K_{\ell,\ell}$ denote the complete bipartite graph with 2ℓ vertices and ℓ^2 edges. In the following, we identify the vertex set of $K_{\ell,\ell}$ with $Z_\ell \times Z_2$, where two vertices are connected by an edge iff they have different second components in $Z_\ell \times Z_2$. The construction of (*d*, *f*)-cluttered orderings for $K_{\ell,\ell}$ with small positive integer *f* is based on two fundamental concepts. Firstly, we introduce the well-known concept of a **Δ**-labelling of a suitable bipartite subgraph from which one gets a decomposition of $K_{\ell,\ell}$ into isomorphic copies of this subgraph. Secondly, we define the concept of a (*d*, *f*)-*movement* which will lead to "locally" defined edge orderings of $K_{\ell,\ell}$. This principle was implicitely used in [6] in case of the complete graph. In case of the complete bipartite graph, we refer to [9].

In the following, $H = (U,E)$ always denotes a bipartite graph with vertex set *U* which is partitioned into

$$
\begin{array}{cc|c}
\bullet_1 & \bullet_2 & \circ_a \\
\bullet_3 & \bullet_4 & \circ_b \\
\hline
\circ_c & \circ_d &
\end{array}
\qquad
H = \begin{array}{c}
\begin{array}{cccccccc} 1 & 2 & 3 & 4 & a & b & c & d \end{array} \\
\left[\begin{array}{cccc|cccc}
1 & 1 & 0 & 0 & 1 & 0 & 0 & 0 \\
0 & 0 & 1 & 1 & 0 & 1 & 0 & 0 \\
1 & 0 & 1 & 0 & 0 & 0 & 1 & 0 \\
0 & 1 & 0 & 1 & 0 & 0 & 0 & 1
\end{array}\right]
\end{array}
\begin{array}{c} \\ a \\ b \\ c \\ d \end{array}
$$

Figure 1. 2-dim. parity code and its parity check matrix.

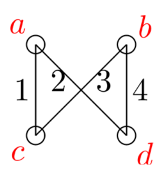

Figure 2. Code as graph.

two subsets denoted by V and W. Any edge of the edge set E contains exactly one point of V and W respectively. Let $\ell = |E|$, then a $\boldsymbol{\Delta}$-labelling of H with respect to V and W is defined to be a map $\Delta : U \to Z_\ell \times Z_2$ with $\Delta(V) \subset Z_\ell \times \{0\}$ and $\Delta(W) \subset Z_\ell \times \{1\}$, where each element of Z_ℓ occurs exactly once in the difference list

$$\Delta(E) := \left(\pi_1\left(\Delta(v) - \Delta(w)\right) \middle| v \in V, w \in W, (v, w) \in E\right). \tag{1}$$

Here, $\pi_1 : Z_\ell \times Z_2 \to Z_\ell$ denotes the projection on the first component. In general, Δ-labellings are a well-known tool for the decomposition of graphs into subgraphs (see [11]). In this context a decomposition is understood to be a partition of the edge set of the graph. In case of the complete bipartite graph, one has the following proposition.

Proposition 1. ([9]) *Let* $H = (U, E)$ *be a bipartite graph,* $\ell = |E|$*, and* $\boldsymbol{\Delta}$ *be a* $\boldsymbol{\Delta}$*-labelling as defined above. Then there is a decomposition of the complete bipartite graph* $K_{\ell,\ell}$ *into isomorphic copies of H.*

For example, **Figure 3** shows $\boldsymbol{\Delta}$-labellings of a graph $H = H(1;1)$ with 3 edges leading to a decomposition of $K_{3,3}$ into isomorphic copies of $H(1;1)$ such as **Figure 4**. Next, in order to move a graph H to an isomorphic copy such as **Figure 5**, we define the concept of a (d, f)-movement which can easily be generalized to arbitrary set system.

Definition 1. Let G be a graph with edge set $E(G) = \{e_0, e_1, \cdots, e_{n-1}\}$, where n is positive integer, and let Σ_0, $\Sigma_1 \subset E(G)$ with $d := |\Sigma_0| = |\Sigma_1|$. For a permutation σ on $\{0, 1, \cdots, n-1\}$ define $V_i^{\sigma,d} := \bigcup_{j=0}^{d-1} e_{\sigma(i+j)}$ for $0 \le i \le n-d$. Then, for some given a positive integer f, and a map σ is called a (d, f)*-movement from* Σ_0 *to* Σ_1 if $\Sigma_0 = \left\{e_{\sigma(j)} \middle| 0 \le j \le d-1\right\}$, $\Sigma_1 = \left\{e_{\sigma(j)} \middle| n-d \le j \le n-1\right\}$, and $\max_i \left|V_i^{\sigma,d}\right| \le f$.

In order to assemble such (d, f)-movements of certain subgraphs to a (d, f)-cluttered ordering, we need some notion of consistency. Let $\varphi : \Sigma_0 \to \Sigma_1$ be any bijection, then a (d, f)-movement σ from Σ_0 to Σ_1 is called consistent with φ if

$$\varphi\left(e_{\sigma(j)}\right) = e_{\sigma(n-d+j)}, \quad \text{for} \quad j = 0, 1, \cdots, d-1. \tag{2}$$

Now, for each $j \in Z_\ell$ one gets an automorphism τ_j of the bipartite graph $K_{\ell,\ell}$ defined by cyclic translation of the vertex set:

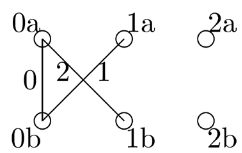

Figure 3. A $\boldsymbol{\Delta}$-labelling of a graph $H(1;1)$ with 3 edges.

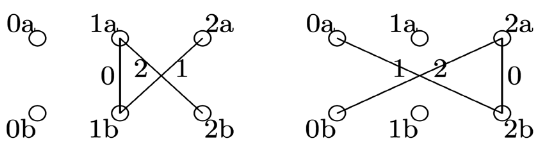

Figure 4. Isomorphic copies of $H(1;1)$.

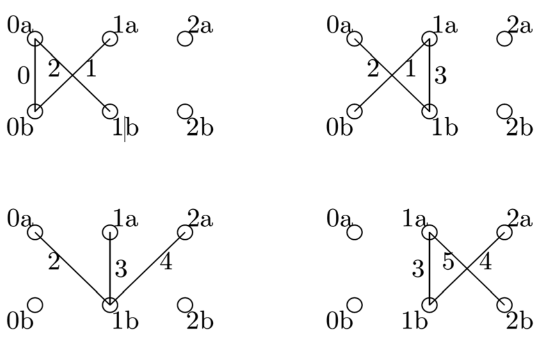

Figure 5. A (3,4)-movement.

$$\tau_j : Z_\ell \times Z_2 \to Z_\ell \times Z_2, \quad \tau_j\left((u,b)\right) := (u+j,b), \tag{3}$$

$(u,b) \in Z_\ell \times Z_2$. Obviously, τ_j induces in a natural way an automorphism of the edge set of $K_{\ell,\ell}$ which we also denote τ_j. Then, $\tau_j\left(E^{(i)}\right) = E^{(i+j)}$ and $\tau_j\left(\Sigma_0^{(i)}\right) = \Sigma_0^{(i+j)}$, $i \in Z_\ell$. Next, we define a subgraph $G^{(0)} \subset K_{\ell,\ell}$ by specifying its edge set $E\left(G^{(0)}\right) := E^{(0)} \cup \Sigma_0^{(\kappa)}$. Let $E\left(G^{(0)}\right) = \left\{e_0^{(0)}, e_1^{(0)}, \cdots, e_{n-1}^{(0)}\right\}$, $n = \ell + d$, where we fix some arbitrary edge ordering. We denote the restriction of the cyclic translation τ_κ to $\Sigma_0^{(0)}$ by $\varphi_\kappa^{(0)}$ which defines a bijection $\varphi_\kappa^{(0)} : \Sigma_0^{(0)} \to \Sigma_0^{(\kappa)}$.

Definition 2. With above notation, a (*d*, *f*)-movement of $G^{(0)}$ from $\Sigma_0^{(0)}$ to $\Sigma_0^{(\kappa)}$ consistent with $\varphi_\kappa^{(0)}$ will be denoted as (d,f)-movement from $\Sigma_0^{(0)}$ consistent with the translation parameter κ.

According to Definition 1, such a (*d*, *f*)-movement is given by some permutation σ of the index set $\{0,1,\cdots,n-1\}$. By applying the cyclic translation τ_i one gets a graph $G^{(i)} := \tau_i\left(G^{(0)}\right)$ with edge set $E\left(G^{(i)}\right) = E^{(i)} \cup \Sigma_0^{(i+\kappa)} = \left\{e_0^{(i)}, e_1^{(i)}, \cdots, e_{n-1}^{(i)}\right\}$, $i \in Z_\ell$. We denote the restriction of τ_κ to $\Sigma_0^{(i)}$ by $\varphi_\kappa^{(i)}$ which defines a bijection

$$\varphi_\kappa^{(i)} : \Sigma_0^{(i)} \to \Sigma_0^{(i+\kappa)}, \quad \varphi_\kappa^{(i)}\left(e^{(i)}\right) = e^{(i+\kappa)}, \quad e^{(i)} \in \Sigma_0^{(i)}. \tag{4}$$

Then σ also defines a (d,f)-movement of $G^{(i)}$ from $\Sigma_0^{(i)}$ to $\Sigma_0^{(i+\kappa)}$ consistent with $\varphi_\kappa^{(i)}$. Using that $e_{\sigma(j)}^{(i)} \in \Sigma_0^{(i)}$, $0 \le j < d$, (see Defintion 1), we get, for $j = 0,1,\cdots,d-1$,

$$e_{\sigma(j)}^{(i+\kappa)} \overset{(4)}{=} \varphi_\kappa^{(i)}\left(e_{\sigma(j)}^{(i)}\right) \overset{(2)}{=} e_{\sigma(n-d+j)}^{(i)} = e_{\sigma(\ell+j)}^{(i)}. \tag{5}$$

Having such a consistent σ, it is easy to construct a (*d*, *f*)-cluttered ordering of $K_{\ell,\ell}$. In short, one orders the edges of $K_{\ell,\ell}$ by first arranging the subgraphs of the decomposition along $E^{(0)}, E^{(\kappa)}, E^{(2\kappa)}, \cdots, E^{((\ell-1)\kappa)}$ and then ordering the edges within each subgraph according to σ.

Proposition 2. ([9]) *Let* $H = (U,E)$, $\ell = |E|$, *be a bipartite graph allowing some* ρ*-labelling, and let* κ *be a translation parameter coprime to* ℓ. *Furthermore, let* $\Sigma_0 \subset E$, $d := |\Sigma_0|$. *If there is a (d, f)-movement from* Σ_0 *consistent with* κ, *then there also is a (d, f)-cluttered ordering for the complete bipartite graph* $K_{\ell,\ell}$.

3. Construction of Cluttered Orderings of $H(h;t)$

In this section, we define an infinite family of bipartite graphs which allow (*d*, *f*)-movements with small *f*. In order to ensure that these (*d*, *f*)-movements are consistent with some translation parameter κ, we impose an additional condition on the Δ-labellings also referred to as wrapped-condition.

Let *h* and *t* be two positive integers. For each parameter *f* and *t*, we define a bipartite graph denoted by $H(h;t) = (U,E)$. Its vertex set *U* is partitioned into $U = V \cup W$ and consists of the following $2h(t+1)$ vertices:

$$V := \left\{v_i \middle| 0 \le i < h(t+1)\right\},$$
$$W := \left\{w_i \middle| 0 \le i < h(t+1)\right\}.$$

The edge set *E* is partitioned into subsets E_s, $0 \le s < t$, defined by

$$E_s' := \left\{\{v_i, w_j\} \middle| s \cdot h \le i, j < s \cdot h + h\right\},$$
$$E_s'' := \left\{\{v_i, w_{h+j}\} \middle| s \cdot h \le j \le i < s \cdot h + h\right\},$$
$$E_s''' := \left\{\{v_{h+i}, w_j\} \middle| s \cdot h \le i \le j < s \cdot h + h\right\},$$
$$E_s := E_s' \cup E_s'' \cup E_s''', \quad \text{for} \quad 0 \le s < t,$$
$$E := \bigcup_{s=0}^{t-1} E_s.$$

Figure 6 shows the edge partition of $H(2;1)$. For the number of edges holds

$$|E| = t \cdot \left(h^2 + \frac{h(h+1)}{2} + \frac{h(h+1)}{2} \right) = th(2h+1).$$

The t subgraphs defined by the edge sets E_s, $0 \le s < t$, and its respective underlying vertex sets are isomorphic to $H(h;1)$. Intuitively speaking, the bipartite graph $H(h;t)$ consists of t "consecutive" copies of $H(h;1)$, where the last h vertices of V and W respectively of one copy are identified with the first h vertices of V and W respectively of the next copy. Traversing these copies with increasing s will define a (d, f)-movement of $H(h;t)$ with small parameter f as is shown in the next proposition.

Proposition 3. ([9]) *Let h, t be pogitive integers. Let* $H(h;t) = (U, E)$, $t \ge 2$, *be the bipartite graph as defined above. Then, there is a (d, f)-movement of* $H(h;t)$ *from* E_0 *to* E_{t-1} *with* $d = h(2h+1)$ *and* $f = 4h$.

By Proposition 1 a **Δ**-labelling of the graph $H(h;t)$ will lead to a decomposition of the complete bipartite graph $K_{\ell,\ell}$ into ℓ isomorphic copies of $H(h;t)$, where $\ell = th(2h+1)$. However, in general there is no (d, f)-movement consistent with some translation parameter κ. To this means, we impose an additional condition on the Δ-labelling. The following definition generalizes and adapts the notion of a wrapped **Δ**-labelling to the bipartite case, which was introduced in [6] for certain subgraphs of the complete graph.

Definition 3. Let $H = (U, E)$, $\ell = |E|$, denote a bipartite graph and let X, $Y \subset U$ with $|X| = |Y|$. A **Δ**-labelling **Δ** is called a wrapped **Δ**-labelling of H relative to X and Y if there exists a $\kappa \in Z$ coprime to ℓ such that

$$\Delta(Y) = \Delta(X) + (\kappa, 0) \tag{6}$$

as multisets in $Z_\ell \times Z_2$. The parameter κ is also referred to as translation parameter of the wrapped **Δ**-labelling.

For the graphs $H = H(h;t)$, we define $X := \{v_i, w_i \mid 0 \le i < h\}$ and $Y := \{v_i, w_i \mid ht \le i < h(t+1)\}$. Furthermore, in the following we only consider wrapped Δ-labellings relative to X and Y for which the stronger condition

$$\Delta(v_{i+ht}) = \Delta(v_i) + (\kappa, 0) \quad \text{and} \quad \Delta(w_{i+ht}) = \Delta(w_i) + (\kappa, 0), \tag{7}$$

hold for $0 \le i < h$. Suppose we have such labelling **Δ** satisfying condition (7). Now, $E^{(i)}$, $i \in Z_\ell$, are isomorphic copies of $H(h;t)$. Furthermore, $\Sigma_0^{(\kappa)}$ is isomorphic to $H(h;1)$ consisting of the first d edges of $E^{(\kappa)}$. From condition (7) follows that the graph $G^{(0)} \subset K_{\ell,\ell}$ with edge set $E\left(G^{(0)}\right) := E^{(0)} \cup \Sigma_0^{(\kappa)}$ can obviously identified with $H(h;t+1)$. In addition, one easily checks that the (d, f)-movement of $G^{(0)} = H(h;t+1)$ from Proposition 3 is consistent with the translation parameter κ.

Proposition 4. ([9]) *Let* h, t *be positive integers. From any wrapped* **Δ***-labelling of* $H(h;t)$, *satisfying condition* (7), *one gets a* (*d*, *f*)*-cluttered ordering of the complete bipartite graph* $K_{\ell,\ell}$ *with* $\ell = th(2h+1)$, $d = h(2h+1)$, *and* $f = 4h$.

4. Sequences of Wrapped Δ-Labellings for $H(1; t)$, $H(2; t)$ and $H(h; 1)$

In this section, we construct some infinite families of such wrapped **Δ**-labellings. By applying Proposition 2 we get explicite (d, f)-cluttered orderings of the corresponding bipartite graphs. For these results in this section, we refer to [9].

4.1. A Sequence for $H(1; t)$

We define a wrapped **Δ**-labelling of $H(1;t)$ for any positive integer t. $H(1;t) = (U, E)$ has $2(t+1)$ vertices

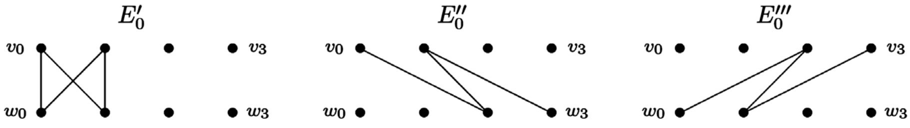

Figure 6. Partition of the edge set of $H(2;1)$.

and $3t$ edges. For a fixed t, we define $\Delta : U \to Z_{3t} \times Z_2$ on the vertex set $U = V \cup W$ as follows:

$$\Delta(v_j) = \begin{cases} (jt, 0), & \text{for } 0 \le j < t, \\ (t^2+1, 0), & \text{for } j = t, \end{cases}$$

$$\Delta(w_j) = \begin{cases} (j(t-1), 1), & \text{for } 0 \le j < t, \\ (t^2+1, 1), & \text{for } j = t, \end{cases}$$

where the integers in the first components are considered modulo $3t$. We now compute the difference list $\Delta(E)$ of δ defined as in (1). Hence each element of Z_{3t} appears in $\Delta(E)$ and the difference condition holds. **Figure 3** illustrates the definition for the case $t = 1$.

Obviously, the wrapped-condition (7) relative to $X = \{v_0, w_0\}$ and $Y = \{v_t, w_t\}$ holds as well and the translation parameter $\kappa = t^2 + 1$ is coprime to $3t$ for any t. Therefore, $\mathbf{\Delta}$ defines the desired wrapped $\mathbf{\Delta}$-labelling of $H(1;t)$.

Theorem 5. ([9]) *Let t be a positive integer. For all t there is a (d, f)-cluttered ordering of the complete bipartite graph* $K_{3t,3t}$ *with* $d = 3$ *and* $f = 4$.

Theorem 6. ([9]) *Let t be a positive integer. For all t there is a (d, f)-cluttered ordering of the complete bipartite graph* $K_{3t,3t}$ *with* $d = 3s + r$ *and* $f = 2(s+1) + r$, $s > 0$, $r = 0,1,2$.

4.2. A Sequence for *H*(2; *t*)

We define a wrapped $\mathbf{\Delta}$-labelling of $H(2;t)$ for any positive integer t. $H(2;t) = (U,E)$ has $4(t+1)$ vertices and $10t$ edges. For a fixed t, a labelling $\mathbf{\Delta}$ is a map $\Delta : U \to Z_{10t} \times Z_2$ on the vertex set $U = V \cup W$. We specify the second component of $\mathbf{\Delta}$ on the vertices $V = (v_0, v_1, \cdots, v_{2t+1})$ sequentially by the following list of $2t + 2$ numbers:

$$c_0, c_0 + a, c_1, c_1 + a, \cdots, c_j, c_j + a, \cdots, c_{t-1}, c_{t-1} + a, c_0 + \kappa, c_0 + a + \kappa,$$

and, on the vertices $W = (w_0, w_1, \cdots, w_{2t+1})$ by, similarly,

$$d_0, d_0 + b, d_1, d_1 + b, \cdots, d_j, d_j + b, \cdots, d_{t-1}, d_{t-1} + b, d_0 + \kappa, d_0 + b + \kappa,$$

where we set

$$\begin{aligned} &a = 6t - 1, \quad c_j = 2jt, \qquad\quad j = 0,1,\cdots,t-1, \\ &b = 6t - 2, \quad d_j = 2j(t-1), \quad j = 0,1,\cdots,t-1, \\ &\kappa = 2t^2 + 1. \end{aligned}$$

All integers are considered modulo $10t$. Note that $|E| = 10t$ and $\kappa = 2t^2 + 1$ are coprime for all t and that the wrapped-condition (7) is obviously fulfilled. Thus, $\mathbf{\Delta}$ defines a wrapped $\mathbf{\Delta}$-labelling.

Theorem 7. ([9]) *Let t be a positive integer. For all t there is a (d, f)-cluttered ordering of the complete bipartite graph* $K_{10t,10t}$ *with* $d = 10$ *and* $f = 8$.

Theorem 8. ([9]) *Let t be a positive integer. For all t there is a (d, f)-cluttered ordering of the complete bipartite graph* $K_{10t,10t}$ *with* $d = 10s + r$ *and* $f = 4(s+1) + \min(r,4)$, $s > 0$, $r = 0,1,\cdots,9$.

4.3. A Sequence for *H*(*h*; 1)

We define in this section a wrapped $\mathbf{\Delta}$-labelling for $H(h;1)$ for any positive integer h. $H(h;1) = (U,E)$ has $4h$ vertices and $h(2h+1)$ edges. We define the $\mathbf{\Delta}$-labelling $\Delta : U \to Z_{h(2h+1)} \times Z_2$ on the vertex set $U = V \cup W$ by specifying the first component of $\mathbf{\Delta}$ on the vertices $V = (v_0, v_1, \cdots, v_{2h-1})$ sequentially by the following list of $2h$ numbers:

$$a_0, a_1, \cdots, a_{h-1}, a_0 + \kappa, a_1 + \kappa, \cdots, a_{h-1} + \kappa,$$

and on the vertices $W = (w_0, w_1, \cdots, w_{2h-1})$ by, similarly,

$$b_0, b_1, \cdots, b_{h-1}, b_0+\kappa, b_1+\kappa, \cdots, b_{h-1}+\kappa,$$

where we set

$$a_0 = 0, \quad a_i = 2i-(2h+1), \qquad i = 1,2,\cdots,h-1,$$
$$b_0 = 0, \quad b_j = -j(2h+1)-1, \quad j = 1,2,\cdots,h-1,$$
$$\kappa = -1.$$

All integers are considered modulo $h(2h+1)$. Obviously, $|E| = h(2h+1)$ and κ are coprime for any positive integer h and the wrapped-condition (7) is fulfilled. **Figure 7** illustrates the definition for the case $h=3$. All numbers in $Z_{h(2h+1)}$ appear exactly once as difference of $\mathbf{\Delta}$ which hence defines a wrapped $\mathbf{\Delta}$-labelling.

Theorem 9. ([9]) *Let h be a positive integer. For all h there is a (d, f)-cluttered ordering of the complete bipartite graph $K_{h(2h+1),h(2h+1)}$ with $d = h(2h+1)$ and $f = 4h$.*

5. Our Result: A Sequence of a Wrapped Δ-Labelling for $H(3;t)$

In this section, we define a wrapped $\mathbf{\Delta}$-labelling of $H(3;t)$ for any positive integer *t*. $H(3;t) = (U,E)$ has $6(t+1)$ vertices and $21t$ edges. For a fixed *t*, a labelling $\mathbf{\Delta}$ is a map $\Delta: U \to Z_{21t} \times Z_2$ on the vertex set $U = V \cup W$. We specify the second component of $\mathbf{\Delta}$ on the vertices $V = (v_0, v_1, \cdots, v_{3t+2})$ sequentially by the following list of $3t+3$ numbers:

$$c_0, c_0+a, c_0+2a, c_1, c_1+a, c_1+2a, \cdots, c_j, c_j+a, c_j+2a, \cdots, c_{t-1}, c_{t-1}+a, c_{t-1}+2a, c_0+\kappa, c_0+a+\kappa, c_0+2a+\kappa,$$

and, on the vertices $W = (w_0, w_1, \cdots, w_{3t+2})$ by, similarly,

$$d_0, d_0+b, d_0+2b, d_1, d_1+b, d_1+2b, \cdots, d_j, d_j+b, d_j+2b, \cdots, d_{t-1}, d_{t-1}+b, d_{t-1}+2b, d_0+\kappa, d_0+b+\kappa, d_0+2b+\kappa,$$

where we set

$$a = 15t-1, \quad c_j = 3jt, \qquad j = 0,1,\cdots,t-1,$$
$$b = 15t-2, \quad d_j = 3j(t-1), \quad j = 0,1,\cdots,t-1,$$
$$\kappa = 3t^2+1.$$

All integers are considered modulo $21t$. Note that $|E| = 21t$ and $\kappa = 3t^2+1$ are coprime for all positive integer *t* and that the wrapped-condition (7) is obviously fulfilled. **Figure 8** illustrates the definition for the case $t = 1$.

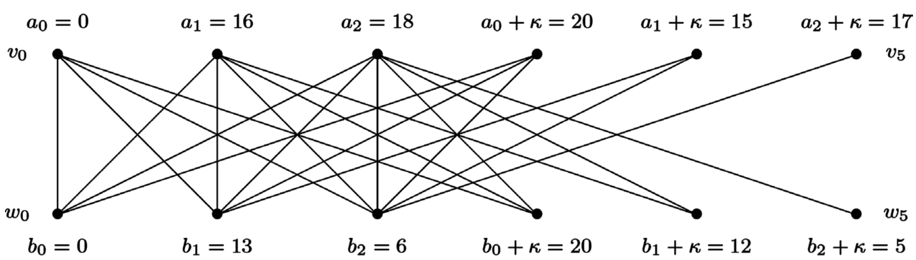

Figure 7. Some wrapped $\mathbf{\Delta}$-labelling of $H(3;1)$, $|E| = 21$, $|V| = 12$, $\kappa = -1$.

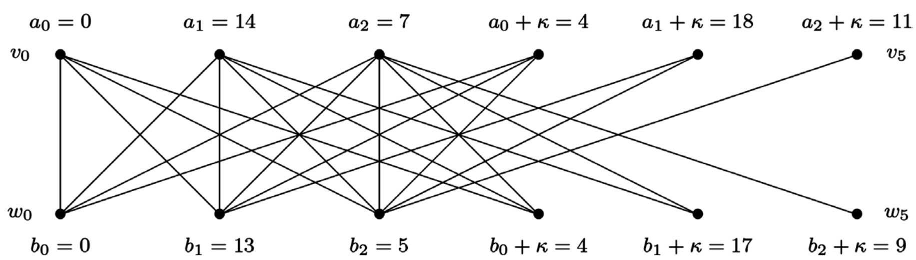

Figure 8. Some wrapped $\mathbf{\Delta}$-labelling of $H(3;1)$, $|E| = 21$, $|V| = 12$, $\kappa = 4$.

We now compute the differences of $\boldsymbol{\Delta}$ using the notation from (1):

$$\begin{aligned}\Delta\left(E_0'\right) &= \big(c_0-d_0, c_0-d_0+(a-b), c_0-d_0+(2a-2b), c_0-d_0+a, c_0-d_0+2a, c_0-d_0-b, c_0-d_0-2b,\\ &\qquad c_0-d_0+(2a-b), c_0-d_0+(a-2b)\big)\\ &= (0,1,2,15t-1,9t-2,6t+2,12t+4,15t,6t+3),\end{aligned}$$

$$\begin{aligned}\Delta\left(E_j'\right) &= \big(c_j-d_j, c_j-d_j+(a-b), c_j-d_j+(2a-2b), c_j-d_j+a, c_j-d_j+2a, c_j-d_j-b,\\ &\qquad c_j-d_j-2b, c_j-d_j+(2a-b), c_j-d_j+(a-2b)\big)\\ &= (3j,3j+1,3j+2,3j+15t-1,3j+9t-2,3j+6t+2,3j+12t+4,3j+15t,3j+6t+3)\\ &\qquad \text{for } j=1,2,\cdots,t-1,\end{aligned}$$

$$\begin{aligned}\Delta\left(E_{j-1}''\right) &= \big(c_{j-1}-d_j, c_{j-1}-d_j+a, c_{j-1}-d_j+2a, c_{j-1}-d_j+(a-b), c_{j-1}-d_j+(2a-b), c_{j-1}-d_j+(2a-2b)\big)\\ &= (3j+18t,3j+12t-1,3j+6t-2,3j+18t+1,3j+12t,3j+18t+2)\\ &\qquad \text{for } j=1,2,\cdots,t-1,\end{aligned}$$

$$\begin{aligned}\Delta\left(E_{j-1}'''\right) &= \big(c_j-d_{j-1}, c_j-d_{j-1}-b, c_j-d_{j-1}-2b, c_j-d_{j-1}+(a-b), c_j-d_{j-1}+(a-2b), c_j-d_{j-1}+(2a-2b)\big)\\ &= (3j+3t-3,3j+9t-1,3j+15t+1,3j+3t-2,3j+9t,3j+3t-1)\\ &\qquad \text{for } j=1,2,\cdots,t-1,\end{aligned}$$

$$\begin{aligned}\Delta\left(E_{t-1}''\right) &= \big(c_{t-1}-d_0-\kappa, c_{t-1}-d_0-\kappa+a, c_{t-1}-d_0-\kappa+2a, c_{t-1}-d_0-\kappa+(a-b), c_{t-1}-d_0-\kappa+(2a-b),\\ &\qquad c_{t-1}-d_0-\kappa+(2a-2b)\big)\\ &= (18t-1,12t-2,6t-3,18t,12t-1,18t+1),\end{aligned}$$

$$\begin{aligned}\Delta\left(E_{t-1}'''\right) &= \big(c_0+\kappa-d_{t-1}, c_0+\kappa-d_{t-1}-b, c_0+\kappa-d_{t-1}-2b, c_0+\kappa-d_{t-1}+(a-b), c_0+\kappa-d_{t-1}+(a-2b),\\ &\qquad c_0+\kappa-d_{t-1}+(2a-2b)\big)\\ &= (6t-2,12t,18t+2,6t-1,12t+1,6t).\end{aligned}$$

We now compute the difference list $\Delta(E)$:

$$\Delta\left(E_0'\right) \supset (0,1,2), \tag{1}$$

$$\Delta\left(\bigcup_{j=1}^{t-1} E_j'\right) \supset \left\{3j,3j+1,3j+2 \,\middle|\, 1\le j\le t-1\right\} = \{3,4,5,\cdots,3t-1\}, \tag{2}$$

$$\Delta\left(\bigcup_{j=1}^{t-1} E_j'''\right) \supset \left\{3j+3t-3,3j+3t-2,3j+3t-1 \,\middle|\, 1\le j\le t-1\right\} = \{3t,3t+1,3t+2,\cdots,6t-4\}, \tag{3}$$

$$\Delta\left(E_{t-1}''\right) \supset (6t-3), \tag{4}$$

$$\Delta\left(E_{t-1}'''\right) \supset (6t-2,6t-1,6t), \tag{5}$$

$$\Delta\left(\bigcup_{j=1}^{t-1} E_{j-1}''\right) \supset \left\{3j+6t-2 \,\middle|\, j=1\right\} = \{6t+1\}, \tag{6}$$

$$\Delta\left(E_0'\right) - (1) \supset (6t+2,6t+3), \tag{7}$$

$$\Delta\left(\bigcup_{j=1}^{t-1} E_{j-1}''\right) - (6) \supset \left\{3j+6t-2 \,\middle|\, 2\le j\le t-1\right\} = \{6t+4,6t+7,6t+10,\cdots,9t-5\}, \tag{8-1}$$

$$\Delta\left(\bigcup_{j=1}^{t-1} E_j'\right) - (2) \supset \left\{3j+6t+2,3j+6t+3 \,\middle|\, 1\le j\le t-2\right\} = \{6t+5,6t+6,6t+8,6t+9,\cdots,9t-4,9t-3\}, \tag{8-2}$$

$$\begin{aligned}&\left(\Delta\left(\bigcup_{j=1}^{t-1}E''_{j-1}\right)-(6)\right)\cup\left(\Delta\left(\bigcup_{j=1}^{t-1}E'_{j}\right)-(2)\right)\\&\quad\supset(8-1)\cup(8-2)\\&\quad=\left\{3j+6t-2\,\middle|\,2\le j\le t-1\right\}\cup\left\{3j+6t+2,3j+6t+3\,\middle|\,1\le j\le t-2\right\}\\&\quad=(6t+4,6t+5,6t+6,6t+7,6t+8,6t+9,6t+10,\cdots,9t-5,9t-4,9t-3),\end{aligned}\tag{8-3}$$

$$\Delta(E'_0)-(1)-(7)\supset(9t-2),\tag{9}$$

$$\Delta\left(\bigcup_{j=1}^{t-1}E'_{j}\right)-(2)-(8-2)\supset\left\{3j+6t+2,3j+6t+3\,\middle|\,j=t-1\right\}=(9t-1,9t),\tag{10}$$

$$\Delta\left(\bigcup_{j=1}^{t-1}E'_{j}\right)-(2)-(8-2)-(10)\supset\left\{3j+9t-2\,\middle|\,1\le j\le t-1\right\}=(9t+1,9t+4,9t+7,\cdots,12t-5),\tag{11-1}$$

$$\Delta\left(\bigcup_{j=1}^{t-1}E'''_{j-1}\right)-(3)\supset\left\{3j+9t-1,3j+9t\,\middle|\,1\le j\le t-1\right\}=(9t+2,9t+3,9t+5,9t+6,\cdots,12t-4,12t-3),\tag{11-2}$$

$$\begin{aligned}&\left(\Delta\left(\bigcup_{j=1}^{t-1}E'_{j}\right)-(2)-(8-2)-(10)\right)\cup\left(\Delta\left(\bigcup_{j=1}^{t-1}E'''_{j-1}\right)-(3)\right)\\&\quad\supset(11-1)\cup(11-2)\\&\quad=\left\{3j+9t-2\,\middle|\,1\le j\le t-1\right\}\cup\left\{3j+9t-1,3j+9t\,\middle|\,1\le j\le t-1\right\}\\&\quad=(9t+1,9t+2,9t+3,9t+4,9t+5,9t+6,\cdots,12t-5,12t-4,12t-3),\end{aligned}\tag{11-3}$$

$$\Delta(E''_{t-1})-(4)\supset(12t-2,12t-1),\tag{12}$$

$$\Delta(E'''_{t-1})-(5)\supset(12t,12t+1),\tag{13}$$

$$\Delta\left(\bigcup_{j=1}^{t-1}E''_{j-1}\right)-(6)-(8-1)\supset\left\{3j+12t-1,3j+12t\,\middle|\,j=1\right\}=(12t+2,12t+3),\tag{14}$$

$$\Delta(E'_0)-(1)-(7)-(9)\supset(12t+4),\tag{15}$$

$$\begin{aligned}&\Delta\left(\bigcup_{j=1}^{t-1}E''_{j-1}\right)-(6)-(8-1)-(14)\supset\left\{3j+12t-1,3j+12t\,\middle|\,2\le j\le t-1\right\}\\&\qquad=(12t+5,12t+6,12t+8,12t+9,\cdots,15t-4,15t-3),\end{aligned}\tag{16-1}$$

$$\Delta\left(\bigcup_{j=1}^{t-1}E'_{j}\right)-(2)-(8-2)-(10)-(11-1)\supset\left\{3j+12t+4\,\middle|\,1\le j\le t-2\right\}=(12t+7,12t+10,\cdots,15t-2),\tag{16-2}$$

$$\begin{aligned}&\left(\Delta\left(\bigcup_{j=1}^{t-1}E''_{j-1}\right)-(6)-(8-1)-(14)\right)\cup\left(\Delta\left(\bigcup_{j=1}^{t-1}E'_{j}\right)-(2)-(8-2)-(10)-(11-1)\right)\supset(16-1)\cup(16-2)\\&\quad=\left\{3j+12t-1,3j+12t\,\middle|\,2\le j\le t-1\right\}\cup\left\{3j+12t+4\,\middle|\,1\le j\le t-2\right\}\\&\quad=(12t+5,12t+6,12t+7,12t+8,12t+9,12t+10,\cdots,15t-4,15t-3,15t-2),\end{aligned}\tag{16-3}$$

$$\Delta(E'_0)-(1)-(7)-(9)-(15)=(15t-1,15t),\tag{17}$$

$$\Delta\left(\bigcup_{j=1}^{t-1}E'_{j}\right)-(2)-(8-2)-(10)-(11-1)-(16-2)\supset\left\{3j+12t+4\,\middle|\,j=t-1\right\}=(15t+1),\tag{18}$$

$$\begin{aligned}&\Delta\left(\bigcup_{j=1}^{t-1}E'_{j}\right)-(2)-(8-2)-(10)-(11-1)-(16-2)-(18)\\&\quad=\left\{3j+15t-1,3j+15t\,\middle|\,1\le j\le t-1\right\}\\&\quad=(15t+2,15t+3,15t+5,15t+6,\cdots,18t-4,18t-3),\end{aligned}\tag{19-1}$$

$$\Delta\left(\bigcup_{j=1}^{t-1} E'''_{j-1}\right)-(3)-(11-2)=\left\{3j+15t+1 \middle| 1\le j\le t-1\right\}=(15t+4,15t+7,\cdots,18t-2), \tag{19-2}$$

$$\begin{aligned}&\left(\Delta\left(\bigcup_{j=1}^{t-1} E'_{j}\right)-(2)-(8-2)-(10)-(11-1)-(16-2)-(18)\right)\cup\left(\Delta\left(\bigcup_{j=1}^{t-1} E'''_{j-1}\right)-(3)-(11-2)\right)\\&=(19-1)\cup(19-2)\\&=\left\{3j+15t-1,3j+15t \middle| 1\le j\le t-1\right\}\cup\left\{3j+15t+1 \middle| 1\le j\le t-1\right\}\\&=(15t+2,15t+3,15t+4,15t+5,15t+6,15t+7,\cdots,18t-4,18t-3,18t-2),\end{aligned} \tag{19-3}$$

$$\Delta\left(E''_{t-1}\right)-(4)-(12)=(18t-1,18t,18t+1), \tag{20}$$

$$\Delta\left(E'''_{t-1}\right)-(5)-(13)=(18t+2), \tag{21}$$

$$\begin{aligned}\Delta\left(\bigcup_{j=1}^{t-1} E''_{j-1}\right)-(6)-(8-1)-(14)-(16-1)&=\left\{3j+18t,3j+18t+1,3j+18t+2 \middle| 1\le j\le t-1\right\}\\&=(18t+3,18t+4,18t+5,\cdots,21t-1).\end{aligned} \tag{22}$$

From this one easily checks that the twenty-two lists cover all numbers in Z_{21t} exactly once. Thus, **Δ** defines a wrapped **Δ**-labelling and by applying Proposition 4 we get the following result.

Theorem 10. *Let t be a positive integer. For all t there is a* (*d*, *f*)*-cluttered ordering of the complete bipartite graph* $K_{21t,21t}$ *with* $d=21$ *and* $f=12$.

Using the same edge ordering of $K_{21t,21t}$ one gets the following theorem by enlarging the window *d*.

Theorem 11. *Let t be a positive integer. For all t there is a* (*d*, *f*)*-cluttered ordering of the complete bipartite graph* $K_{21t,21t}$ *with* $d=21s+r$ *and* $f=6(s+1)+\min(r,6)$, $s>0$, $r=0,1,\cdots,20$.

For example, we get a (21, 12)-cluttered ordering of $K_{21t,21t}$. For the graphs $K_{21t,21t}$, this is a much better ordering than the (21, 16)-cluttered ordering from Theorem 6.

6. Conclusion

In conclusion, we give a new sequence for construction of wrapped **Δ**-labellings. **Figure 7** and **Figure 8** are the same as a graph, but they are different as a sequence. Cluttered orderings given by two sequences construct the different orderings for the complete bipartite graph $K_{21,21}$.

Acknowledgements

We thank the Editor and the referee for their comments.

References

[1] Hellerstein, L., Gibson, G., Karp, R., Katz, R. and Patterson, D. (1994) Coding Techniques for Handling Failures in Large Disk Arrays. *Algorithmica*, **12**, 182-208. http://dx.doi.org/10.1007/BF01185210

[2] Chen, P., Lee, E., Gibson, G., Katz, R. and Ptterson, D. (1994) RAID: High-Performance, Reliable Secondary Storage. *ACM Computing Surveys*, **26**, 145-185. http://dx.doi.org/10.1145/176979.176981

[3] Chee, Y., Colbourn, C. and Ling, A. (2000) Asymptotically Optimal Erasure-Resilient Codes for Large Disk Arrays. *Discrete Applied Mathematics*, **102**, 3-36. http://dx.doi.org/10.1016/S0166-218X(99)00228-0

[4] Cohen, M. and Colbourn, C. (2000) Optimal and Pessimal Orderings of Steiner Triple Systems in Disk Arrays. *Lecture Notes in Computer Science*, **1776**, 95-104. http://dx.doi.org/10.1007/10719839_10

[5] Cohen, M. and Colbourn, C. (2001) Ordering Disks for Double Erasure Codes. *Proceedings of the Thirteenth Annual ACM Symposium on Parallel Algorithms and Architectures*, 229-236.

[6] Cohen, M., Colbourn, C. and Froncek, D. (2001) Cluttered Orderings for the Complete Graph. *Lecture Notes in Computer Science*, **2108**, 420-431. http://dx.doi.org/10.1007/3-540-44679-6_48

[7] Cohen, M. and Colbourn, C. (2004) Ladder Orderings of Pairs and RAID Performance. *Discrete Applied Mathematics*, **138**, 35-46. http://dx.doi.org/10.1016/S0166-218X(03)00268-3

[8] Adachi, T. and Uehara, H. (2014) Construction of Wrapped *ρ*-Labellings for RAID. *Journal of Mathematics and Sys-*

tem Science, **4**, 750-754.

[9] Mueller, M., Adachi, T. and Jimbo, M. (2005) Cluttered Orderings for the Complete Bipartite Graph. *Discrete Applied Mathematics*, **152**, 213-228. http://dx.doi.org/10.1016/j.dam.2005.06.005

[10] Adachi, T. (2007) Optimal Ordering of the Complete Tripartite Graph $K_{9,9,9}$. *Proceedings of the Fourth International Conference on Nonlinear Analysis and Convex Analysis*, 1-10.

[11] Bosák, J. (1990) Decompositions of Graphs. Kluwer Academic Publishers, Dordrecht.

Applied Mathematics, 2015, 6, 206-220
Published Online January 2015 in SciRes. http://www.scirp.org/journal/am
http://dx.doi.org/10.4236/am.2015.61020

On a Problem of an Infinite Plate with a Curvilinear Hole inside the Unit Circle

F. S. Bayones, B. M. Alharbi

Department of Mathematics, Faculty of Science, Taif University, Taif, KSA
Email: F.S.Bayones@hotmail.com, shobee33@gmail.com

Received 8 January 2015; accepted 26 January 2015; published 29 January 2015

Abstract

In this work, we used the complex variable methods to derive the Goursat functions for the first and second fundamental problem of an infinite plate with a curvilinear hole C. The hole is mapped in the domain inside a unit circle by means of the rational mapping function. Many special cases are discussed and established of these functions. Also, many applications and examples are considered. The results indicate that the infinite plate with a curvilinear hole inside the unit circle is very pronounced.

Keywords

Complex Variable Method, An Infinite Plate, Curvilinear Hole, Conformal Mapping, Goursat Functions

1. Introduction

Many intangible phenomena can be found in nature-like magnetic field, electricity and heat. These phenomena cannot be presented mathematically in the real plane. The complex plane plays an important role in presenting these intangible phenomena. Also, many mathematical problems cannot be solved in the real plane; their solutions can be found in the complex plane.

The considerable mathematical difficulties which arise during any attempt to solve plane elastic problems necessitate the search for practical methods of solution. The first use and development of the methods of complex function theory in two-dimensional elastic problems were made by Muskhelishvili (see [1]), and their ideas were expounded in their latter books (see [2]-[4]). The development of the theory was based on the complex representation of the general solution of the equations of the plane theory of elasticity. This complex representation has been found very useful for the effective solution of the plane elastic problems.

Contact and mixed problems in the theory of elasticity have been recognized as a rich and challenging subject

How to cite this paper: Bayones, F.S. and Alharbi, B.M. (2015) On a Problem of an Infinite Plate with a Curvilinear Hole inside the Unit Circle. *Applied Mathematics*, **6**, 206-220. http://dx.doi.org/10.4236/am.2015.61020

for study (see Popov [5], Sabbah [6] and Atkin and Fox [7]). These problems can be established from the initial value problems or from the boundary value problems, or from the mixed problems (see Colton and Kress [8] and Abdou [9]). Also, many different methods are established for solving the contact and mixed problems in elastic and thermoelastic problems; the books edited by Noda [10], Hetnarski [11], Parkus [12] and Popov [5] contain many different methods to solve the problems in the theory of elasticity in one, two and three dimensions.

Several authors wrote about the boundary value problems and their applications in many different sciences (see [7] [13]-[15]). Form these problems, we established contact and mixed problems (see [8] [16]). Complex variable method used to express the solutions of these problems in the form of power series applied Laurent's theorem (see [8] [17]-[19]). The extensive literature on the topic is now available and we can only mention a few recent interesting investigations in [20]-[24].

The first and second fundamental problems in the plane theory of elasticity are equivalent to finding analytic functions $\phi_1(z)$ and $\psi_1(z)$ of one complex argument $z = x + iy$.

These functions satisfy the boundary conditions

$$k\phi_1(t) - t\overline{\phi_1^{\backslash}}(t) - \overline{\psi_1}(t) = f(t) \tag{1}$$

where $\phi_1(t)$ and $\psi_1(t)$ are two analytic functions; t denotes the affix of a point on the boundary. In the first fundamental problem $k = -1$, $f(t)$ is a given function of stresses, while in the second fundamental problem

$$\begin{gathered} k = \chi = \frac{(\lambda + 3\mu)}{\lambda + \mu} \\ \lambda = \frac{E}{(1-2v)(1+v)} \end{gathered} \tag{2}$$

And $f = 2\mu g$ is a given function of the displacement; λ and μ are called the Lame constants.

Let the complex potentials $\phi_1(t)$ and $\psi_1(t)$ take the form

$$\phi_1(\zeta) = -\frac{X + iY}{2\pi(1+\chi)} \ln\zeta + c\Gamma\zeta + \phi(\zeta) \tag{3}$$

$$\psi_1(\zeta) = \chi\frac{(X - iY)}{2\pi(1+\chi)} \ln\zeta + c\Gamma^*\zeta + \psi(\zeta) \tag{4}$$

where X, Y are the components of the resultant vector of all external forces acting on the boundary and Γ, Γ^* are constants; generally complex functions $\phi(\zeta), \psi(\zeta)$ are single-valued analytic functions within the region inside the unit circle γ and $\phi(\infty) = 0$.

Take the conformal mapping which mapped the domain of the curvilinear hole C on the domain inside a unit circle γ by the rational function

$$z = w(\zeta),\ |\zeta| < 1, c > 0. \tag{5}$$

and $w'(\zeta)$ does not vanish or become infinite to conform the curvilinear hole of an infinite elastic plate onto the domain inside a unit circle γ *i.e.*

$$w'(\zeta) \neq 0, \infty. \tag{6}$$

2. Conformal Mapping

Consider the rational mapping on the domain inside a unit circle γ by the rational function

$$z = w(\zeta) = \frac{\zeta^3 + m\zeta}{\zeta - n},\ |n| < 1,\ |\zeta| < 1, \tag{7}$$

where, m and n are complex number $n = n_1 + in_2$, $m = m_1 + im_2$, Equation (7) must satisfy the condition Equation (6).

For determining the tax parameters x and y, we put $\zeta = \rho e^{i\theta}$, $|\rho| = 1$ in Equation (7) to get

$$x + iy = \frac{(\cos 3\theta + m_1 \cos\theta - m_2 \sin\theta) + i(\sin 3\theta + m_1 \sin\theta + m_2 \cos\theta)}{(\cos\theta - n_1) + i(\sin\theta - n_2)} \tag{8}$$

Then

$$x = \frac{\cos 2\theta + m_1 - n_1(\cos 3\theta + m_1 \cos\theta - m_2 \sin\theta) + n_1(\sin 3\theta + m_1 \sin\theta + m_2 \cos\theta)}{(\cos\theta - n_1)^2 + (\sin\theta - n_2)^2} \tag{9}$$

$$y = \frac{\sin 2\theta + m_2 + n_2(\cos 3\theta + m_1 \cos\theta - m_2 \sin\theta) - n_1(\sin 3\theta + m_1 \sin\theta + m_2 \cos\theta)}{(\cos\theta - n_1)^2 + (\sin\theta - n_2)^2} \tag{10}$$

Also,

$$z' = w'(\zeta) = \frac{2\zeta^3 - 3n\zeta^2 - mn}{(\zeta - n)^2}.$$

To obtain the critical points, we consider

$$2\zeta^3 - 3n\zeta^2 - mn = 0 \tag{11}$$

this linear equation of three order, the roots of this equation must be under 1.
The following graphs give the different shapes of the rational mapping (7), see **Figure 1**.

3. The Components of Stresses

It is known that, the components of stresses are given by, see [1]

$$\sigma_{xx} + \sigma_{yy} = 4\operatorname{Re}\{\phi'(z)\} \tag{12}$$

$$\sigma_{yy} - \sigma_{xx} + i\sigma_{xy} = 2\{\bar{z}\phi''(z) + \psi'(z)\} \tag{13}$$

Hence, we have

$$\sigma_{yy} = \operatorname{Re}\{2\phi'(z) + M(z,\bar{z})\},\ M(z,\bar{z}) = \bar{z}\phi''(z) + \psi'(z) \tag{14}$$

$$\sigma_{xx} = \operatorname{Re}\{2\phi'(z) - M(z,\bar{z})\},\ M(z,\bar{z}) = \bar{z}\phi''(z) + \psi'(z) \tag{15}$$

and

$$\sigma_{xy} = 2\operatorname{Im}\{\bar{z}\phi''(z) + \psi'(z)\} = 2\operatorname{Im}\{M(z,\bar{z})\} \tag{16}$$

4. Goursat Functions

To obtain the tow complex potential functions (Goursat functions) by using the conformal mapping (7) in the boundary condition (6). We write the expression $\dfrac{w(\zeta)}{\overline{w'(\zeta)}}$ in the form,

$$\frac{w(\zeta)}{\overline{w'(\zeta)}} = \alpha(\zeta) + \overline{\beta(\zeta)} \tag{17}$$

where,

$$\alpha(\zeta) = \frac{h}{(\zeta - n)},\ \overline{\beta(\zeta)} = \frac{w(\zeta)}{\overline{w'(\zeta)}} - \frac{h}{\zeta - n} \tag{18}$$

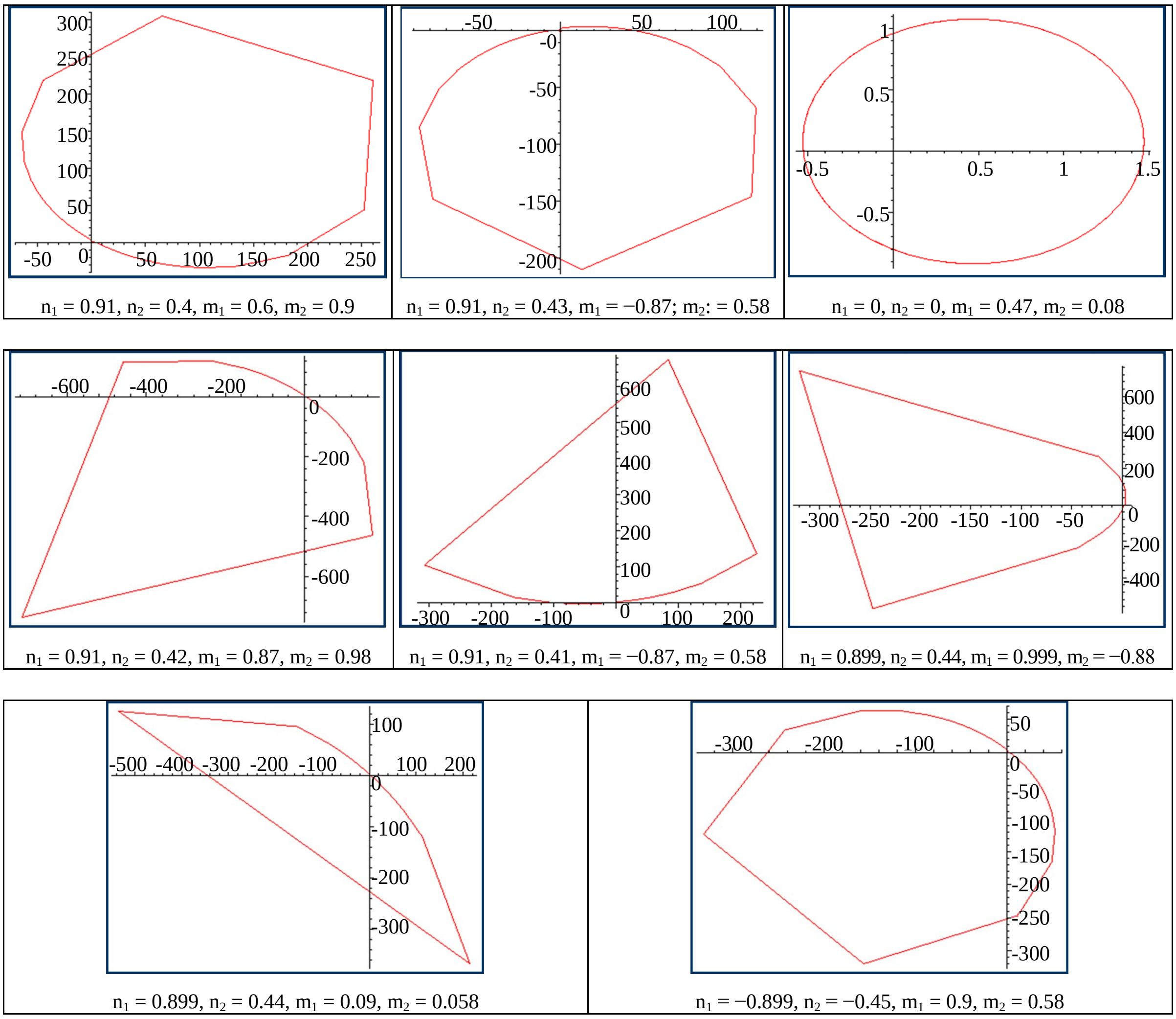

Figure 1. The different shapes of the rational mapping (7).

$\beta\left(\zeta^{-1}\right)$ is a regular function for $|\zeta|<1$.

In order to separate the singularity, we use the definition of mapping, to have

$$\frac{w(\zeta)}{\overline{\overline{w'(\zeta)}}}=\frac{\zeta^3+m\zeta}{\zeta-n}\cdot\frac{\zeta(1-n\zeta)^2}{\left(2-3n\zeta-mn\zeta^3\right)}=\frac{1}{\zeta-n}\cdot\frac{\zeta^2\left(\zeta^2+m\right)(1-n\zeta)^2}{\left(2-3n\zeta-mn\zeta^3\right)} \tag{19}$$

The term $\left(2-3n\zeta-mn\zeta^3\right)$ in the are has no singular point while $(\zeta-n)$ has a singularity at $\zeta=n$. where

$$\overline{w'(\zeta)}=\frac{\left(2-3n\zeta-mn\zeta^3\right)}{\zeta(1-n\zeta)^2} \tag{20}$$

To determine h form Equation (19), we can write the form

$$\frac{w(\sigma)}{\overline{\overline{w'(\sigma)}}}=\frac{1}{\sigma-n}\cdot\frac{\sigma^2\left(\sigma^2+m\right)(1-n\sigma)^2}{\left(2-3n\sigma-mn\sigma^3\right)}. \tag{21}$$

By using the residues in this equating we have

$$h = \frac{n^2\left(n^2+m\right)\left(1-n^2\right)^2}{\left(2-3n^2-mn^4\right)}. \tag{22}$$

Using Equation (3) and Equation (4) in Equation (1), we get

$$k\phi(\sigma)-\alpha(\sigma)\overline{\phi'(\sigma)}-\overline{\psi_*(\sigma)}=G(\sigma) \tag{23}$$

where

$$\psi_*(\sigma)=\psi(\sigma)+\beta(\sigma)\phi'(\sigma) \tag{24}$$

$$G(\sigma)=F(\sigma)-ck\Gamma\sigma+\frac{c\overline{\Gamma^*}}{\sigma}+N(\sigma)\alpha(\sigma)+N(\sigma)\overline{\beta(\sigma)} \tag{25}$$

$$N(\sigma)=\left[c\overline{\Gamma}-\frac{\sigma(X-iY)}{2\pi(1+\chi)}\right],\quad F(\sigma)=f(t) \tag{26}$$

Assume that the function $F(\sigma)$ with its derivatives must satisfy the Holder condition. Our aim is to determine the functions $\phi(\zeta)$ and $\psi(\zeta)$ for the various boundary value problems. For this multiply both sides of Equation (23) by $\frac{\mathrm{d}\sigma}{2\pi i(\sigma-\zeta)}$, where ζ is any point in the interior of γ and integral over the circle, we obtain

$$\frac{k}{2\pi i}\int_\gamma\frac{\phi(\sigma)}{\sigma-\zeta}\mathrm{d}\sigma-\frac{1}{2\pi i}\int_\gamma\frac{\alpha(\sigma)\overline{\phi'}(\sigma)}{\sigma-\zeta}\mathrm{d}\sigma-\frac{1}{2\pi i}\int_\gamma\frac{\overline{\psi_*}(\sigma)}{\sigma-\zeta}\mathrm{d}\sigma=\frac{1}{2\pi i}\int_\gamma\frac{G(\sigma)}{\sigma-\zeta}\mathrm{d}\sigma \tag{27}$$

Using Equations (24)-(26) in Equation (27) then applying the properties of Cauchy integral, to have

$$\frac{k}{2\pi i}\int_\gamma\frac{\phi(\sigma)}{\sigma-\zeta}\mathrm{d}\sigma=-k\phi(\zeta) \tag{28}$$

and

$$\frac{1}{2\pi i}\int_\gamma\frac{\alpha(\sigma)\overline{\phi'}(\sigma)}{\sigma-\zeta}\mathrm{d}\sigma=\frac{chb}{n-\zeta} \tag{29}$$

$$\frac{1}{2\pi i}\int_\gamma\frac{N(\sigma)\alpha(\sigma)}{(\sigma-\zeta)}\mathrm{d}\sigma=\frac{N(n)h}{n-\zeta} \tag{30}$$

Also,

$$\frac{1}{2\pi i}\int_\gamma\frac{G(\sigma)}{(\sigma-\zeta)}\mathrm{d}\sigma=A(\zeta)-\frac{c\overline{\Gamma^*}}{\zeta}+\frac{hN(n)}{(n-\zeta)} \tag{31}$$

where,

$$A(\zeta)=\frac{1}{2\pi i}\int_\gamma\frac{F(\sigma)}{(\sigma-\zeta)}\mathrm{d}\sigma,\quad N(\sigma)=\left[c\overline{\Gamma}-\frac{\sigma(X-iY)}{2\pi(1+\chi)}\right]. \tag{32}$$

From the above, Equation (27) becomes

$$-k\phi(\zeta)=A(\zeta)+\frac{h}{n-\zeta}\left(cb+N(n)\right)-\frac{c\overline{\Gamma^*}}{\zeta} \tag{33}$$

To determined b, where b are complex constants, differentiating Equation (33) with respect to ζ and substituting in Equation (29), we get

$$\frac{1}{2\pi i}\int_{\gamma}\frac{\alpha(\sigma)}{(\sigma-\zeta)}\left[-\overline{A'(\sigma)}-c\Gamma^{*}\sigma^{2}-\frac{h\sigma^{2}}{(n\sigma-1)^{2}}\left(c\bar{b}+\overline{N(n)}\right)\mathrm{d}\sigma\right]=\frac{ckhb}{(n-\zeta)} \tag{34}$$

Substituting Equation (18) in Equation (34), then using the properties of Cauchy integral and applying the reside theorem at the singular points, we obtain

$$ckb+\overline{A'(n)}+c\Gamma^{*}n^{2}+\upsilon h\left(c\bar{b}+\overline{N(n)}\right)=0 \tag{35}$$

where

$$\upsilon=\frac{n^{2}}{\left(1-n^{2}\right)^{2}} \tag{36}$$

The last equation can be written in the form

$$ckb+\upsilon hc\bar{b}=E \tag{37}$$

where,

$$E=-\overline{A'(n)}-c\Gamma^{*}n^{2}-\upsilon h\overline{N(n)} \tag{38}$$

taking the complex conjugate of Equation (37), we get

$$ck\bar{b}+\upsilon hcb=\bar{E} \tag{39}$$

form Equation (37) and Equation (39), we have

$$b=\frac{kE-\upsilon h\bar{E}}{c\left(k^{2}-\upsilon^{2}h^{2}\right)} \tag{40}$$

To obtain the complex function $\psi(\zeta)$ we have form Equation (23) after substituting the expression of $\psi(\sigma)$ and $G(\sigma)$, and taking the complex conjugate of the resulting equation after using the expression of $\overline{\beta(\sigma)}$ to yields,

$$\psi(\sigma)=-\overline{F(\sigma)}+ck\bar{\Gamma}\sigma^{-1}-c\Gamma^{*}\sigma+k\overline{\phi(\sigma)}-\overline{\alpha(\sigma)}\phi_{*}(\sigma)-\frac{\overline{w(\sigma)}}{w'(\sigma)}\phi_{*}(\sigma)+\frac{h\sigma}{(1-n\sigma)}\phi_{*}(\sigma) \tag{41}$$

where,

$$\phi_{*}(\sigma)=\phi'(\sigma)+\overline{N(\sigma)},\quad \overline{N(\sigma)}=\left[c\Gamma-\frac{\sigma^{-1}(X+iY)}{2\pi(1+\chi)}\right] \tag{42}$$

and calculate sum residue, we obtain multiplying both sides of Equation (41) by $\frac{1}{2\pi i(\sigma-\zeta)}$, where ζ is any point in the interior of γ and integrating over the circle, then using the properties of Cauchy's integral and calculating the sum residue, we obtain

$$\psi(\zeta)=ck\bar{\Gamma}\zeta^{-1}-\frac{\overline{w(\zeta)}}{w'(\zeta)}\phi_{*}(\zeta)+\frac{h\zeta}{(1-n\zeta)}\phi_{*}\left(n^{-1}\right)+B(\zeta)-B \tag{43}$$

where,

$$B(\zeta)=\frac{1}{2\pi i}\int_{\gamma}\frac{\overline{F(\sigma)}}{(\sigma-\zeta)}\mathrm{d}\sigma, \tag{44}$$

and

$$B=\frac{1}{2\pi i}\int_{\gamma}\frac{\overline{F(\sigma)}}{\sigma}\mathrm{d}\sigma. \tag{45}$$

5. Special Cases

Now, we are in a position to consider several cases:

1) Let $m=0, n\neq 0$, we get the mapping function represent of the hole is an ellipse, see **Figure 2**

$$z=w(\zeta)=\frac{\zeta^3}{\zeta-n} \tag{46}$$

by let

$$z'=0\Rightarrow 2\zeta^3-3n\zeta^2=0.$$

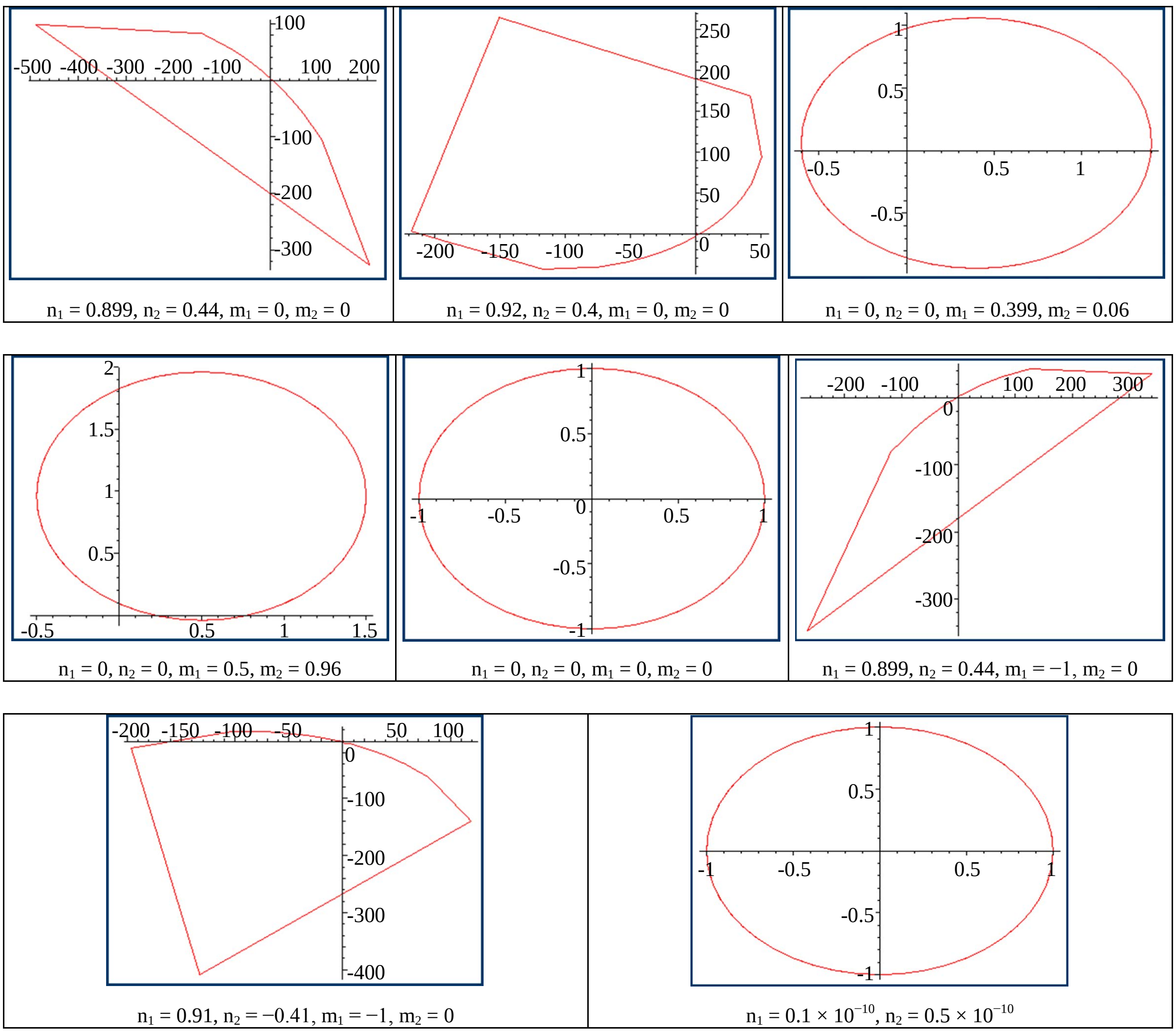

Figure 2. The different shapes of the rational mapping for special cases.

Then (33) and (43) becomes

$$h=\frac{n^4\left(1-n^2\right)^2}{2-3n^2}$$

$$-k\phi(\zeta)=A(\zeta)-\frac{c\overline{\Gamma^*}}{\zeta}+\frac{n^4\left(1-n^2\right)^2}{\left(2-3n^2\right)(n-\zeta)}\left[N(n)+\frac{kE-h\upsilon\bar{E}}{k^2-h^2\upsilon^2}\right] \tag{47}$$

$$-k\phi(\zeta)=A(\zeta)-\frac{c\overline{\Gamma^*}}{\zeta}+\frac{n^4\left(1-n^2\right)^2}{\left(2-3n^2\right)(n-\zeta)}\left[N(n)+\frac{kE-\frac{n^6\bar{E}}{\left(2-3n^2\right)}}{k^2-\frac{n^{12}}{\left(2-3n^2\right)^2}}\right].$$

Also,

$$\psi(\zeta)=B(\zeta)+\frac{ck\bar{\Gamma}}{\zeta}-\frac{w\left(\zeta^{-1}\right)}{w'(\zeta)}\phi_*(\zeta)+\frac{n^4\left(1-n^2\right)^2\zeta}{\left(2-3n^2\right)(1-n\zeta)}\phi_*\left(n^{-1}\right)-B. \tag{48}$$

where

$$E=-\overline{A'(n)}-c\Gamma^*n^2-\frac{n^6}{2-3n^2}\overline{N(n)}$$

2) For $n=0, 0\le m\le 1$, we get the mapping function represent of the hole is an ellipse, see **Figure 2**

$$\begin{gathered} z=\frac{\zeta^3+m\zeta}{\zeta}=\zeta^2+m \\ z'=0\Rightarrow 2\zeta=0 \end{gathered} \tag{49}$$

then

$$\zeta=\mathrm{e}^{i\alpha},\ \ \mathrm{e}^{i\alpha}=\cos\alpha+i\sin\alpha.$$

Then (33) and (43) becomes

$$h=0$$

$$-k\phi(\zeta)=A(\zeta)-\frac{c\overline{\Gamma^*}}{\zeta} \tag{50}$$

$$\psi(\zeta)=B(\zeta)+\frac{ck\bar{\Gamma}}{\zeta}-\frac{1+m\zeta^2}{2\zeta^3}\phi_*(\zeta)-B \tag{51}$$

where

$$E=-\overline{A'(n)}-c\Gamma^*n^2,\ \ n=0.$$

3) Let $m=n=0$, we get the mapping function represent of the hole is an ellipse, see **Figure 2**

$$z=\frac{\zeta^3}{\zeta}=\zeta^2 \tag{52}$$

$$z'=0\Rightarrow 2\zeta=0$$

$$\zeta=\mathrm{e}^{i\alpha},\ \ \mathrm{e}^{i\alpha}=\cos\alpha+i\sin\alpha$$

Then (33) and (43) becomes

$$h = 0$$

$$-k\phi(\zeta) = A(\zeta) - \frac{c\overline{\Gamma^*}}{\zeta} \tag{53}$$

$$\psi(\zeta) = B(\zeta) + \frac{ck\overline{\Gamma}}{\zeta} - \frac{1}{2\zeta^3}\phi_*(\zeta) - B \tag{54}$$

$$E = -\overline{A'(n)} - c\Gamma^* n^2,\ n = 0.$$

4) Let $m = -1$, where $m_1 = -1, m_2 = 0$ we get the mapping function represent of the hole is an ellipse, see **Figure 2**

$$z = \frac{\zeta^3 - \zeta}{\zeta - n} \tag{55}$$

$$z' = 0 \Rightarrow 2\zeta^3 - 3n\zeta^2 + n = 0$$

Then (33) and (43) becomes

$$h = \frac{n^2\left(n^2-1\right)\left(1-n^2\right)^2}{2-3n^2+n^4}$$

$$-k\phi(\zeta) = A(\zeta) - \frac{c\overline{\Gamma^*}}{\zeta} + \frac{n^2\left(n^2-1\right)\left(1-n^2\right)^2}{\left(2-3n^2+n^4\right)(n-\zeta)}\left[N(n) + \frac{kE - \dfrac{n^4\left(n^2-1\right)\overline{E}}{\left(2-3n^2+n^4\right)}}{k^2 - \dfrac{n^8\left(n^2-1\right)^2}{\left(2-3n^2+n^4\right)^2}}\right] \tag{56}$$

Also,

$$\psi(\zeta) = B(\zeta) + \frac{ck\overline{\Gamma}}{\zeta} - \frac{w\left(\zeta^{-1}\right)}{w'(\zeta)}\phi_*(\zeta) + \frac{n^2\left(n^2-1\right)\left(1-n^2\right)^2\zeta}{\left(2-3n^2+n^4\right)(1-n\zeta)}\phi_*\left(n^{-1}\right) - B \tag{57}$$

where

$$E = -\overline{A'(n)} - c\Gamma^* n^2 + \frac{n^4\left(n^2-1\right)}{2-3n^2+n^4}\overline{N(n)}$$

5) Let $m = -n^2$, we get the mapping function represent of the hole is an ellipse, see **Figure 2**

$$z = \frac{\zeta^3 - n^2\zeta}{\zeta - n} = \zeta^2 + n\zeta \tag{58}$$

$$z' = 0 \Rightarrow 2\zeta + n = 0$$

$$\zeta = -\frac{n}{2}$$

Then (33) and (43) becomes

$$h = 0$$

$$-k\phi(\zeta) = A(\zeta) - \frac{c\overline{\Gamma^*}}{\zeta} \tag{59}$$

Also,

$$\psi(\zeta) = B(\zeta) + \frac{ck\overline{\Gamma}}{\zeta} - \frac{w(\zeta^{-1})}{w'(\zeta)}\phi_*(\zeta) - B \tag{60}$$

$$E = -\overline{A'(n)} - c\Gamma^* n^2 + \frac{n^4(n^2+1)}{2-3n^2+n^4}\overline{N(n)}$$

6. Applications

In this section we study some applications:

1) For $k=-1, \Gamma = \frac{p}{4}, \Gamma^* = -\frac{1}{2}pe^{-2i\theta}$ and $X = Y = f = 0$, we have the case of infinite plate stretched at infinity by the application of a uniform tensile stress of intensity p, making an angle θ with the x-axis. The plate weakened by the curvilinear hole C which is free from stresses (see **Figure 3**, **Figure 4** ($n_1 = 0.001$, $n_2 = 0.002l$, $m_1 = 0.025$, $m_2 = 0.03I$, $c = 2$, $p = 0.25$)). Then the functions in (33) and (43) become

$$f = 0 \Rightarrow A(\zeta) = 0 \tag{61}$$

$$N(n) = \left[c\overline{\Gamma} - \frac{n(X - iY)}{2\pi(1+\chi)}\right] = \frac{cp}{4} \tag{62}$$

$$E = \frac{2cn^2 pe^{-2i\theta} - \upsilon hcp}{4}, \quad \overline{E} = \frac{2cn^2 pe^{2i\theta} - \upsilon hcp}{4} \tag{63}$$

$$cb = \frac{kE - \upsilon h\overline{E}}{(k^2 - \upsilon^2 h^2)} = \frac{-E - \upsilon h\overline{E}}{(1 - \upsilon^2 h^2)} \tag{64}$$

$$\phi(\zeta) = \frac{cpe^{2i\theta}}{2\zeta} + \frac{chp}{4(n-\zeta)}\left(1 + \frac{ch\upsilon - 2cn^2 e^{-2i\theta} - 2h\upsilon cn^2 e^{2i\theta} + ch^2\upsilon^2}{1 - h^2\upsilon^2}\right). \tag{65}$$

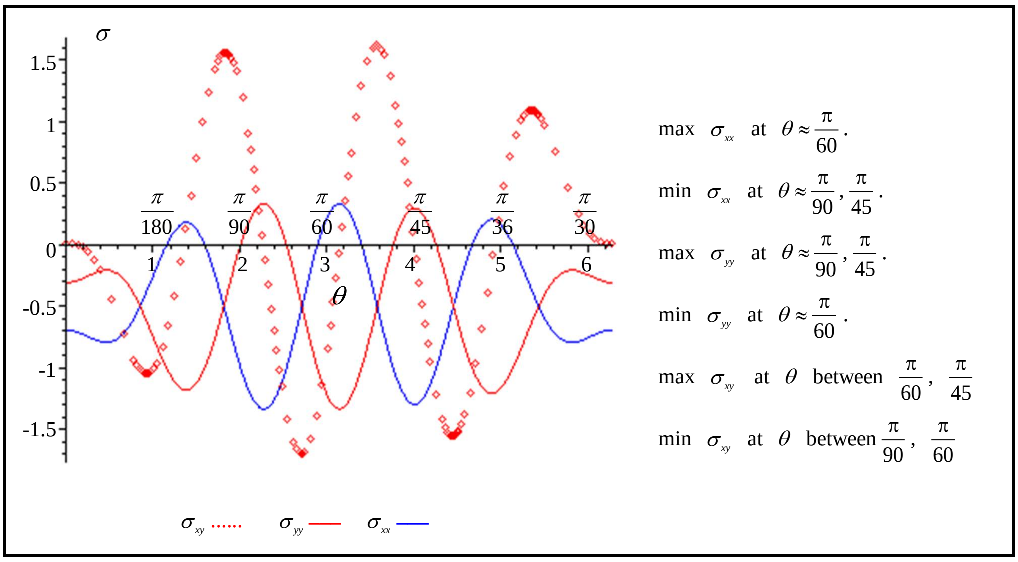

Figure 3. The relation between components of stresses and the angle made on the x-axis.

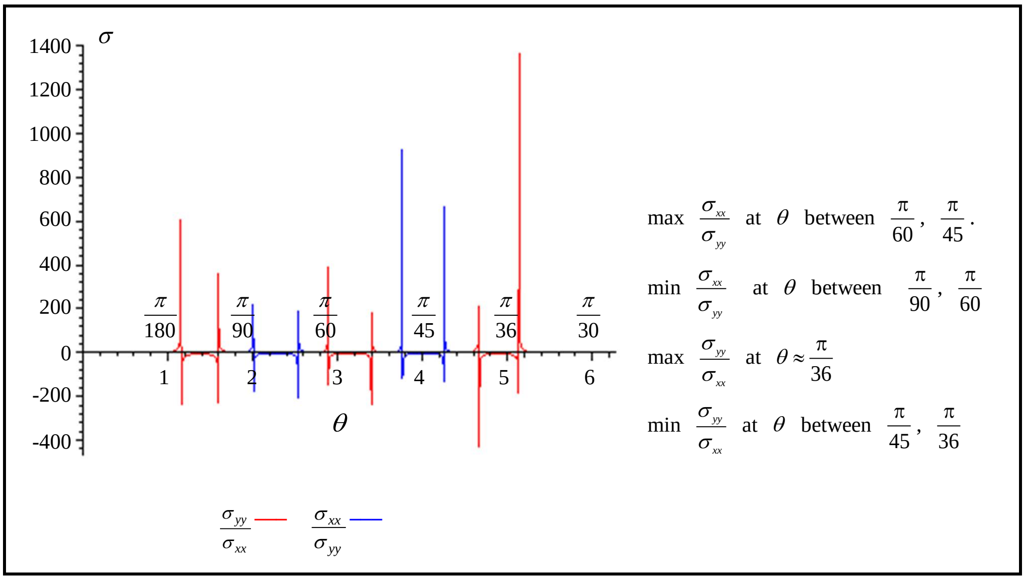

Figure 4. The ratio of vertical to horizontal stresses.

$$\psi(\zeta) = -\frac{cp}{4\zeta} - \frac{w(\zeta^{-1})}{w'(\zeta)}\phi_*(\zeta) + \frac{h\zeta}{(1-n\zeta)}\phi_*(n^{-1}) \tag{66}$$

where

$$\phi_*(\zeta) = \phi'(\zeta) + \frac{cp}{4}.$$

2) For $k=-1$, $\Gamma = \Gamma^* = X = Y = 0$ and $f = Pt$, where P is a real constant (see **Figure 5**, **Figure 6** ($n_1 = 0.001, n_2 = 0.002I, m_1 = 0.025, m_2 = 0.03I, c = 2, p = 0.25$)).

Then the functions in (33) and (43) become

$$f = Pt \Rightarrow f = \frac{Pc(\sigma^3 + m\sigma)}{(\sigma - n)} \tag{67}$$

$$\bar{f} = \frac{cP(1 + m\sigma^2)}{\sigma^2(1 - n\sigma)} \tag{68}$$

$$A(\zeta) = \frac{cP}{2\pi i}\int_\gamma \frac{\sigma^3 + m\sigma}{(\sigma - n)(\sigma - \zeta)}\mathrm{d}\sigma = \frac{cP(n^3 + mn)}{(n - \zeta)} \tag{69}$$

$$A'(\zeta) = \frac{cP(n^3 + mn)}{(n - \zeta)^2}, \quad \overline{A'(\zeta)} = \frac{cP\zeta^2(n^3 + mn)}{(n\zeta - 1)^2}$$

$$\overline{A'(n)} = \frac{cPn^2(n^3 + mn)}{(n^2 - 1)^2}, \quad N(n) = 0 \tag{70}$$

$$E = -\frac{cPn^2(n^3 + mn)}{(n^2 - 1)^2} = \bar{E} \tag{71}$$

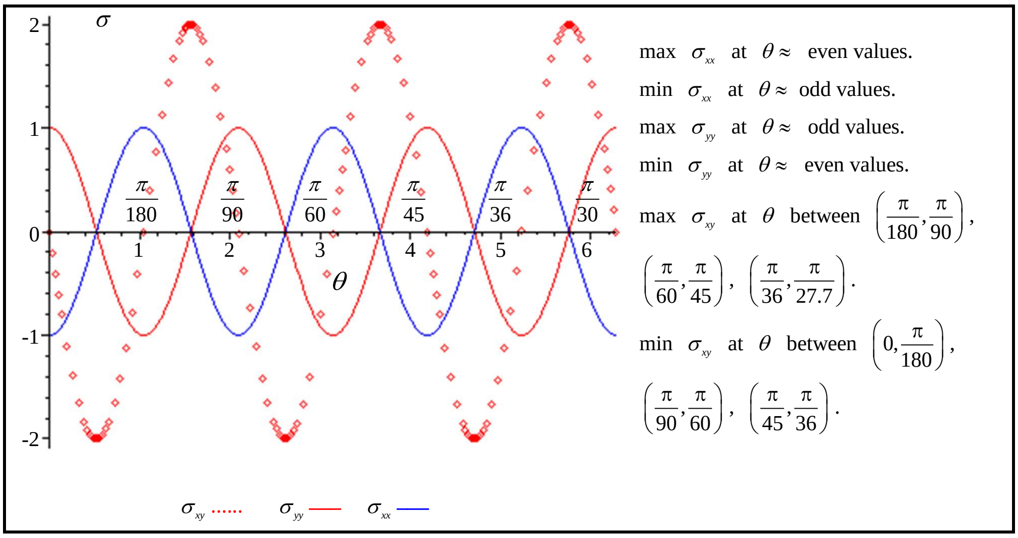

Figure 5. The relation between components of stresses and the angle made on the x-axis.

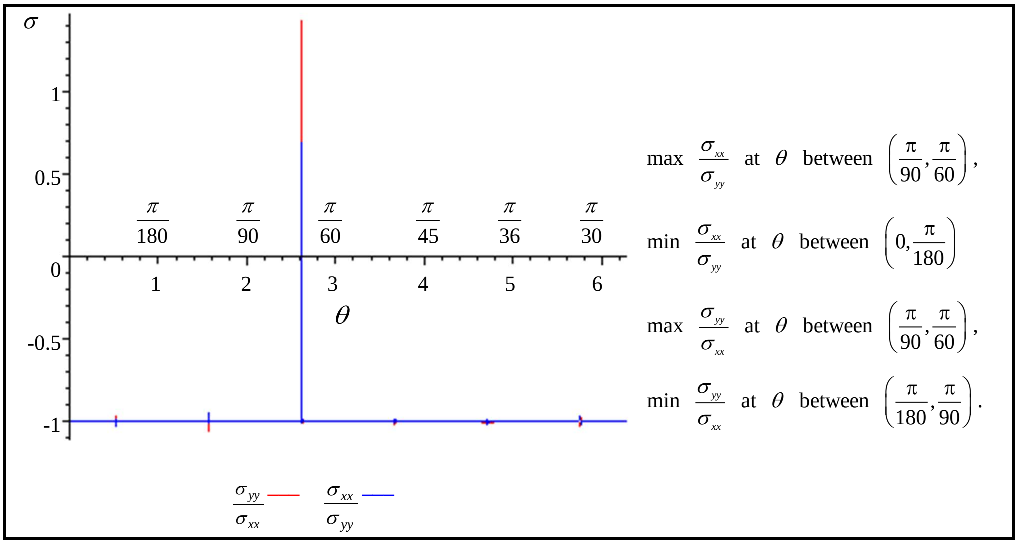

Figure 6. The ratio of vertical to horizontal stresses.

$$cb = \frac{cPn^2\left(n^3+mn\right)}{(1-\upsilon h)\left(n^2-1\right)^2} \tag{72}$$

$$\phi(\zeta) = \frac{cP\left(n^3+mn\right)}{(n-\zeta)} + \frac{hcPn^2\left(n^3+mn\right)}{(n-\zeta)(1-\upsilon h)\left(n^2-1\right)^2} \tag{73}$$

$$\psi(\zeta) = -cP\left(n+\frac{1}{\zeta^2}\right) - \frac{w\left(\zeta^{-1}\right)}{w'(\zeta)}\phi'(\zeta) + \frac{h\zeta}{(1-n\zeta)}\phi'\left(n^{-1}\right) \tag{74}$$

where

$$B(\zeta) = \frac{1}{2\pi i}\int_\gamma \frac{\overline{F(\sigma)}}{(\sigma-\zeta)}\mathrm{d}\sigma = \frac{cP}{2\pi i}\int_\gamma \frac{\left(1+m\sigma^2\right)}{\sigma^2(1-n\sigma)(\sigma-\zeta)}\mathrm{d}\sigma = -\frac{cP(1+n\zeta)}{\zeta^2}$$

$$B=\frac{cP}{2\pi i}\int_{\gamma}\frac{\left(1+m\sigma^{2}\right)}{\sigma^{3}\left(1-n\sigma\right)}\mathrm{d}\sigma=2cP\left(m+n^{2}\right),\ \phi_{*}\left(\zeta\right)=\phi'\left(\zeta\right).$$

3) For $k=\chi,\ \Gamma=\Gamma^{*}=f=0$ (see **Figure 7**, **Figure 8** ($n_1=0.001,\ n_2=0.002I,\ m_1=0.025,\ m_2=0.03I,\ c=2,\ x=0.25,\ X=2,\ Y=2$)). Then the functions in (33) and (43) become

$$f=0\Rightarrow A\left(\zeta\right)=0 \tag{75}$$

$$N\left(n\right)=-\frac{n\left(X-iY\right)}{2\pi\left(1+\chi\right)} \tag{76}$$

$$E=\frac{\upsilon hn\left(X+iY\right)}{2\pi\left(1+\chi\right)},\ \bar{E}=\frac{\upsilon hn\left(X-iY\right)}{2\pi\left(1+\chi\right)} \tag{77}$$

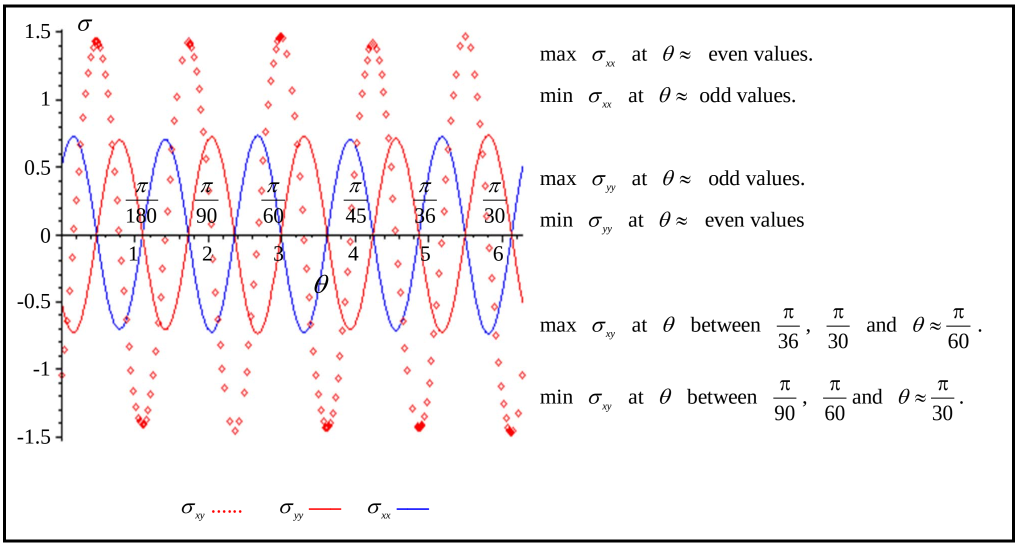

Figure 7. The relation between components of stresses and the angle made on the x-axis.

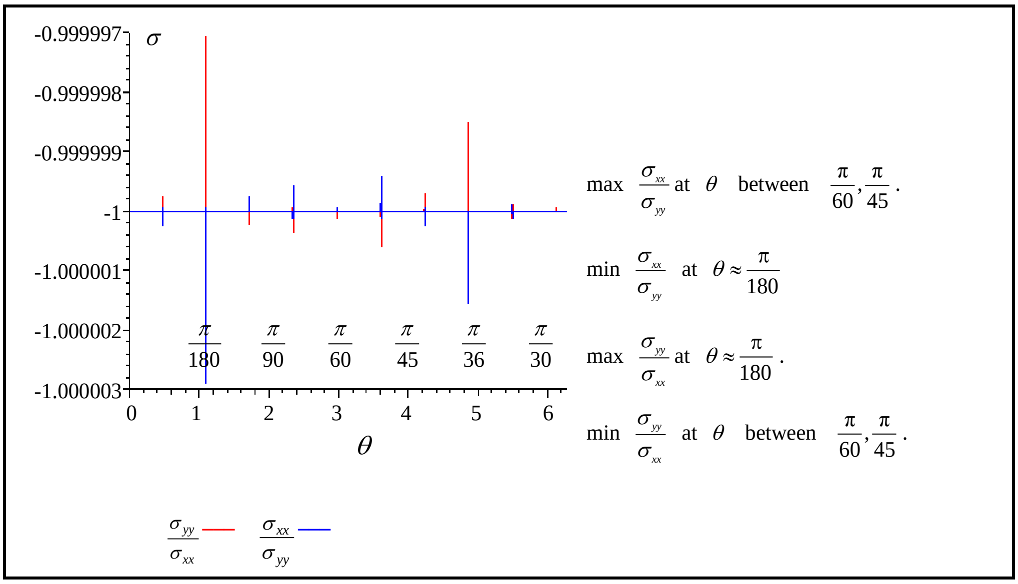

Figure 8. The ratio of vertical to horizontal stresses.

$$cb = \frac{\chi h \upsilon n (X + iY) - nh^2 \upsilon^2 (X - iY)}{2\pi (1+\chi)(\chi^2 - h^2 \upsilon^2)} \tag{78}$$

$$-\chi \phi(\zeta) = \frac{h}{(n-\zeta)} \left(\frac{\chi h \upsilon n (X + iY) - nh^2 \upsilon^2 (X - iY)}{2\pi (1+\chi)(\chi^2 - h^2 \upsilon^2)} - \frac{n(X - iY)}{2\pi (1+\chi)} \right)$$

$$\phi(\zeta) = \frac{-1}{\chi} \frac{hn}{2\pi (1+\chi)(n-\zeta)} \left(\frac{\chi h \upsilon (X + iY)}{(\chi^2 - h^2 \upsilon^2)} - (X - iY) \left(1 + \frac{h^2 \upsilon^2}{(\chi^2 - h^2 \upsilon^2)} \right) \right) \tag{79}$$

$$\psi(\zeta) = -\frac{w(\zeta^{-1})}{w'(\zeta)} \phi_*(\zeta) + \frac{h\zeta}{(1-n\zeta)} \phi_*(n^{-1}) \tag{80}$$

where

$$\phi_*(\zeta) = \phi'(\zeta) - \frac{(X + iY)}{2\pi (1+\chi)\zeta}.$$

References

[1] Muskhelishvili, N.I. (1953) Some Basic Problems of Mathematical Theory of Elasticity. Noordroof, Holland.

[2] Spiegel. M.R. (1964) Theory and Problems of Complex Variables, Schaum's Outline Series. McGraw-Hill, New York.

[3] Rubenfeld, L.A. (1985) A First Course in Applied Complex Variables. John Wiley & Sons, New York.

[4] Bieberbach, L. (1953) Conformal Mapping. Chelsea Publishing Company, New York.

[5] Popov, G.Ya. (1982) Contact Problems for a Linearly Deformable Functions. Odessa, Kiev.

[6] Sabbah, A.S., Abdou, M.A. and Ismail, A.S. (2002) An Infinite Plate with a Curvilinear Hole and Flowing Heat. *Proc. Math. Phys. Soc. Egypt*.

[7] Atkin, R.J. and Fox, N. (1990) An Introduction to the Theory of Elasticity. Longman, Harlow.

[8] Colton, D. and Kress, R. (1983) Integral Equation Method in Scattering Theory. John Wiley, New York.

[9] Abdou, M.A. (2003) On Asymptotic Method for Fredholm-Volterra Integral Equation of the Second Kind in Contact Problems. *Journal of Computational and Applied Mathematics*, **154**, 431-446. http://dx.doi.org/10.1016/S0377-0427(02)00862-2

[10] Noda, N. and Hetnarski Yoshinobu Tanigowa, R.B. (2003) Thermal Stresses. Taylor and Francis, UK.

[11] Hetnarski, R.B. (2004) Mathematical Theory of Elasticity. Taylor and Francis, London.

[12] Parkus, H. (1976) Thermoelasticity. Springer-Verlag, New York.

[13] Gakhov, F.D. (1966) Boundary Value Problems. General Publishing Company, Ltd., Canada

[14] Ciarlet, P.G., Schultz, M.H. and Varga, R.S. (1967) Numerical Methods of High-Order Accuracy for Nonlinear Boundary Value Problems. I. One Dimensional Problem. *Numerische Mathematik*, **9**, 394-430.

[15] Zebib, A. (1984) A Chebyshev Method for the Solution of Boundary Value Problems. *Journal of Computational Physics*, **53**, 443-455. http://dx.doi.org/10.1016/0021-9991(84)90070-6

[16] Saito, S. and Yamamto, M. (1989) Boundary Value Problems of Quasilinear Ordinary Differential Systems on a Finite Interval. *Math. Japon.*, **34**, 447-458.

[17] Abdou, M.A. (1994) First and Second Fundamental Problems for an Elastic Infinite Plate with a Curvilinear Hole. *Alex. Eng. J.*, **33**, 227-233.

[18] Abdou, M.A. (2002) Fundamental Problems for an Infinite Plate with a Curvilinear Hole Having Infinite Poles. *Applied Mathematics and Computation*, **125**, 177-193.

[19] Abdou, M.A. and Khamis, A.K. (2000) On a Problem of an Infinite Plate with a Curvilinear Hole Having Three Poles and Arbitrary Shape. *Bulletin of the Calcutta Mathematical Society*, **92**, 309-322.

[20] Abd-Alla, A.M., Abo-Dahab, S.M. and Bayones, F.S. (2013) Propagation of Rayleigh Waves in Magneto-Thermo-Elastic Half-Space of a Homogeneous Orthotropic Material under the Effect of Rotation, Initial Stress and Gravity

Field. *Journal of Vibration and Control*, **19**, 1395-1420. http://dx.doi.org/10.1177/1077546312444912

[21] Abd-Alla, A.M. and Abo-Dahab, S.M. (2012) Effect of Rotation and Initial Stress on an Infinite Generalized Magneto-Thermoelastic Diffusion Body with a Spherical Cavity. *Journal of Thermal Stresses*, **35**, 892-912. http://dx.doi.org/10.1080/01495739.2012.720209

[22] Abd-Alla, A.M., Abd-Alla, A.N. and Zeidan, N.A. (2000) Thermal Stresses in a Non-Homogeneous Orthotropic Elastic Multilayered Cylinder. *Journal of Thermal Stresses*, **23**, 413-428.

[23] Abd-Alla, A.M., Mahmoud, S.R., Abo-Dahab, S.M. and Helmy, M.I. (2011) Propagation of S-Wave in a Non-Homogeneous Anisotropic Incompressible and Initially Stressed Medium under Influence of Gravity Field. *Applied Mathematics and Computation*, **217**, 4321-4332. http://dx.doi.org/10.1016/j.amc.2010.10.029

[24] Abd-Alla, A.M., Mahmoud, S.R. and AL-Shehri, N.A. (2011) Effect of the Rotation on a Non-Homogeneous Infinite Cylinder of Orthotropic Material. *Applied Mathematics and Computation*, **217**, 8914-8922.

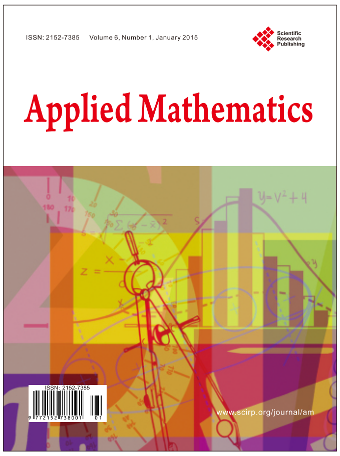

Call for Papers

Applied Mathematics (AM)

ISSN Print: 2152-7385 ISSN Online: 2152-7393
http://www.scirp.org/journal/am

Applied Mathematics **(AM)** is an international journal dedicated to the latest advancement of applied mathematics. The goal of this journal is to provide a platform for scientists and academicians all over the world to promote, share, and discuss various new issues and developments in different areas of applied mathematics.

Subject Coverage

All manuscripts must be prepared in English, and are subject to a rigorous and fair peer-review process. Accepted papers will immediately appear online followed by printed hard copy. The journal publishes original papers including but not limited to the following fields:

- Applied Probability
- Applied Statistics
- Approximation Theory
- Chaos Theory
- Combinatorics
- Complexity Theory
- Computability Theory
- Computational Methods in Mechanics and Physics
- Continuum Mechanics
- Control Theory
- Cryptography
- Discrete Geometry
- Dynamical Systems
- Elastodynamics
- Evolutionary Computation
- Financial Mathematics
- Fuzzy Logic
- Game Theory
- Graph Theory
- Information Theory
- Inverse Problems
- Linear Programming
- Mathematical Biology
- Mathematical Chemistry
- Mathematical Economics
- Mathematical Physics
- Mathematical Psychology
- Mathematical Sociology
- Matrix Computations
- Neural Networks
- Nonlinear Processes in Physics
- Numerical Analysis
- Operations Research
- Optimal Control
- Optimization
- Ordinary Differential Equations
- Partial Differential Equations
- Probability Theory
- Statistical Finance
- Stochastic Processes
- Theoretical Statistics

We are also interested in: 1) Short Reports—2-5 page papers where an author can either present an idea with theoretical background but has not yet completed the research needed for a complete paper or preliminary data; 2) Book Reviews—Comments and critiques.

Notes for Intending Authors

Submitted papers should not have been previously published nor be currently under consideration for publication elsewhere. Paper submission will be handled electronically through the website. All papers are refereed through a peer review process. For more details about the submissions, please access the website.

Website and E-mail

http://www.scirp.org/journal/am **E-mail: am@scirp.org**

What is SCIRP?

Scientific Research Publishing (SCIRP) is one of the largest Open Access journal publishers. It is currently publishing more than 200 open access, online, peer-reviewed journals covering a wide range of academic disciplines. SCIRP serves the worldwide academic communities and contributes to the progress and application of science with its publication.

What is Open Access?

All original research papers published by SCIRP are made freely and permanently accessible online immediately upon publication. To be able to provide open access journals, SCIRP defrays operation costs from authors and subscription charges only for its printed version. Open access publishing allows an immediate, worldwide, barrier-free, open access to the full text of research papers, which is in the best interests of the scientific community.

- High visibility for maximum global exposure with open access publishing model
- Rigorous peer review of research papers
- Prompt faster publication with less cost
- Guaranteed targeted, multidisciplinary audience

Scientific
Research
Publishing

Website: http://www.scirp.org

Subscription: sub@scirp.org

Advertisement: service@scirp.org